AD-A040 130 PARKS COLL OF SAINT LOUIS UNIV CAHOKIA ILL F/G 1/3
APPLICATIONS OF THE SHOCK PULSE TECHNIQUE TO HELICOPTER DIAGNOS--ETC(U)
FEB 75 T C MAYER, E F COVILL, J A GEORGE DAAJ01-72-A-0027
USAAVSCOM-TR-77-21 NL

UNCLASSIFIED

1 OF 3
AD
A040 130

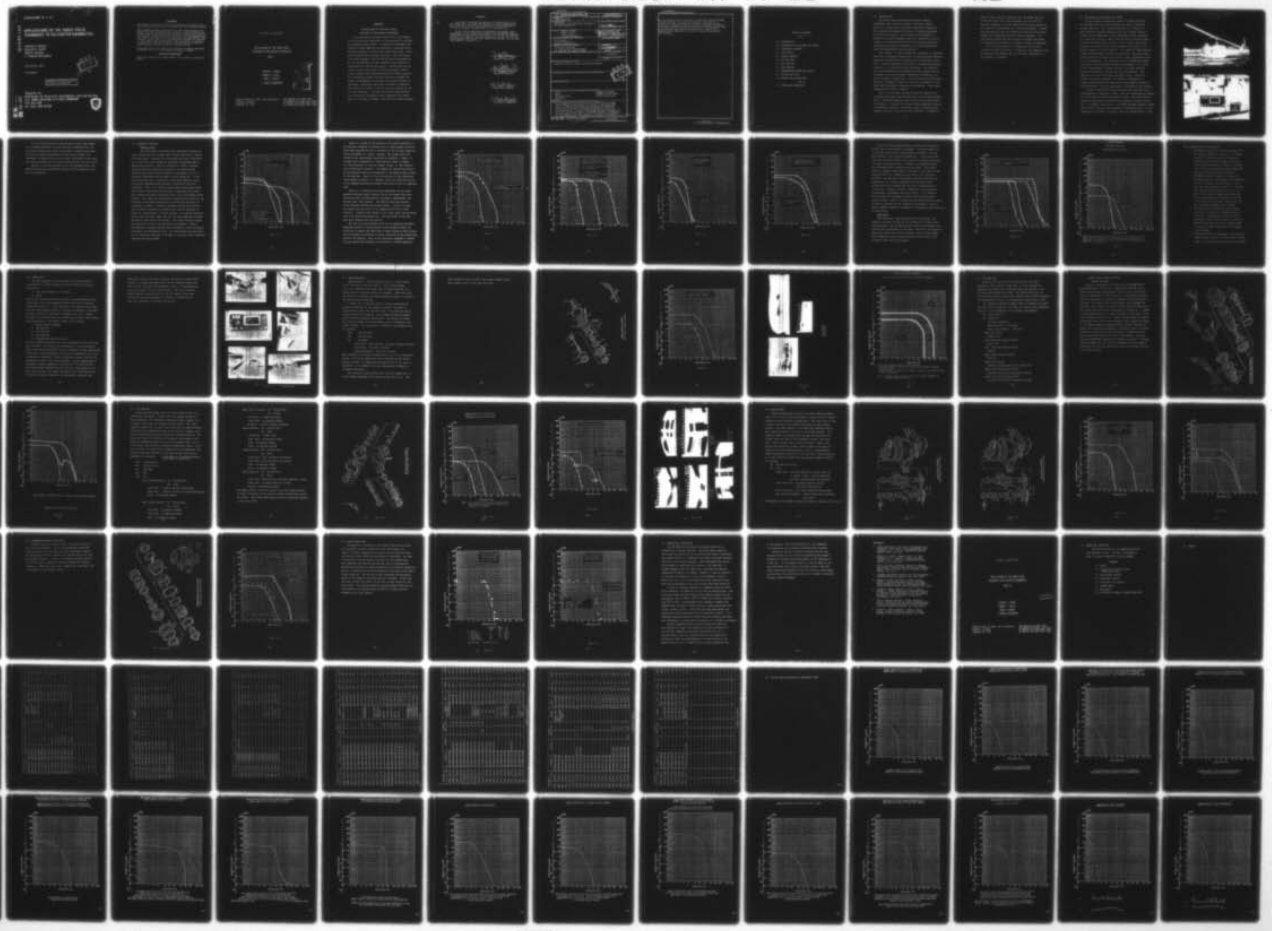

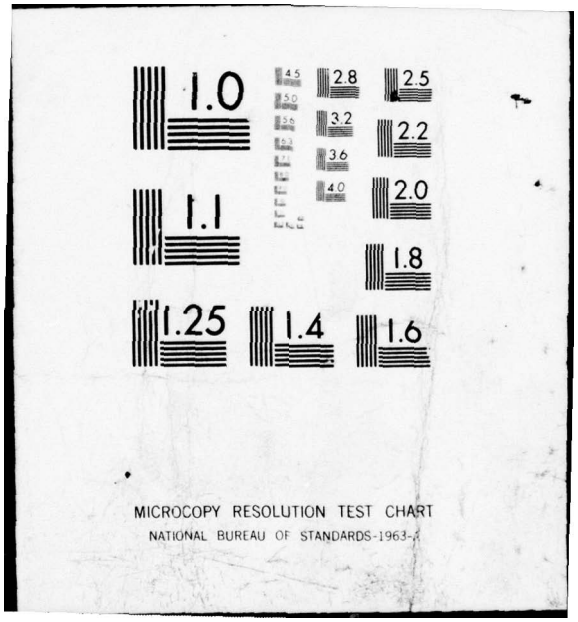
1.0
1.1
1.25
1.4
1.6
1.8
2.0
2.2
2.5
2.8
3.2
3.6
4.0
4.5
5.0
5.6
MICROCOPY RESOLUTION TEST CHART
NATIONAL BUREAU OF STANDARDS-1963-A

USAAVSCOM TR 77-21



# APPLICATIONS OF THE SHOCK PULSE TECHNIQUES TO HELICOPTER DIAGNOSTICS

Timothy C. Mayer
Edward F. Covill
John A. George
J. Thomas Harrington



24 February 1975

Final Report.



Prepared for
Directorate for Research, Development, and Engineering
U.S. ARMY AVIATION SYSTEMS COMMAND
P.O. Box 209
St. Louis, MO 63166

## DISCLAIMERS

The findings in this report are not to be construed as an official Department of the Army position unless so designated by other authorized documents.

When Government drawings, specifications, or other data are used for any purpose other than in connection with a definitely related Government procurement operation, the United States Government thereby incurs no responsibility nor any obligation whatsoever; and the fact that the Government may have formulated, furnished, or in any way supplied the said drawings, specifications, or other data is not to be regarded by implication or otherwise as in any manner licensing the holder or any other person or corporation, or conveying any rights or permission, to manufacture, use, or sell any patented invention that may in any way be related thereto.

Trade names cited in this report do not constitute an official endorsement or approval of the use of such commercial hardware or software.

## DISPOSITION INSTRUCTIONS

Destroy this report when no longer needed. Do not return it to the originator.

# F I N A L  R E P O R T

## APPLICATIONS OF THE SHOCK PULSE TECHNIQUE TO HELICOPTER DIAGNOSTICS

## PART I

TIMOTHY C. MAYER
EDWARD F. COVILL
JOHN A. GEORGE
J. THOMAS HARRINGTON

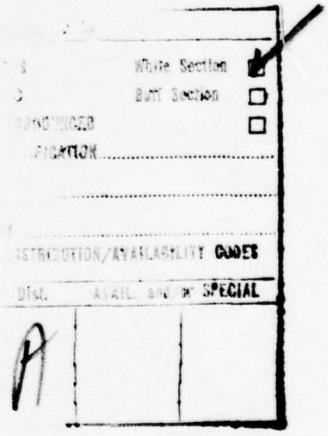


PARKS COLLEGE OF SAINT LOUIS UNIVERSITY
CAHOKIA, ILLINOIS
FEBRUARY 24, 1975

BOA DAAJ01-72-A-0027 (P6C)
DO DAAJ01-72-A-0027-0001 (P6C)
DO DAAJ01-72-A-0027-0002 (P6C)

## ABSTRACT

APPLICATIONS OF THE SHOCK PULSE
TECHNIQUE TO HELICOPTER DIAGNOSTICS

An investigation has been carried out on the feasibility of shock pulse techniques in the detection of failures in helicopter power trains. A standard off-the-shelf SKF Industries model MEPA-10A was employed to construct shock emission envelopes of shock rate versus shock level. Data was collected from the hanger bearings of the tail rotor drive shaft assembly, the $42^{o}$ and $90^{o}$ gear box assemblies, and the transmission and mast assemblies as installed on operational UH-1 series helicopters. Further data was obtained on the OH-58 as well as from helicopters at Fort Rucker, Alabama with implanted bearings of known condition. The correlation between the shock emission envelopes and degree of degradation as revealed by teardown analysis is described. Laboratory tests were conducted to determine the condition of gears in the $42^{o}$ gear box through the use of shock emissions. The shock pulse meter shows promise for its ability to separate those components with normal wear, or the onset of damage, from those with severe damage.

FOREWARD

This report presents the results of the analysis of the SKF Industries, Inc. MEPA-10A Shock Pulse Meter conducted by Parks College of Saint Louis University with SKF Industries of King of Prussia, Pennsylvania, as a subcontractor.

Parks College gratefully acknowledges the support and assistance of the United States Army Aviation Systems Command (USAAVSCOM) Flight Operations Division, St. Louis, MO; Hawthorn Aviation, Fort Rucker, AL; Bell Helicopter Co., Ft. Worth, TX; United States Army Flight Test Board, Fort Rucker, AL; and the 102d USARFFAC, Cahokia, IL.

Mr. Timothy C. Mayer
Research Associate

Mr. Edward F. Covill
Research Associate

Dr. John A. George
Technical Director

J. Thomas Harrington
Director of Research

Unclassfied

SECURITY CLASSIFICATION OF THIS PAGE *(When Data Entered)*

# REPORT DOCUMENTATION PAGE

READ INSTRUCTIONS BEFORE COMPLETING FORM

| | |
|---|---|
| 1. REPORT NUMBER: USAAVSCOM TR-77-21 | 2. GOVT ACCESSION NO. |
| 3. RECIPIENT'S CATALOG NUMBER | |
| 4. TITLE *(and Subtitle)*: Applications of the Shock Pulse Technique to Helicopter Diagnostics. | 5. TYPE OF REPORT & PERIOD COVERED: Final Report. |
| | 6. PERFORMING ORG. REPORT NUMBER |
| 7. AUTHOR(s): Timothy C. Mayer, Edward F. Covill, John A. George, J. Thomas Harrington | 8. CONTRACT OR GRANT NUMBER(s): DAAJ01-A-0027 (P6C); DAAJ01-72-A-0027-0001(P6C); DAAJ01-72-A-0027-0002(P6C) |
| 9. PERFORMING ORGANIZATION NAME AND ADDRESS: Parks College, St. Louis University, Cahokia, Illinois 62206 | 10. PROGRAM ELEMENT, PROJECT, TASK AREA & WORK UNIT NUMBERS |
| 11. CONTROLLING OFFICE NAME AND ADDRESS: Directorate for RDandE., U.S. Army Aviation Systems Command, P.O. Box 209 St. Louis, MO 63166 | 12. REPORT DATE: 24 February 1975 |
| | 13. NUMBER OF PAGES: 270 (217 p.) |
| 14. MONITORING AGENCY NAME & ADDRESS *(if different from Controlling Office)* | 15. SECURITY CLASS. *(of this report)*: unclassified |
| | 15a. DECLASSIFICATION/DOWNGRADING SCHEDULE |

16. DISTRIBUTION STATEMENT *(of this Report)*

Approved for public release; distribution unlimited.



17. DISTRIBUTION STATEMENT *(of the abstract entered in Block 20, if different from Report)*

18. SUPPLEMENTARY NOTES

19. KEY WORDS *(Continue on reverse side if necessary and identify by block number)*

Shock
Pulses
Helicopter Rotors
Helicopters
Drives
Diagnostic Equipment
AIDAPS Test Bed Program
Condition Monitoring

20. ABSTRACT *(Continue on reverse side if necessary and identify by block number)*

An investigation has been carried out on the feasibility of shock pulse techniques in the detection of failures in helicopter power trains. A standard off-the-shelf SKF Industries model MEPA-10A was employed to construct shock emission envelopes of shock rate versus shock level. Data was collected from the hanger bearings of the tail rotor drive shaft assembly, the 42° and 90° gear box assemblies, and the transmission and mast assemblies as installed on operational UH-1 series helicopters. Further data was obtained on the OH-58 as NEXT page

DD FORM 1 JAN 73 1473 EDITION OF 1 NOV 65 IS OBSOLETE

49250 only

unclassified

SECURITY CLASSIFICATION OF THIS PAGE *(When Data Entered)*

well as from helicopters at Fort Rucker, Alabana with implanted bearings of known condition. The correlation between the shock emission envelopes and degree of degredation as revealed by teardown analysis is described. Laboratory tests were conducted to determine the condition of the gears in the 42° gear box through the use of shock emissions. The shock pulse meter shows promise for its ability to separate those components with normal wear, or the onset of damage, from those with severe damage.

TABLE OF CONTENTS

Part I



Part II

## 1.0 INTRODUCTION

The United States Army Aviation Systems Command (USAAVSCOM) has an ongoing program to develop a system which will automatically accomplish inspection, diagnostic, and prognostic maintenance functions on related subsystems of the UH-1 helicopter. This program, called AIDAPS, is intended to provide equipment which will contribute to an increase in the tactical mobility of Army aviation operations and provide an effective reduction in aircraft maintenance costs and maintenance related accidents.

Past efforts [1-4] have included the collection of vibration data with a subsequent analysis of the resulting Power Spectral Densities to determine the condition of the helicopter power train. Another approach, particularly in determining bearing condition, is to use shock pulse techniques. The technique and instrumentation were developed by AB SKF, Sweden and are available in the United States through SKF Industries, Inc., King of Prussia, Pennsylvania. Parks College was placed under contract to AVSCOM to conduct an intensive evaluation of the shock pulse diagnostic technique to helicopters. This report summarizes the effort to date[5-8].

Part I of the report briefly reviews the operation of the shock pulse meter and the generation of the shock emission curve. The shock emission curve is the basic starting point for analysis. Findings of the preliminary laboratory analysis on bearings as well as a laboratory study in detecting gear damage on the UH-1 42$^{o}$ gear box are presented. A summary is

given of data which was collected from the hanger bearings of the tail rotor drive shaft assembly, the $42^{o}$ and $90^{o}$ gear box assemblies, and the transmission and mast assemblies as installed on operational UH-1 series helicopters. Further data was obtained from the AIDAPS helicopters at Fort Rucker, Alabama with implanted bearings of known condition. The correlation between the shock emission envelopes and degree of degradation as revealed by teardown analysis is described.

Part II of the report is a compilation of all data collected during this effort. In addition, the complete study in detecting gear damage, made by SKF under subcontract to the College is included.

## 2.0 EXPLANATION OF THE MEPA-10A SYSTEM

As an alternative diagnostic method in bearing analysis, the SKF MEPA-10A shock pulse technique was used to determine bearing condition. The technique employed is to construct a shock emission envelope containing the rate of shock emission as well as the measurement of the amplitude of shock developed by a particular bearing. When a bearing race or rolling element contains a discrete fault, such as a pit or spall, the contact between this fault and the rolling elements will result in repetitive impacts of short duration. As a result of these impacts, a shock wave propagates through the structure. The shock pulse travels through the bearing and causes a pulse displacement input to an accelerometer. The equipment used in the MEPA-10A system includes a 38 KHZ resonance response accelerometer. The output of the accelerometer is passed through a high gain amplifier tuned at the resonant frequency of the accelerometer. This amplifier acts as a very sharp band-pass filter. After the signal is suitably processed, the output is displayed on a counter which provides the frequency of peaks above any desired peak amplitudes. No other processing is required for the analysis.

A graph is made of the shock emissions and from this data a determination of condition is made. With the accelerometer attached, an initial rate and value evaluation is made. The rate found becomes the first point plotted on the ordinate at a shock level of one. A threshold varing dial, on the MEPA-10A meter housing, ranges from a level of one to ten thousand on a logrithmic scale. As the threshold is increased, successive rates are plotted until a curve

SHOCK PULSE TECHNIQUE AS A DIAGNOSTIC

TOOL FOR HELICOPTERS

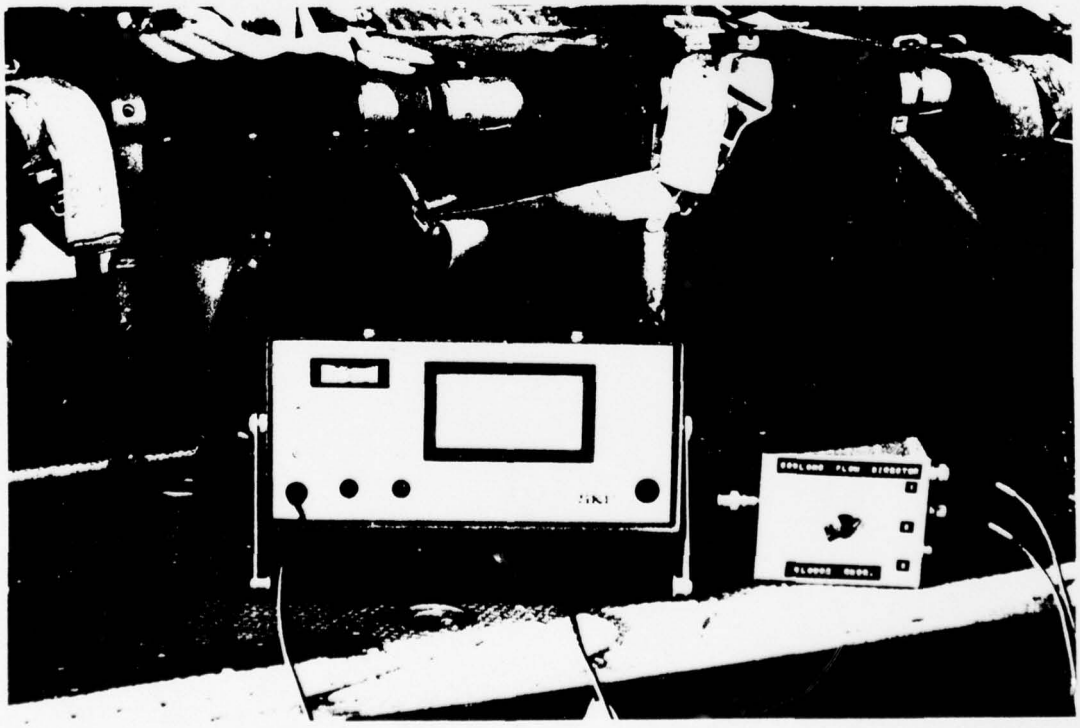

Fig 1

crosses the abscissa. The value at the intercept becomes the highest potentiometer level at which at least one shock pulse per second can be measured. Rate values are in pulses per second and shock level obtained is in relation to the displacement of the accelerometer used. The curves drawn are evaluated by their general curve form and the magnitude of rates and/or levels obtained.

The meter is logrithmicly integrated and the movement is approximately $90^{o}$. Since a logrithmic scale is employed, the reading from $0^{o}$ to $80^{o}$'s of movement corresponds to 0 to 1000 on the meter, while the remaining $10^{o}$'s consists of readings 1000 to 10,000. Because of this situation, and that the first point plotted is dependent on one reading along the ordinate, needle swing may cause difficulty in initial rate determination. This does not affect the shock level and yields no overall impediment in determining bearing condition.

SKF Industries indicates in their operator's manual, included with the MEPA-10A, that all curves plotted are a variation of three general forms 1) one with high rates and relatively low levels - an apparent indication of foreign matter in the lubricant of the bearing, 2) a curve shape of low rates and levels of shock values which reach a relatively high degree - a curve slope indicative of a bearing with insufficient lubricant or possible element damage. 3) a curve with both significantly high values in rate and level - the amount of "filling out" of this curve would be proportionate to the extent which the damage is encountered in the bearing. (Fig. 2.0)

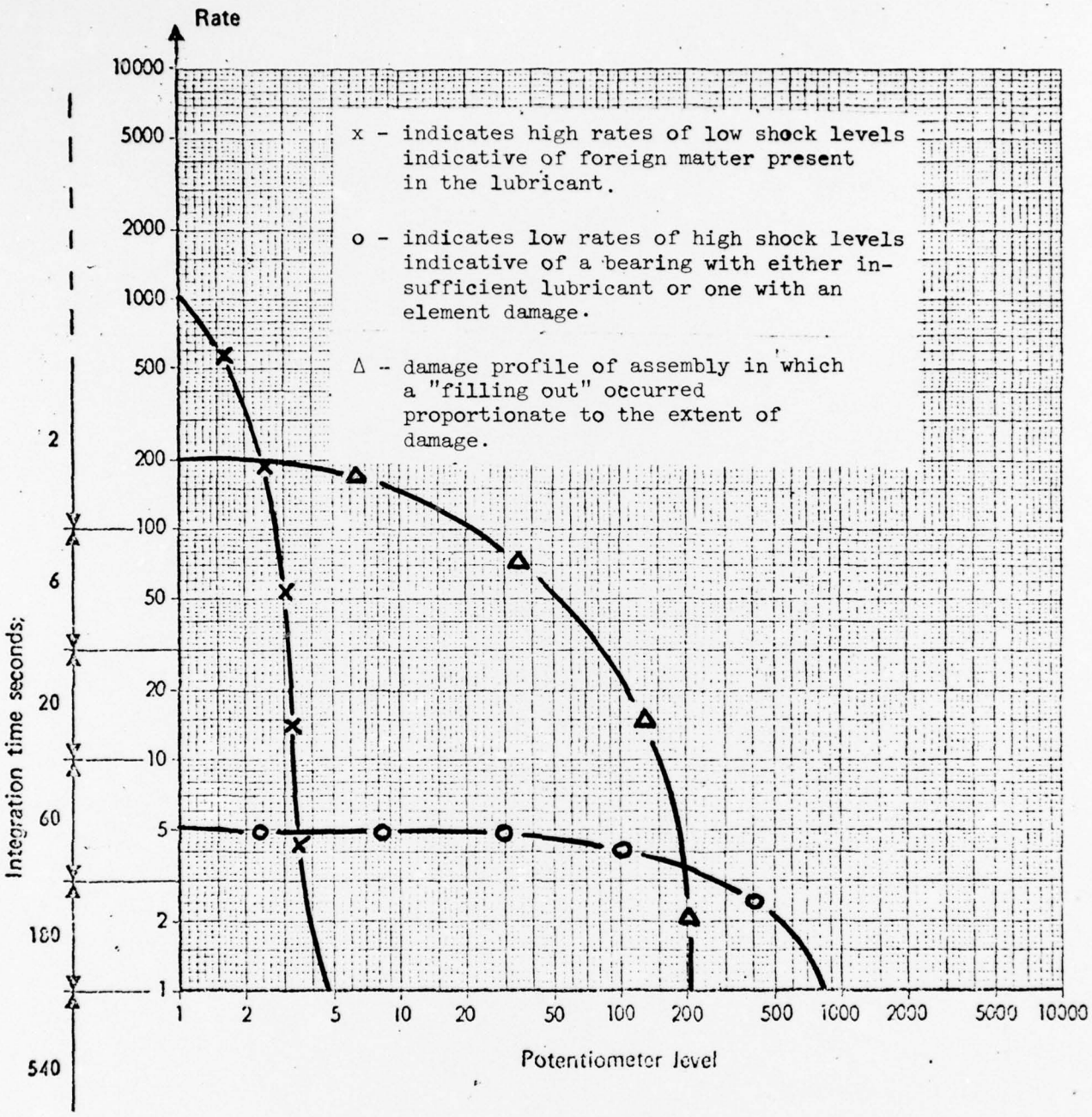
Rate
10000
5000
2000
1000
500
200
100
50
20
10
5
2
1
x - indicates high rates of low shock levels indicative of foreign matter present in the lubricant.
o - indicates low rates of high shock levels indicative of a bearing with either insufficient lubricant or one with an element damage.
Δ - damage profile of assembly in which a "filling out" occurred proportionate to the extent of damage.
Integration time seconds:
2
6
20
60
180
540
1
2
5
10
20
50
100
200
500
1000
2000
5000
10000
Potentiometer level

Fig. 2.0

Of the curves plotted on bearings with either known damage or of unknown condition, no case has been documented which fit the precise theoretical forms as described. Although the amount and type of damage approximates the theoretical shapes, the assessment of damage relies on an overall evaluation of the curve, any slope irregularities, as well as magnitude of rate and values.

Because of size and portability of the equipment used, the MEPA-10A shock pulse method was operated in both laboratory and field environments.

## 3.0 LABORATORY FINDINGS

### Bearing Tests

The first use of the shock pulse technique performed by Parks College was on an AIDAPS test aircraft operated at Granite City Army Depot. Although this was technically not a laboratory use, it was the first attempt to establish the methods used in shock pulse analysis. Data was collected in order to become familiar with the technique of analysis, to identify areas where further study could profitably be undertaken, and to investigate consistency and accuracy of data collection. It was found that there was a difference in the shock emission curves of good and degraded hanger bearings installed on the UH-1H helicopter (Fig. 3.0). Several questionable areas arose during this initial phase which precipitated a laboratory study under more closely controlled conditions than a field environment could provide. This study was undertaken to determine the nature of the different curve shapes which could be plotted and evaluate the threshold of damage. A MEPA-10A analyzer coupled with several other pieces of electronic equipment were used on bearings rotating at, approximately, constant speeds. All bearings analyzed were of the same type, make, and size as those employed as hanger bearings on UH-1 series helicopters. The hanger bearing fixture was identical to that of an operational helicopter. Several accelerometer attaching methods were evaluated in order to achieve consistent and reproducible data. An oscilloscope was used keyed to the rotational frequency in attempt to correlate shock emissions depicted with known damage.

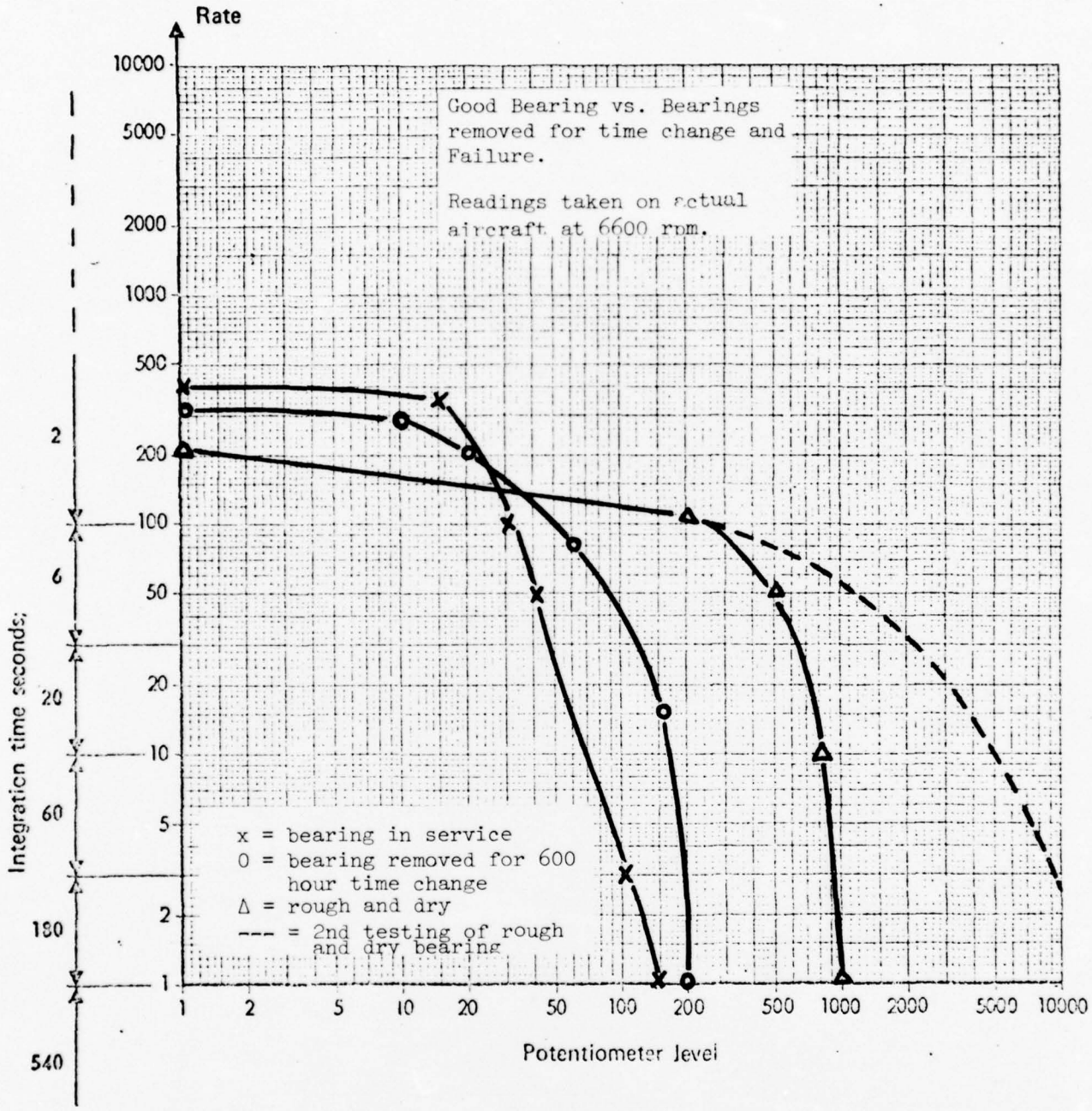
Rate
10000
5000
2000
1000
500
200
100
50
20
10
5
2
1
Good Bearing vs. Bearings removed for time change and Failure.
Readings taken on actual aircraft at 6600 rpm.
x = bearing in service
0 = bearing removed for 600 hour time change
Δ = rough and dry
--- = 2nd testing of rough and dry bearing
Integration time seconds
2
6
20
60
180
540
1
2
5
10
20
50
100
200
500
1000
2000
5000
10000
Potentiometer level

Fig. 3.0

Figure 3.1 shows the differences in the shock emissions of new bearings compared to bearings with an unserviceable condition which were rejected for use in aircraft by the US Army inspection facility USAAVNS, Ft. Rucker, Alabama. The higher rates and levels of the unserviceable bearings are apparent. Figure 3.2 is made from a comparison of three specific types of damage: 1) Dirty lubricant, 2) Rolling element damage, 3) "Dry bearing" with insufficient lubricant. The damage was induced artifically on new bearings which are represented on the graph as data scatter of new bearings. There is little correlation to the theoretical curve shapes of Figure 2.0. However, again the rates and levels of the damaged bearings are greater than those of new or undamaged ones.

Figure 3.3 illustrates the speed dependence of the shock emission envelope using a bearing run at two speeds with other conditions such as accelerometer attachment, temperature, and bearing load, held constant. The bearing used had lubricant which contained foreign particulate matter. Figure 3.4 shows the change that can occur in the damage profile over a time interval. A bearing with damage to the "inner race" was monitored over a 100 minute continuous run. The conditions of the test were held constant over this period.

The use of an oscilloscope as an aid in depicting the shock emissions proved of little relative value because of both the difficulty in keying the amplitude of sweep traces to shock levels and the problem of isolating a single revolution of the inner/outer races of the bearing. Very little additional diagnostic information was gained and therefore not employed in further analysis.

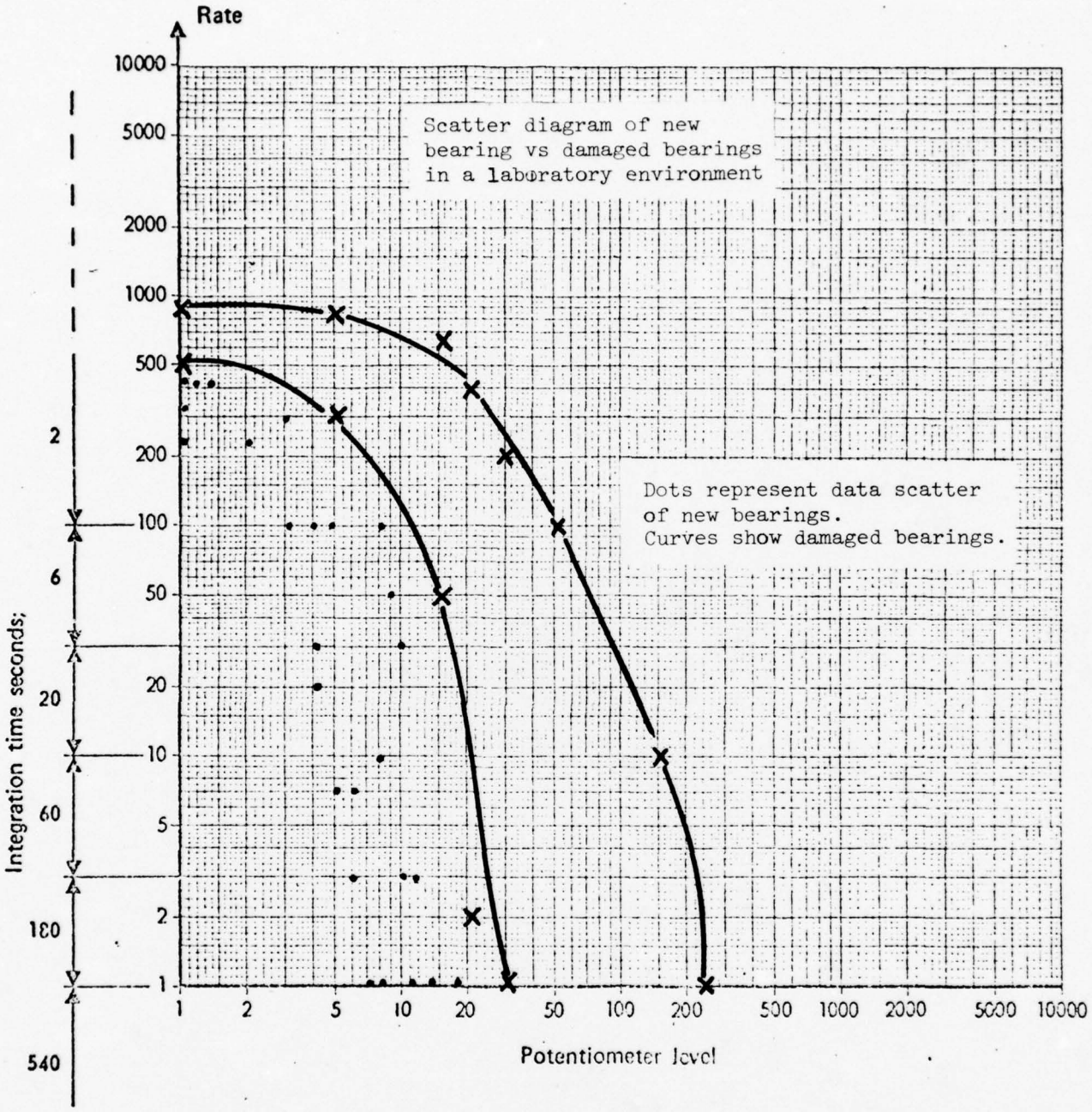
Rate
10000
5000
2000
1000
500
200
100
50
20
10
5
2
1
Scatter diagram of new
bearing vs damaged bearings
in a laboratory environment
Dots represent data scatter
of new bearings.
Curves show damaged bearings.
Integration time seconds;
2
6
20
60
180
540
1
2
5
10
20
50
100
200
500
1000
2000
5000
10000
Potentiometer level

Fig. 3.1

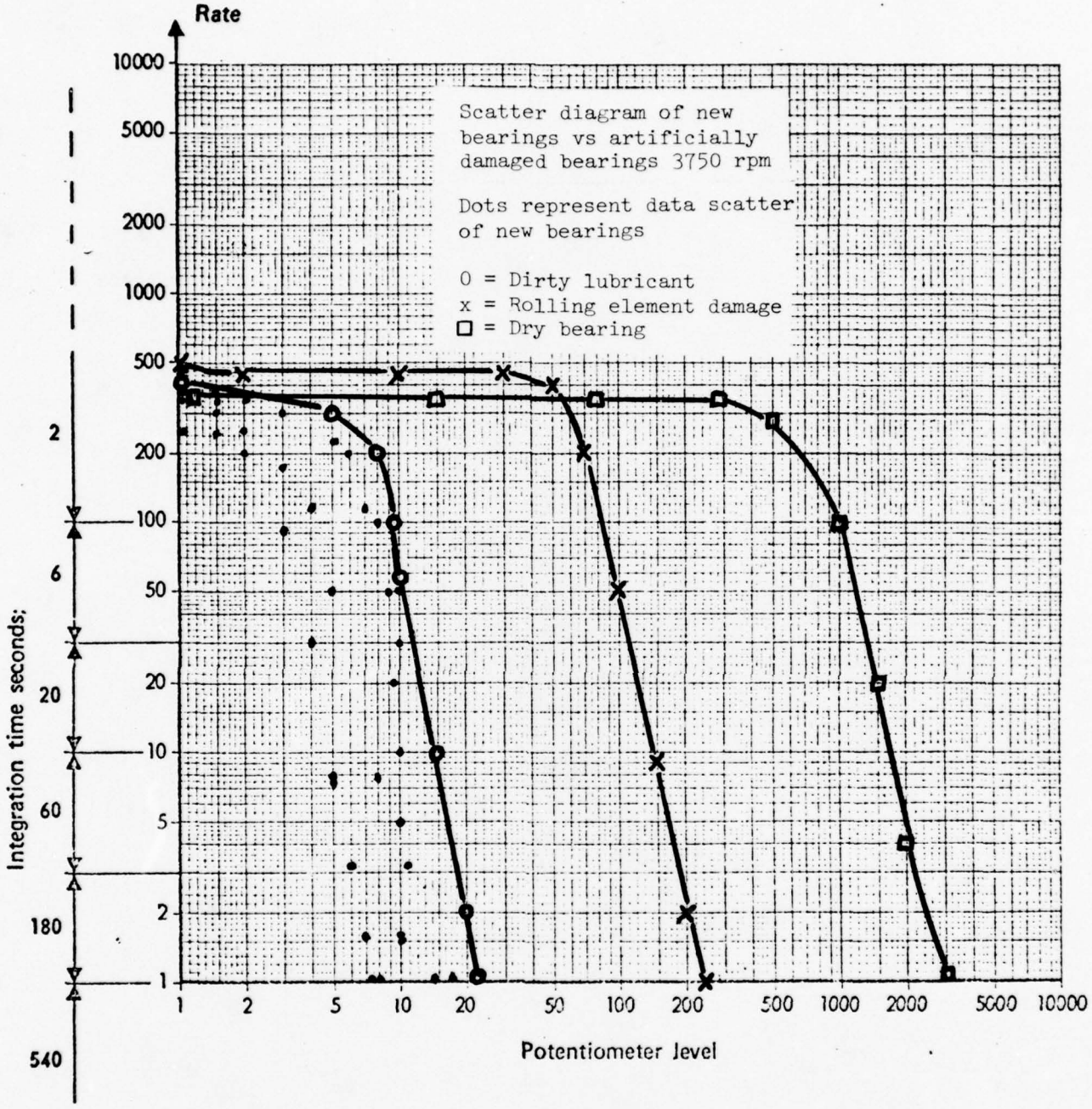
Rate
10000
5000
2000
1000
500
200
100
50
20
10
5
2
1
Scatter diagram of new bearings vs artificially damaged bearings 3750 rpm
Dots represent data scatter of new bearings
0 = Dirty lubricant
x = Rolling element damage
□ = Dry bearing
Integration time seconds;
2
6
20
60
180
540
1
2
5
10
20
50
100
200
500
1000
2000
5000
10000
Potentiometer level

Fig. 3.2

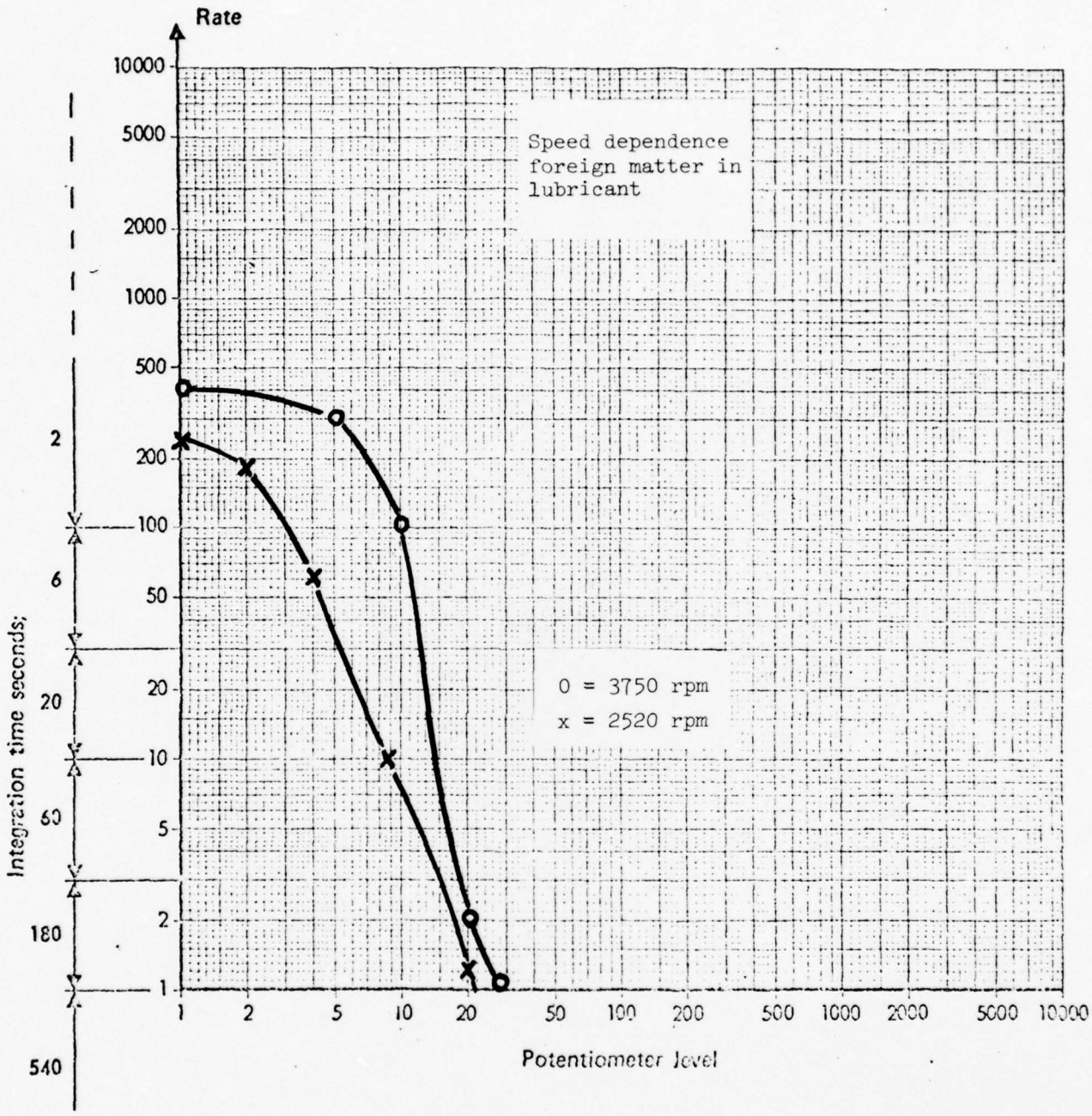
Rate
10000
5000
2000
1000
500
200
100
50
20
10
5
2
1
Speed dependence
foreign matter in
lubricant
0 = 3750 rpm
x = 2520 rpm
Integration time seconds;
2
6
20
60
180
540
1
2
5
10
20
50
100
200
500
1000
2000
5000
10000
Potentiometer level

Fig. 3.3

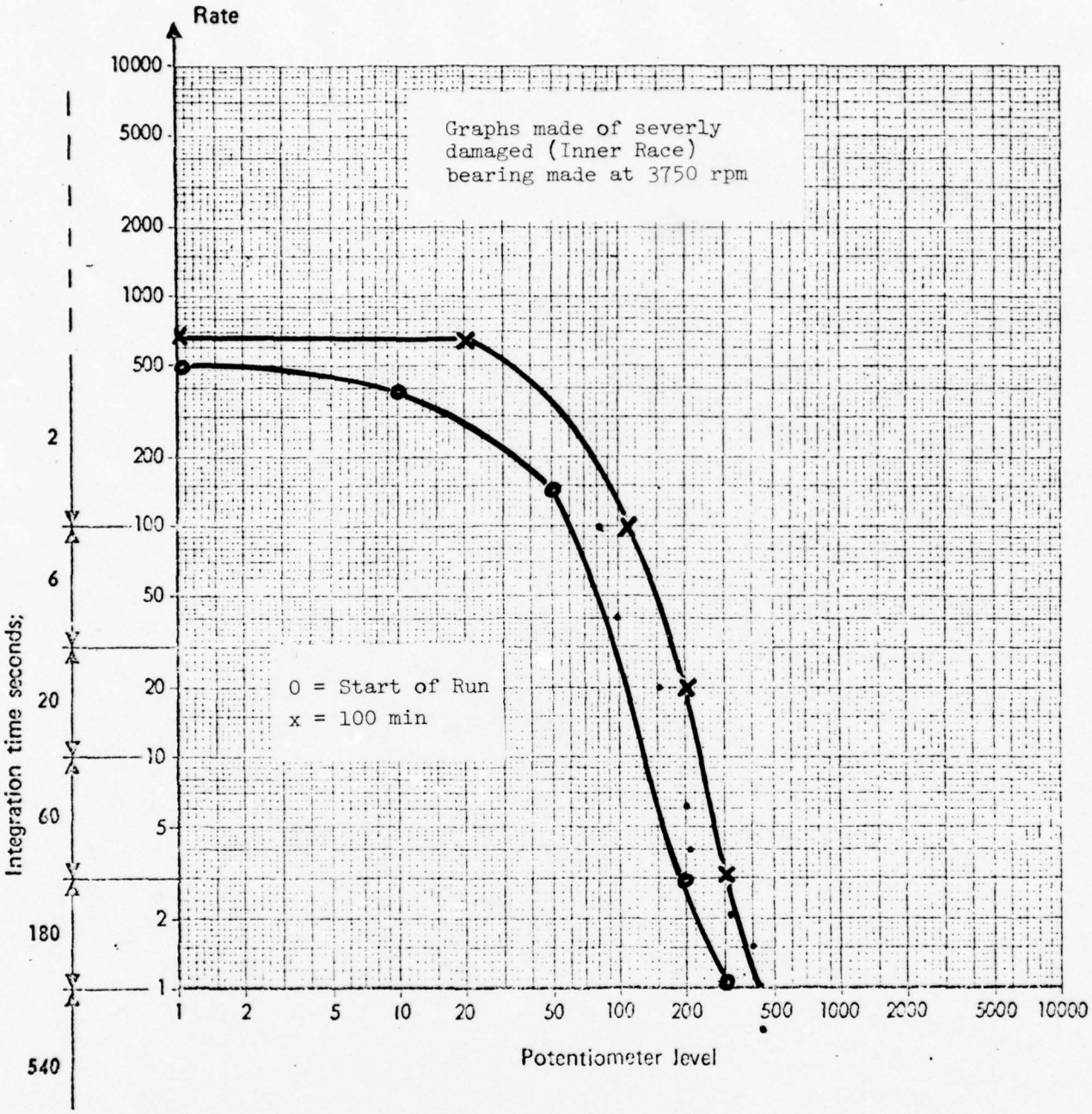
Rate
10000
5000
2000
1000
500
200
100
50
20
10
5
2
1
Graphs made of severly
damaged (Inner Race)
bearing made at 3750 rpm
0 = Start of Run
x = 100 min
Integration time seconds;
2
6
20
60
180
540
1
2
5
10
20
50
100
200
500
1000
2000
5000
10000
Potentiometer level

Fig. 3.4

One of the first problems which confronted the gathering of data was in accelerometer attachment. A device similar to a vice grip pliers with an accelerometer attached to one jaw was included in the equipment accessories. It was found that using the vice grip device did not allow for enough consistency to insure reproducible data. A number of attachment methods were employed before a suitable one was found. The present device, a pressure clamp which is attached to the lands of the mounting bolts for a component, was used on all field test aircraft. By designing five separate attaching fixtures, designated as VD 1-5,most components with bearings can be quickly and easily analyzed and yet assure reproducibility of the data. Figure 3.5 shows a comparison of variations of accelerometer attachments that were tested. It is apparent that the type of attachment strongly influences the shock emission curve. Figure 3.6 shows the same hanger bearing tested on both an aircraft and the laboratory environment. This indicates damage thresholds determined by laboratory tests would not be appropriate.

Gear Tests

SKF Industries, under subcontract to the College, was tasked to evaluate the ability of the MEPA-10A to detect gear sourced shocks. The College provided technical assistance and monitored the performance of the task. Three UH-1 helicopter 42 degree gear boxes with several different types of gear damage were subjected to shock pulse monitoring during runs at two different loads and at two speeds.

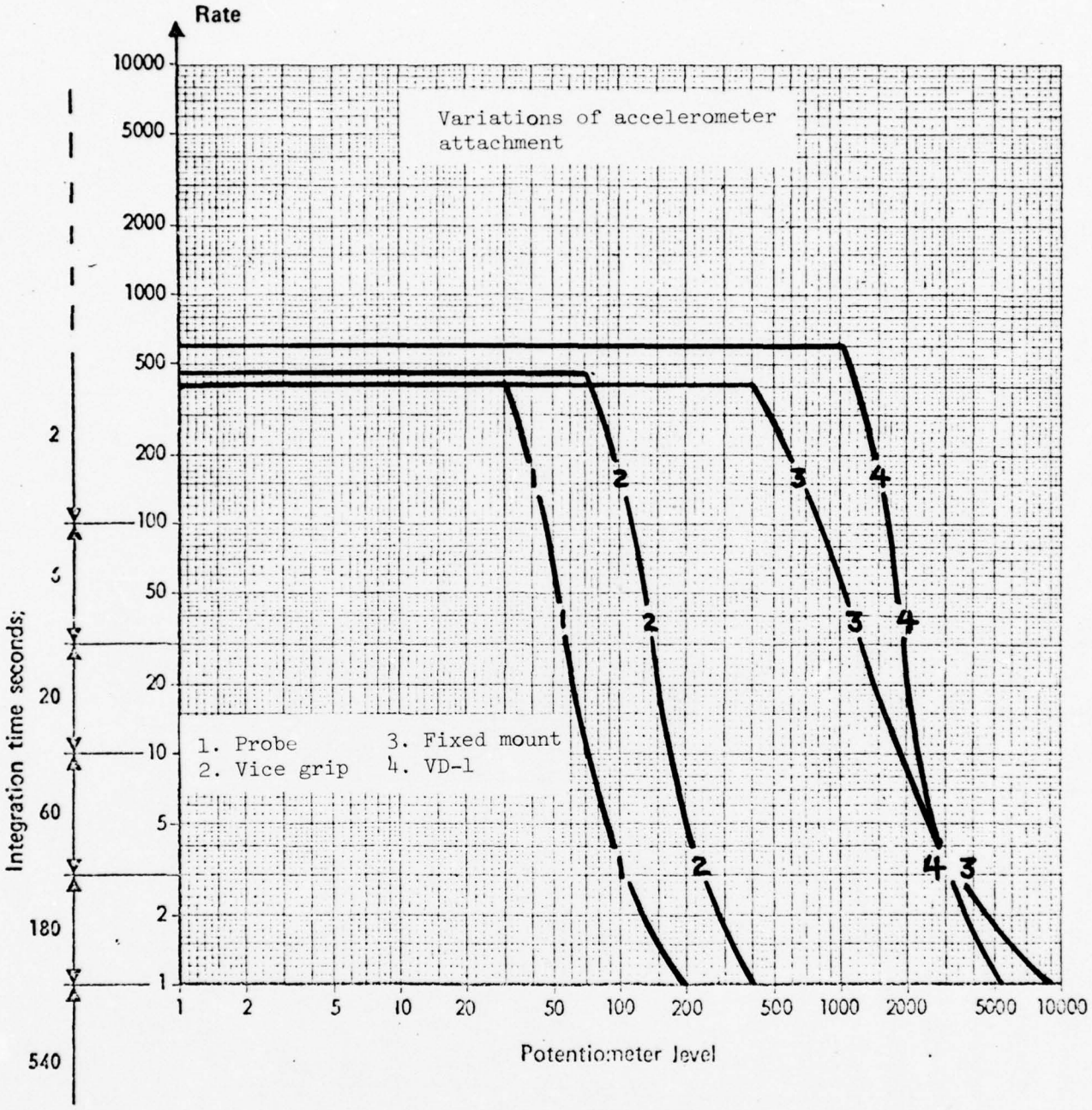
Rate
10000
5000
2000
1000
500
200
100
50
20
10
5
2
1
Variations of accelerometer attachment
1. Probe
2. Vice grip
3. Fixed mount
4. VD-1
Integration time seconds:
2
5
20
60
180
540
1
2
5
10
20
50
100
200
500
1000
2000
5000
10000
Potentiometer level

Figure 3.5

4 HANGER BEARINGS

UH-1H TAIL #66-01087

TEST CONDUCTED 28 NOV 1973

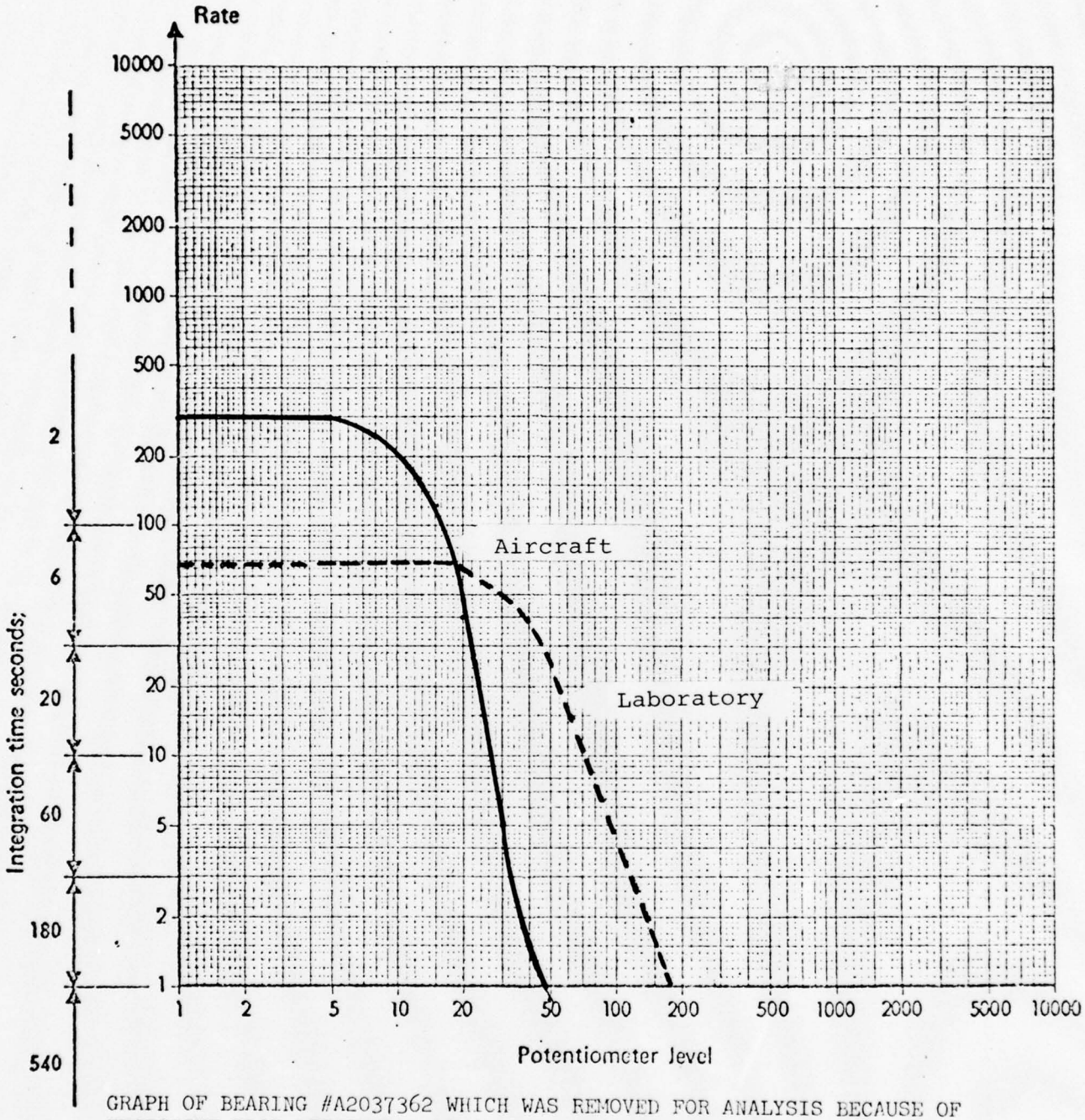


GRAPH OF BEARING #A2037362 WHICH WAS REMOVED FOR ANALYSIS BECAUSE OF EXCESSIVE PLAY DISCOVERED BY AN AIRCRAFT TECHNICAL INSPECTOR - ONE GRAPH MADE ON AIRCRAFT, THE OTHER IN LABORATORY AT APPROXIMATELY THE SAME RPM. (14 DEC 1973).

Fig. 3.6

The following has been determined:

1. The MEPA-10A as used can supply warnings as to the onset of damage in a gear box. If damage originates in the bearings, an indication directly correlated with damage is received. If the damage originates in gears, the indication is due to the sensing of particulate contaminant passing through the bearings.
2. The MEPA-10A appears capable of detecting a secondary effect of gear damage in an operating $42^{O}$ UH-1 helicopter gear box since, in this gear box, the lubricant is captive in the gear box. Metal chips and particles are the products of the mesh of damaged gear teeth and tend to pass through the bearings as the oil in the gear box circulates. Shock level and rate increases accompany their passage.
3. The shock pulse technique has again proven successful in isolating a damaged bearing in a gear box. Standard shock pulse analysis techniques (shock emission profile) using the MEPA-10A were not found in the present study to provide a direct indication of the degree of gear damage.
4. Vibrational velocity measurement, analyzing the signal either in three, two and one-half octave bands, or one-third octave analysis of the audio-

frequency spectrum has failed to provide any consistent indication of damage.

Figure 3.7 illustrates the ability of the shock pulse technique to isolate foreign matter present in the lubricant of a 42° gear box run on a laboratory test facility. The foreign matter was a result of debris from damaged gears implanted in the assembly.

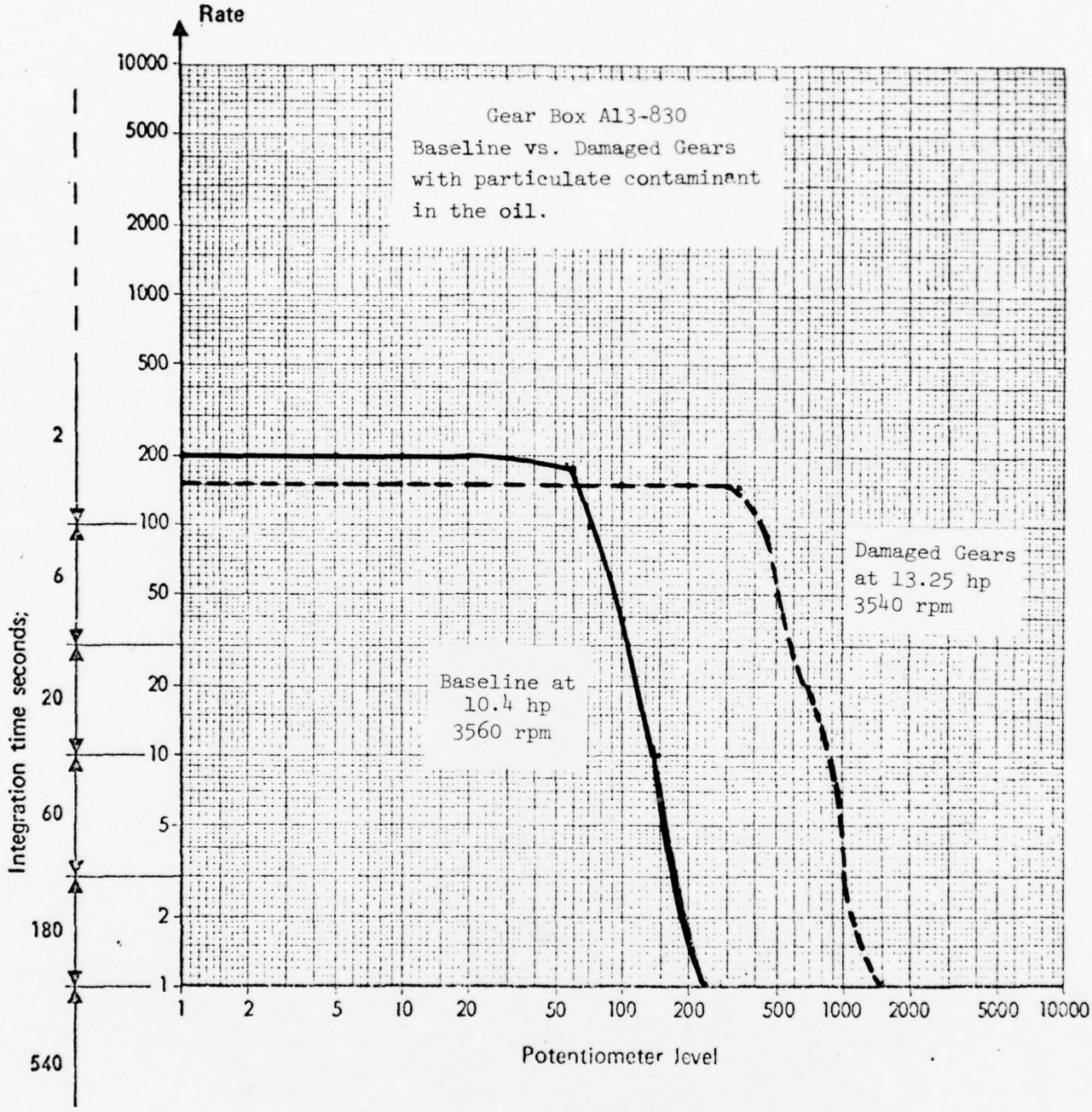
Rate
10000
5000
2000
1000
500
200
100
50
20
10
5
2
1
Gear Box A13-830
Baseline vs. Damaged Gears
with particulate contaminant
in the oil.
Damaged Gears
at 13.25 hp
3540 rpm
Baseline at
10.4 hp
3560 rpm
Integration time seconds;
2
6
20
60
180
540
1
2
5
10
20
50
100
200
500
1000
2000
5000
10000
Potentiometer level

Fig. 3.7

## 4.0 FIELD STUDY

The data presented in this section are selected typical evaluations of various components analyzed from the following helicopters:

1) UH-1 series models H, D, M and C
2) OH-58

Shock pulse signatures were made using a standard MEPA-10A shock pulse meter and all accelerometer mounts were with a pressure clamp device (VD 1-5). Each individual type component was tested with the accelerometer mounted as closely as possible in the same position relative to the bearing assembly (Fig. 4.0). Except as noted, all aircraft were run at 6600 rpm $N_2$ with no anti-torque pedal application. The areas of study are as follows:

1) Hanger bearing assembly
2) $42^{o}$ gear box
3) $90^{o}$ gear box
4) Mast bearing
5) Transmission input drive quill

This by no means represents all of the components which could have been analyzed. All testing was completed on a non-interference basis with military aircraft, Active and Reserve, normal operational scheduling. The accelerometer mounts were designed with this non-interference constraint in mind so component removal would not be necessary to install the testing fixture. Certain assemblies of the hanger bearing assemblies, $42^{o}$ gear box, $90^{o}$ gear box and mast bearing were removed from the aircraft, disassembled to inspect the bearings, and damage correlated with shock depictions. In addition, whenever possible the replacement component was

analyzed to verify that shock emission returned to a lower state. Section 7.0 (Tables and Appendices) of this report contains the bulk of data collected from assemblies tested. A representative group is reviewed in this summary report. The level of shock pulse emissions coupled with its rate and general curve form plotted on each type component is viewed in relation to the same type component to evaluate the bearing.

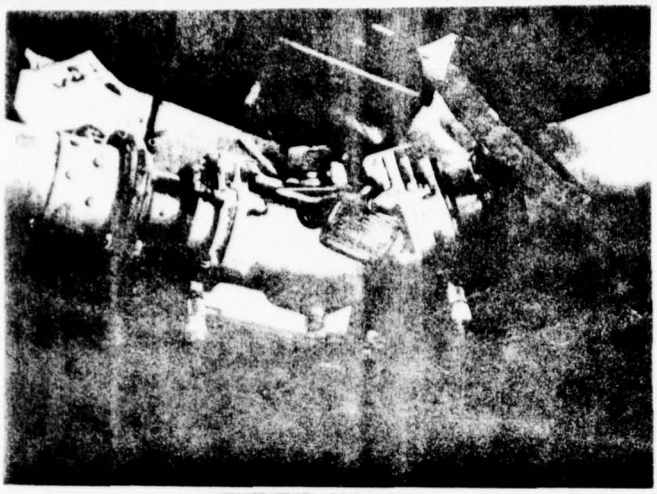

42° Gear Box

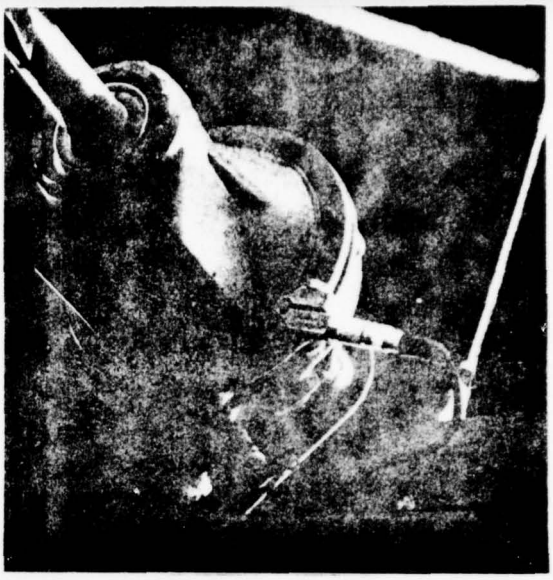

90° Gear Box


Drive Quill

Mast Bearing

Hanger Bearing

Fig. 4.0

## 4.1 HANGER BEARINGS

Approximately 72 hanger bearings (Fig. 4.1) were tested on UH-1 and OH-58 type helicopters. The following graph (Fig. 4.2) represents one taken from a typical analysis of a hanger bearing which was found to be damaged. After the graph was plotted, a teardown and damage summary was made to correlate the plotted shock emissions.

A shock rate of 340 and level of 700 was considered excessive at the time of the analysis, however, the level is significantly lower than the mean level of the 1800 for hanger bearings removed for testing. This hanger bearing had damage which could be classified as marginal. The ability to detect the onset of damage is of significant value in predicting component failure. The following is a summary of the damage found at teardown·

FSN· 3110-911-8384

PN: 204-040-600-9

SN: A20-44891

Outer Race· Metal Fatigue, Pitting, Flaking Corrosion

Inner Race· Corrosion, Pitting

Rolling Elements: Corrosion, Pitting

When viewing the pictorial evidence (Fig. 4.3), it is relatively simple to correlate damage with shock emissions on the single bearing fixture. By comparing the graph of new or "O" time replacement, it is possible to see the appearance of damage vs undamaged components.

The extensive hanger bearing data has been summarized in a single damage-assessment shock emision curve (Fig. 4.4). The

data indicates a new or normal wear hanger bearing would have a shock level of less than 500 units.

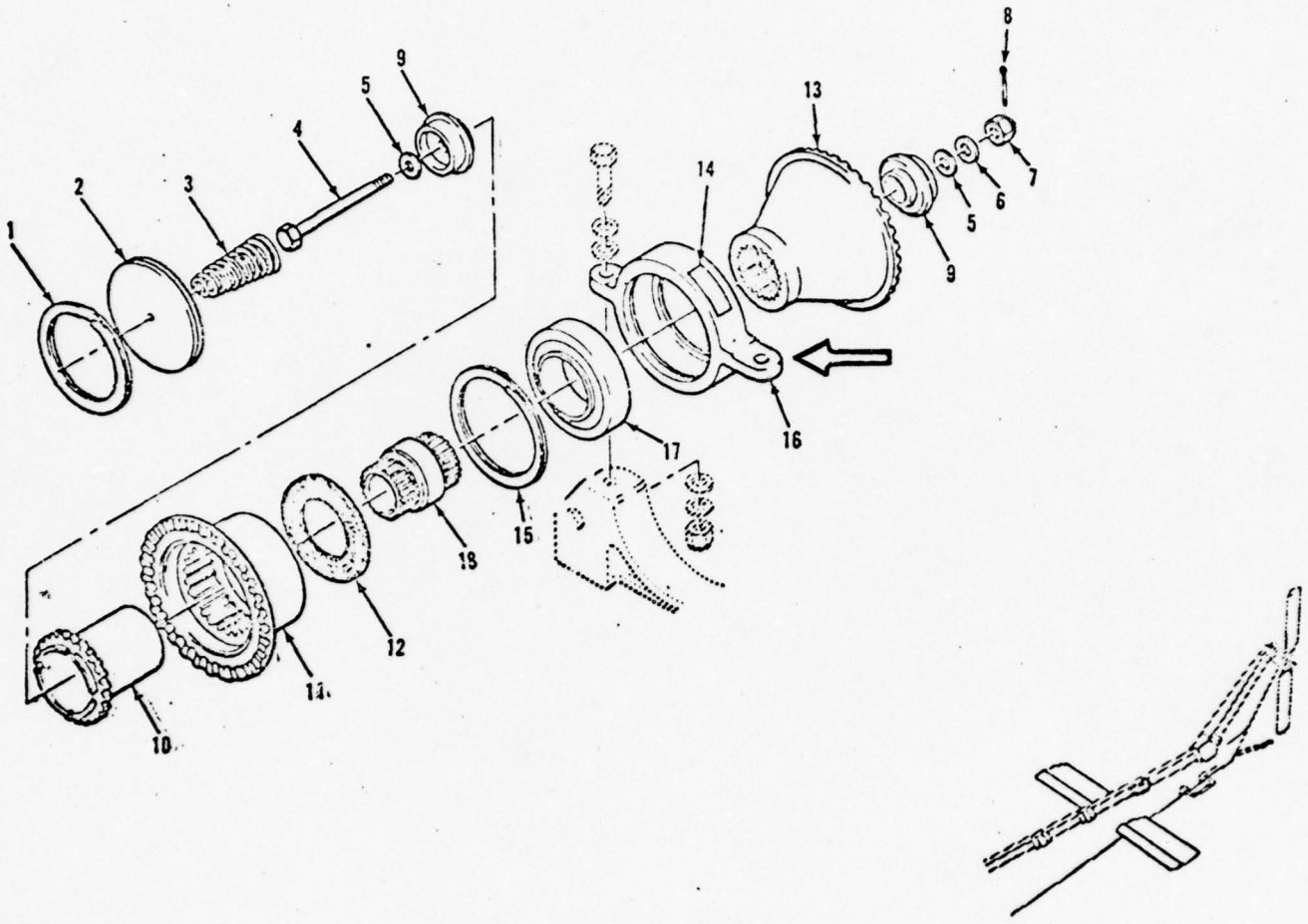


HANGER BEARING ASSEMBLY

ARROW DENOTES SENSOR LOCATION

Fig. 4.1
-25-

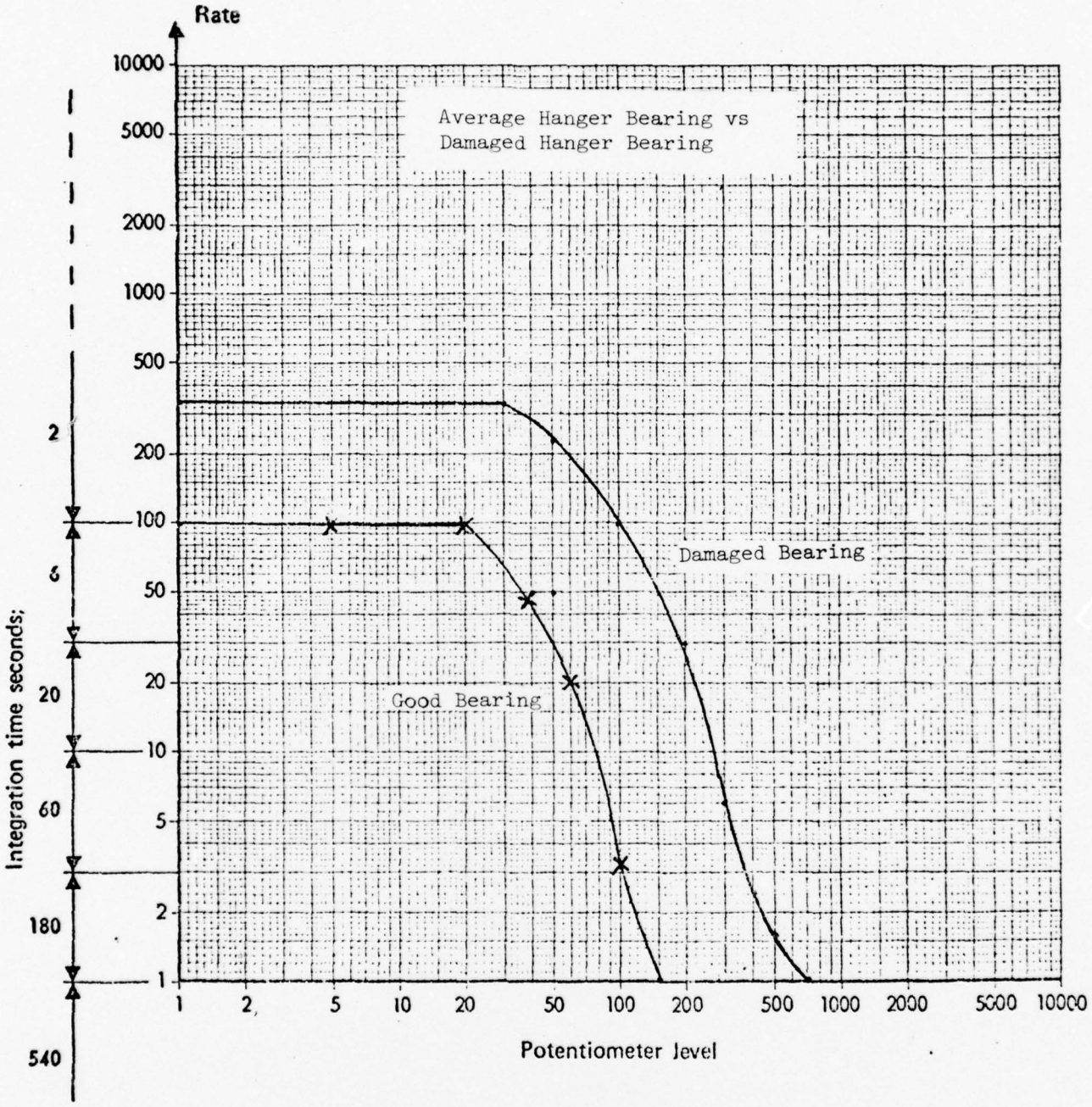
Rate
10000
5000
2000
1000
500
200
100
50
20
10
5
2
1
Average Hanger Bearing vs
Damaged Hanger Bearing
Damaged Bearing
Good Bearing
Integration time seconds;
2
6
20
60
180
540
1
2
5
10
20
50
100
200
500
1000
2000
5000
10000
Potentiometer level

Fig. 4.2


Hanger Bearing
P/N A20-44891
A/C 65-9519

Fig. 4.3

GRAPH FOR BEARING ASSEMBLIES

ANALYZED IN FIELD EVALUATION OF SHOCK PULSE TECHNIQUES

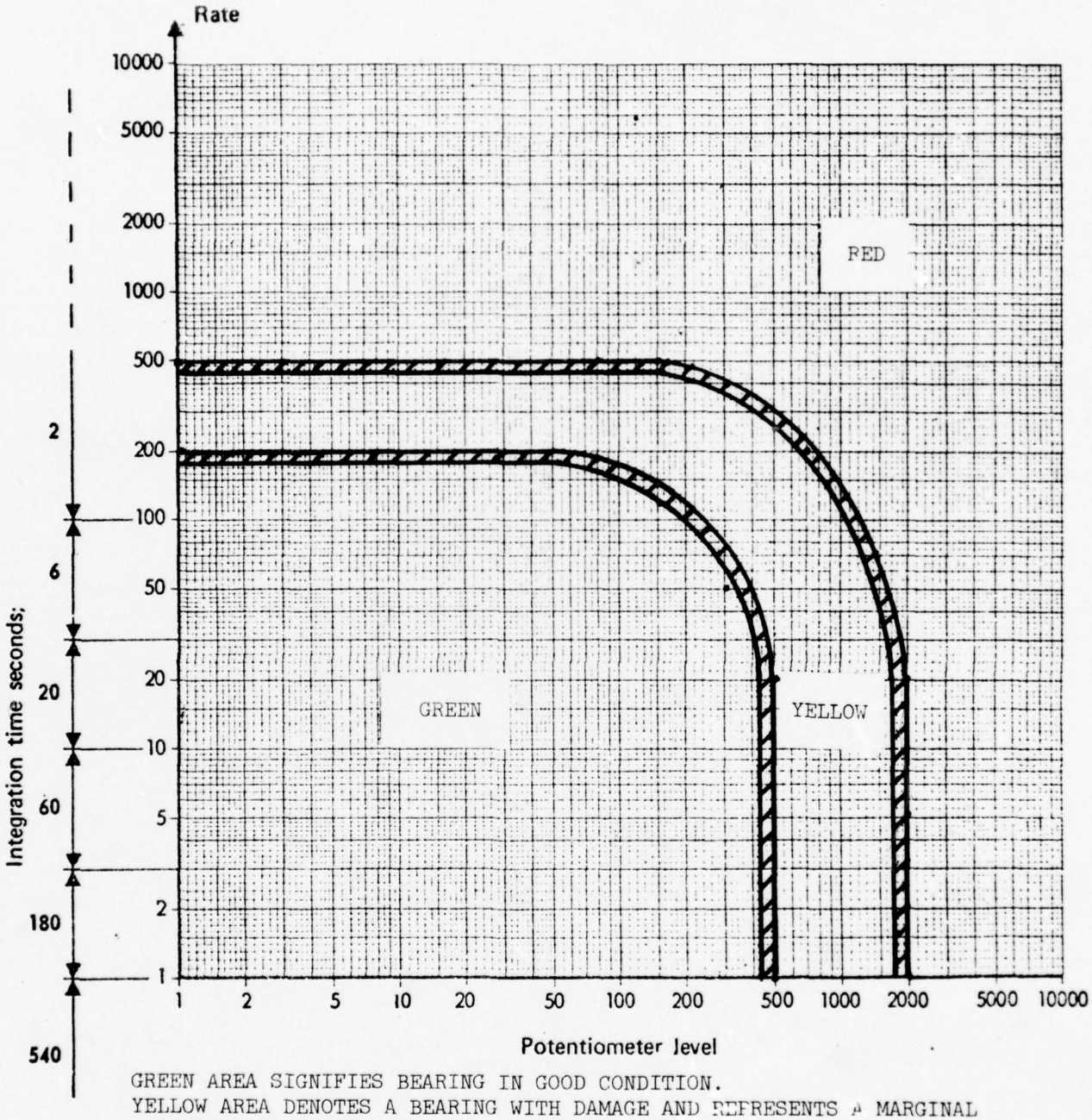


GREEN AREA SIGNIFIES BEARING IN GOOD CONDITION.
YELLOW AREA DENOTES A BEARING WITH DAMAGE AND REPRESENTS A MARGINAL CONDITION AREA.
RED AREA SIGNIFIES A BEARING WITH DAMAGE IN EXCESS OF THAT WHICH WE FEEL WOULD BE ACCEPTABLE.

NOTE: SPECIFIC LIMITS OF COLORED AREAS COULD CHANGE, DEPENDING ON A GREATER COLLECTION OF DATA.

Fig. 4.4

## 4.2 $42^{o}$ GEAR BOX

Forty two $42^{o}$ gear box drive quills (Fig. 4.5) were evaluated. The following graph (Fig. 4.6) and teardown information was taken from a component which was typical of the $42^{o}$ gear boxes removed for study. The output drive quill of this gear box showed a higher than average rate of shock emissions of approximately 300 and a correspondingly higher level of 200.

The following summary of damage found at teardown correlates with the graphs plotted for the input and output quill assemblies. Figure 4.7 is a photograph of the damaged subassemblies.

PN: 204-04-003-37

SN: #ABB-1101

Two Prior Overhauls

Usage Since New - 1725 hours

Usage Since Overhaul - 148 hours

Input Gear #27427

Pattern low

Input Outer Ball Bearing #56073

Small Pits

Input Inner Ball Bearing #56073

Few pits

Input Roller Bearing #210073

Few pits

Output Gear #27821

Pattern too high and too far towards toe

Output Outer Ball Bearing #56775

Corrosion and pitting throughout bearing

Output Inner Ball Bearing #56775

Corrosion and pitting throughout bearing

Output Roller Bearing #209959

Radial scratches

Figure 4.6 represents a $42^{o}$ gear box with damage which progressed during a test run. A duplex ball bearing, with a single shallow spall approximately 0.08" x 0.08" in the outer race, was implanted in a $42^{o}$ gear box. Of particular interest was the observation of progressive damage while the test was in progress. The shape of the shock emission curve changed continuously over a period of minutes in both rate and shock level. The Figure shows two curves developed on a single run. A change in slope takes place (A), a sharp increase in rate (B-C), a continual change in slope (C-D). Without shutting down the engine, the second curve (E-F-G) was developed. After engine shut-down, an oil sample analysis revealed traces of metal, although not beyond that considered acceptable. The dotted line is an extrapolation of the initial slope and gives an indication of the shock level stabilizing at a factor of ten higher. Two more runs were made which essentially repeated curve E-F-G. Teardown analysis showed that the original degradation had not changed noticeably but that new spalls were found on the outer race and on one ball bearing.

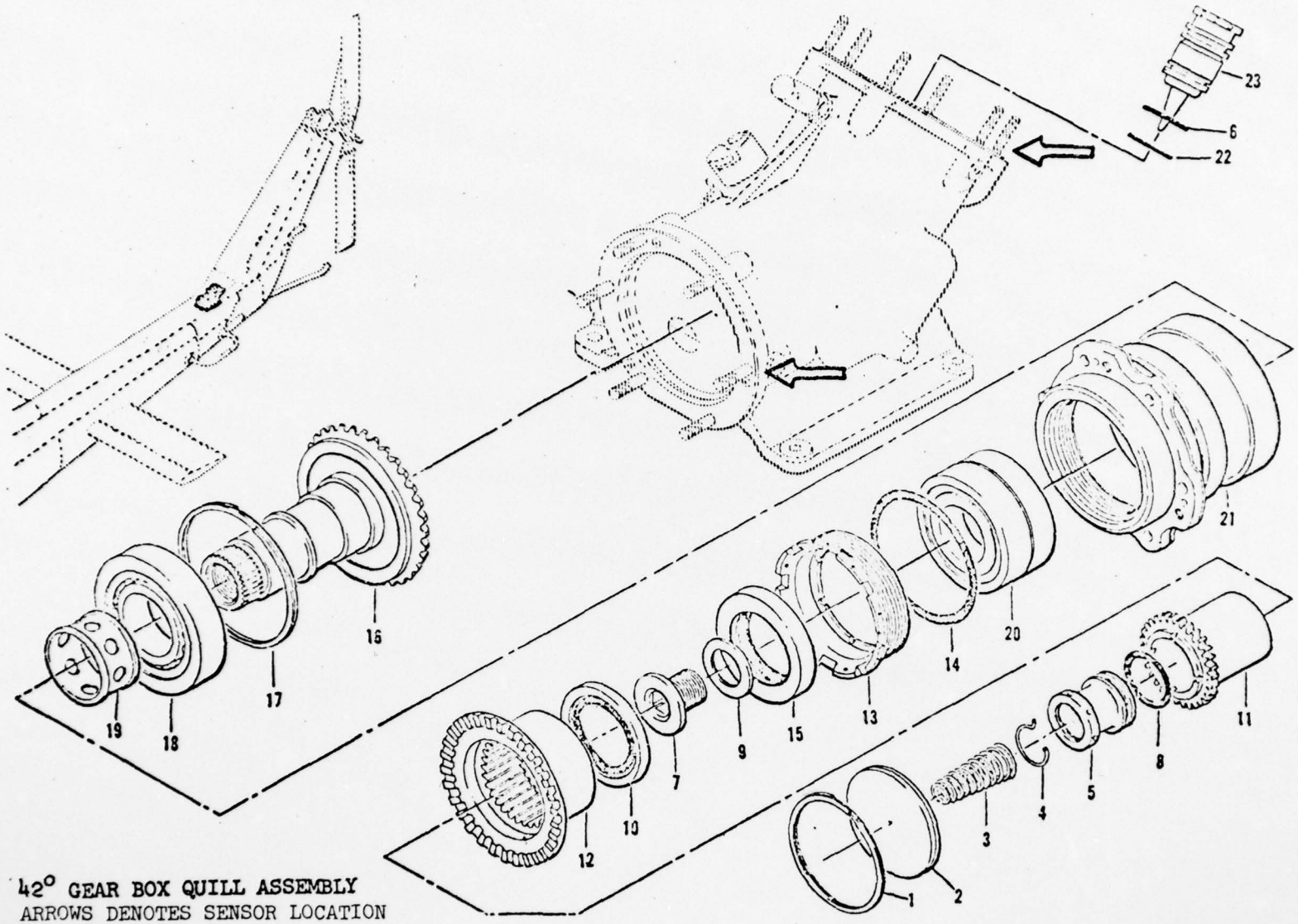


$42^{o}$ GEAR BOX QUILL ASSEMBLY
ARROWS DENOTES SENSOR LOCATION

Fig. 4.5

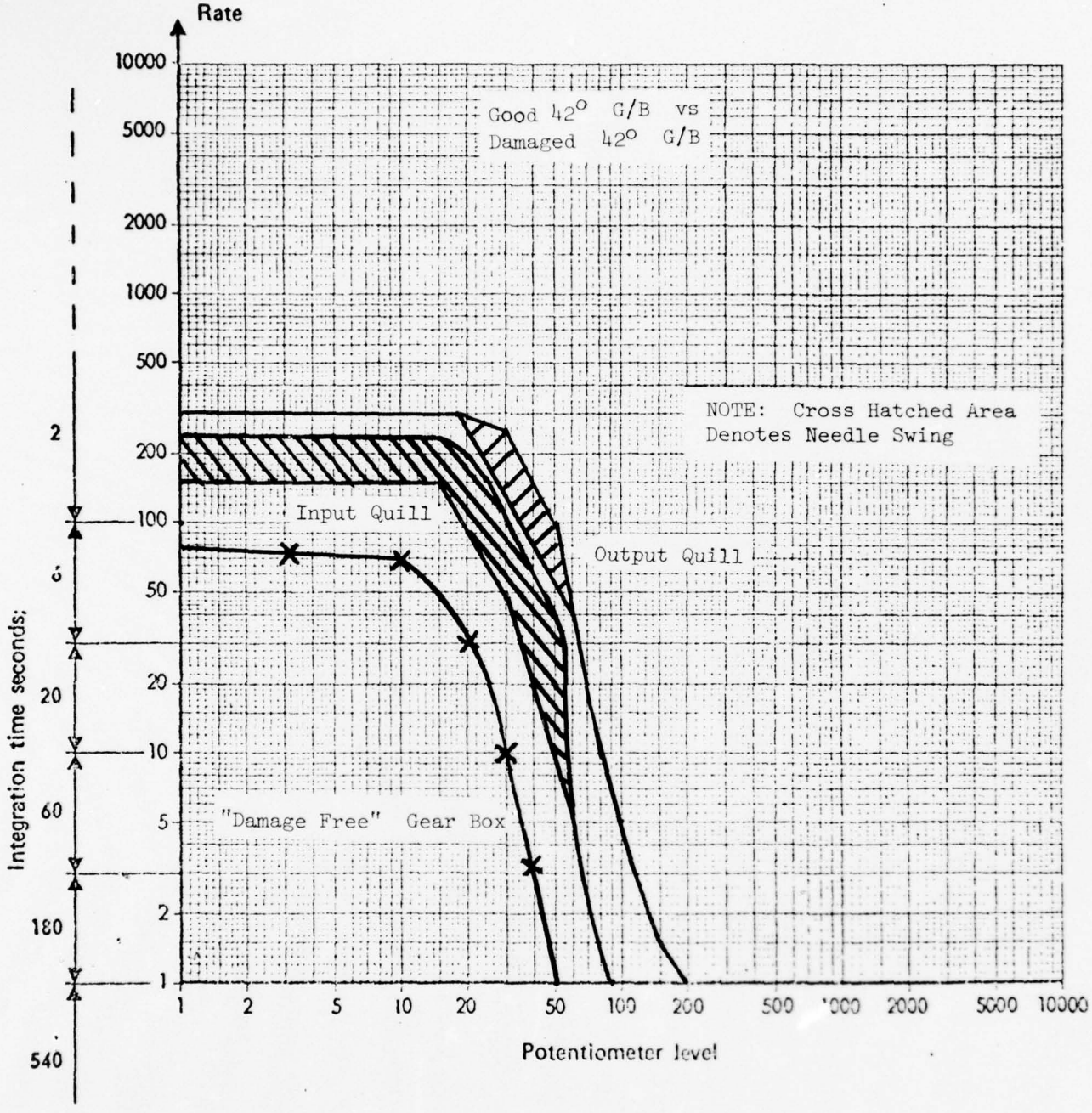
Rate
10000
5000
2000
1000
500
200
100
50
20
10
5
2
1
Good 42° G/B vs
Damaged 42° G/B
NOTE: Cross Hatched Area
Denotes Needle Swing
Input Quill
Output Quill
"Damage Free" Gear Box
Integration time seconds:
2
6
20
60
180
540
1
2
5
10
20
50
100
200
500
1000
2000
5000
10000
Potentiometer level

Fig. 4.6

ABB-1101
Output, Inner Bearing,
Corrosion on Ball

ABB-1101
Output, Outer Bearing,
Corrosion and Pitting
on Oute. Race

ABB-1101
Output, Inner Bearing,
Corrosion Damage on
Outer Race

Fig. 4.7

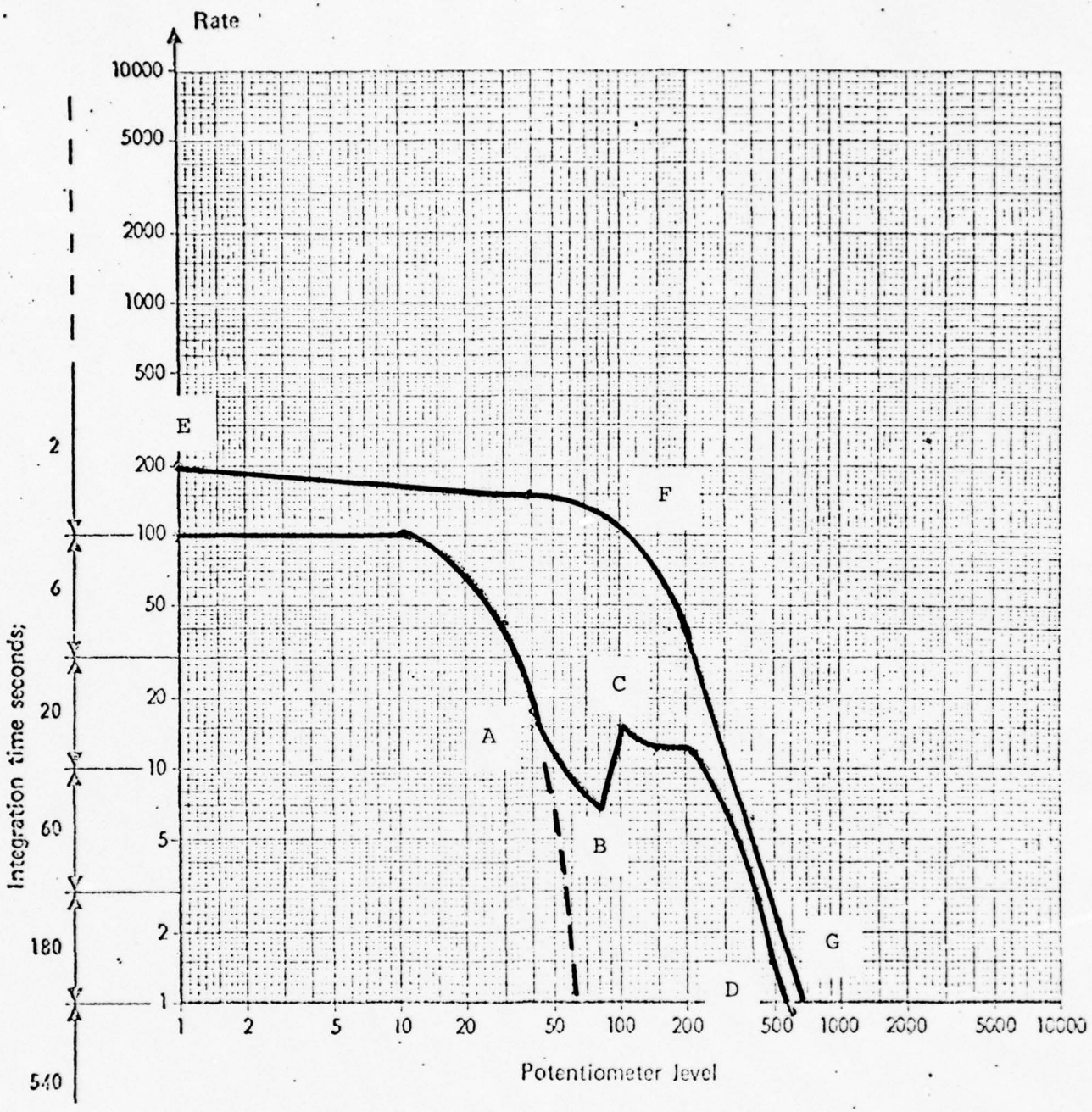


42° GEARBOX IMPLANTED WITH A SPALLED DUPLEX BALL BEARING

EVIDENCE OF DAMAGE PROGRESSING

Fig. 4.8

## 4.3 90° GEAR BOX

Twelve 90° gear boxes (Fig. 4.9) were tested on UH-1 and OH-58 type helicopters. Figure 4.10 is a summary diagram of shock emissions. Two assemblies indicate either a higher rate or higher level than the average of those tested. The curve labeled "damage free" is taken from a gear box of known condition installed on an AIDAPS helicopter at Fort Rucker, Alabama. One of the tested gear boxes was removed for teardown analysis. The principle reason for removing the component was because of the shape and progressing nature of the curve plotted (Fig. 4.11). A curve which, when plotted, developes successively higher x intercepts (levels) is indicative of damage which is progressing. The following data was compiled at the time the gear box was disassembled for analysis: Photographs of the damaged elements can be seen in Figure 4.12.

FSN: 1615-918-2677

PN: 204-040-012-13

SN: ABC-5688

TSN: 588

TSO: 400

Small Duplex Bearing: PN: 204-040-424-1

SN: 21262

Outer Race: 2 Spalls, Burred Around Edges

Inner Race: 3 Spalls, Evidence of False Brinnelling

Balls: No Apparent Damage

Small Duplex Bearing: PN: 204-040-424-1

SN: 21262

Outer Race: No Apparent Damage

Inner Race: No Apparent Damage

Balls: No Apparent Damage

Small Roller Bearing: PN: 204-040-406-1

SN: 203462

Outer Race: 2 Small Scratches

Inner Race: No Apparent Damage

Rollers: 1 Roller Slightly Scratched

Duplex Bearing: PN: 204-040-143-1

SN: 12620

Outer Race: 1 Small Spall

Inner Race: No Apparent Damage

Cage: No Apparent Damage

Balls: No Apparent Damage

Duplex Bearing: PN: 204-040-143-1

SN: 12620

Outer Race: Mild Corrosion and Pitting

Inner Race: Mild Corrosion and Pitting

Cage: No Apparent Damage

Balls: No Apparent Damage

Roller Bearing: PN: 204-040-407-3

SN: 23475

Outer Race: Mild Pitting, Scratches Parallel to Race

Inner Race: Scratches Parallel to Race

Rollers: No Apparent Damage

The damage found in the outer race of the Small Duplex Bearing SN 21262 is spalling of the nature of sharp burred edges around the spalls. The burred edges would cause the indication apparent in the curve plots.

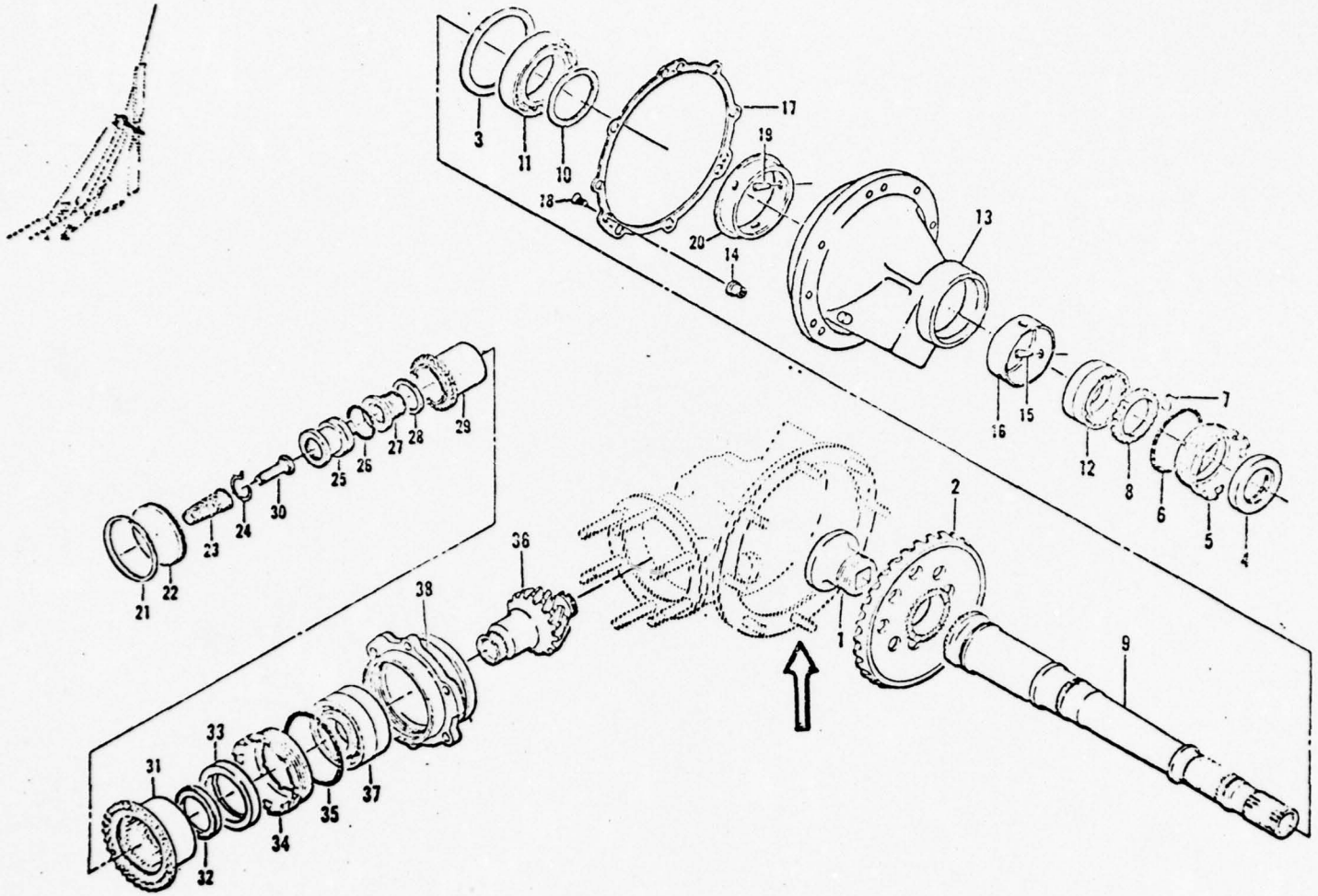


90° GEAR BOX QUILL ASSEMBLY
ARROW DENOTES SENSOR LOCATION

Fig. 4.9

SUMMARY CHART OF 10 90° GEAR BOX
ASSEMBLIES SHOWING DATA SCATTER

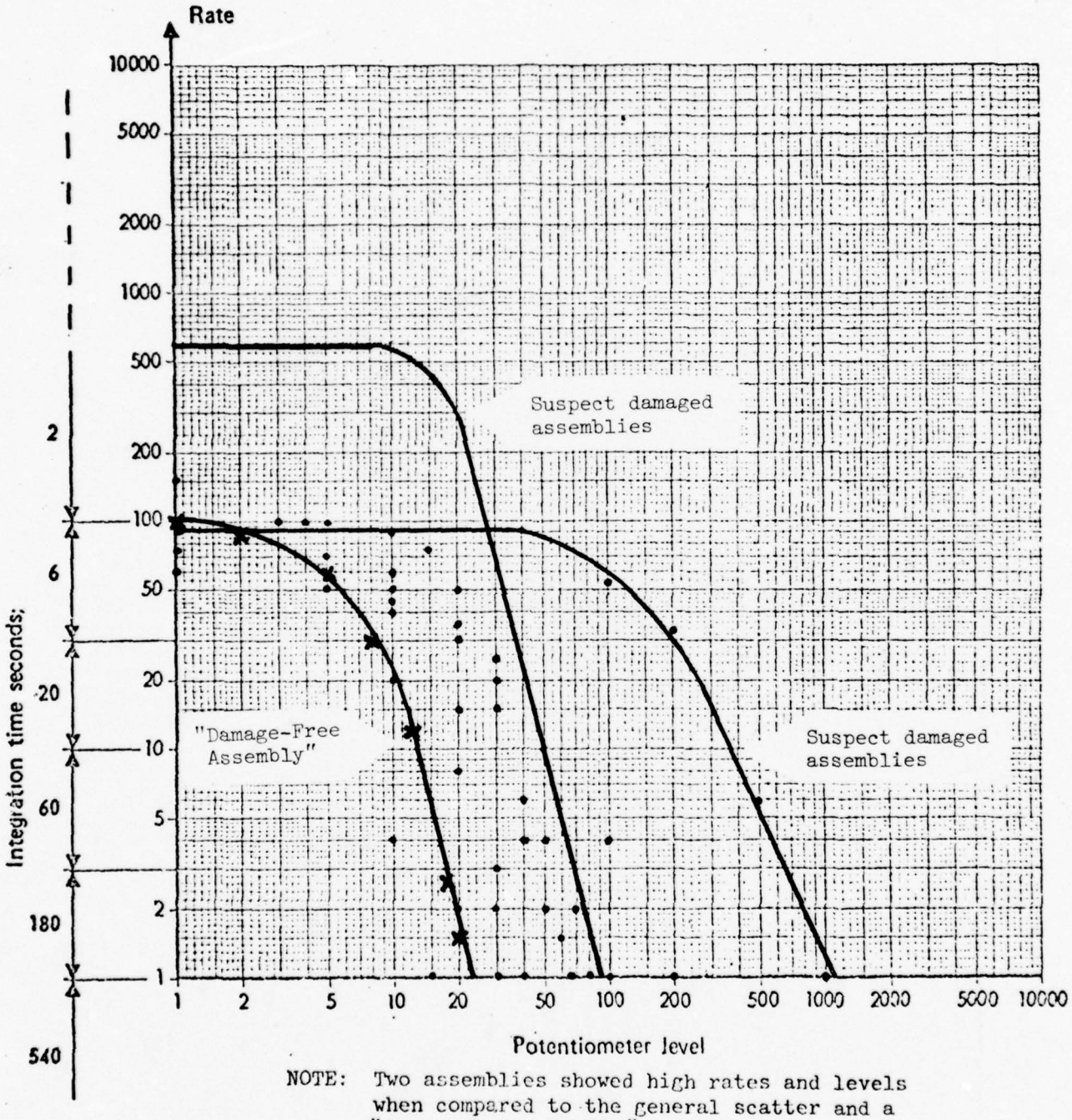


NOTE: Two assemblies showed high rates and levels when compared to the general scatter and a "damage-free assembly".

Fig. 4.10

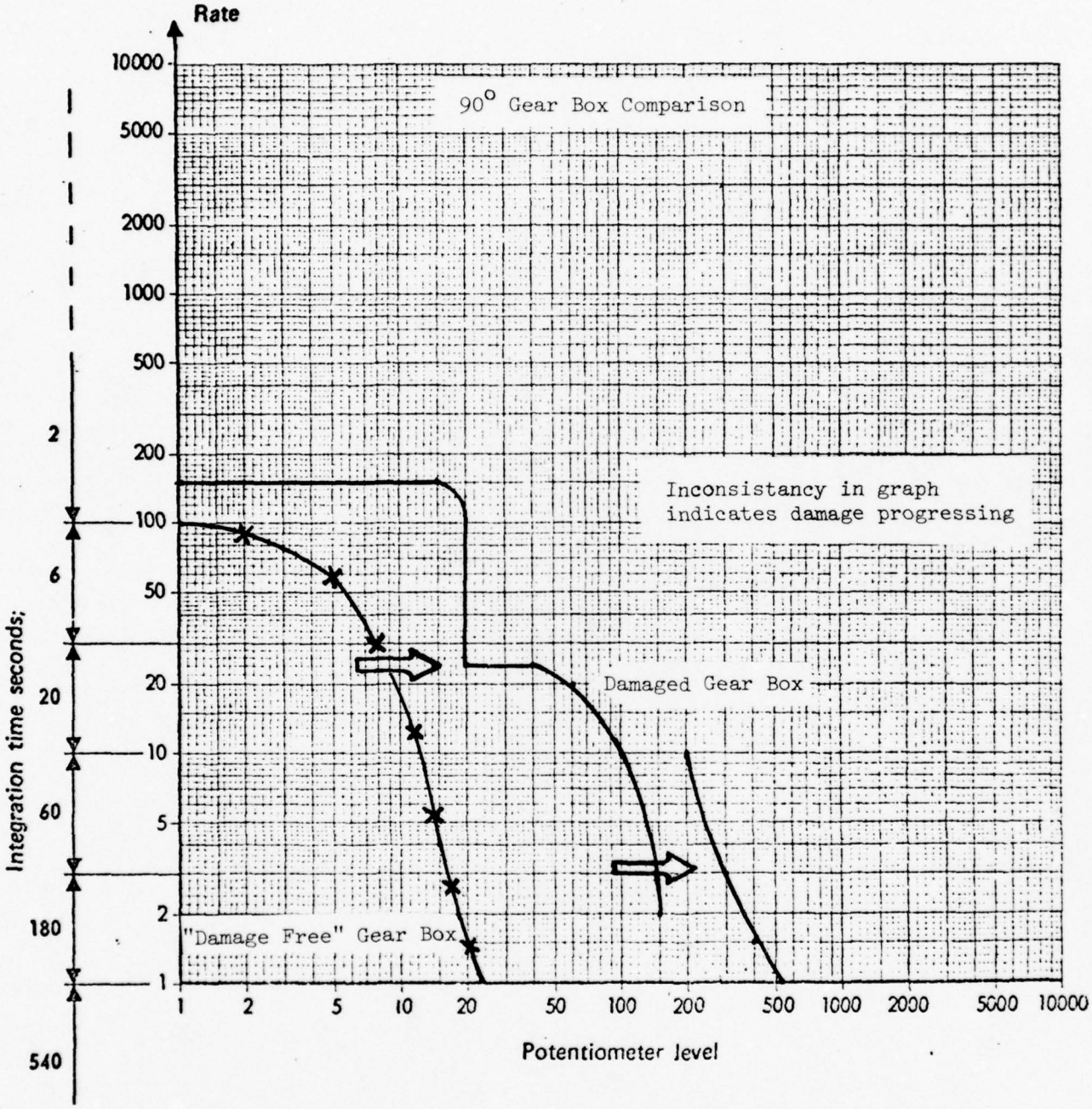
Rate
10000
5000
2000
1000
500
200
100
50
20
10
5
2
1
90° Gear Box Comparison
Inconsistancy in graph
indicates damage progressing
Damaged Gear Box
"Damage Free" Gear Box
Integration time seconds;
2
6
20
60
180
540
1
2
5
10
20
50
100
200
500
1000
2000
5000
10000
Potentiometer level

Fig. 4.11

Small Duplex Bearing
S/N 21262
Outer Race

Small Duplex Bearing
S/N 21262
Inner Race

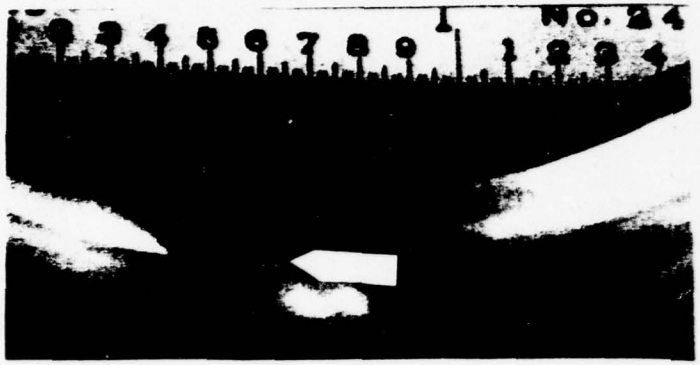

Duplex Bearing
S/N 12620
Outer Race

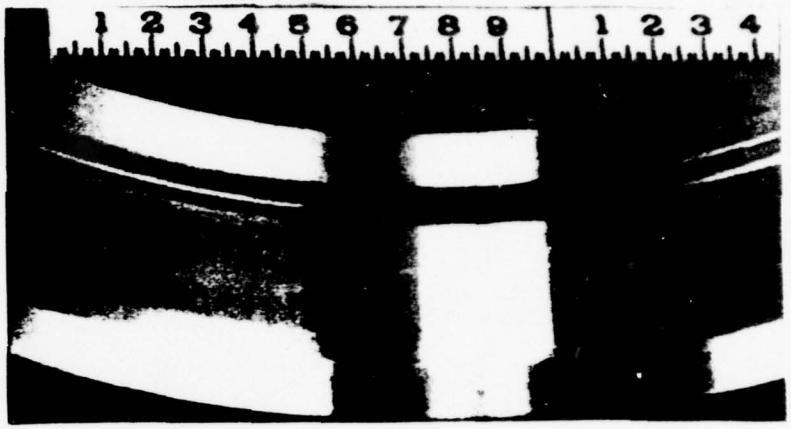

Roller Bearing
S/N 23475
Outer Race

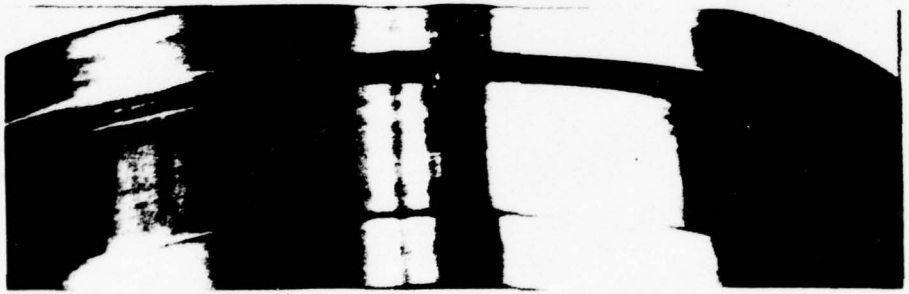

Roller Bearing
S/N 23475
Inner Race



Fig. 4.12

## 4.4 MAST BEARING

Fourteen graphs were plotted on the mast bearing assembly (Fig. 4.13) of UH-1 series helicopter. Figure 4.14 is a scatter diagram of nine different transmissions. The solid line is that recorded from one of the AIDAPS helicopters at Fort Rucker, Alabama. This mast bearing is of known good condition having been inspected prior to its use in the AIDAPS program. The assembly chosen for teardown was the same one which had the highest level and rate of the components tested. The graph (Fig. 4.15) was made over a 40 minute period. After a new bearing was installed, another test was made on the same aircraft with the replacement bearing. New "O" time bearings showed significant reduction in rate and level from the bearing as it was initially tested with the following damage revealed at teardown:

PN· 204-040-136-7-21335

SN· 613m

Outer Race: Scratches parallel to outer race 1 cm in length. scuffs, false brinnelling and heat discoloration and corrosion.

Inner Race Ring: Scratches paralled to race mild heat discoloration.

Inner Race Ring: Very light scratches and pitting.

Ball and Cage Assembly: Several balls have scratches and nicks.

Photographs of the damaged elements are shown in Figures 4.16 and 4.17.

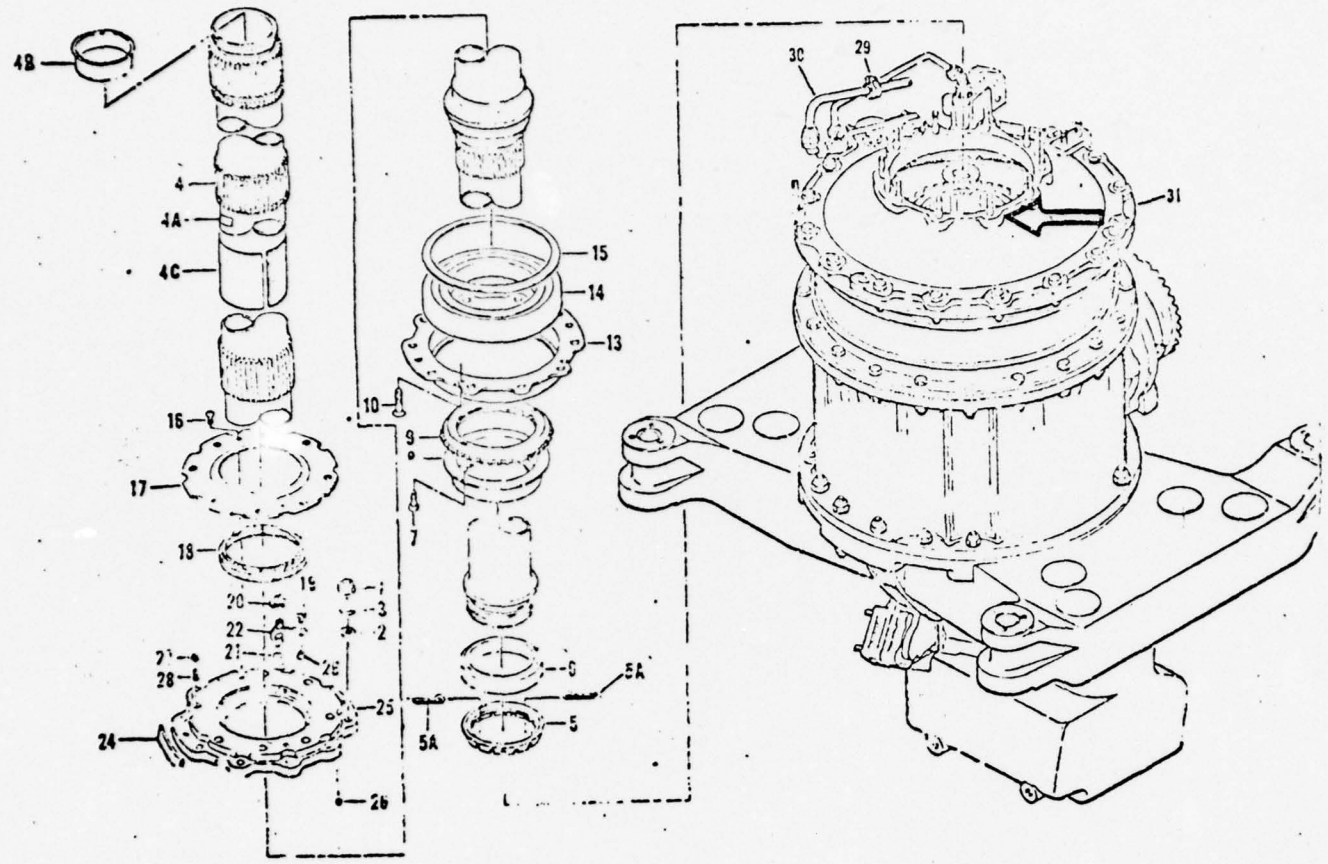


Fig. 4.13
-42-

MAST BEARING ASSEMBLY
ARROW DENOTES SENSOR LOCATION

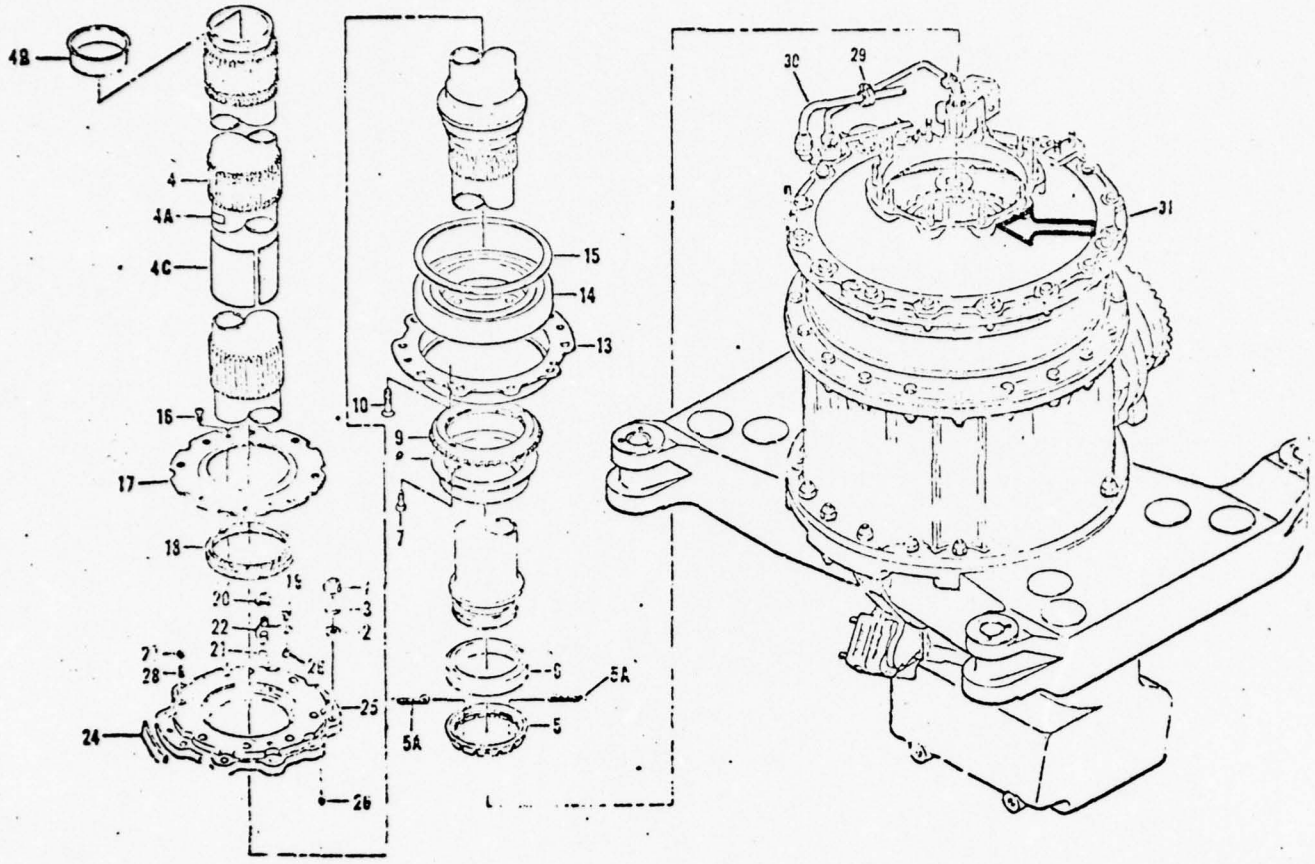


Fig. 4.13
-42-

MAST BEARING ASSEMBLY
ARROW DENOTES SENSOR LOCATION

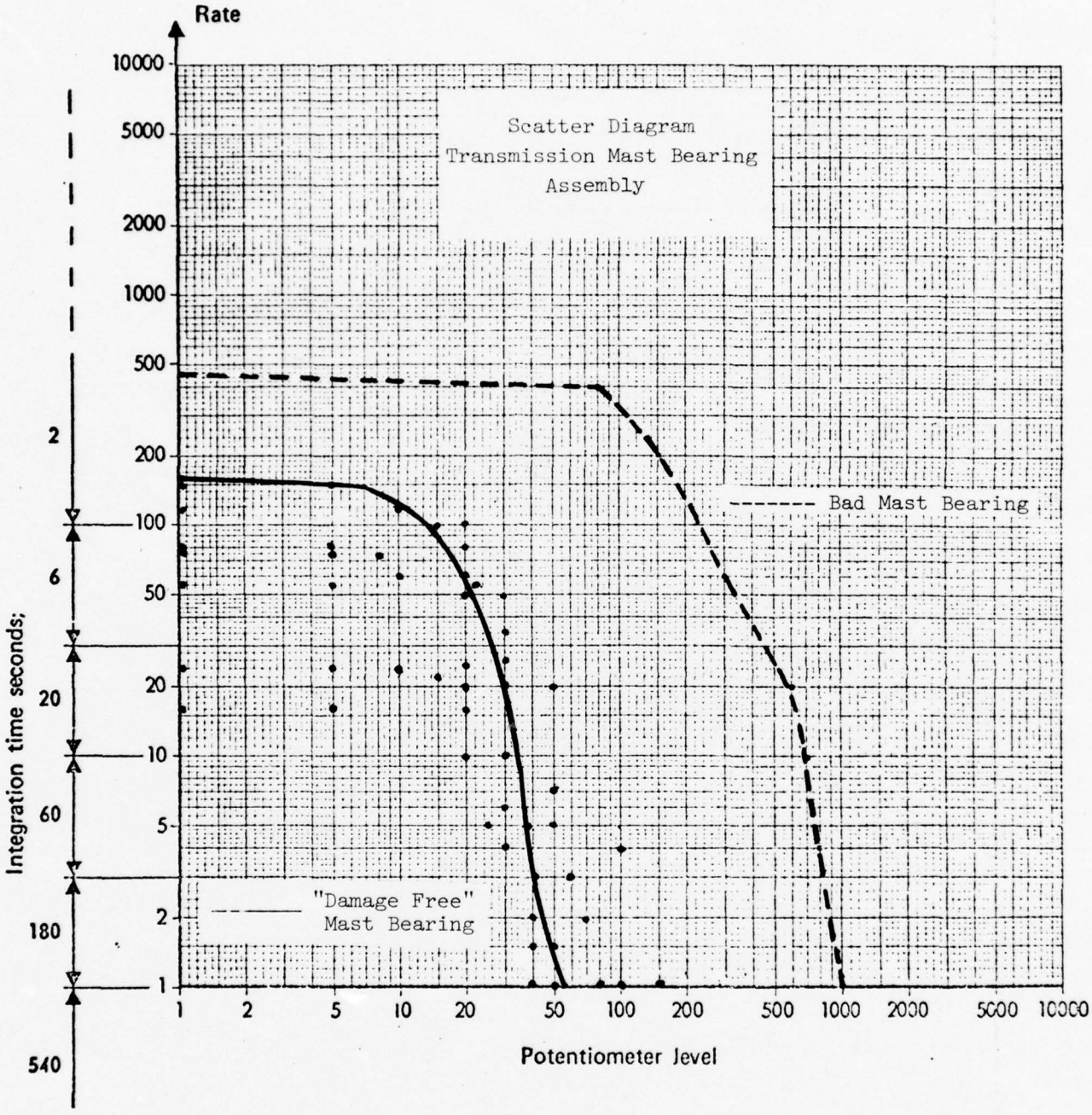
Rate
10000
5000
2000
1000
500
200
100
50
20
10
5
2
1
Scatter Diagram
Transmission Mast Bearing
Assembly
Bad Mast Bearing
"Damage Free"
Mast Bearing
Integration time seconds;
2
6
20
60
180
540
1
2
5
10
20
50
100
200
500
1000
2000
5000
10000
Potentiometer level

Fig. 4.14

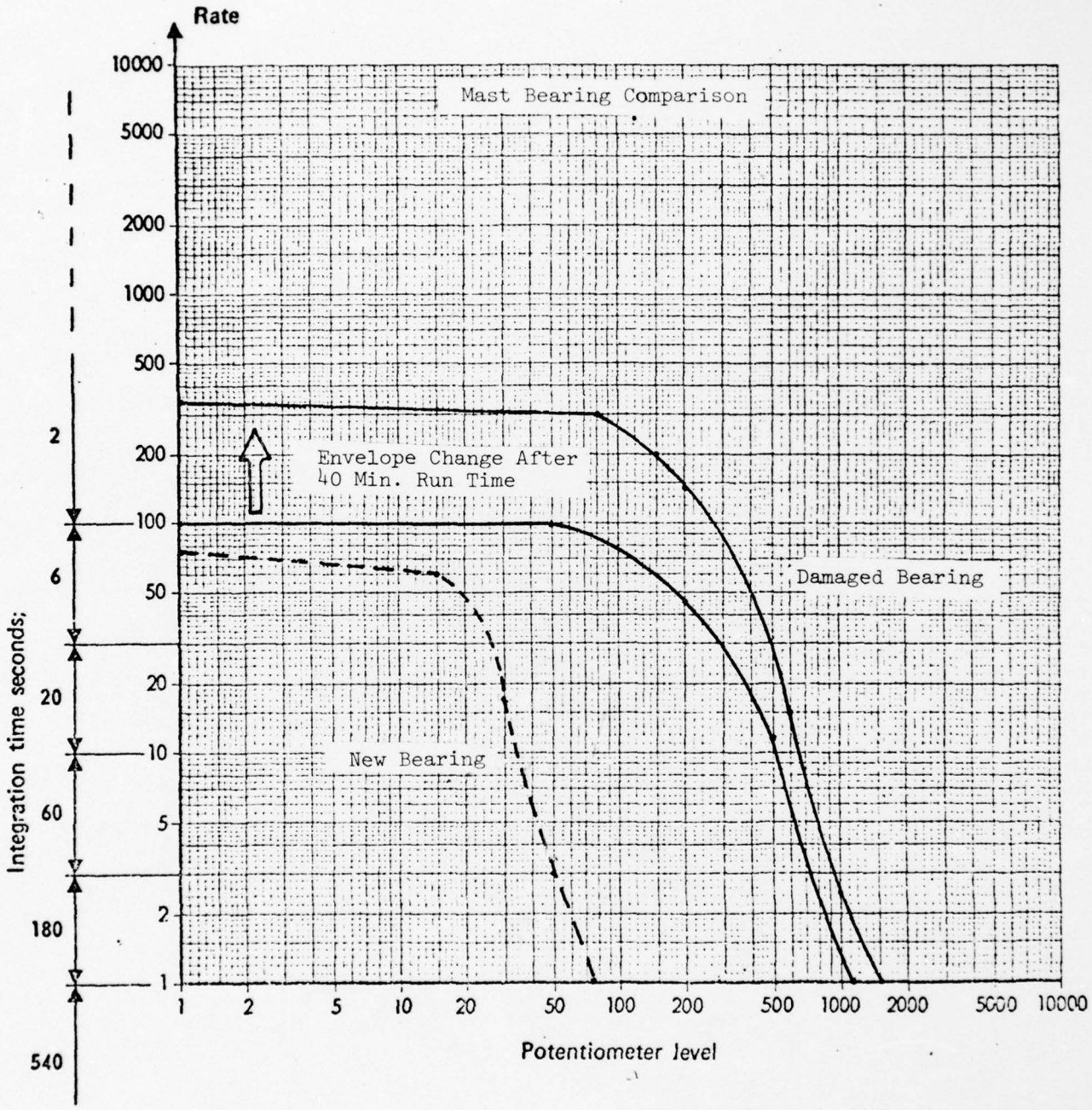
Rate
10000
5000
2000
1000
500
200
100
50
20
10
5
2
1
Mast Bearing Comparison
Envelope Change After
40 Min. Run Time
Damaged Bearing
New Bearing
Integration time seconds:
2
6
20
60
180
540
1
2
5
10
20
50
100
200
500
1000
2000
5000
10000
Potentiometer level

Fig. 4.15

MAST BEARING
Serial No. 613M

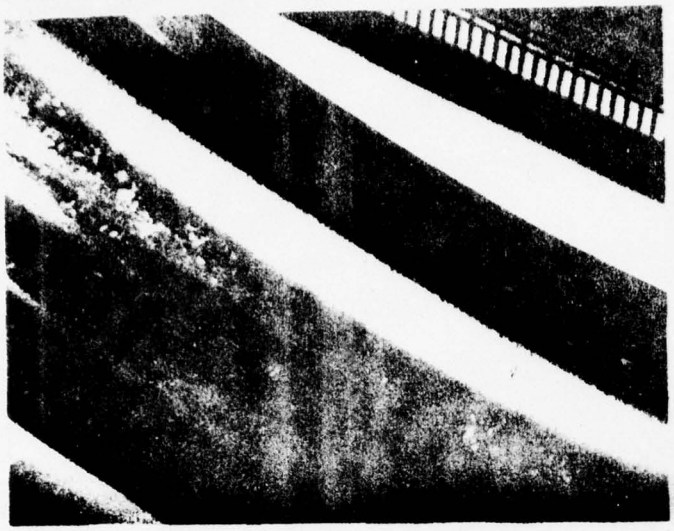

FALSE BRINELLING ON
OUTER RACE

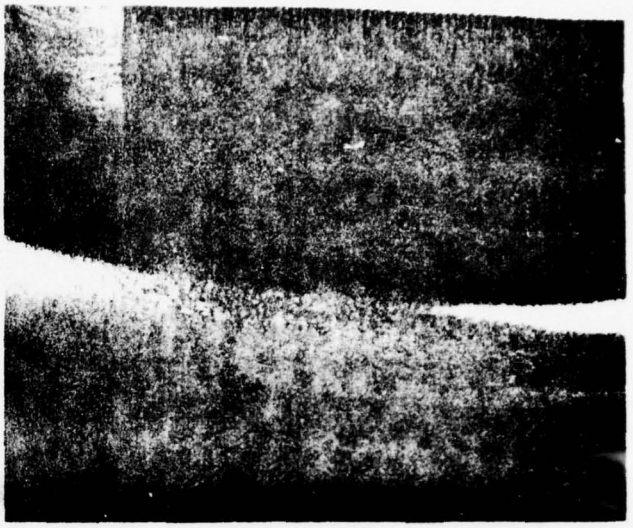

PITTING ON OUTER RACE

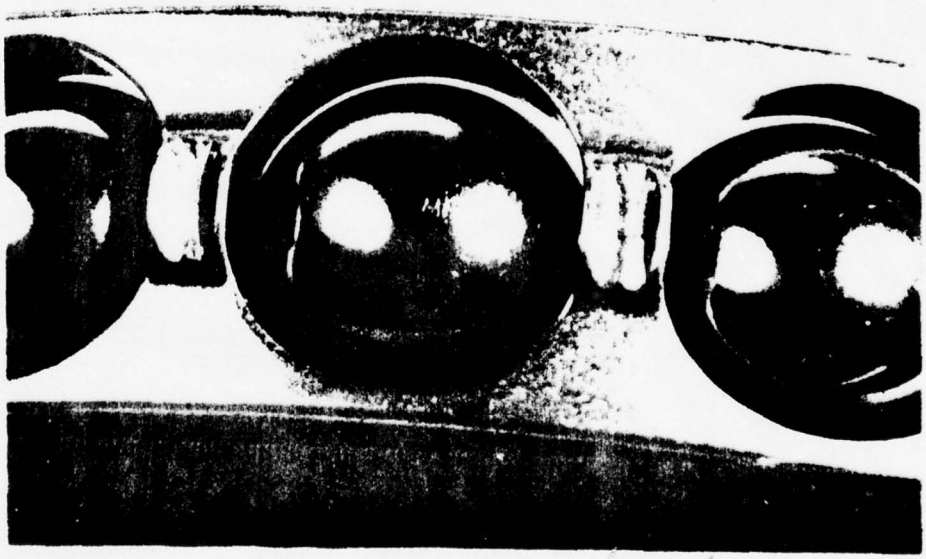

SCORING ON BALLS

Fig. 4.16

MAST BEARING
Serial No. 613M

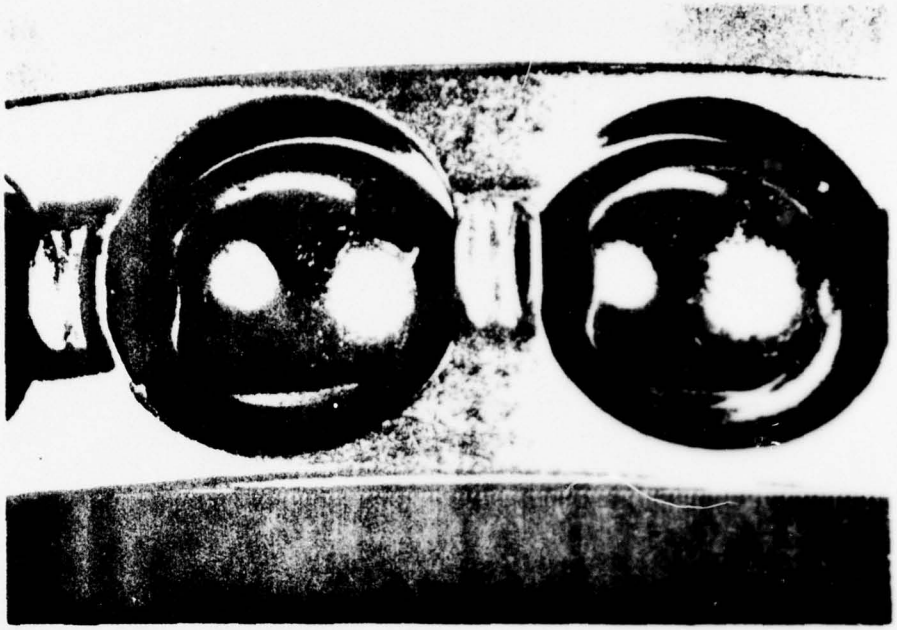

SCORING ON BALLS

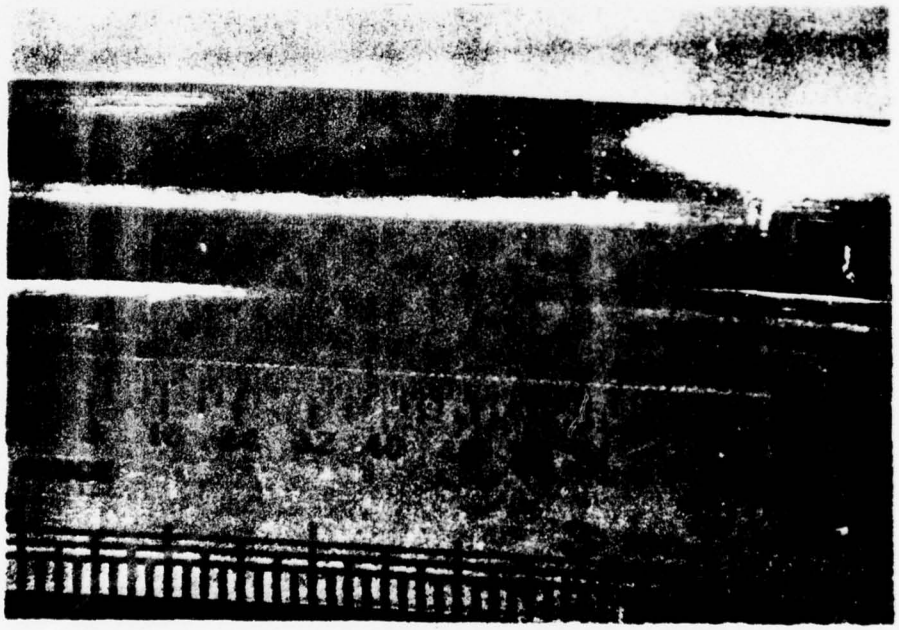

NICKS AND SCRATCHES
ON INNER RACE

Fig. 4.17

## 4.5 TRANSMISSION INPUT DRIVE QUILL

Thirteen input drive quills (Fig. 4.18) were tested on UH-1 series helicopters. One of the assemblies tested had relatively high rate and levels of shock emissions, however, the transmission was not removed for teardown due to the time and expense involved. Figure 4.19 presents the data scatter of all input quill assemblies tested including the suspect component. Again the curve label "damage-free" was taken from a helicopter in the AIDAPS program.

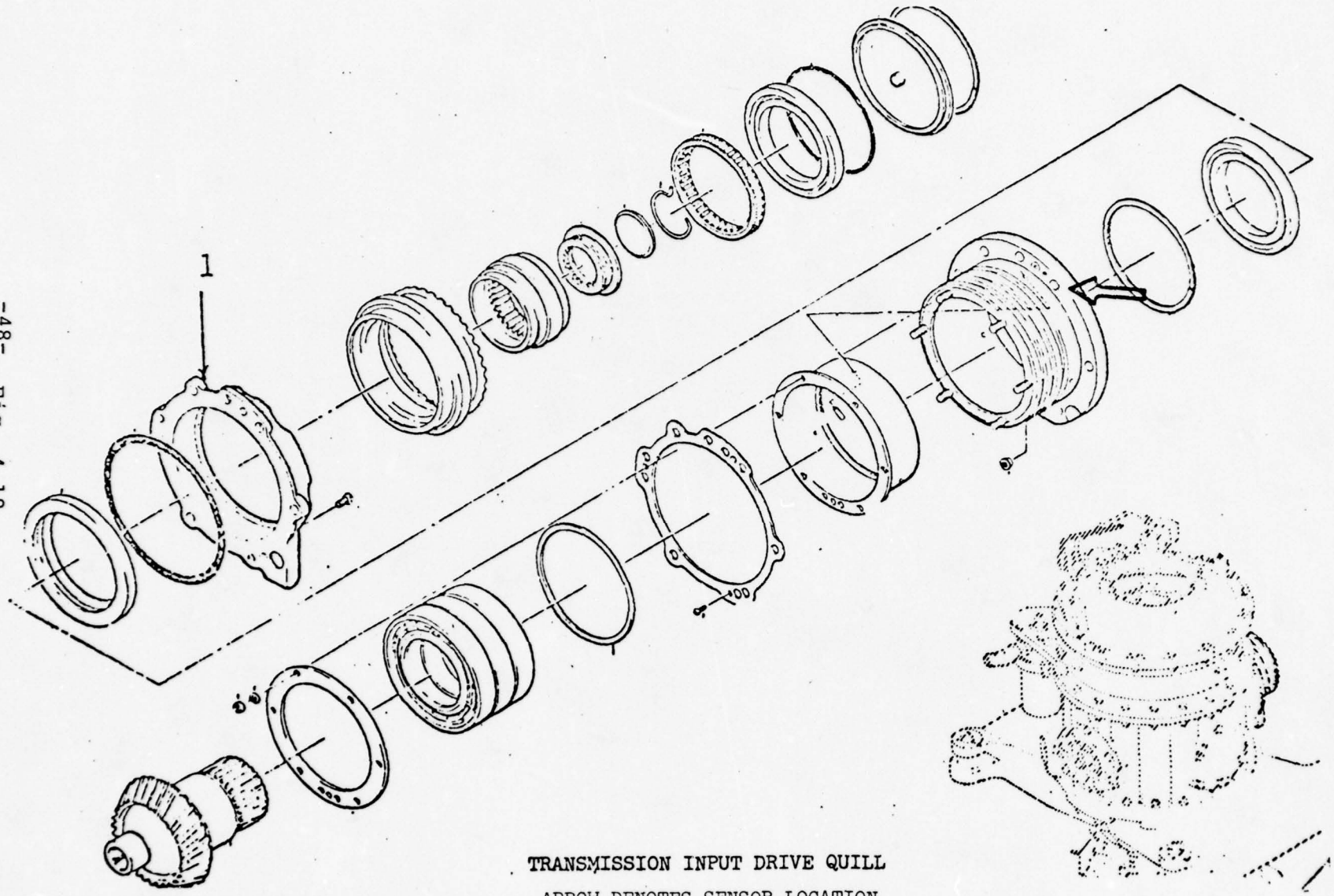


TRANSMISSION INPUT DRIVE QUILL

ARROW DENOTES SENSOR LOCATION



Fig. 4.18

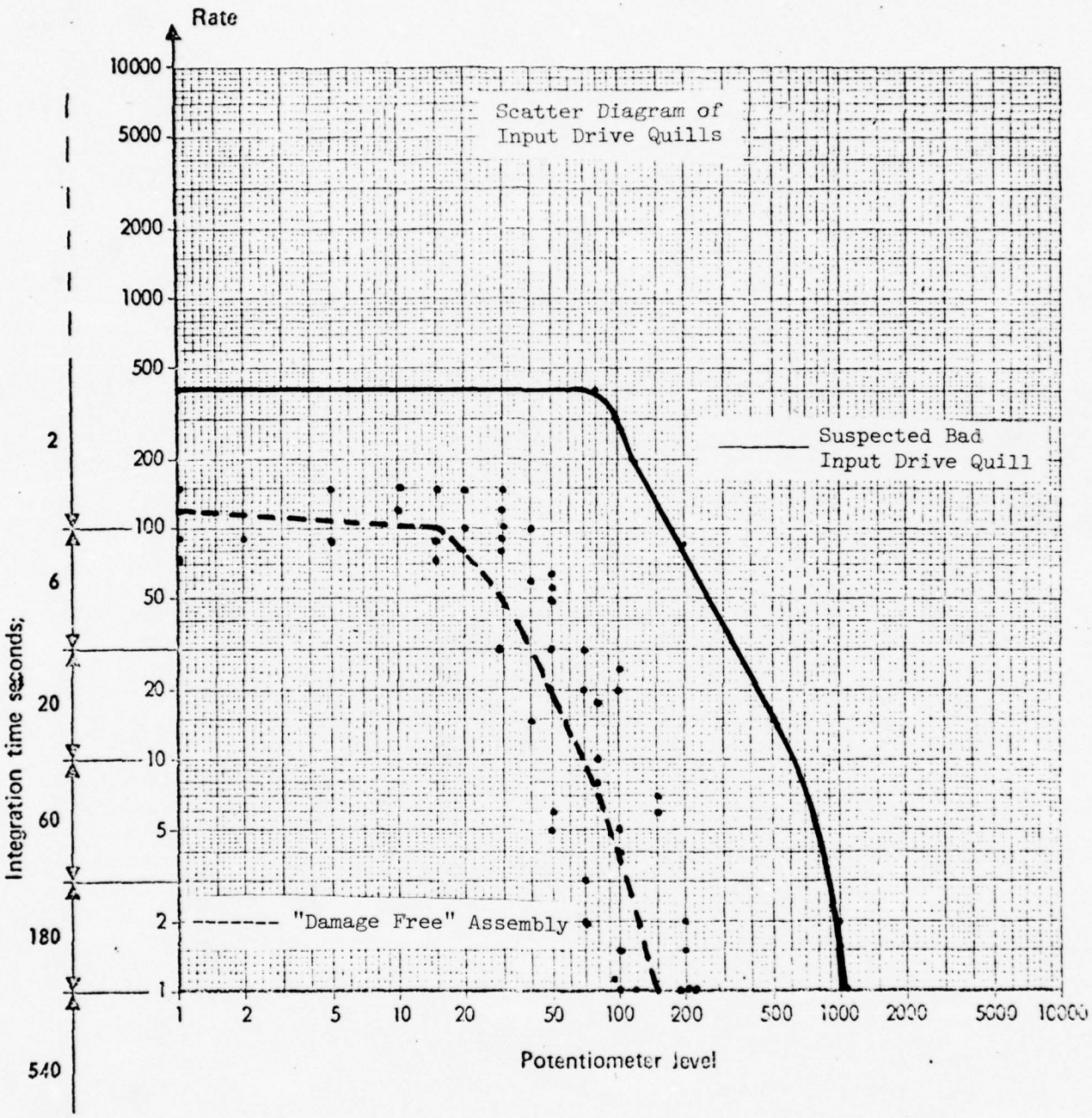
Rate
10000
5000
2000
1000
500
200
100
50
20
10
5
2
1
Scatter Diagram of
Input Drive Quills
Suspected Bad
Input Drive Quill
"Damage Free" Assembly
Integration time seconds;
2
6
20
60
180
540
1
2
5
10
20
50
100
200
500
1000
2000
5000
10000
Potentiometer level

Fig. 4.19

## 5.0 FLIGHT TESTS DATA

Although not a contractual requirement, data was collected with the MEPA 10A under conditions other than ground runs. Figure 5.0 shows a comparison of ground, hover-in-ground effect, low and high speed flight and autorotation conditions. All data collected was from the input drive quill of the transmission. This component was selected because the ease of accelerometer mounting and security of cables from moving and rotating assemblies. Figure 5.1 compares two UH-1H helicopters at the same "high speed" flight condition. The various flight conditions had negligible effect on the shape of the shock emission envelope. Flight data fell well within the scatter of the bulk of data tested for the input quill. More testing would be required before advancing any conclusions as to optimum sensor location or flight profiles necessary for a test program.

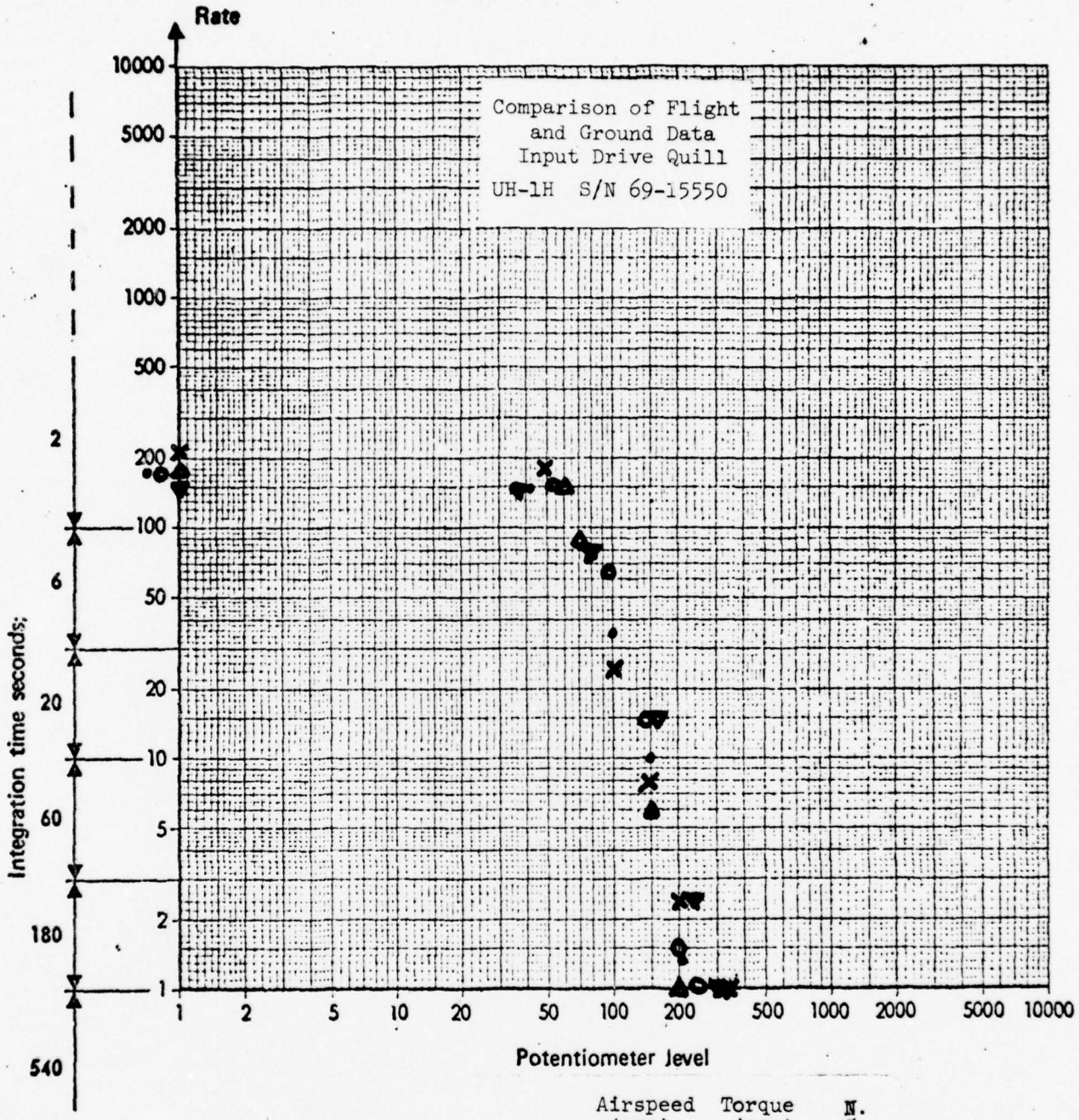


| | | Airspeed (KTS) | Torque (PSI) | N. % |
|---|---|---|---|---|
| ● | Ground | -- | 10 | 86.0 |
| 0 | Hover IGE | -- | 25 | 91.8 |
| Δ | Low Speed | 75 | 18 | 90.0 |
| ∇ | High Speed | 110 | 31 | 91.0 |
| x | Autorotation | 80 | 0 | 72.0 |

$N_2$= 6600 rpm  Altitude 3000 ft.



Fig. 5.0

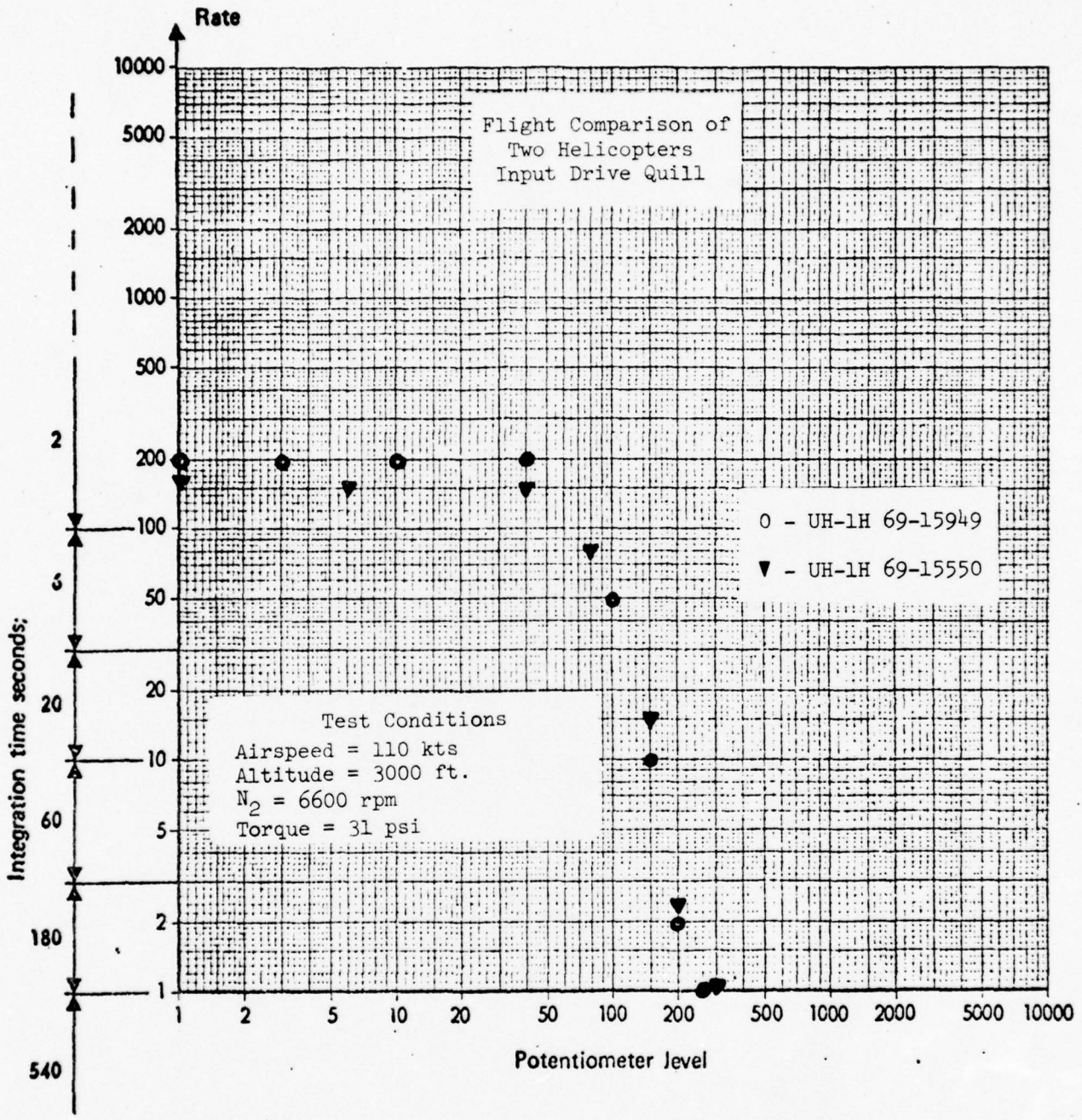
Rate
10000
5000
2000
1000
500
200
100
50
20
10
5
2
1
Integration time seconds:
2
5
20
60
180
540
Flight Comparison of
Two Helicopters
Input Drive Quill
O - UH-1H 69-15949
▼ - UH-1H 69-15550
Test Conditions
Airspeed = 110 kts
Altitude = 3000 ft.
$N_2$ = 6600 rpm
Torque = 31 psi
1
2
5
10
20
50
100
200
500
1000
2000
5000
10000
Potentiometer level

Fig. 5.1

## 6.0 RESULTS AND CONCLUSIONS

The SKF MEPA-10A has shown its effectiveness and reliability as a bearing analyzer. The shock pulse technique has proven its values as a quick and accurate means to determine the general health of a component by plotting the shock emission profile of non-friction bearings. When components were tested and reviewed in comparison with others of the same type, it becomes apparent that the shock pulse technique can separate assemblies by degree's of damage. However, it was not possible to localize the damage as to the rolling elements, inner or outer race. etc. All of the damage which was revealed at tear-down was correlatable to the data plotted from shock emissions.

In over 150 studies conducted on assemblies with the shock pulse technique, the MEPA-10A did not have any malfunctions. The conditions which prevailed during field testing ranged from approximately -30°C to +40°C (-14°F to 104°F) and relative humidity from 30% to 100%. Accelerometers were exposed to exhaust gas temperatures in excess of 200°C and the g forces associated with flight, without failure. Some difficulty was experienced with cables and fittings although not of a significant nature. A recommended ongoing program of flight tests will require some hardware refinement to insure system reliability in a flight environment.

Several assemblies which contain antifriction bearings were analyzed to insure the feasibility of data collection on all aircraft components regardless of bearing size or rotational speed. The only limiting factor to the shock pulse technique is that the accelerometer be located either on the bearing fixture or at a location with a direct mechanical path

to the bearing. With few exceptions all the assemblies on a helicopter can be rapidly and effectively analyzed.

Efforts to realize a method of diagnostics for gear analysis proved to be of value in determining the possible existence of foreign particulate matter in the lubricant of a gear box. If the damage present on a set of gears is the type that debris will result from tooth contact, then the shock pulse method appears to have the ability to show damage by evaluating the particulate matter as it passes in transient through a bearing assembly.

REFERENCES


1. James Provenzano, John Games, Al Wyrostek, Art Ostheimer, Jack Young, "UH-1H AIDAPS Test Bed Program," Vol. I and II; USAAVSCOM Technical Report 72-18, Aug. 1972.

2. Robert R. Butcher, Russel Kirby, Jr., John Nakakihara, T.C. Watkins, "UH-1H Test Bed Program," Vol. I and II; USAAVSCOM Technical Report 72-19, June 1972.

3. John A. George, Richard M. Andres, J. Thomas Harrington, "Parks College UH-1H AIDAPS Program," Parks College of Saint Louis University, Final Report, Jan. 1975.

4. "AIDAPS Development Program, 2nd Interim Report," USAAVSCOM Technical Report 74-50, Nov. 1974.

5. Edward F. Covill, Timothy C. Mayer, John A. George, "Preliminary Evaluation of the Shock Pulse Technique to the UH-1 Series Helicopter," Parks College of Saint Louis University, Jan, 1974.

6. Timothy C. Mayer, Edward F. Covill, John A. George, J. Thomas Harrington, "Field Evaluation Of the Shock Pulse Technique to the UH-1 Series Helicopter," Parks College of Saint Louis University, June 1974.

7. John A. George, Timothy C. Mayer, Edward F. Covill, "Evaluation of the Shock Pulse Technique to the UH-1 Series Helicopter," 45th Shock and Vibration Symposium, Dayton, Ohio, Oct. 1974.

8. Timothy C. Mayer, Edward F. Covill, John A. George, "Shock Pulse Meter Analysis," Parks College of Saint Louis University, Oct. 1974.

# FINAL REPORT

# APPLICATIONS OF THE SHOCK PULSE TECHNIQUE TO HELICOPTER DIAGNOSTICS

## PART II

TIMOTHY C. MAYER
EDWARD F. COVILL
JOHN A. GEORGE
J. THOMAS HARRINGTON

PARKS COLLEGE OF SAINT LOUIS UNIVERSITY
CAHOKIA, ILLINOIS
FEBRUARY 24, 1975

BOA DAAJ01-72-A-0027 (P6C)
DO DAAJ01-72-A-0027-0001 (P6C)
DO DAAJ01-72-A-0027-0002 (P6C)

## 7.0 TABLES AND APPENDICES

The following section is a compilation of all data gathered to date. The data is arranged in order to provide readability with the report.

CONTENTS

## 7.1 TABLES

| Aircraft # | Type | Position | Serial # | Hours TBN | Hours TSO | Comment | Date | Rate | Level |
|---|---|---|---|---|---|---|---|---|---|
| 13740 | UH-1H | 42° Gearbox Input Quill | AB-1097 | | | | Nov.27,1973 | 100 | 65 |
| 13740 | UH-1H | 42° Gearbox Output Quill | AB-1097 | | | | Nov.27,1973 | 75 | 55 |
| 16197 | UH-1H | 42° Gearbox Input Quill | BBB-289 | | 225 | | Nov.27,1973 | 150 | 80 |
| 16197 | UH-1H | 42° Gearbox Output Quill | BBB-289 | | 225 | | Nov.27,1973 | 85 | 80 |
| 66-01087 | UH-1H | 42° Gearbox Input Quill | B13-3886 | | 727 | | Nov.28,1973 | 150 | 70 |
| 15949 | UH-1H | 42° Gearbox Input Quill | B13-5346 | | | | Nov.28,1973 | 150 | 110 |
| 15949 | UH-1H | 42° Gearbox Output Quill | B13-5346 | | | | Nov.28,1973 | 75 | 110 |
| 59519 | UH-1M | 42° Gearbox Input Quill | ABB-1742 | | | | Nov.30,1973 | 220 | 50 |
| 59519 | UH-1M | 42° Gearbox Output Quill | ABB-1742 | | | | Nov.30,1973 | 200 | 40 |
| 15200 | UH-1M | 42° Gearbox Input Quill | ABB-6012 | 298 | 298 | * | Dec.6,1973 | 600 | 200 |
| 15200 | UH-1M | 42° Gearbox Output Quill | ABB-6012 | 298 | | * | Dec.6,1973 | 110 | 150 |
| 69-15771 | UH-1H | 42° Gearbox Input Quill | ABB-2667 | | 1042 | Excessive Needle Swing * | Dec.6,1973 | 300 | 150 |
| 69-15771 | UH-1H | 42° Gearbox Output Quill | ABB-2667 | | | Excessive Needle Swing * | Dec.6,1973 | 250 | 300 |
| 66-15190 | UH-1M | 42° Gearbox Input Quill | AB-1101 | | 148 | Excessive Needle Swing * | Dec.12,1973 | 250 | 90 |
| 66-15190 | UH-1M | 42° Gearbox Output Quill | AB-1101 | | 148 | Excessive Needle Swing * | Dec.12,1973 | 300 | 195 |
| 66-16879 | UH-1H | 42° Gearbox Output Quill | B13-3800 | | 569 | Excessive Needle Swing * | Dec.13,1973 | 500 | 195 |
| BC14 | UH-1H | 42° Gearbox Input Quill | B13-9881 | | | Data Scatter 3 Runs | June13,1974 | 140/190 | 100/160 |
| BC13 | UH-1H | 42° Gearbox | B13-4312 | | | | June13,1974 | 75 | 50 |
| BC13 | UH-1H | 42° Gearbox Input Quill | B13-8282 | | | | June 14,1974 | 200 | 700 |
| BC14 | UH-1H | 42° Gearbox | | | | | June 14,1974 | 200 | 70 |
| BC14 | UH-1H | 42° Gearbox | | | | | June 14,1974 | 25 | 80 |



* Removed for Analysis

| Aircraft # | | Position | Serial # | Hours | | Comment | Date | Rate | Level |
|---|---|---|---|---|---|---|---|---|---|
| # | Type | | | TSN | TSO | | | | |
| BC14 | UH-1H | 42° Gearbox | | | | | June 14,1974 | 175 | 30 |
| 15550 | UH-1H | 42° Gearbox Output Quill | B13-2929 | 1324 | New | | July 30,1974 | 25 | 80 |
| 15550 | UH-1H | 42° Gearbox Input Quill | B13-2929 | 1324 | New | | July 30,1974 | 100 | 90 |
| 13740 | UH-1H | 42° Gearbox Output Quill | A13-1097 | 173 | 0 | | July 31,1974 | 75 | 60 |
| 13740 | UH-1H | 42° Gearbox Input Quill | A13-1097 | 173 | 0 | | July 31,1974 | 75 | 60 |
| 60529 | UH-1H | 42° Gearbox Output Quill | A13-1639 | 75 | 0 | | Aug. 1,1974 | 350 | 320 |
| 60529 | UH-1M | 42° Gearbox Input Quill | A13-1639 | 75 | 0 | | Aug. 1,1974 | 35 | 75 |
| 15200 | UH-1M | 42° Gearbox Output Quill | B13-8818 | 24 | 0 | | Aug. 1,1974 | 150 | 30 |
| 15200 | UH-1M | 42° Gearbox Input Quill | B13-8818 | 24 | 0 | | Aug. 1,1974 | 40 | 80 |
| 59884 | UH-1D | 42° Gearbox Input Quill | B13-9384 | | 626 | | Aug. 5,1974 | 25 | 80 |
| 60630 | UH-1C | 42° Gearbox Output Quill | B13-3243 | 1735 | 939 | * | Aug. 6,1974 | 625 | 300 |
| 60630 | UH-1C | 42° Gearbox Input Quill | B13-3243 | 1735 | 939 | * | Aug. 6,1974 | 100 | 40 |
| 15071 | UH-1C | 42° Gearbox Input Quill | | | | | Aug. 6,1974 | 85 | 50 |
| 15071 | UH-1C | 42° Gearbox Output Quill | BBB-1894 | | 237 | | Aug. 6,1974 | 80 | 80 |
| 59519 | UH-1M | 42° Gearbox Input Quill | ABB-742 | | 171 | | Aug. 8,1974 | 110 | 43 |
| 59519 | UH-1M | 42° Gearbox Output Quill | ABB-742 | | 171 | | Aug. 8,1974 | 100 | 40 |
| 15091 | UH-1M | 42° Gearbox Input Quill | B-13-646 | | | | Aug. 9,1974 | 30 | 40 |
| 16354 | UH-1H | 42° Gearbox Input Quill | B13-6564 | | | | Aug.12,1974 | 35 | 60 |
| 16354 | UH-1H | 42° Gearbox Output Quill | B13-6564 | | | | Aug.12,1974 | 150 | 320 |
| 16779 | UH-1D | 42° Gearbox Output Quill | B13-6509 | | | | Aug.14,1974 | 100 | 75 |
| 16779 | UH-1D | 42° Gearbox Input Quill | B13-6509 | | | | Aug.14,1974 | 10 | 40 |

* Removed for Analysis

| Aircraft # | | | | Hours | | | | | |
|---|---|---|---|---|---|---|---|---|---|
| # | Type | Position | Serial # | TSN | TSO | Comment | Date | Rate | Level |
| 38784 | UH-1H | Mast Bearing | | | | Portside Position | May 21,1974 | 90 | 70 |
| 38784 | UH-1H | Mast Bearing | | | | Front Position | May 23,1974 | 65 | 70 |
| 38784 | UH-1H | Mast Bearing | | | | Starboard Position | May 23,1974 | 95 | 60 |
| 38784 | UH-1H | Mast Bearing | | | | AFT Position | May 23,1974 | 90 | 150 |
| BC13 | UH-1H | Mast Bearing | | | | | June 14,1974 | 160 | 55 |
| 60529 | UH-1M | Mast Bearing | 574D | | | | Aug. 1,1974 | 75 | 50 |
| 60630 | UH-1C | Mast Bearing | | 1686 | | | Aug. 6,1974 | 55 | 80 |
| 15071 | UH-1C | Mast Bearing | 613-N | 1260 | | * | Aug. 6,1974 | 450 | 1000 |
| 59771 | UH-1H | Mast Bearing | 7377A | | | | Aug. 7,1974 | 75 | 40 |
| 59519 | UH-1M | Mast Bearing | MRC 3192 | | | | Aug. 8,1974 | 25 | 50 |
| 16354 | UH-1H | Mast Bearing | FAF 3393A | | | | Aug.12,1974 | 150 | 60 |
| 16779 | UH-1D | Mast Bearing | FAF 190x | | | | Aug.14,1974 | 80 | 100 |
| 01087 | UH-1H | Mast Bearing | 167-S | | | | Aug.16,1974 | 17 | 55 |
| 15071 | UH-1C | Mast Bearing | H9-2965 | | | New Bearing | Dec. 3,1974 | 75 | 75 |



* Removed for Analysis

| Aircraft # | Type | Position | Serial # | Hours TSN | Hours TSO | Comment | Date | Rate | Level |
|---|---|---|---|---|---|---|---|---|---|
| 15550 | UH-1H | 90° Gear Box | ABC-5688 | 588 | 400 | Progressing Damage * | July 30,1974 | 150 | 650 |
| 13740 | UH-1H | 90° Gear Box | B13-8168 | 106 | 0 | | July 31,1974 | 100 | 70 |
| 60529 | UH-1M | 90° Gear Box | ABC-2892 | 75 | 0 | | Aug. 1,1974 | 600 | 70 |
| 15200 | UH-1M | 90° Gear Box | A-133069 | 10 | 0 | | Aug. 1,1974 | 100 | 55 |
| 59884 | UH-1D | 90° Gear Box | B13-5077 | | 626 | | Aug. 5,1974 | 70 | 95 |
| 60630 | UH-1C | 90° Gear Box | B13-9937 | | 12 | | Aug. 6,1974 | 95 | 40 |
| 15071 | UH-1C | 90° Gear Box | B13-3307 | | 6 | | Aug. 6,1974 | 150 | 30 |
| 59519 | UH-1M | 90° Gear Box | B13-8655 | | 171 | | Aug. 8,1974 | 100 | 40 |
| 16354 | UH-1H | 90° Gear Box | A13-369 | | | | Aug.12,1974 | 150 | 15 |
| 16779 | UH-1D | 90° Gear Box | B12-8663 | | | | Aug.14,1974 | 70 | 200 |
| 21418 | OH-58A | 90° Gear Box | | | | T/R 6180 rpm | Sept.18,1974 | 45 | 125 |
| BC13 | UH-1H | 90° Gear Box | Sample N-5 | | | Sanitized | Dec 5,1974 | 100 | 25 |

* Removed for Analysis

| Aircraft # | | | | Hours | | | | | |
|---|---|---|---|---|---|---|---|---|---|
| # | Type | Position | Serial # | TSN | TSO | Comment | Date | Rate | Level |
| BC13 | UH-1H | Input Drive Quill | ABU-11067 | | | | June 14,1974 | 150 | 150 |
| 60630 | UH-1C | Input Drive Quill | | | | | Aug. 6,1974 | 150 | 100 |
| 15071 | UH-1C | Input Drive Quill | | | | | Aug. 6,1974 | 400 | 1100 |
| 59771 | UH-1H | Input Drive Quill | | | | | Aug. 7 1974 | 90 | 100 |
| 59519 | UH-1M | Input Drive Quill | | | | | Aug. 8,1974 | 150 | 200 |
| 16354 | UH-1H | Input Drive Quill | | | | | Aug.12,1974 | 150 | 150 |
| 16779 | UH-1D | Input Drive Quill | | | | | Aug.14,1974 | 75 | 120 |
| 01087 | UH-1H | Input Drive Quill | | | | | Aug.16,1974 | 140 | 150 |
| 5550 | UH-1H | Input Drive Quill | | | | Torque 0 psi | Sept.17,1974 | 230 | 290 |
| 5550 | UH-1H | Input Drive Quill | | | | Torque 0 psi | Sept.17,1974 | 170 | 220 |
| 5550 | UH-1H | Input Drive Quill | | | | Torque 0 psi | Sept.17,1974 | 200 | 290 |
| 15949 | UH-1H | Input Drive Quill | | | | Low Power | Sept.19,1974 | 150 | 160 |
| 15949 | UH-1H | Input Drive Quill | | | | High Power | Sept.19,1974 | 200 | 270 |
| | | | | | | | | | |
| | | | | | | | | | |
| | | | | | | | | | |
| | | | | | | | | | |
| | | | | | | | | | |
| | | | | | | | | | |
| | | | | | | | | | |
| | | | | | | | | | |

| Aircraft # | | Position | Serial # | Hours | | Comment | Date | Rate | Level |
|---|---|---|---|---|---|---|---|---|---|
| # | Type | | | TSN | TSO | | | | |
| 16264 | UH-1H | #3 Hanger Bearing | A20-67523 | 806 | 404 | Removed * | Nov.13,1973 | 340 | 600 |
| 16264 | UH-1H | #4 Hanger Bearing | A20-60933 | | | | Nov.13,1973 | 100 | 85 |
| 59771 | UH-1D | #3 Hanger Bearing | A20-69969 | | | | Nov.14,1973 | 185 | 90 |
| 59771 | UH-1D | #4 Hanger Bearing | A20-23720 | | | | Nov.14,1973 | 150 | 65 |
| 13740 | UH-1H | #3 Hanger Bearing | A20-27256 | | | | Nov.14,1973 | 100 | 45 |
| 13740 | UH-1H | #4 Hanger Bearing | A20-44738 | | 306 | | Nov.14,1973 | 150 | 52 |
| 16264 | UH-1H | #3 Hanger Bearing | A20-55994 | | | new bearing (replacement) | Nov.19,1973 | 175 | 95 |
| 16197 | UH-1H | #3 Hanger Bearing | A20-48180 | | 225 | | Nov.27,1973 | 240 | 110 |
| 16197 | UH-1H | #4 Hanger Bearing | A20-19152 | | 225 | | Nov.27,1973 | 120 | 70 |
| 13740 | UH-1H | #3 Hanger Bearing | A20-27256 | | | repeat hanger 11/14/73 | Nov.27,1973 | 150 | 45 |
| 13740 | UH-1H | #4 Hanger Bearing | A20-44738 | | | repeat hanger 11/14/73 | Nov.27,1973 | 100 | 60 |
| 66-01087 | UH-1H | #3 Hanger Bearing | A20-43391 | | 488 | Removed * | Nov.28,1973 | 300 | 900 |
| 66-01087 | UH-1H | #4 Hanger Bearing | A20-37362 | | 501 | Aircraft * | Nov.28,1973 | 300 | 45 |
| 66-01087 | UH-1H | #4 Hanger Bearing | A20-37362 | | 501 | Laboratory * | Nov.28,1973 | 65 | 170 |
| 15949 | UH-1H | #3 Hanger Bearing | A20-64495 | | 427 | Removed * | Nov.28,1973 | 150 | 1800 |
| 15949 | UH-1H | #4 Hanger Bearing | A20-64906 | | 427 | Removed * | Nov.28,1973 | 295 | 550 |
| 59519 | UH-1M | #1 Hanger Bearing | A20-44891 | | | | Nov.30,1973 | 95 | 700 |
| 59519 | UH-1M | #2 Hanger Bearing | A20-57910 | | | | Nov.30,1973 | 150 | 200 |
| 59519 | UH-1M | #3 Hanger Bearing | A20-11446 | | | Removed-Excessive Needle Swing * | Nov.30.;973 | 300 | 1200 |
| 66-01087 | UH-1H | #3 Hanger Bearing | A20-10705 | | | new bearing (replacement) | Nov.30,1973 | 200 | 80 |
| 15949 | UH-1H | #3 Hanger Bearing | | | | new bearing (replacement) | Nov.30,1973 | 200 | 70 |



* Removed for Analysis

| Aircraft # | | | | Hours | | | | | |
|---|---|---|---|---|---|---|---|---|---|
| # | Type | Position | Serial # | TSN | TSO | Comment | Date | Rate | Level |
| 15949 | UH-1H | #4 Hanger Bearing | | | | New bearing (replacement) | Nov.30,1973 | 320 | 50 |
| 15200 | UH-1M | #1 Hanger Bearing | A20-29105 | | 143 | | Dec.6,1973 | 170 | 60 |
| 15200 | UH-1M | #2 Hanger Bearing | A20-22817 | | 143 | | Dec.6,1973 | 55 | 50 |
| 15200 | UH-1M | #3 Hanger Bearing | A20-10877 | | 143 | | Dec.6,1973 | 185 | 50 |
| 66-15190 | UH-1M | #1 Hanger Bearing | A20-56617 | | 80 | | Dec.12,1973 | 200 | 400 |
| 66-15190 | UH-1M | #2 Hanger Bearing | A20-46146 | | 80 | | Dec.12,1973 | 100 | 150 |
| 66-15190 | UH-1M | #3 Hanger Bearing | A20-53737 | | 80 | | Dec.12,1973 | 60 | 55 |
| 66-16879 | UH-1H | #3 Hanger Bearing | A20-26745 | | 403 | Removed for Analysis * | Dec.12,1973 | 250 | 2500 |
| 66-16879 | UH-1H | #4 Hanger Bearing | A20-31225 | | 403 | Removed for Analysis * | Dec.12,1973 | 300 | 6000 |
| 38784 | UH-1H | #3 Hanger Bearing | A20-36705 | 1166 | 646 | 6600 * | May 21,1974 | 150 | 1500 |
| 38784 | UH-1H | #3 Hanger Bearing | A20-36705 | | | 4600 | May 21,1974 | 80 | 1000 |
| 38484 | UH-1H | #4 Hanger Bearing | A20-31435 | | | 4600 | May 21,1974 | 225 | 4800 |
| 38784 | UH-1H | #4 Hanger Bearing | A20-31435 | | | 6600 * | May 21,1974 | 225 | 7000 |
| BC14 | UH-1H | #3 Hanger Bearing | | | | Left Pedal | June 13,1974 | 35 | 65 |
| BC14 | UH-1H | #4 Hanger Bearing | | | | Left Pedal | June 13,1974 | 300 | 1000 |
| BC14 | UH-1H | #4 Hanger Bearing | | | | Right Pedal | June 13,1974 | 300 | 1000 |
| BC14 | UH-1H | #4 Hanger Bearing | | | | Neutral Pedal | June 13,1974 | 300 | 700 |
| BC13 | UH-1H | #4 Hanger Bearing | A20-34779 | | | | June 13,1974 | 120 | 100 |
| BC13 | UH-1H | #3 Hanger Bearing | | | | | June 13,1974 | 45 | 150 |
| BC14 | UH-1H | #4 Hanger Bearing | | | | Flight Idle | June 13,1974 | 220 | 200 |
| BC14 | UH-1H | #4 Hanger Bearing | | | | 6400 Full Rt.Pedal | June 13,1974 | 240 | 900 |



* Removed for Analysis

| Aircraft # | Type | Position | Serial # | Hours TSN | Hours TSO | Comment | Date | Rate | Level |
|---|---|---|---|---|---|---|---|---|---|
| BC14 | UH-1H | #3 Hanger Bearing | | | | Flight Idle | June 13,1974 | 150 | 25 |
| BC14 | UH-1H | #3 Hanger Bearing | | | | 6400 Full Rt.Pedal | June 13,1974 | 90 | 50 |
| BC13 | UH-1H | Hanger Bearing | | | | Damage Free Assy | June 14,1974 | 100 | 50 |
| BC13 | UH-1H | #3 Hanger Bearing | | | | | June 14,1974 | 65 | 150 |
| 13740 | UH-1H | #3 Hanger Bearing | | | | | July 31,1974 | 120 | 60 |
| 13740 | UH-1H | #4 Hanger Bearing | | | | | July 31,1974 | 140 | 30 |
| 60529 | UH-1M | #3 Hanger Bearing | A20-64529 | 75 | 0 | * | Aug. 1,1974 | 400 | 800 |
| 60529 | UH-1M | #2 Hanger Bearing | A20-52529 | | 0 | | Aug. 1,1974 | 250 | 80 |
| 15200 | UH-1M | #3 Hanger Bearing | | | 167 | | Aug. 1,1974 | 130 | 50 |
| 15200 | UH-1M | #2 Hanger Bearing | | | 167 | | Aug. 1,1974 | 300 | 80 |
| 15200 | UH-1M | #1 Hanger Bearing | | | 167 | | Aug. 1,1974 | 340 | 160 |
| 59884 | UH-1D | #3 Hanger Bearing | | | | | Aug. 5,1974 | 150 | 20 |
| 60630 | UH-1C | #1 Hanger Bearing | | | | | Aug. 6,1974 | 300 | 70 |
| 15071 | UH-1C | #3 Hanger Bearing | | | | | Aug. 6,1974 | 320 | 850 |
| 60630 | UH-1C | #3 Hanger Bearing | | | | | Aug. 6,1974 | 160 | 150 |
| 60630 | UH-1C | #2 Hanger Bearing | | | | | Aug. 6,1974 | 100 | 40 |
| 15071 | UH-1C | #2 Hanger Bearing | A20-15990 | | 237 | * | Aug. 6,1974 | 300 | 3000 |
| 15071 | UH-1C | #1 Hanger Bearing | A20-66943 | | 237 | | Aug. 6,1974 | 65 | 50 |
| 59519 | UH-1M | #2 Hanger Bearing | A20-57910 | | 171 | | Aug. 8,1974 | 120 | 70 |
| 59519 | UH-1M | #3 Hanger Bearing | A20-26938 | | 27 | | Aug. 8,1974 | 150 | 50 |
| 59519 | UH-1M | #1 Hanger Bearing | A20-44891 | 2219 | 194 | | Aug. 8,1974 | 340 | 700 |

* Removed for Analysis

| Aircraft # | Type | Position | Serial # | Hours TSN | Hours TSO | Comment | Date | Rate | Level |
|---|---|---|---|---|---|---|---|---|---|
| 15091 | UH-1M | #1 Hanger Bearing | | | | | Aug. 9,1974 | 200 | 600 |
| 21418 | OH-58A | #6 Hanger Bearing | | | | T/R 6180 rpm | Sept.18,1974 | 40 | 150 |
| 21418 | OH-58A | #5 Hanger Bearing | | | | T/R 6180 rpm | Sept.18,1974 | 100 | 70 |
| 21418 | OH-58A | #4 Hanger Bearing | | | | T/R 6180 rpm | Sept.18,1974 | 75 | 60 |
| 21418 | OH-58A | #3 Hanger Bearing | | | | T/R 6180 rpm | Sept.18,1974 | 190 | 40 |
| 21418 | OH-58A | #2 Hanger Bearing | | | | T/R 6180 rpm | Sept.18,1974 | 75 | 75 |
| 21418 | OH-58A | #1 Hanger Bearing | | | | T/R 6180 rpm | Sept.18,1974 | 90 | 67 |
| 15949 | UH-1H | #1 Hanger Bearing | A20-55389 | 943 | 500 | Removed For Analysis * | Sept.23,1974 | 250 | 1200 |



* Removed for Analysis

## 7.2 INITIAL FAMILIARIZATION AND LABORATORY TESTS

INITIAL FAMILIARIZATION ON THE NUMBER FOUR
HANGER BEARING OF AIRCRAFT UH-1H, 67-17223

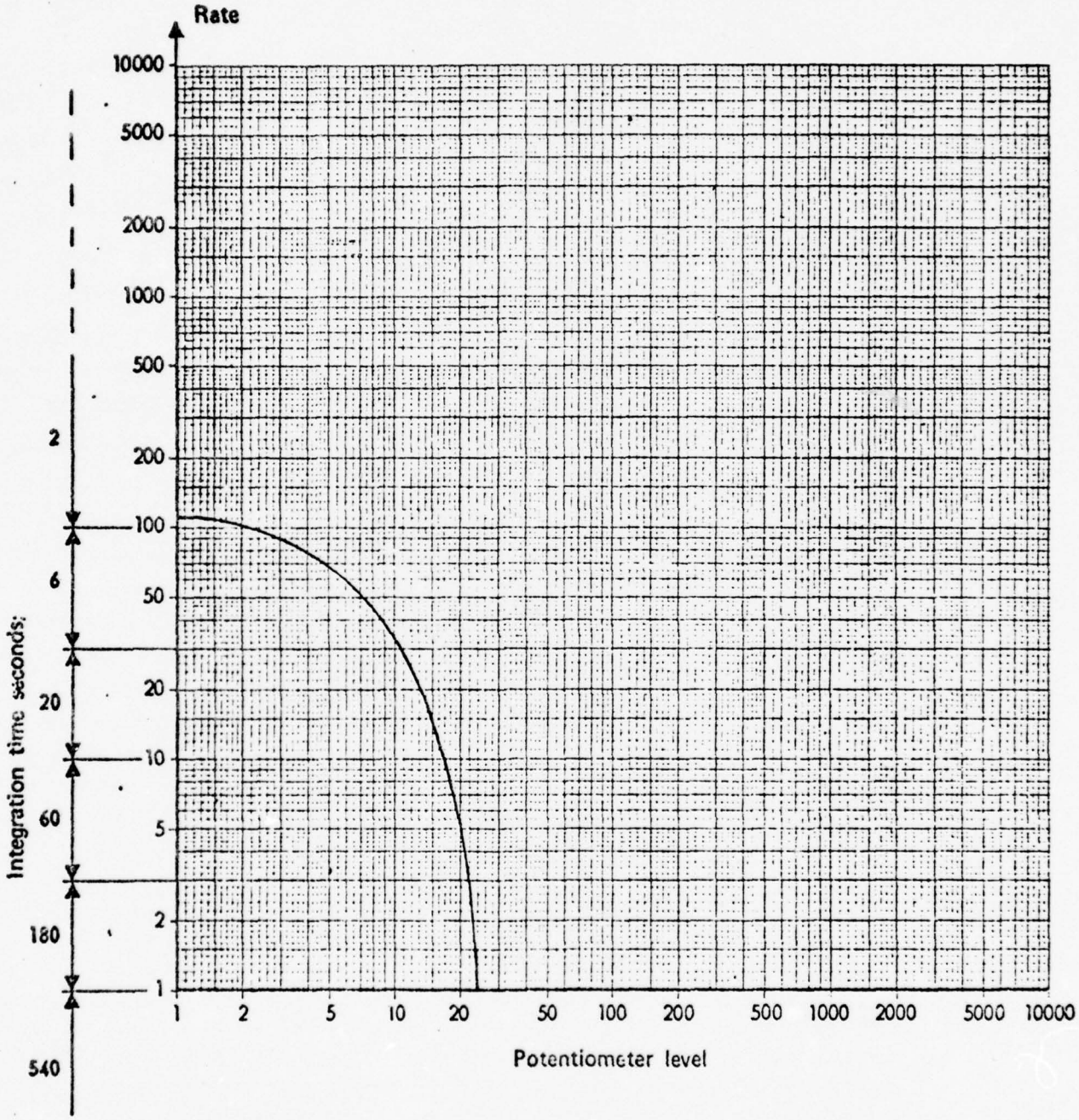


BEARING APPEARS IN GOOD CONDITION WITH
MODERATE TO LOW RATE/POTENTIOMETER LEVELS

INITIAL FAMILIARIZATION ON NUMBER THREE
HANGER BEARING OF AIRCRAFT UH-1H, 67-17223

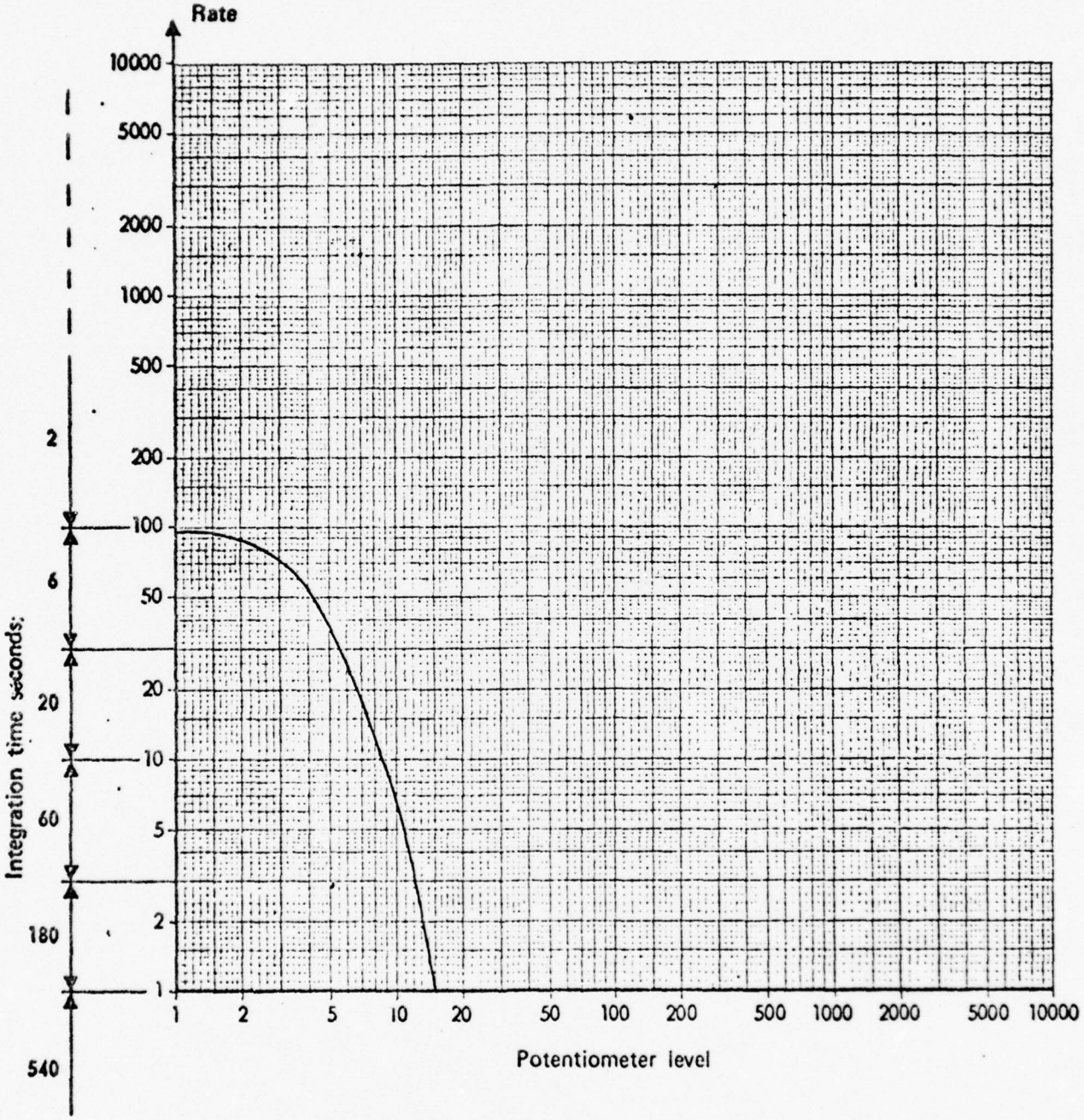


BEARING APPEARS IN GOOD CONDITION WITH
MODERATE TO LOW RATE/POTENTIOMETER LEVELS

ADDITIONAL FAMILIARIZATION ON THE NUMBER THREE HANGER BEARING OF AIRCRAFT UH-1H, 67-17223 TEST PERFORMED ON THE SAME BEARING AS DEPICTED IN FIG. 5 BUT PERFORMED BY ANOTHER INDIVIDUAL

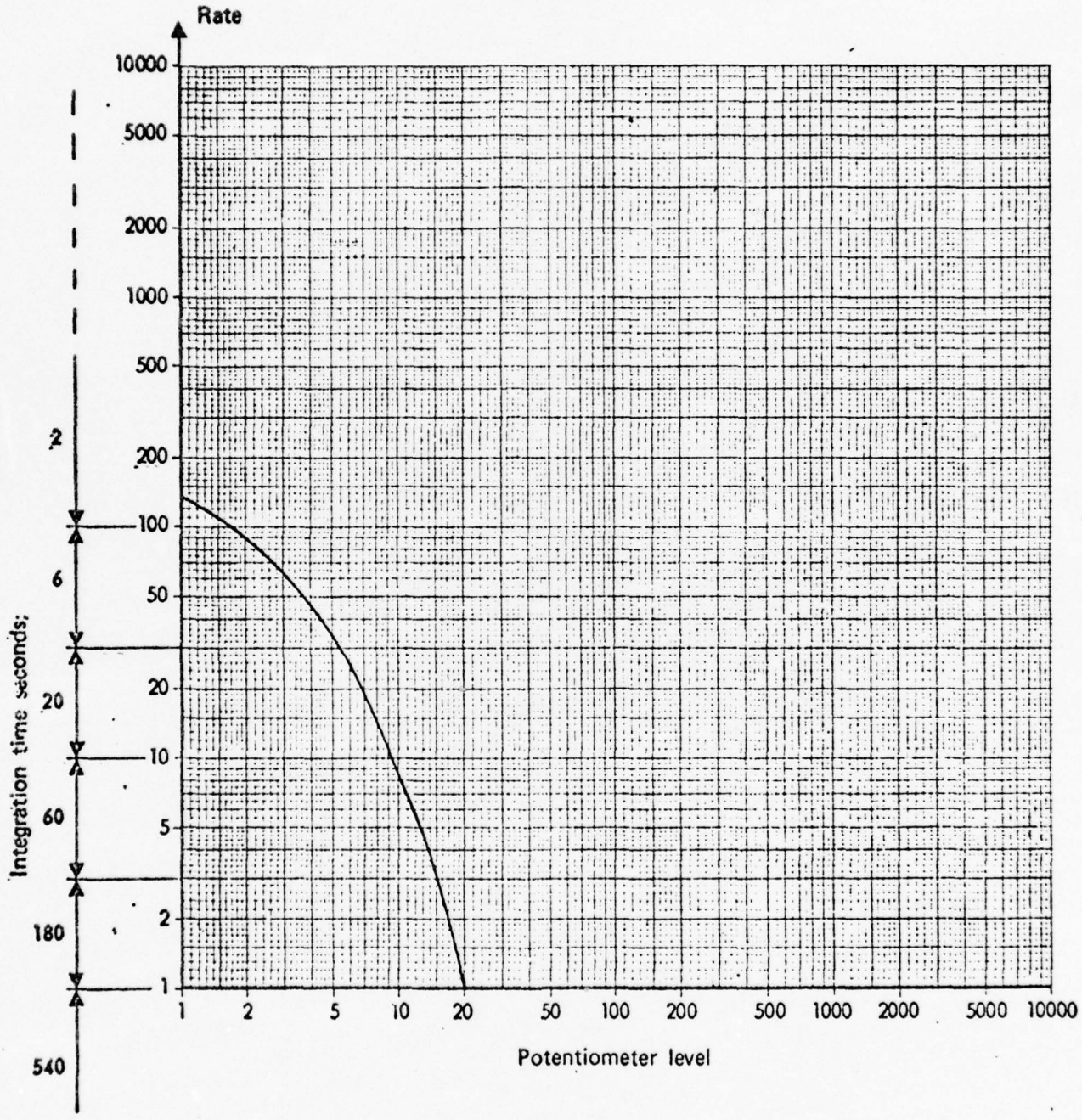


PLOT SHOWS BASIC SIMILARITY AND LEVEL PORTRAYALS EVEN THOUGH THEY WERE PERFORMED BY TWO DIFFERENT PEOPLE

INITIAL FAMILIARIZATION ON THE OUTPUT DRIVE QUILL
BEARING OF THE 42° GEAR BOX OF AIRCRAFT UH-1H, 67-17223

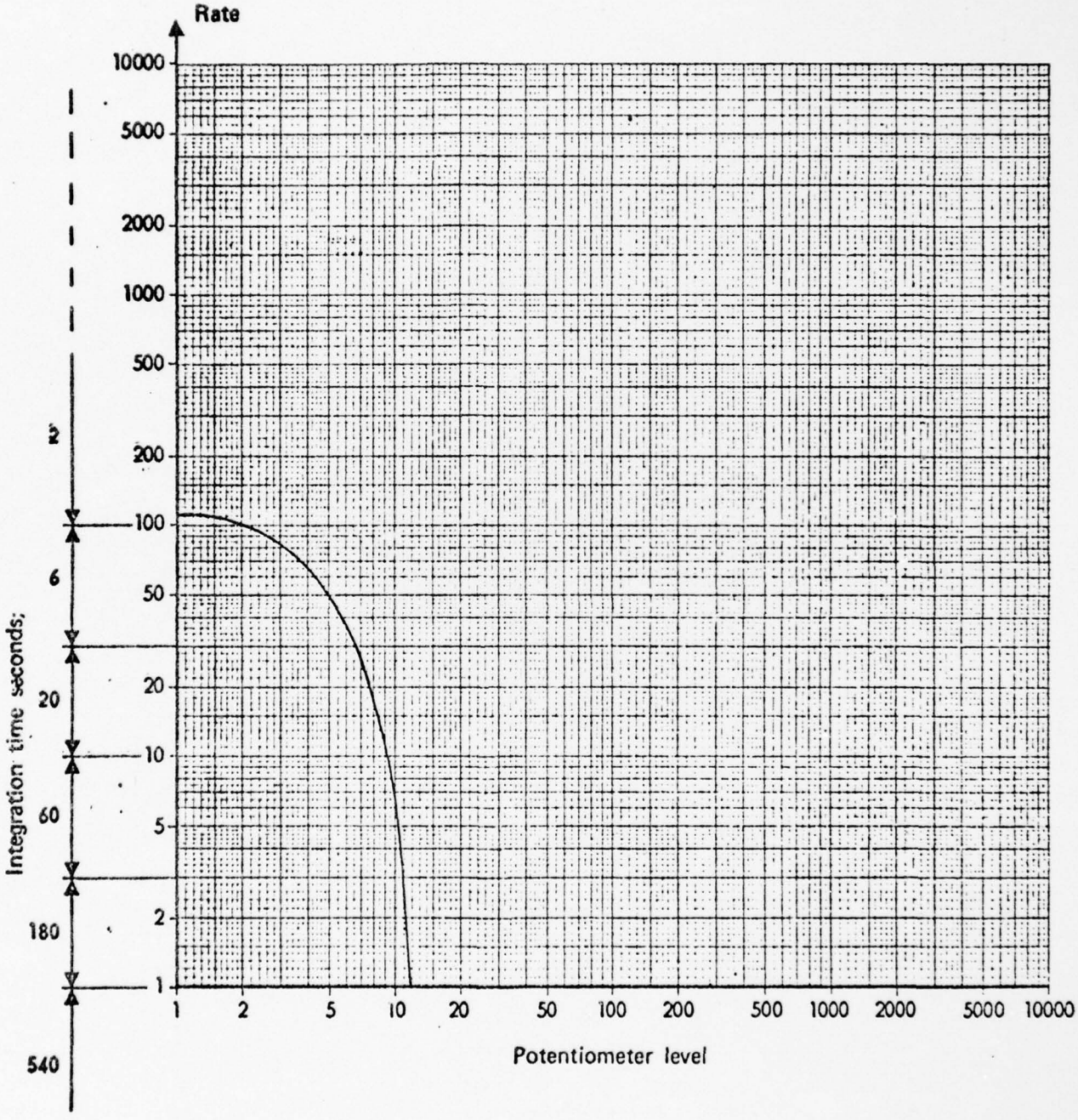


MODERATE LEVELS OF RATE/POTENTIOMETER DEPICTION
INDICATIVE OF BEARING IN GOOD CONDITION

INITIAL FAMILIARIZATION ON THE NUMBER ONE
HANGER BEARING OF AIRCRAFT UH-1H, 67-17223

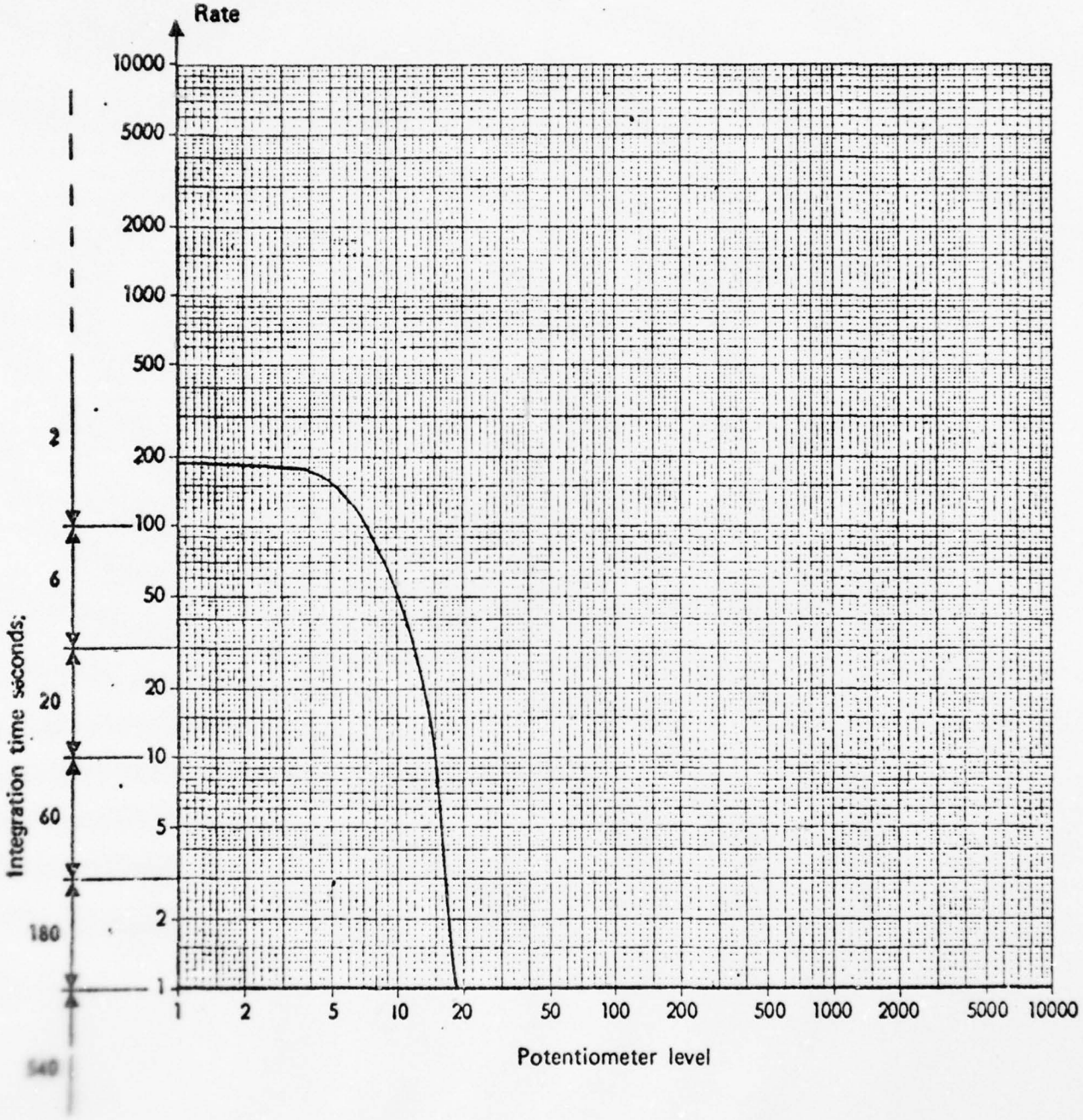


BEARING APPEARS IN GOOD CONDITION
WITH MODERATE TO LOW RATE/POTENTIOMETER LEVELS

TEST OF BEARING USED ON THE TAIL ROTOR STIKE TEST PERFORMED BY BAGANOFF INDUSTRIES TO DETERMINE CONDITION FOR LATER AIRCRAFT USE
TEST PERFORMED ON AIRCRAFT UH-1H, 66-17138

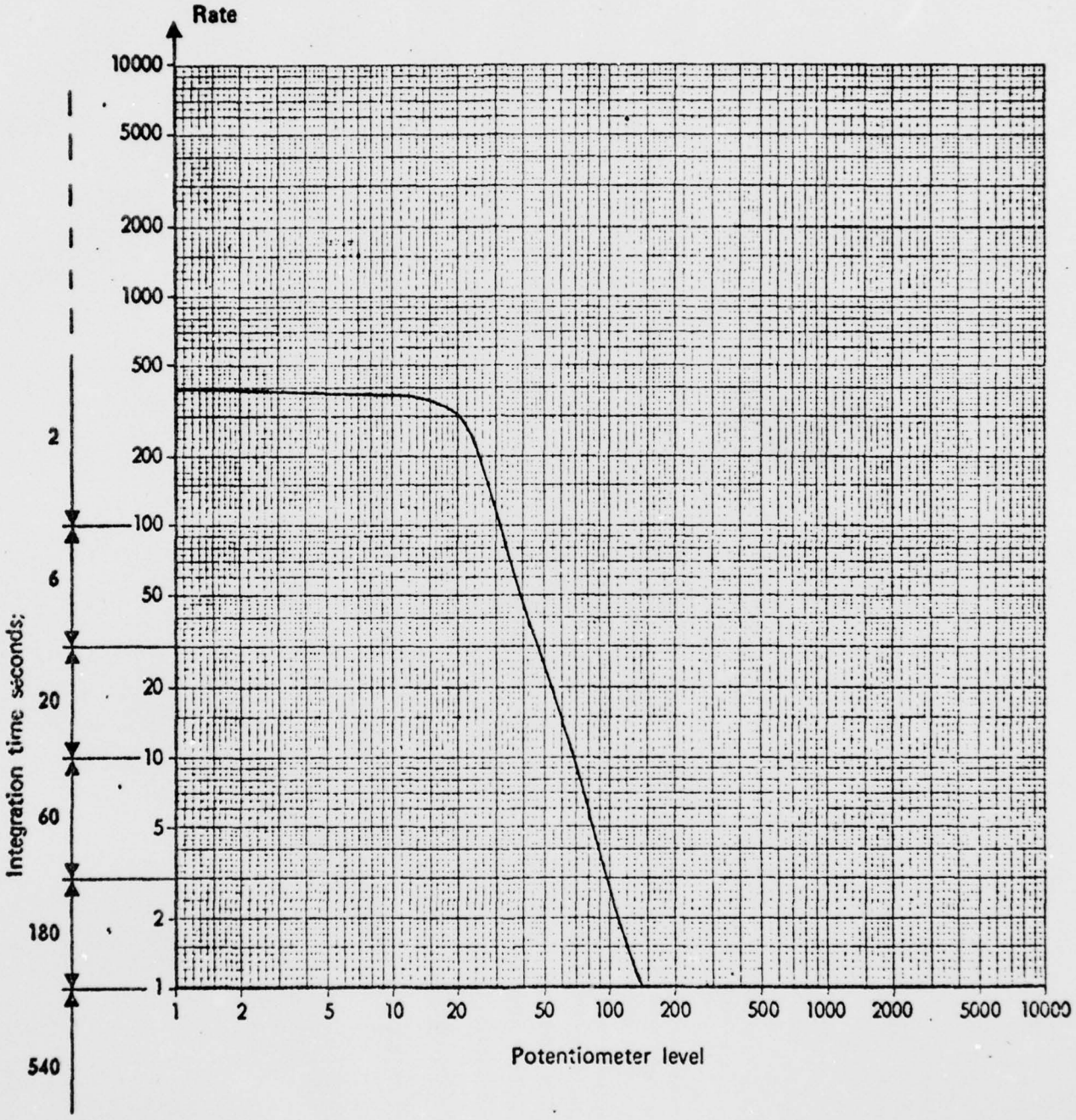


BEARING APPEARS IN GOOD CONDITION WITH
ONLY MODERATE RATE/POTENTIOMETER LEVELS

TEST PERFORMED WITH BEARING IN THE NUMBER THREE HANGER POSITION

TEST ON BEARING WHICH WAS DESCRIBED AS BEING REMOVED BECAUSE OF 600 HOUR TIME CHANGE ON UNSERVICEABLE TAG-MATERIAL

BEARING APPEARS TO STILL BE IN SERVICEABLE CONDITION AND RATE/POTENTIOMETER LEVELS DO NOT INDICATE TOO HIGH FOR USE

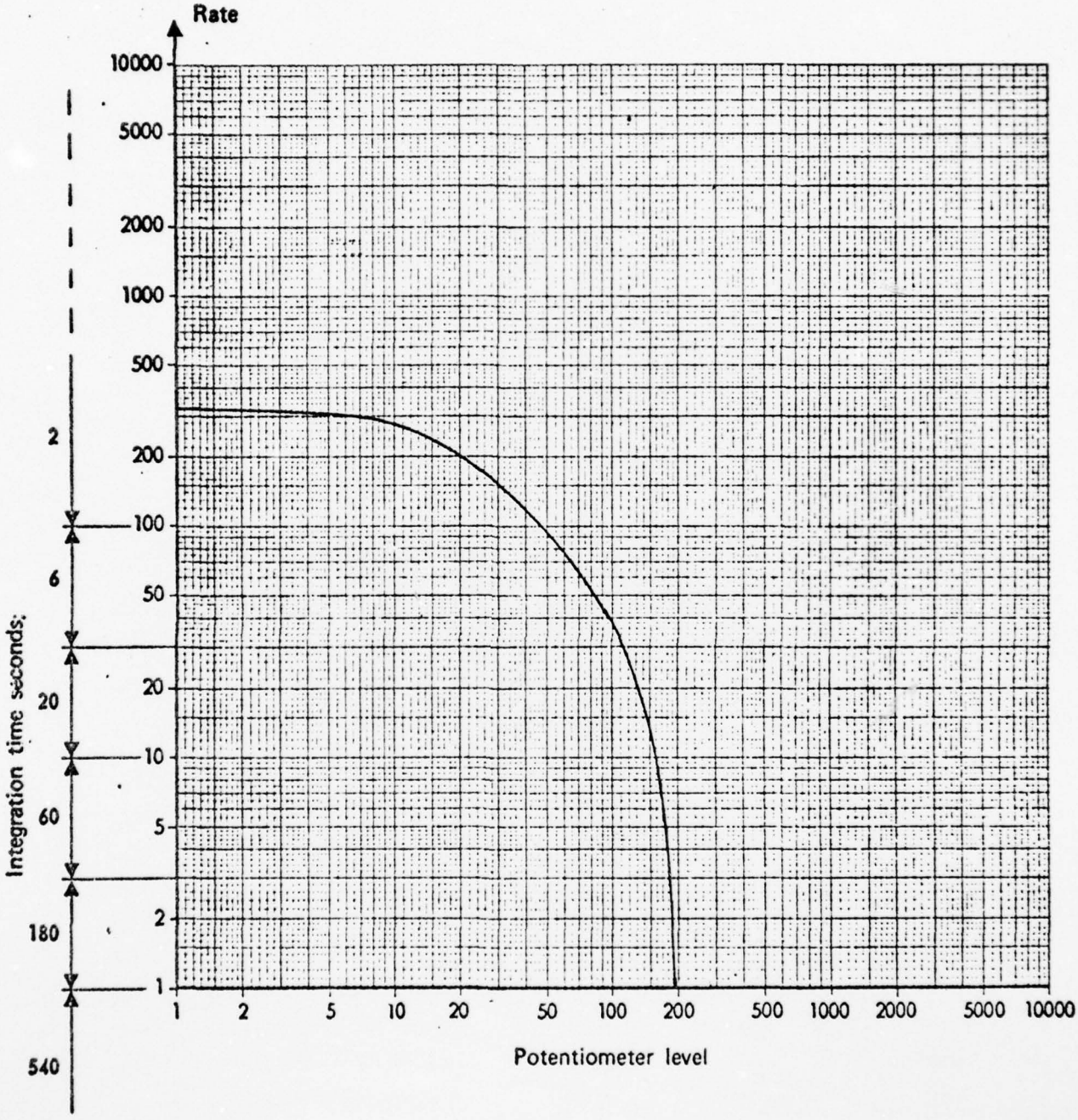


TEST PERFORMED ON BEARING IN THE NUMBER THREE HANGER POSITION

**THIS GRAPH DEPICTS THE BEARING USED IN CONJUNCTION WITH A BEARING TEST BY BAGANOFF ASSOCIATES**

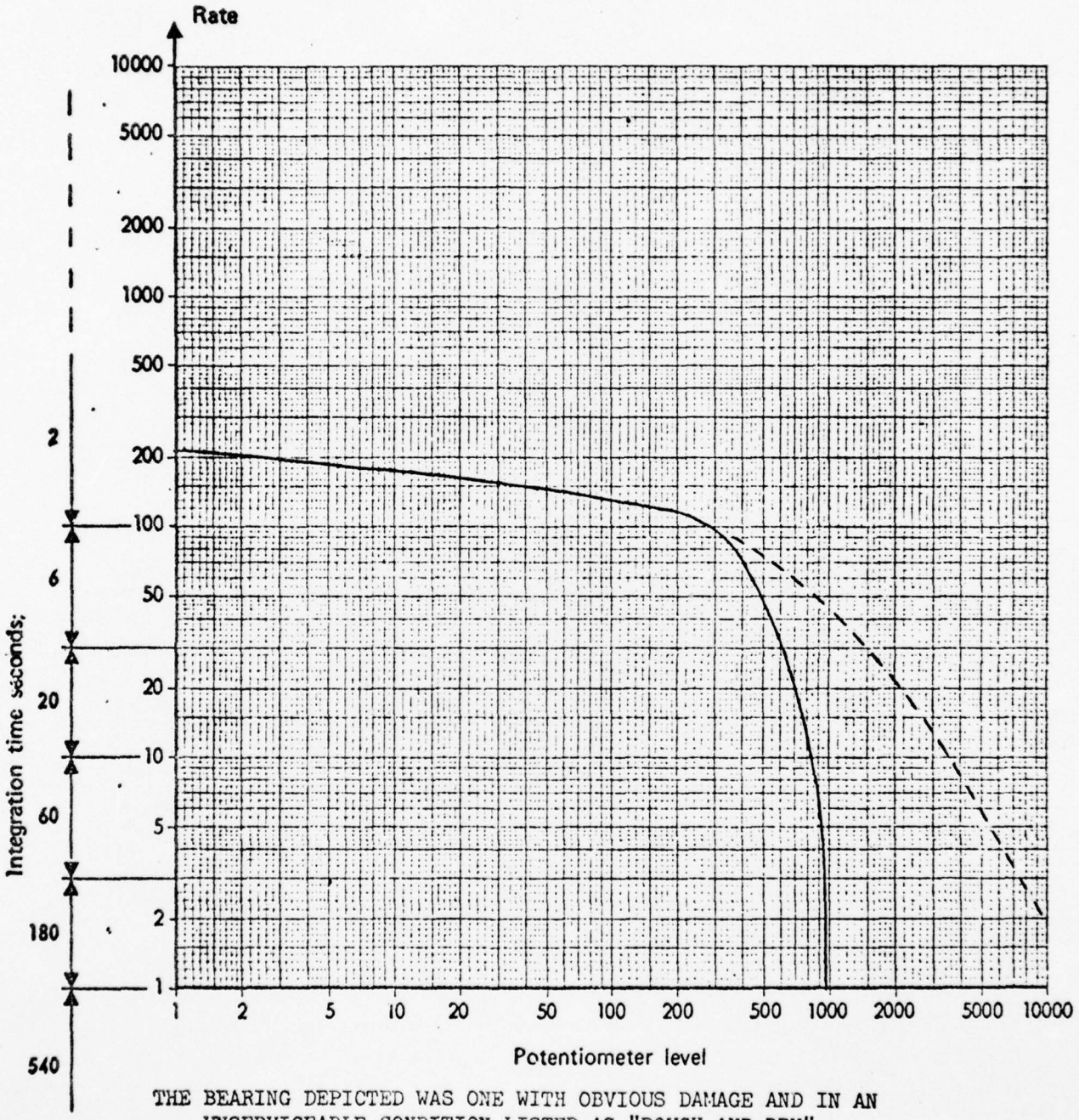


THE BEARING DEPICTED WAS ONE WITH OBVIOUS DAMAGE AND IN AN UNSERVICEABLE CONDITION LISTED AS "ROUGH AND DRY". THREE CURVES WERE PLOTTED ON THE SAME BEARING, ALL OF WHICH SHOW CLEARLY THE DAMAGE IN THE HIGH POTENTIOMETER LEVELS, WHICH IN SOME CASES SEEMED TO EXTEND TO INFINITY, INDICATIVE OF SEVERE ROLLING ELEMENT DAMAGE.

THIS GRAPH DEPICTS THE BEARING USED IN CONJUNCTTON
WITH A BEARING TEST BY BAGANOFF ASSOCIATES

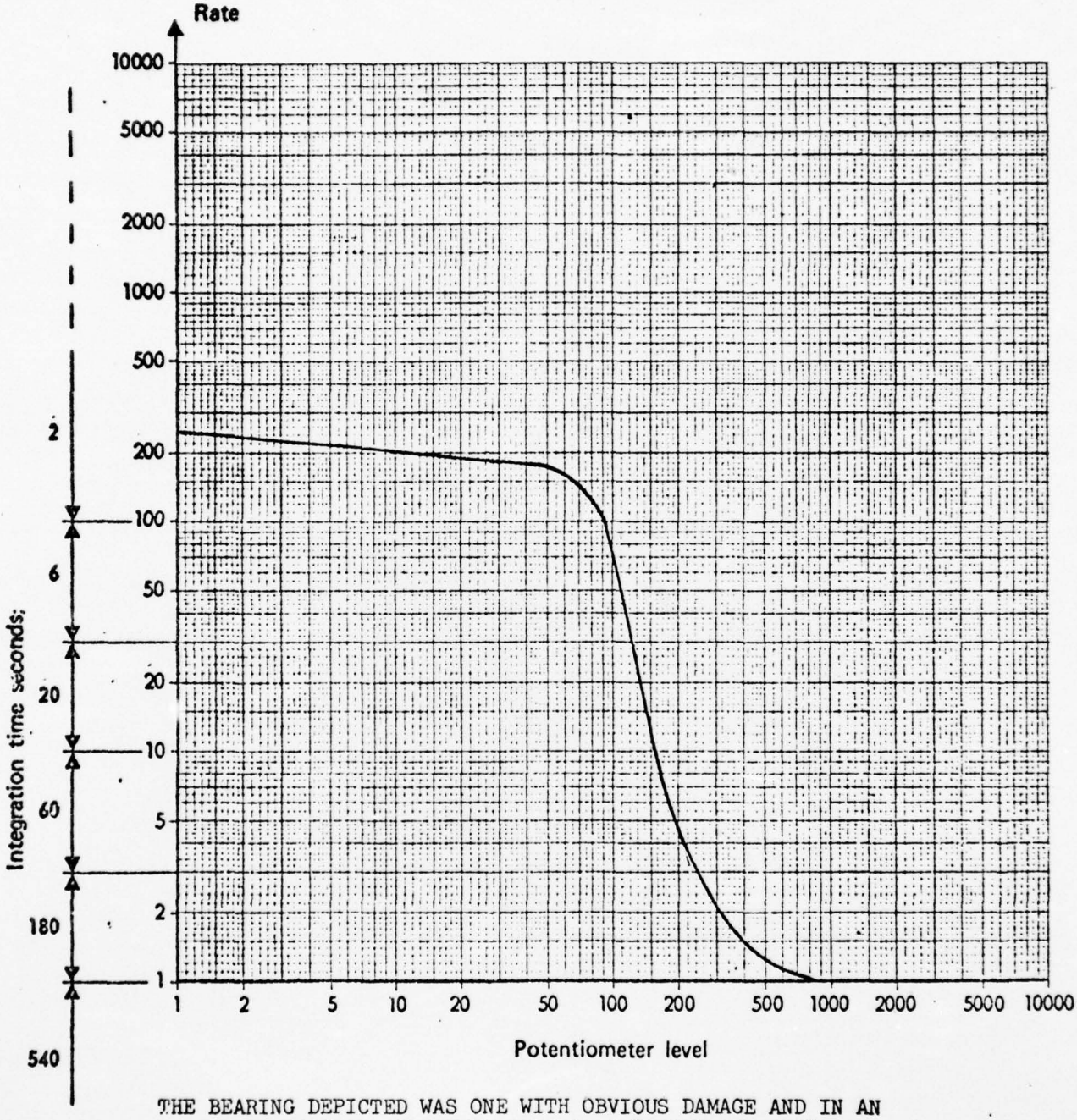


THE BEARING DEPICTED WAS ONE WITH OBVIOUS DAMAGE AND IN AN UNSERVICEABLE CONDITION LISTED AS "ROUGH AND DRY".

THREE CURVES WERE PLOTTED ON THE SAME BEARING, ALL OF WHICH SHOW CLEARLY THE DAMAGE IN THE HIGH POTENTIOMTER LEVELS, WHICH IN SOME CASES SEEMED TO EXTEN [illegible] ROLLING ELEMENT DAMAGE.

FLIGHT TEST ON THE OUTPUT DRIVE QUILL OF THE
42° GEAR BOX OF AIRCRAFT UH-1H, 66-17138

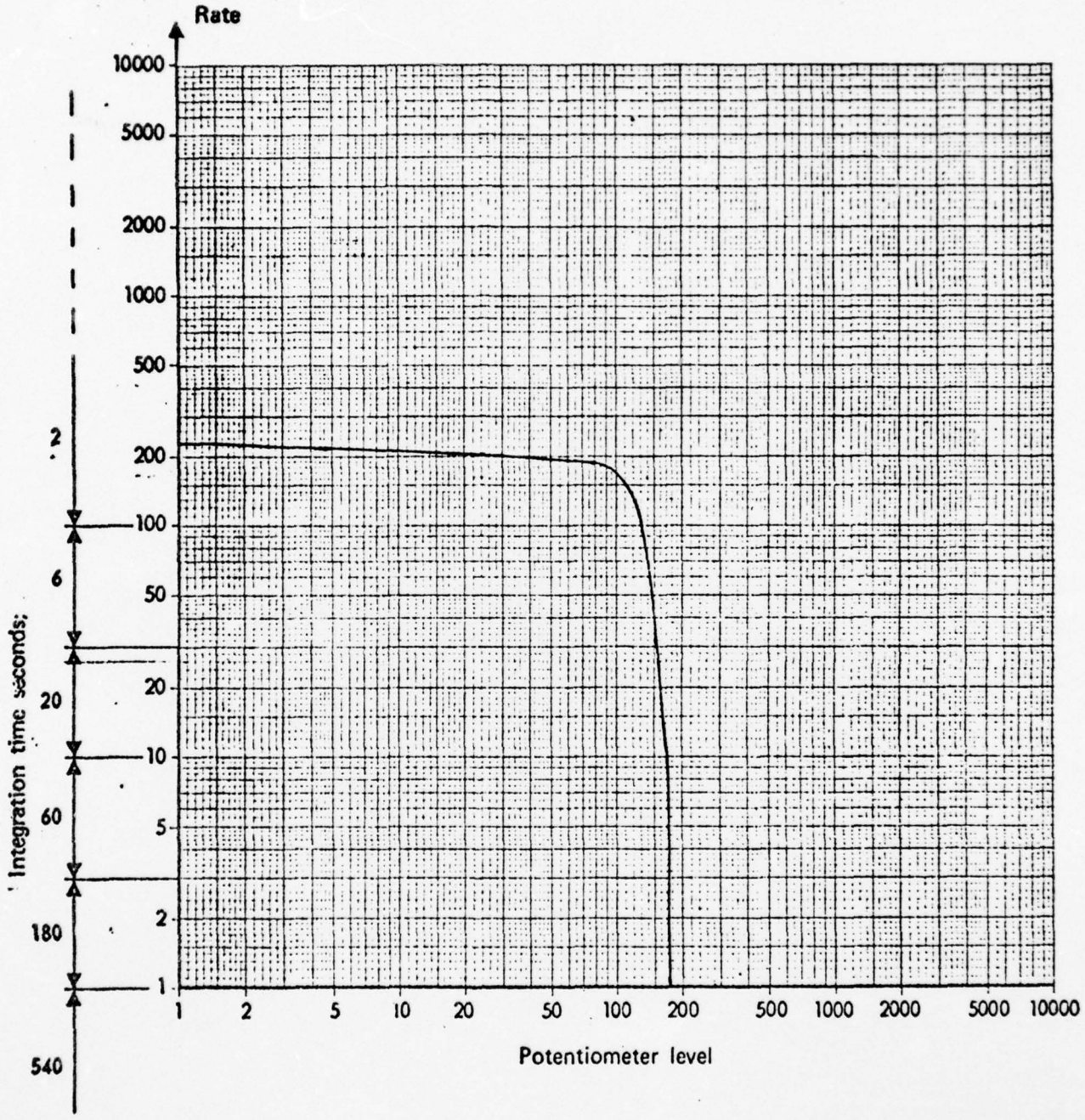


TEST CONDUCTED AT HOVER IN-GROUND EFFECT.
TORQUE VALUE OF 30 PSI AND N1 VALUE OF 92.8%, 6600 ENGINE RPM

(NOTE HIGH POTENTIOMETER LEVEL OF 190 WHEN COMPARED TO 42° GEAR BOX TEST WHEN NOT CONFIGURED FOR FLIGHT TEST)

HOVER CONDITION IN GROUND AFFECT

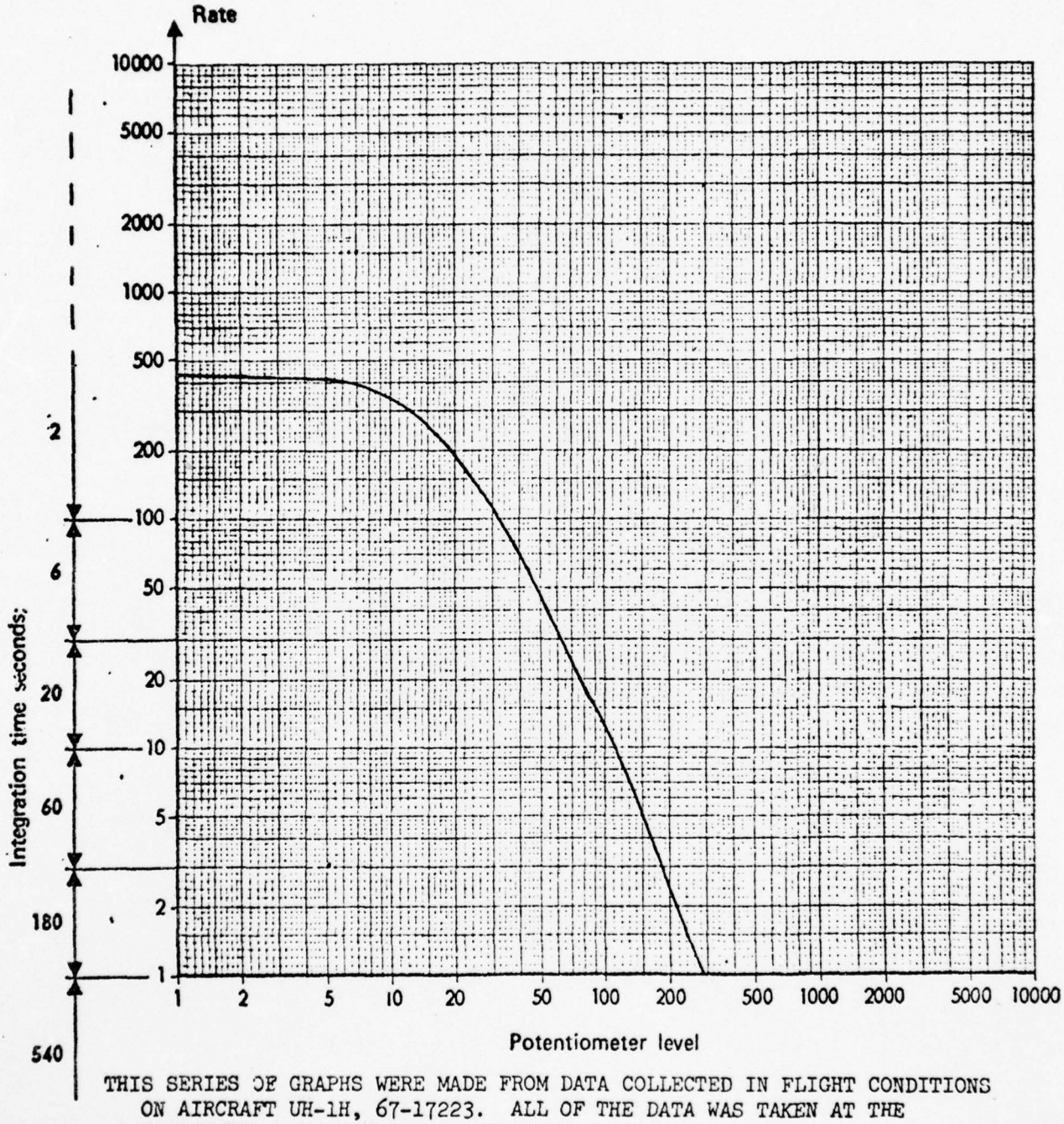


THIS SERIES OF GRAPHS WERE MADE FROM DATA COLLECTED IN FLIGHT CONDITIONS ON AIRCRAFT UH-1H, 67-17223. ALL OF THE DATA WAS TAKEN AT THE OUTPUT DRIVE QUILL AND CAN BE COMPARED TO PREVIOUS GRAPHS OF THE SAME BEARING ELEMENT.

FLIGHT CONDITIONS OF 75 KNOTS AT 22 LBS. TORQUE

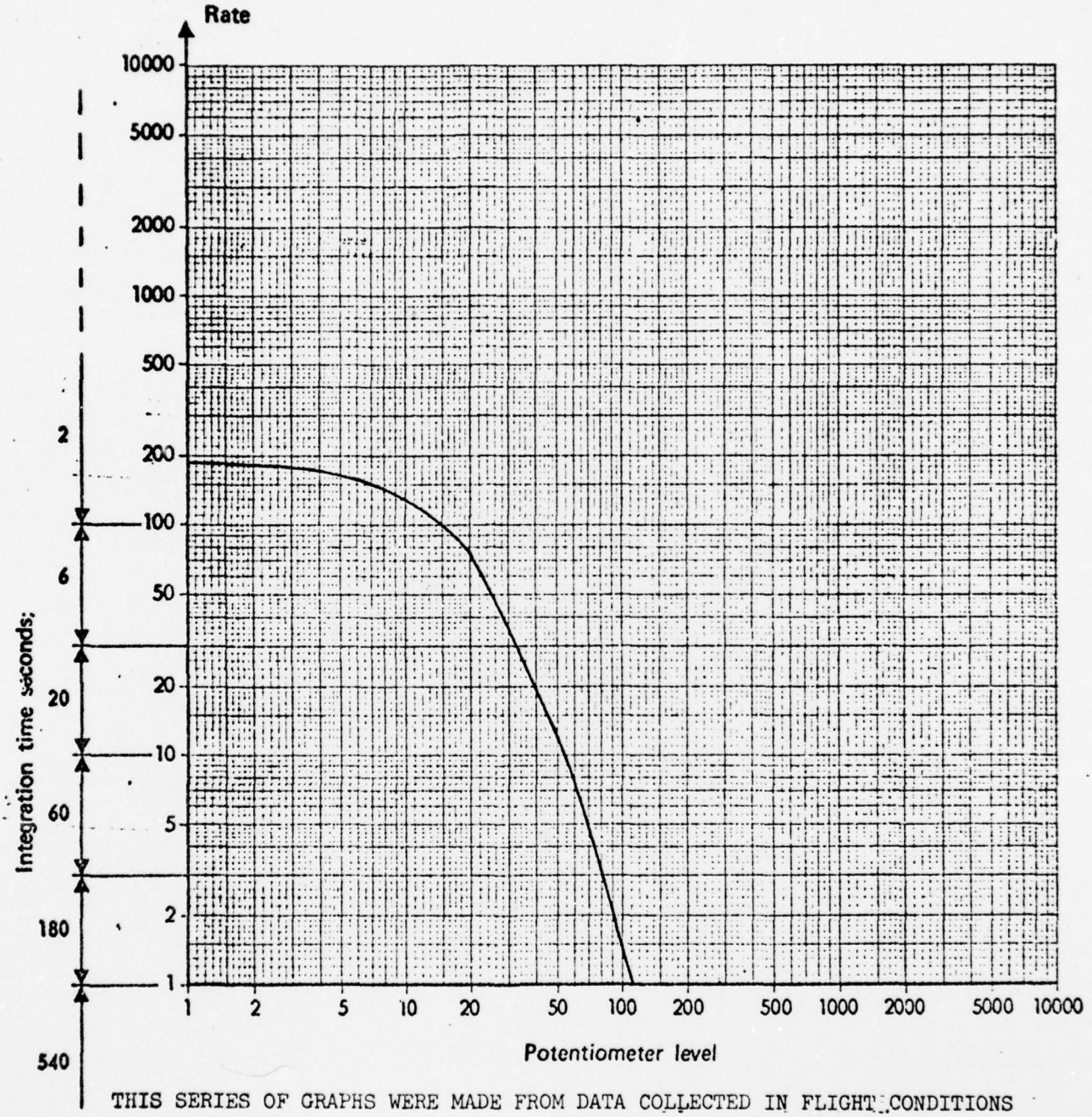


THIS SERIES OF GRAPHS WERE MADE FROM DATA COLLECTED IN FLIGHT CONDITIONS ON AIRCRAFT UH-1H, 67-17223. ALL OF THE DATA WAS TAKEN AT THE OUTPUT DRIVE QUILL AND CAN BE COMPARED TO PREVIOUS GRAPHS OF THE SAME BEARING ELEMENT.

FLIGHT TEST CONDUCTED AT LOW FLIGHT SPEED
(APPROX. 88 kts) AT TORQUE VALUE OF 25 psi AND
91.0% ni, 6600 ENGINE RPM

TEST PERFORMED ON 42° GEAR BOX OUTPUT DRIVE
QUILL BEARING OF AIRCRAFT UH-1H, 66-17138

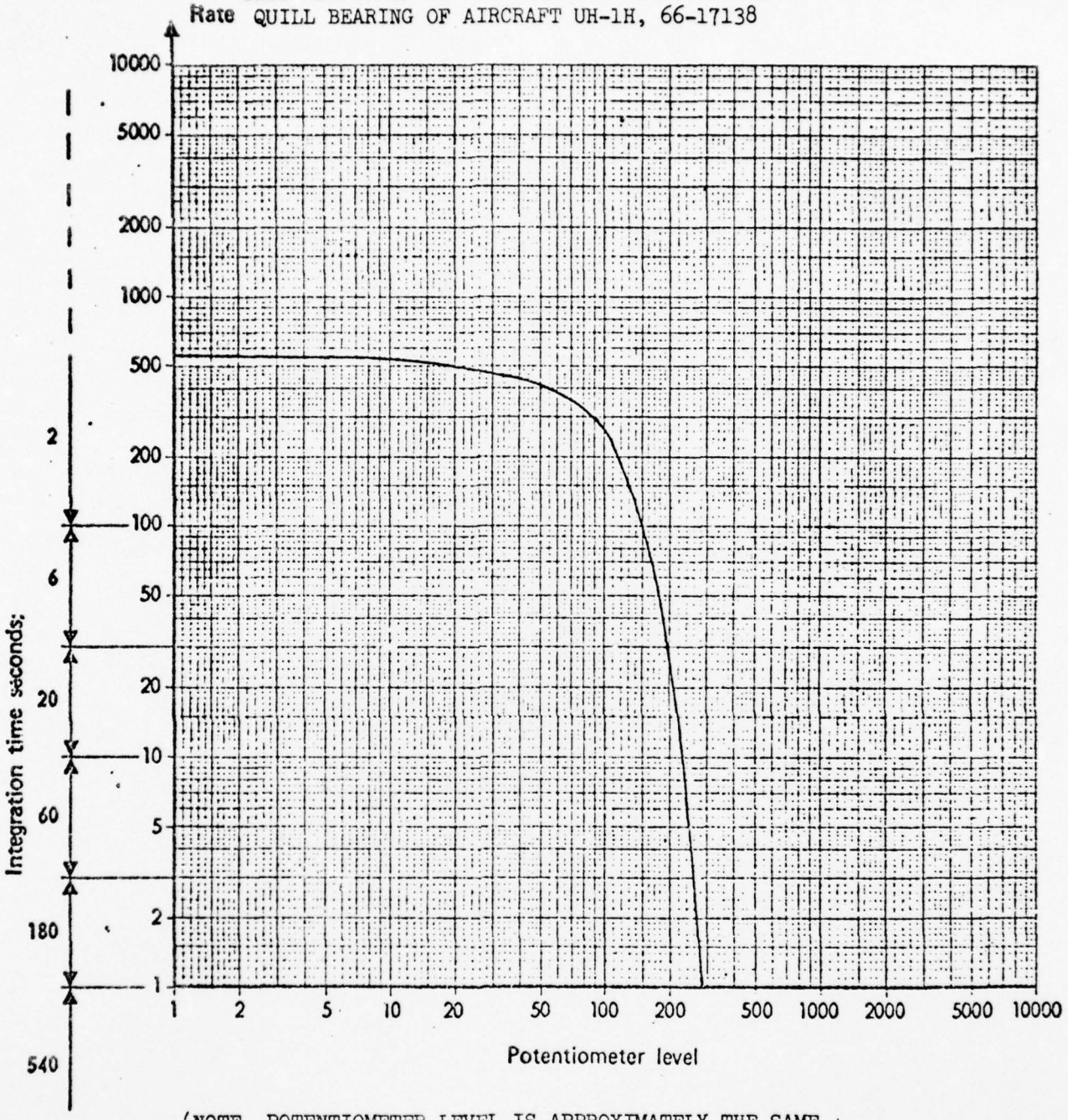


(NOTE, POTENTIOMETER LEVEL IS APPROXIMATELY THE SAME AS IN HOVER TEST OF THE SAME BEARING PACKAGE, HOWEVER, THE RATE LEVEL HAS INCREASED SIGNIFICANTLY)

FLIGHT CONDITIONS OF 95 KNOTS AT 25 LBS. TORQUE

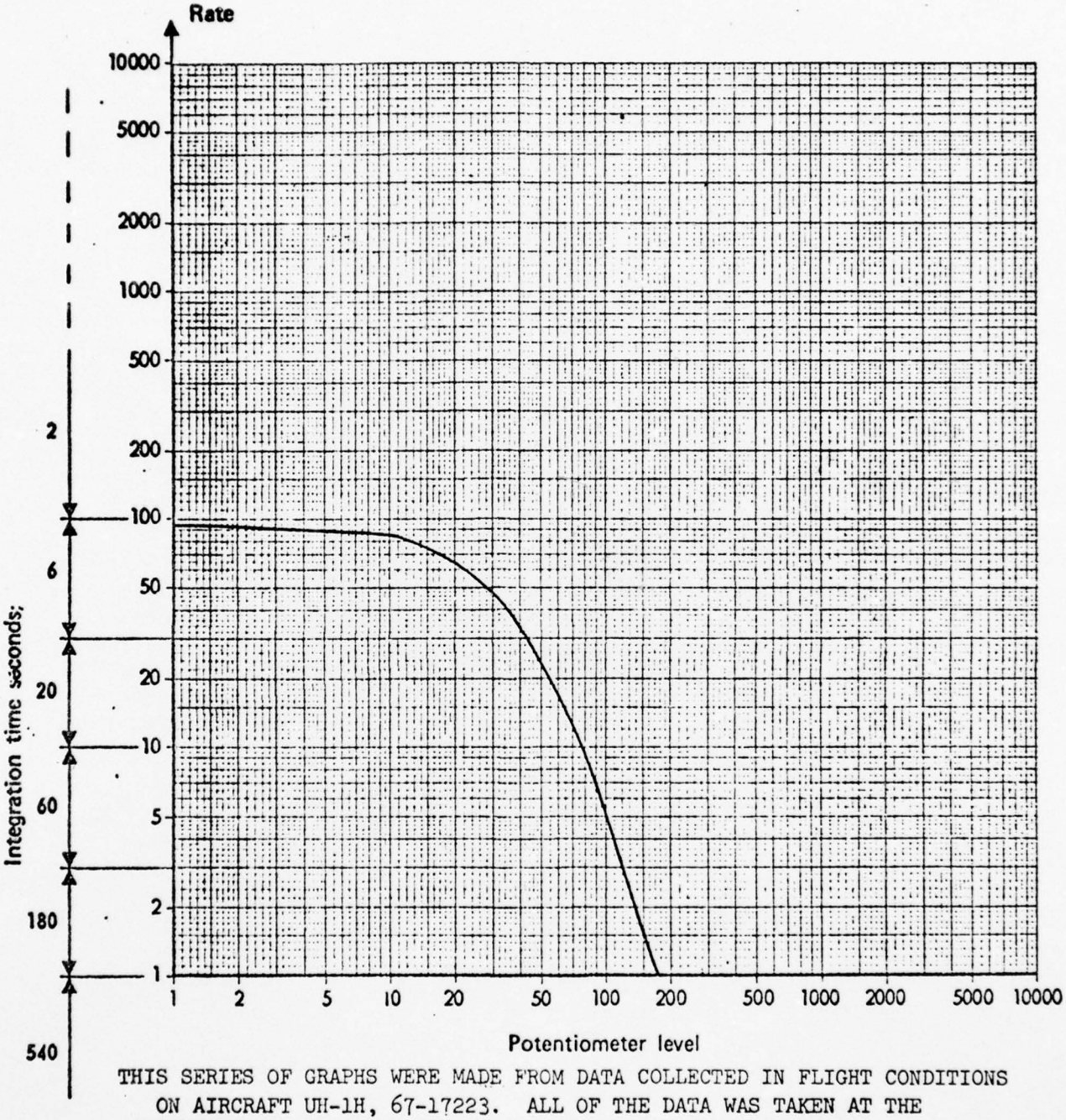


THIS SERIES OF GRAPHS WERE MADE FROM DATA COLLECTED IN FLIGHT CONDITIONS ON AIRCRAFT UH-1H, 67-17223. ALL OF THE DATA WAS TAKEN AT THE OUTPUT DRIVE QUILL AND CAN BE COMPARED TO PREVIOUS GRAPHS OF THE SAME BEARING ELEMENT.

TEST PLOT WITH CABLE OUTSIDE AIRCRAFT UH-1H
66-17138 ON 42° GEAR BOX OUTPUT QUILL BEARING

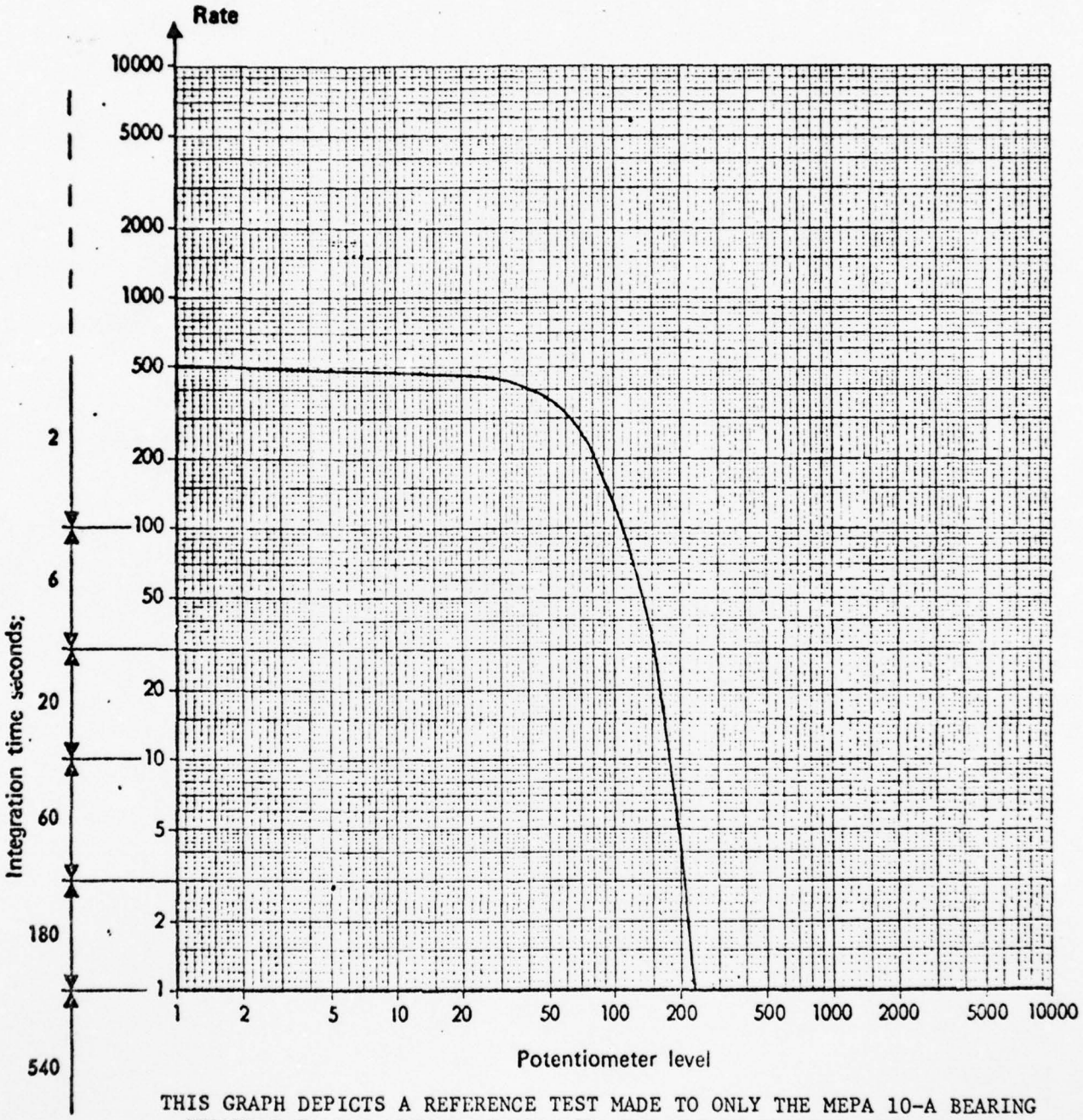


THIS GRAPH DEPICTS A REFERENCE TEST MADE TO ONLY THE MEPA 10-A BEARING ANALYZER IN ITS CONFIGURATION USED FOR FLIGHT TESTING, THE REASON FOR THIS TEST WAS TO DETERMINE TO WHAT EXTENT THE CABLE INSTALLATION INSIDE THE TAIL BOOM MADE, IF ANY

THE CONCLUSION DRAWN AT THIS TIME IS THAT ITS INSTALLATION INSIDE OR OUT YIELDED THE SAME CURVE FORM

TEST PERFORMED ON THE 42° GEAR BOX

OF AIRCRAFT, UH-1H 66-17138

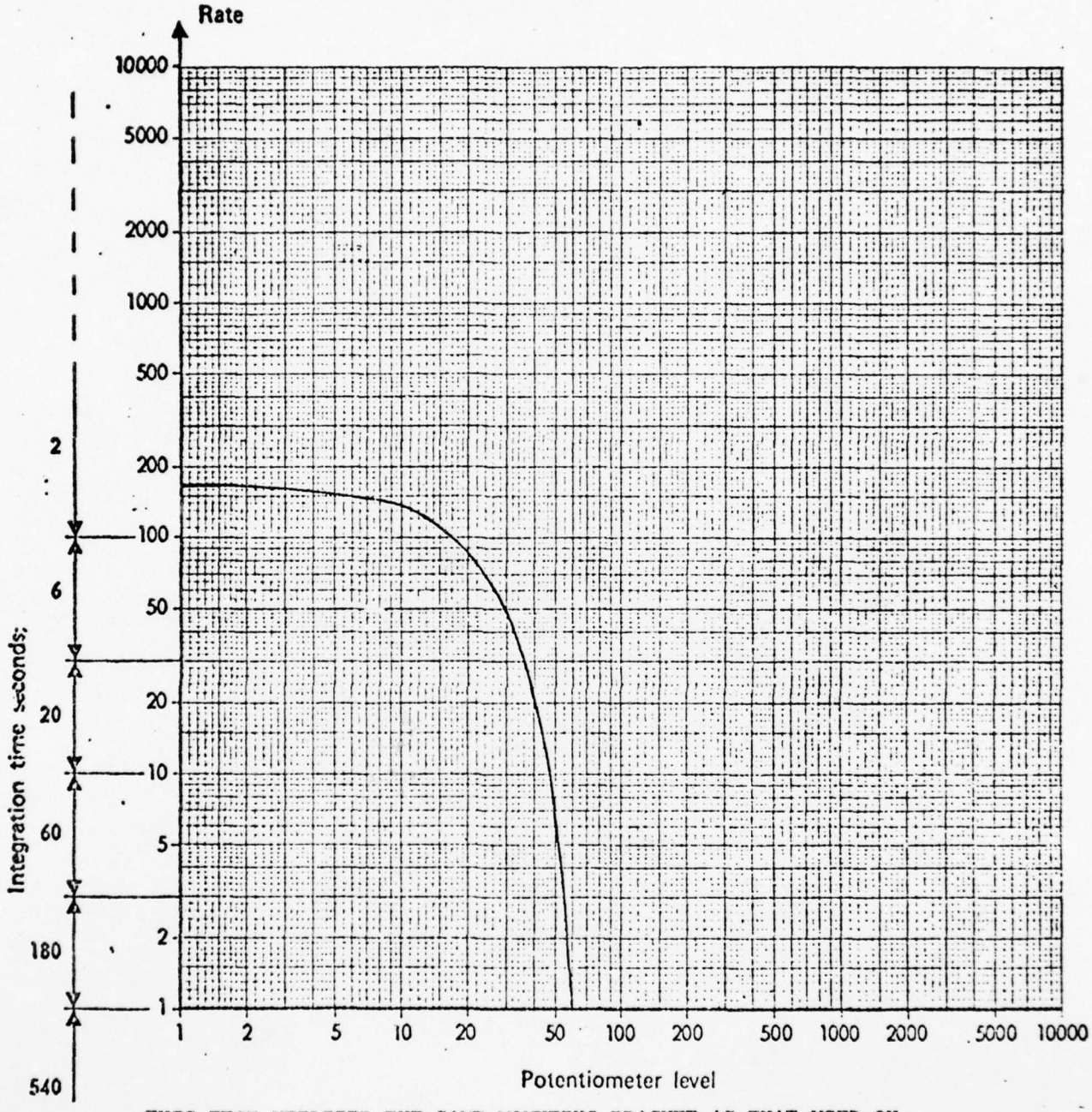


THIS TEST UTILIZED THE SAME MOUNTING BRACKET AS THAT USED ON THE FLIGHT TESTS ON THE BEARING ANALYZER, HOWEVER, THE CABLE WHICH CAME WITH THE SKF BEARING ANALYZER WAS USED IN LIEU OF THE CABLE CONFIGURATION EMPLOYED FOR FLIGHT TESTING

THE CURVE DEPICTS THE SAME SHAPE AS IN THE FLIGHT CONFIGURATION TESTING, HOWEVER, IN FLIGHT CONFIGURATION THE RATE/POTENTIOMENTER IS APPROXIMATELY TRIPLED

NORMALIZATION CURVE NEW BEARING

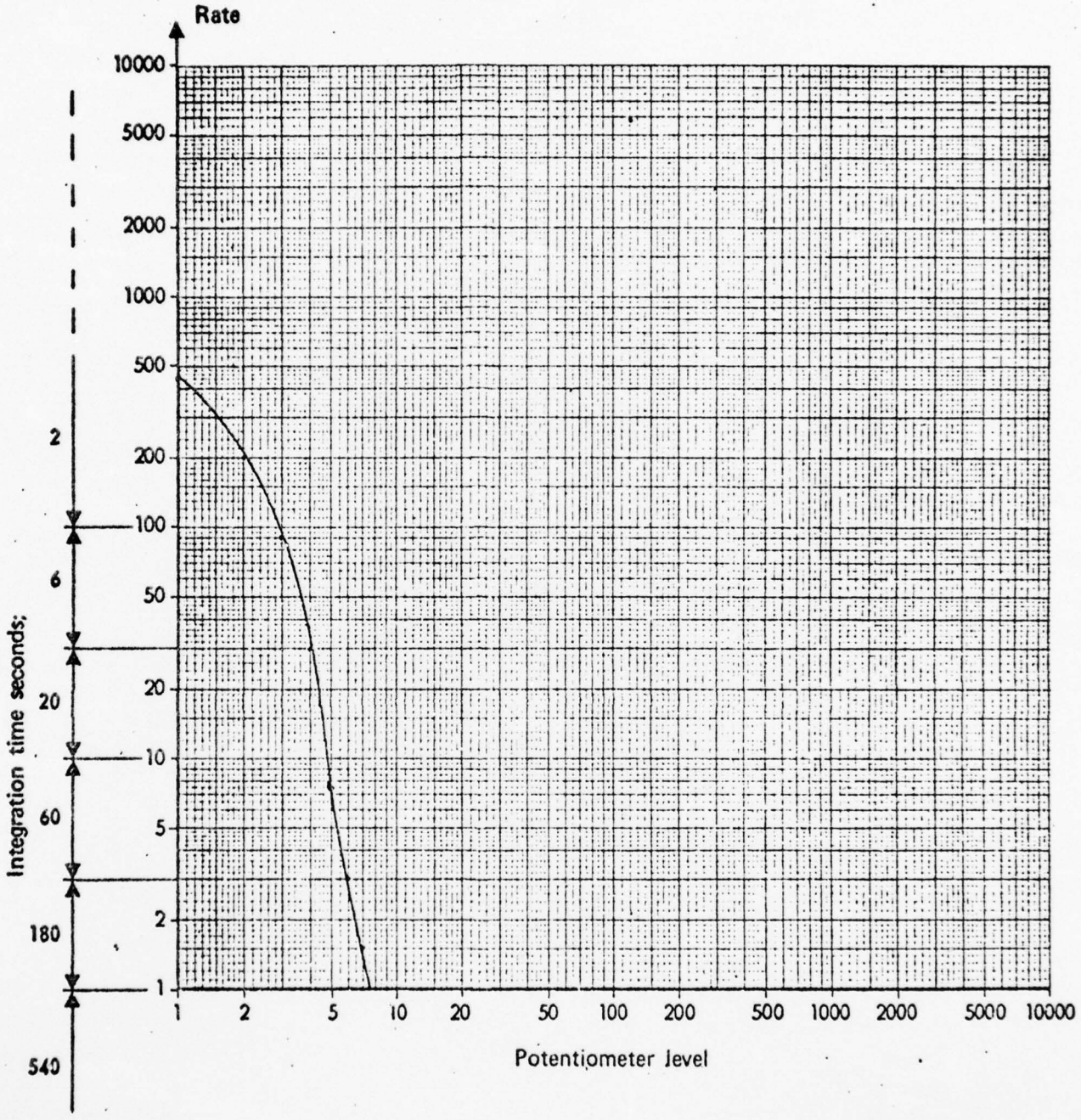


a)

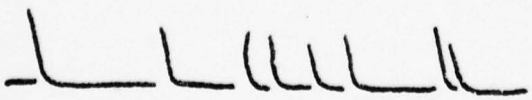

b)

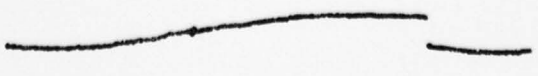

# FOREIGN MATTER IN BEARING LUBRICATION

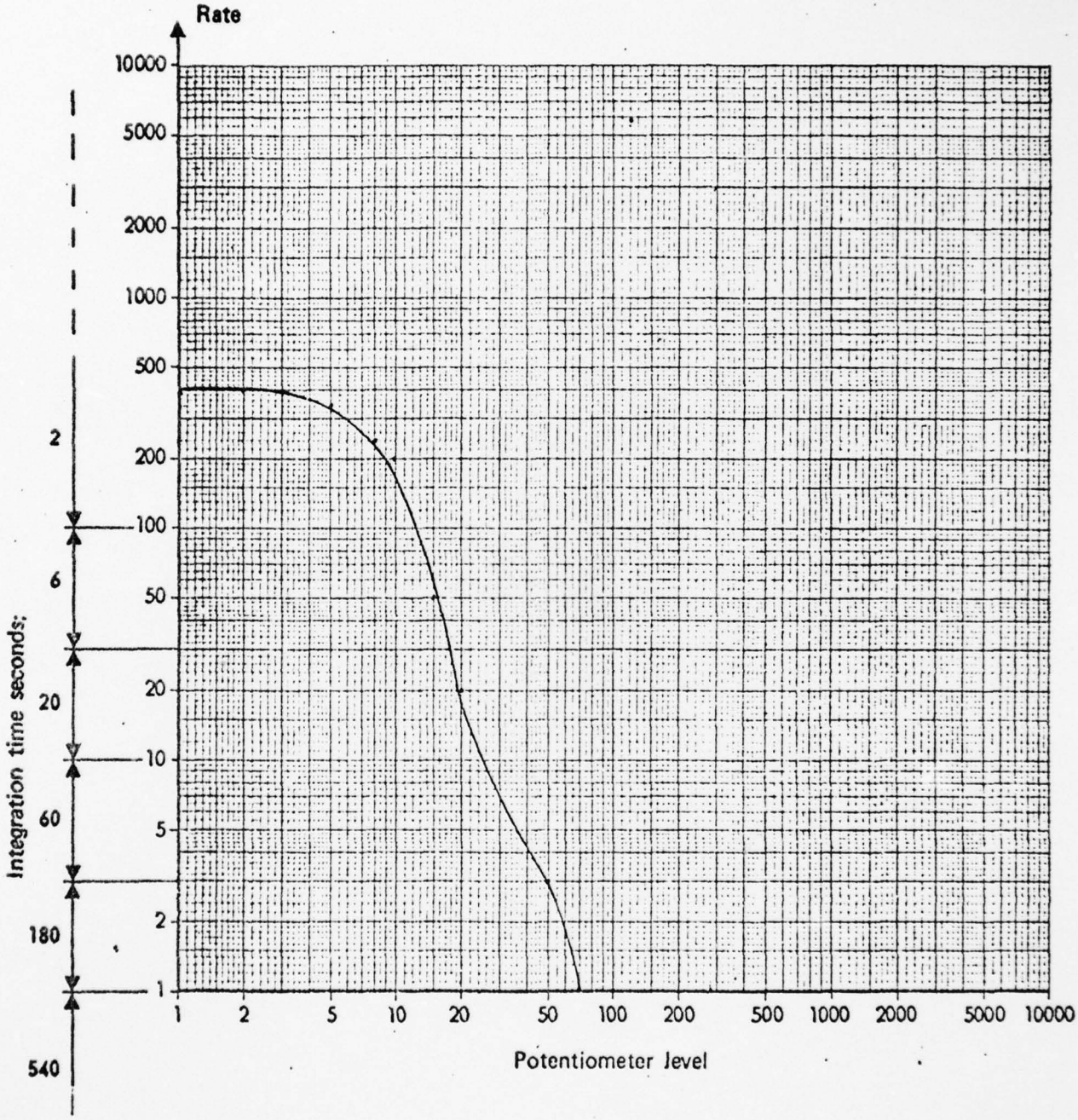


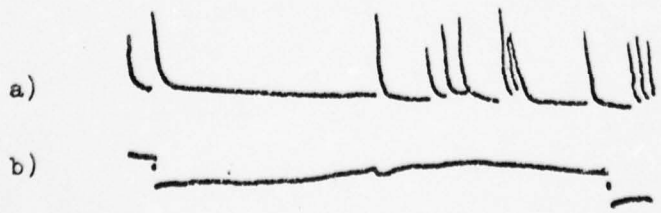

AD-A040 130 PARKS COLL OF SAINT LOUIS UNIV CAHOKIA ILL F/G 1/3
APPLICATIONS OF THE SHOCK PULSE TECHNIQUE TO HELICOPTER DIAGNOS--ETC(U)
FEB 75 T C MAYER, E F COVILL, J A GEORGE DAAJ01-72-A-0027
UNCLASSIFIED USAAVSCOM-TR-77-21 NL

2 OF 3
AD
A040 130

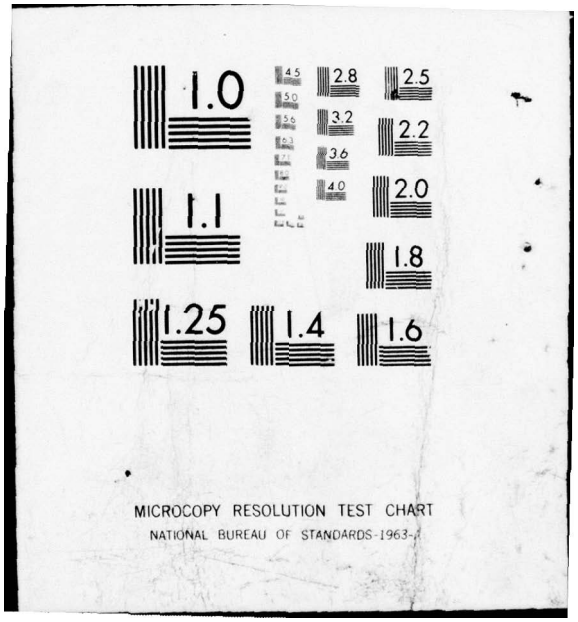
1.0
1.1
1.25
1.4
1.6
1.8
2.0
2.2
2.5
2.8
3.2
3.6
4.0
4.5
5.0
5.6
MICROCOPY RESOLUTION TEST CHART
NATIONAL BUREAU OF STANDARDS-1963-A

# NORMALIZATION CURVE NEW BEARING

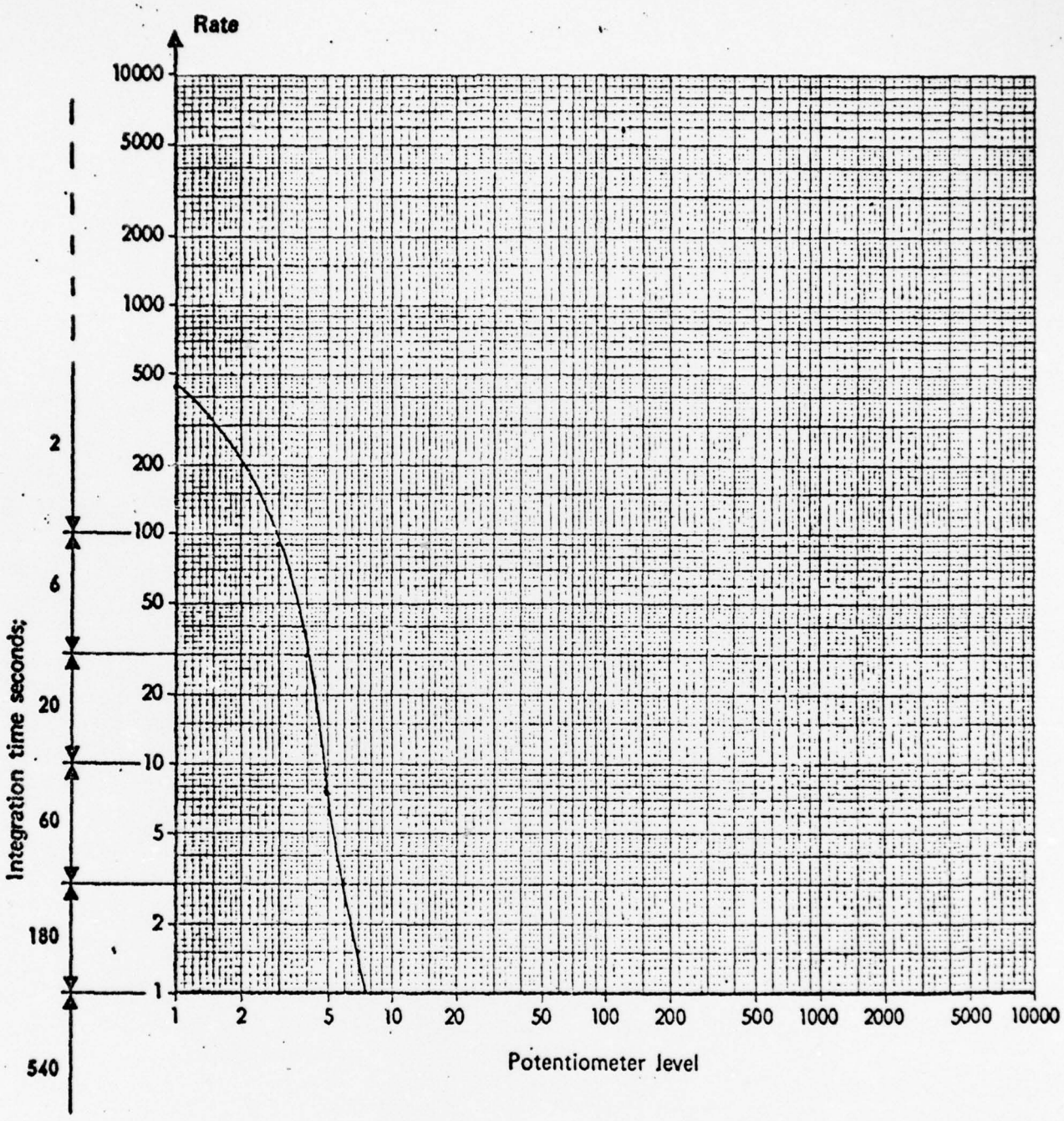


a)

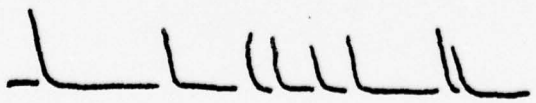

b)

DRY BEARING

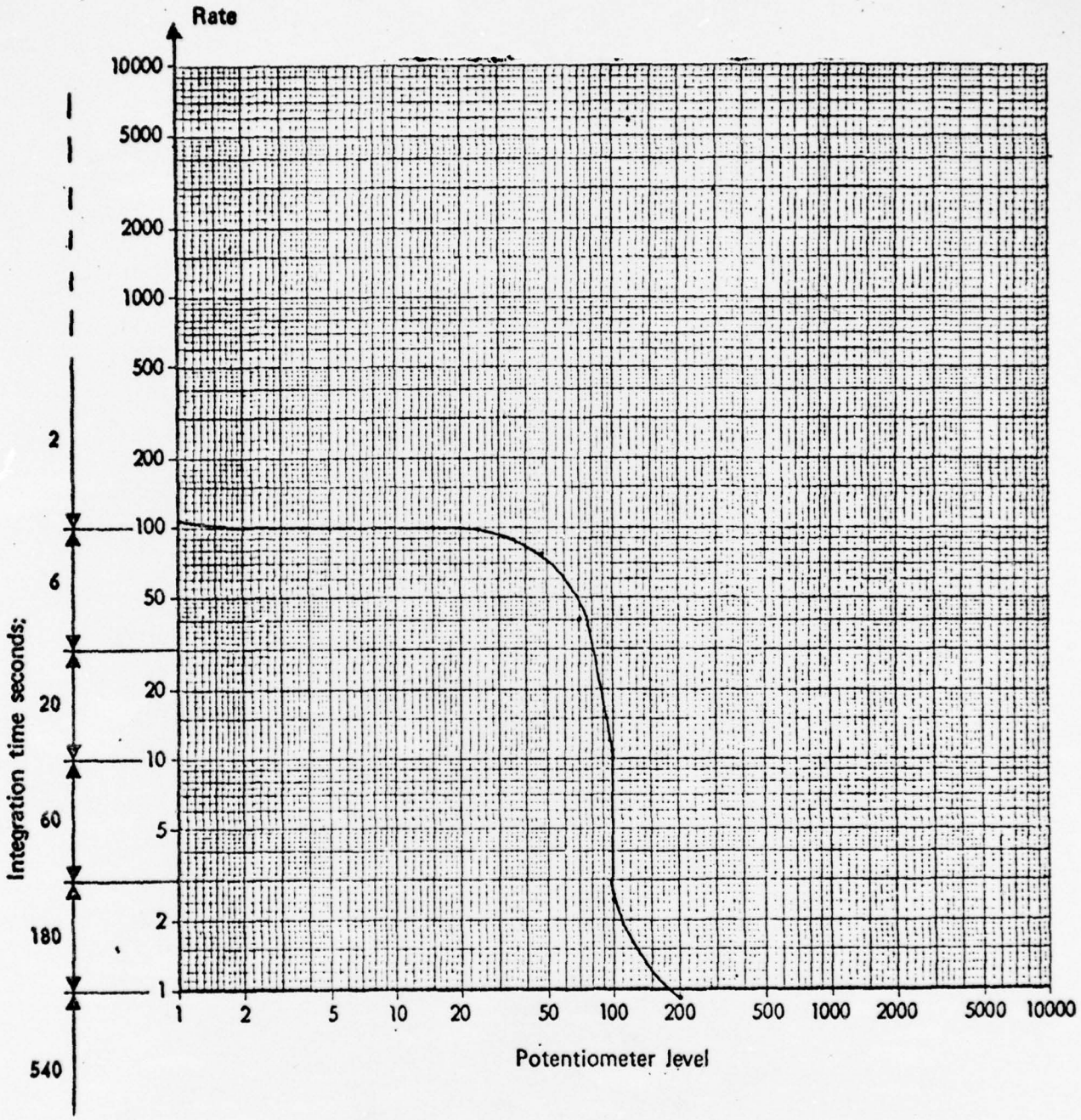


a)

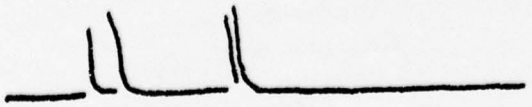

b)

NORMALIZATION CURVE NEW BEARING

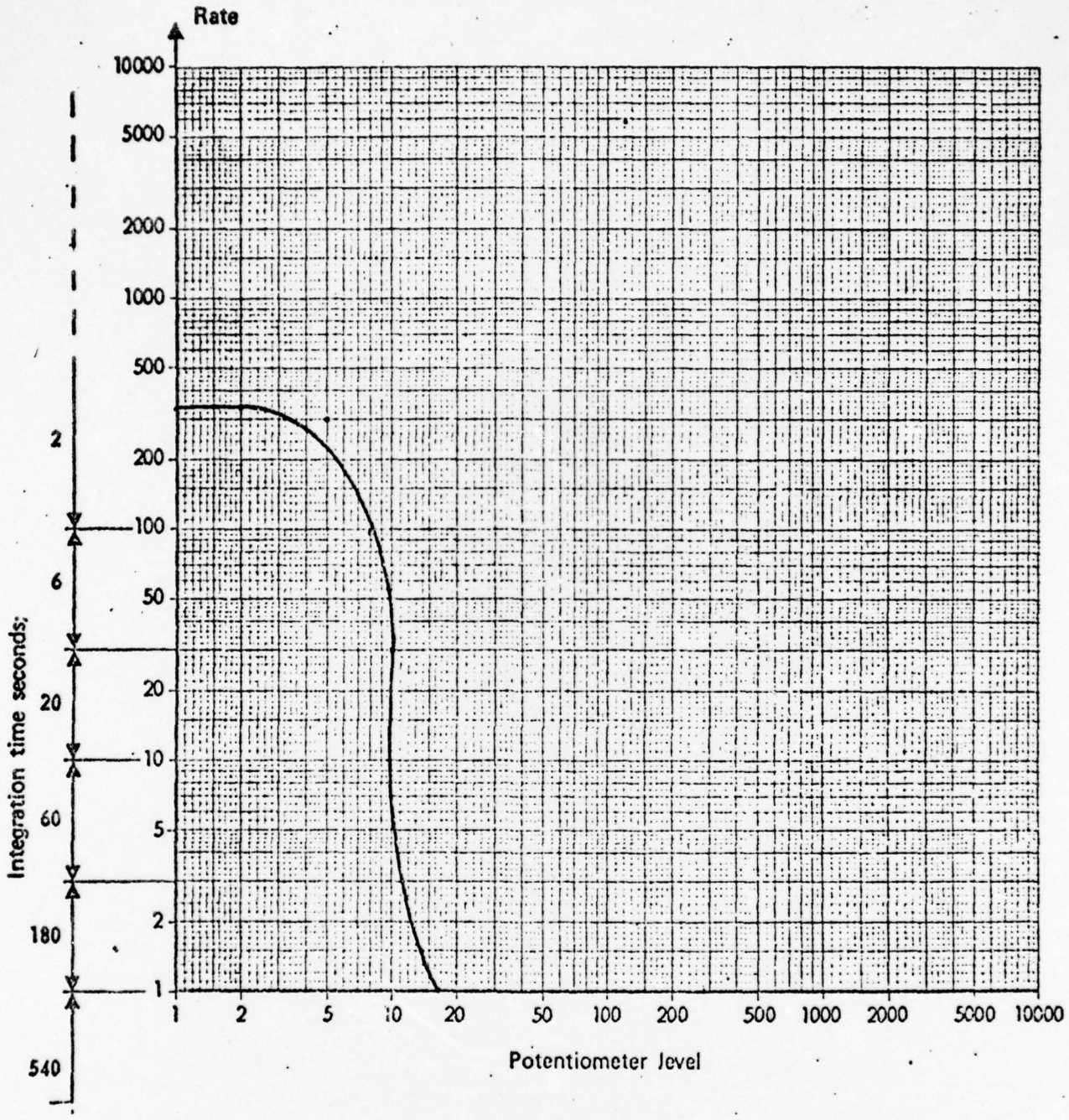


a)

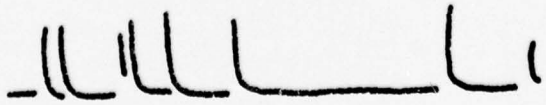

b)

# INNER RACE DAMAGES

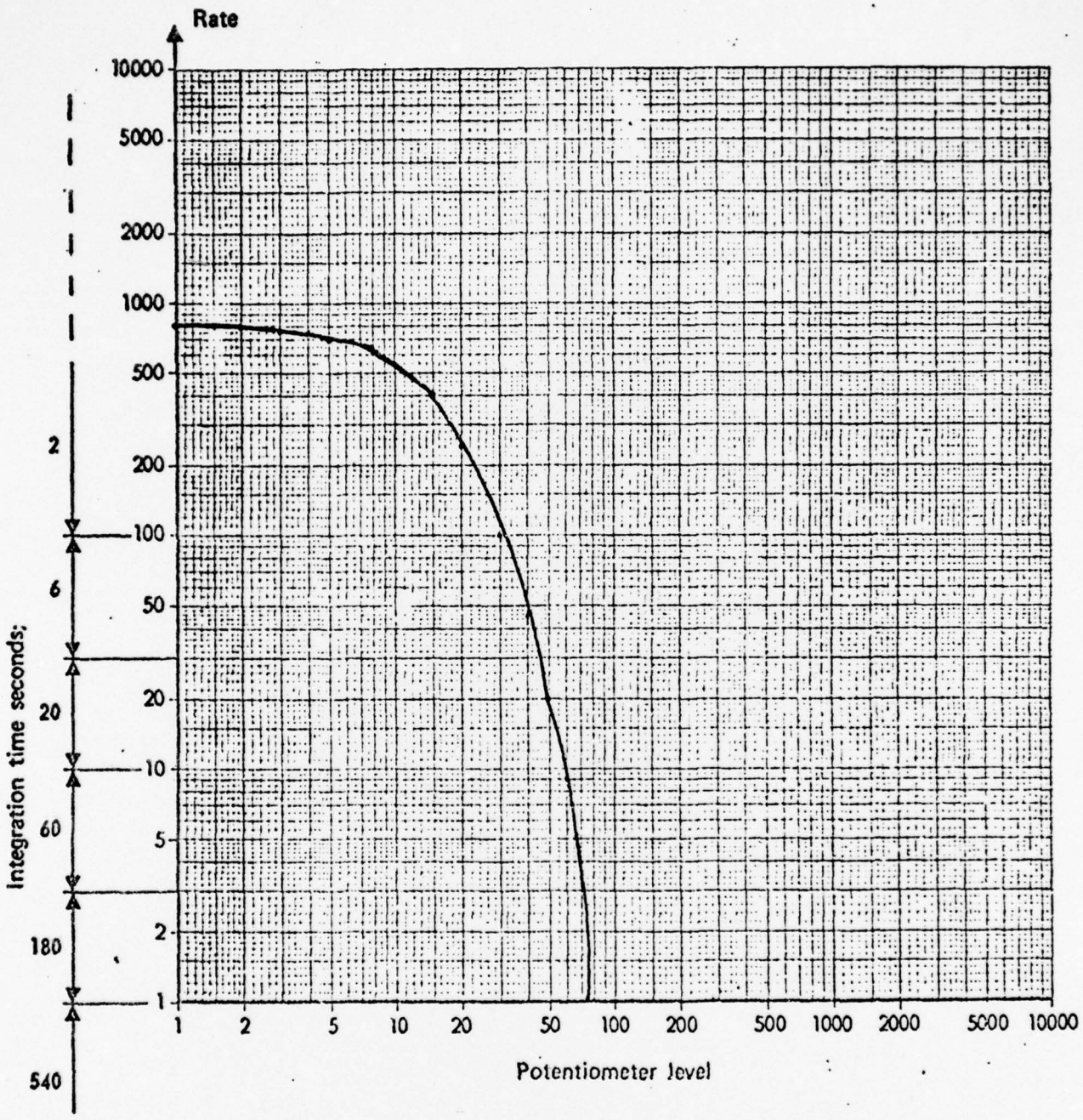


a)

b)

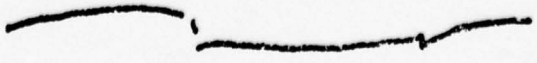

# NORMALIZATION CURVE NEW BEARING

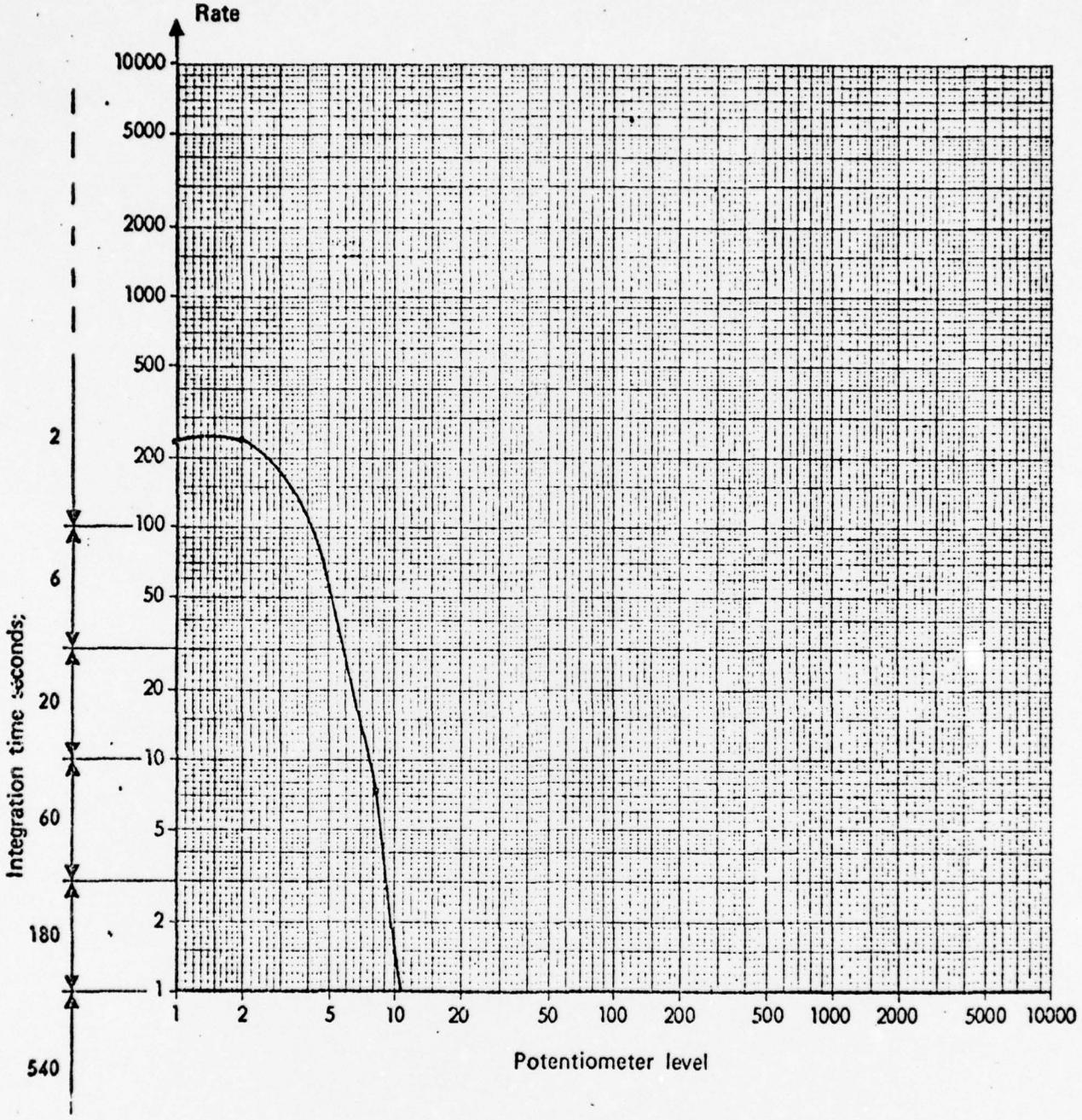


a)

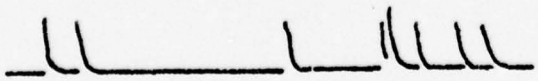

b)

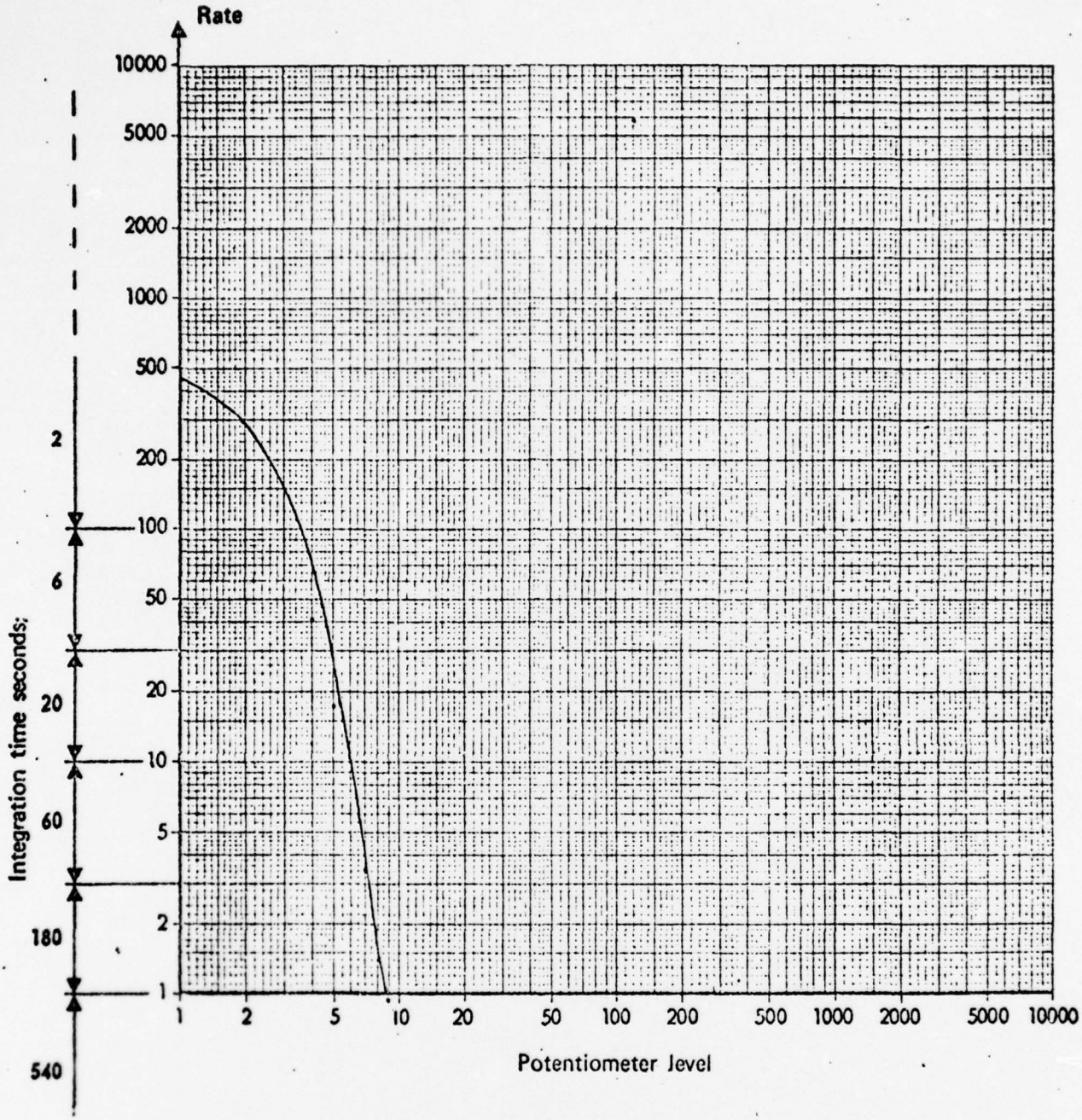
Rate
10000
5000
2000
1000
500
200
100
50
20
10
5
2
1
Integration time seconds:
2
6
20
60
180
540
1
2
5
10
20
50
100
200
500
1000
2000
5000
10000
Potentiometer level

a)

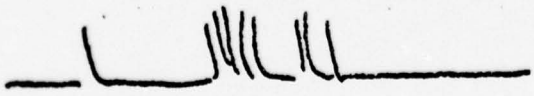

b)

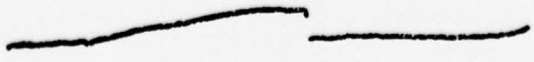

NORMALIZATION CURVE NEW BEARING

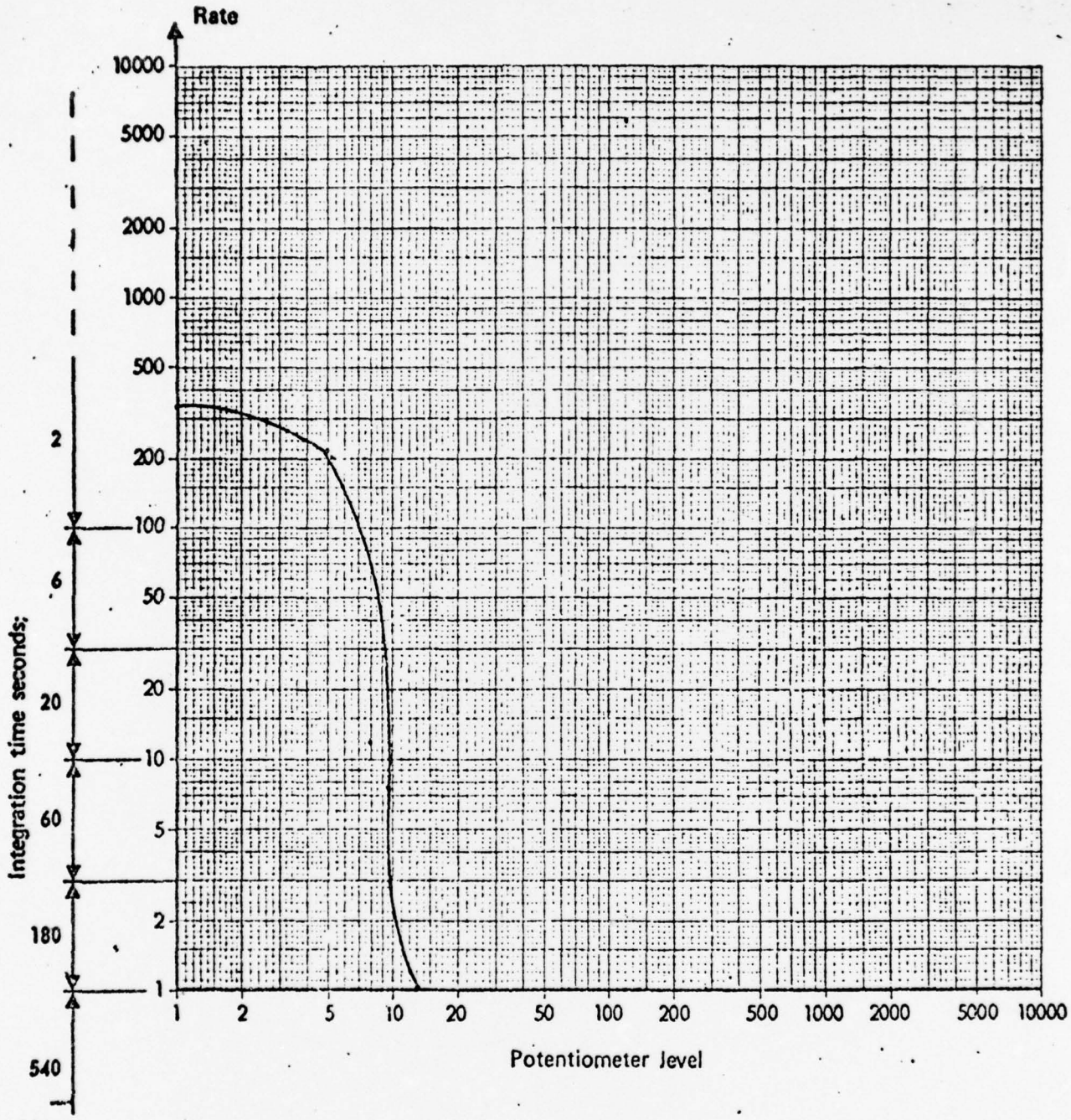


a)

b)

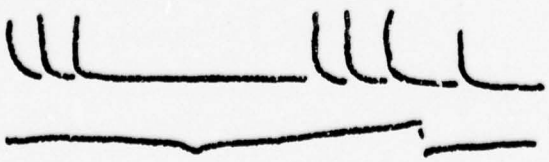

ROLLING ELEMENT DAMAGE

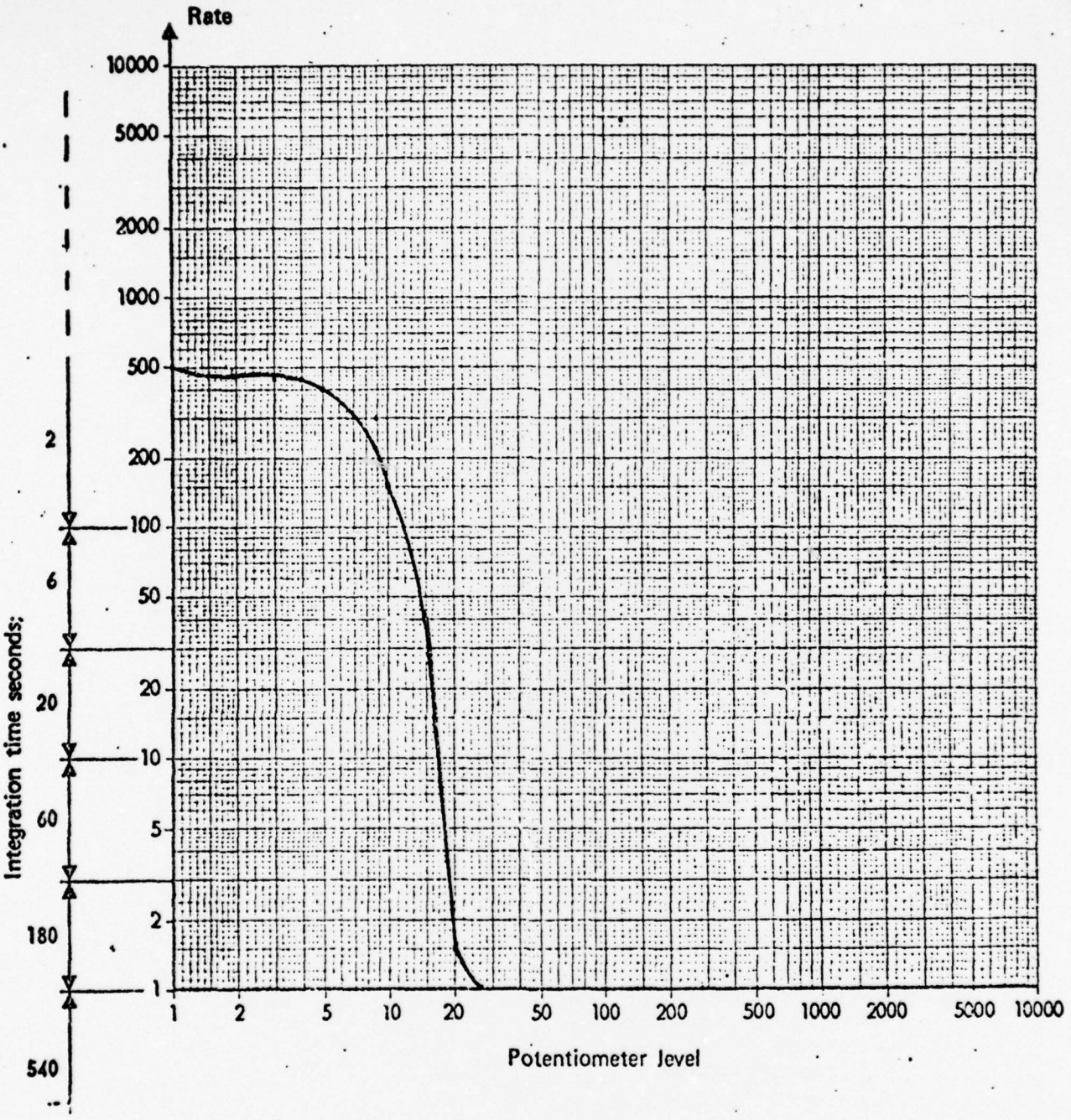


a)

b)

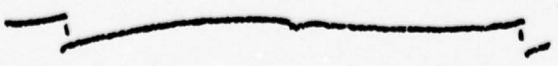

START OF TIME TEST

FIGS. 3.6A - 3.6D SHOWS BEARING WITH SEVERE DAMAGE TO INNER RACE, SHOCK READINGS TAKEN AT INTERVALS OF 30, 60 and 100 MIN. ACCELEROMETER ATTACHMENT WITH VICE GRIPS AND 3750 RPM

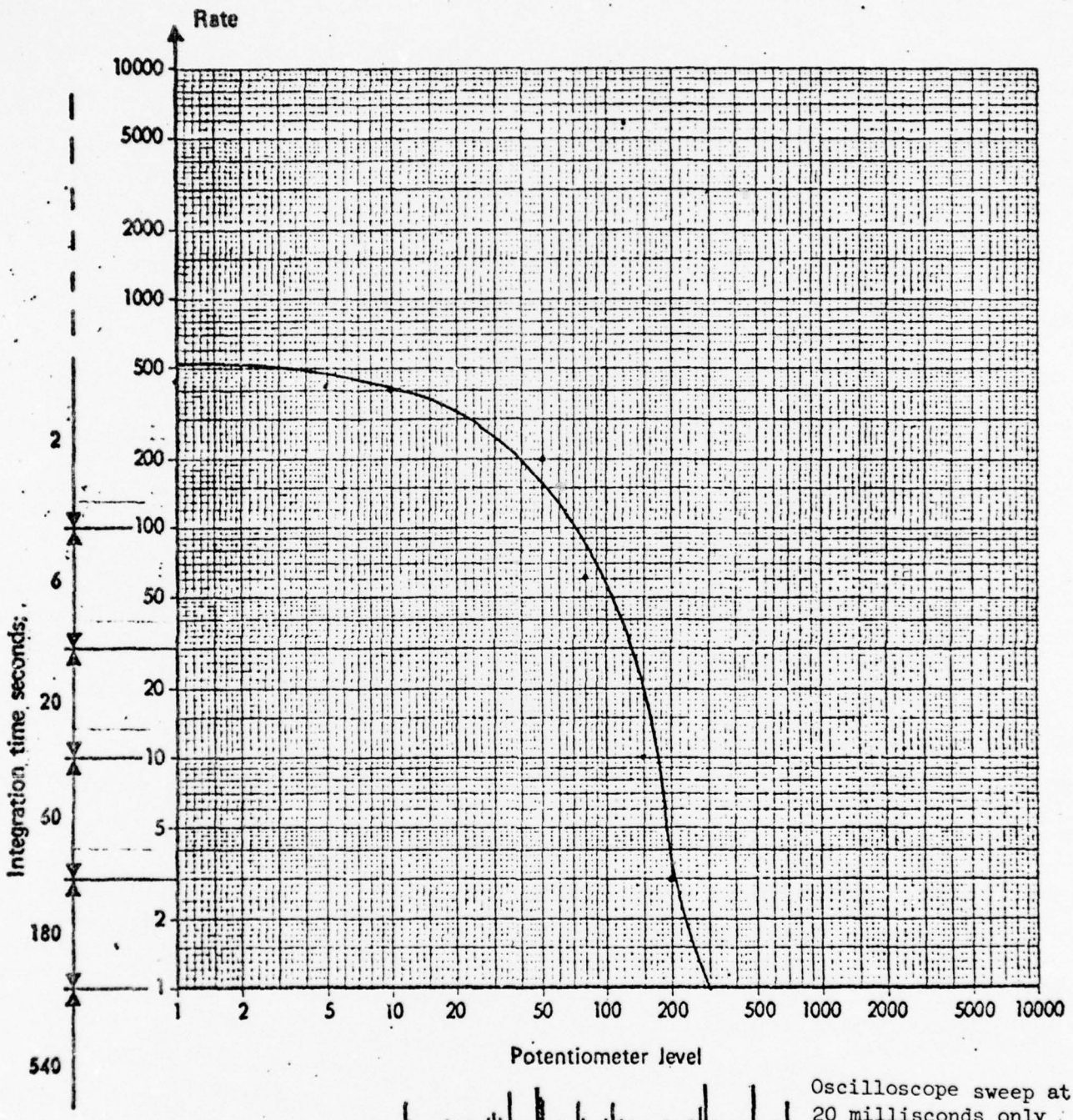


a) 

Oscilloscope sweep at 20 millisconds only quantity not amplitude of shock emission can be considered.

b) 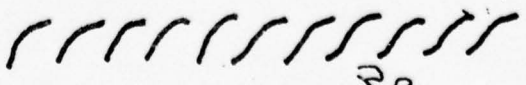

Each curve represents one revolution.

AFTER 30 MIN. RUNNING TIME

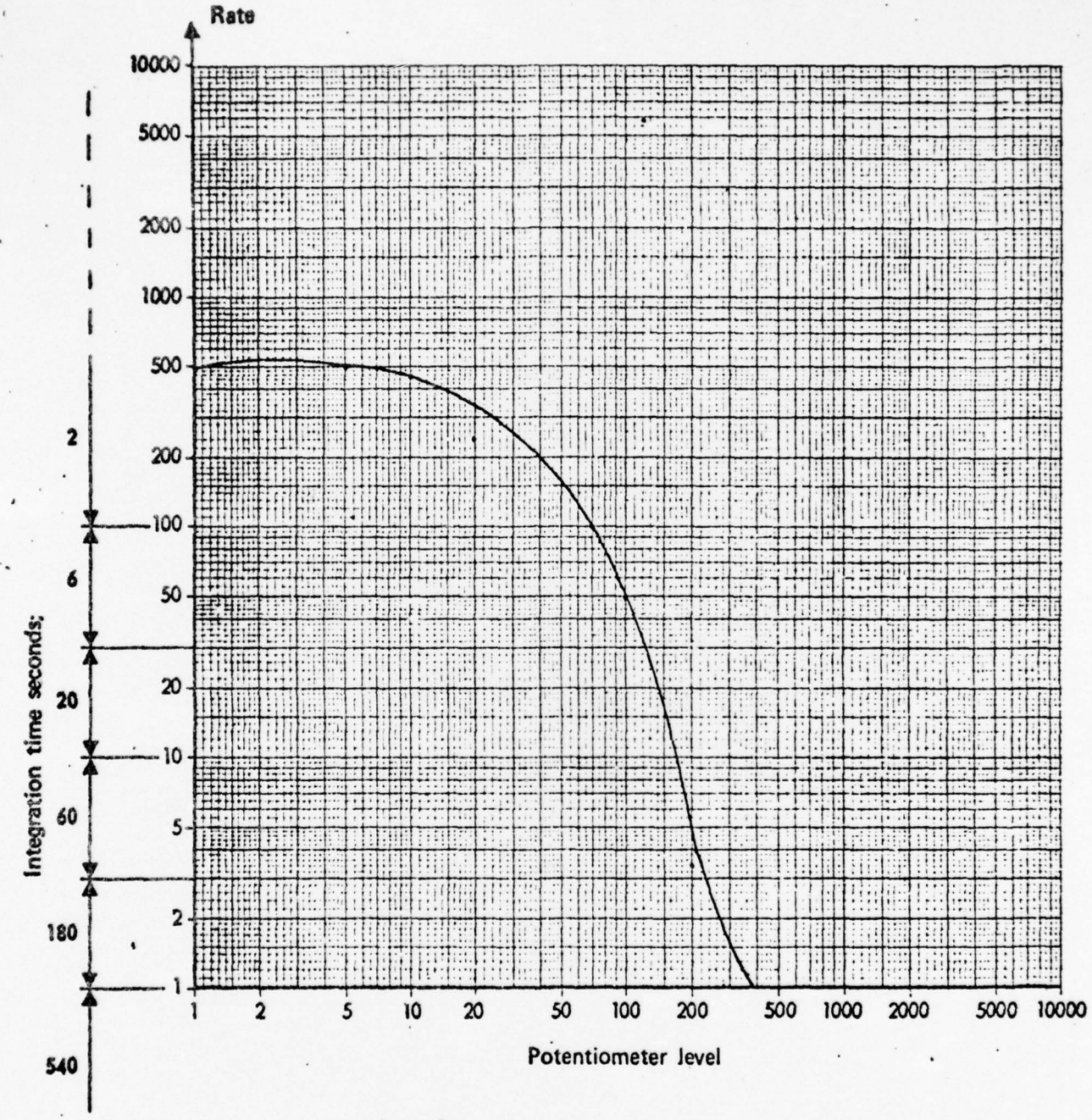


a) 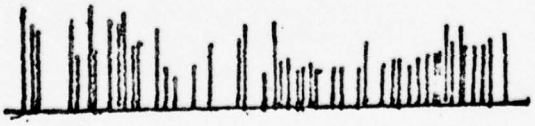

Oscilloscope sweep at 20 milliseconds only quantity not amplitude of shock emission can be considered.

b) 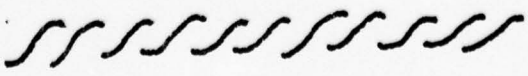

Each curve represents one revolution.

AFTER 60 MIN. RUNNING TIME

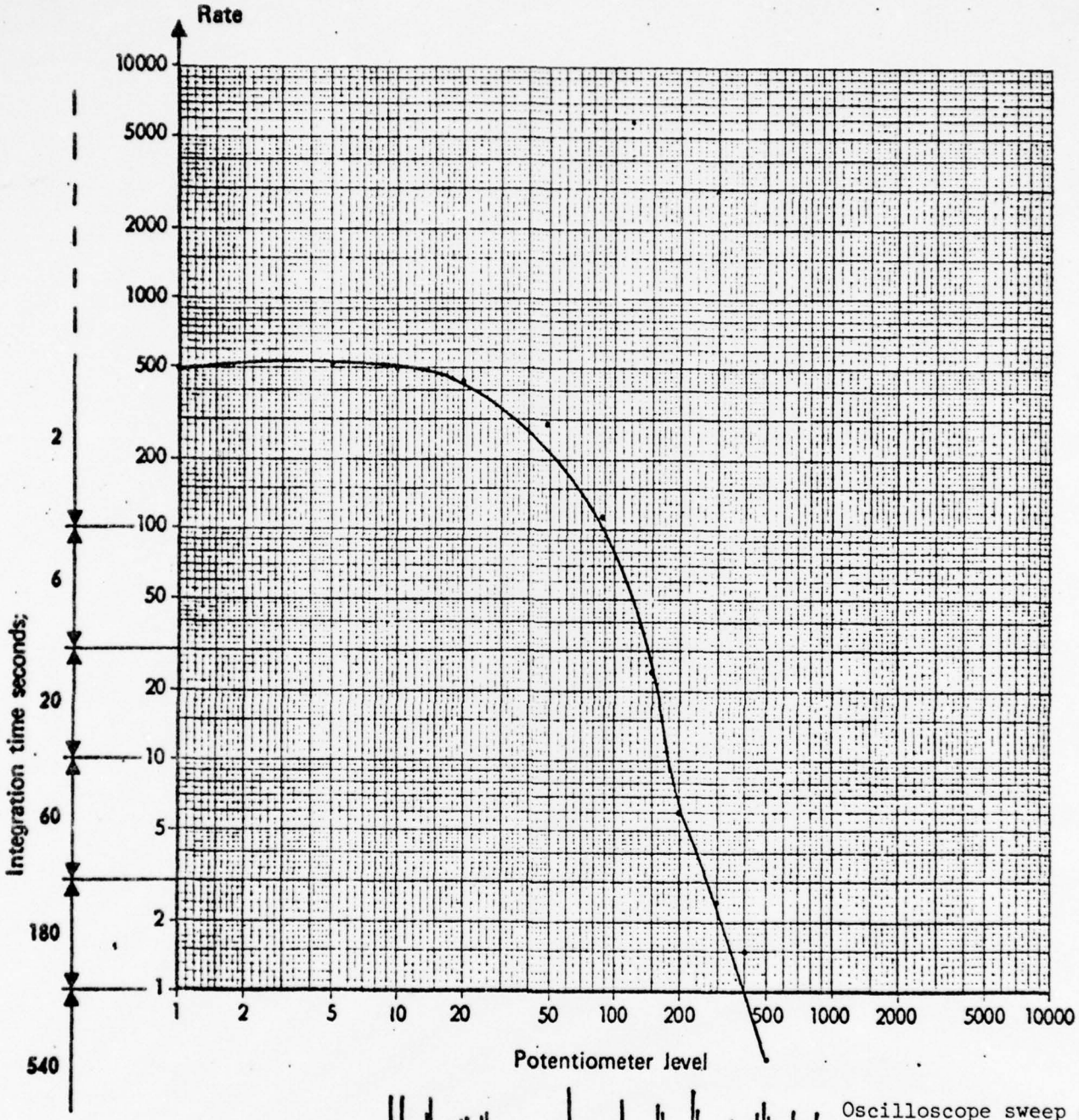


a)

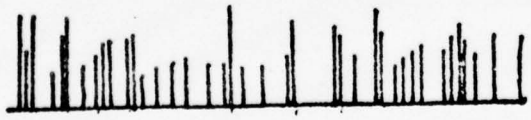

Oscilloscope sweep at 20 milliseconds only quantity not amplitude of shock emission can be considered.

b)

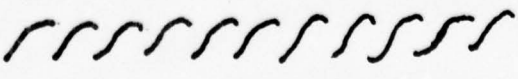

Each curve represents one revolution.

CONCLUDING READING AFTER 100 MIN. RUNNING TIME

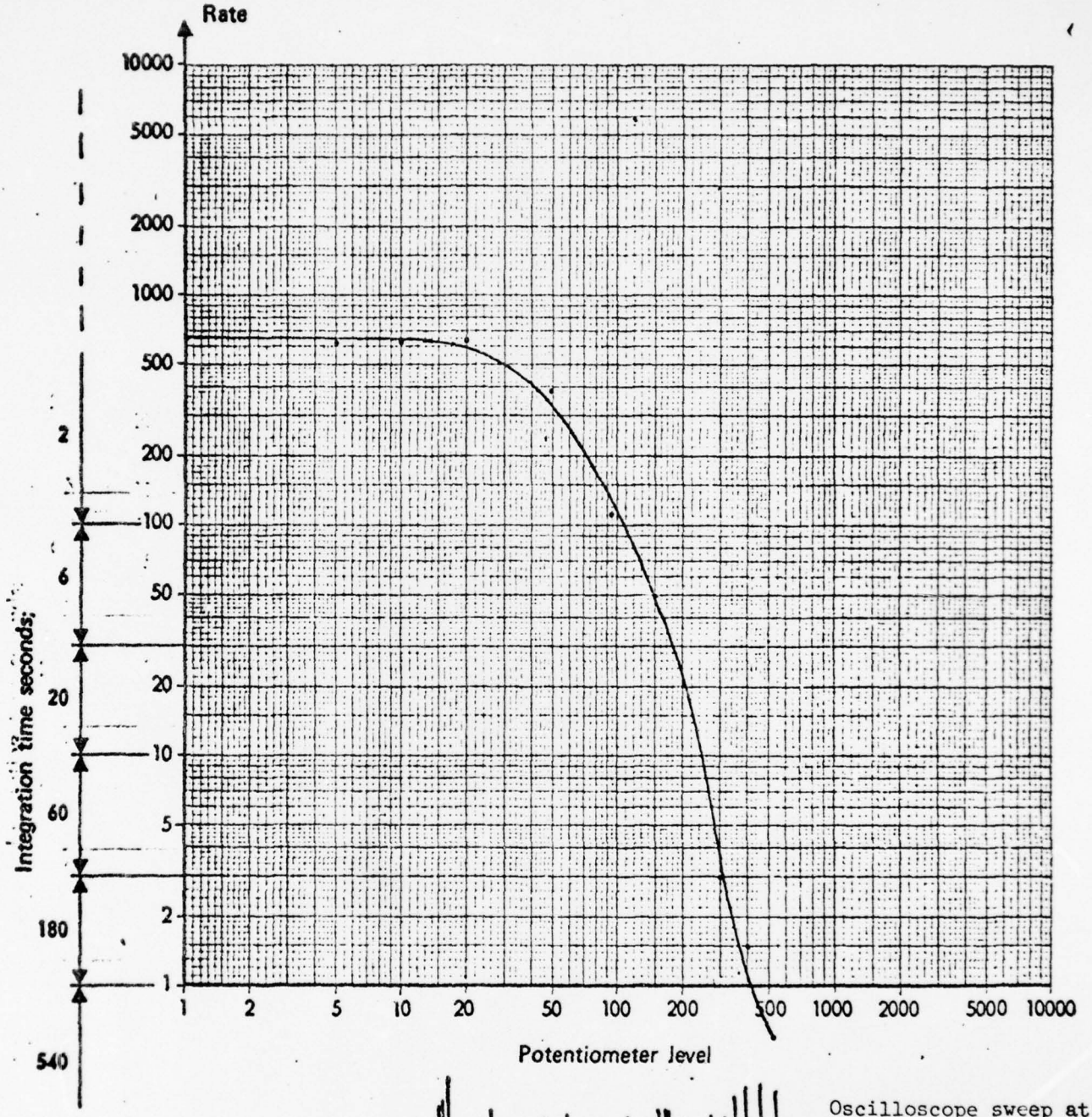


a)

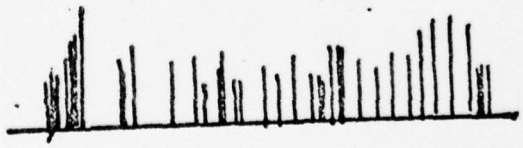

Oscilloscope sweep at 20 milliseconds only quantity not amplitude of shock emission can be considered.

b)

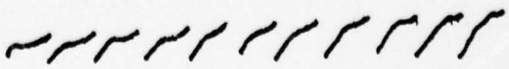

Each curve represents one revolution.

DIRTY LUBRICANT - 2520 RPM

FIGS. 3.7a AND 3.7b DEPICTS THE SAME BEARING WITH IDENTICAL ACCELEROMETER ATTACHMENT RUN AT 2520 AND 3750 RPM's RESPECTIVELY. RPM INCREASED APPROXIMATELY 50% AND IN THIS INSTANCE BOTH RATE AND LEVEL INCREASED WITH THE RPM INCREASE AS GRAPHED.

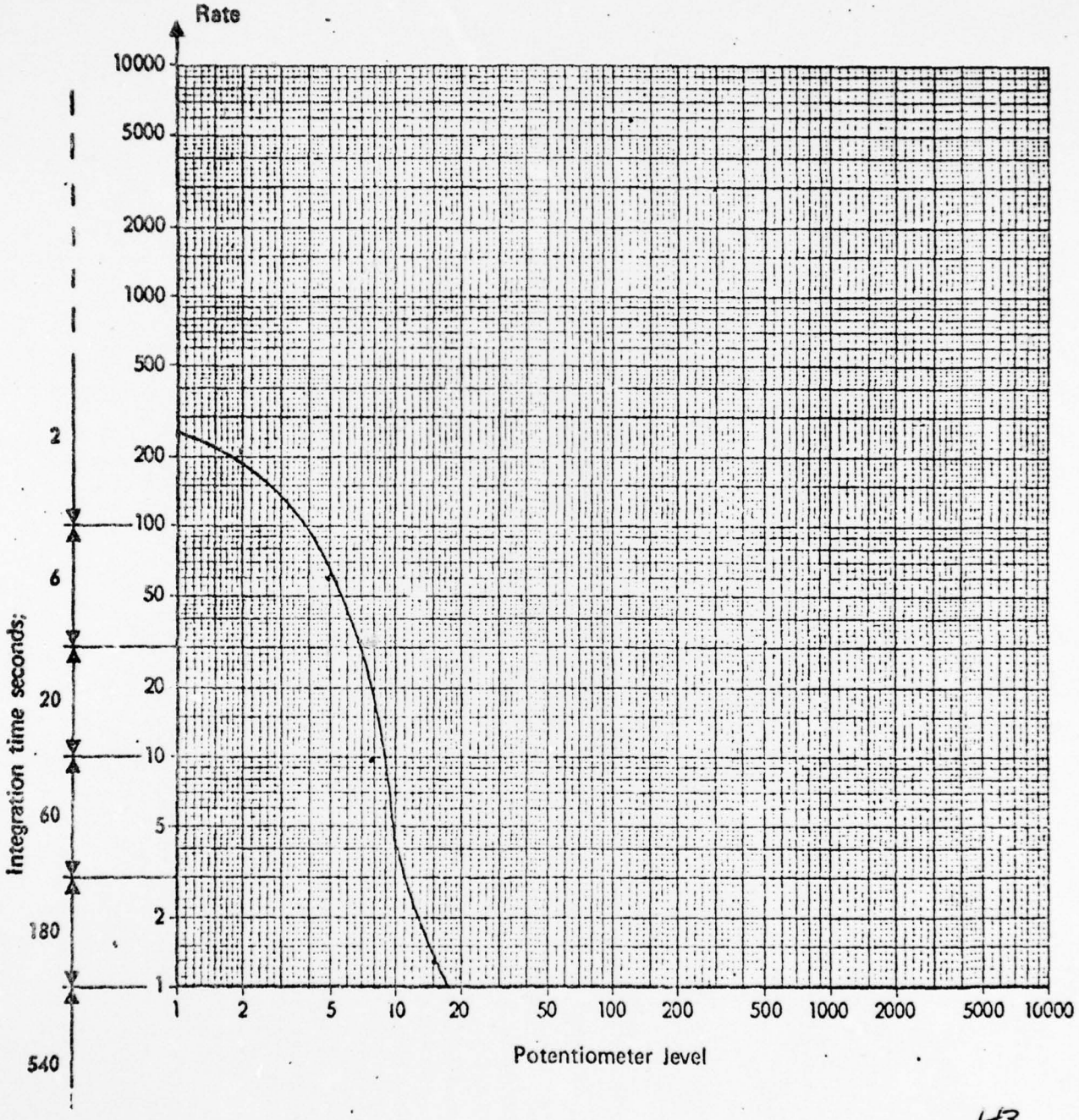


43

a)

b)

DIRTY LUBRICANT 3750 RPM

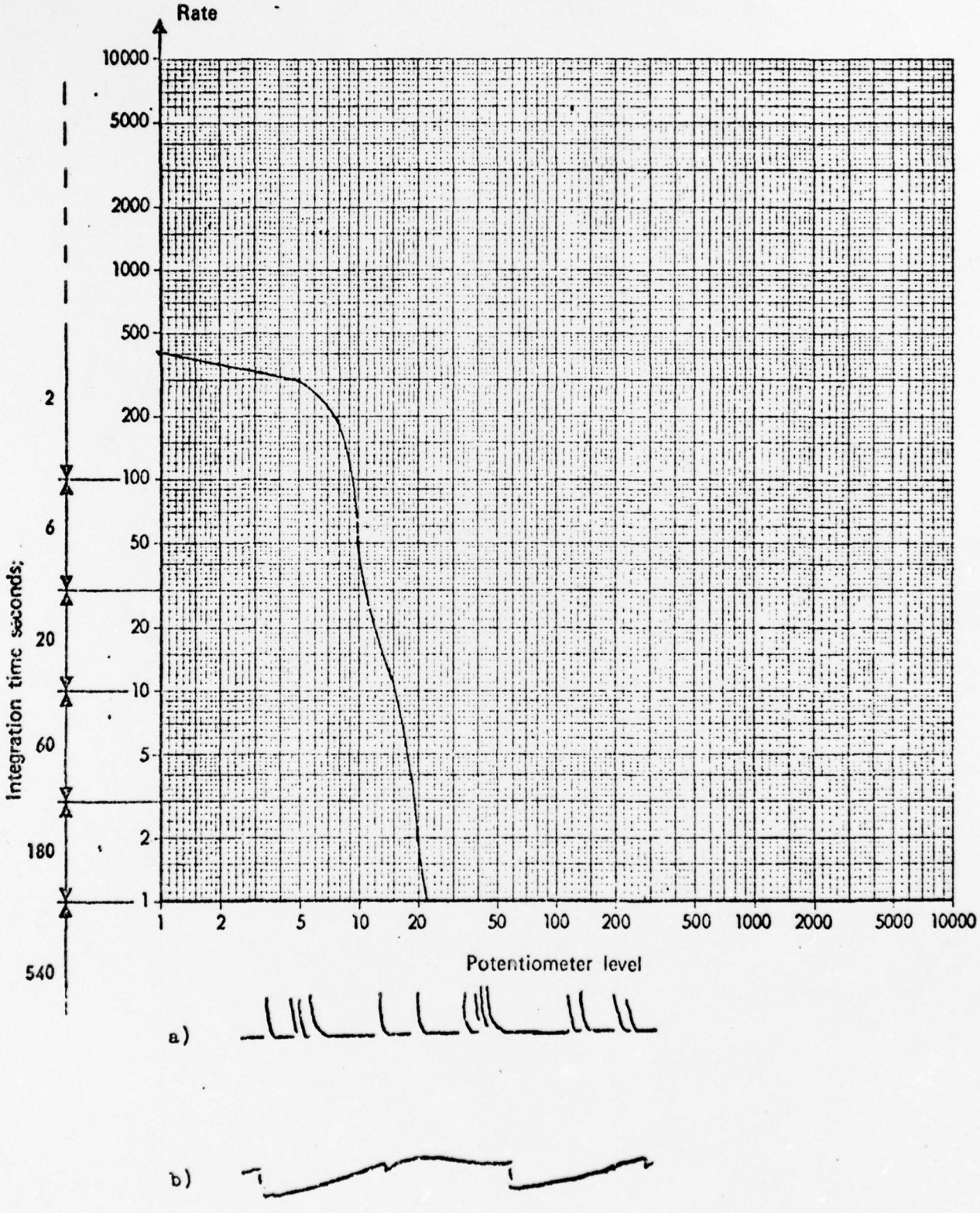

NEW BEARING

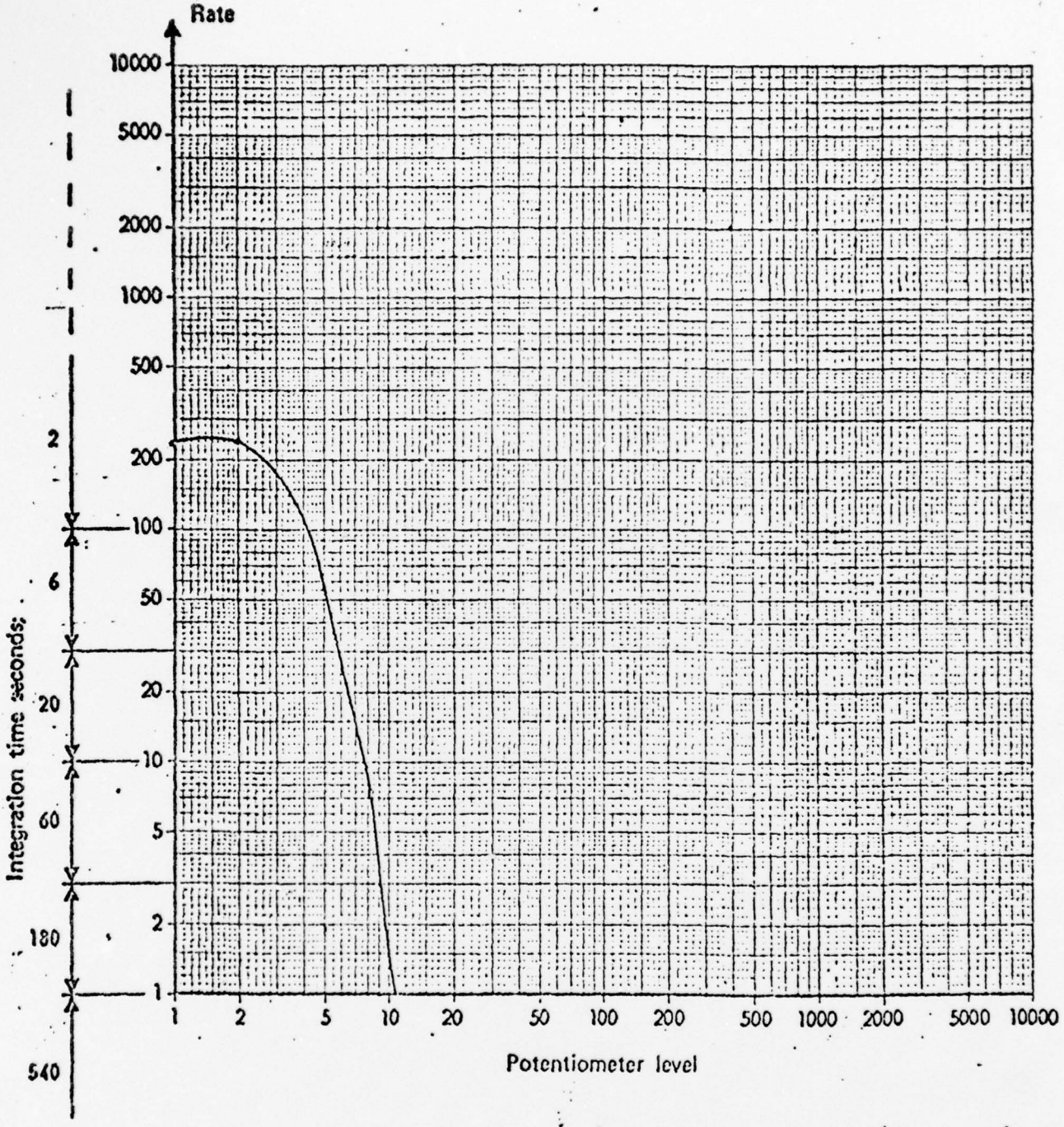


a)

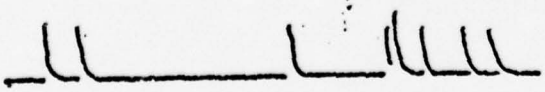

b)

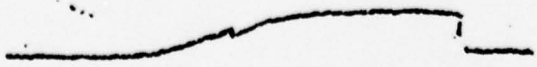

# ROLLING ELEMENT DAMAGE

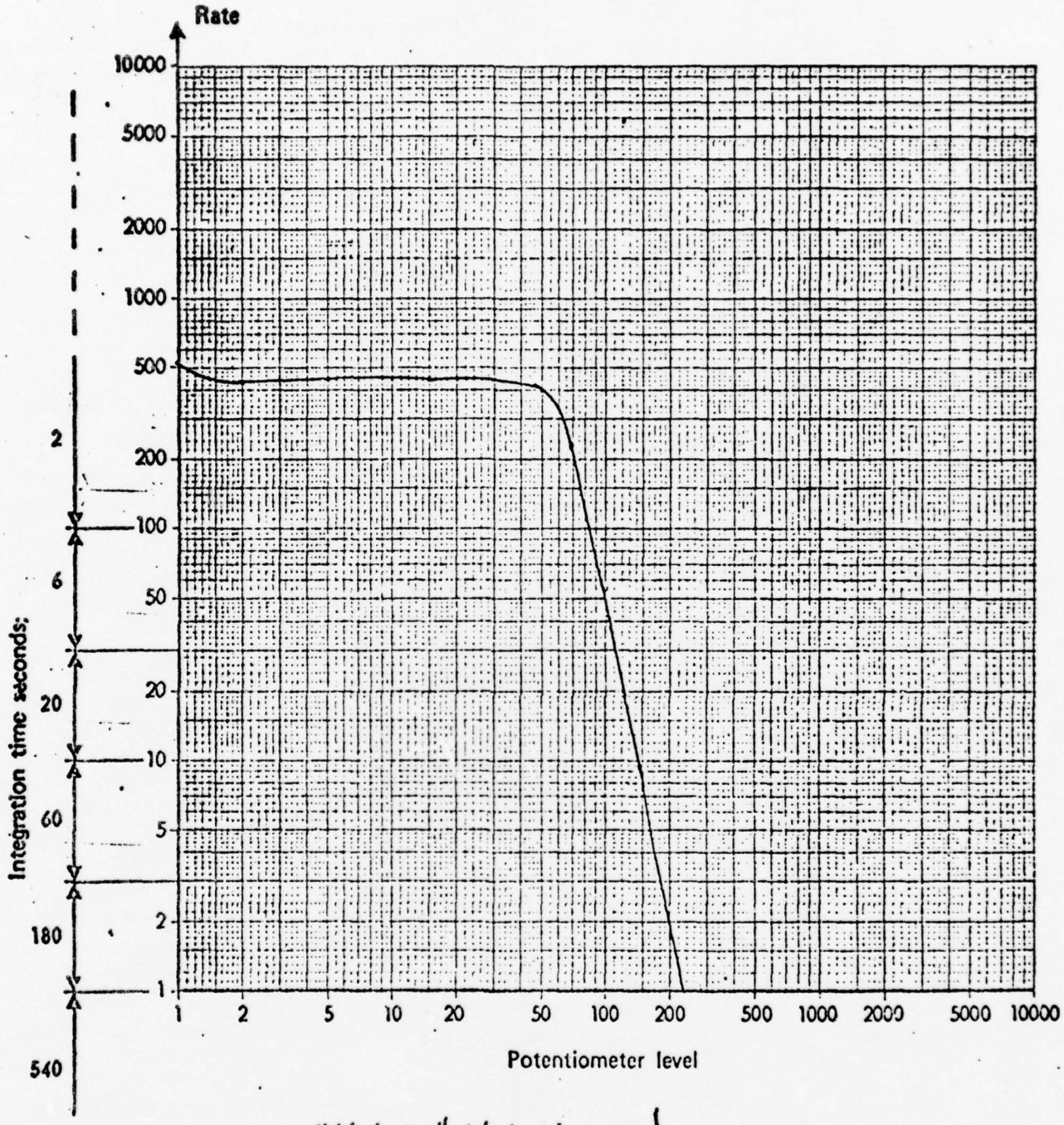


a)

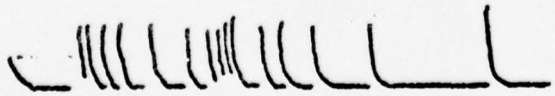

b)

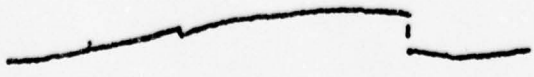

# DIRTY LUBRICANT

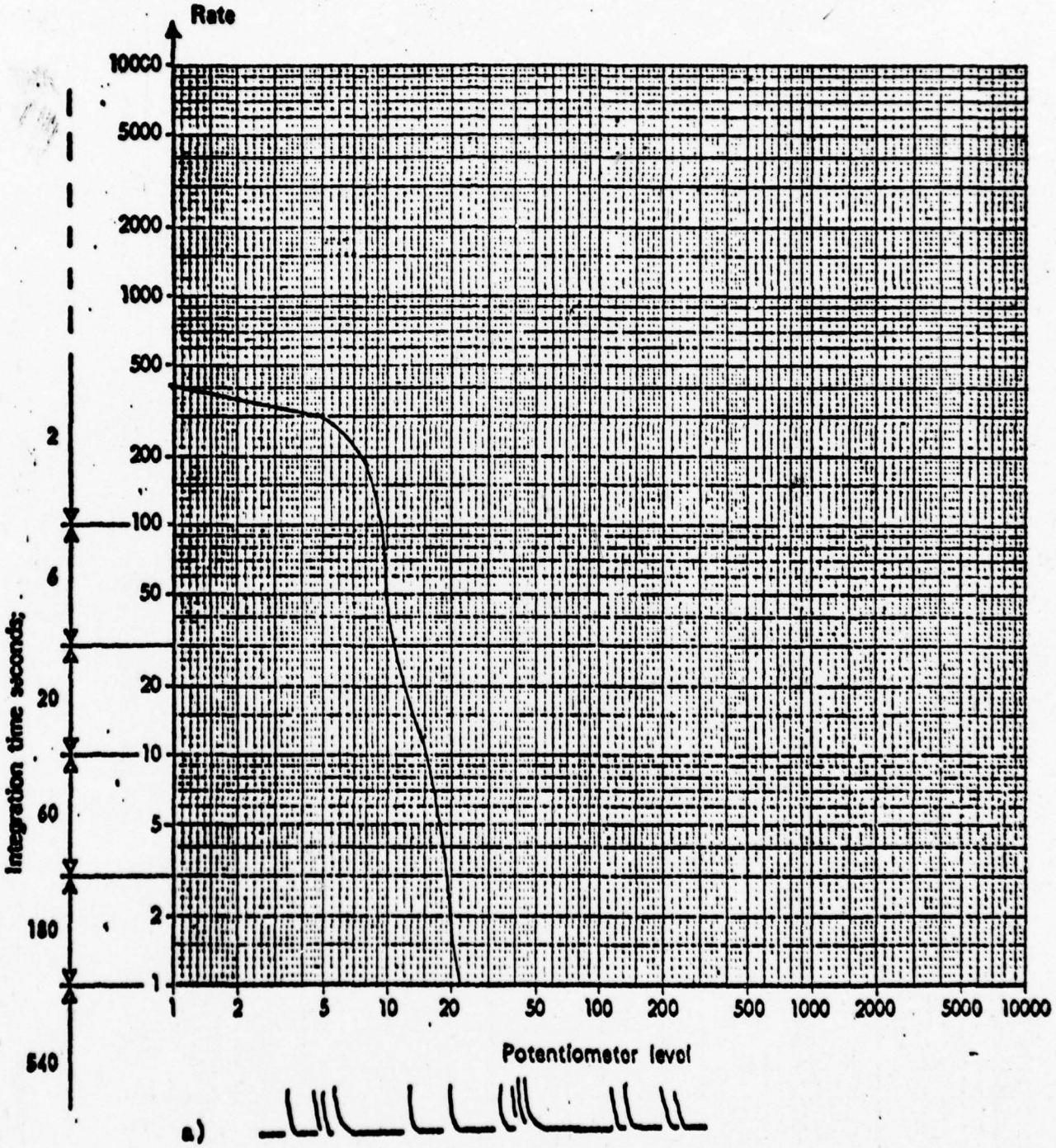


a)



b)

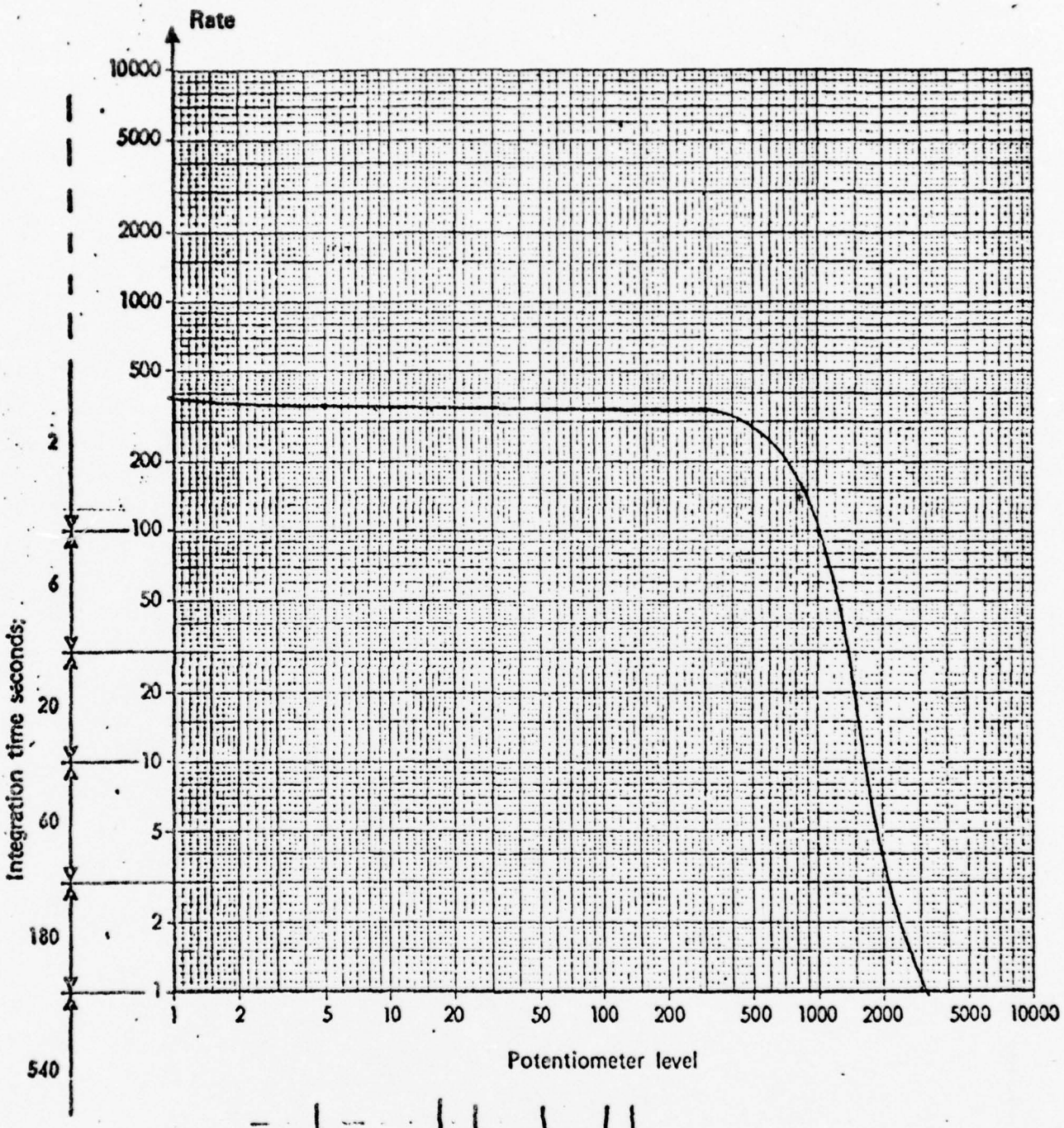
Rate
10000
5000
2000
1000
500
200
100
50
20
10
5
2
1
Integration time seconds:
2
6
20
60
180
540
1
2
5
10
20
50
100
200
500
1000
2000
5000
10000
Potentiometer level

a)

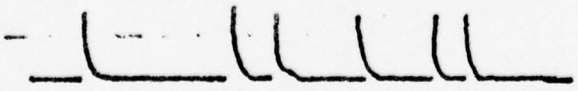

b)

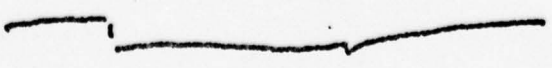

# VARIATIONS OF ACCELEROMETER ATTACHMENT

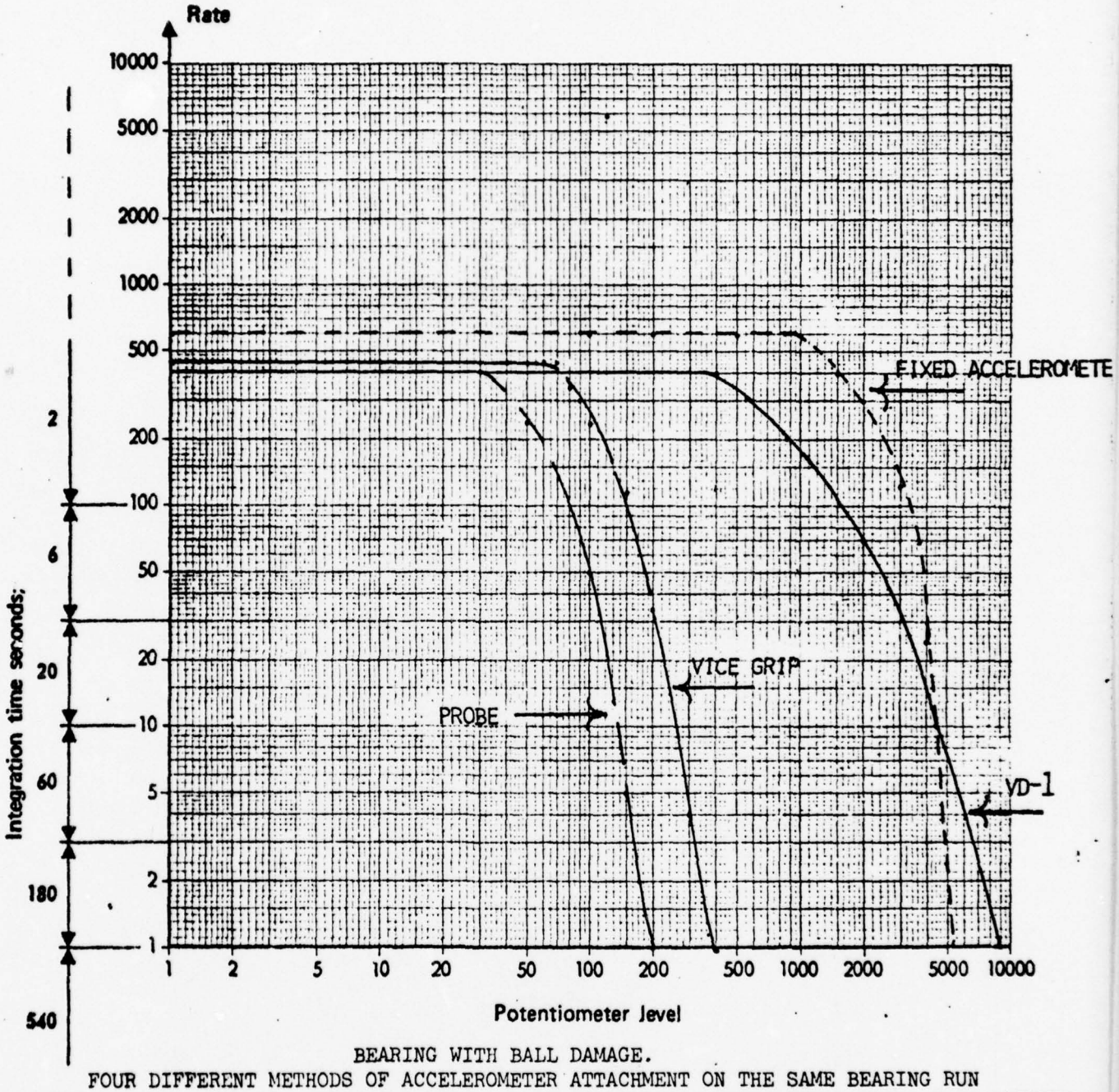


BEARING WITH BALL DAMAGE.
FOUR DIFFERENT METHODS OF ACCELEROMETER ATTACHMENT ON THE SAME BEARING RUN AT A CONSTANT RPM. (3700) THE RATES VARY LESS THAN POTENTIOMETER LEVELS WHICH VARY BETWEEN 200 and 9000.

NEEDLE SWING ERROR IN INITIAL RATE PLOT

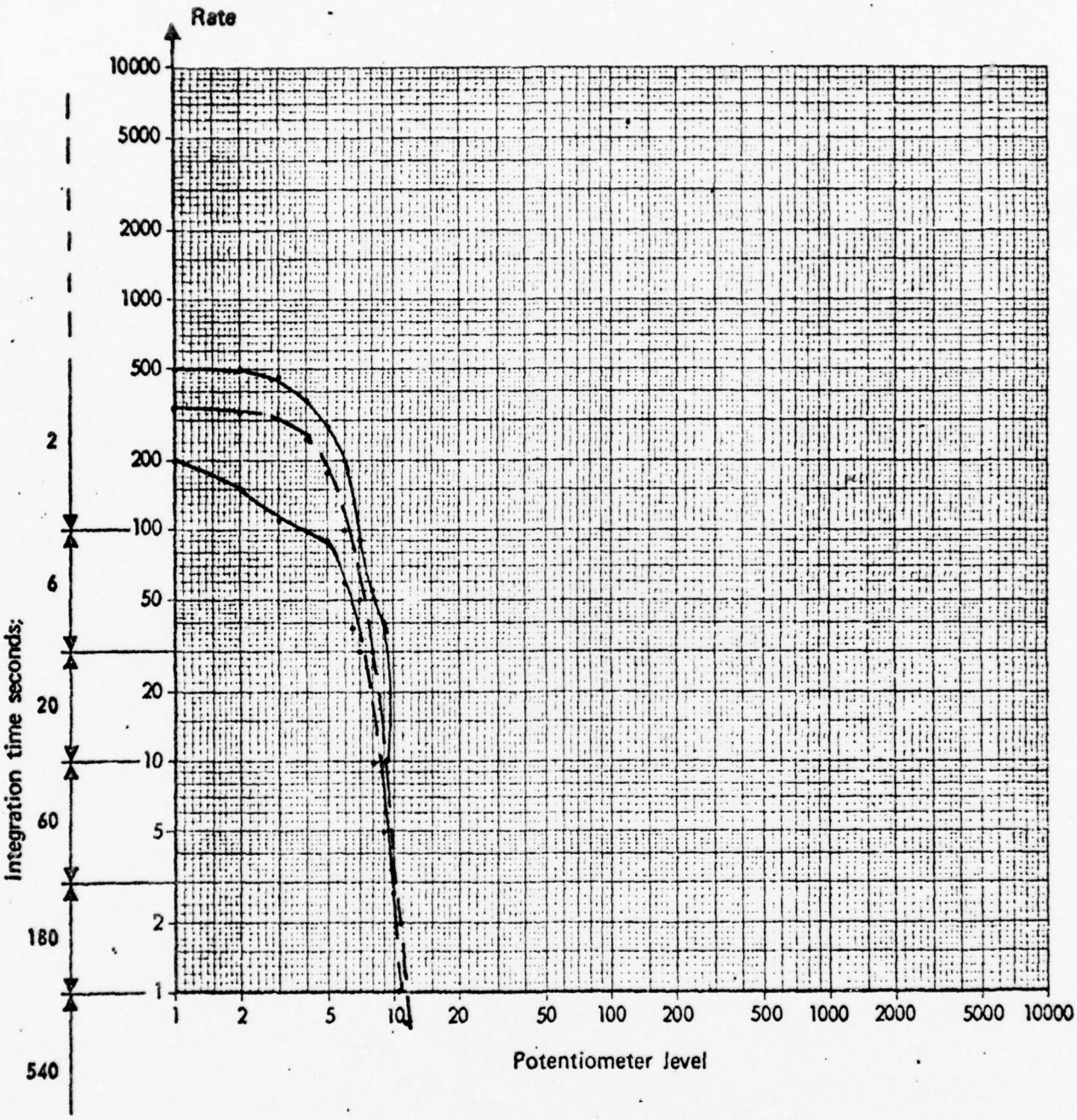

## 7.3 ACCELEROMETER MOUNTS

VICE GRIP ACCELEROMETER MOUNT

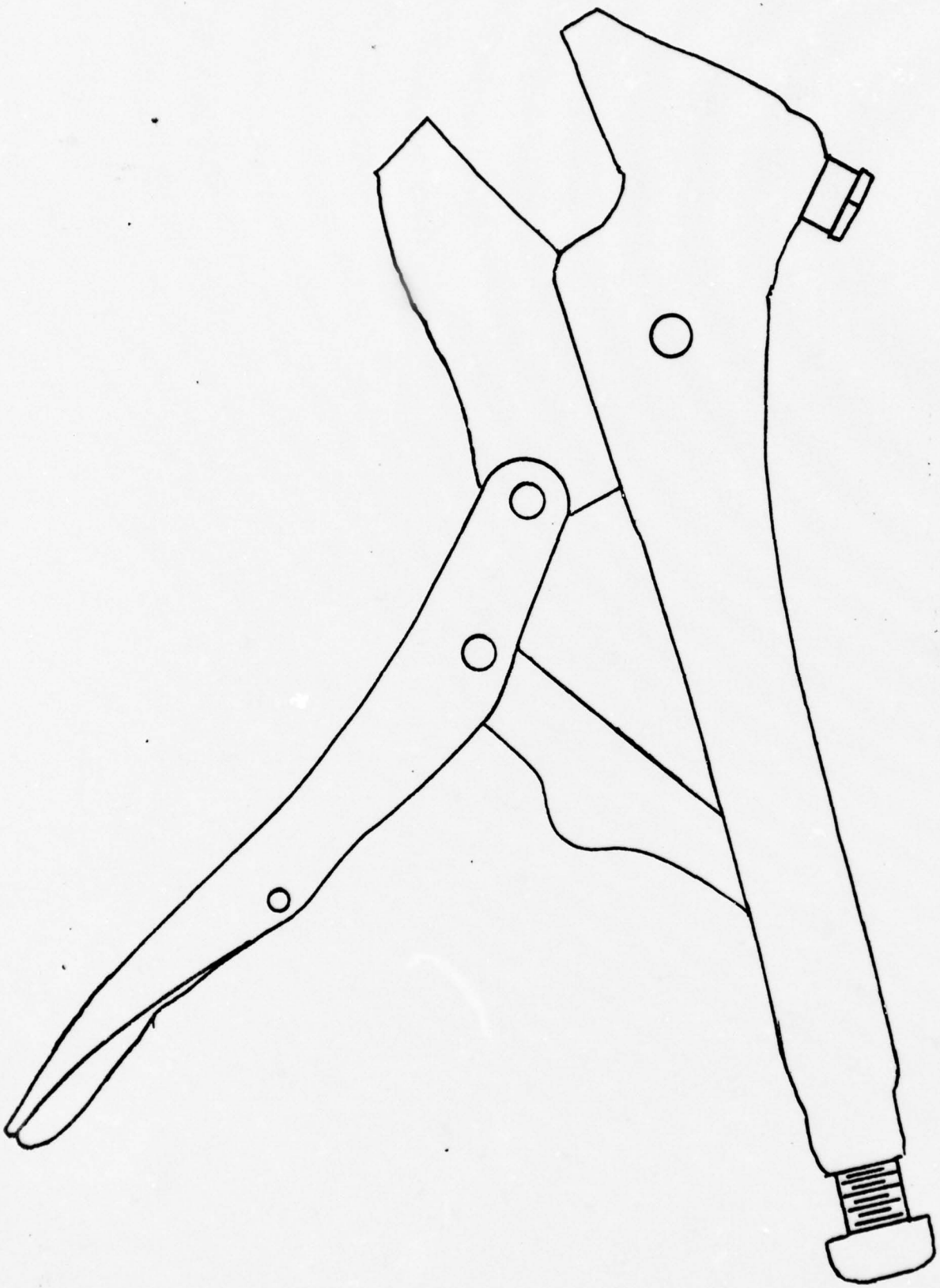

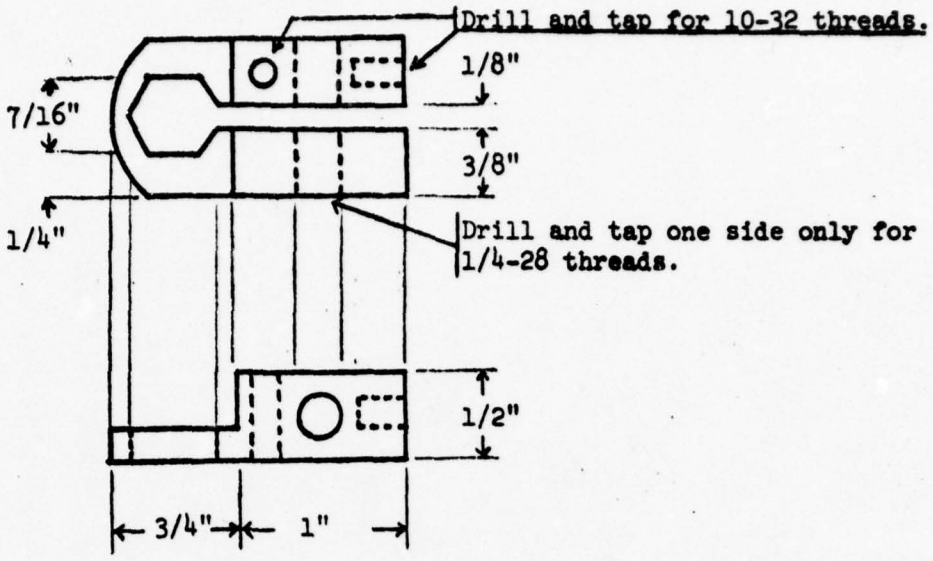


VD-1 accelerometer mount.

Accelerometer mounts VD-3 thru VD-5 differ from the pictured mounts in the dimensions of the aperture of the fixture that fits over the lands of the nuts in the bearing assembly. The sizes of nuts which can be accommodated with the VD 1-5 are 5/16, 3/8, 7/16, 9/16 with the VD-2 affixed to the washers used on the mounting bolts of a bearing fixture.

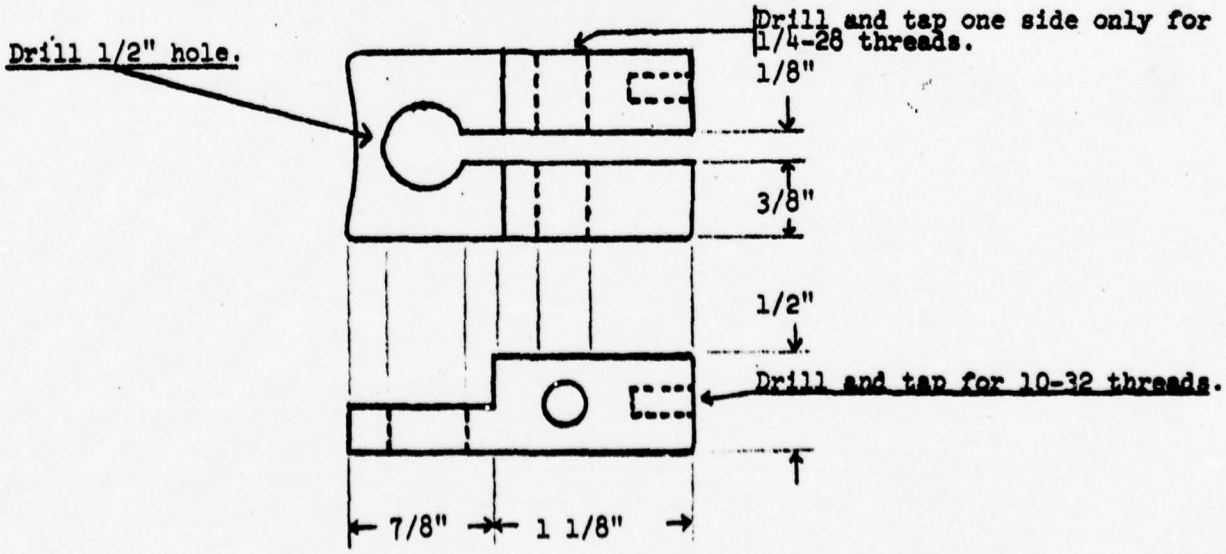


VD-2 accelerometer mount.

## 7.4 FIELD DATA (local)

NUMBER 3 HANGER BEARING UH-1H

TAIL #16264

TEST CONDUCTED 13 NOV 1973 AT BI STATE AIRPORT

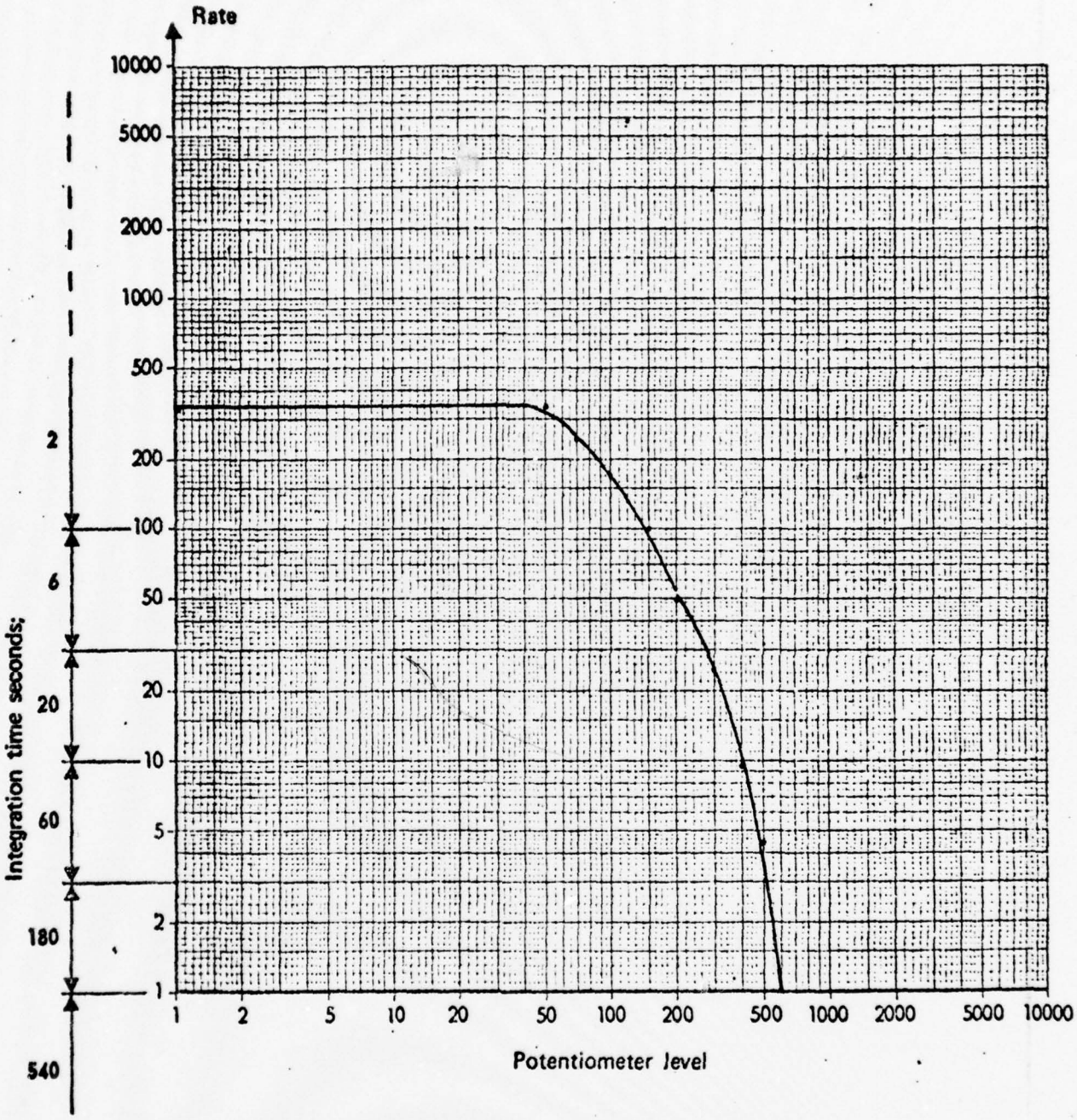


BEARING SERIAL #A20-67523 REMOVED FOR PHYSICAL ANALYSIS.

NUMBER 4 HANGER BEARING

UH-1H TAIL #16264

TEST CONDUCTED 13 NOV 1973 AT BI-STATE AIRPORT

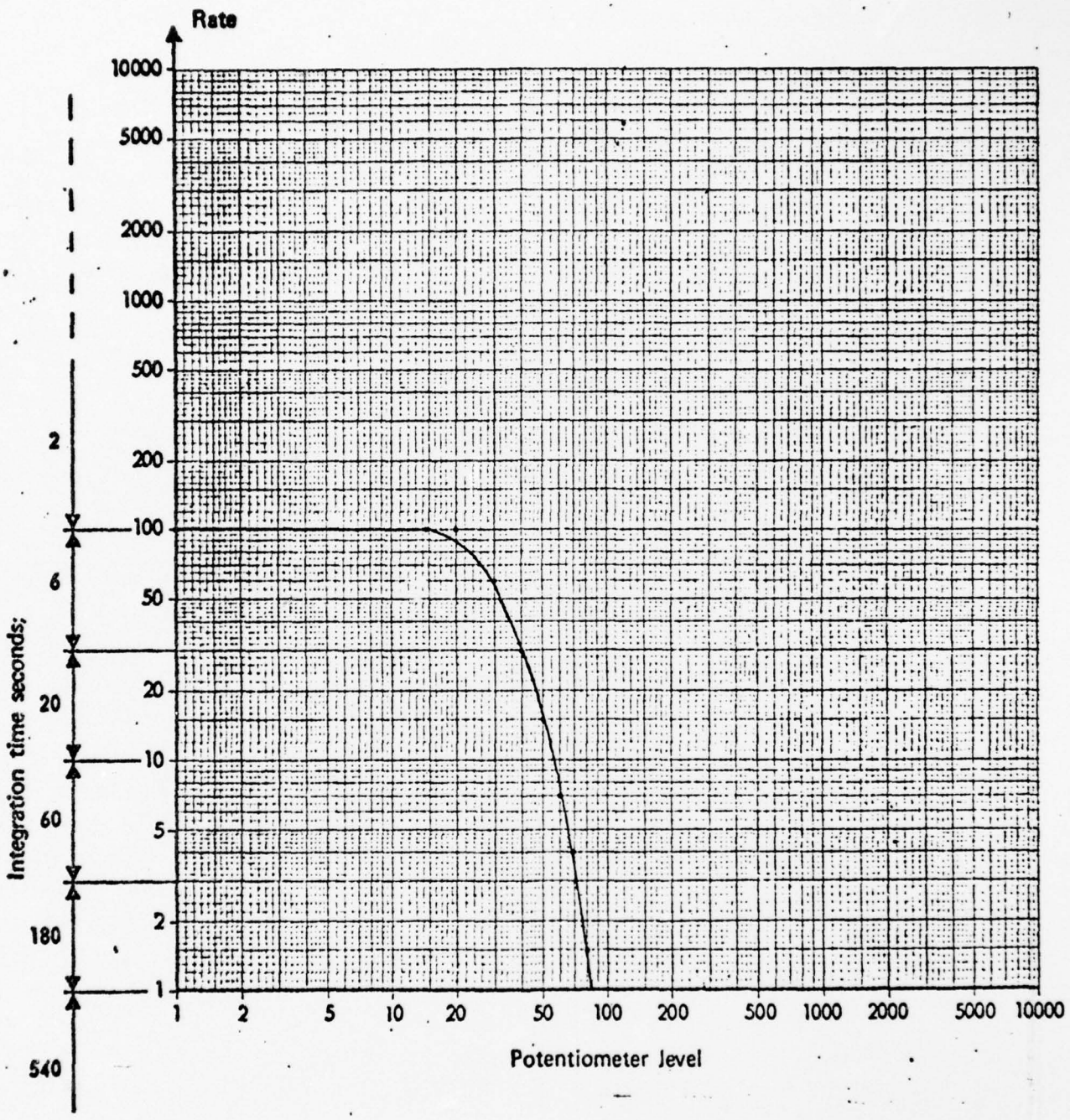

NUMBER 3 HANGER BEARING

UH-1D TAIL #59771

TEST CONDUCTED 14 NOV 1973 AT BI-STATE AIRPORT

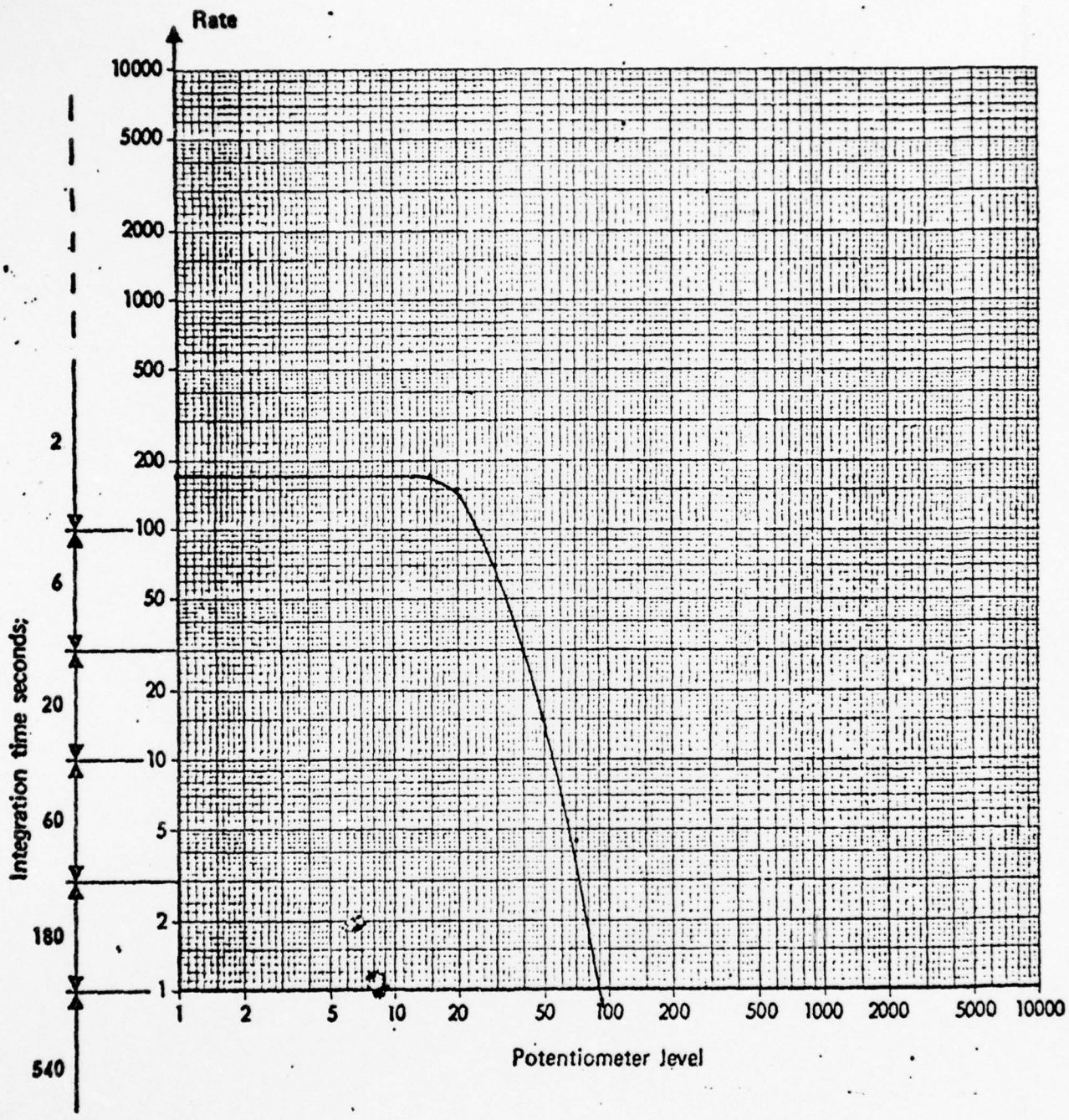

NUMBER 4 HANGER BEARING

UH-1D TAIL #59771

TEST CONDUCTED 14 NOV 1973 AT BI-STATE AIRPORT

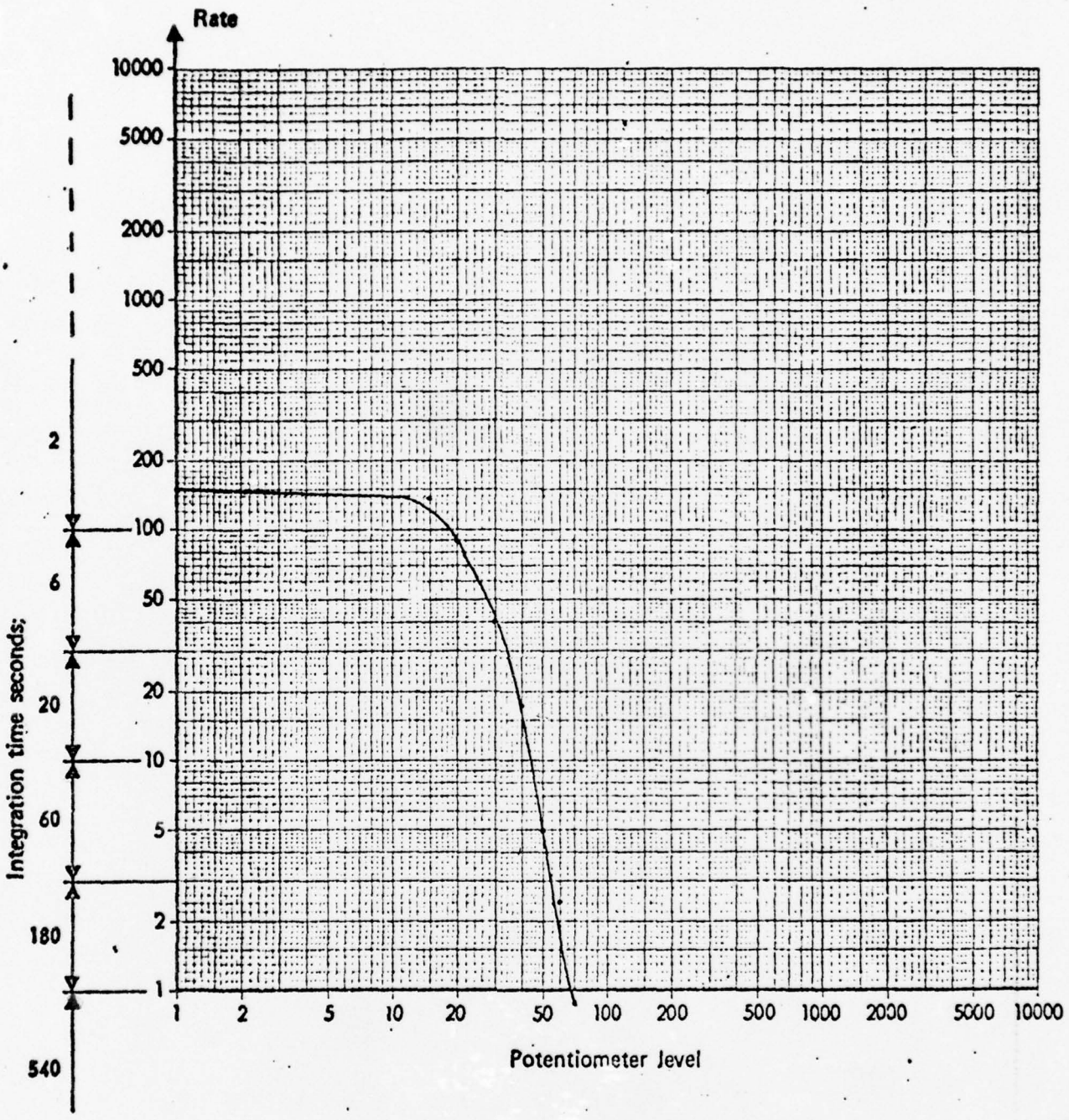

NUMBER 3 HANGER BEARING

UH-1H TAIL #13740

TEST CONDUCTED 14 NOV 1973 AT BI-STATE AIRPORT

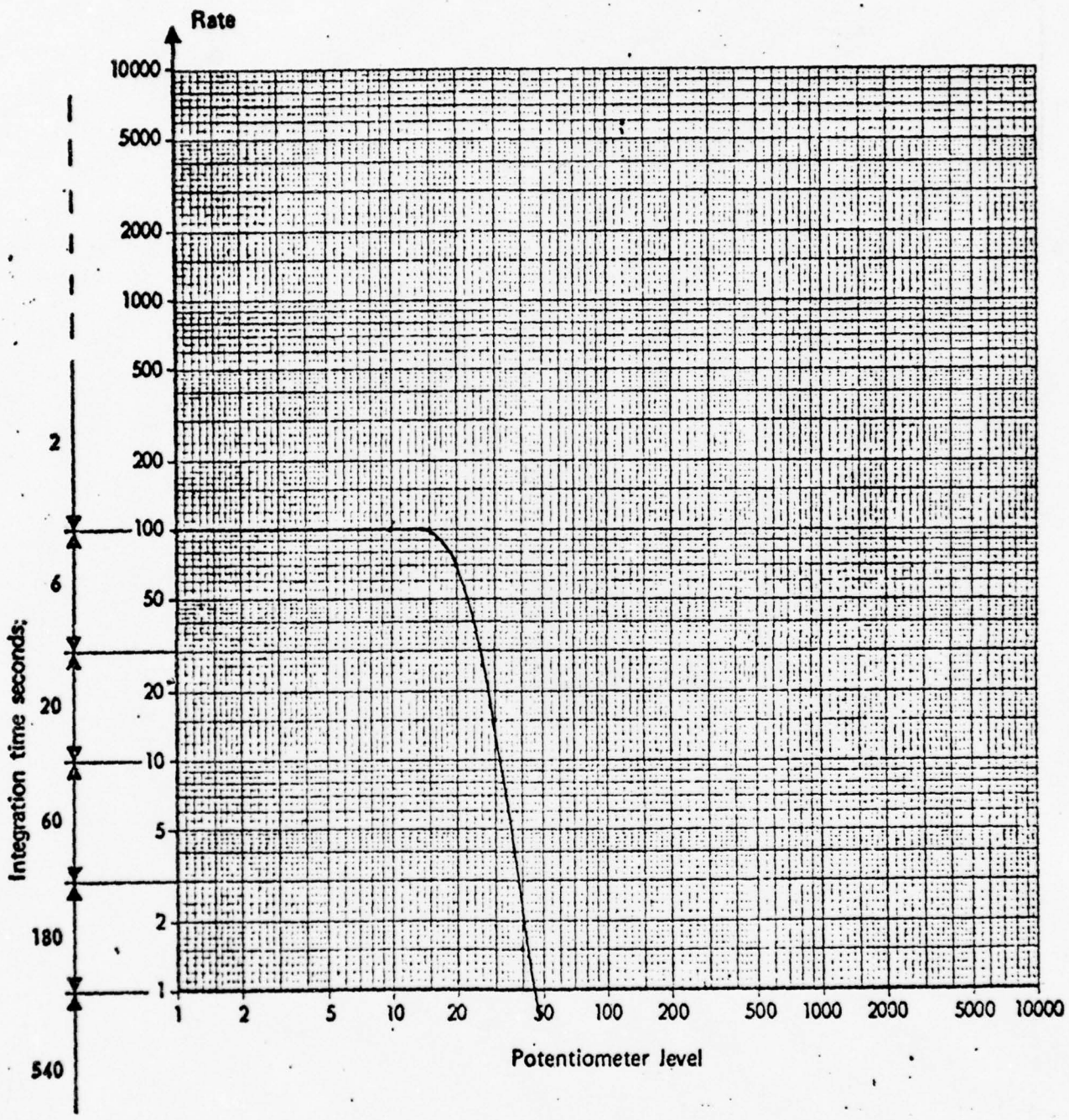

NUMBER 4 HANGER BEARING

UH-1H TAIL #13740

TEST CONDUCTED 14 NOV 1973 AT BI-STATE AIRPORT

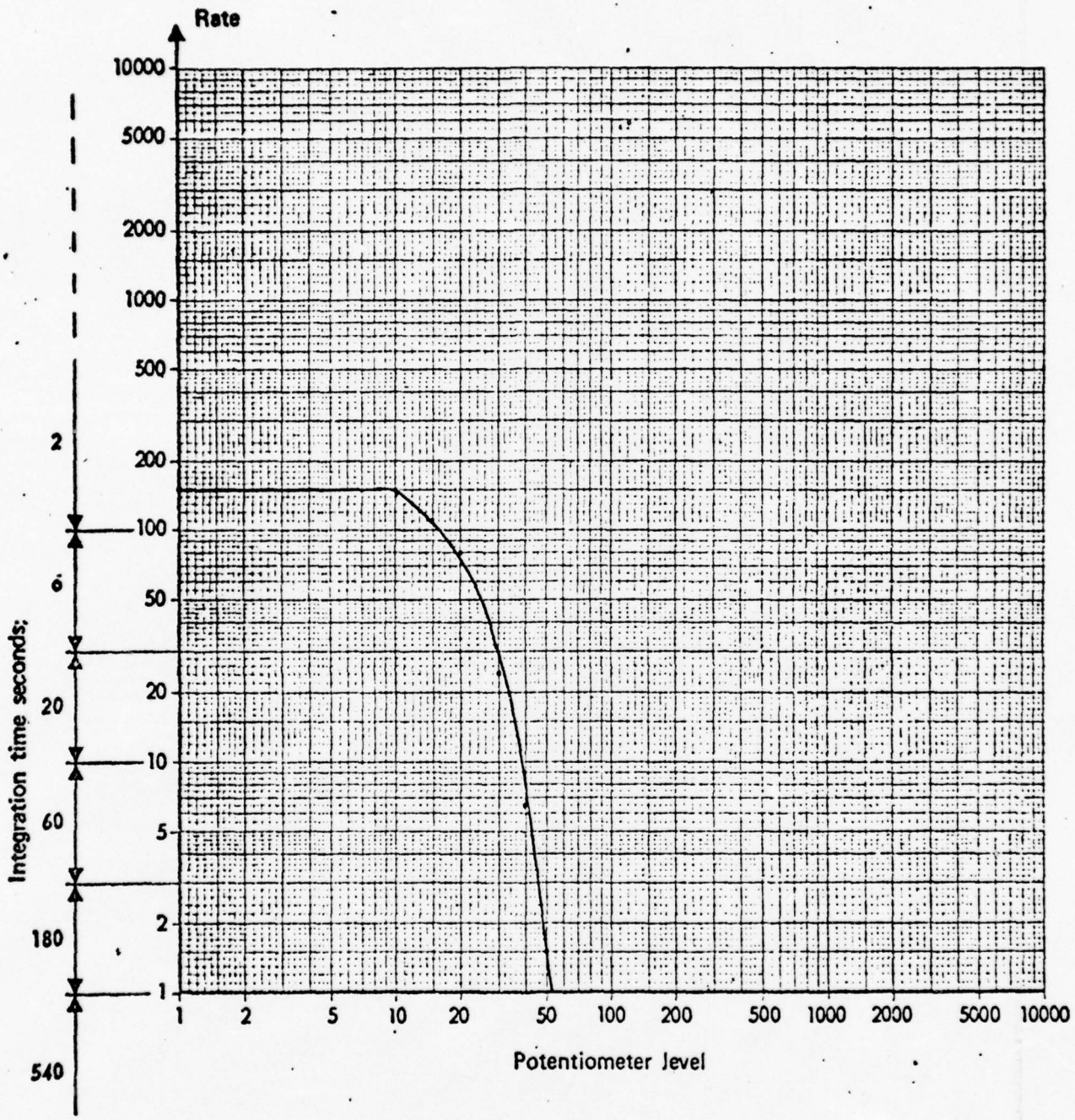

NUMBER 3 HANGER BEARING UH-1H

TAIL #16264

TEST CONDUCTED 19 NOV 1973 AT BI STATE AIRPORT

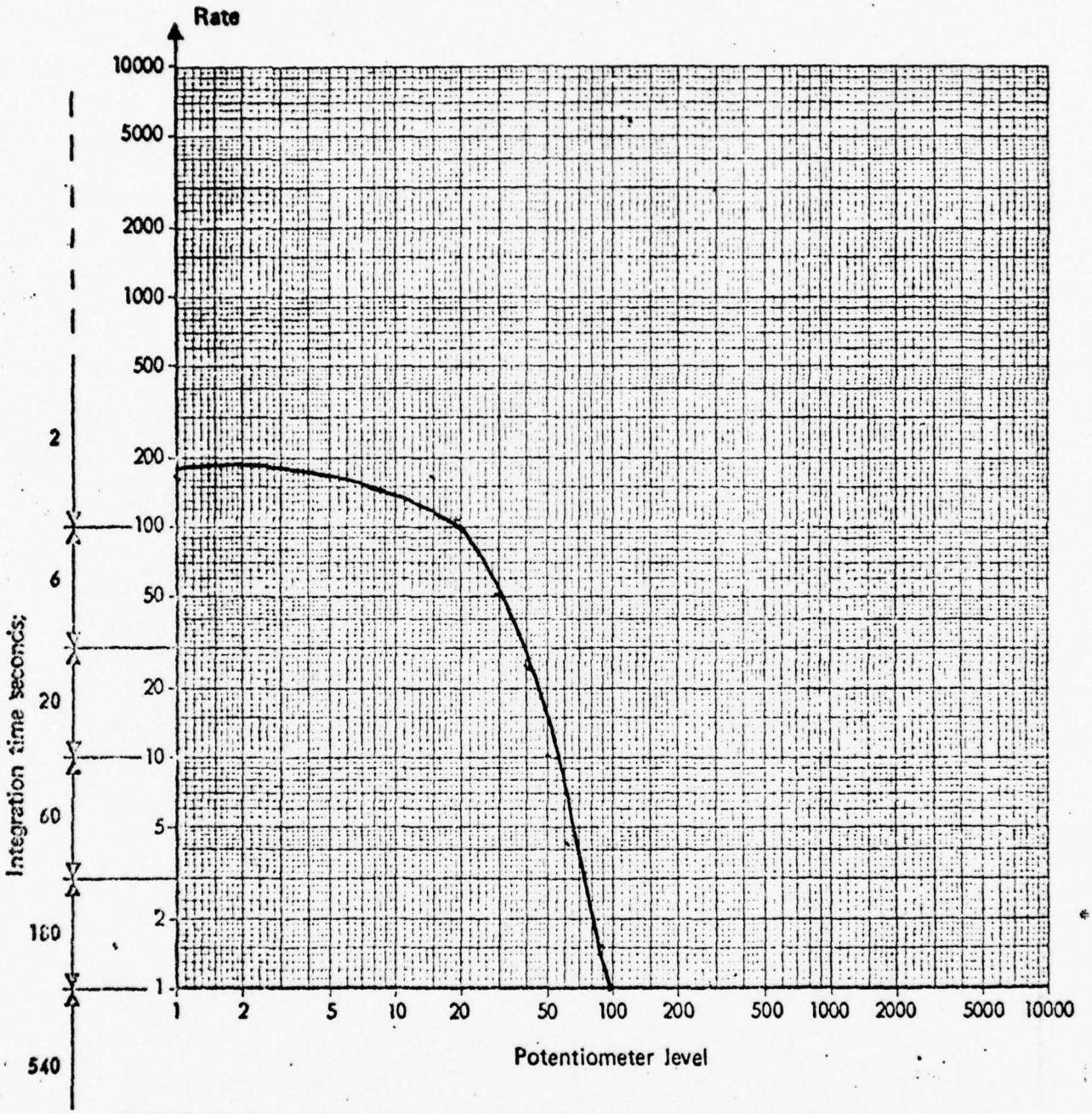


REPEAT OF #3 HANGER BEARING POSITION AFTER INSTALLATION OF NEW BEARING.

NUMBER 3 HANGER BEARING

UH-1H TAIL #16197

TEST CONDUCTED 27 NOV 1973 AT SCOTT AFB

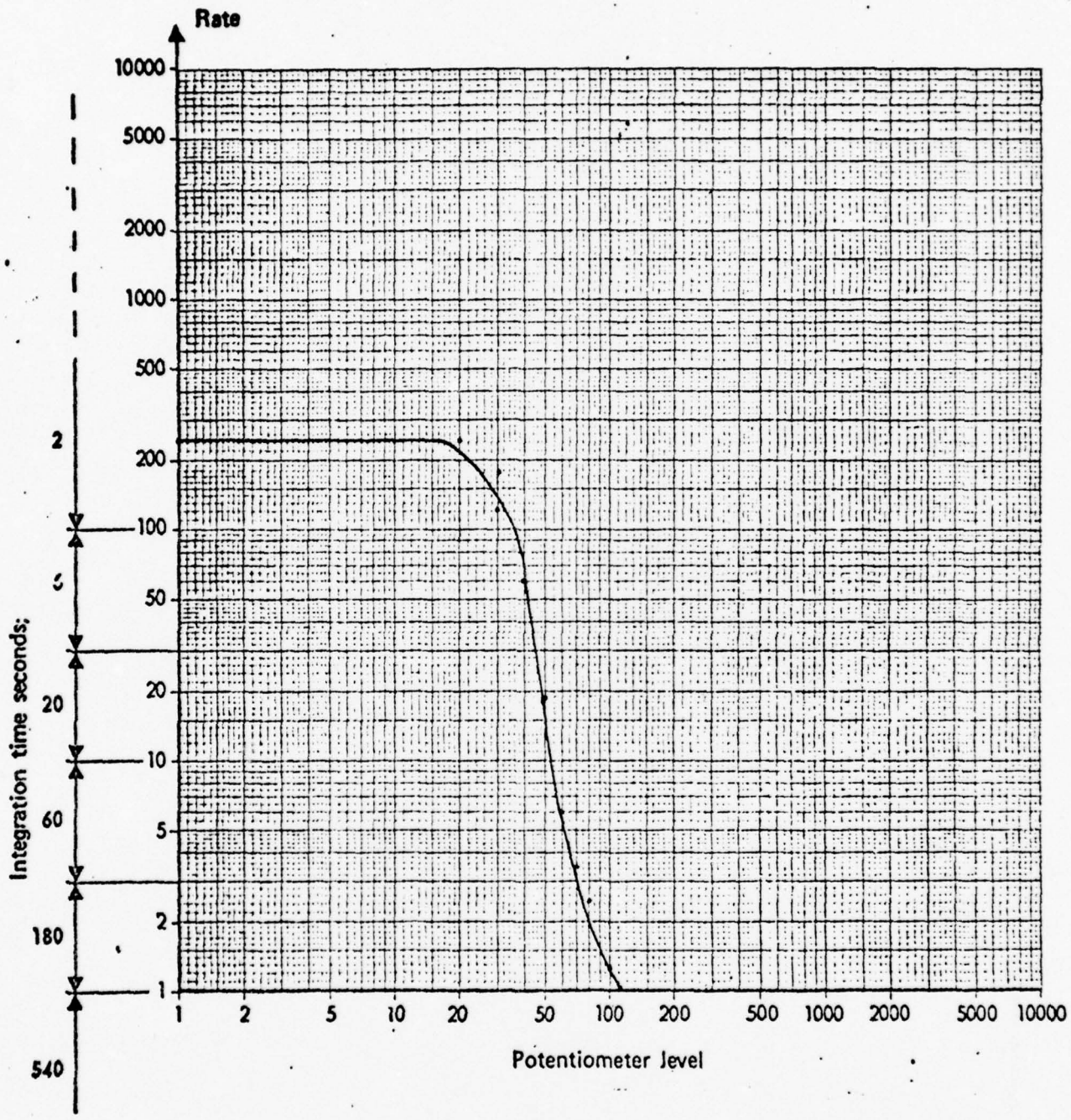

NUMBER 4 HANGER BEARING

UH-1H TAIL #16197

TEST CONDUCTED 27 NOV 1973 AT SCOTT AFB

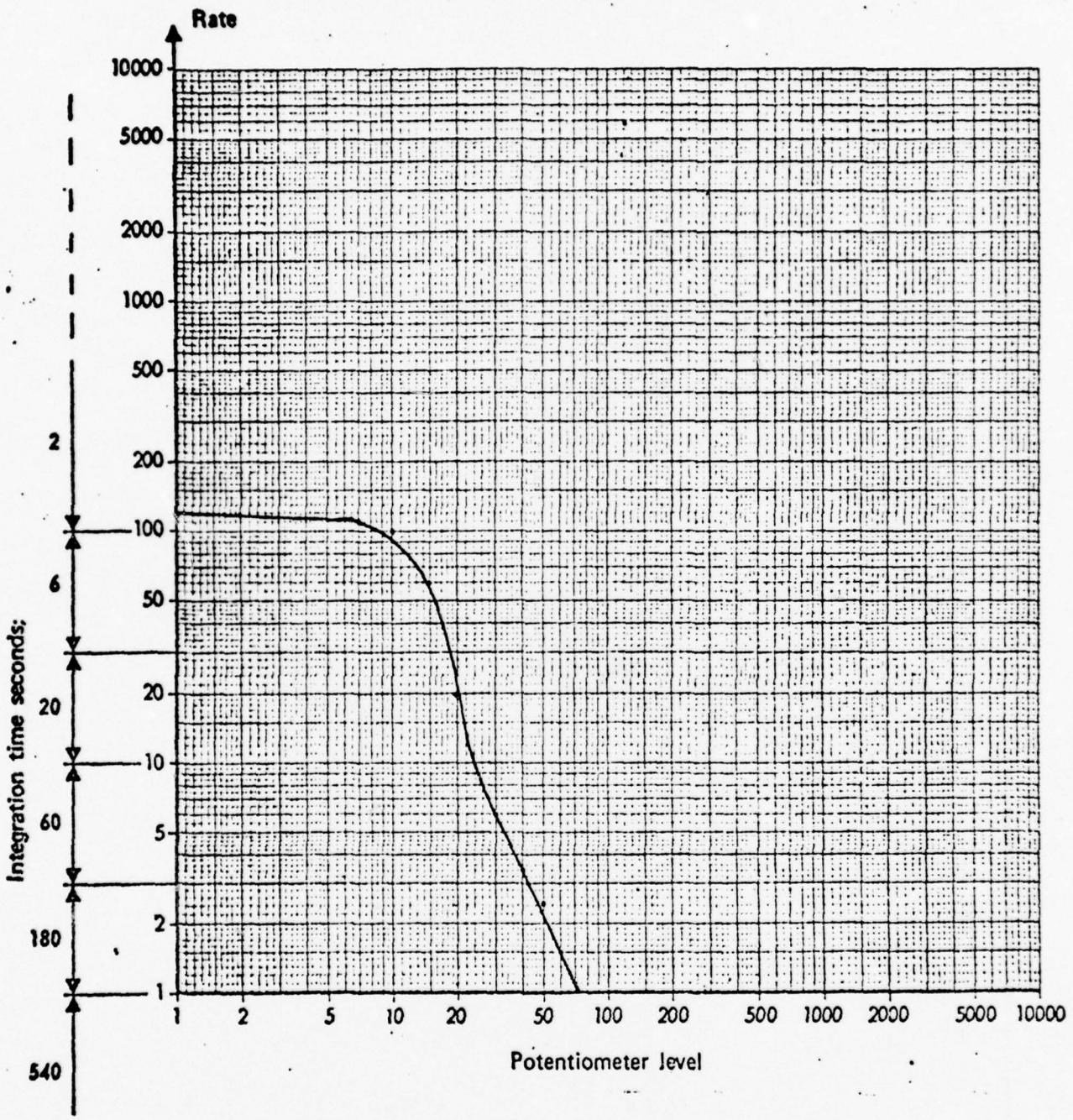

NUMBER 3 HANGER BEARING UH-1H

TAIL #13740

TEST CONDUCTED 27 NOV 1973 AT SCOTT AFB

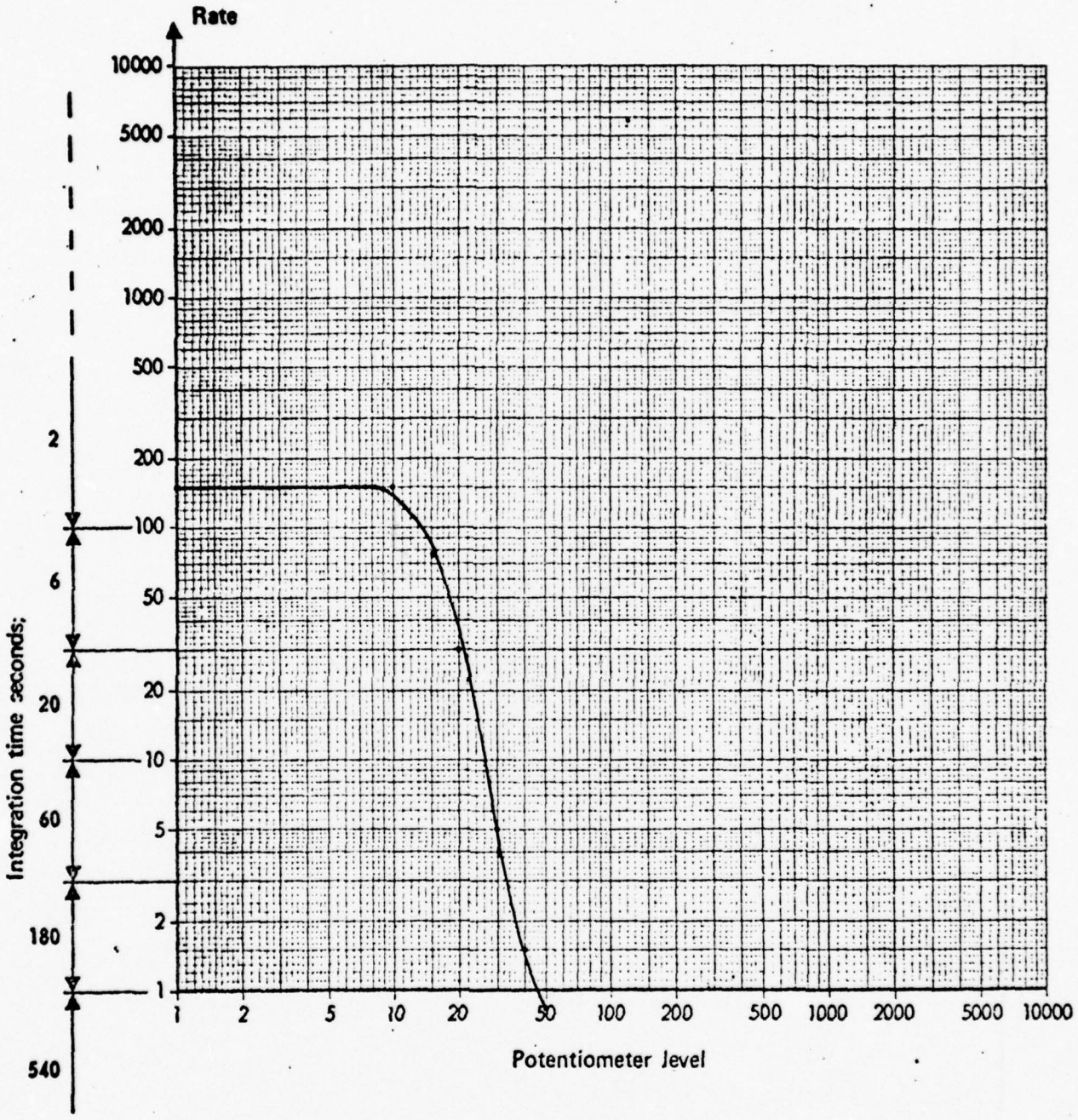

NUMBER 4 HANGER BEARING UH-1H

TAIL #13740

TEST CONDUCTED 27 NOV 1973 AT SCOTT AFB

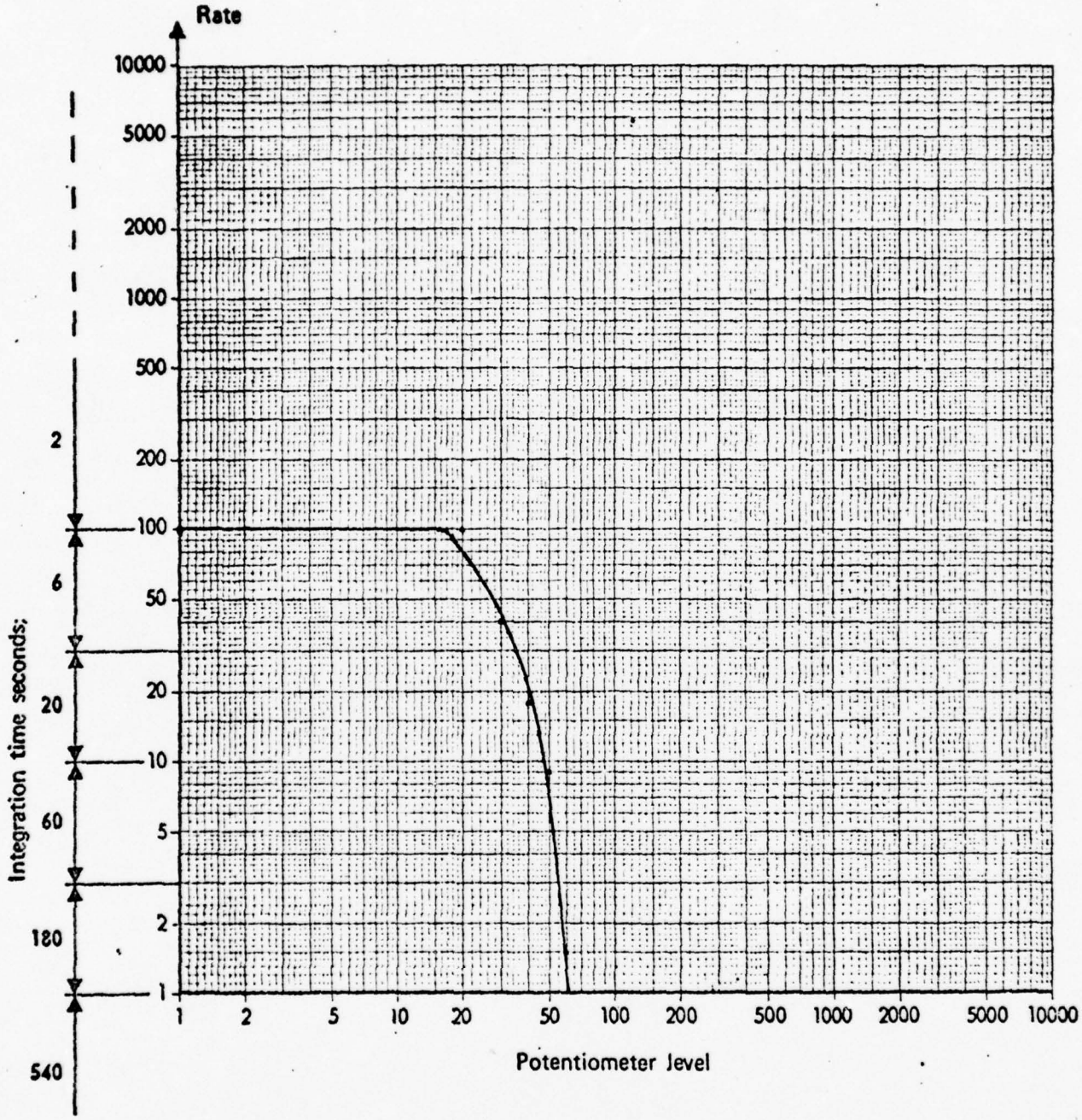

NUMBER 3 HANGER BEARING UH-1H

TAIL #66-01087

TEST CONDUCTED 28 NOV 1973 AT SCOTT AFB

BEARING SERIAL #A20-43391

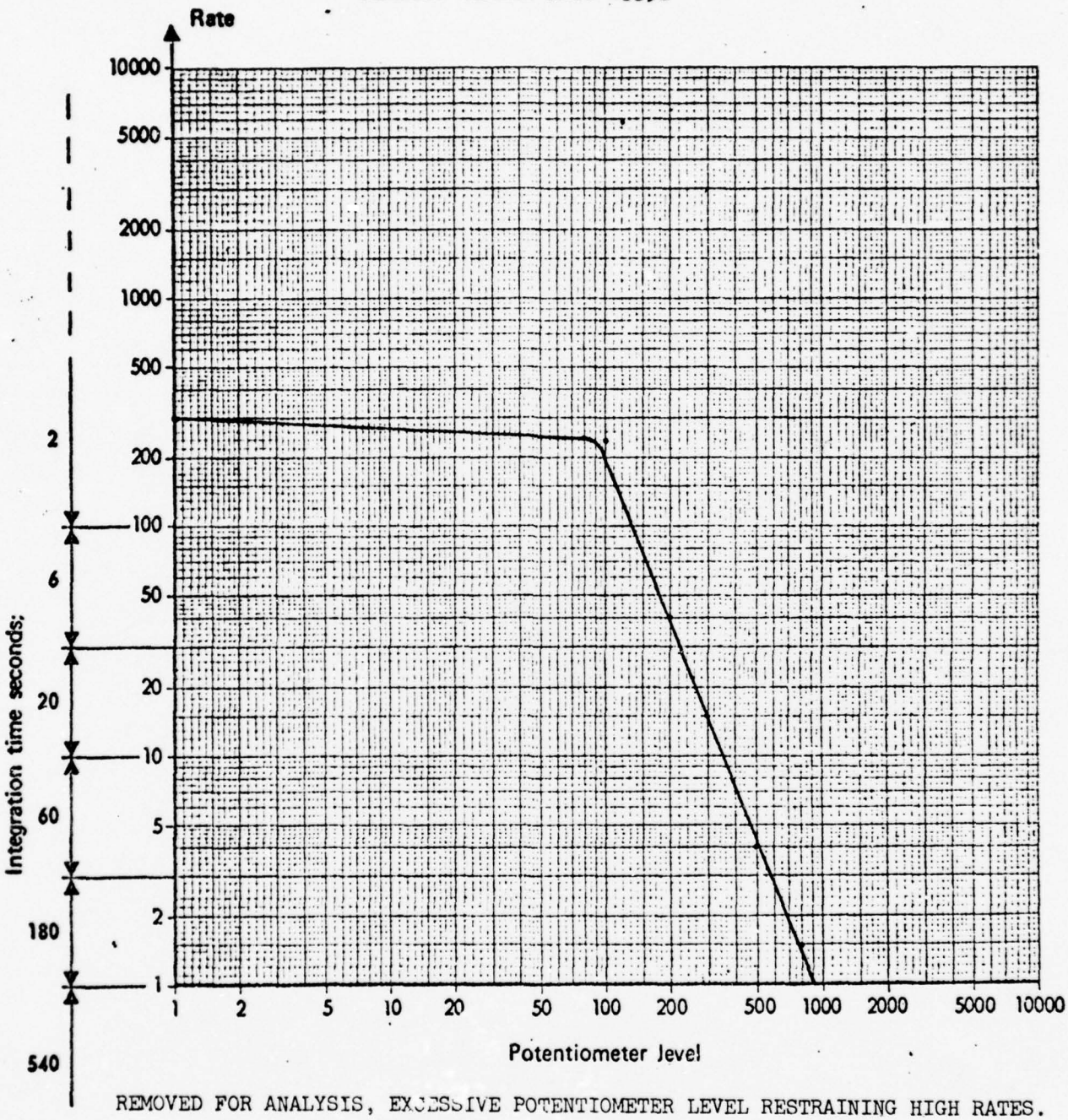


REMOVED FOR ANALYSIS, EXCESSIVE POTENTIOMETER LEVEL RESTRAINING HIGH RATES.

4 HANGER BEARINGS

UH-1H TAIL #66-01087

TEST CONDUCTED 28 NOV 1973

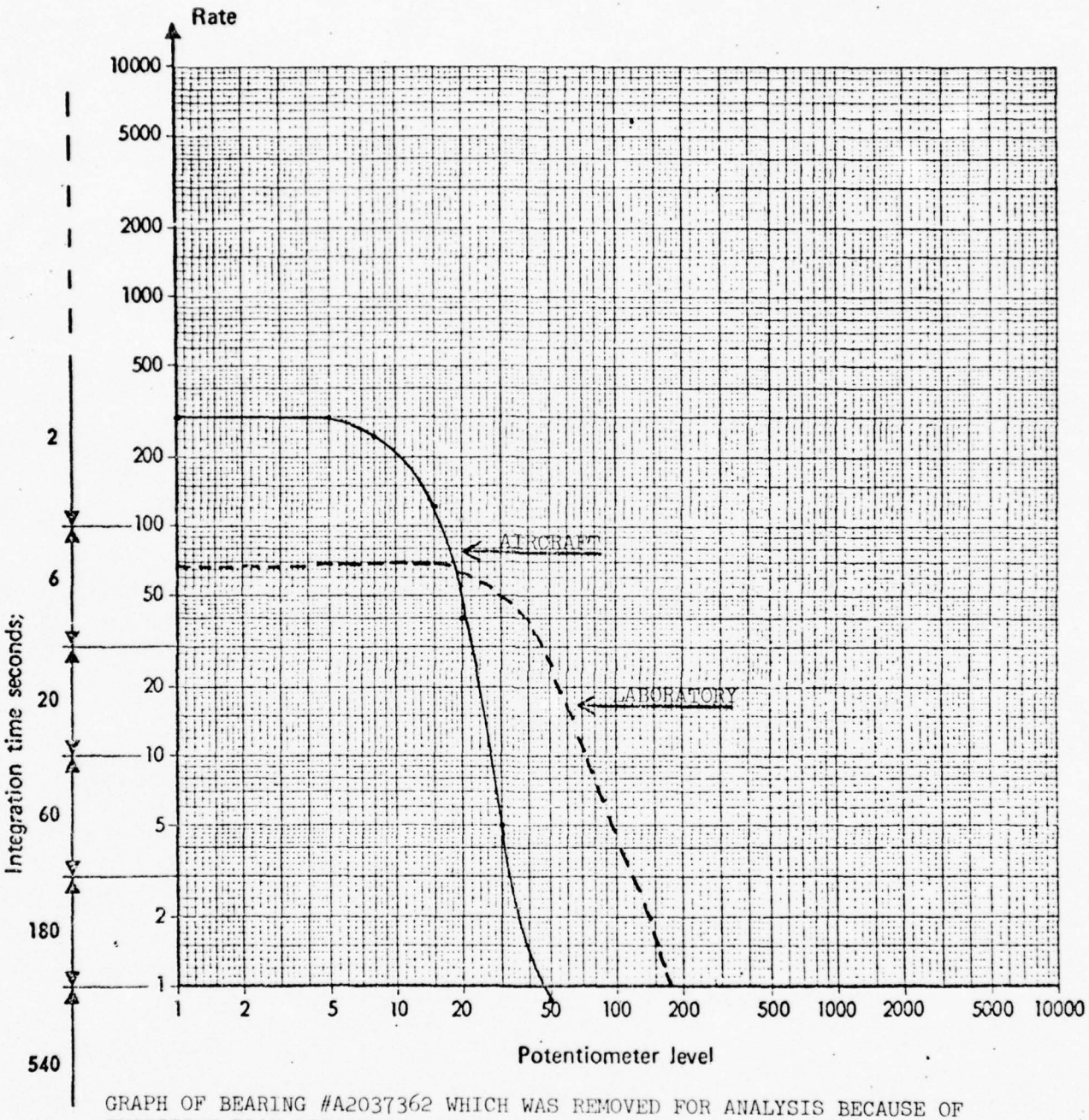


GRAPH OF BEARING #A2037362 WHICH WAS REMOVED FOR ANALYSIS BECAUSE OF EXCESSIVE PLAY DISCOVERED BY AN AIRCRAFT TECHNICAL INSPECTOR - ONE GRAPH MADE ON AIRCRAFT, THE OTHER IN LABORATORY AT APPROXIMATELY THE SAME RPM. (14 DEC 1973).

NUMBER 3 HANGER BEARING UH-1H

TAIL #15949

TEST CONDUCTED 28 NOV 1973 AT SCOTT AFB

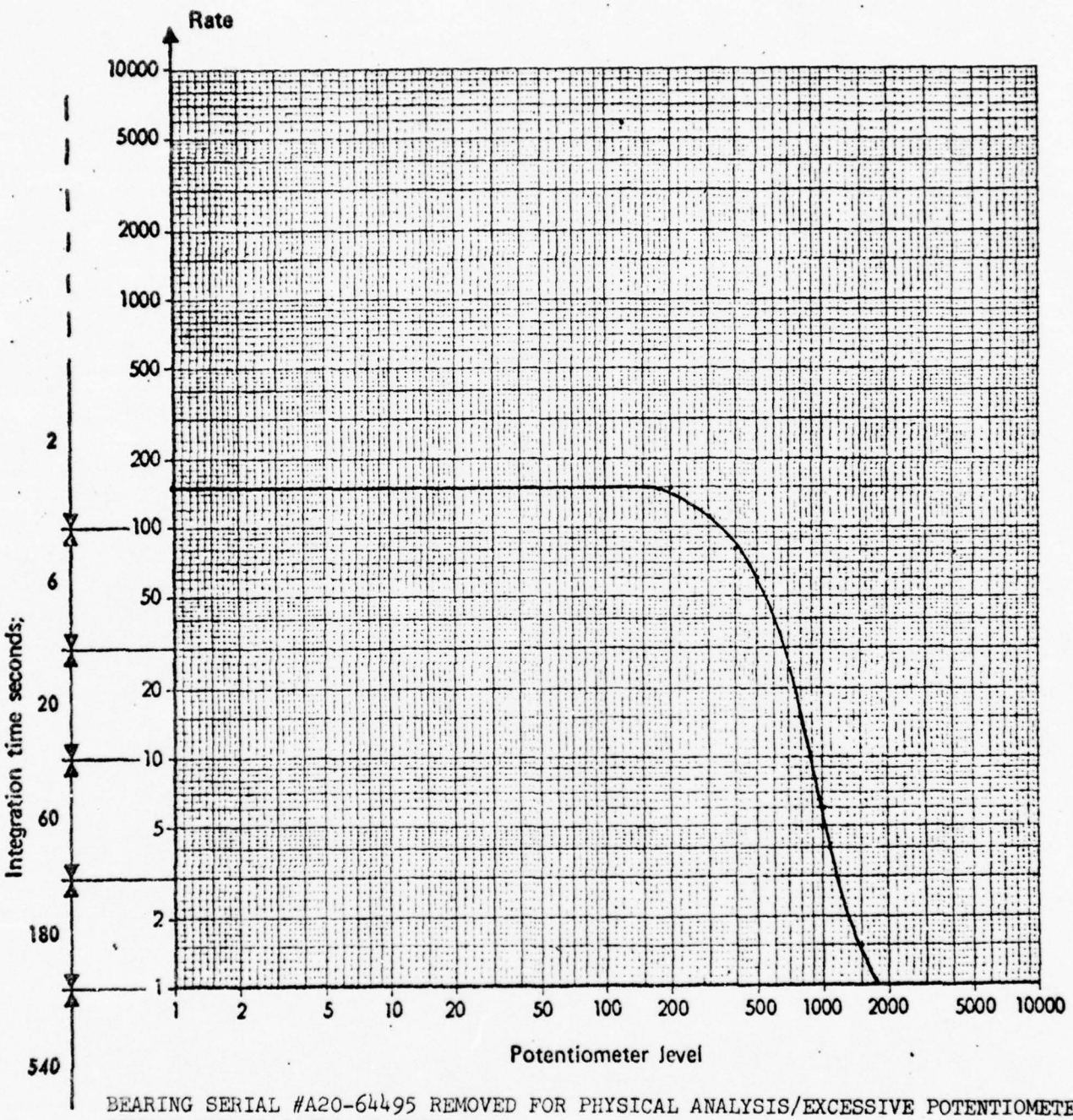


BEARING SERIAL #A20-64495 REMOVED FOR PHYSICAL ANALYSIS/EXCESSIVE POTENTIOMETER LEVELS NORMAL RATES OF SHOCK.

NUMBER 4 HANGER BEARING UH-1H

TAIL # 15949

TEST CONDUCTED 28 NOV 1973 AT SCOTT AFB

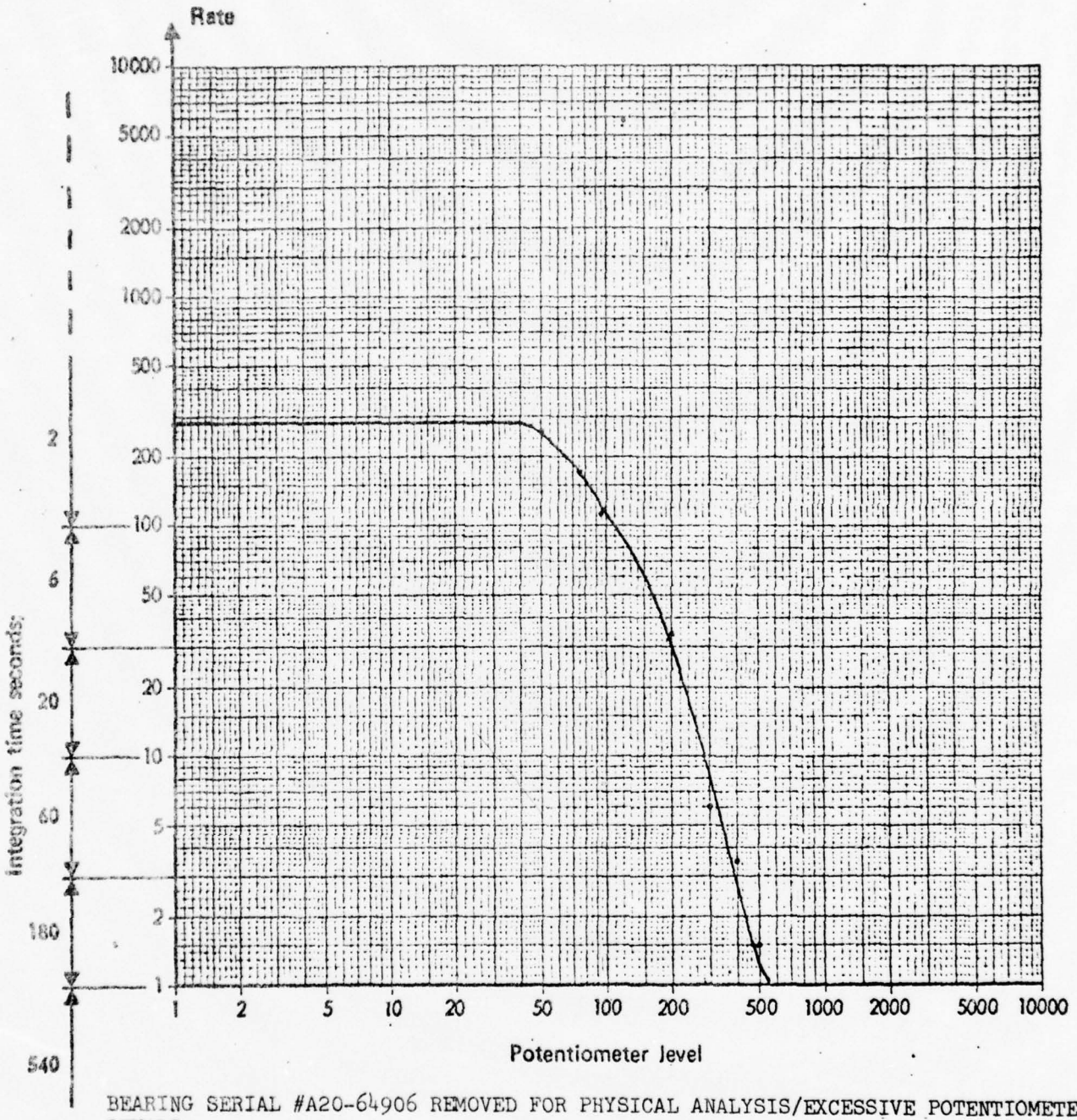


BEARING SERIAL #A20-64906 REMOVED FOR PHYSICAL ANALYSIS/EXCESSIVE POTENTIOMETER LEVELS.

NUMBER 1 HANGER BEARING

UH-1M TAIL #59519

TEST CONDUCTED 30 NOV 1973 AT SCOTT AFB

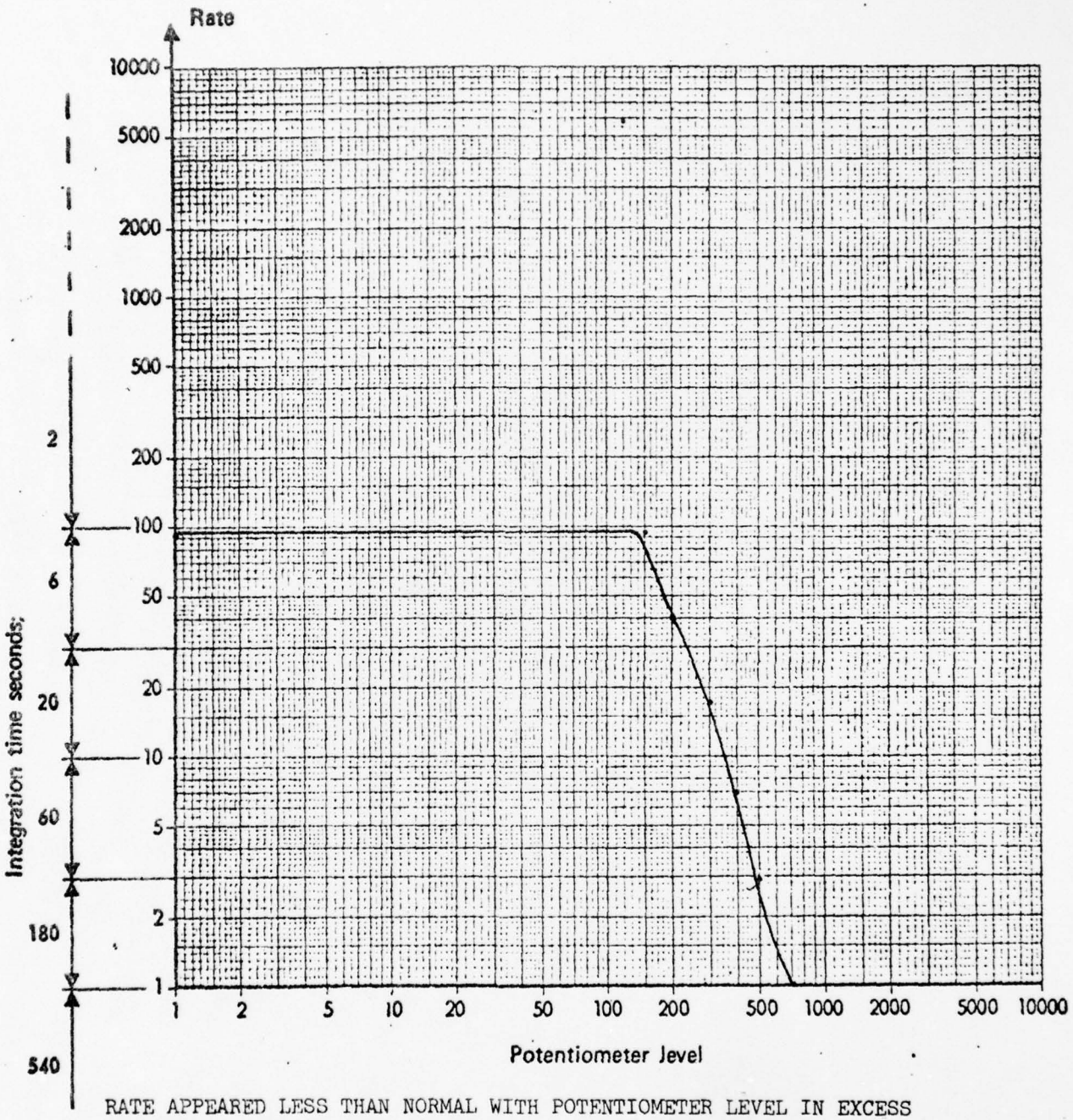


RATE APPEARED LESS THAN NORMAL WITH POTENTIOMETER LEVEL IN EXCESS OF NORMAL. BEARING WAS NOT REMOVED FOR PHYSICAL ANALYSIS.

NUMBER 2 HANGER BEARING

UH-1M TAIL #59519

TEST CONDUCTED 30 NOV 1973 AT SCOTT AFB

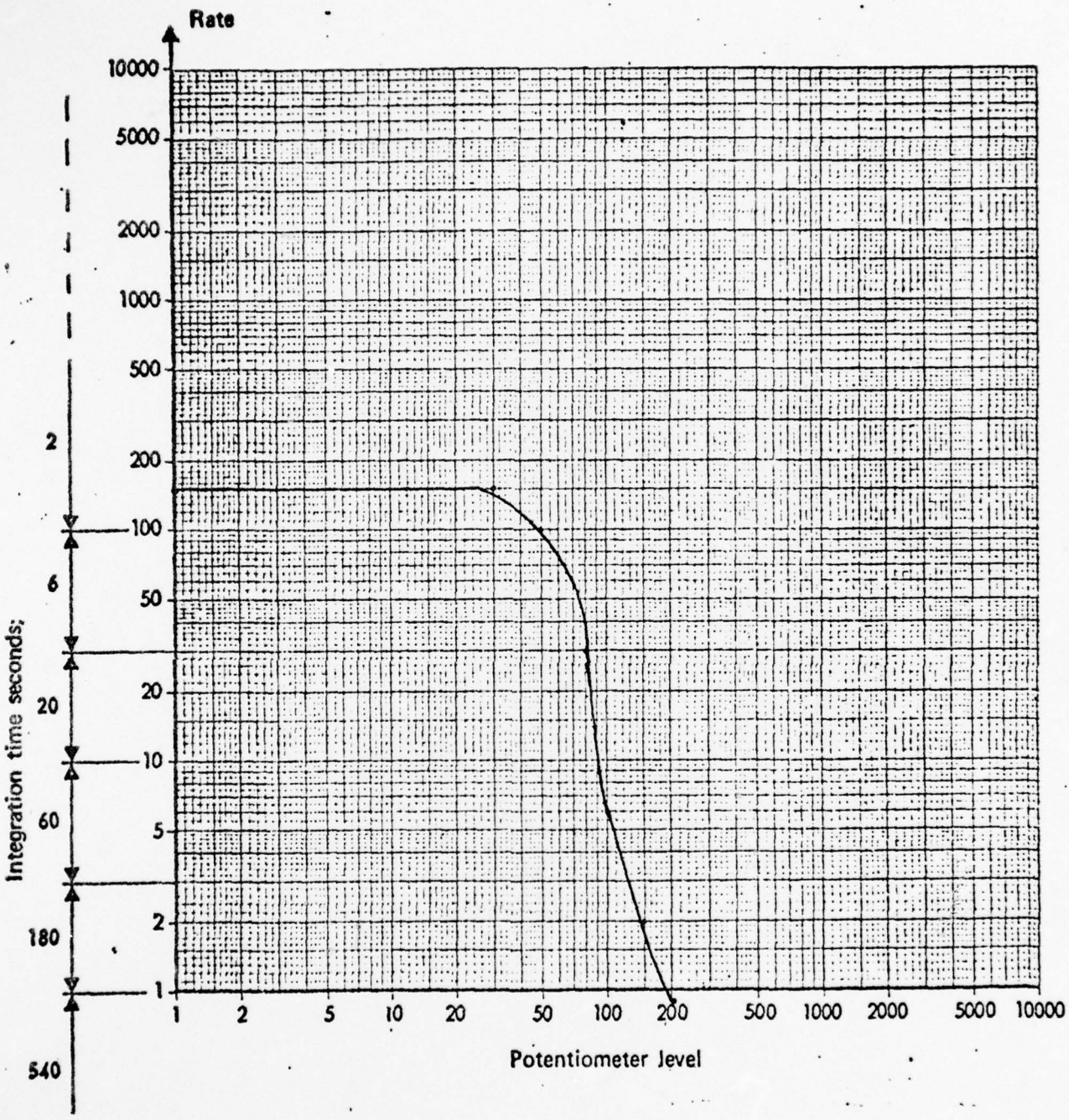

NUMBER 3 HANGER BEARING

UH-1M TAIL #59519

BEARING SERIAL #A20-11446

TEST CONDUCTED 30 NOV 1973 AT SCOTT AFB

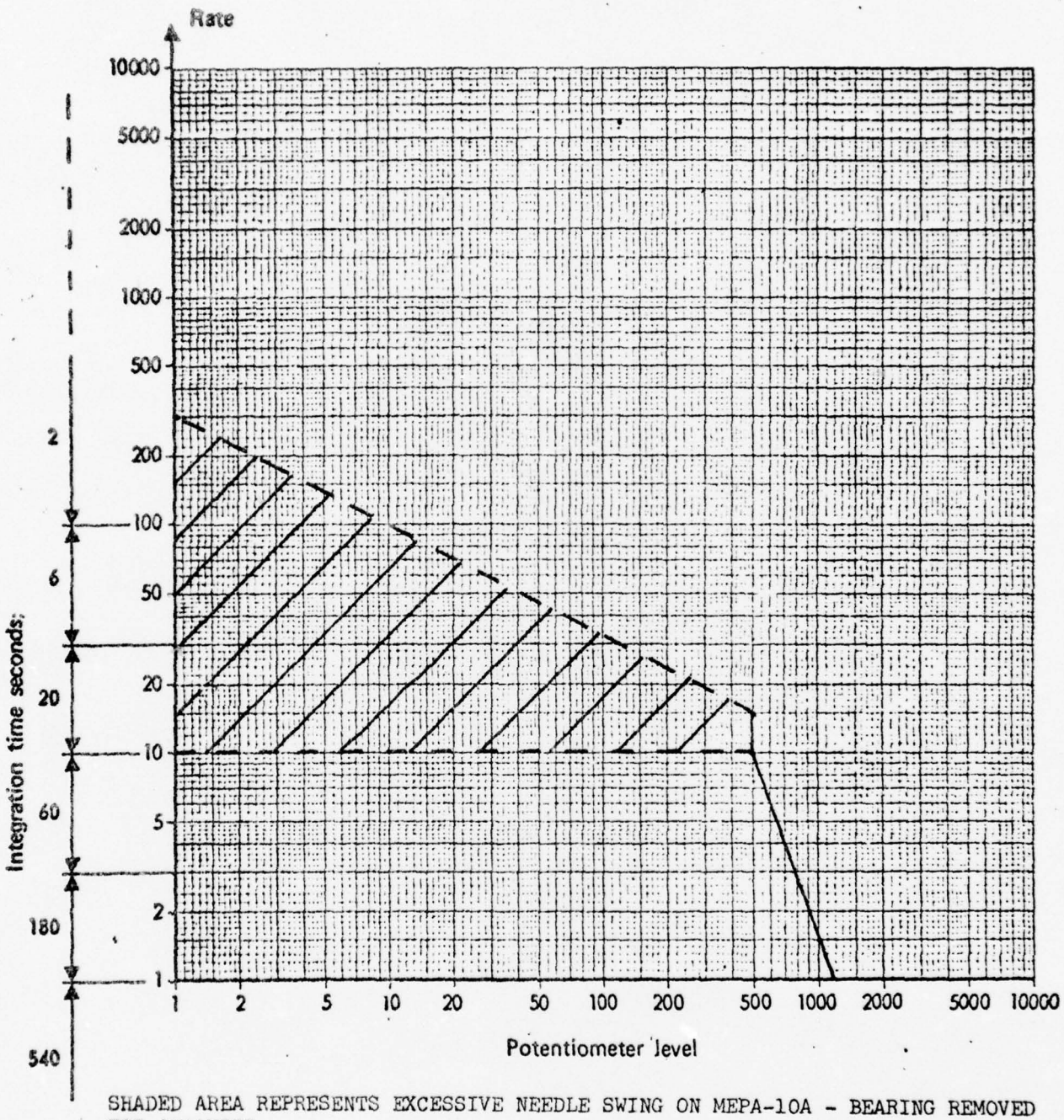


SHADED AREA REPRESENTS EXCESSIVE NEEDLE SWING ON MEPA-10A - BEARING REMOVED FOR ANALYSIS.

NUMBER 3 HANGER BEARING (NEW BEARING)

UH-1H TAIL #66-1087

TEST CONDUCTED 30 NOV 1973 AT SCOTT AFB

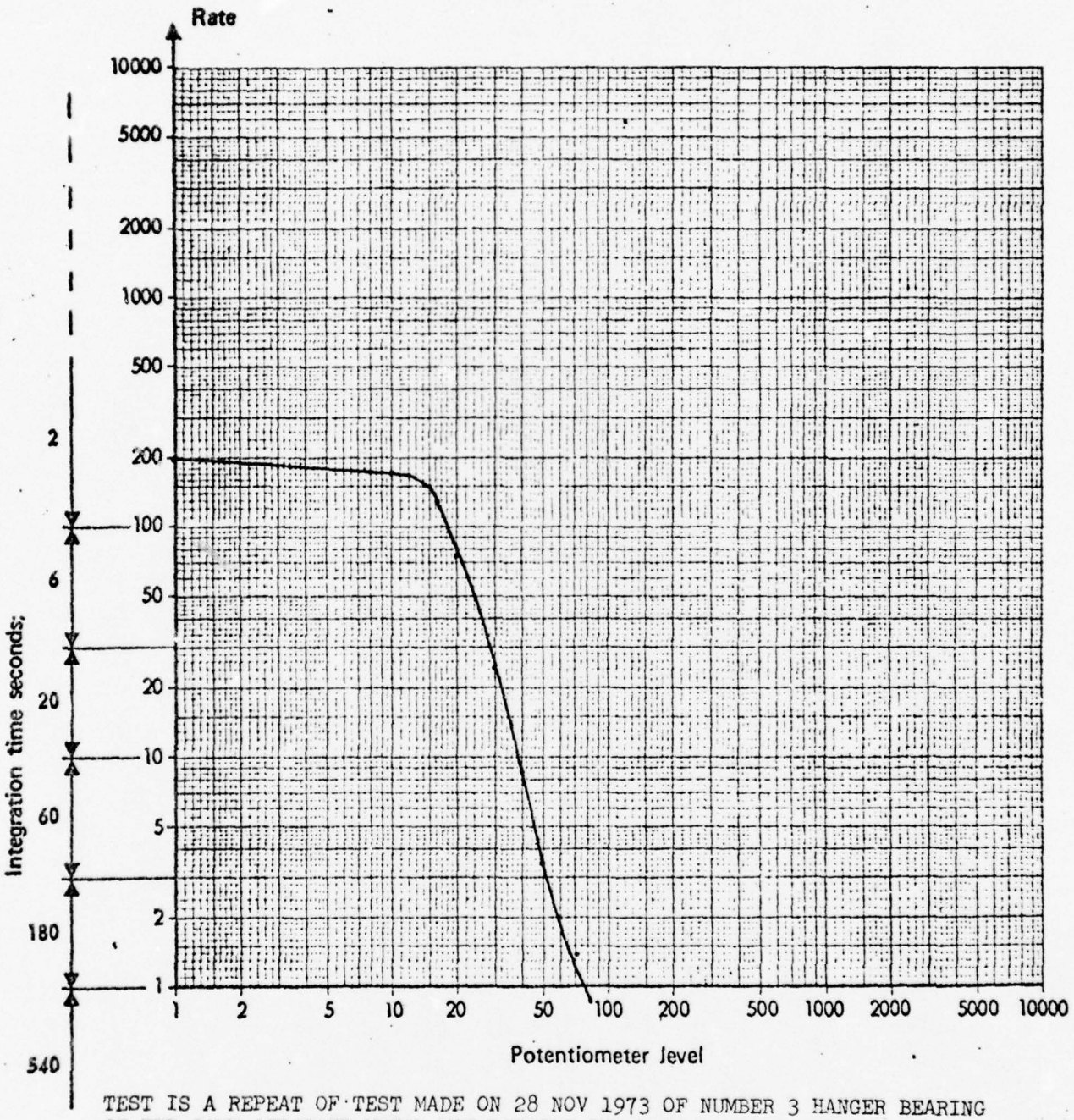


TEST IS A REPEAT OF TEST MADE ON 28 NOV 1973 OF NUMBER 3 HANGER BEARING OF THE SAME AIRCRAFT WHICH WAS REMOVED FOR TEAR DOWN ANALYSIS.

NUMBER 3 HANGER BEARING UH-1H (NEW BEARING)

TAIL #15949

TEST CONDUCTED 30 NOV 1973 AT SCOTT AFB

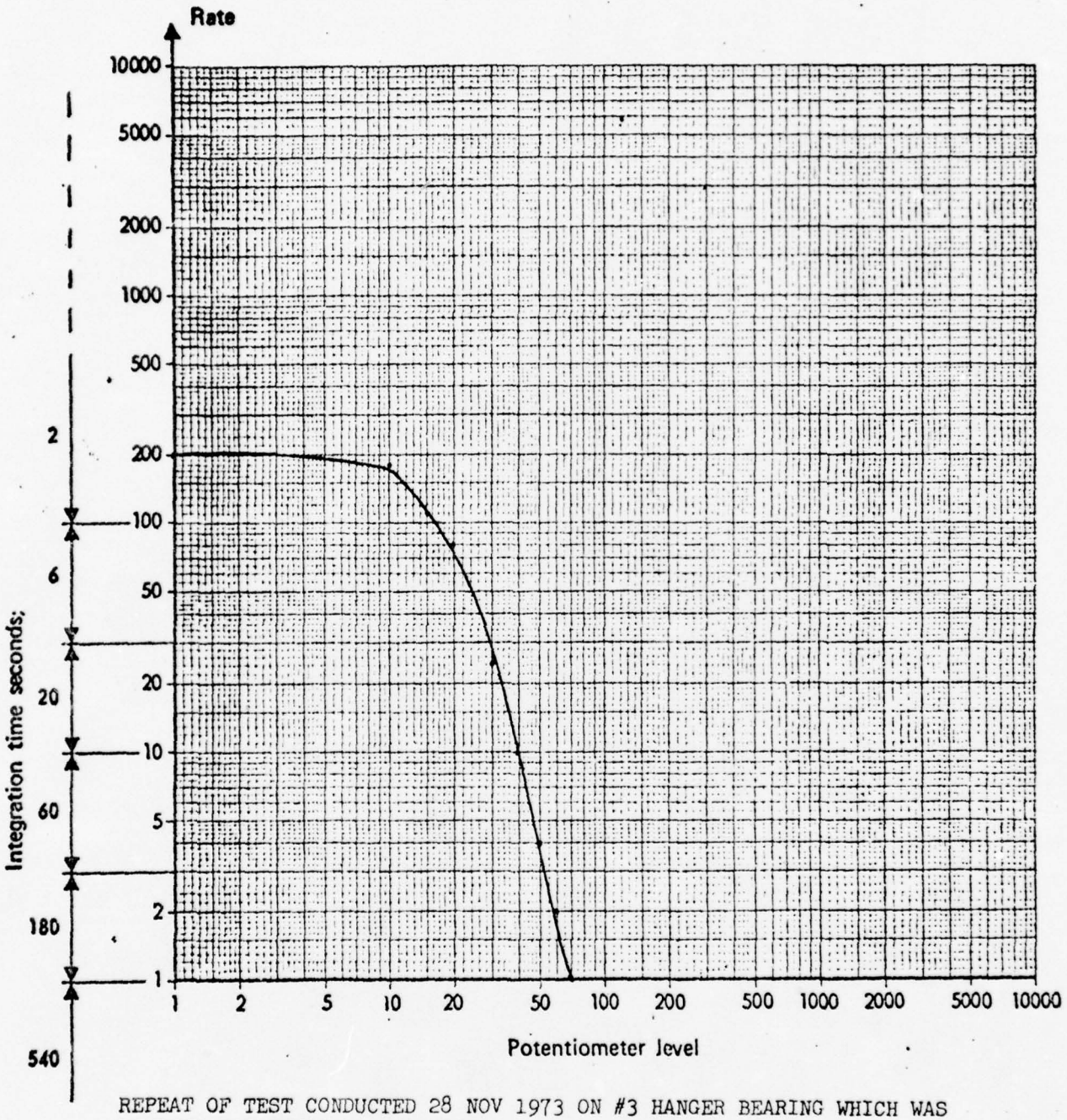


REPEAT OF TEST CONDUCTED 28 NOV 1973 ON #3 HANGER BEARING WHICH WAS REMOVED FOR PHYSICAL ANALYSIS.

NUMBER 4 HANGER BEARING UH-1H (NEW BEARING)

TAIL #15949

TEST CONDUCTED 30 NOV 1973 AT SCOTT AFB

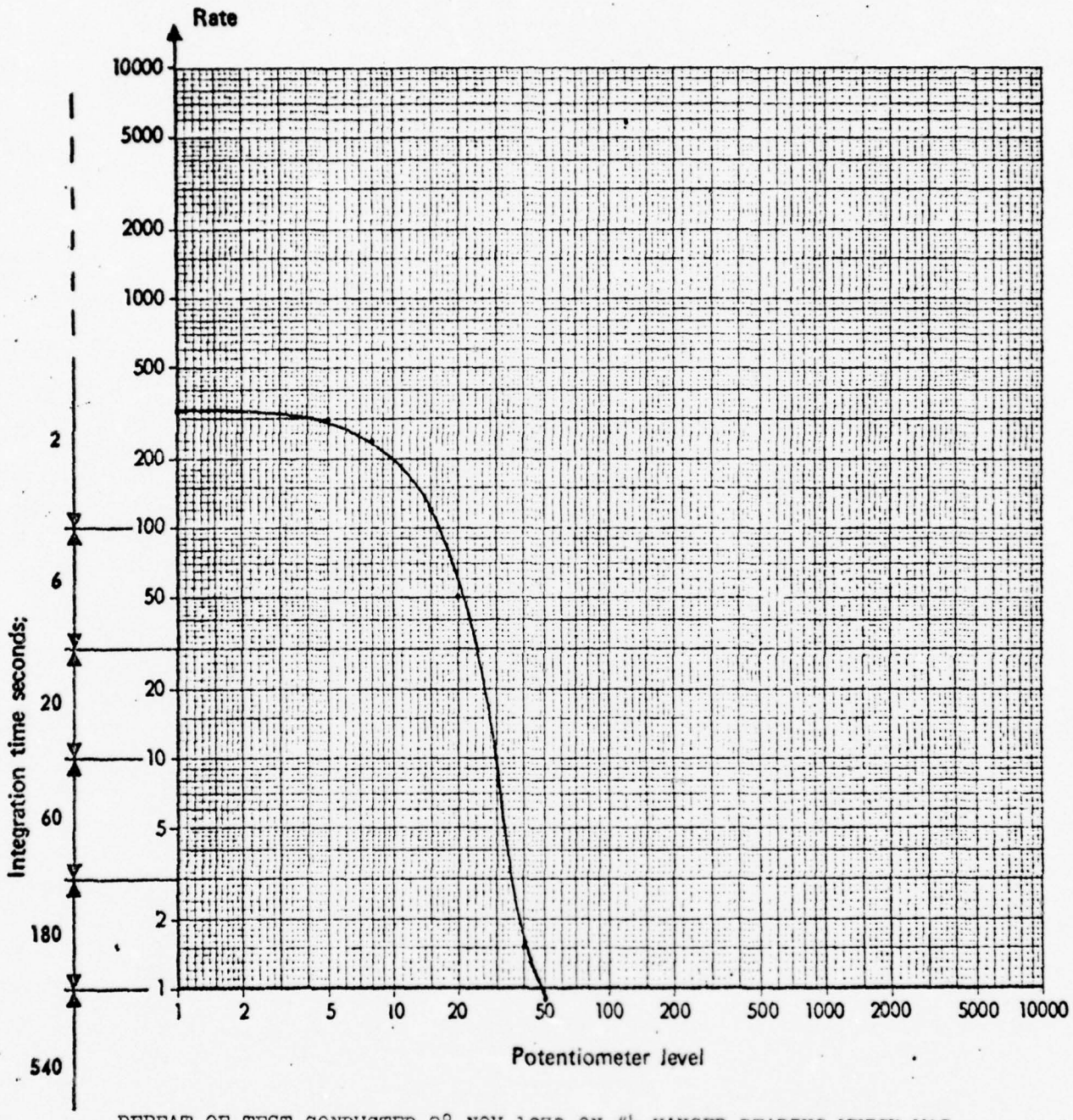


REPEAT OF TEST CONDUCTED 28 NOV 1973 ON #4 HANGER BEARING WHICH WAS REMOVED FOR PHYSICAL ANALYSIS.

NUMBER 1 HANGER BEARING

UH-1M TAIL #15200

TEST CONDUCTED 6 DEC 1973 AT SCOTT AFB

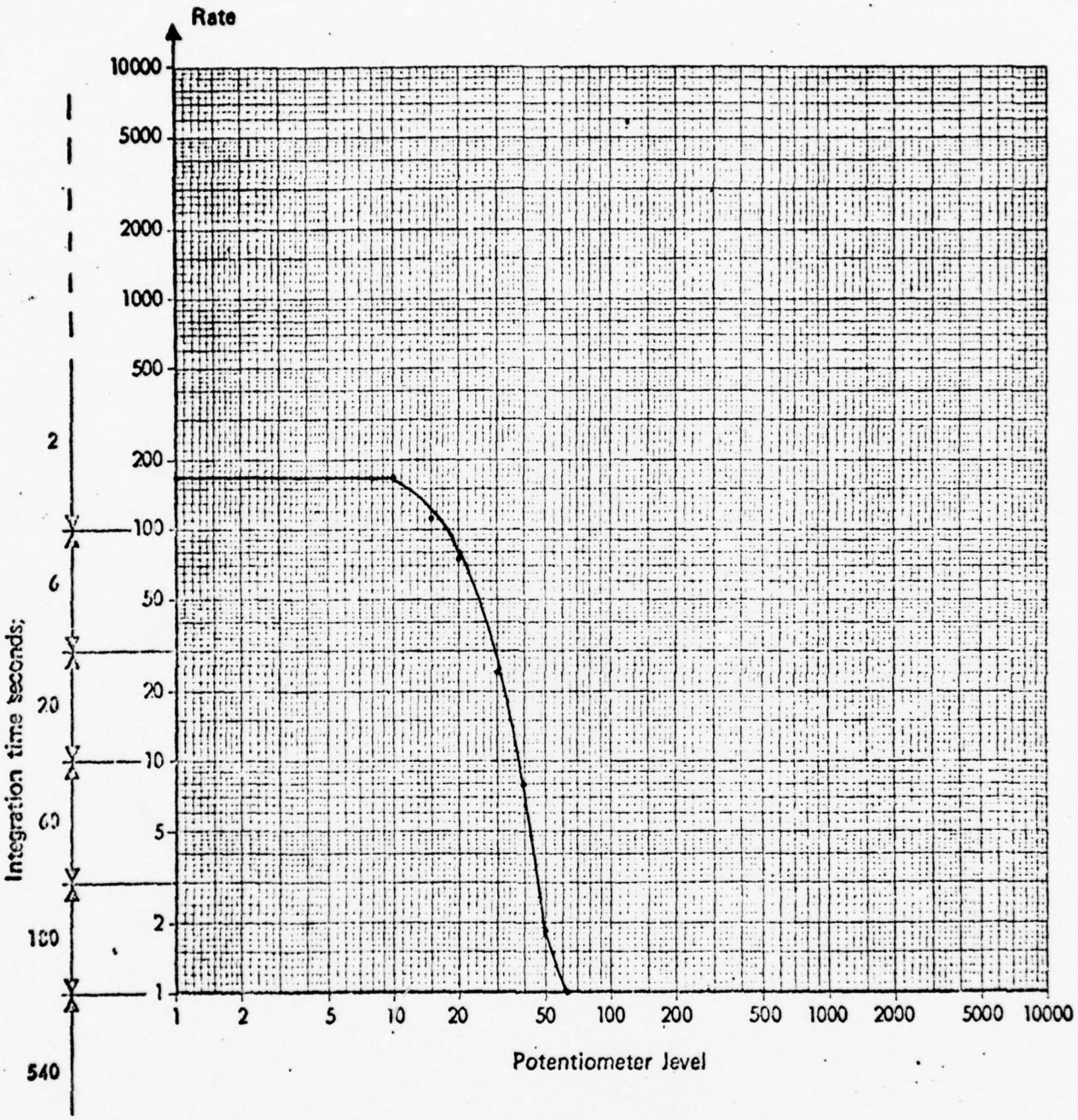

NUMBER 2 HANGER BEARING

UH-1M TAIL #15200

TEST CONDUCTED 6 DEC 1973 AT SCOTT AFB

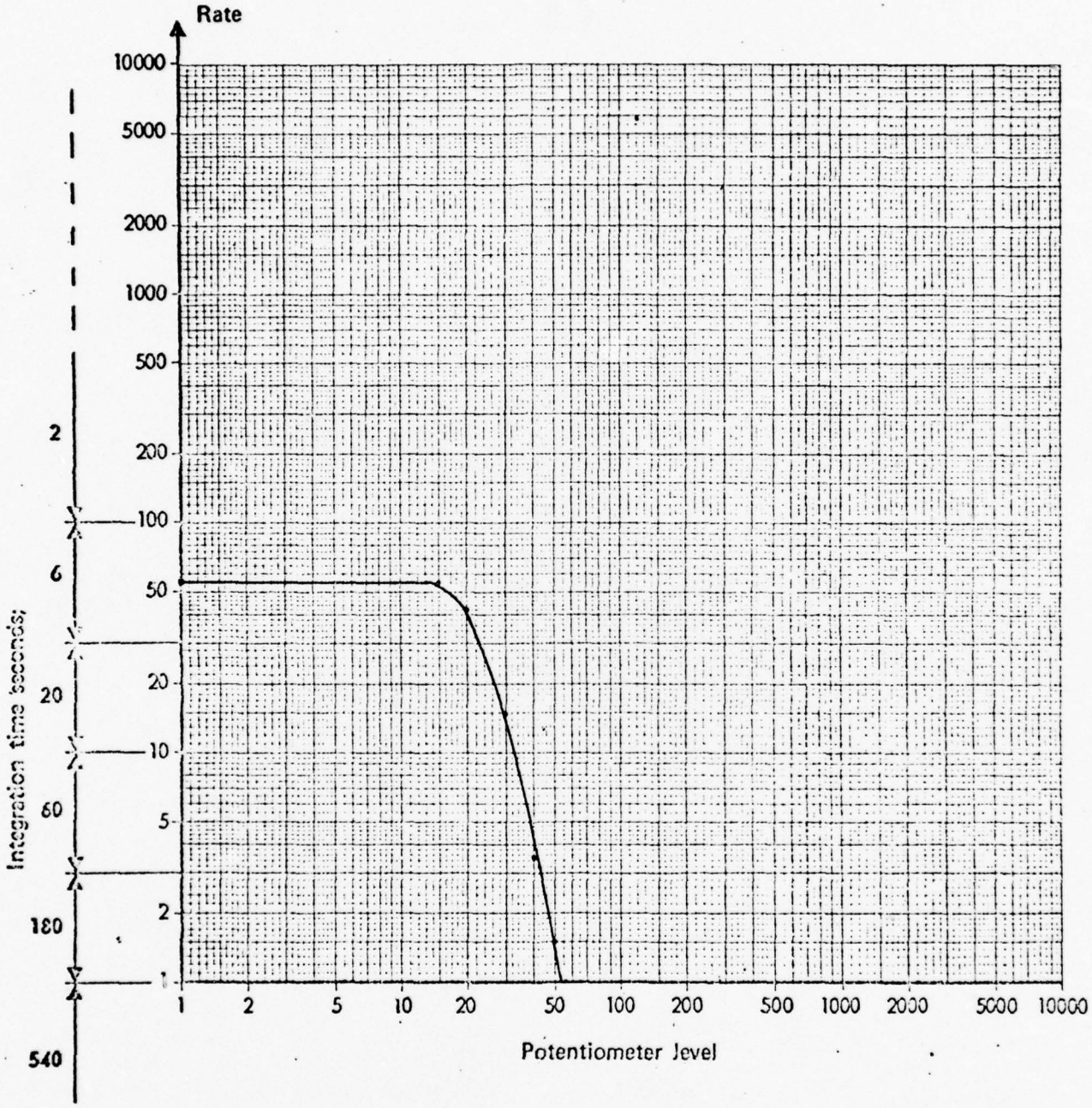

NUMBER 3 HANGER BEARING

UH-1M TAIL #15200

TEST CONDUCTED 6 DEC 1973 AT SCOTT AFB

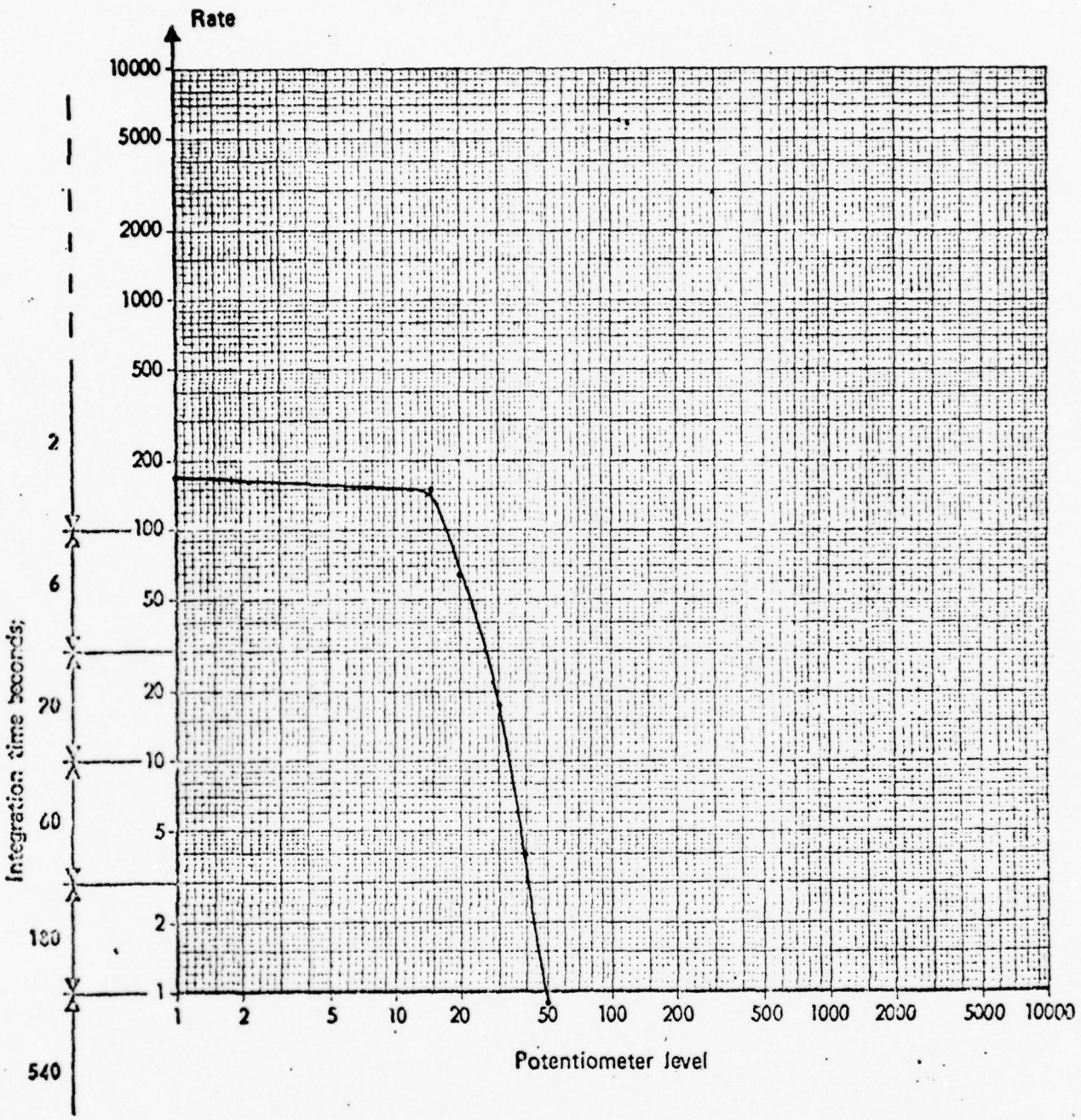

NUMBER 1 HANGER BEARING

UH-1M TAIL #66-15190

TEST CONDUCTED 12 DEC 1973 AT BI-STATE AIRPORT

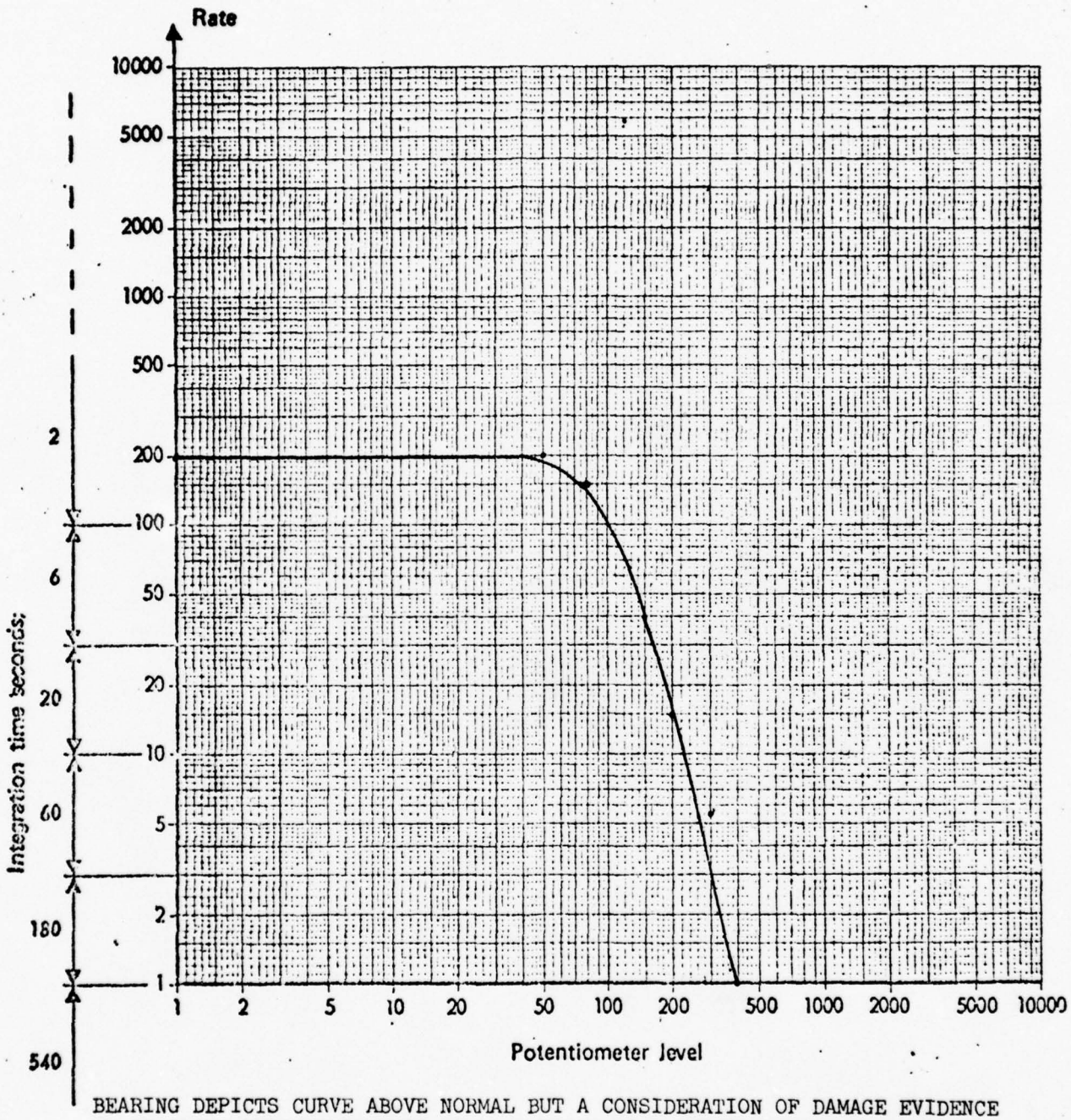


BEARING DEPICTS CURVE ABOVE NORMAL BUT A CONSIDERATION OF DAMAGE EVIDENCE IN TEARDOWN INSPECTION MUST BE MADE PRIOR TO A DETERMINATION THIS BEARING IS EXCESSIVELY DAMAGED.

NUMBER 2 HANGER BEARING

UH-1M TAIL #66-15190

TEST CONDUCTED 12 DEC 1973 AT BI-STATE AIRPORT

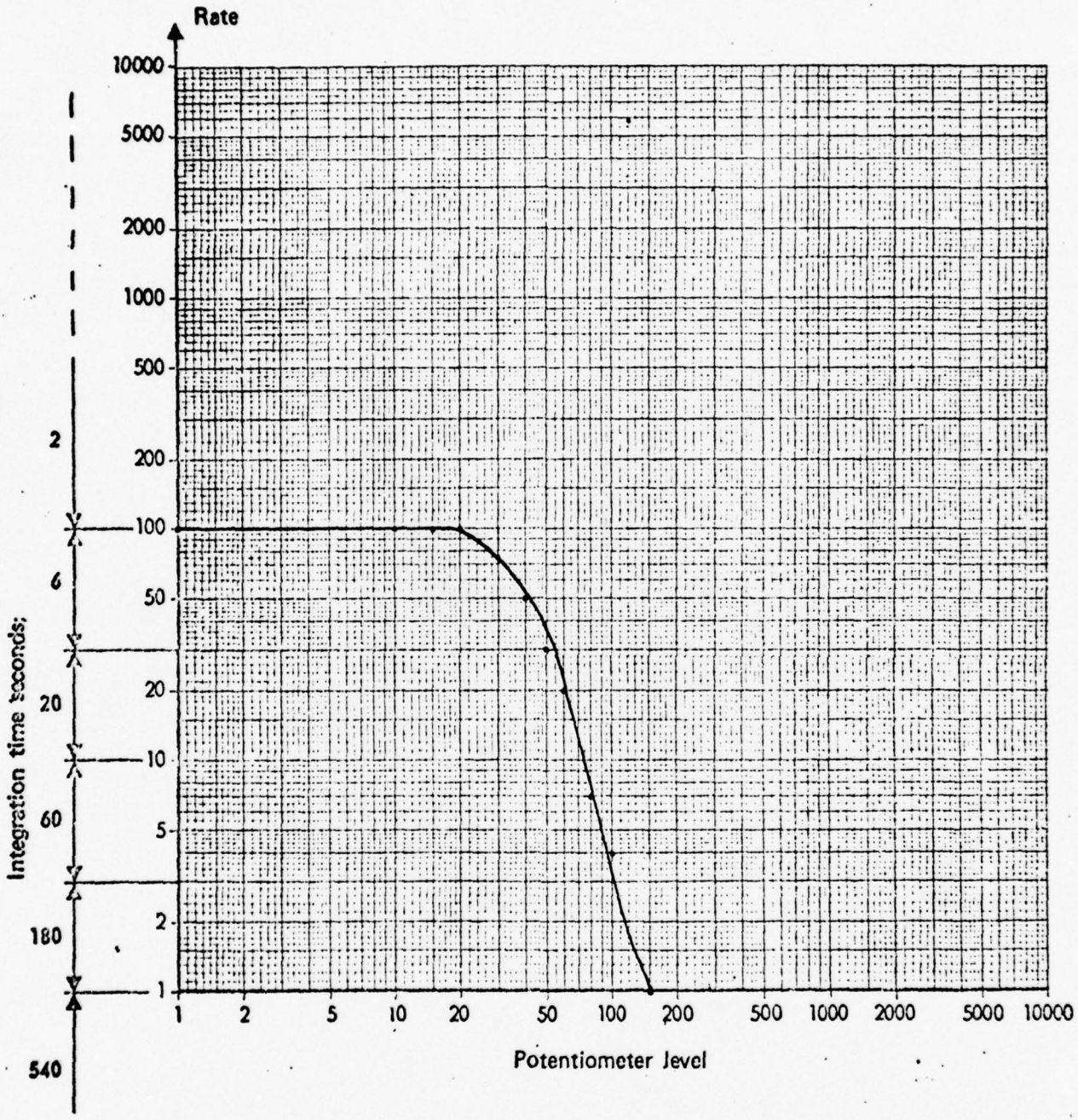


BEARING SHOWED NORMAL RATE AND VALUE.

NUMBER 3 HANGER BEARING

UH-1M TAIL #66-15190

TEST CONDUCTED 12 DEC 1973 AT BI-STATE AIRPORT

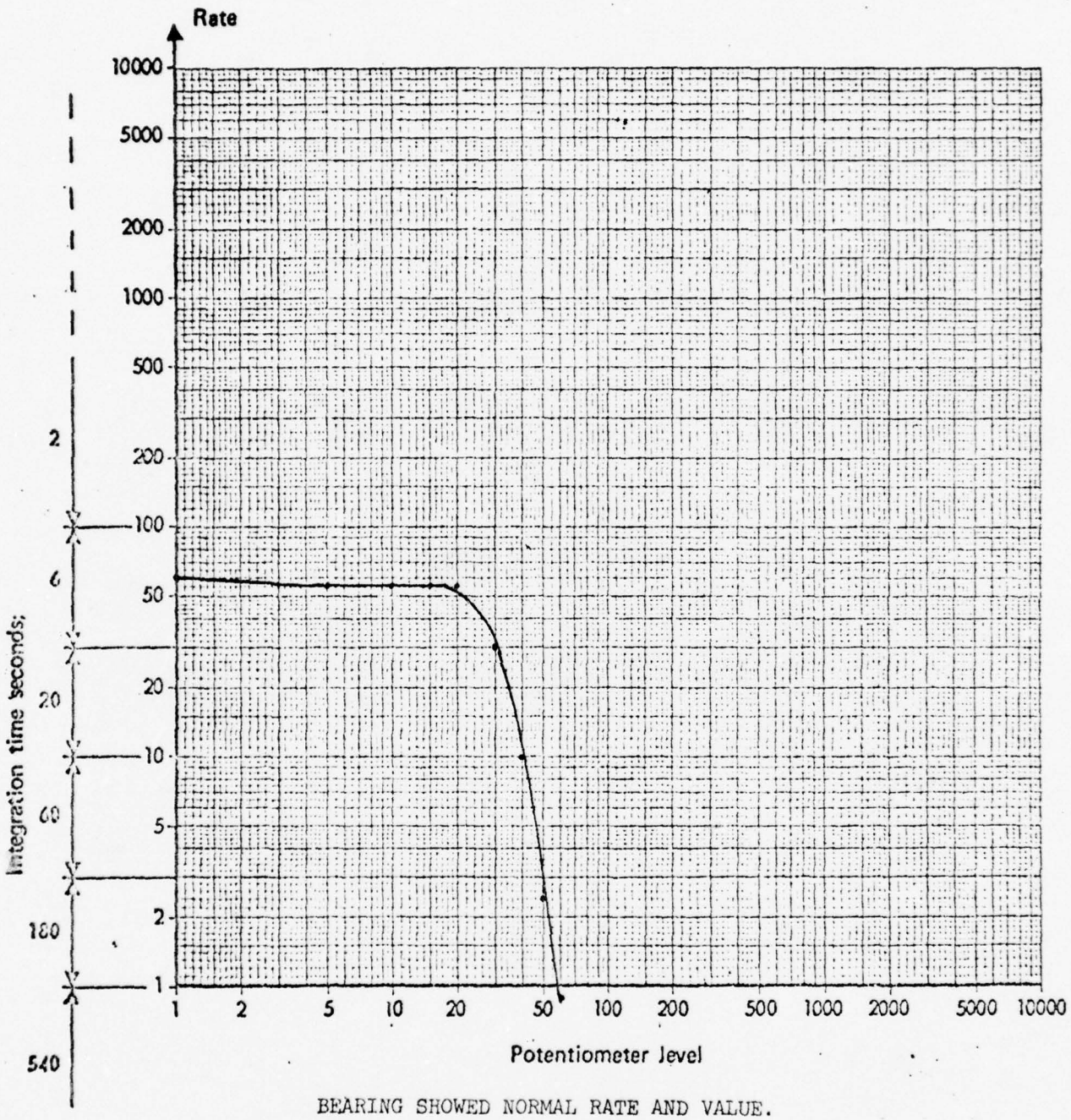


BEARING SHOWED NORMAL RATE AND VALUE.

NUMBER 3 HANGER BEARING

UH-1H TAIL #66-16879

BEARING SERIAL #A20-26745

TEST CONDUCTED 12 DEC 1973 AT BI-STATE AIRPORT

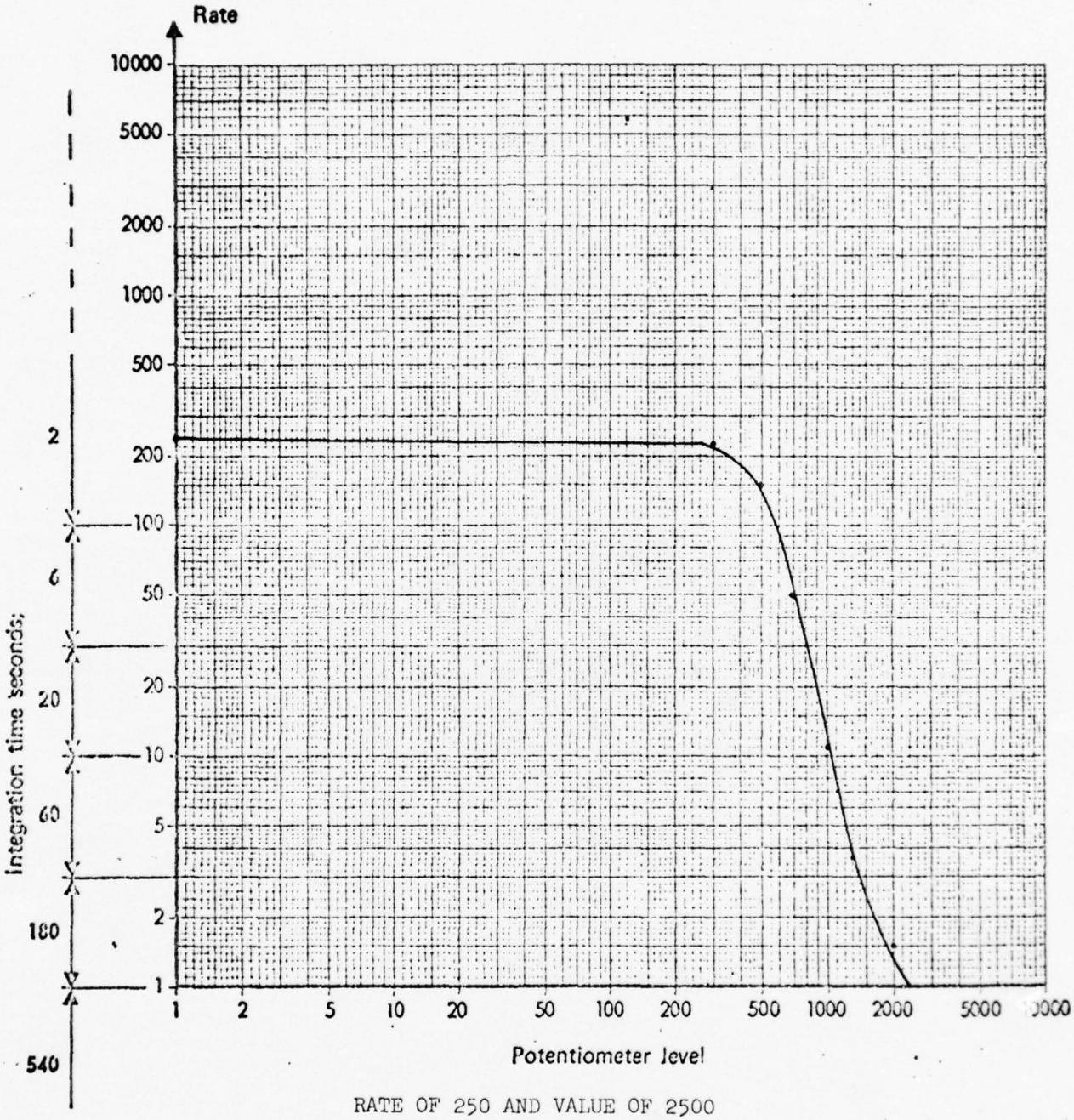


RATE OF 250 AND VALUE OF 2500
BEARING REMOVED FOR ANALYSIS

NUMBER 4 HANGER BEARING

UH-1H TAIL #66-16879

BEARING SERIAL #A20-31225

TEST CONDUCTED 12 DEC 1973 AT RI-STATE AIRPORT

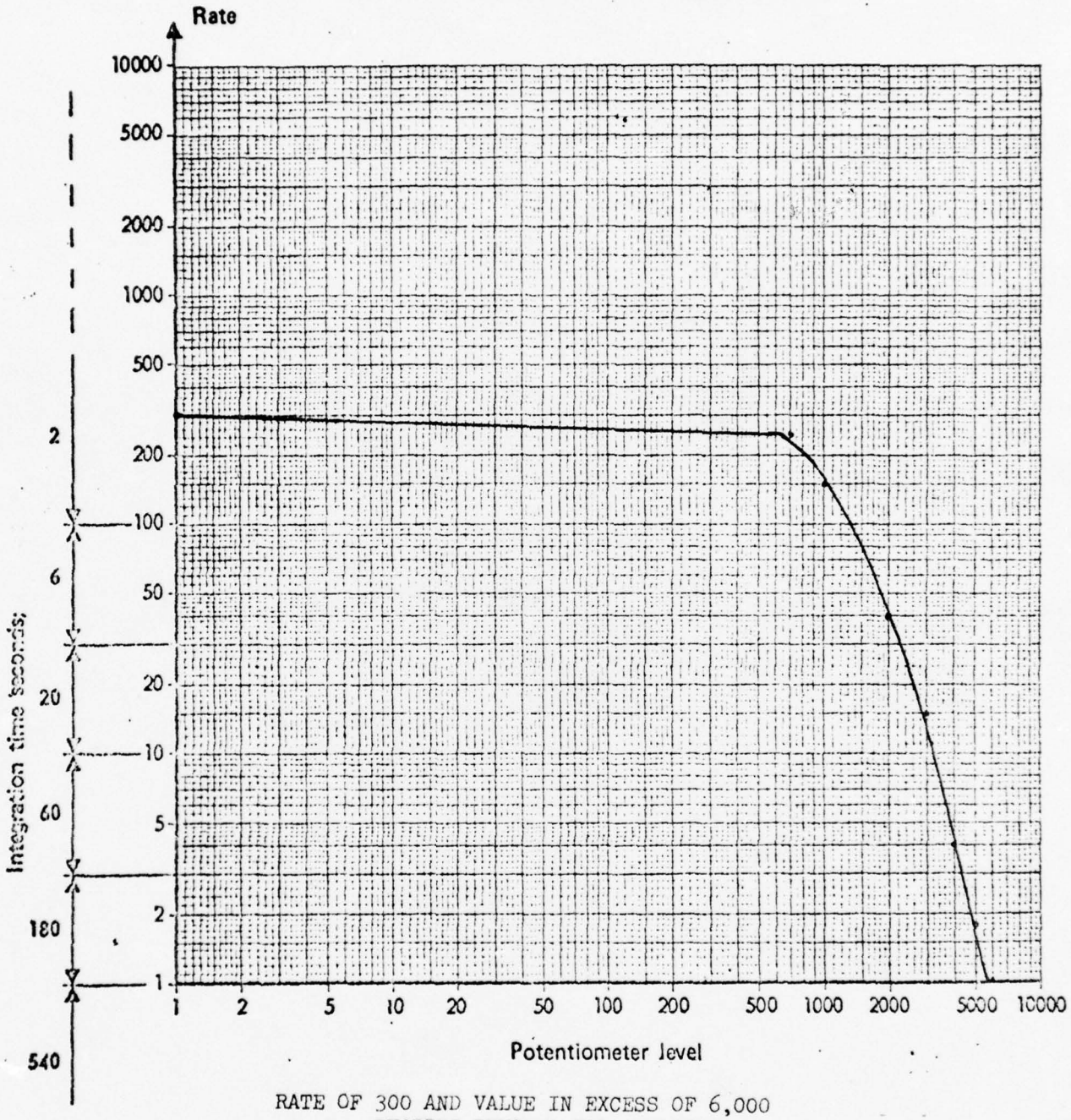


RATE OF 300 AND VALUE IN EXCESS OF 6,000
BEARING REMOVED FOR ANALYSIS

#3 Hanger Bearing
SN A20-36705

A/C 63-8784
6600 RPM $N_2$

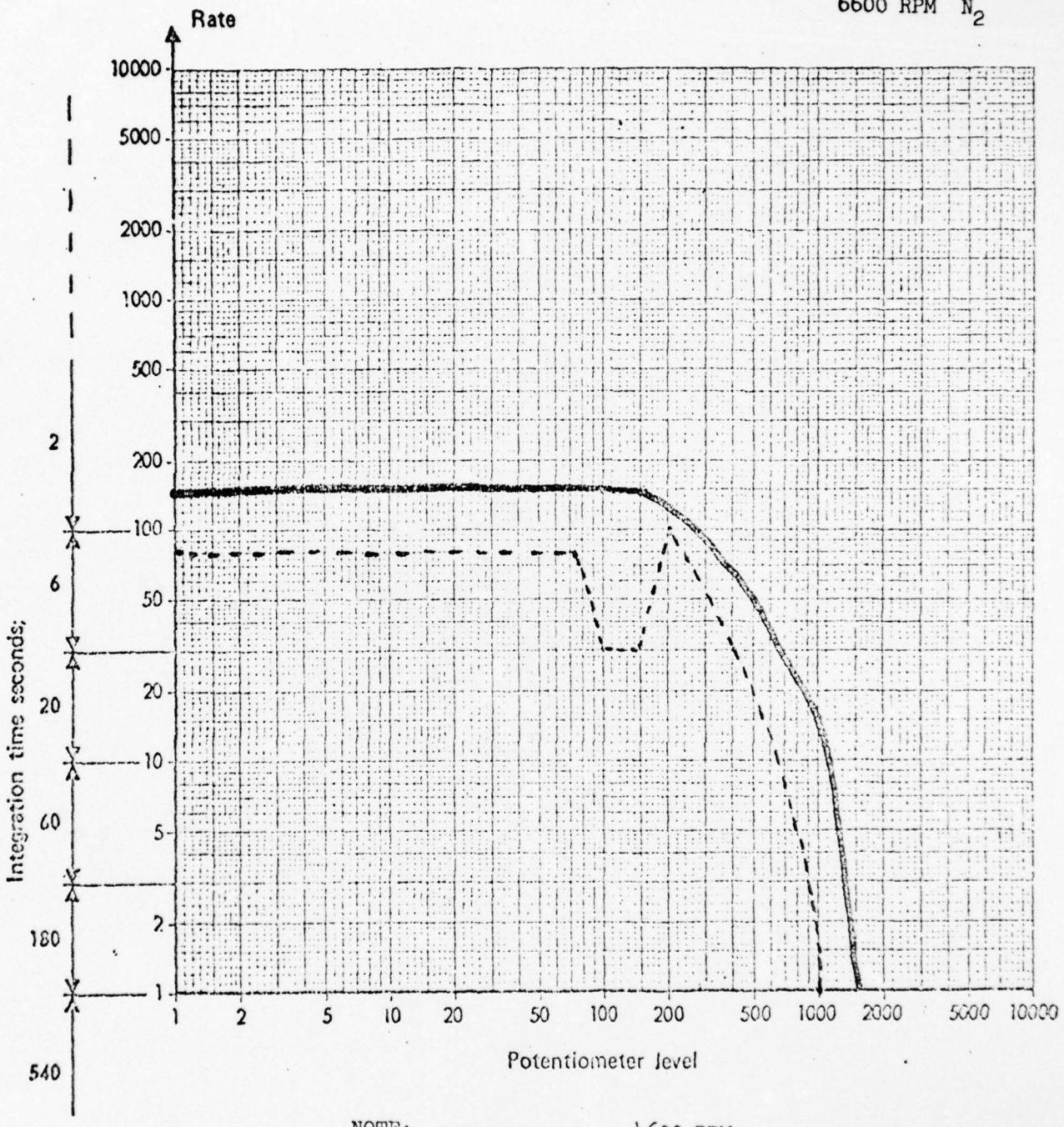


NOTE: ---------- 4600 RPM

_____ 6600 RPM

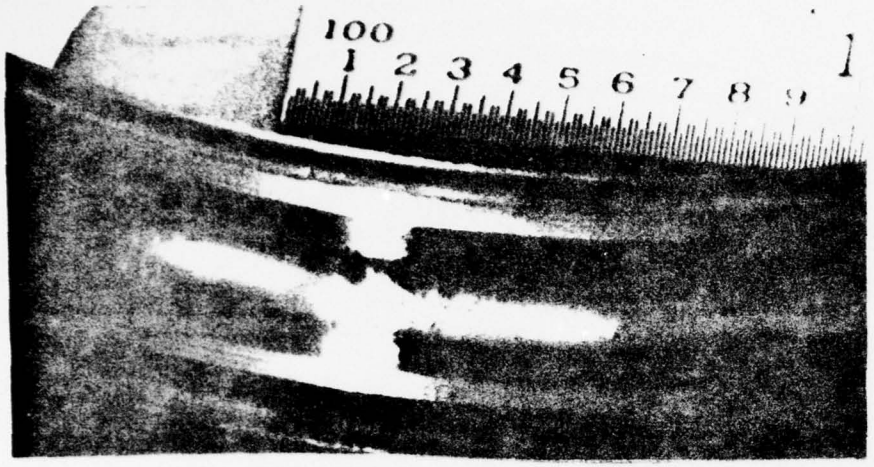


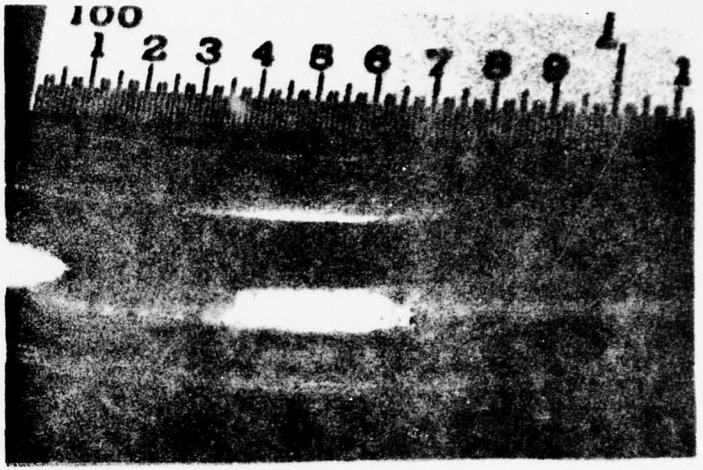


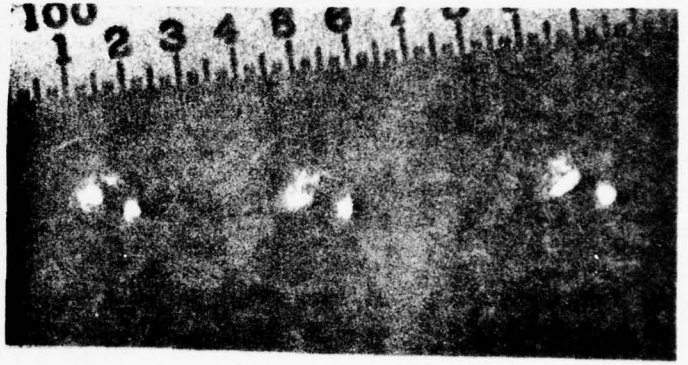


Hanger Bearing
S/N A20-36705
A/C 63-8784

# 4 Hanger Bearing

SN A20-31435

A/C 63-8784

6600 RPM $N_2$

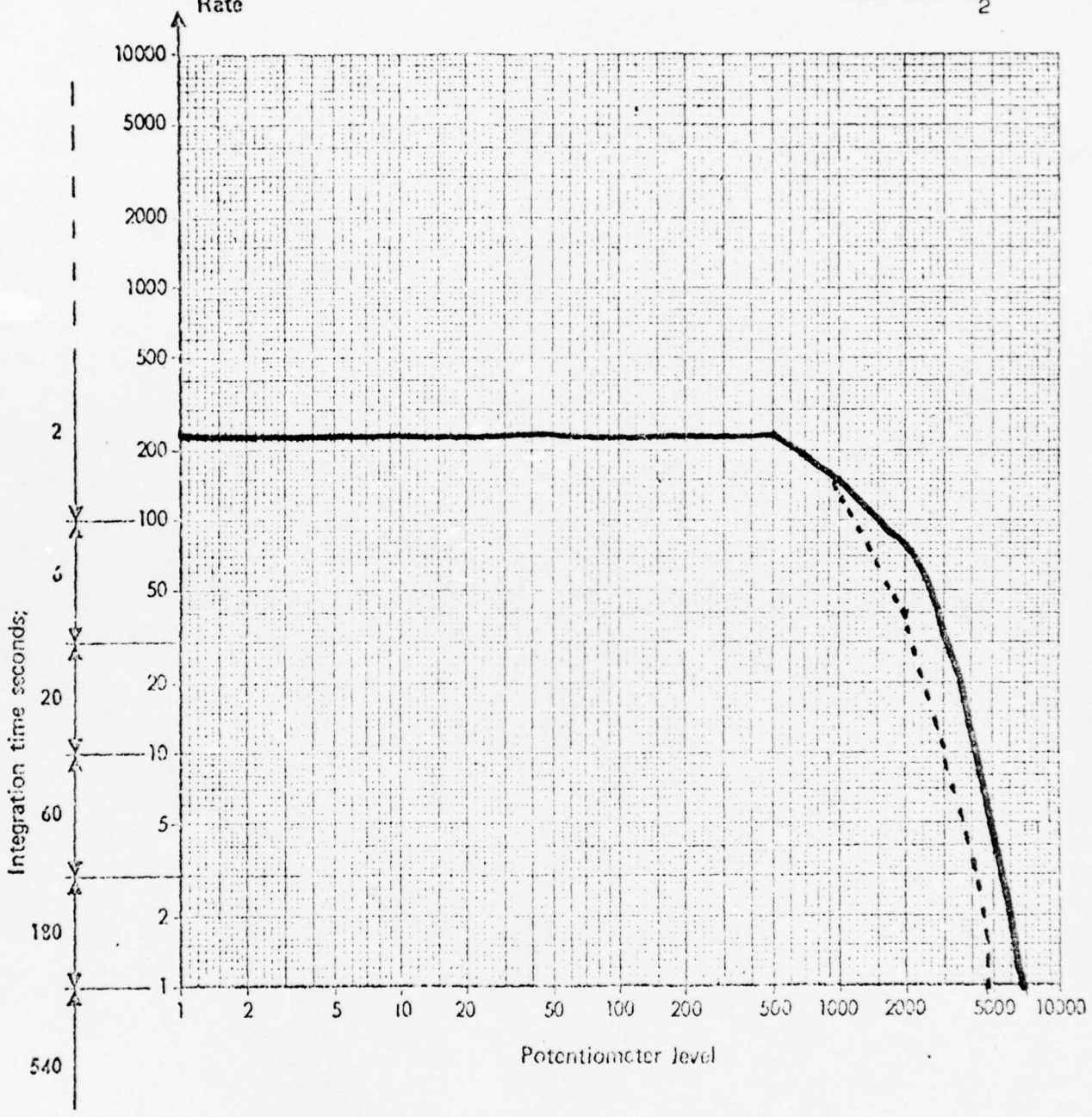


NOTE: _____ 6600

---------- 4600


Hanger Bearing
S/N A20-31435
A/C 63-8784

#3 Hanger Bearing
#4 Hanger Bearing

A/C 64-13740 UH-1H
6600 RPM $N_2$

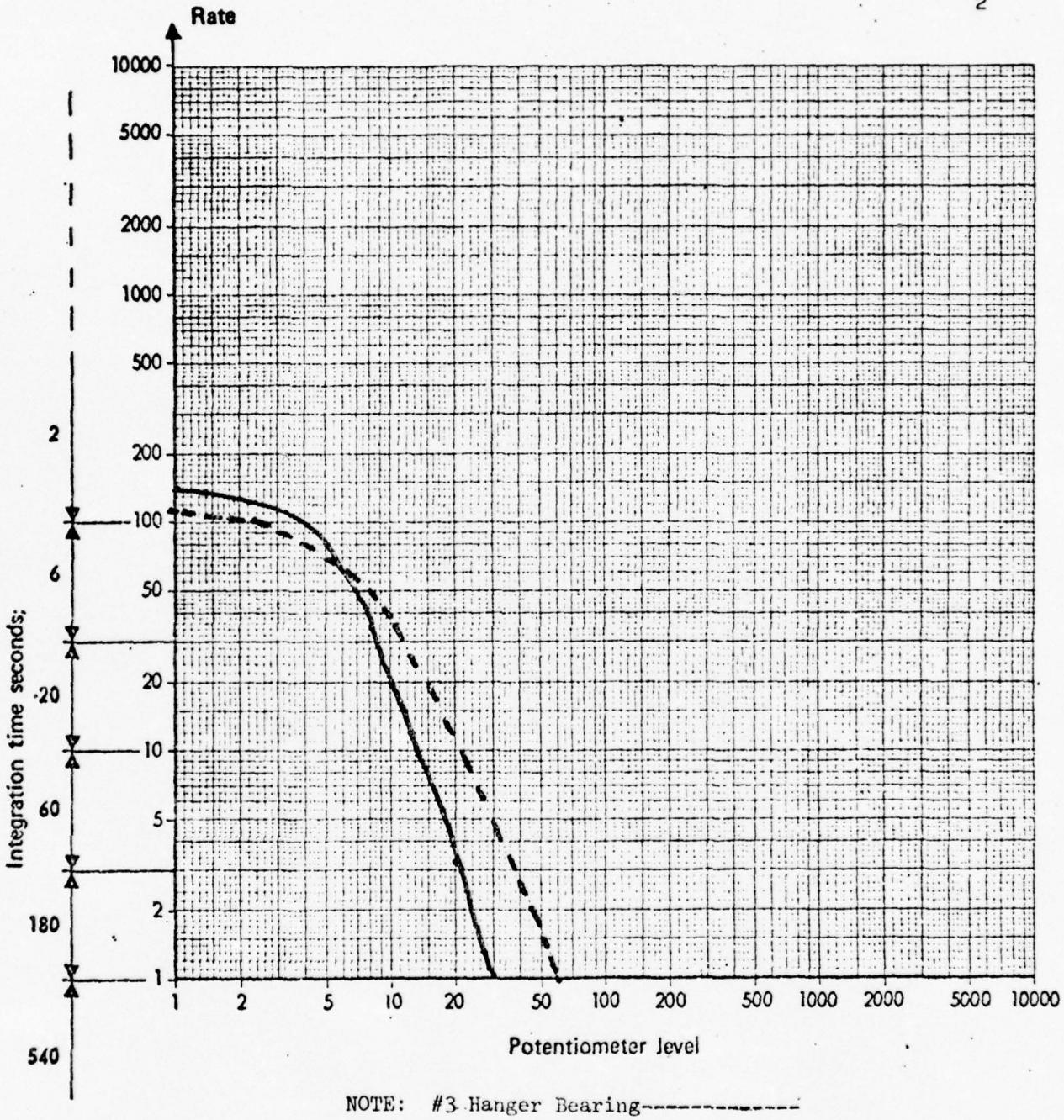


NOTE: #3 Hanger Bearing----------
#4 Hanger Bearing_____

281st Aviation Company Bi State Airport 1 Aug 74

#1 Hanger Bearing
#2 Hanger Bearing
#3 Hanger Bearing

A/C 66-15200 UH-1M
6600 RPM $N_2$

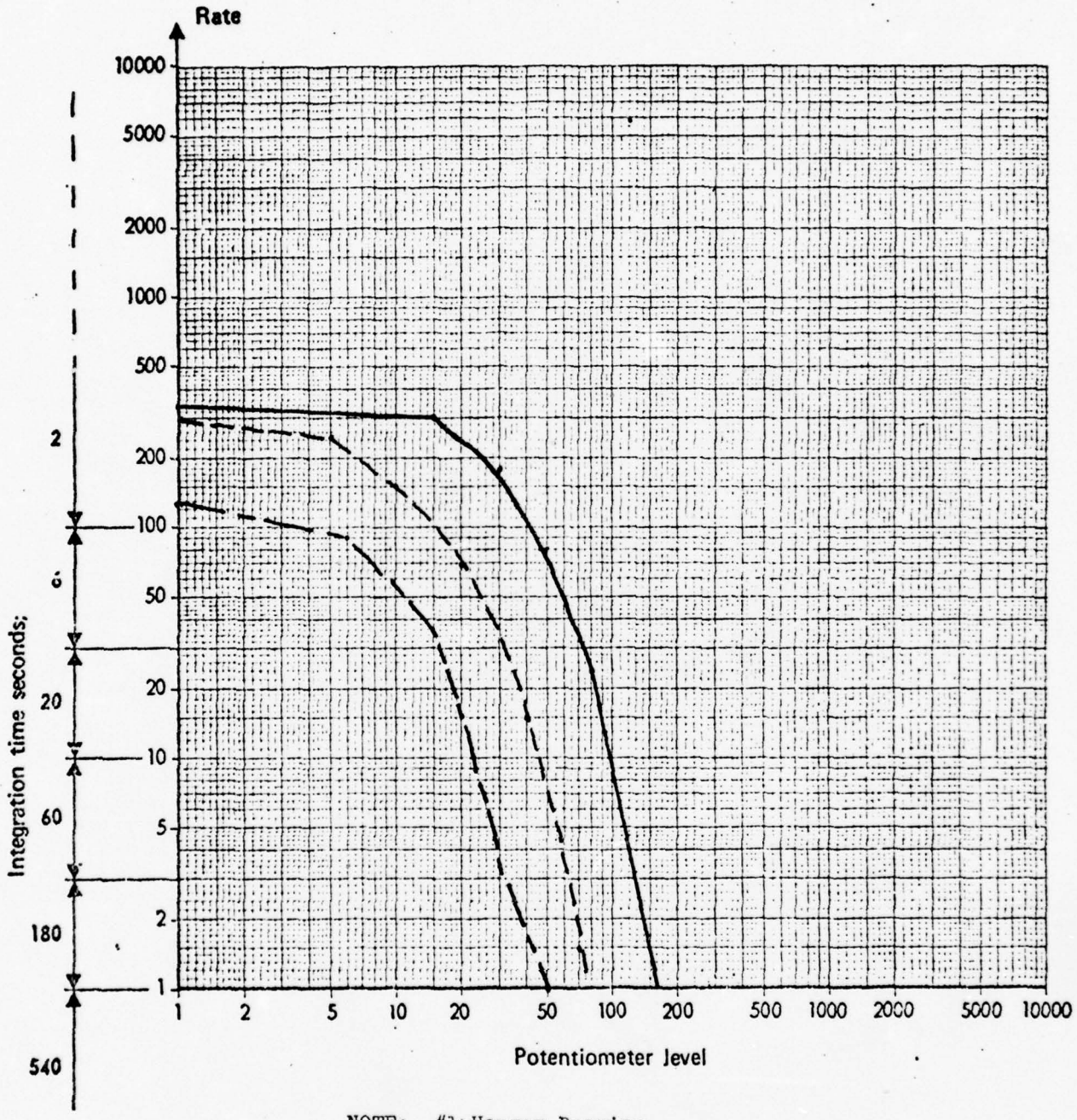


NOTE: #1 Hanger Bearing_____
#2 Hanger Bearing----------
#3 Hanger Bearing _____ - _____ - _____

281st Aviation Company Bi State Airport 8 Aug 74

#1 Hanger Bearing A20-44891
#2 Hanger Bearing A20-57910
#3 Hanger Bearing A20-26938

A/C 65-9519 UH-1M
6600 RPM $N_2$

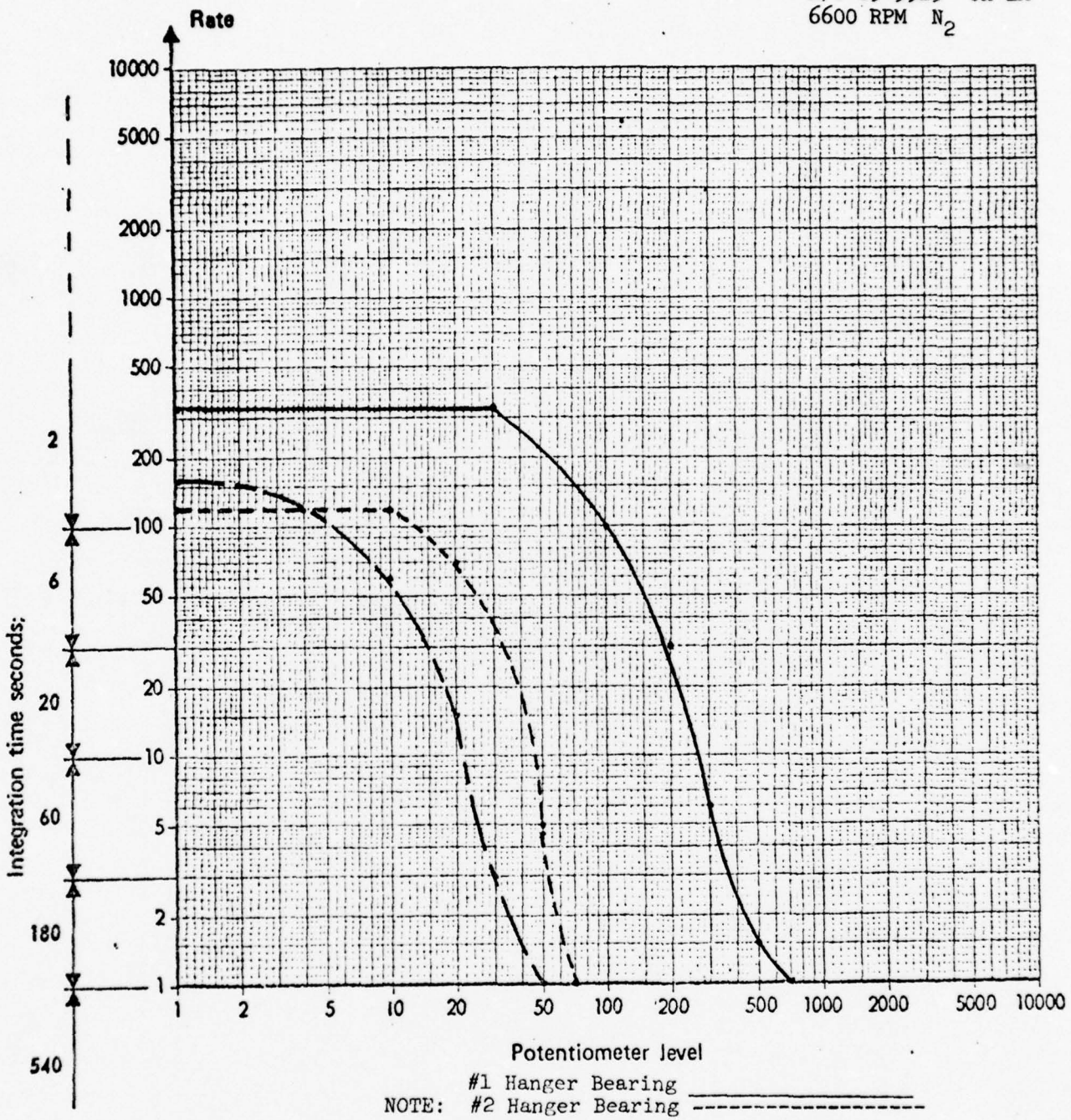


NOTE: #1 Hanger Bearing _____
#2 Hanger Bearing ----------
#3 Hanger Bearing ___ - ___ - ___ -

#1 Hanger Bearing

A/C UH-1M 66-15091
6600 RPM $N_2$

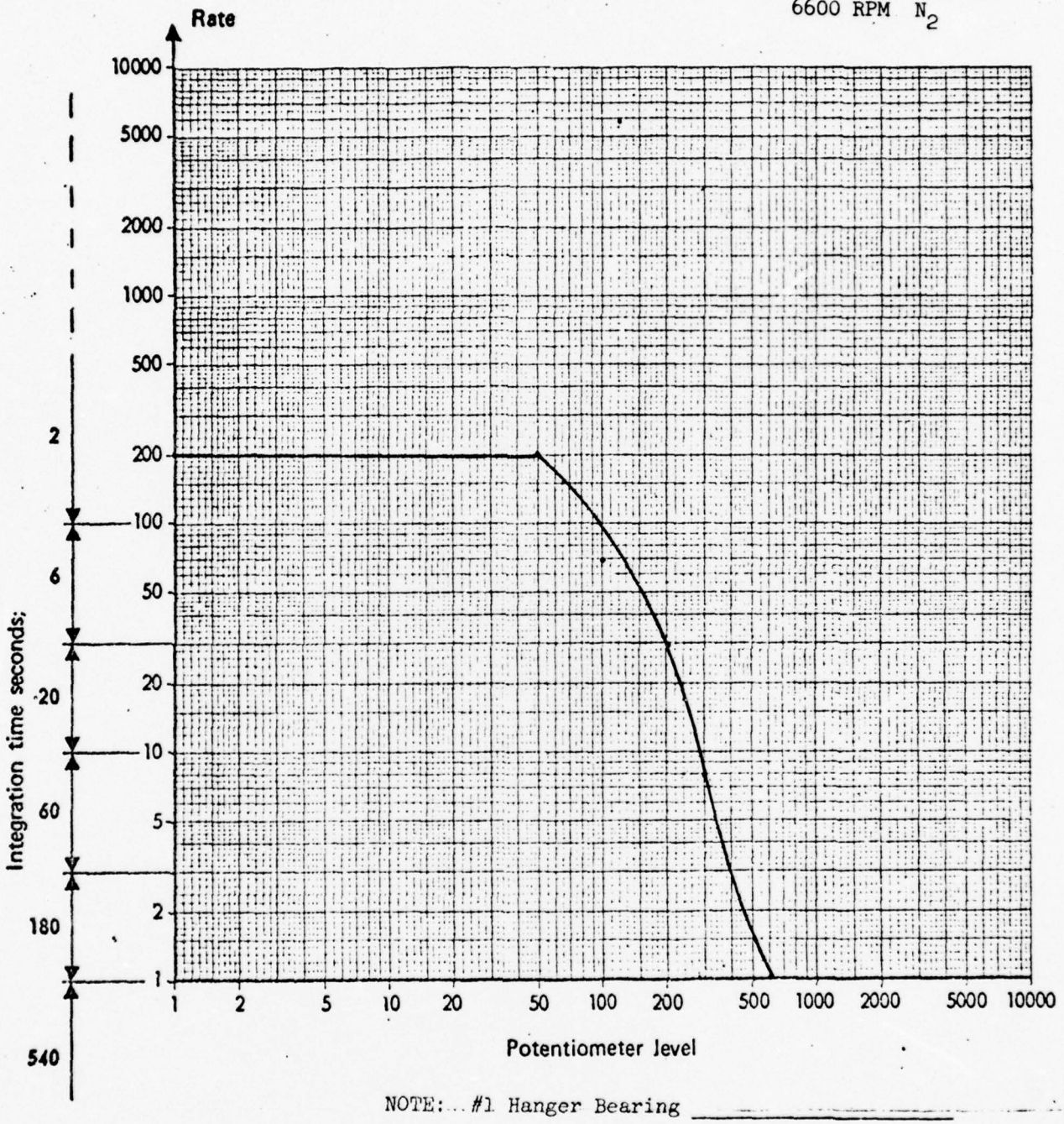


NOTE: #1 Hanger Bearing

#3 Hanger Bearing A20-64529
#2 Hanger Bearing A20-52529

A/C 66-0529 UH-1M
6600 RPM $N_2$

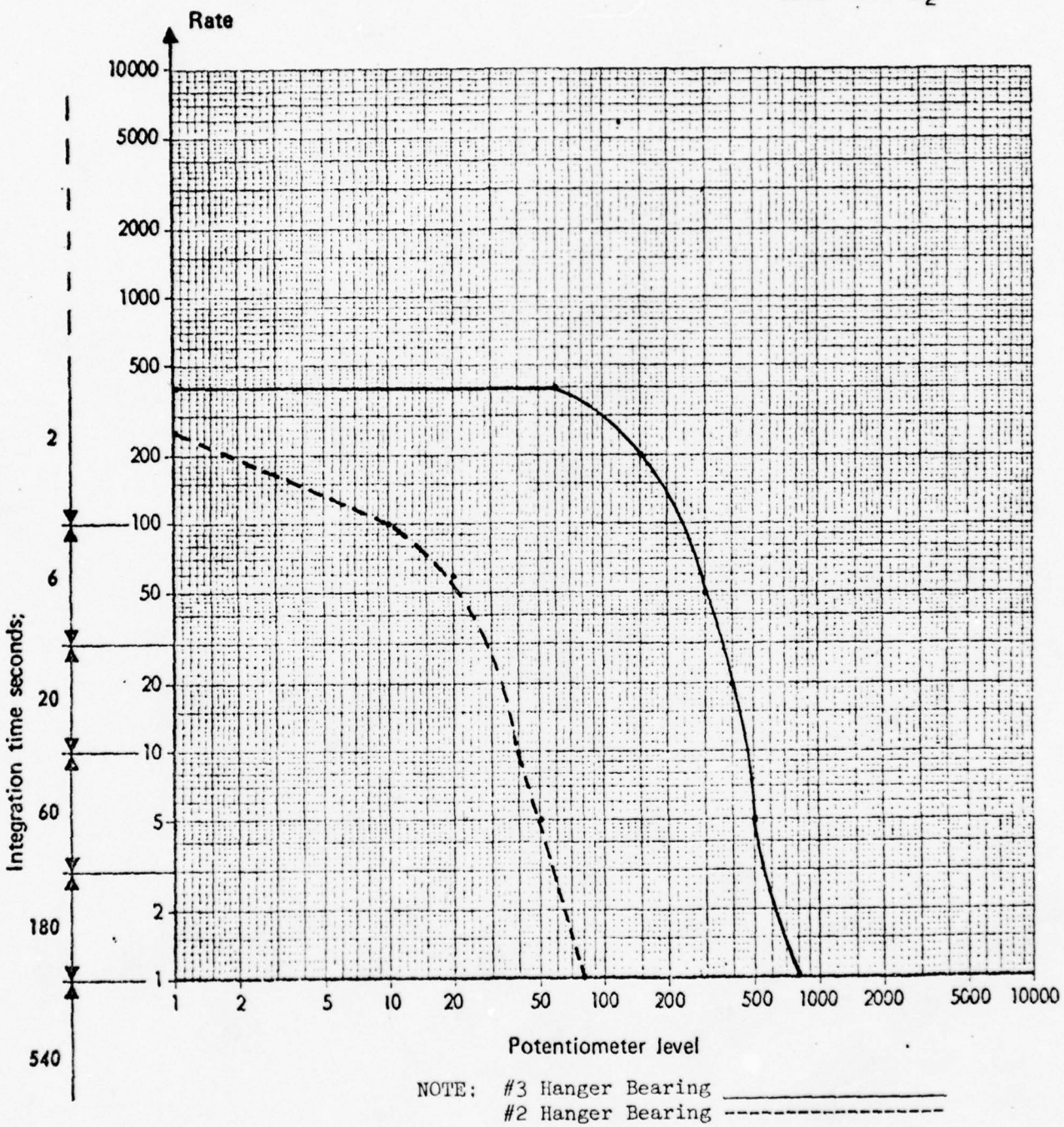


NOTE: #3 Hanger Bearing _____
#2 Hanger Bearing ----------

#3 Hanger Bearing A20-43493

A/C 65-9884 UH-1D
6600 RPM $N_2$

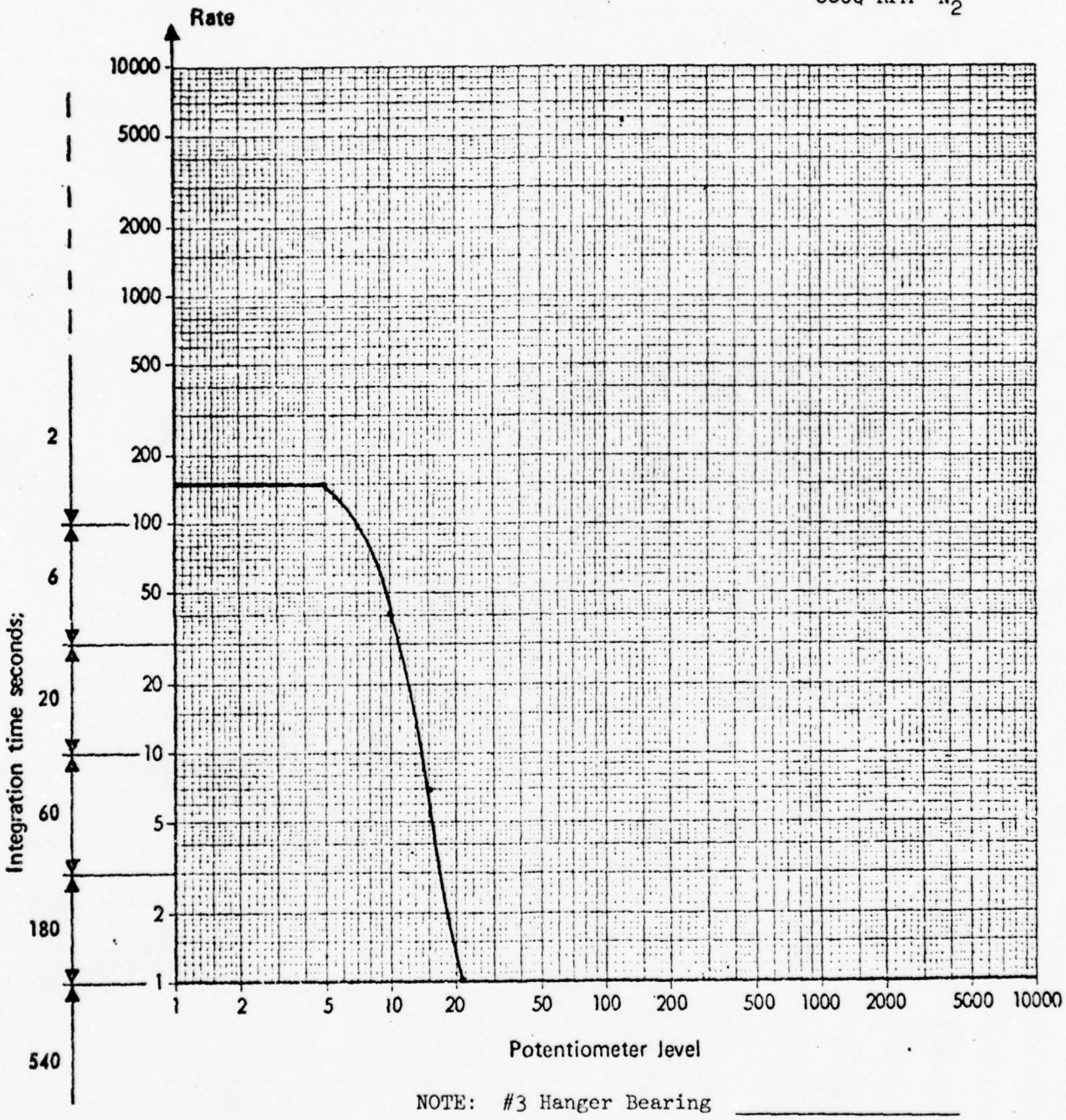


NOTE: #3 Hanger Bearing _____

#2 Hanger Bearing
#3 Hanger Bearing

A/C UH-1C 60630
6600 RPM $N_2$

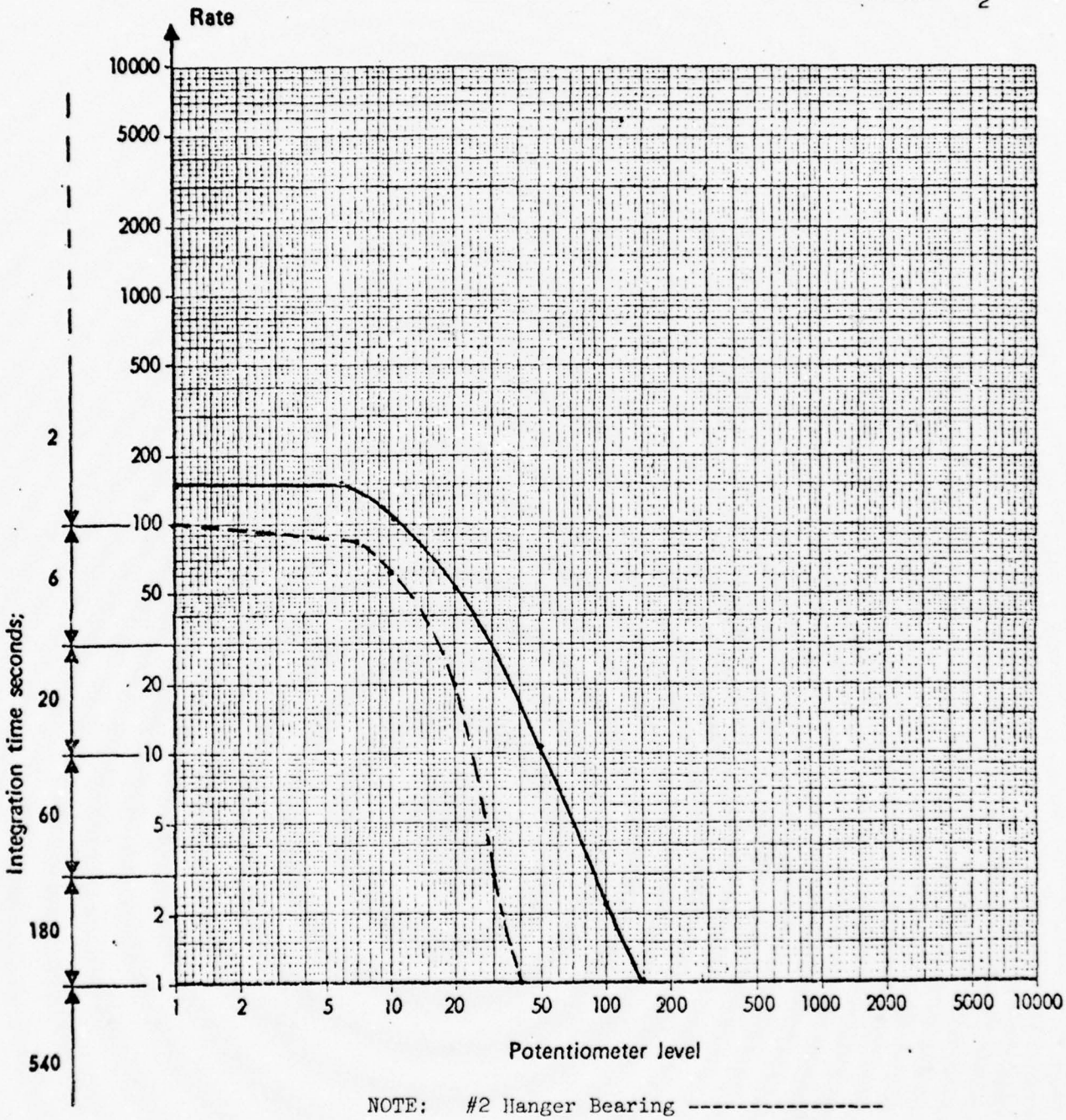


NOTE: #2 Hanger Bearing ----------
#3 Hanger Bearing _____

#1 Hanger Bearing
#2 Hanger Bearing A20-15990
#3 Hanger Bearing A20-31517

A/C 66-15071 UH-1C
6600 RPM $N_2$

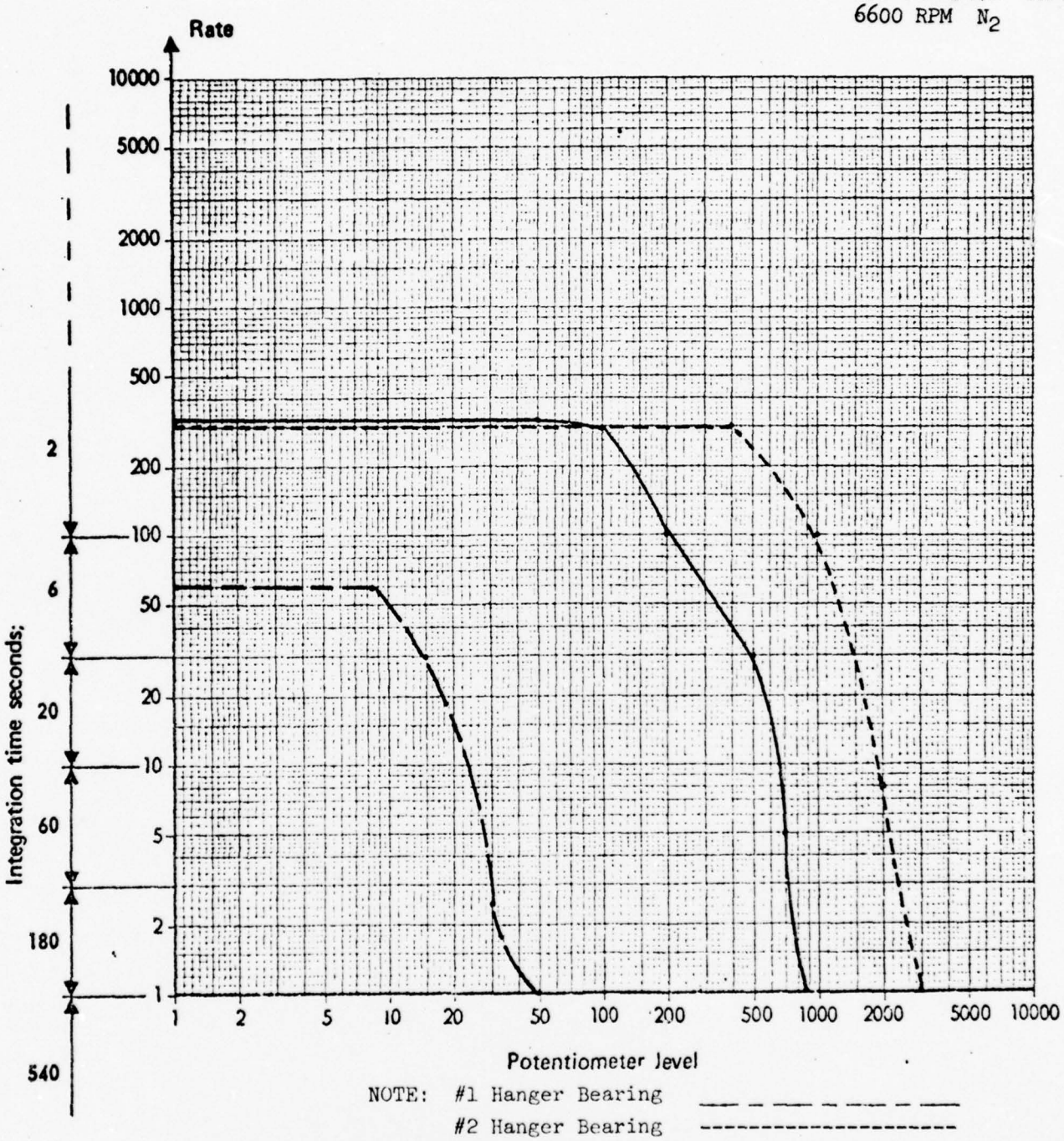


NOTE: #1 Hanger Bearing _ _ _ _ _ _ _
#2 Hanger Bearing ----------
#3 Hanger Bearing _____

#1 Hanger Bearing

A/C UH-1C 60630
6600 RPM $N_2$

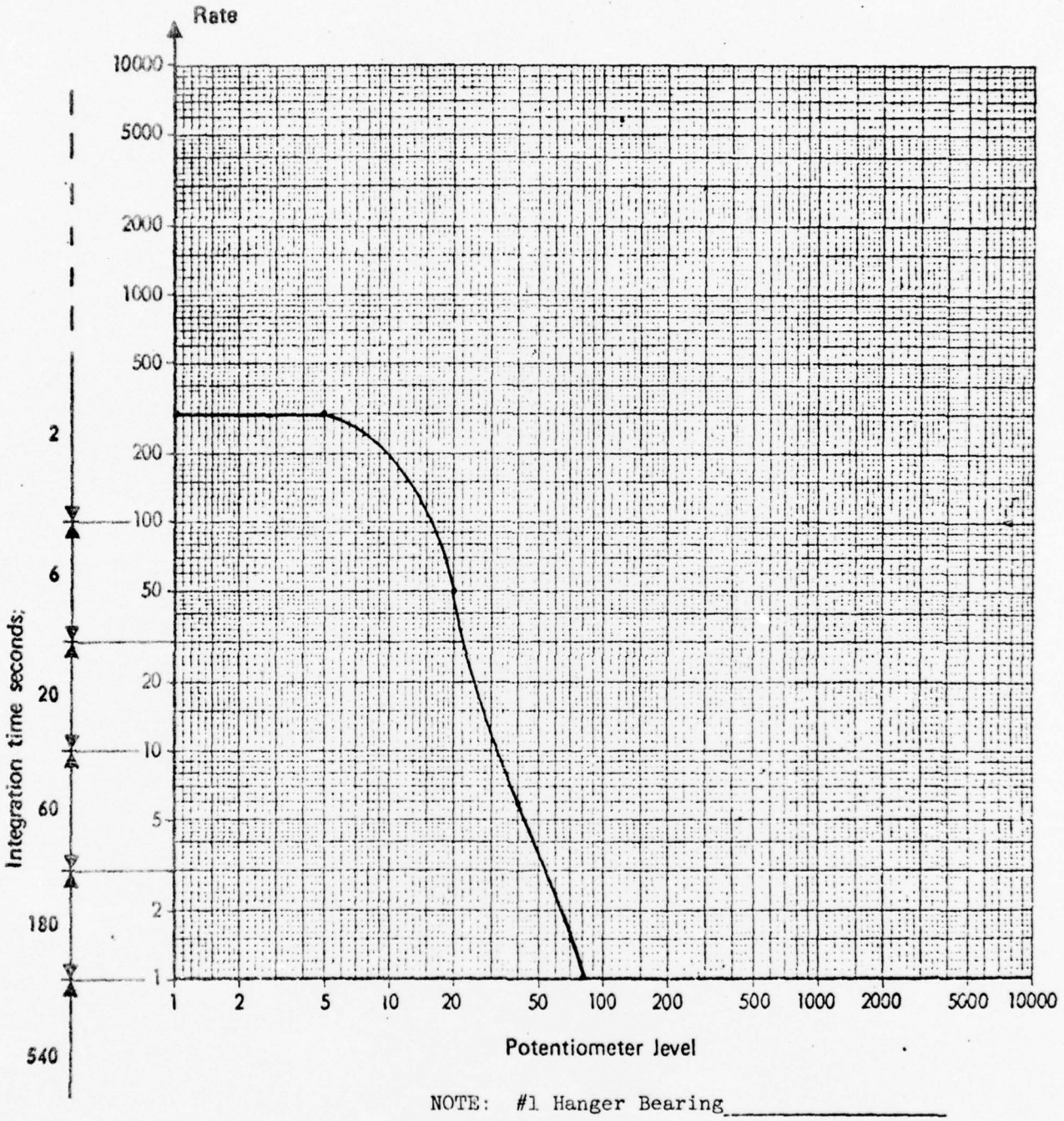


NOTE: #1 Hanger Bearing_____

#1 Hanger Bearing
SN A20-55389

A/C 69-15949
6600 RPM $N_2$

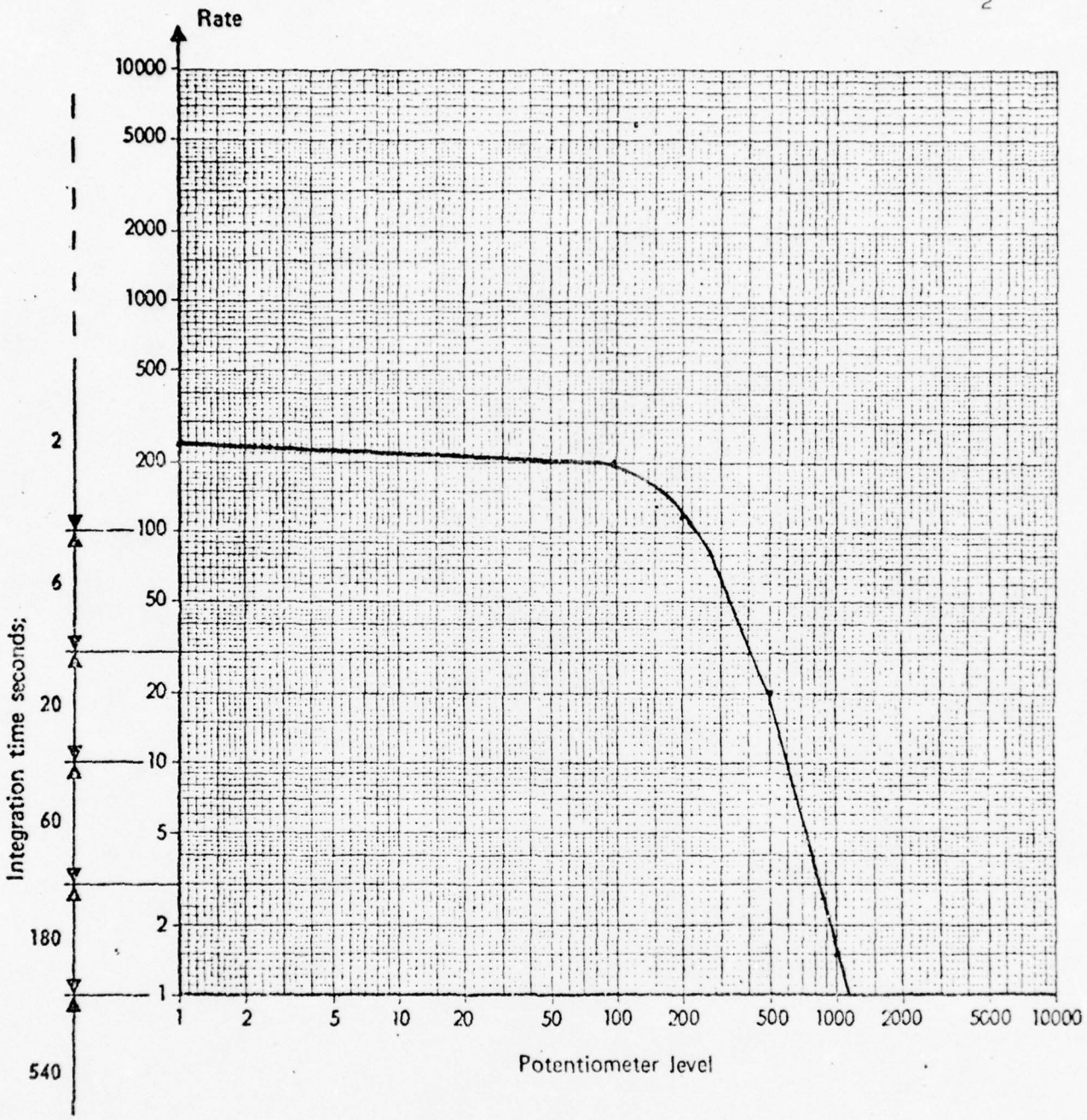


Hanger Bearing
P/N A20-55389
A/C 69-15949

42° GEARBOX

UH-1H TAIL #13740

TEST CONDUCTED 27 NOV 1973 AT SCOTT AFB

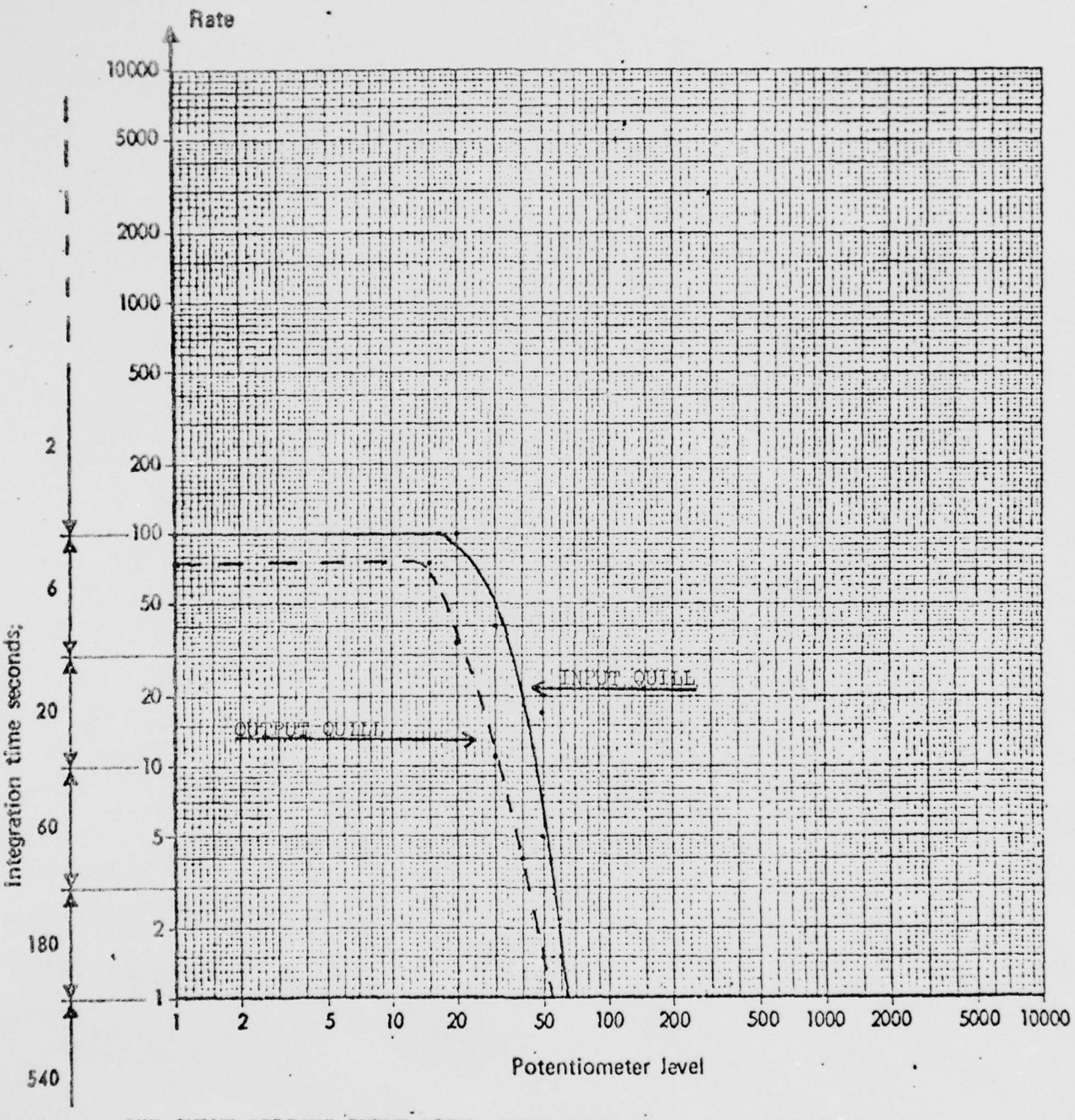


ONE CURVE DEPICTS INPUT DIRVE QUILL, THE OTHER THE OUTPUT DRIVE QUILL

42° GEARBOX

UH-1H TAIL #16197

TEST CONDUCTED 27 NOV 1973 AT SCOTT AFB

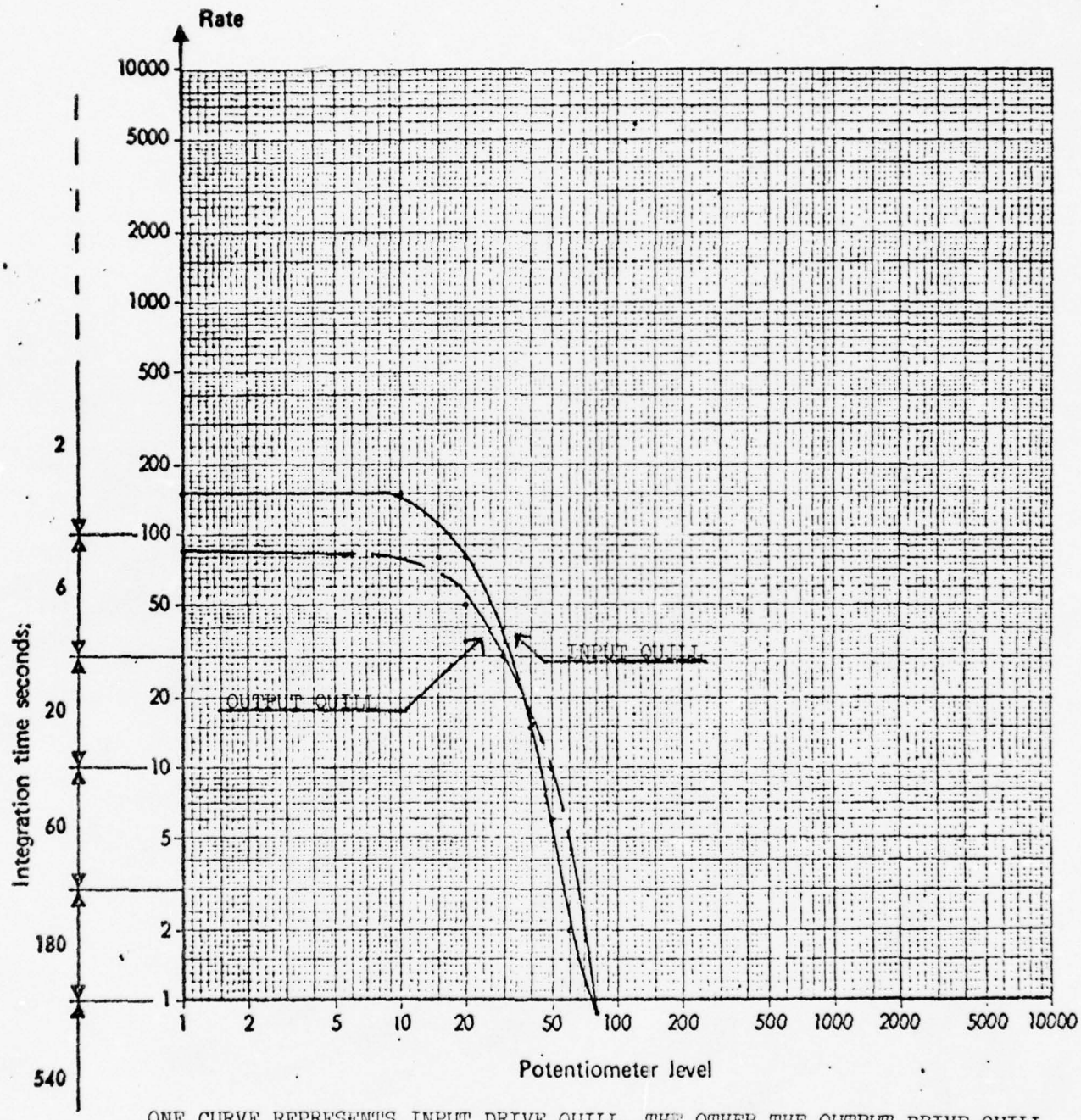


ONE CURVE REPRESENTS INPUT DRIVE QUILL, THE OTHER THE OUTPUT DRIVE QUILL.

42° GEARBOX

UH-1H TAIL #66-01087

INPUT DRIVE QUILL

TEST CONDUCTED 28 NOV 1973 AT SCOTT AFB

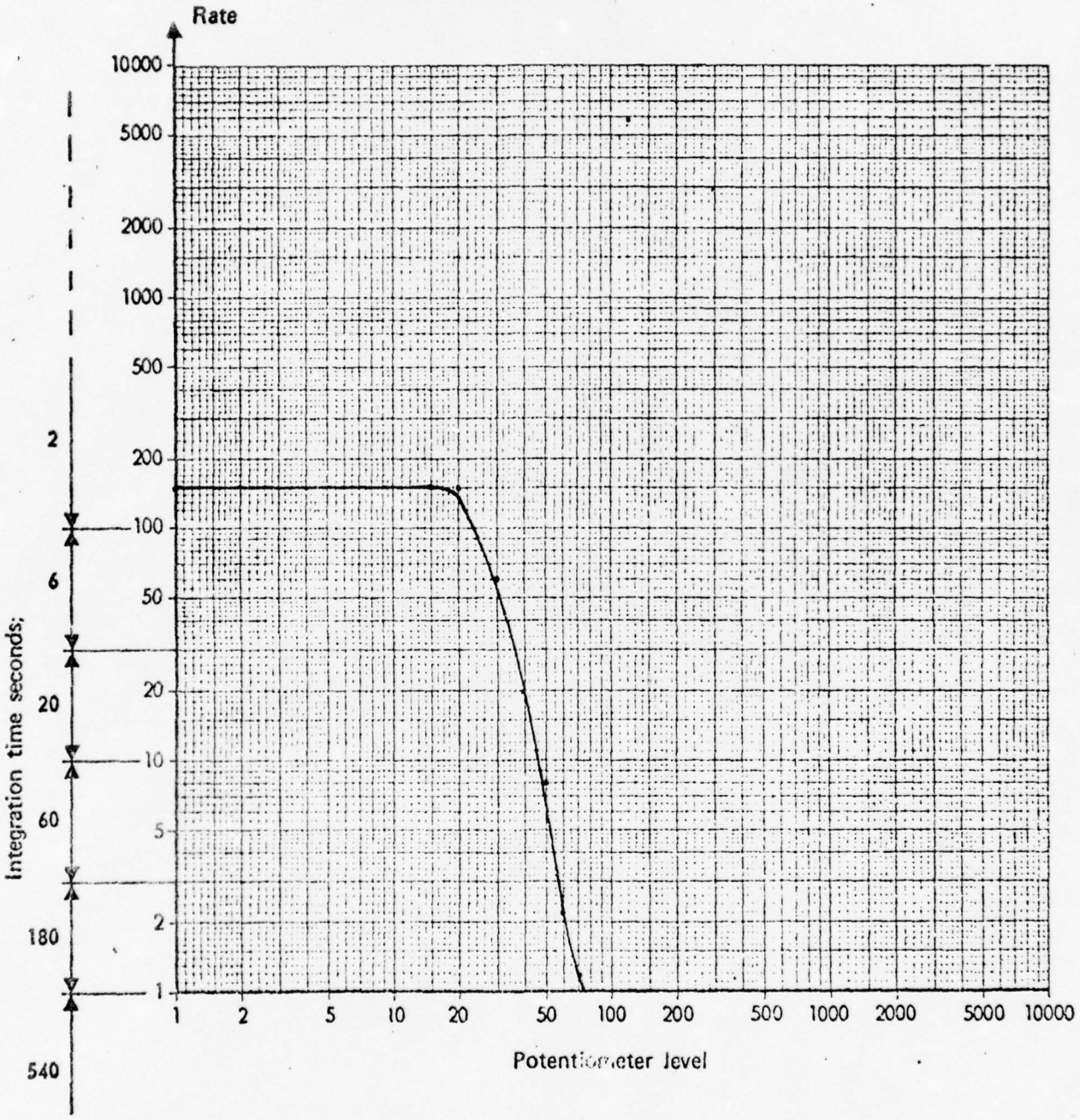

42° GEARBOX

UH-1H TAIL #15949

TEST CONDUCTED 28 NOV 1973 AT SCOTT AFB

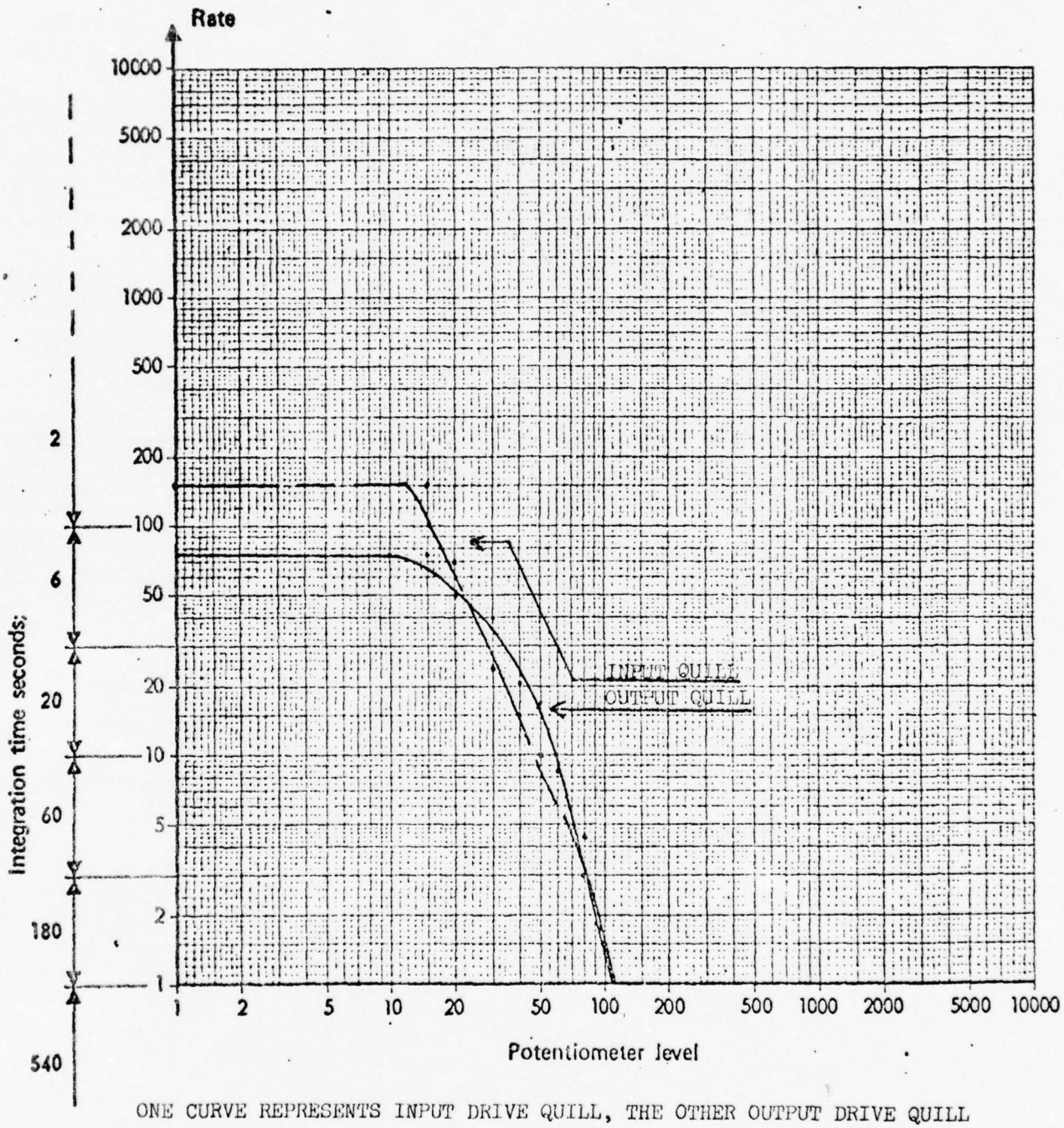


ONE CURVE REPRESENTS INPUT DRIVE QUILL, THE OTHER OUTPUT DRIVE QUILL

42° GEARBOX UH-1M TAIL #59519

TEST CONDUCTED 30 NOV 1973 AT SCOTT AFB

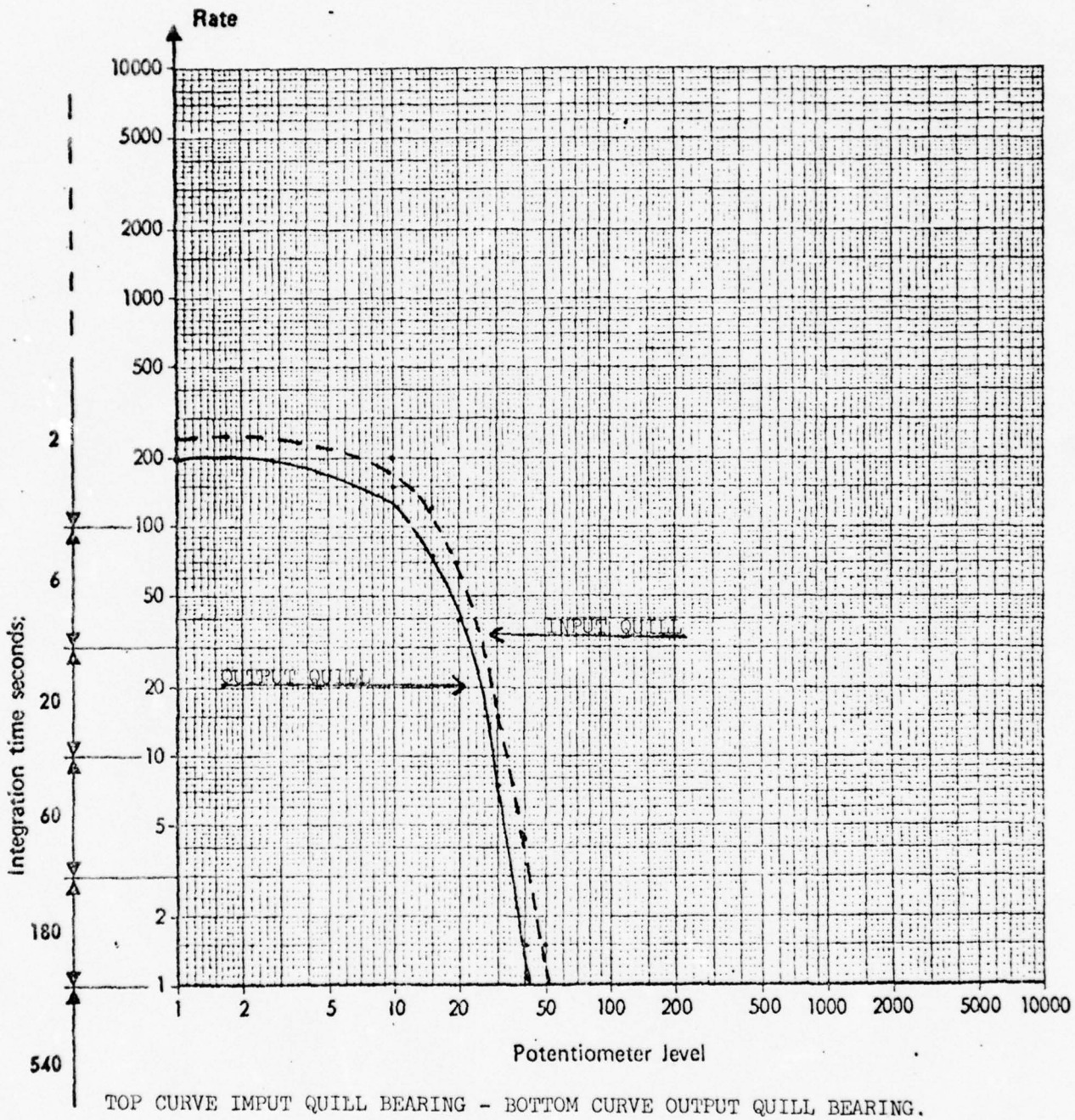


TOP CURVE IMPUT QUILL BEARING - BOTTOM CURVE OUTPUT QUILL BEARING.

42° GEARBOX

UH-1M TAIL #15200

TEST CONDUCTED 6 DEC 1973 AT SCOTT AFB

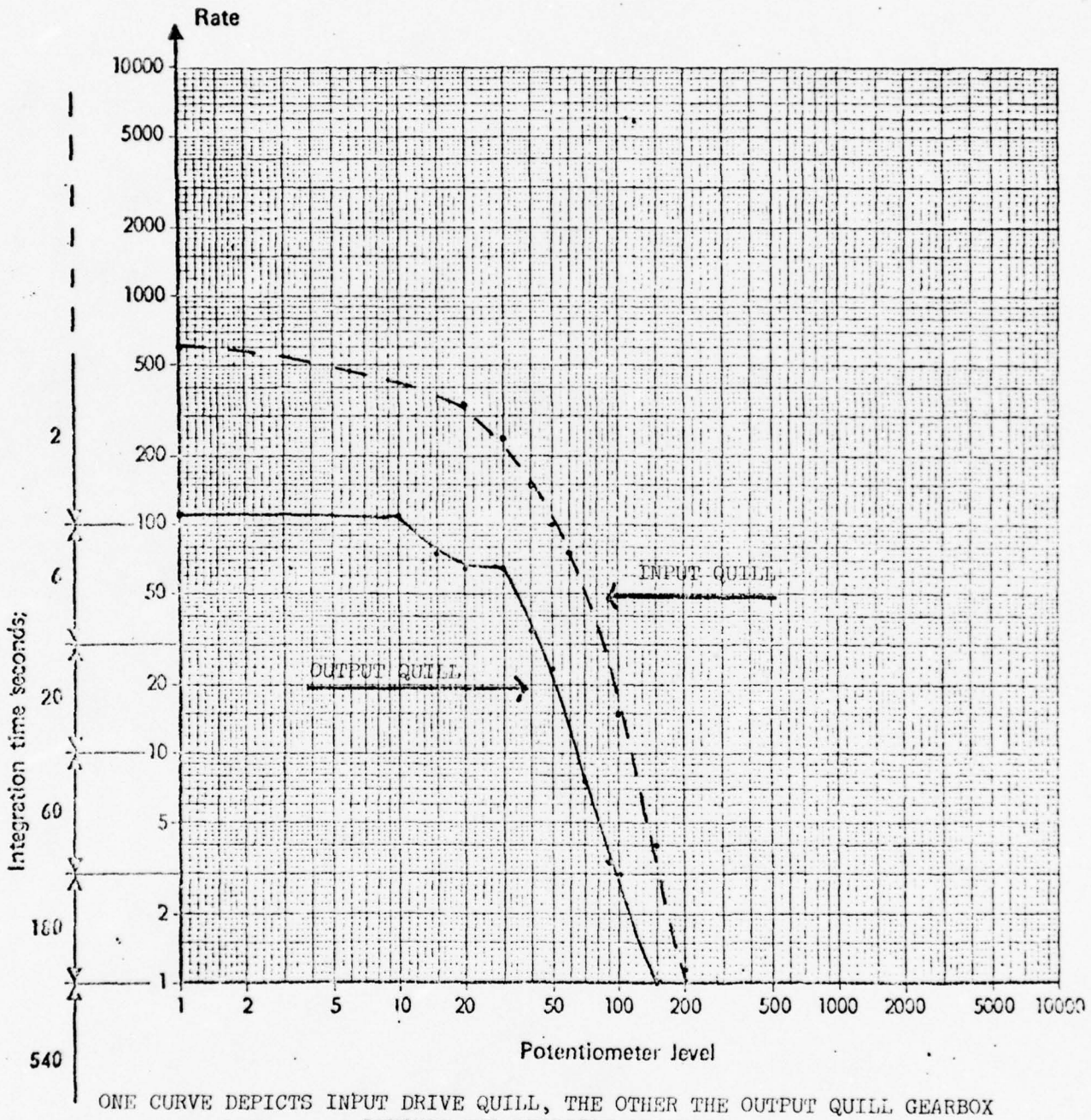


ONE CURVE DEPICTS INPUT DRIVE QUILL, THE OTHER THE OUTPUT QUILL GEARBOX REMOVED FOR TEARDOWN ANALYSIS.

ABB6012 - GEARBOX SERIAL NUMBER

42° GEARBOX

UH-1H TAIL #69-15771

TEST CONDUCTED 6 DEC 1973 AT SCOTT AFB

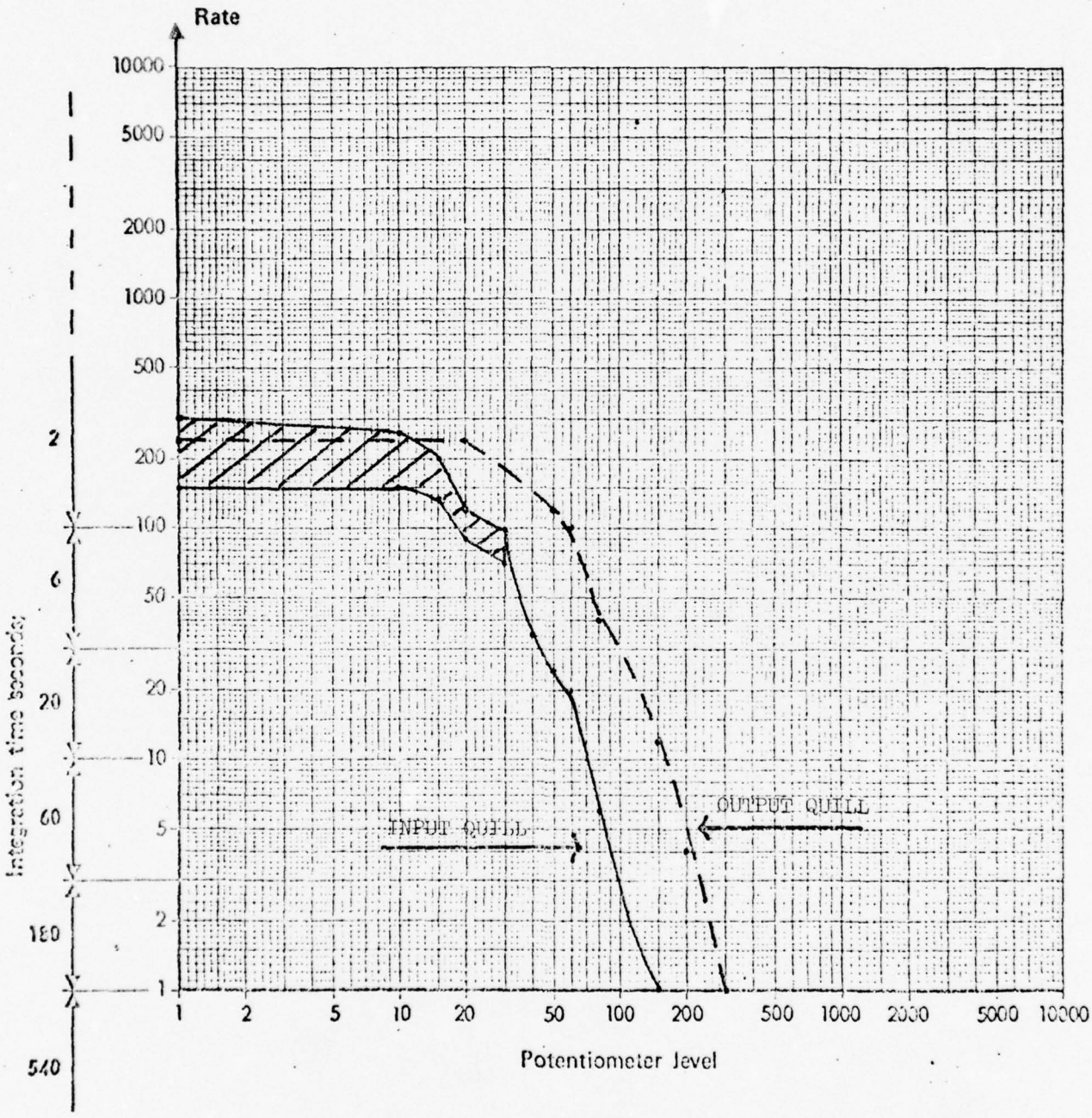


ONE CURVE REPRESENTS INPUT QUILL, THE OTHER THE OUTPUT QUILL GEARBOX REMOVED FOR TEARDOWN ANALYSIS.

NOTE: SCALPED AREA DENOTES NEEDLE SWING.

ABB2667 - GEARBOX SERIAL NUMBER

42° GEARBOX

UH-1H TAIL #66-16879

TEST CONDUCTED 13 DEC 1973

AT BI-STATE AIRPORT

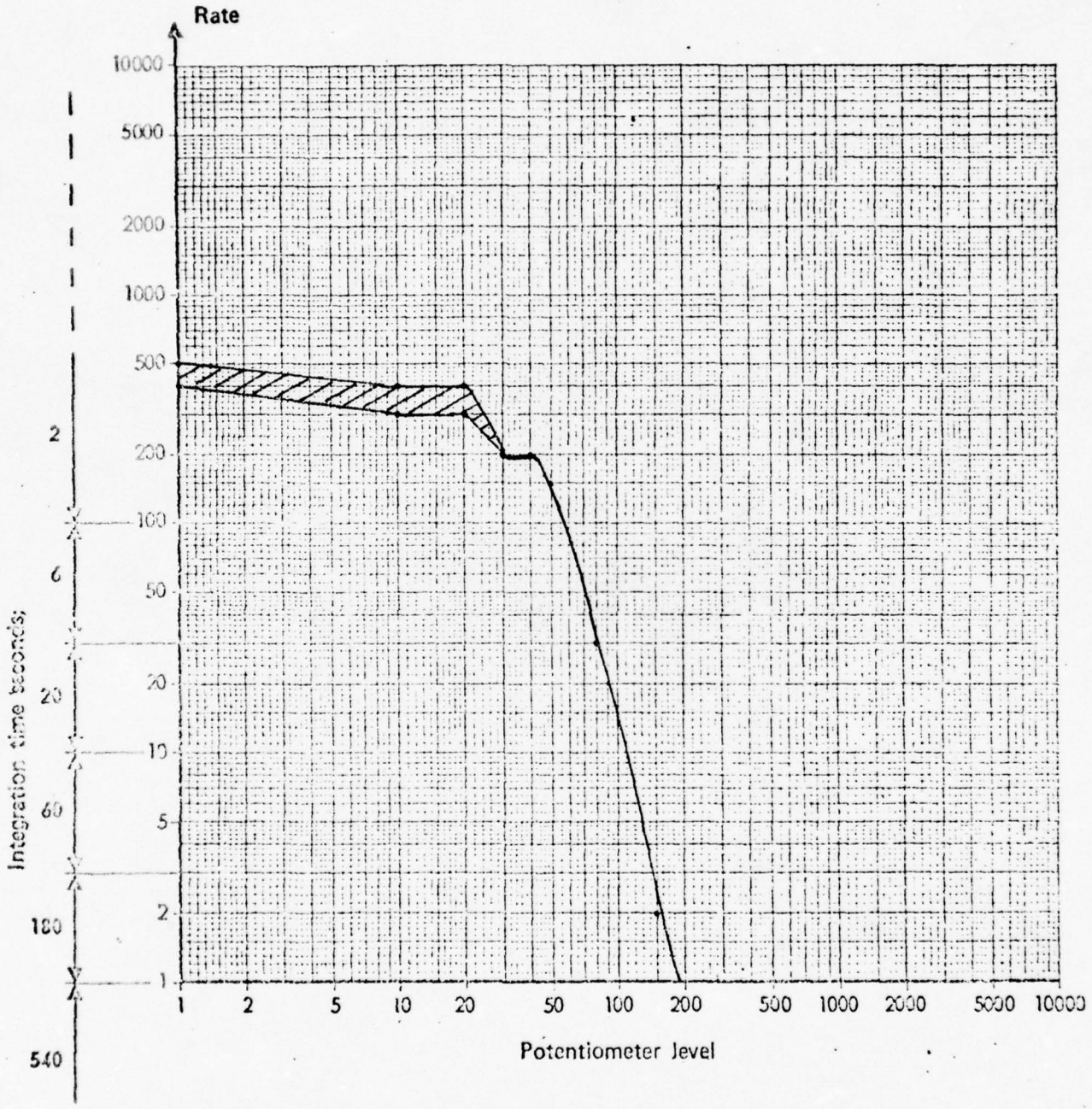


CURVE REPRESENTS THE OUTPUT DRIVE QUILL. GEARBOX REMOVED FOR TEARDOWN ANALYSIS.

NOTE: SCALPED AREA DENOTES NEEDLE SWING.

GEARBOX B13-3800

42° GEARBOX

UH-1M TAIL #66-15190

TEST CONDUCTED 12 DEC 1973 AT BI-STATE AIRPORT

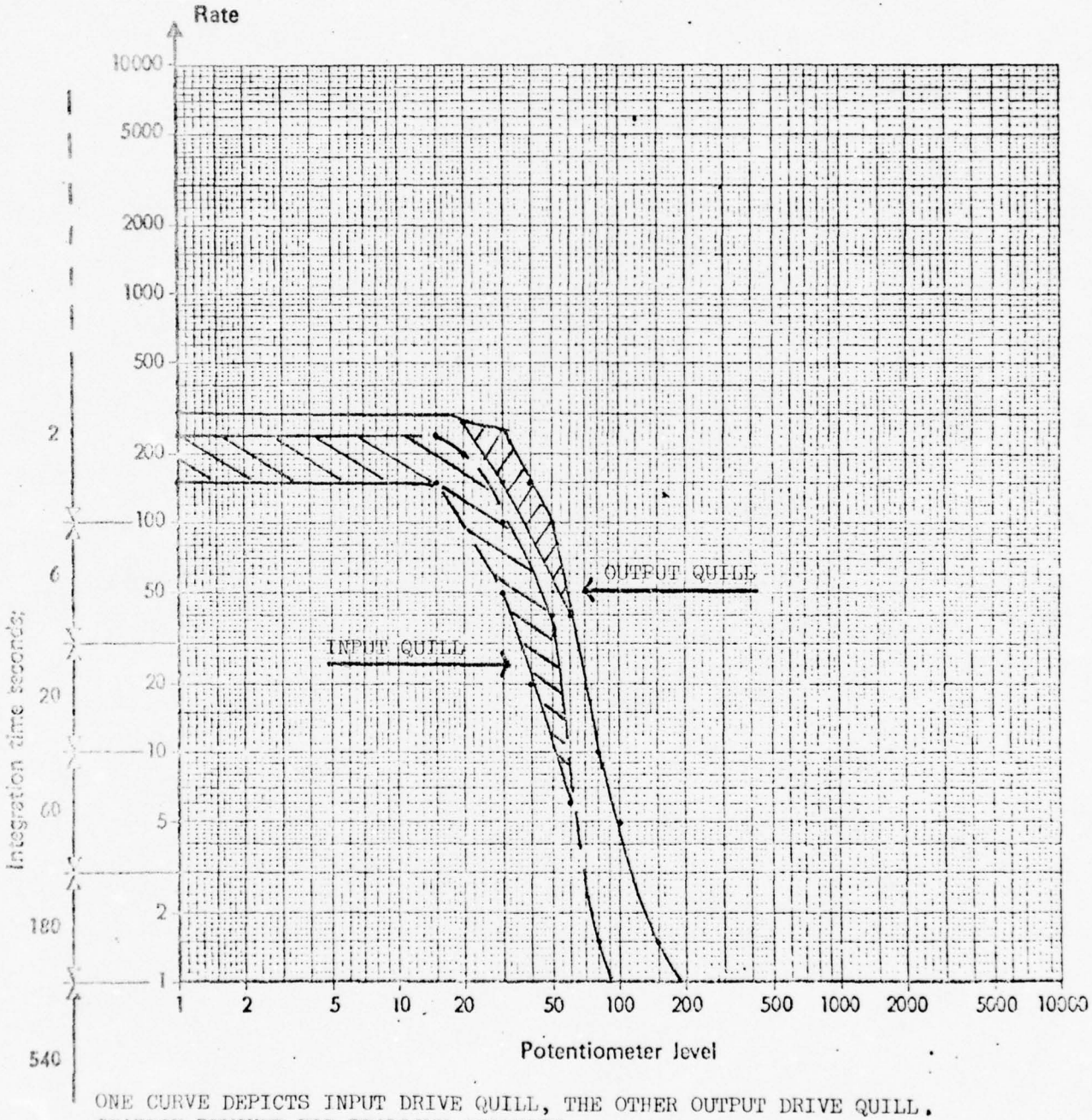


ONE CURVE DEPICTS INPUT DRIVE QUILL, THE OTHER OUTPUT DRIVE QUILL. GEARBOX REMOVED FOR TEARDOWN ANALYSIS.

NOTE: SCALPED AREA DENOTES NEEDLE SWING.

AB 1101 GEARBOX SERIAL NUMBER

281st Aviation Company Bi State Airport 6 Aug 74

90° Gear Box
42° Gear Box Input
42° Gear Box Output

A/C 60630 UH-1C
6600 RPM $N_2$

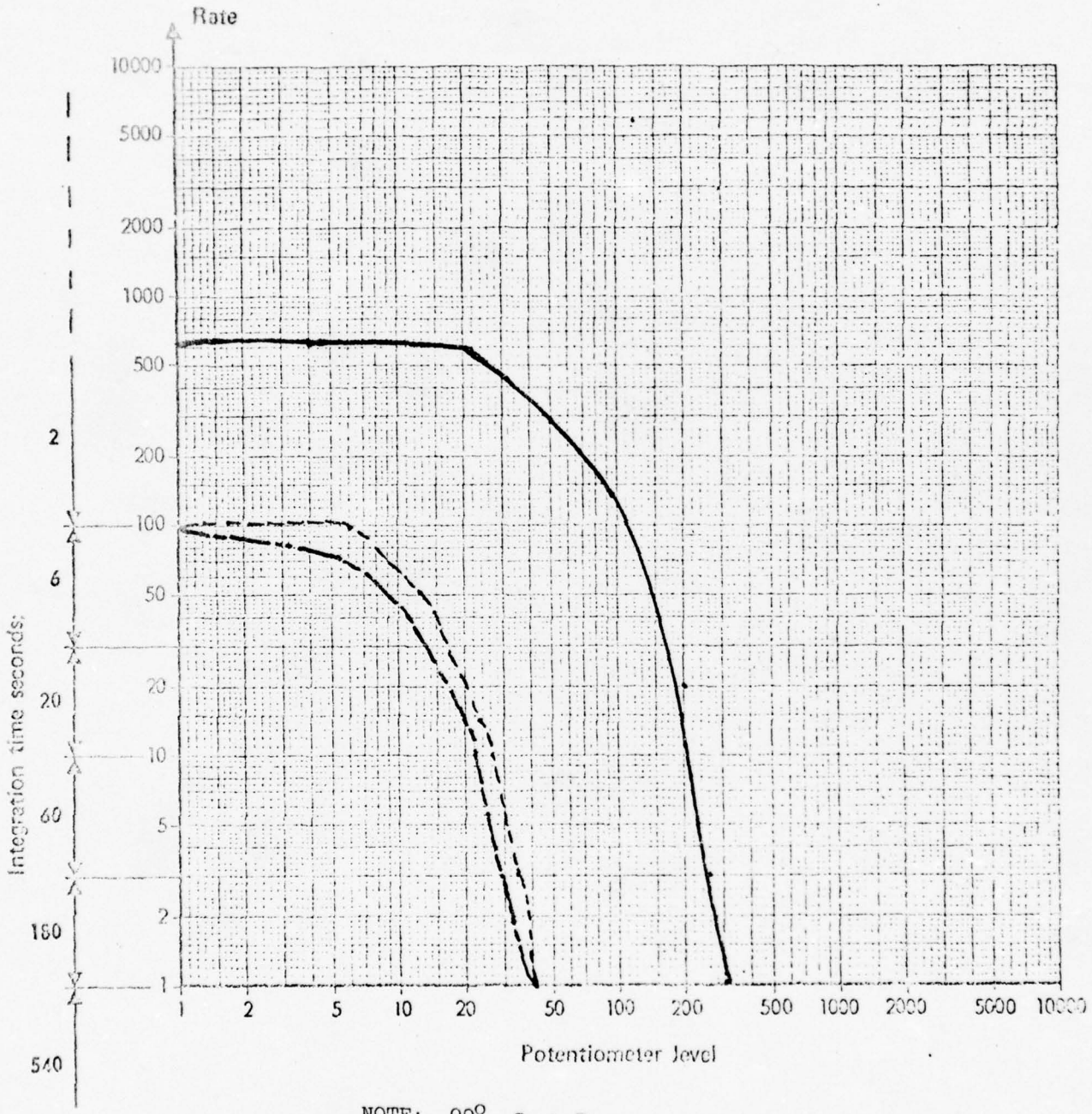


NOTE: 90° Gear Box _____
42° Gear Box Input - - - - - - - -
42° Gear Box Output _____

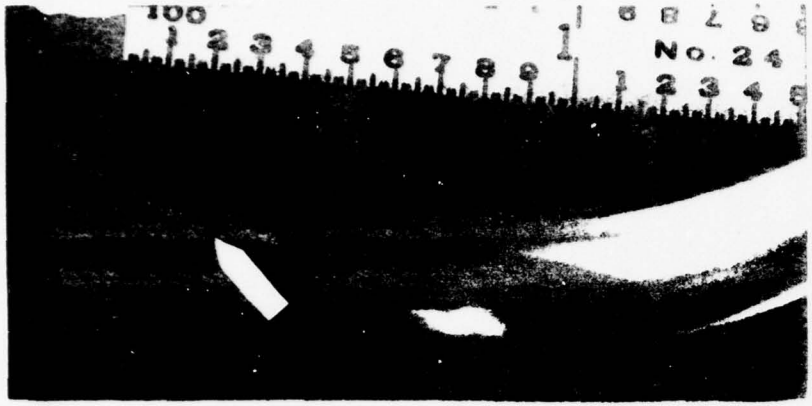


Duplex Ball Bearing
S/N 8199-H-2
Outer Race

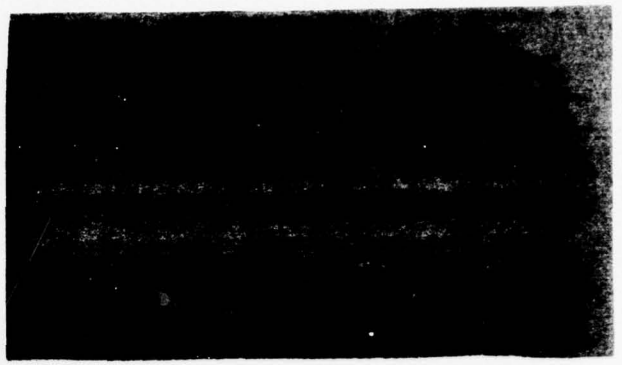

Duplex Ball Bearing
S/N 8199-H-2
Cage

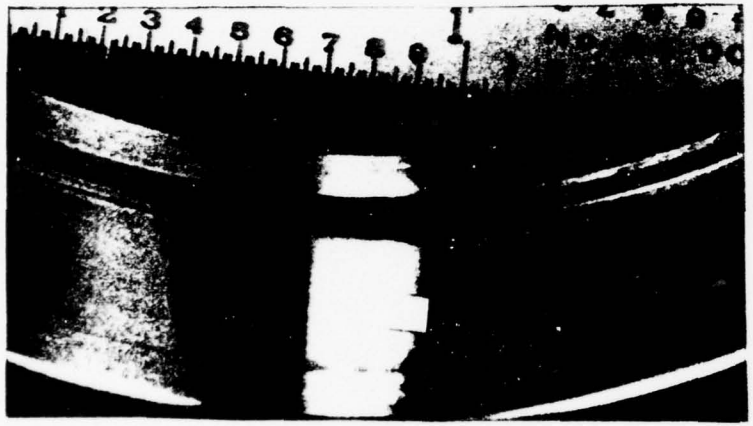

Roller Bearing
S/N 147403
Outer Race

Roller Bearing
S/N 147403
Rollers

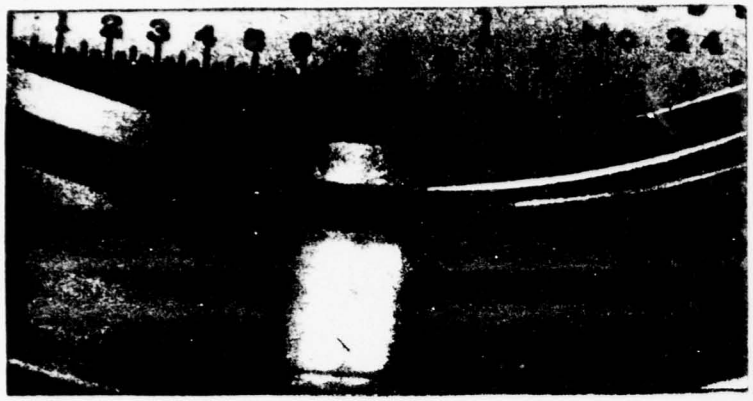

Roller Bearing
S/N 21020
Outer Race

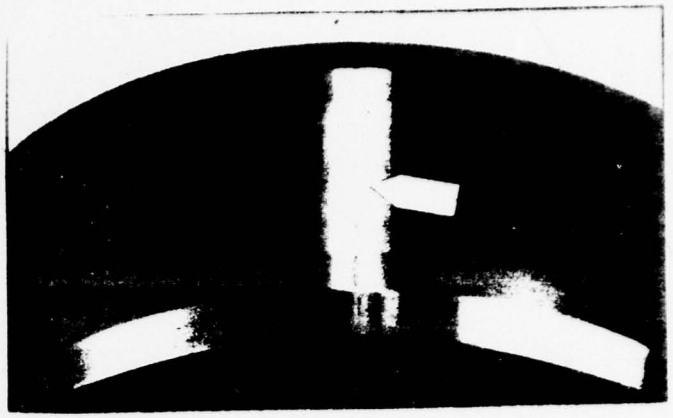

Roller Bearing
S/N 21020
Inner Race

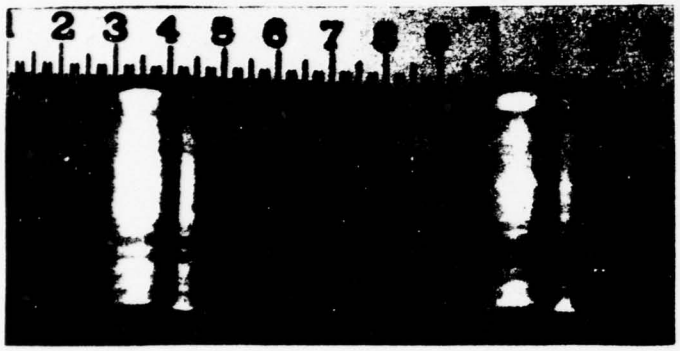

Roller Bearing
S/N 21020
Rollers

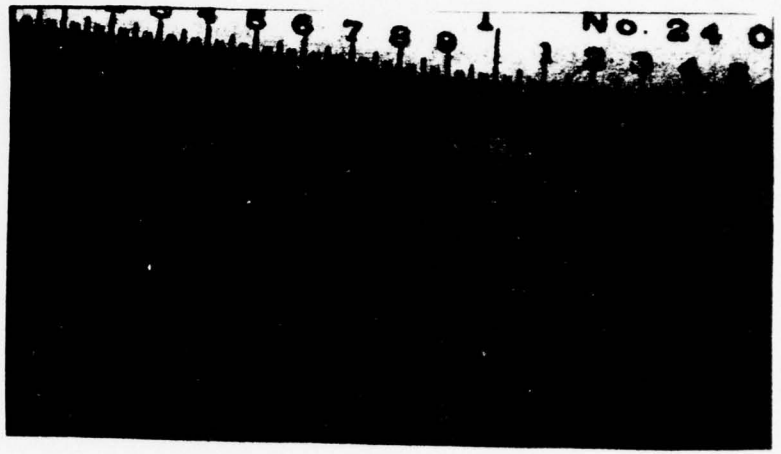

Duplex Ball Bearing
S/N 8199-H-1
Cage

Duplex Ball Bearing
S/N 8112-H-1
Outer Race

Duplex Ball Bearing
S/N 8112-H-1
Inner Race

Duplex Ball Bearing
S/N 8112-H-1
Cage

Duplex Ball Bearing
S/N 8112-H-2
Outer Race

42° Gear Box Input } Portside
42° Gear Box Output }
90° Gear Box Case Half Mount Bolt

A/C 69-15550 UH1H
6600 RPM $N_2$

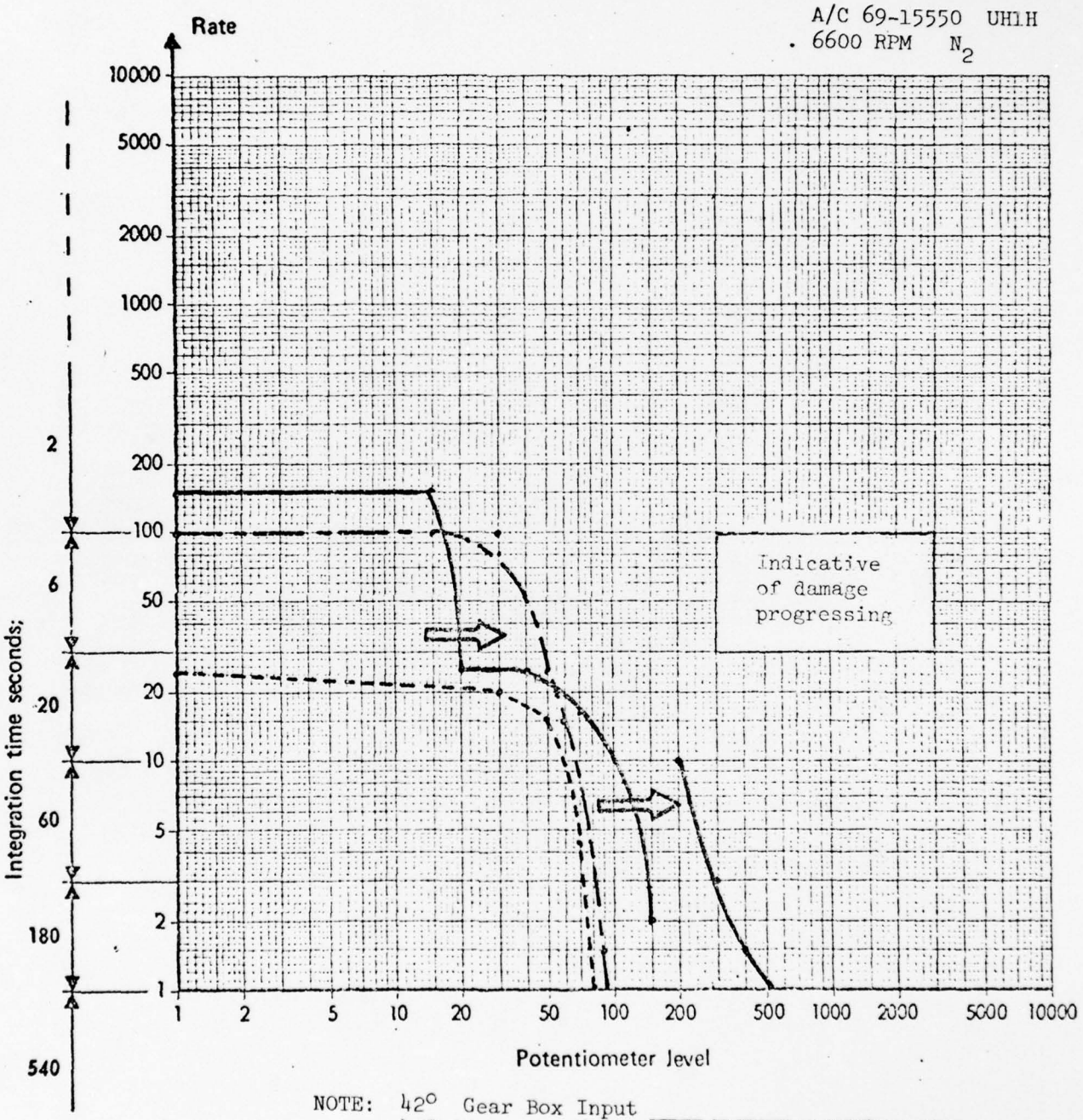


NOTE: 42° Gear Box Input _ _ _ _ _ _ _ _ _ _
42° Gear Box Output ----------
90° Gear Box _____

SUMMARY CHART OF 10 90° GEAR BOX
ASSEMBLIES SHOWING DATA SCATTER

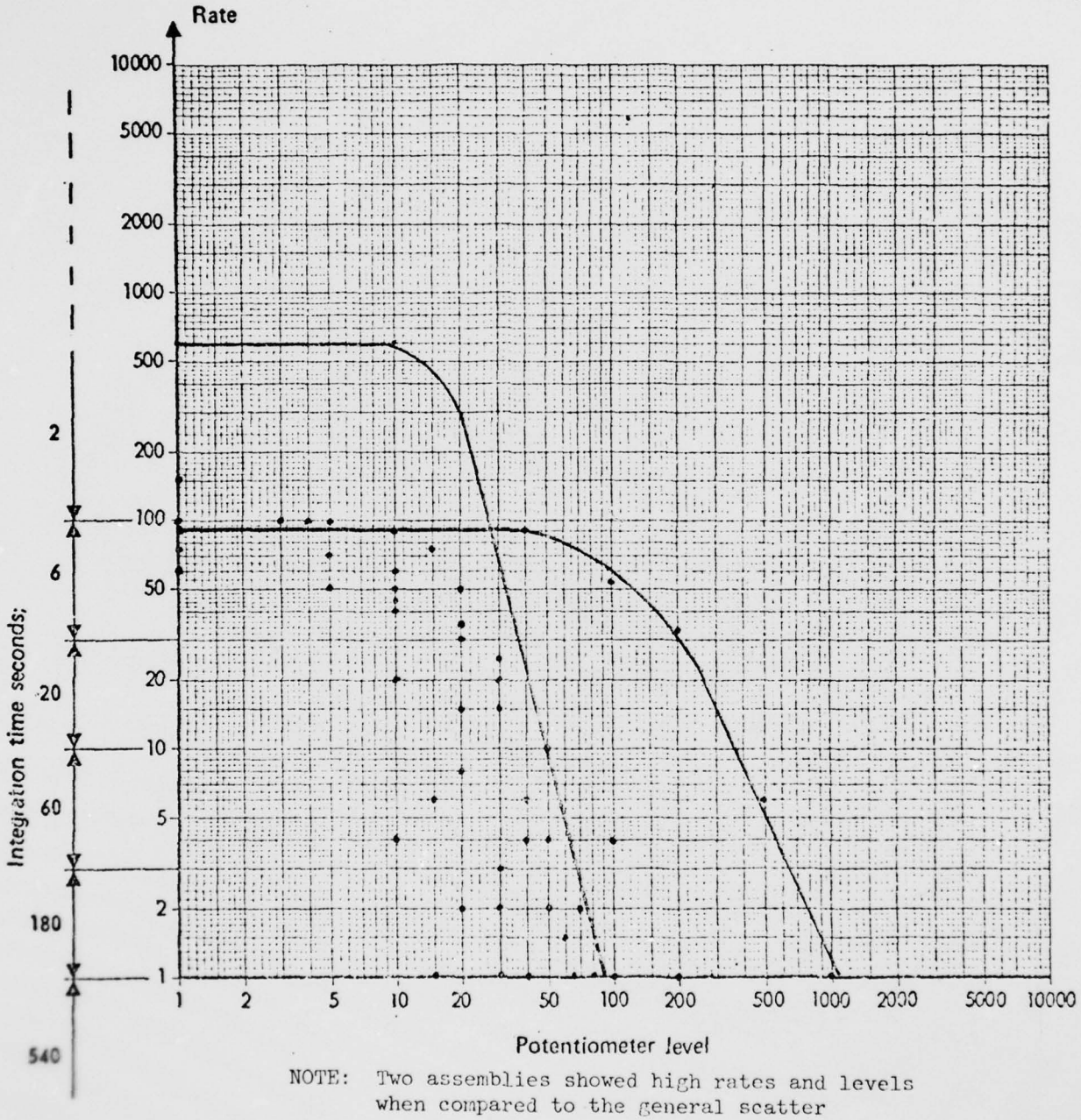


NOTE: Two assemblies showed high rates and levels when compared to the general scatter

90° Gear Box A 133069
42° Gear Box Input B138813
42° Gear Box Output

A/C 66-15200 UH-1H
6600 RPM $N_2$

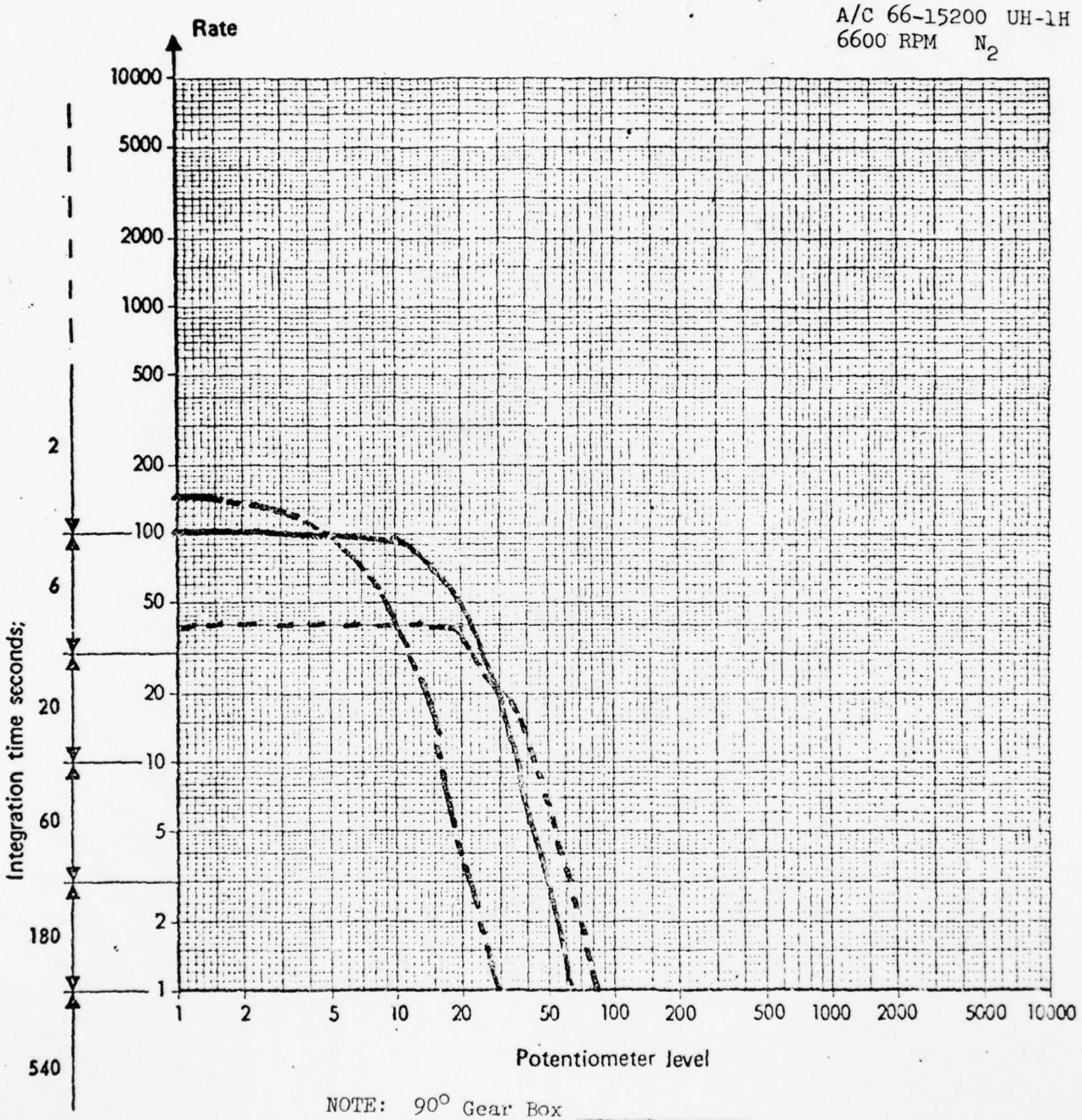


NOTE: 90° Gear Box _____
42° Gear Box Input ---------
42° Gear Box Output ____ - ____ - ____

42° Gear Box Input A131639

90° Gear Box ABC 2892

42° Gear Box Output

A/C 66-0529 UH-1M
6600 RPM $N_2$

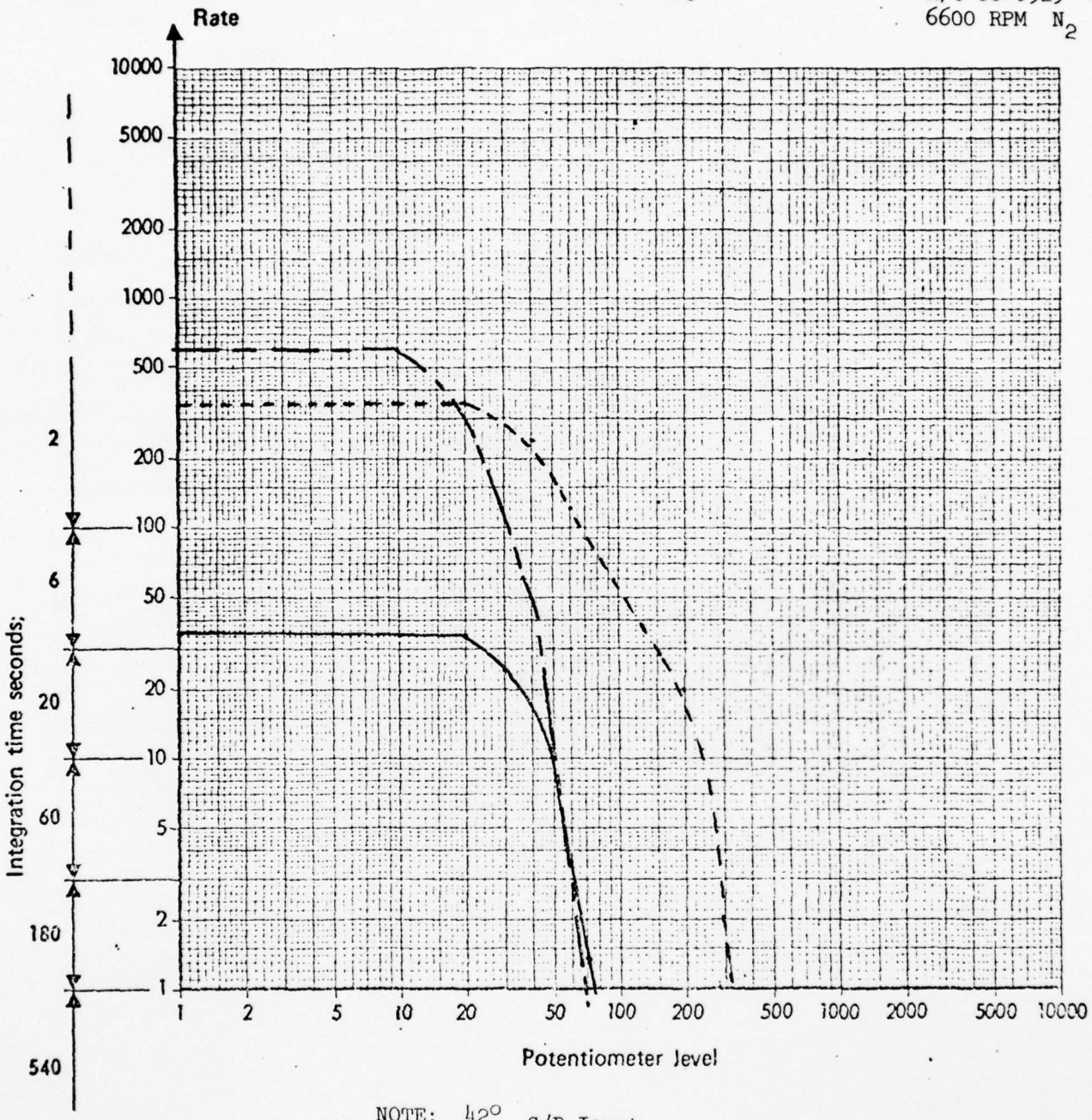


NOTE: 42° G/B Input _____

90° G/B _____ - _____ - _____

42° G/B Output ----------

#3 Hanger Bearing A 2064529
#2 Hanger Bearing A 2052529
Mast Bearing

A/C 66-0529 UH-1M
6600 RPM $N_2$

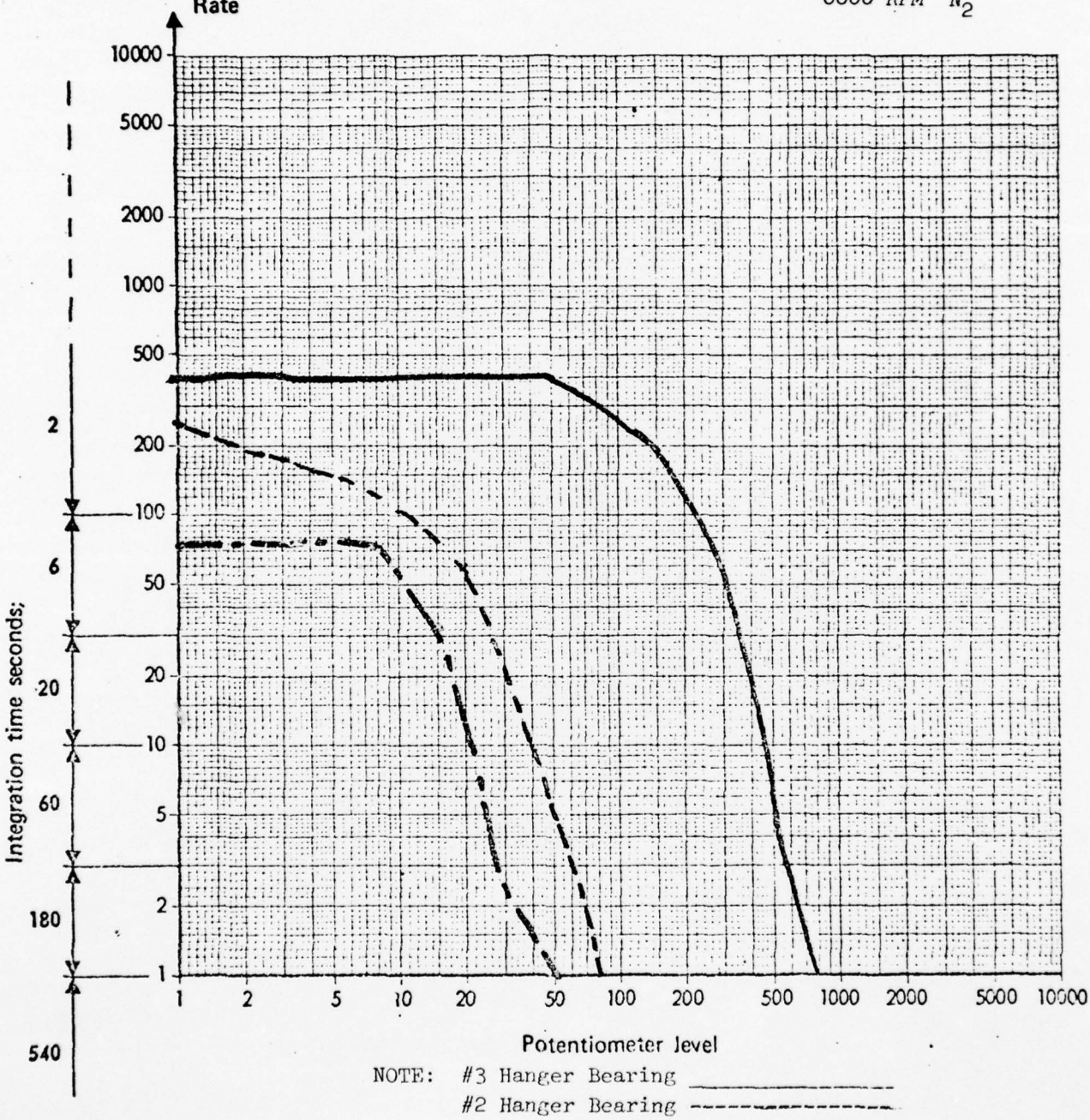


NOTE: #3 Hanger Bearing _____
#2 Hanger Bearing ----------
Mast Bearing _____ _ ____ _ _____ _ ____

281st Aviation Company Bi State Airport 5 Aug 1974
#3 Hanger Bearing A20-43493
42° Gear Box Input B13-9384
90° Gear Box B13-5077

A/C 65-9884 UH-1D
6600 RPM $N_2$

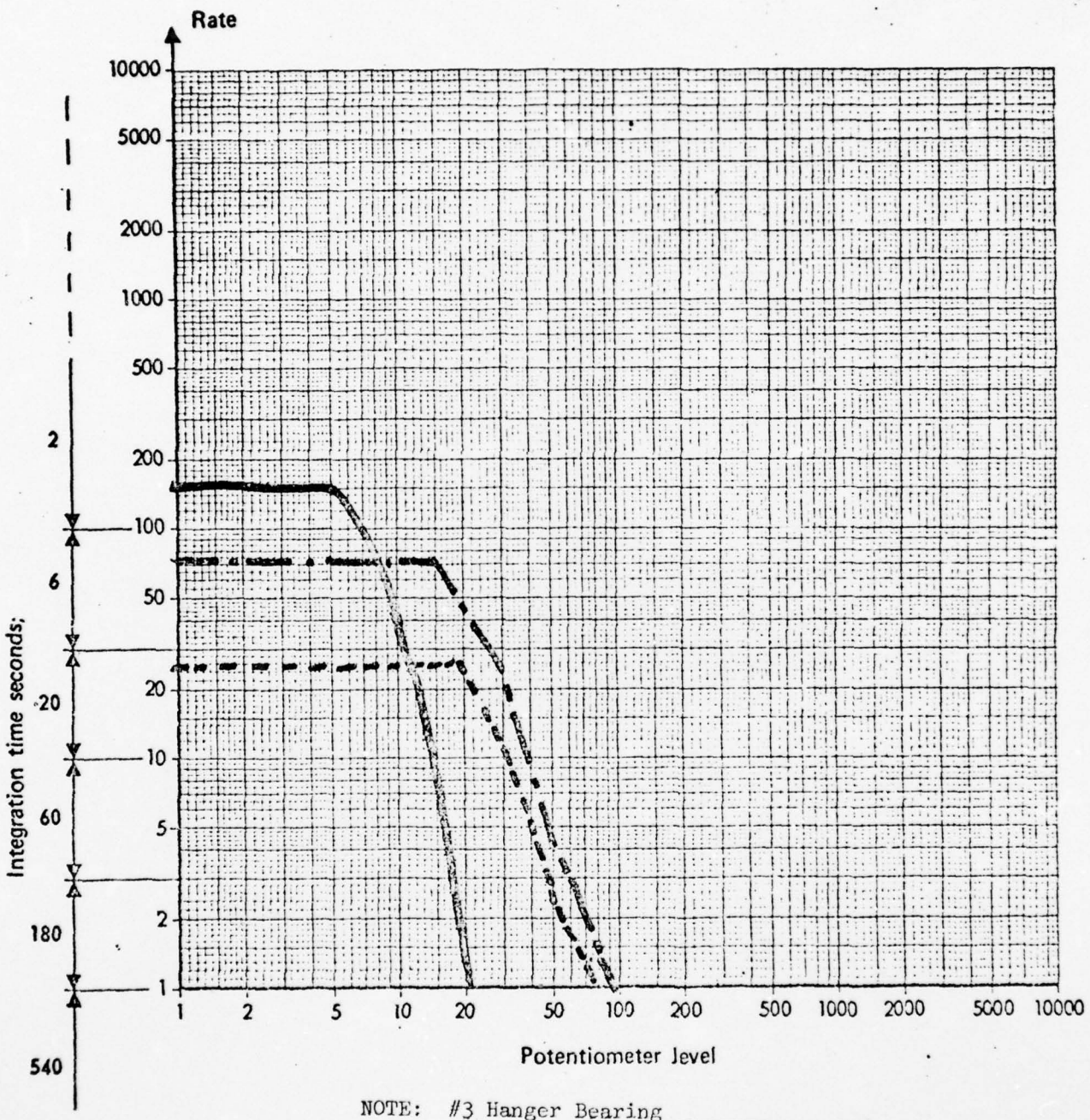


NOTE: #3 Hanger Bearing _____
42° Gear Box Input - - - - - - - - - - - -
90° Gear Box _____ - - _____ - - _____

281st Aviation Company Bi State Airport 6 Aug 74

#1 Hanger Bearing

Input Drive Quill

A/C UH-1C 60630
6600 RPM $N_2$

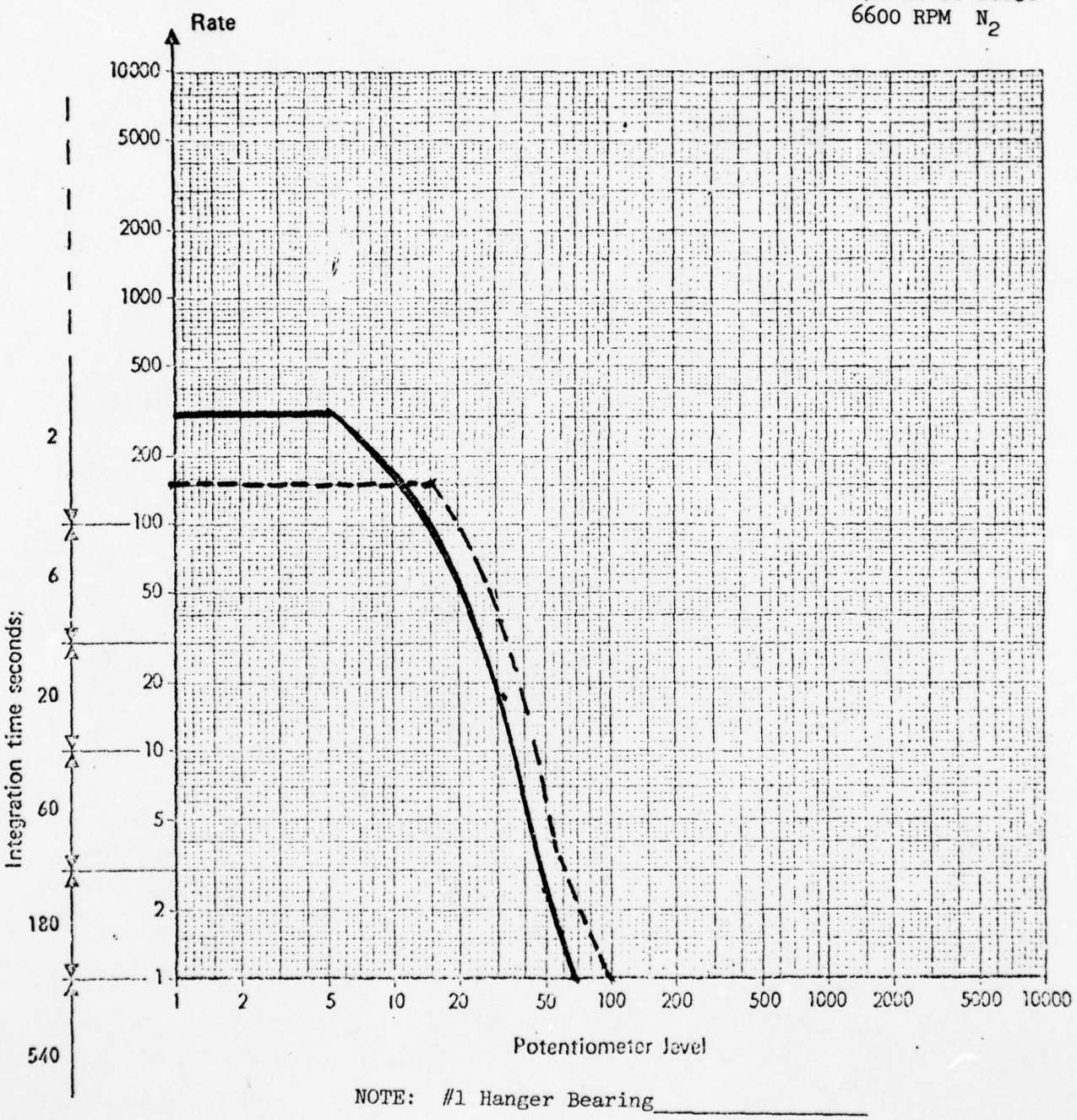


NOTE: #1 Hanger Bearing_____

Drive Quill ----------

281st Aviation Company - Bi State Airport 7 Aug 74

Mast Bearing
Input Drive

A/C 65-9771 UH-1H
6600 RPM $N_2$

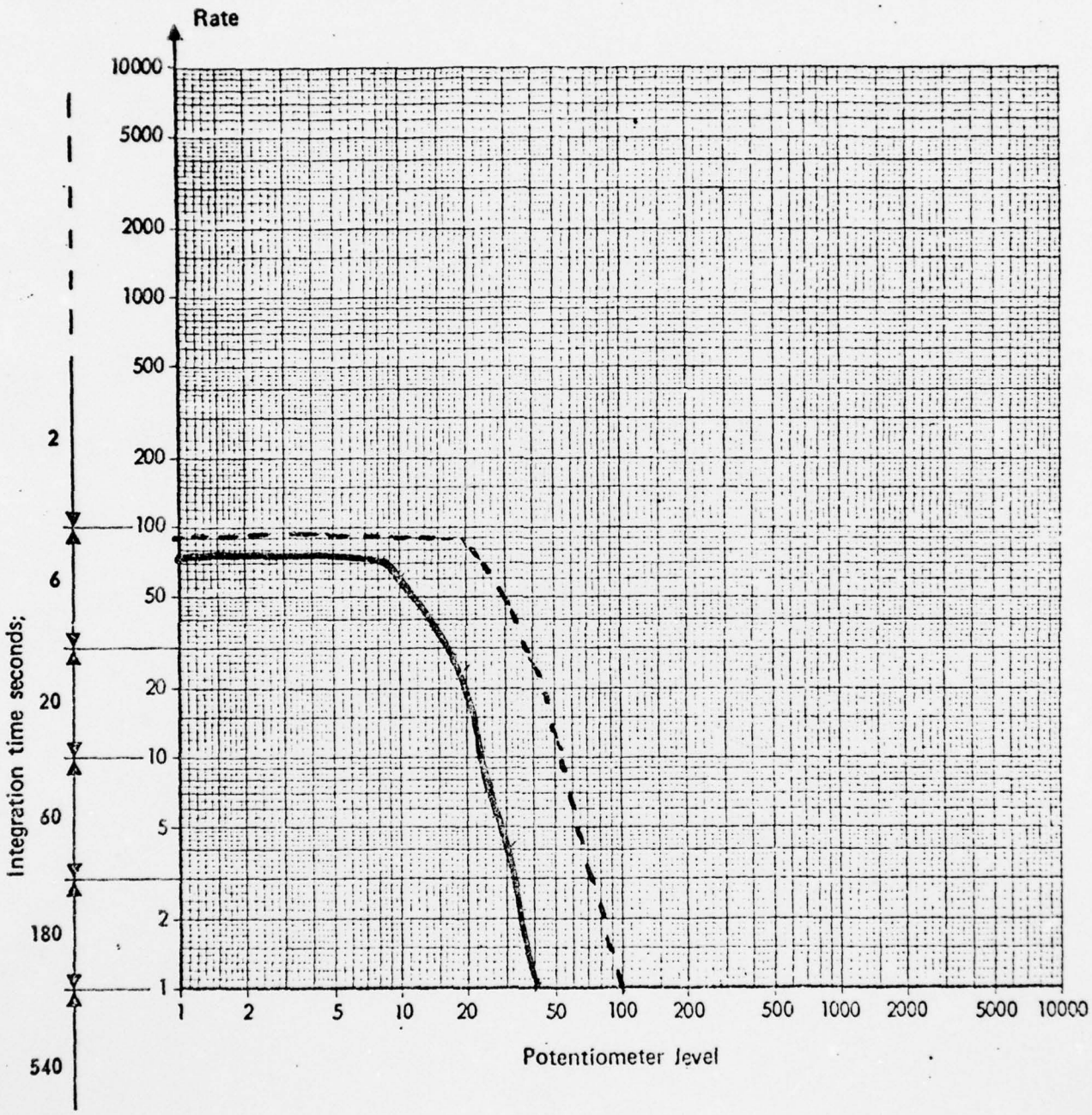


NOTE: Mast Bearing _____

Input Drive----------

281st Aviation Company Bi State Airport 6 Aug 74

#2 Hanger Bearing

#3 Hanger Bearing

Mast Bearing

A/C UH-1C 60630
6600 RPM $N_2$

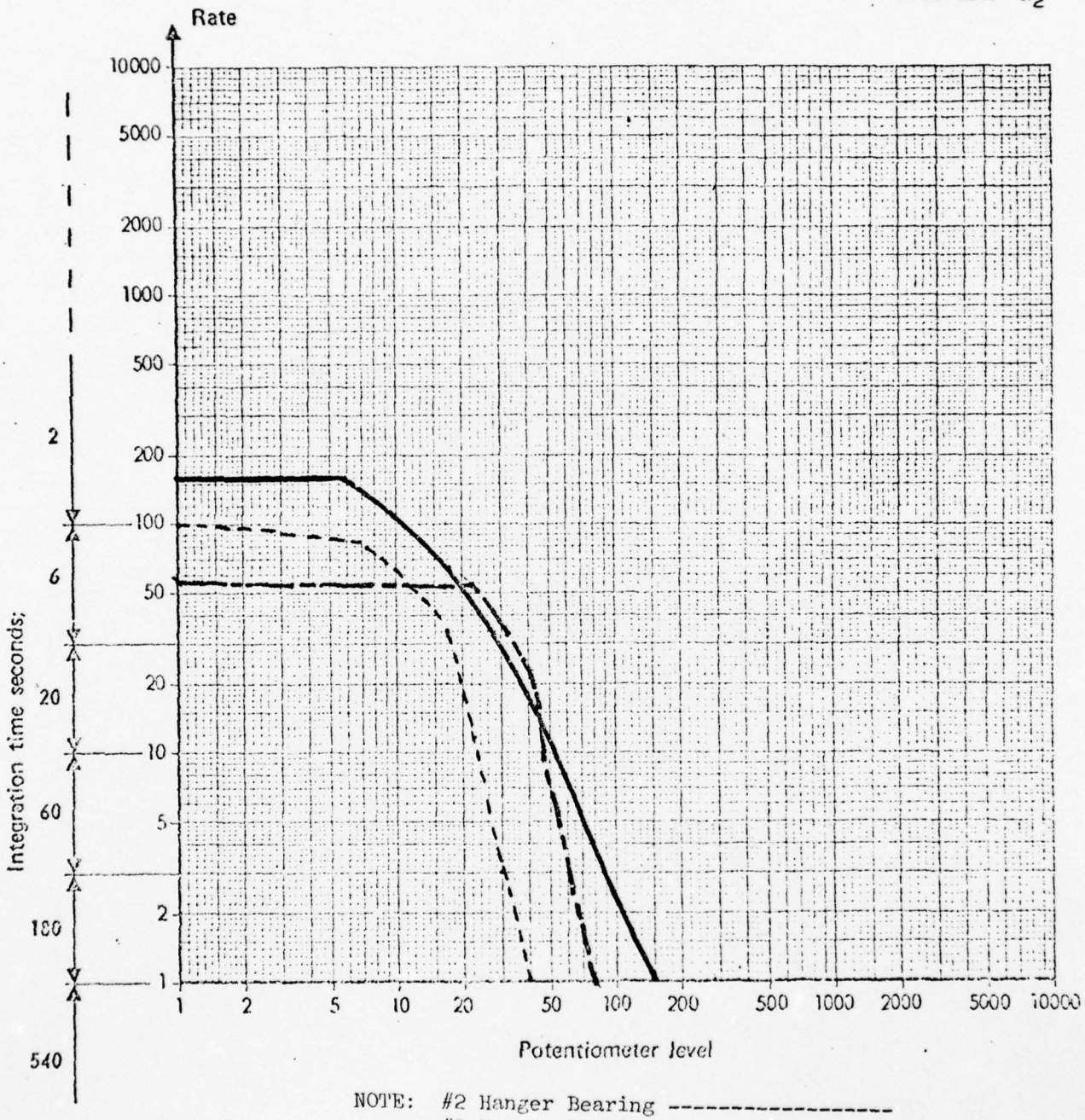


NOTE: #2 Hanger Bearing ----------
#3 Hanger Bearing _____
Mast _____ - _____ - _____ . _____

281st Aviation Company Bi State Airport 6 Aug 74

#1 Hanger Bearing

Mast Bearing

A/C 66-15071 UH-1C
6600 RPM $N_2$

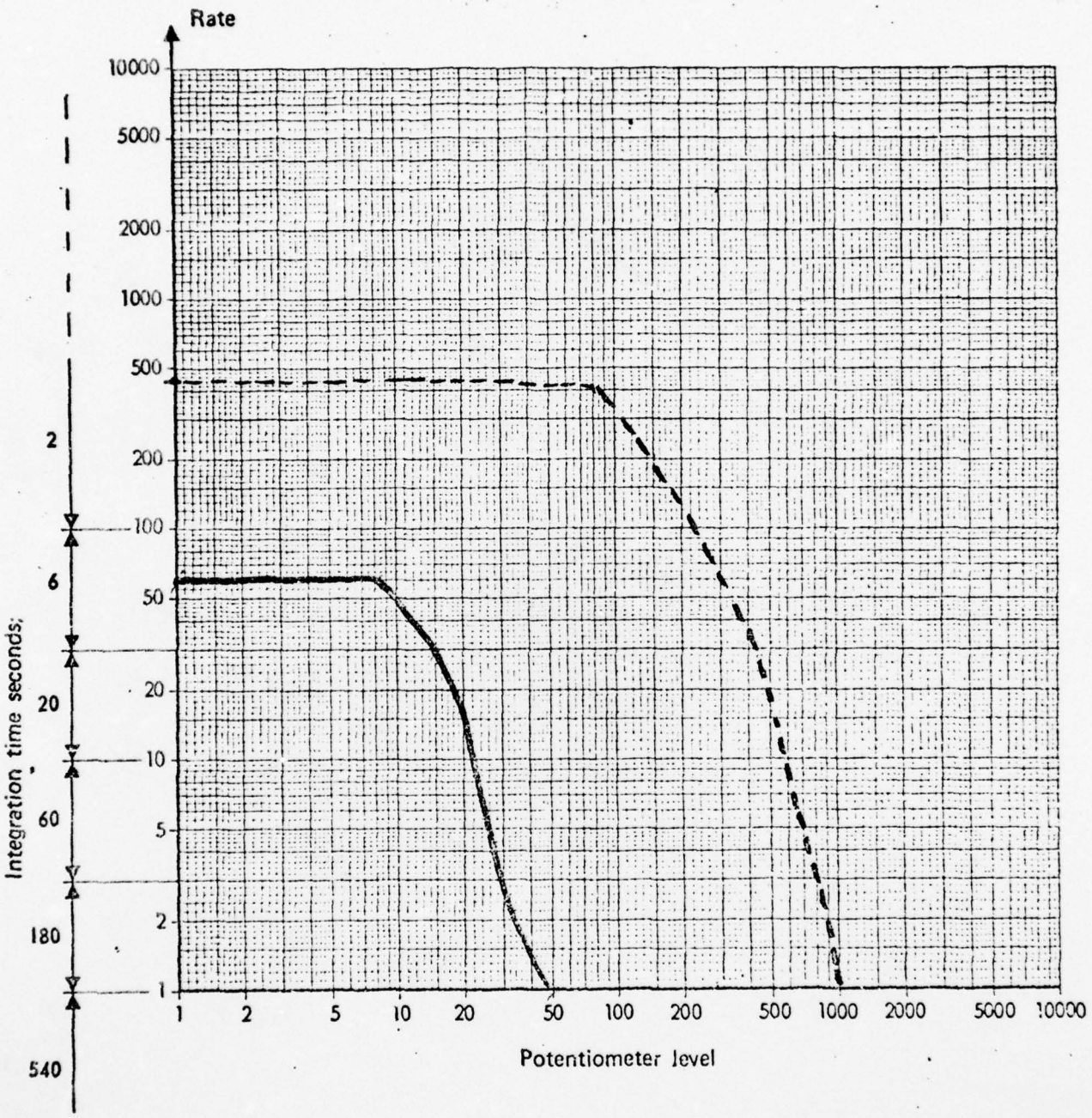


NOTE: #1 Hanger Bearing _____

Mast Bearing ----------

281st Aviation Company Bi State Airport 6 Aug 74

90° Gear Box B13-3307
42° Gear Box Output BBB-1894
#2 Hanger Bearing A20-15990

A/C 66-15071 UH-1C
6600 RPM $N_2$

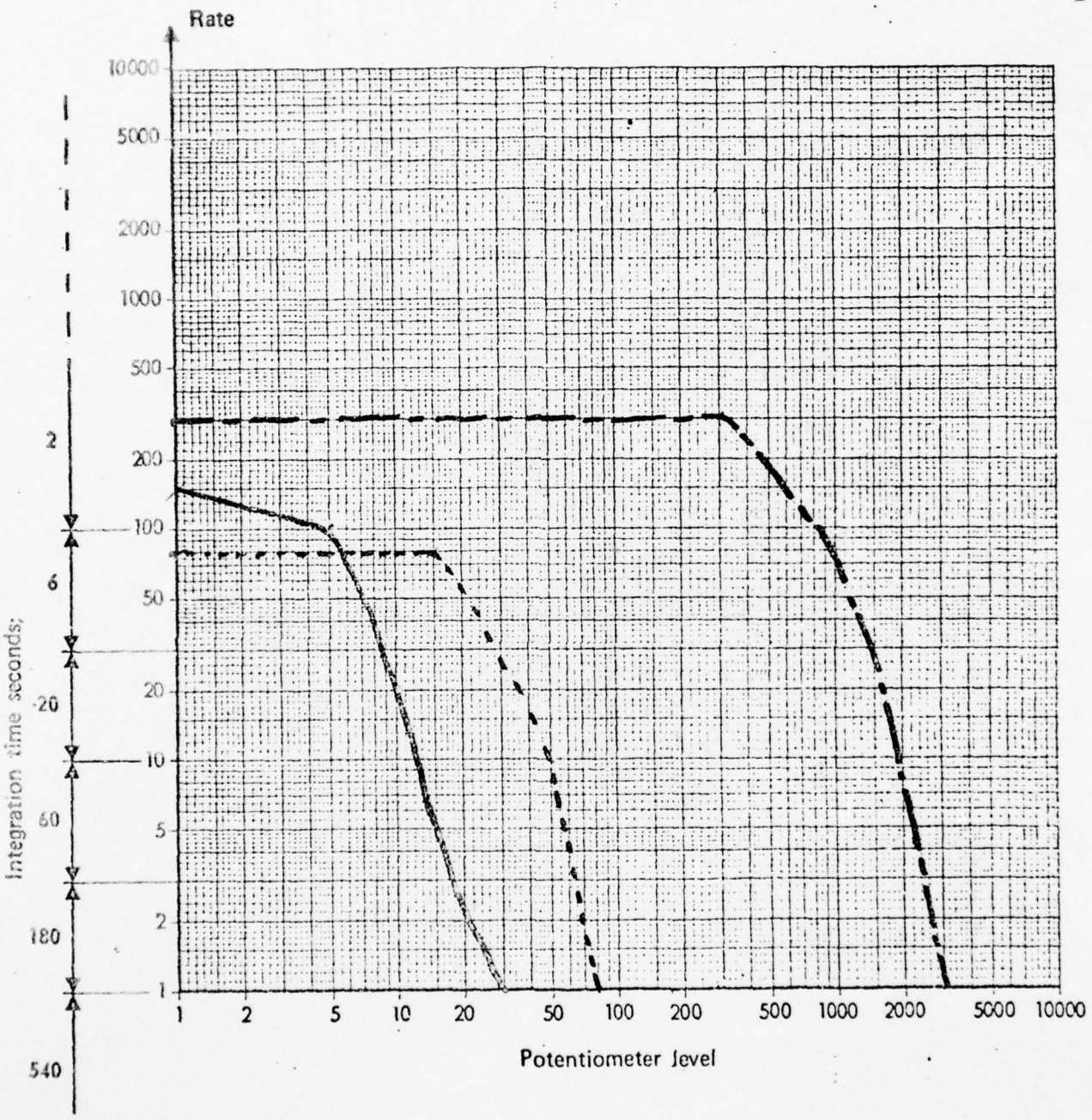


NOTE: 90° G/B _____
42° G/B output----------
#2 Hanger Bearing____ - _____ - _____

42° Gear Box Input . BBB-1894
#3 Hanger Bearing A20-31517
Input Drive Quill

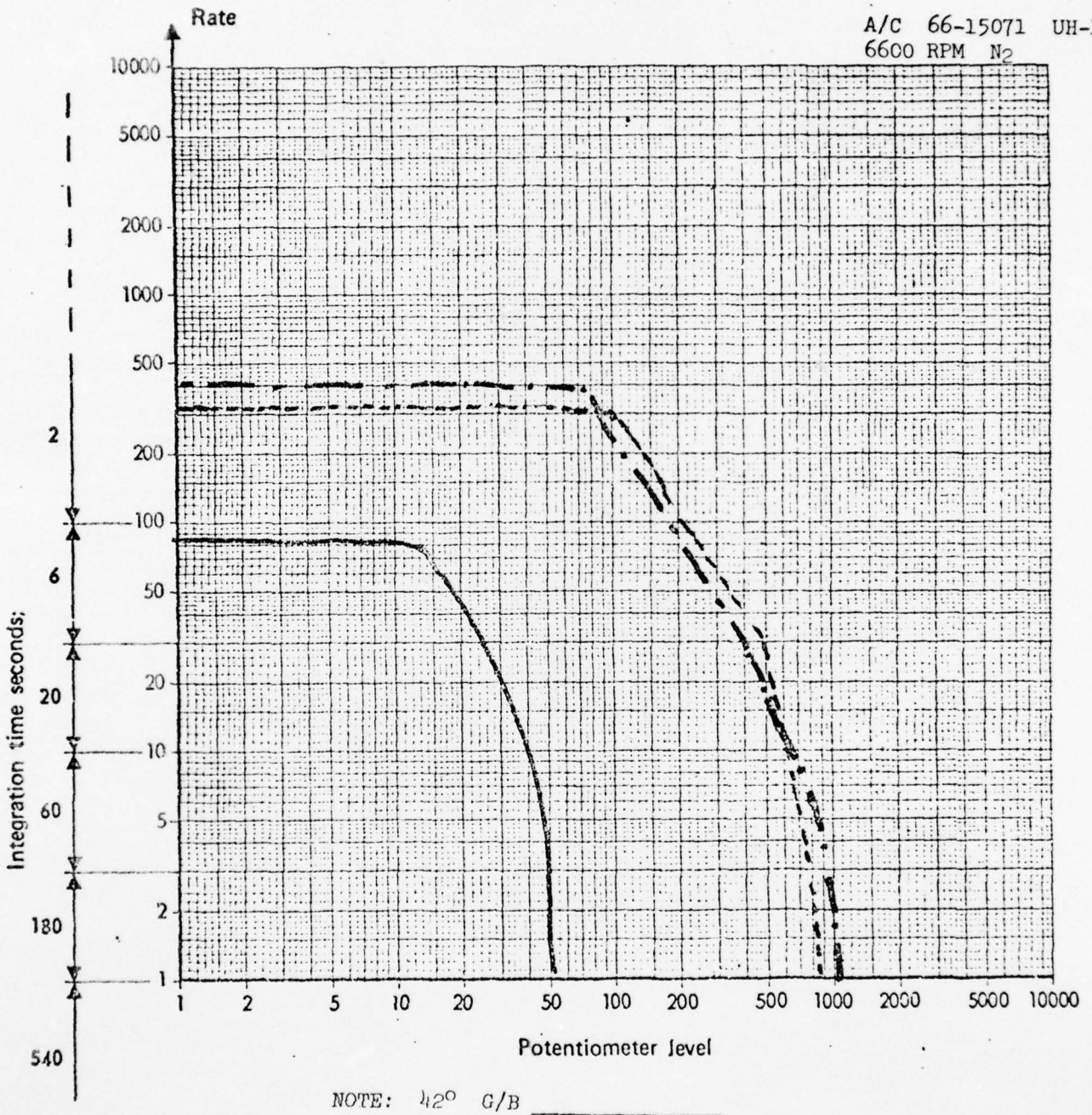


NOTE: 42° G/B _____
#3 Hanger Bearing -------
Input Drive Quill _____ - _____ - _____

90° Gear Box
#3 Hanger Bearing
#2 Hanger Bearing

A/C 65-9519 UH-1M
6600 RPM $N_2$

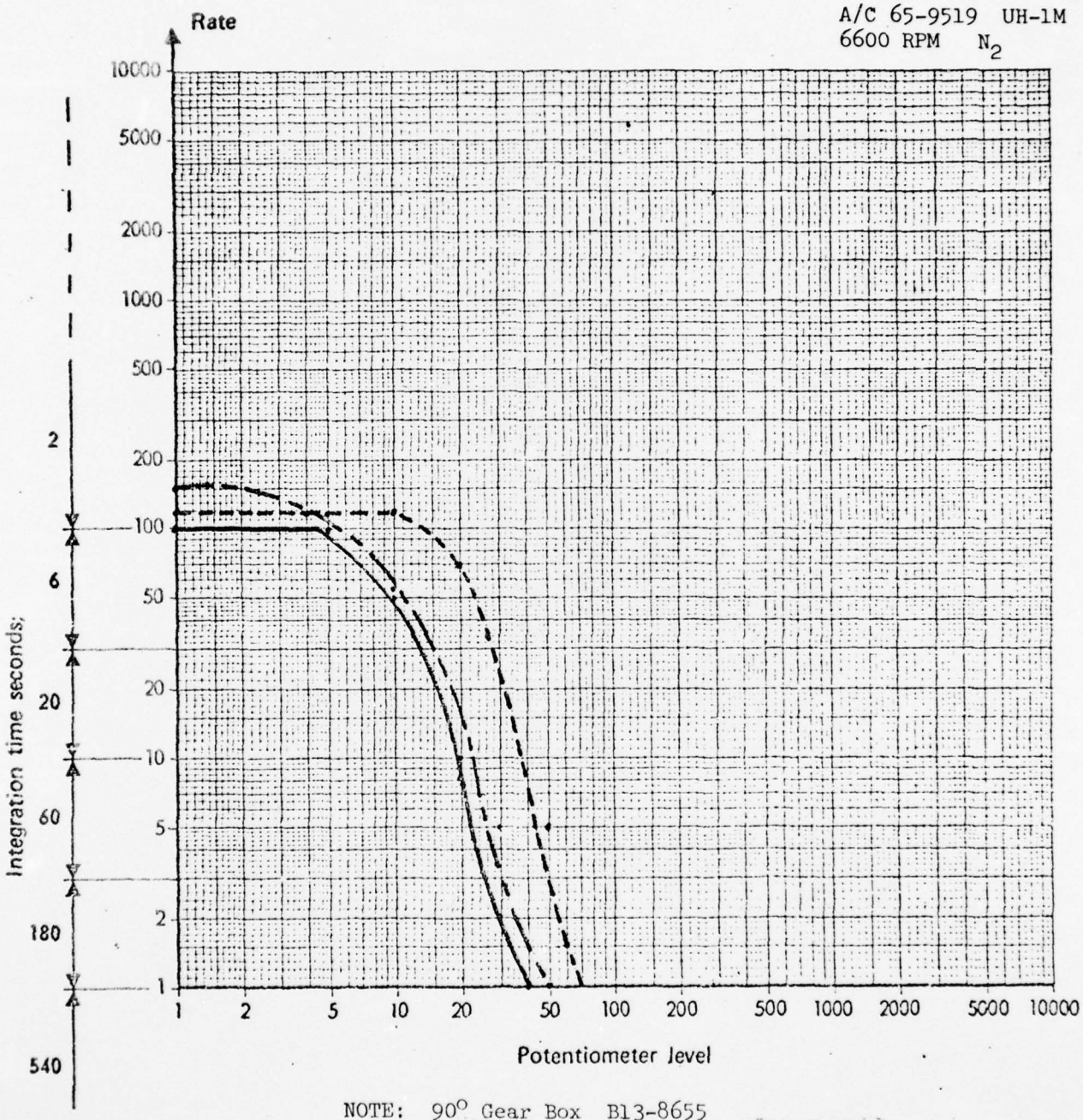


NOTE: 90° Gear Box B13-8655 _____
#3 Hanger Bearing A20-26938 ____ _ ____ _ ____
#2 Hanger Bearing A20-57910 ----------

281st Aviation Company Bi State Airport 8 Aug 74

Input Drive Quill

Mast Bearing

A/C UH-1M 65-9519
6600 RPM $N_2$

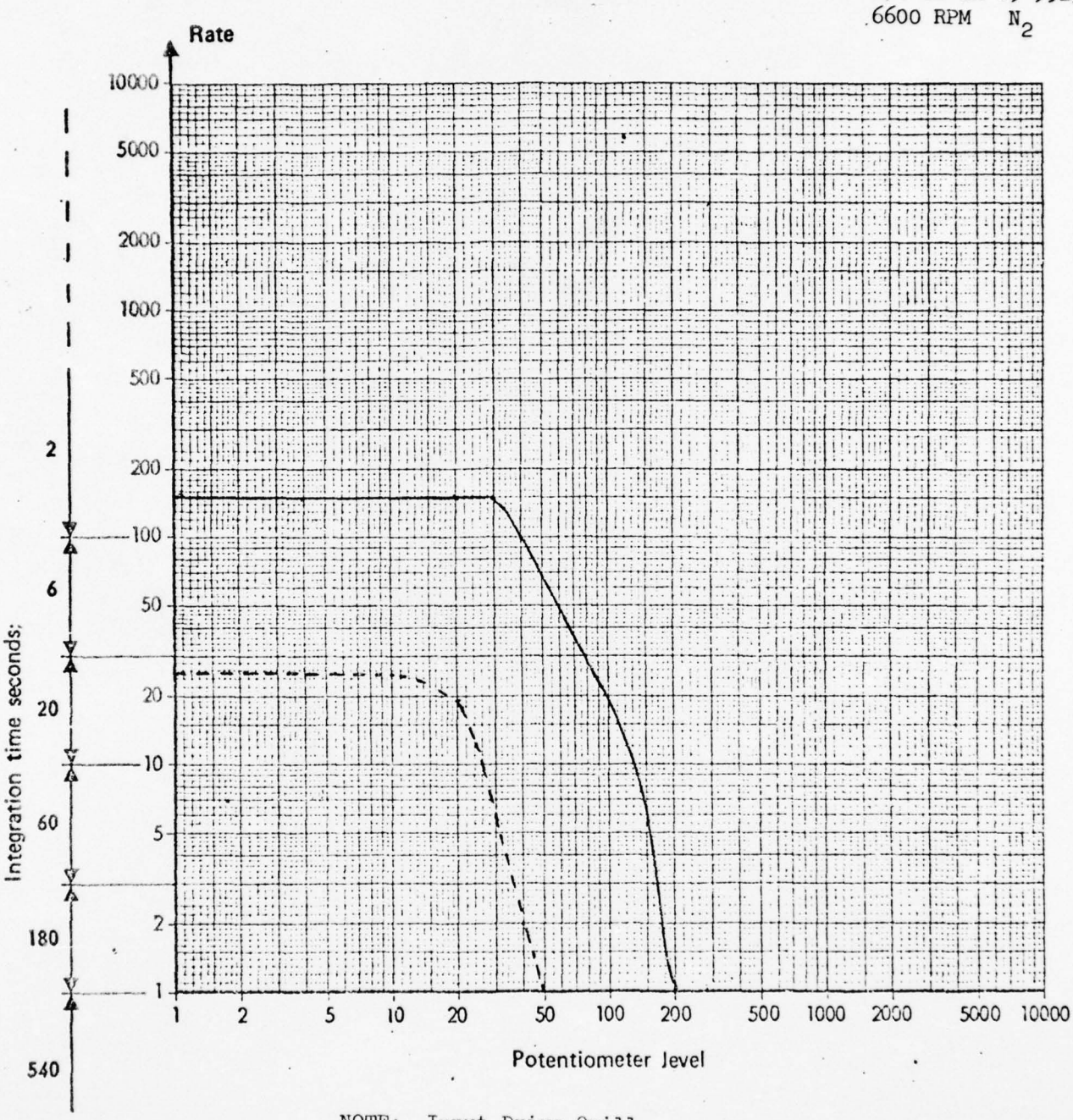


NOTE: Input Drive Quill_____

Mast Bearing ----------

281st Aviation Company Bi State Airport 9 Aug 74

42° Gear Box Input
#1 Hanger Bearing

A/C UH-1M 66-15091
6600 RPM $N_2$

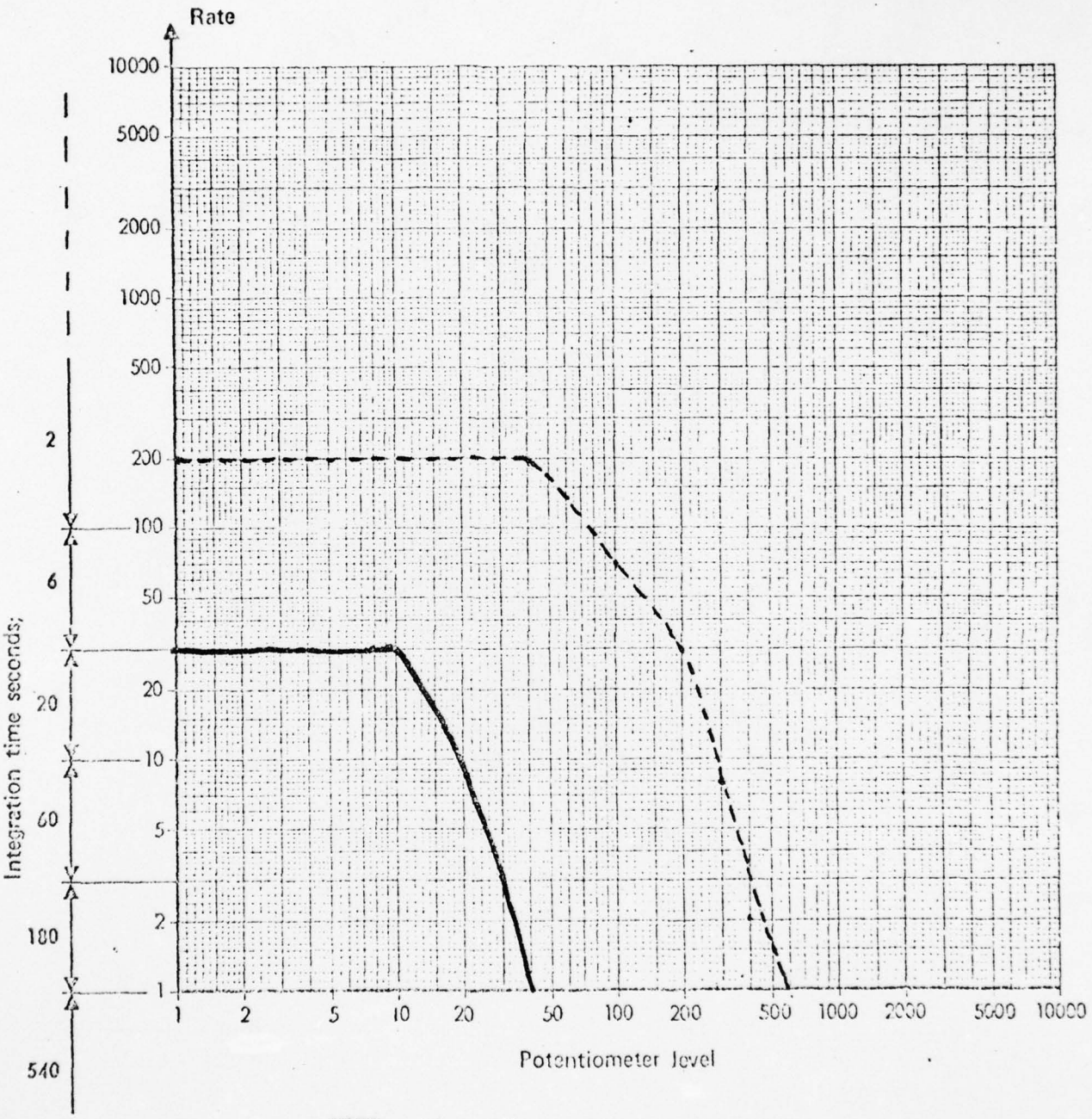


NOTE: Aircraft tested while raining
42° G/B input_____
#1 Hanger Bearing----------

AD-A040 130 PARKS COLL OF SAINT LOUIS UNIV CAHOKIA ILL F/G 1/3
APPLICATIONS OF THE SHOCK PULSE TECHNIQUE TO HELICOPTER DIAGNOS--ETC(U)
FEB 75 T C MAYER, E F COVILL, J A GEORGE DAAJ01-72-A-0027
UNCLASSIFIED USAAVSCOM-TR-77-21 NL

3 OF 3
AD
A040 130

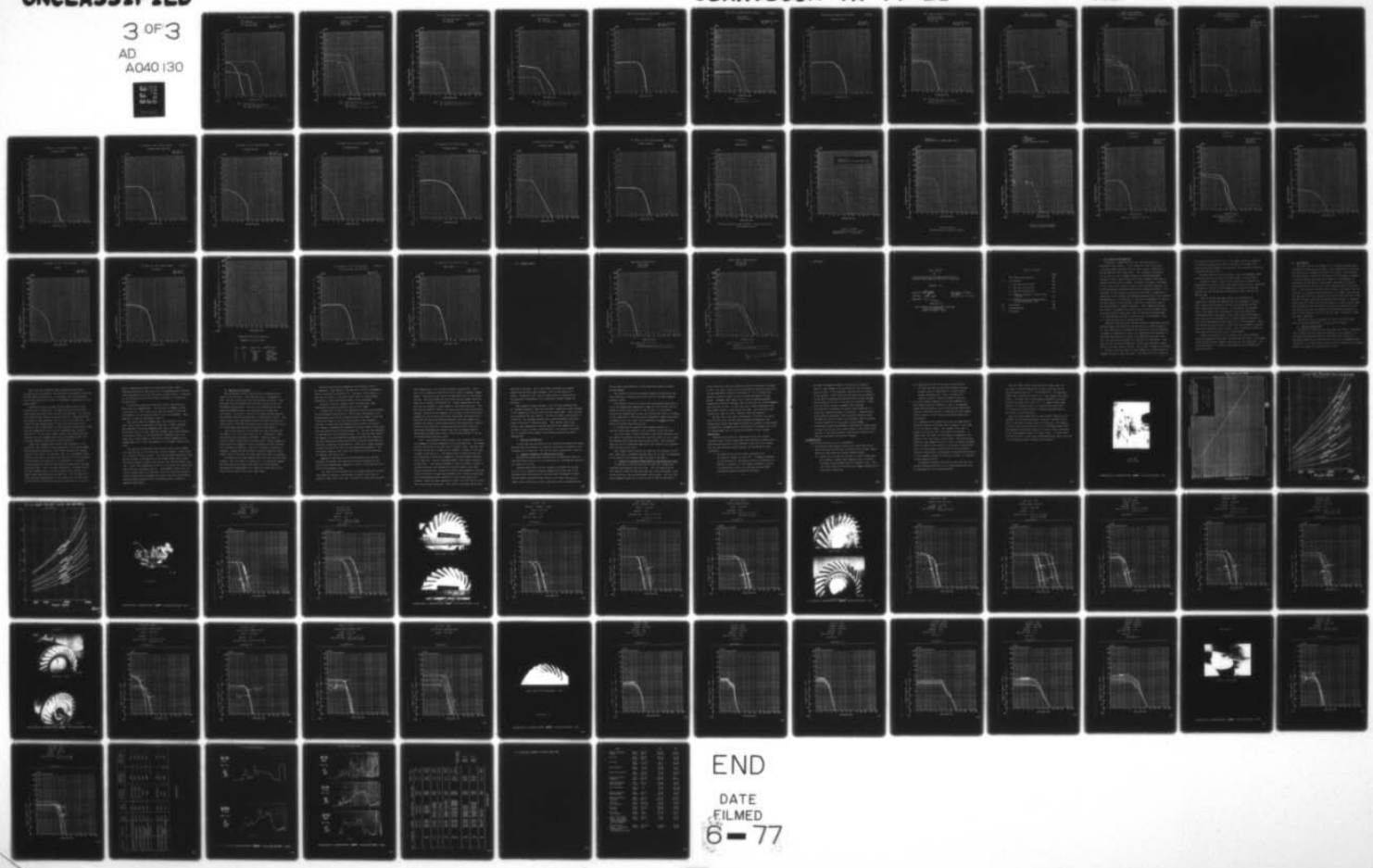

END

DATE
FILMED
6-77

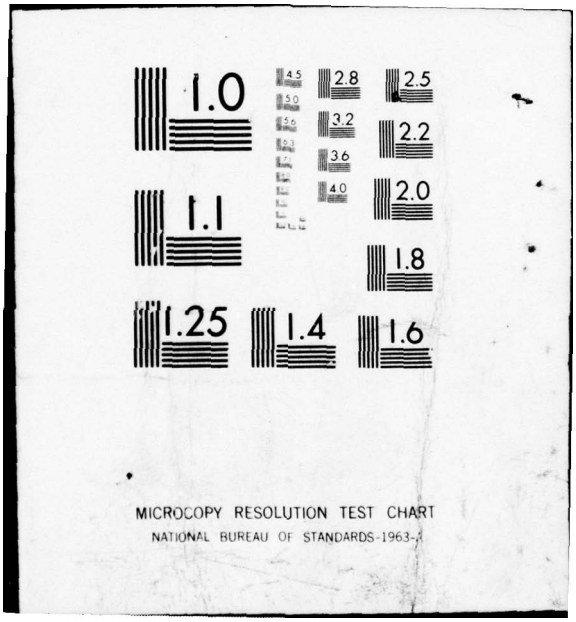
1.0
1.1
1.25
1.4
1.6
1.8
2.0
2.2
2.5
2.8
3.2
3.6
4.0
4.5
5.0
5.6
MICROCOPY RESOLUTION TEST CHART
NATIONAL BUREAU OF STANDARDS-1963-A

281st Aviation Company Bi State Airport 12 Aug 74

90° Gear Box
42° Gear Box Output
42° Gear Box Input

A/C UH-1H 70-16354
6600 RPM $N_2$

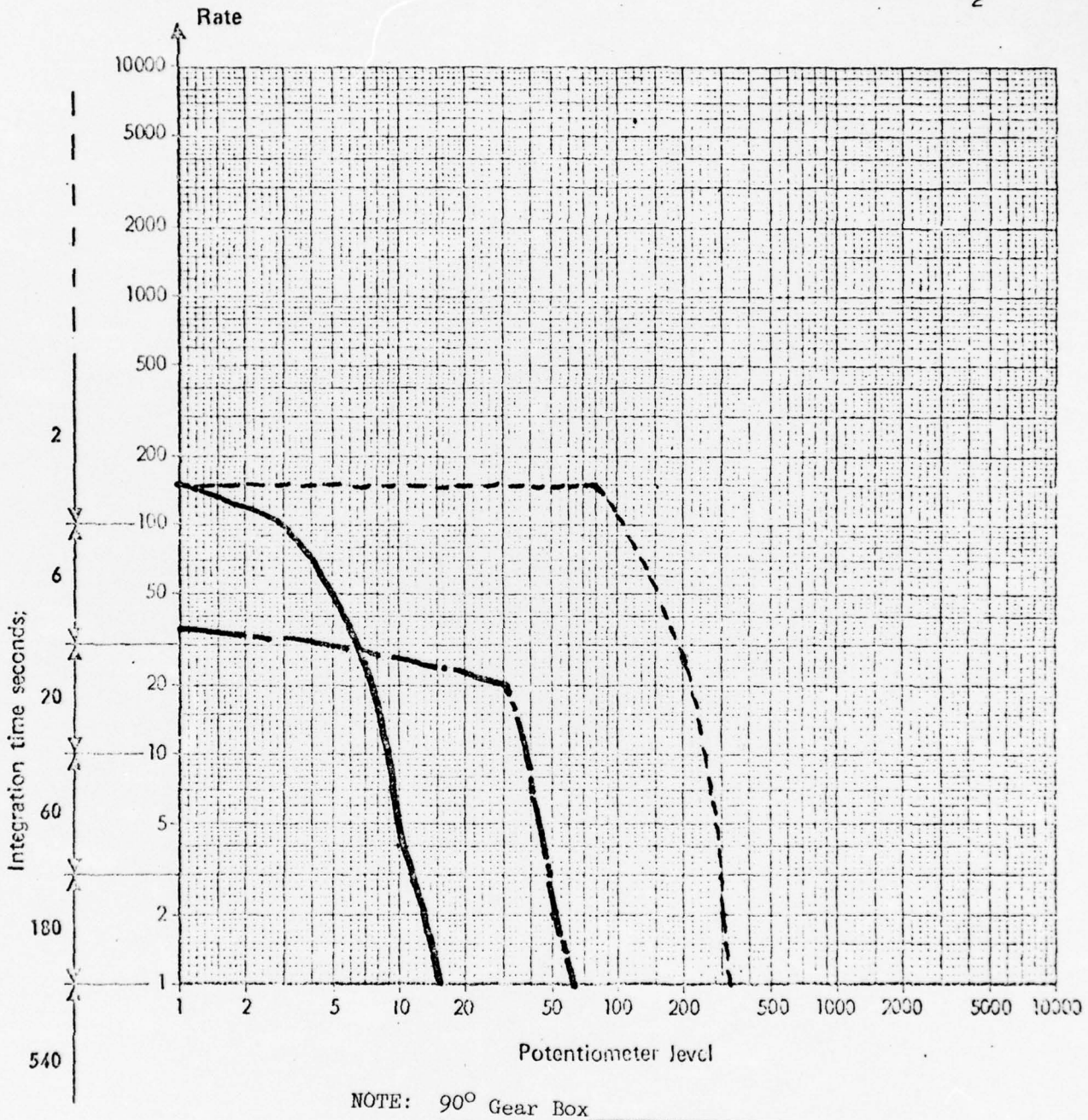


NOTE: 90° Gear Box _____
42° Gear Box Output ---------
42° Gear Box Input _____ - _____ - _____

Generator Drive Gear
Input Drive
Mast Bearing

A/C UH-1H 70-16354

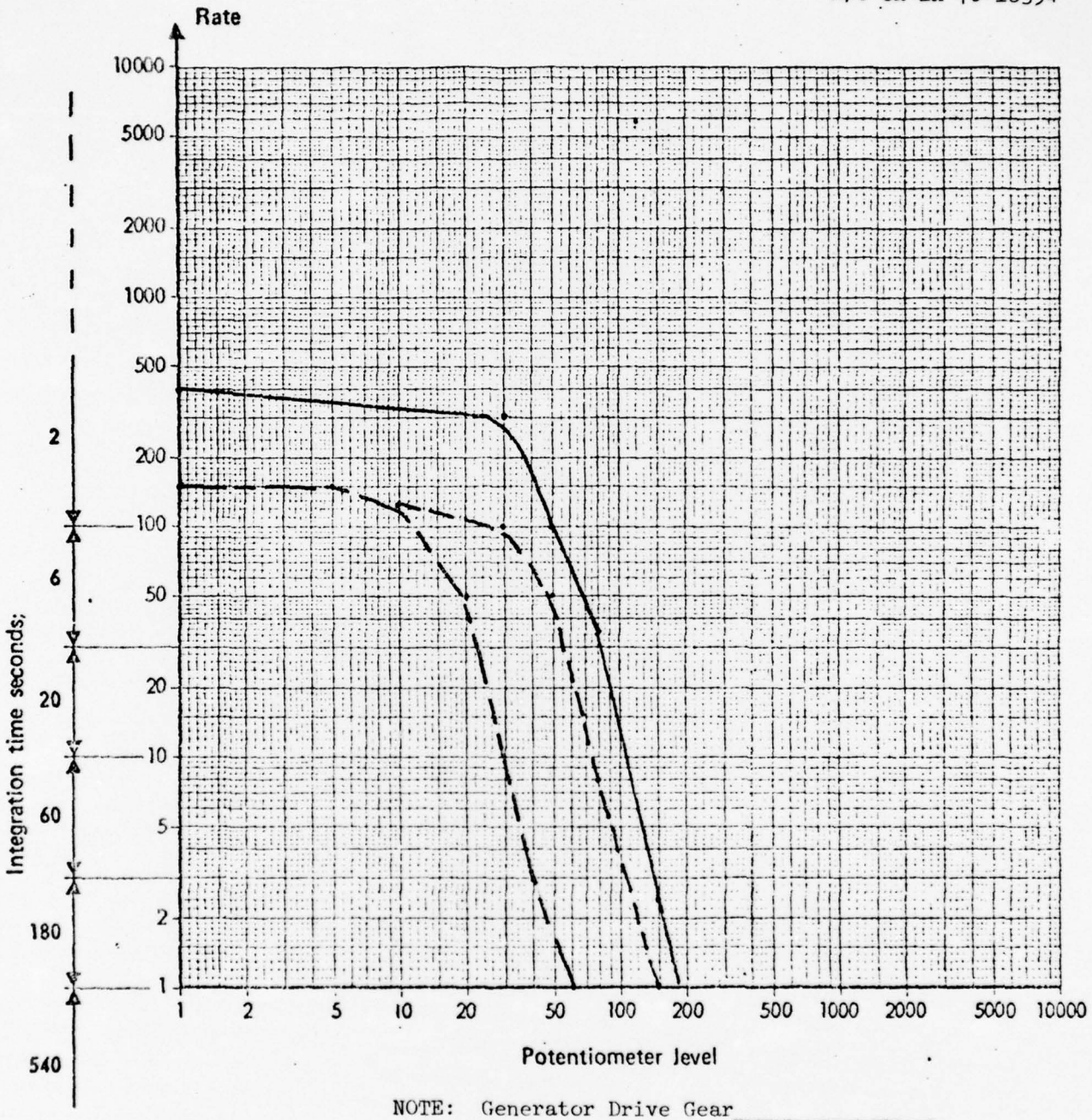


NOTE: Generator Drive Gear_____
Input Drive----------
Mast Bearing_____ - _____ - _____

42° Gear Box Output
Mast Bearing

A/C UH-1D 66-16779
6600 RPM $N_2$

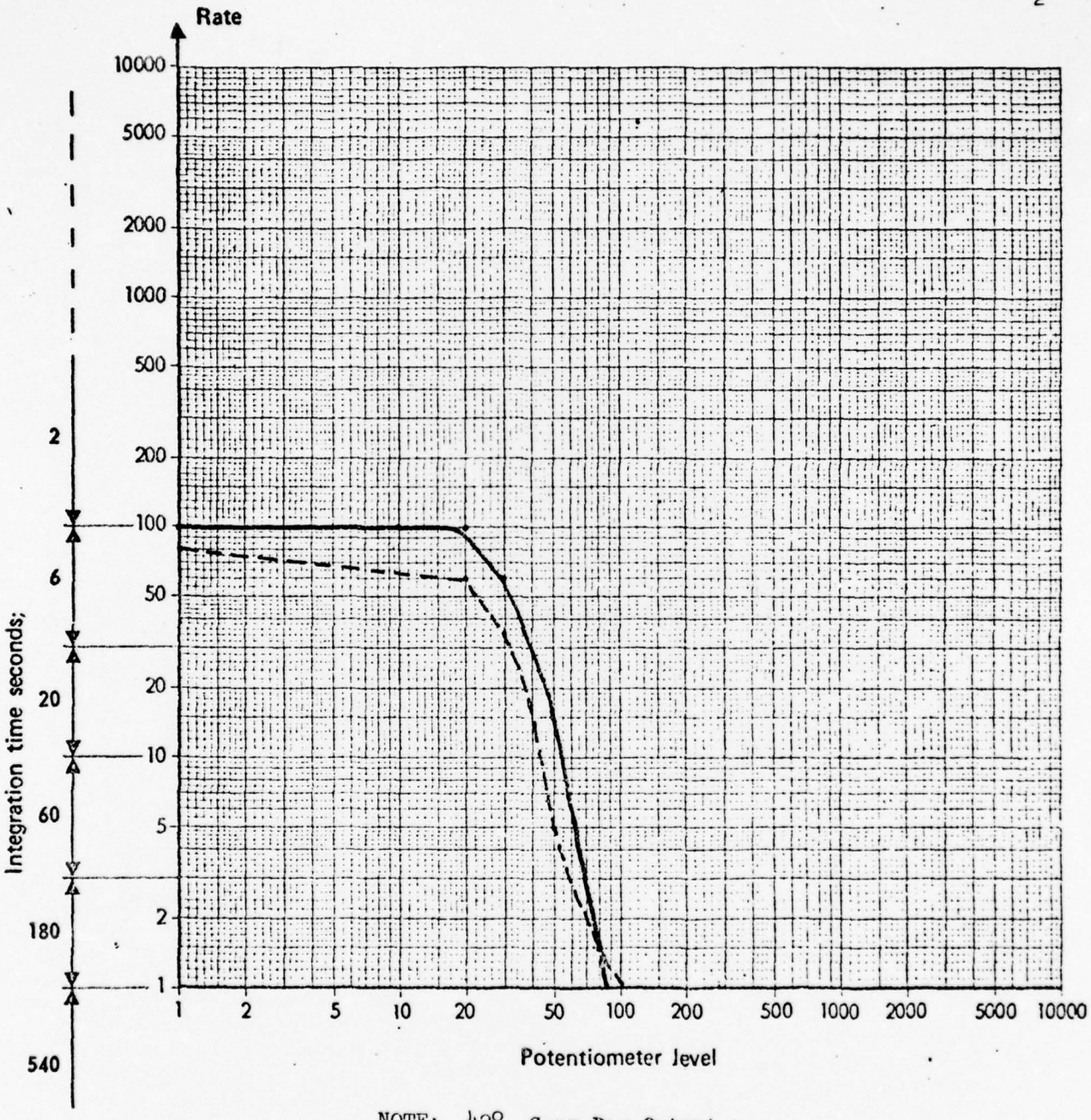


NOTE: 42° Gear Box Output_____
Mast Bearing----------

281st Aviation Company Bi State Airport 14 Aug 74

90° Gear Box
42° Gear Box Input

A/C UH-1D 66-16779
6600 RPM $N_2$

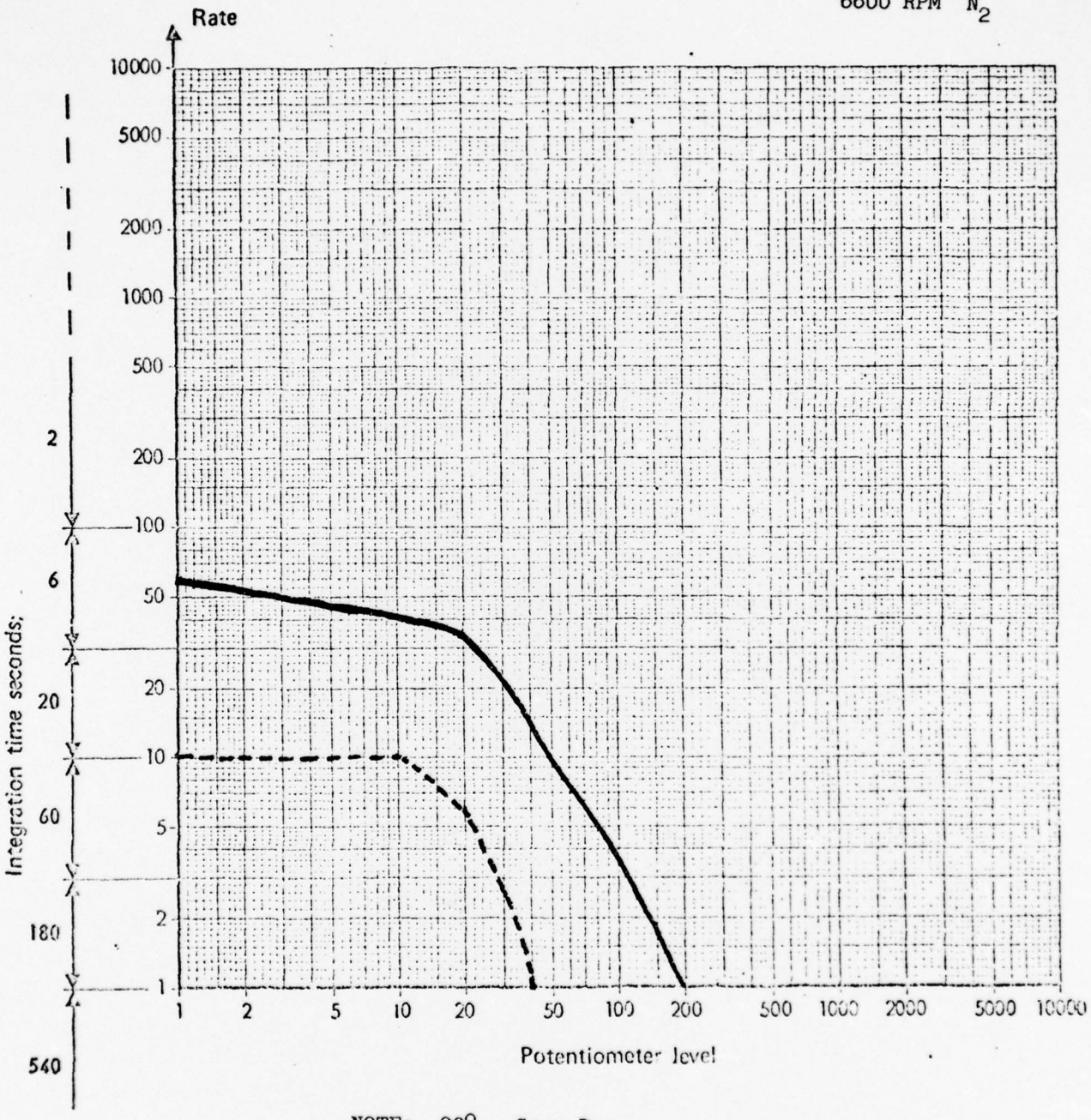


NOTE: 90° Gear Box_____
42° Gear Box----------

Input Drive Quill

A/C UH-1D 66-16779
6600 RPM $N_2$

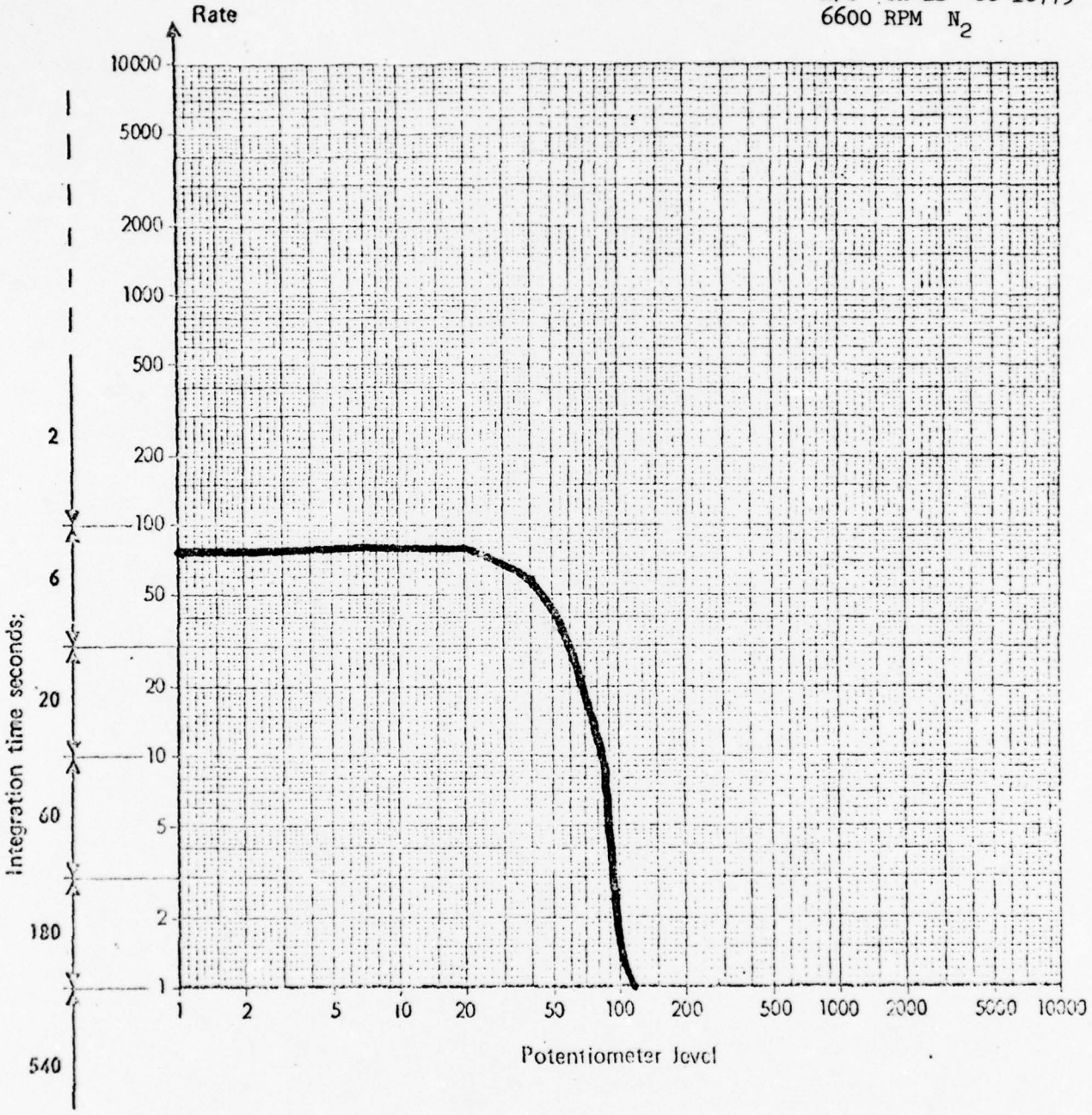

Mast Bearing
Input Drive Quill

A/C 66-01087 UH-1H
6600 RPM $N_2$

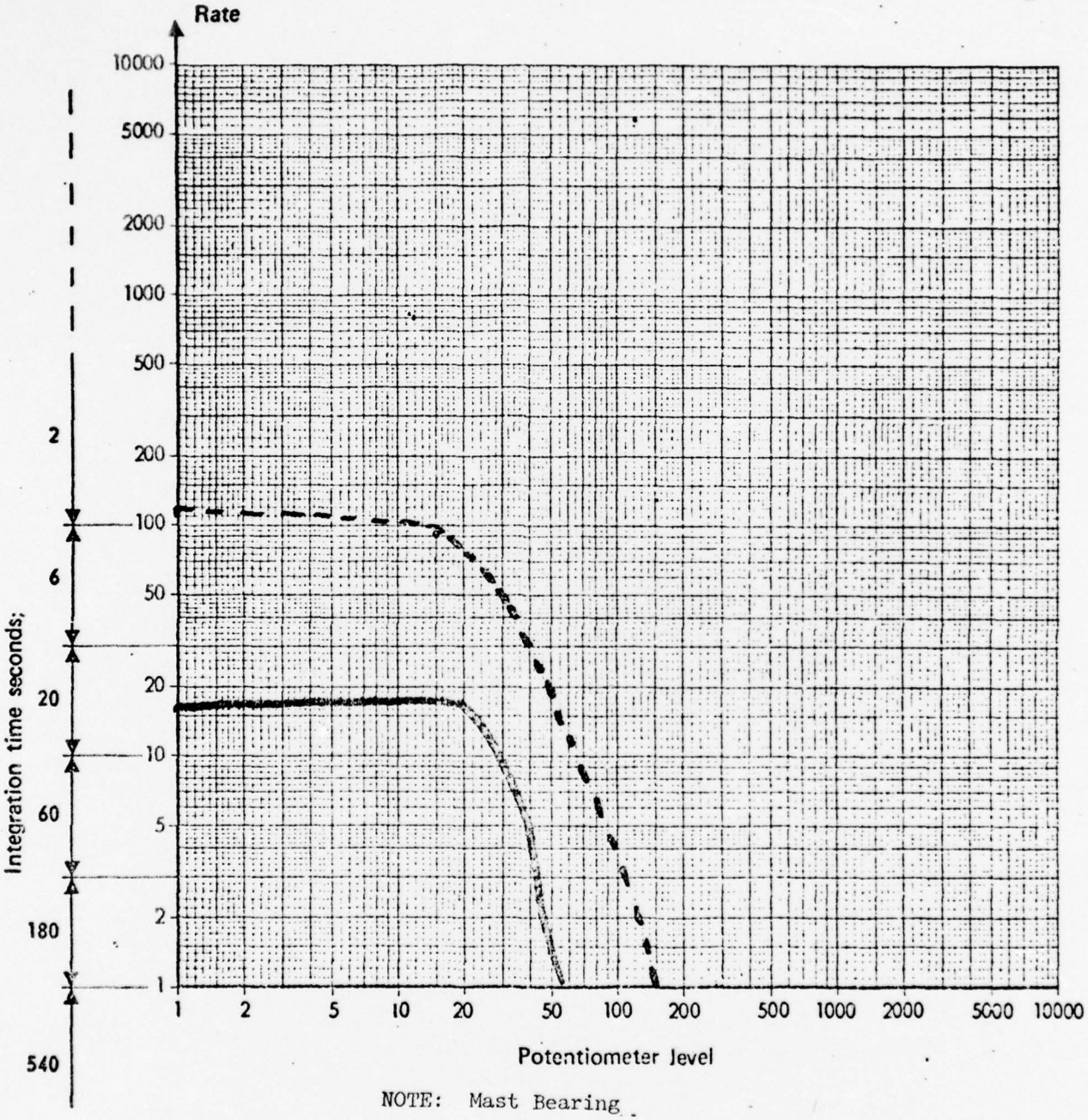


NOTE: Mast Bearing
Input Drive Quill----------

Input Drive Quill

A/C 63-8784
6600 RPM $N_2$

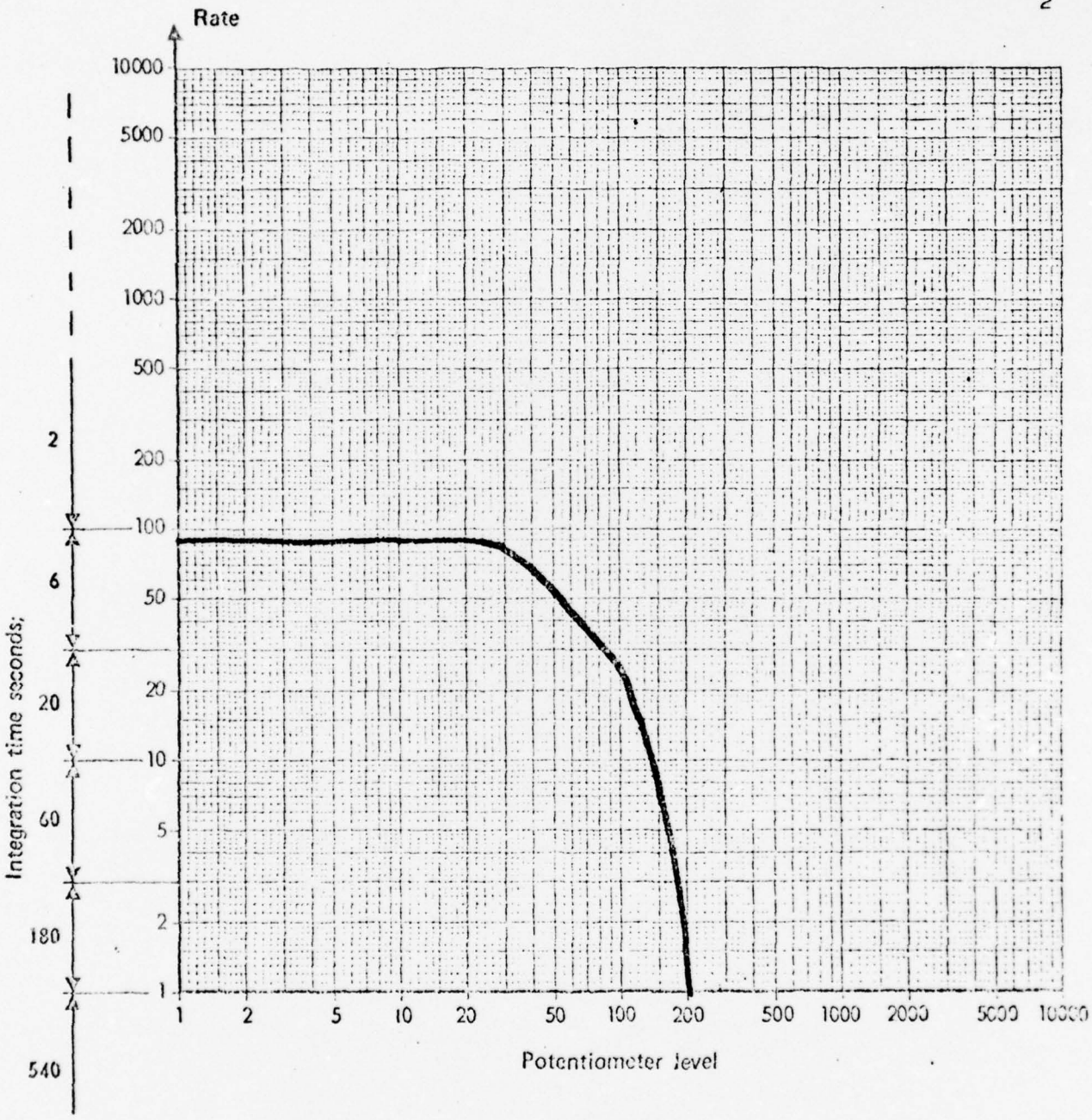

281st Aviation Company Bi State Airport 31 July 1974

42° Gear Box Input
42° Gear Box Output
90° Gear Box

A/C 64-13740 UH-1H
6600 RPM $N_2$

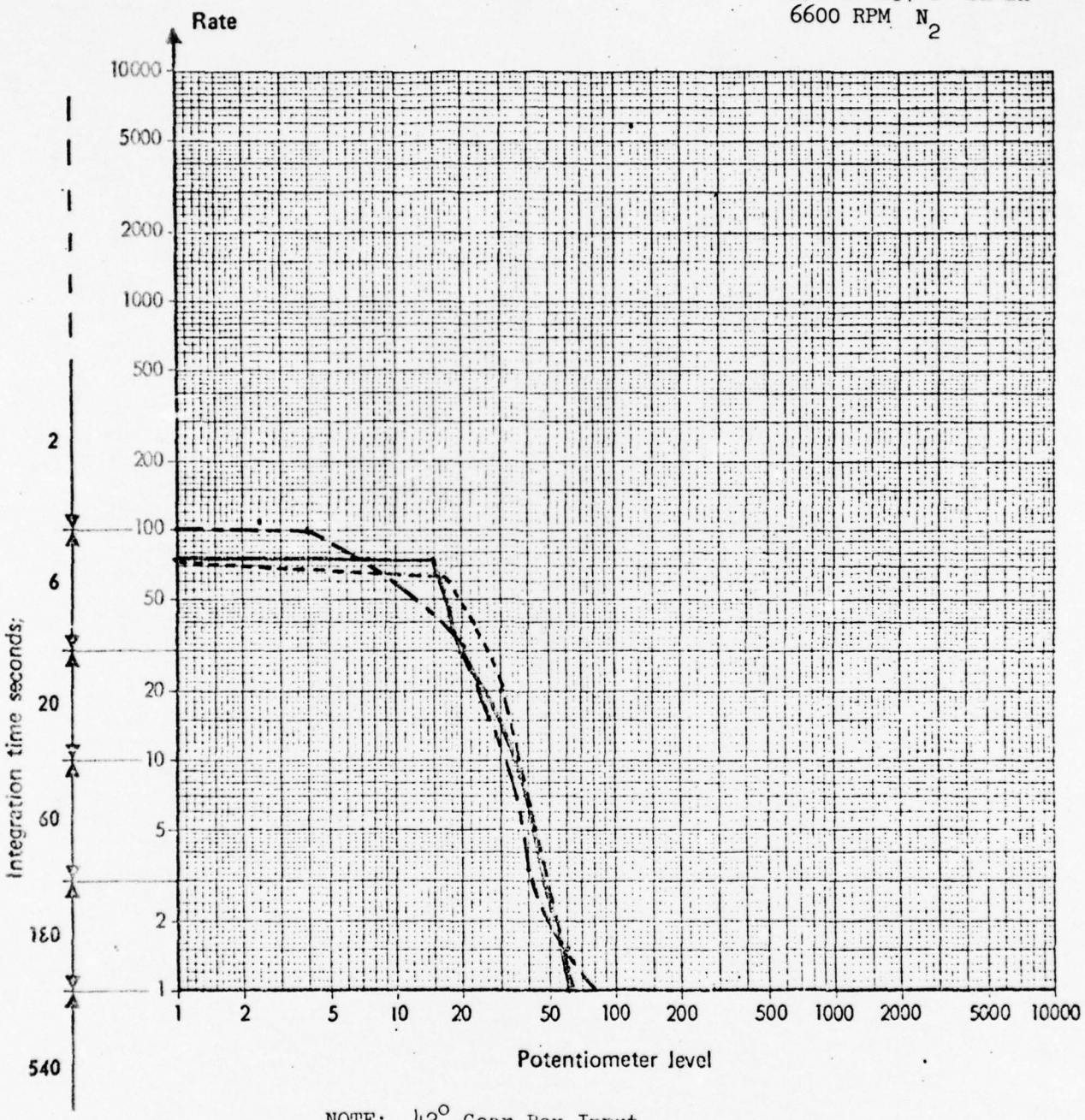


NOTE: 42° Gear Box Input _____
42° Gear Box Output - - - - - - - - - - - -
90° Gear Box _____ _ _____ _ _____ _ _____

AVSCOM FLIGHT DETACHMENT
St. Louis International Airport

18 Sep 74

OH-58-A
A/C# 72-21418
T/R 6180 RPM
Main Rotor 350 RPM
$N_2$ - 103%

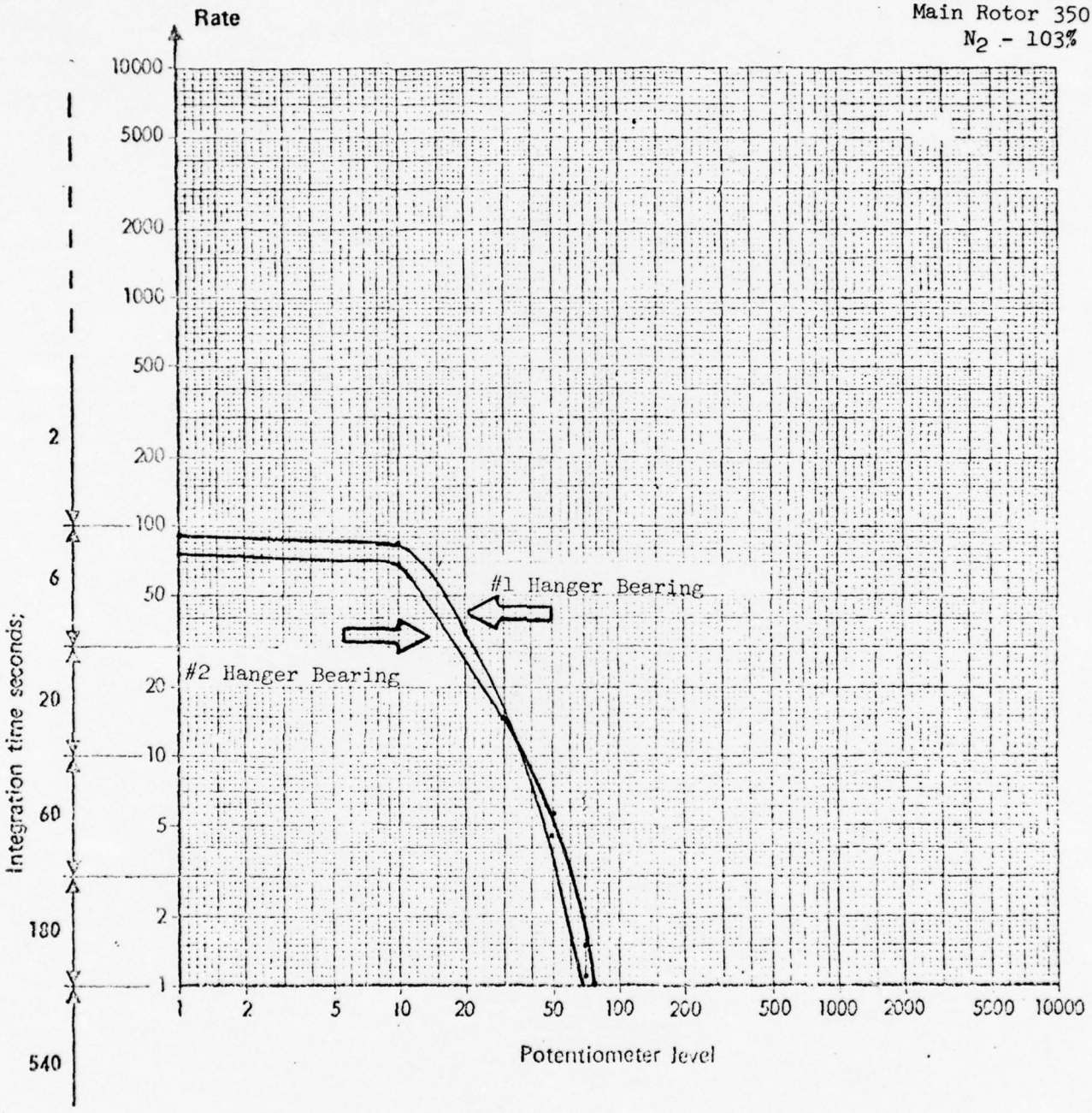

AVSCOM FLIGHT DETACHMENT
St. Louis International Airport

18 Sep 74

Hanger Bearings

OH-58A
A/C# 72-21418
T/R 6180 RPM
Main Rotor 350 RPM
$N_2$ - 103%

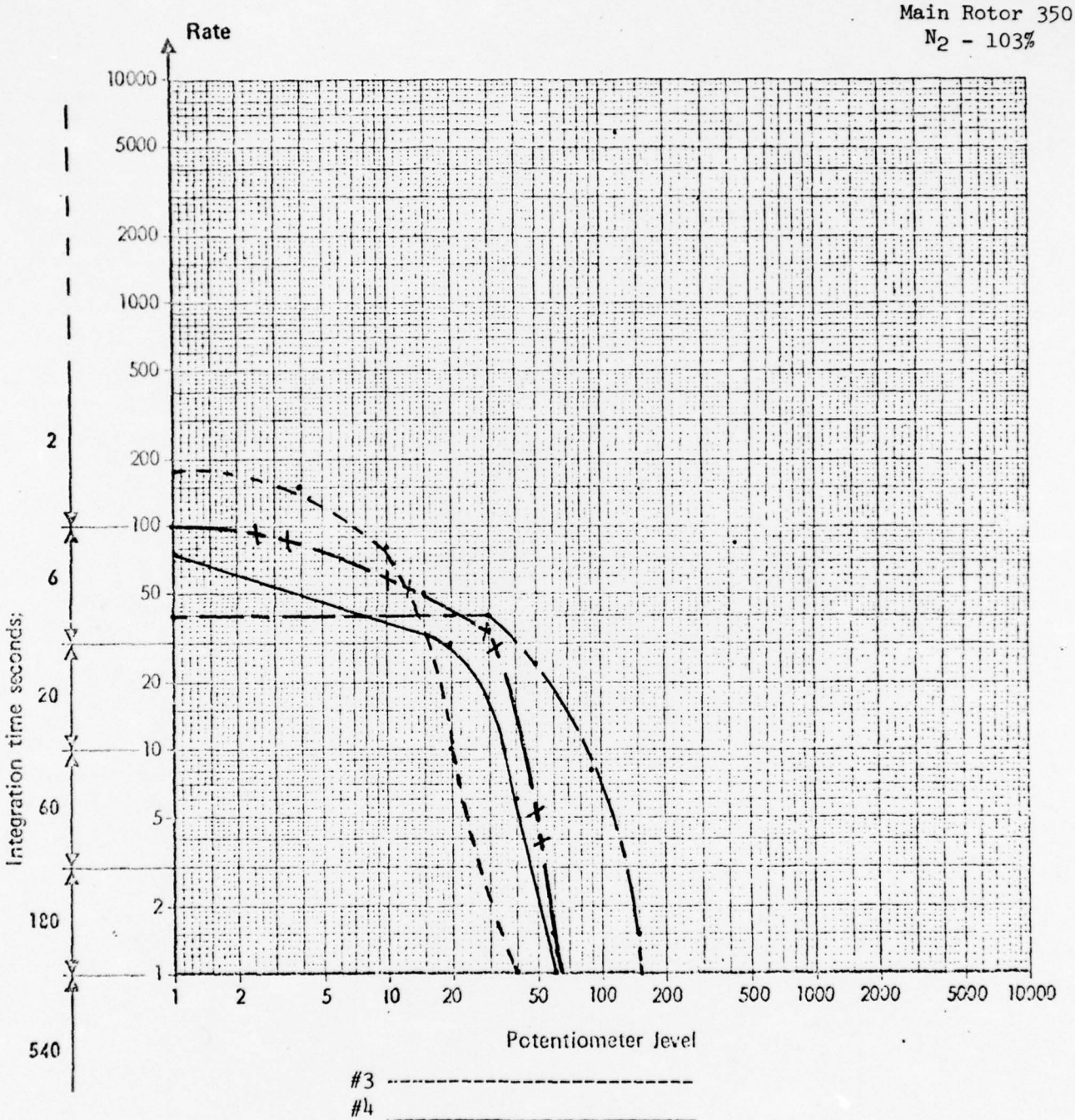


#3 ----------
#4 _____
#5 ___xx_____xx_____xx_____
#6 _ ____ _ ____ _ ____ _ ____

AVSCOM FLIGHT DETACHMENT

ST. LOUIS INTERNATIONAL AIRPORT

18 Sep 74

90° Gear Box

OH-58A
A/C# 72-21418
T/R 6180 RPM
Main Rotor 350 RPM
$N_2$ - 103%

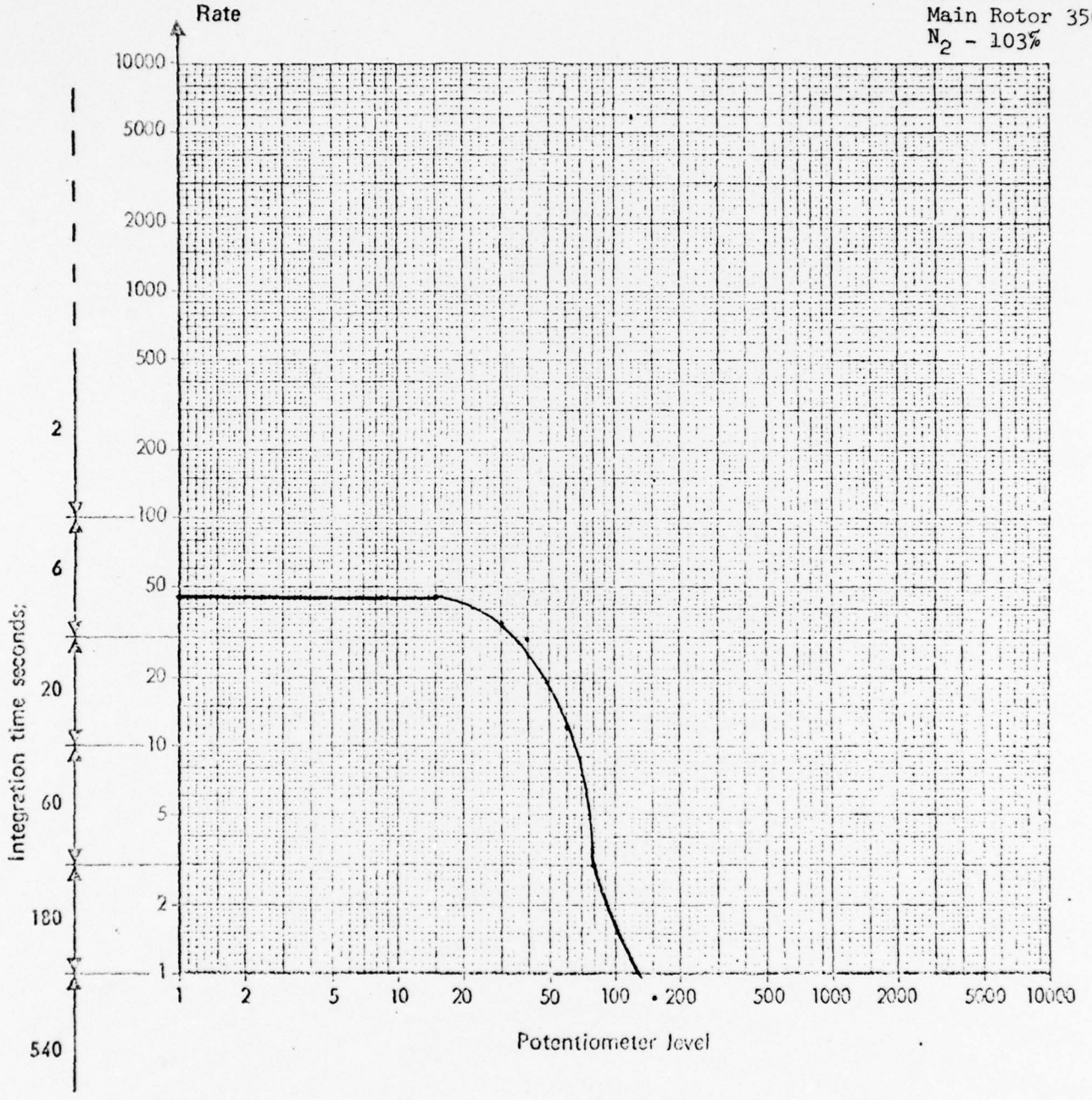

## 7.5 FIELD DATA (Ft. Rucker)

Ft. Rucker, Al. (U.S. Army Test Board) 13 Jun 74

#3 Hanger Bearing

A/C - BC 13
6600 RPM $N_2$

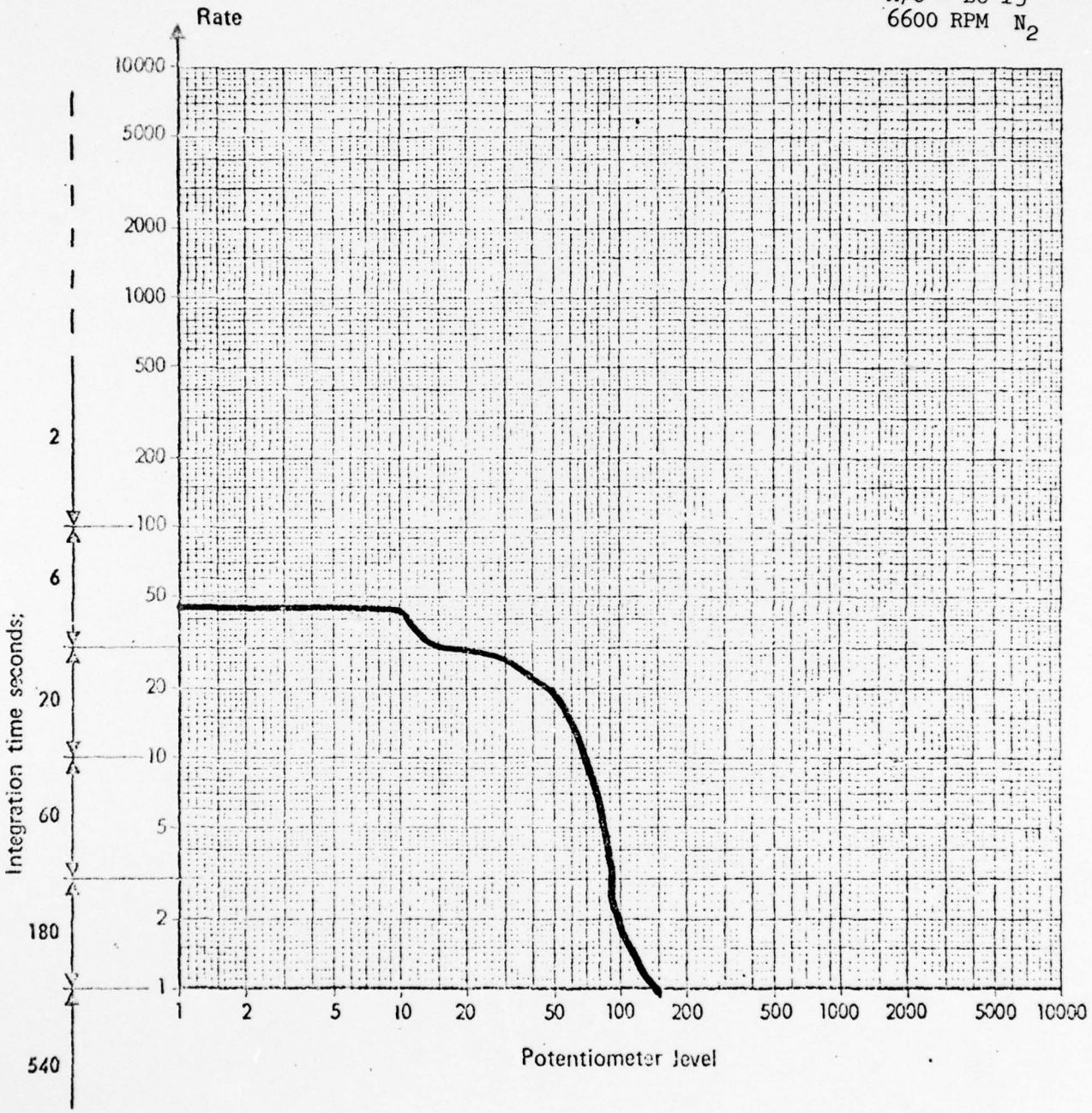

Ft. Rucker Al. (U.S. Army Test Board) 13 Jun 74

#4 Hanger Bearing A20-34779

A/C - BC 13
6600 RPM $N_2$

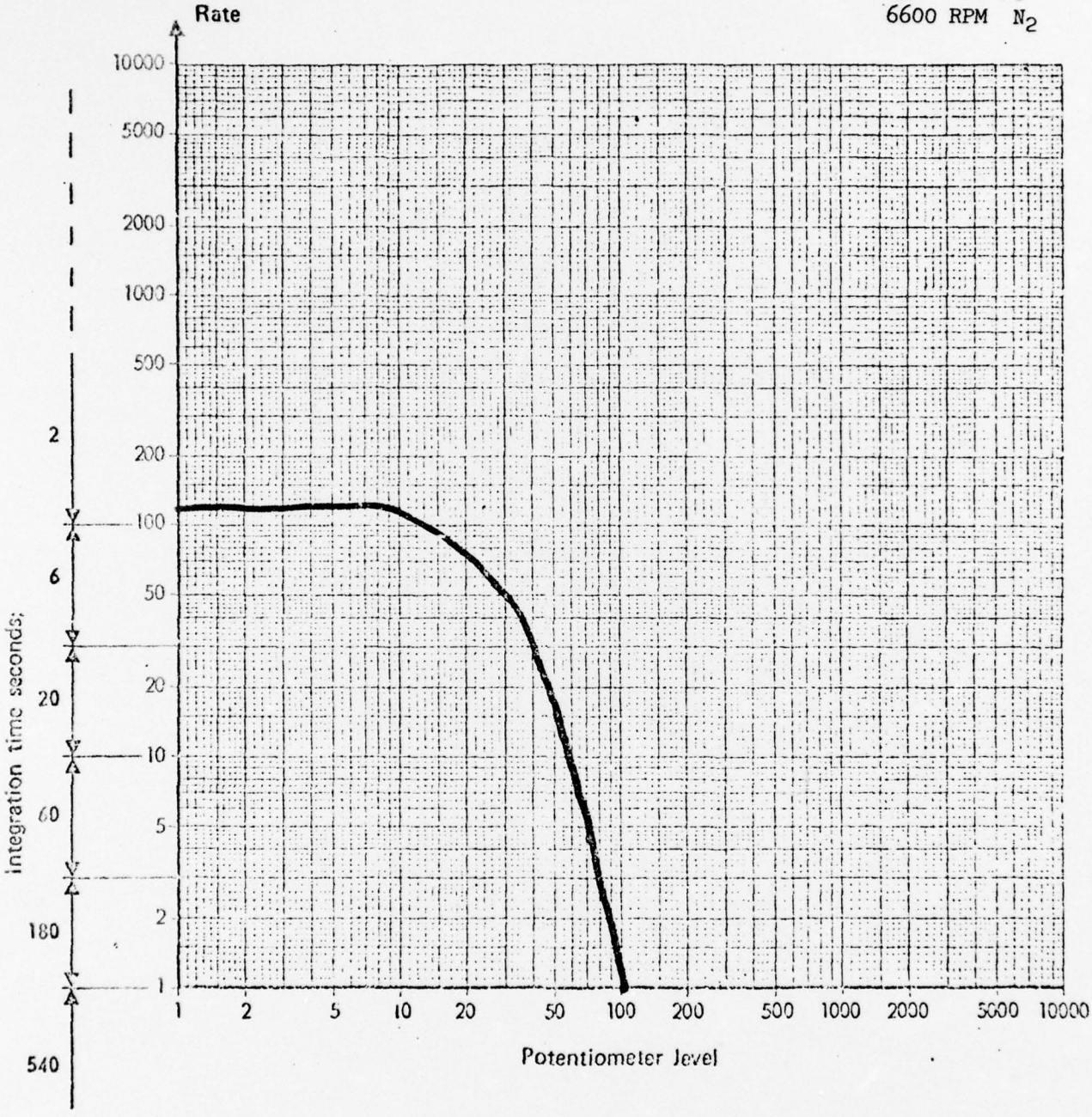

Ft. Rucker, Al. (U.S. Army Test Board) 13 Jun 74

#3 Hanger Bearing

A/C - BC 14
6400 RPM $N_2$ full right pedal

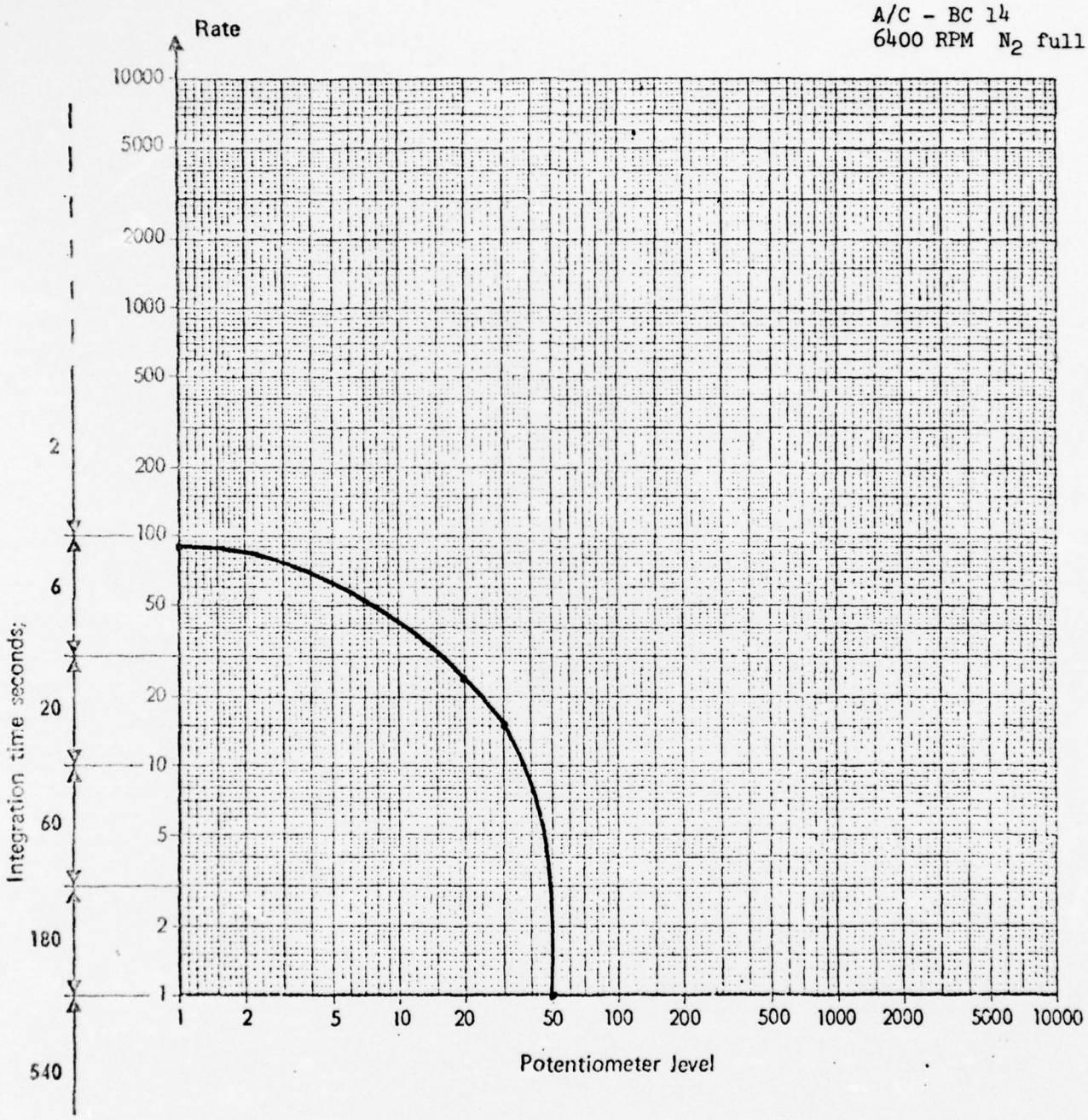

Ft. Rucker, Al. (U.S. Army Test Board) 13 June 74

#3 Hanger Bearing

A/C - BC 14
Flight Idle

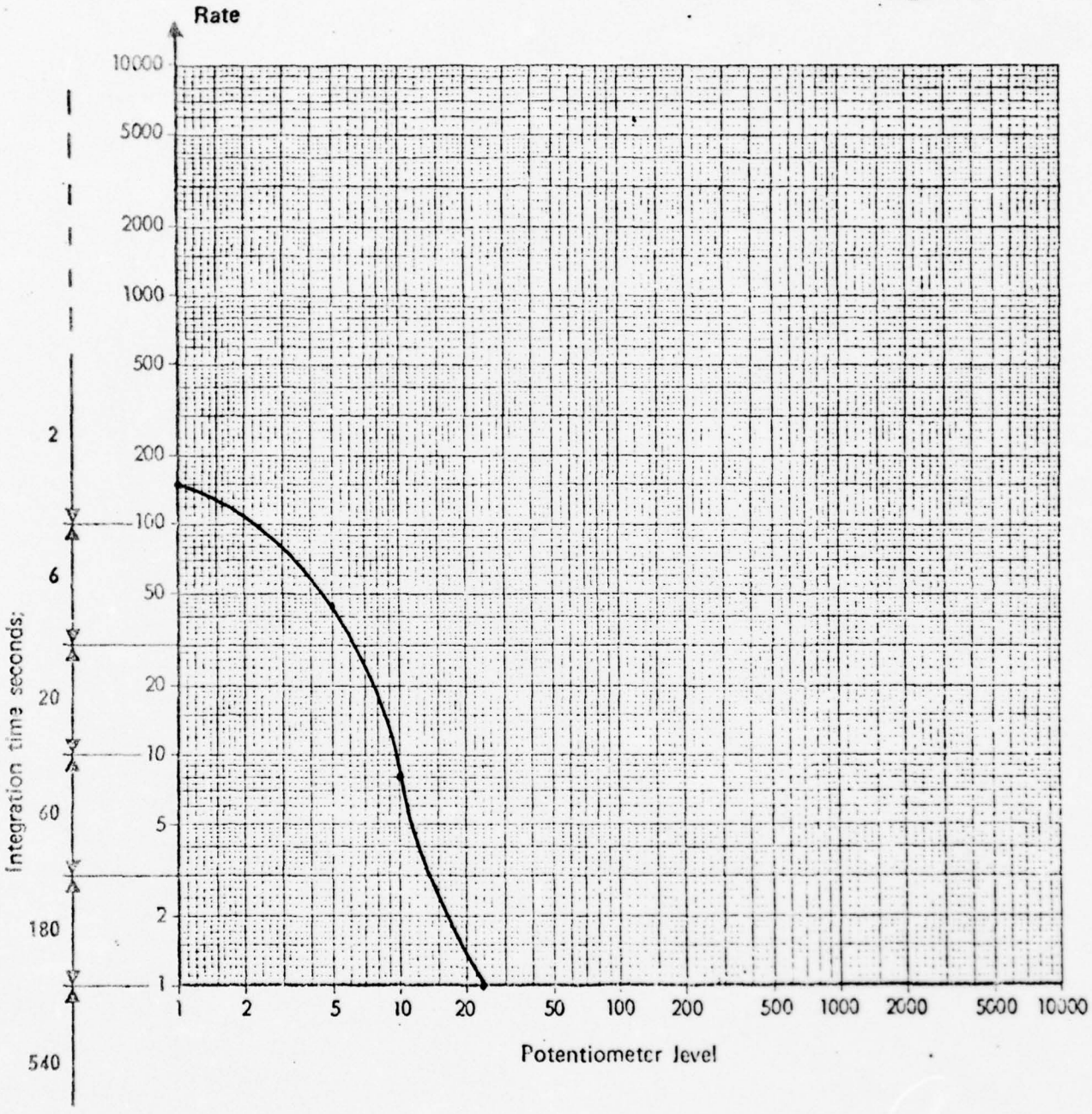

Ft. Rucker,Al. (U.S. Army Test Board) 13 Jun 74

#4 Hanger Bearing

A/C - BC 14
6400 RPM $N_2$ full left pedal

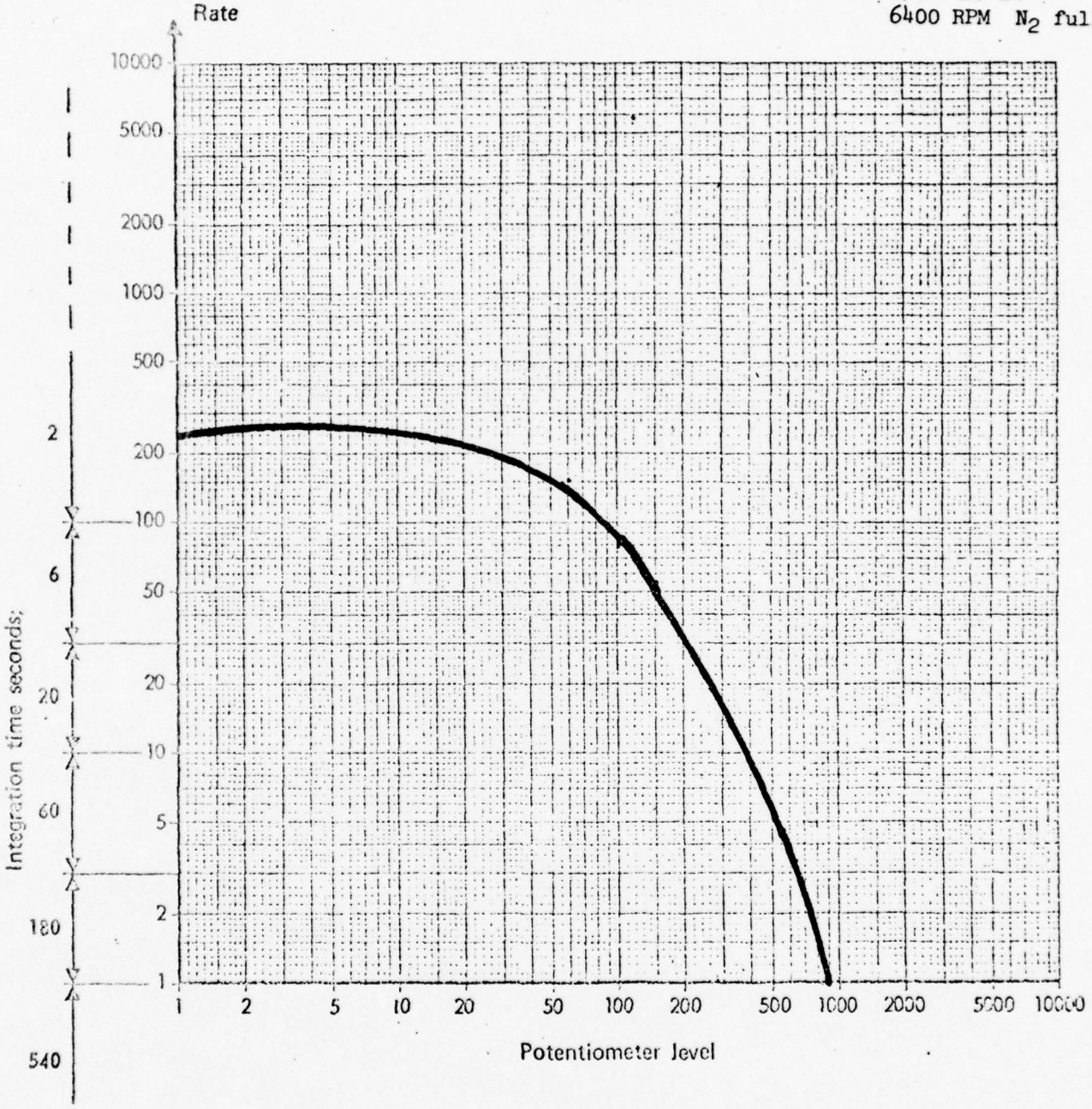

Ft. Rucker, Al. (U.S. Army Test Board) 13 Jun 74

#4 Hanger Bearing A/C - BC 14
Flight Idle

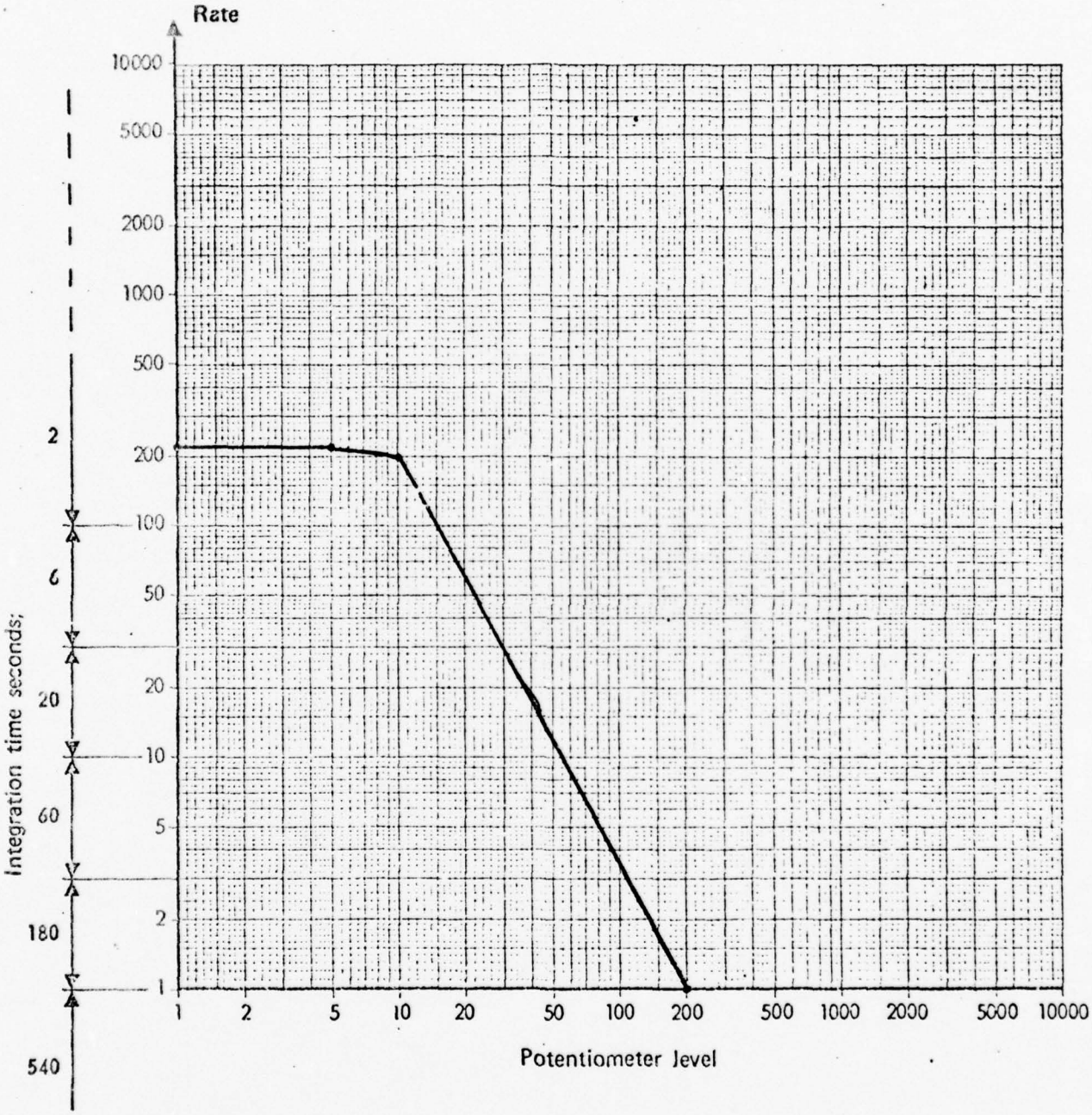

Ft. Rucker, Al. (U.S. Army Test Board) 14 Jun 74

#3 Hanger Bearing

A/C - BC 13
6600 RPM $N_2$

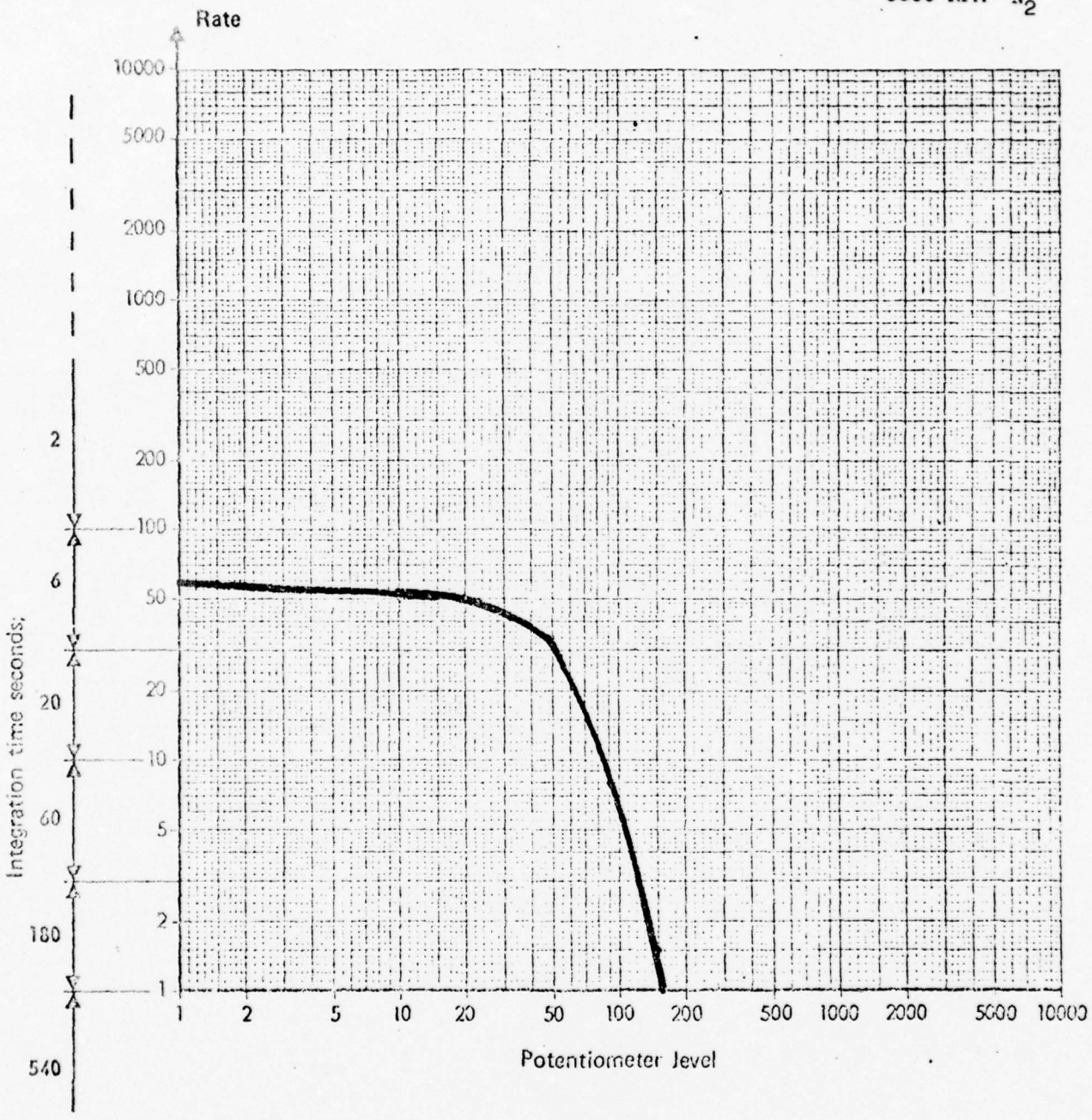

Ft. Rucker, Al. 14 June 74

Hanger Bearing

A/C BC 13
6600 RPM $N_2$

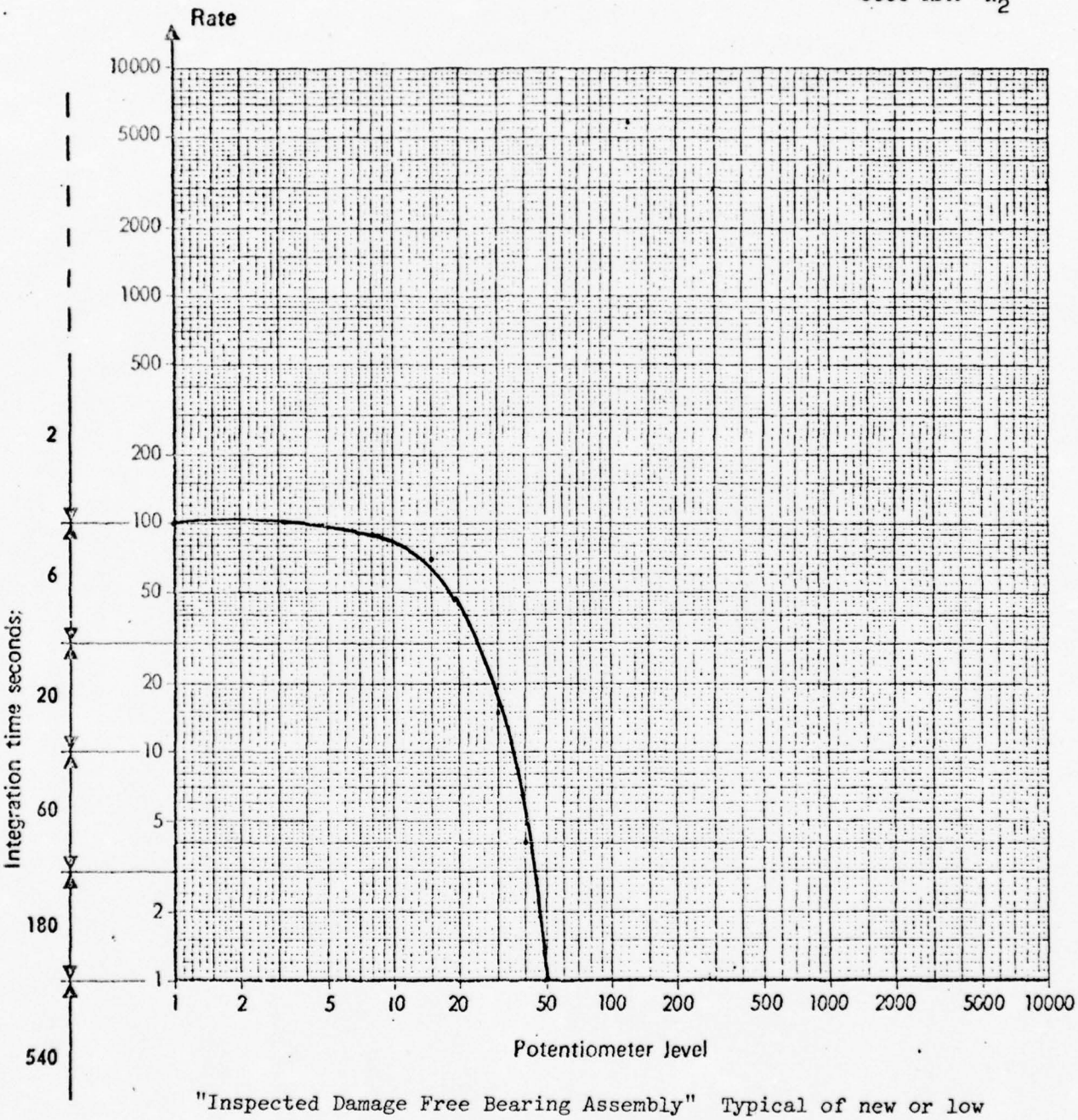


"Inspected Damage Free Bearing Assembly" Typical of new or low time assemblies tested.

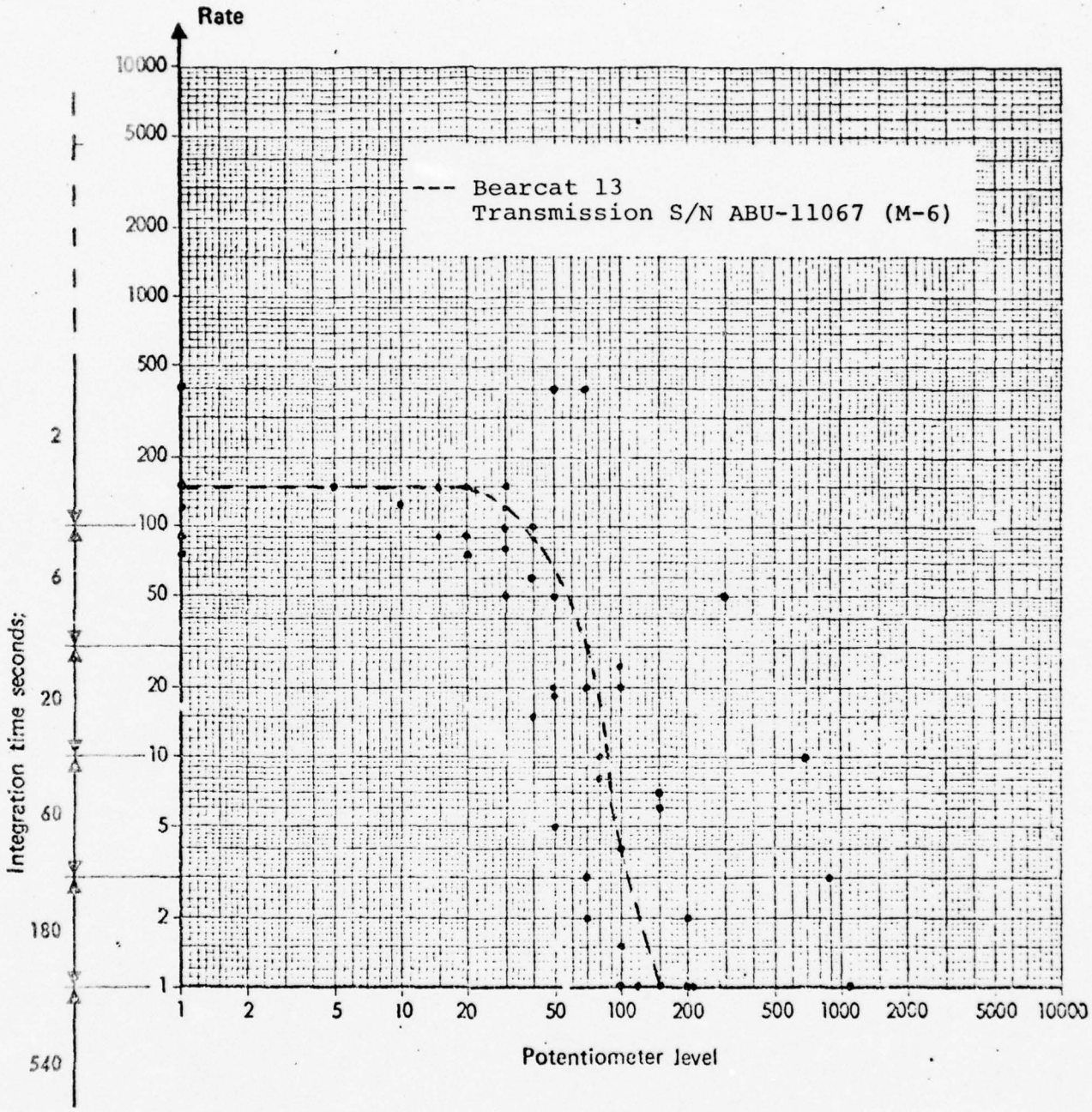


Scatter Diagram

Transmission Input Drive Quill;
Ground Runs, $N_2$ = 6600 RPM.

--- Bearcat 13
Transmission S/N ABU-11067 (M-6)

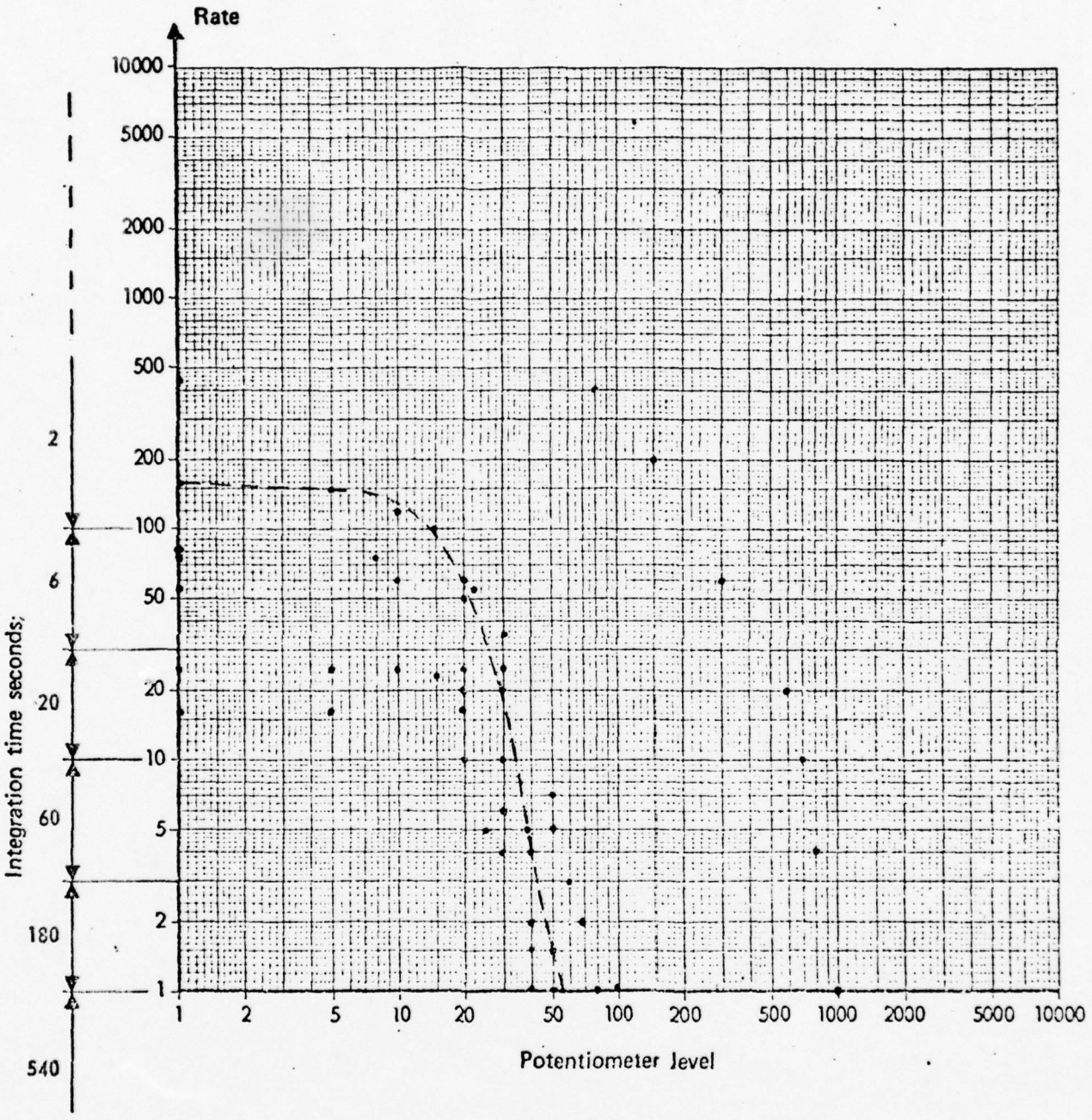


Scatter Diagram
Transmission Mast Bearing Assembly

. Aft
Δ Starboard
∇ Forward
x Port (Normal Attachment)

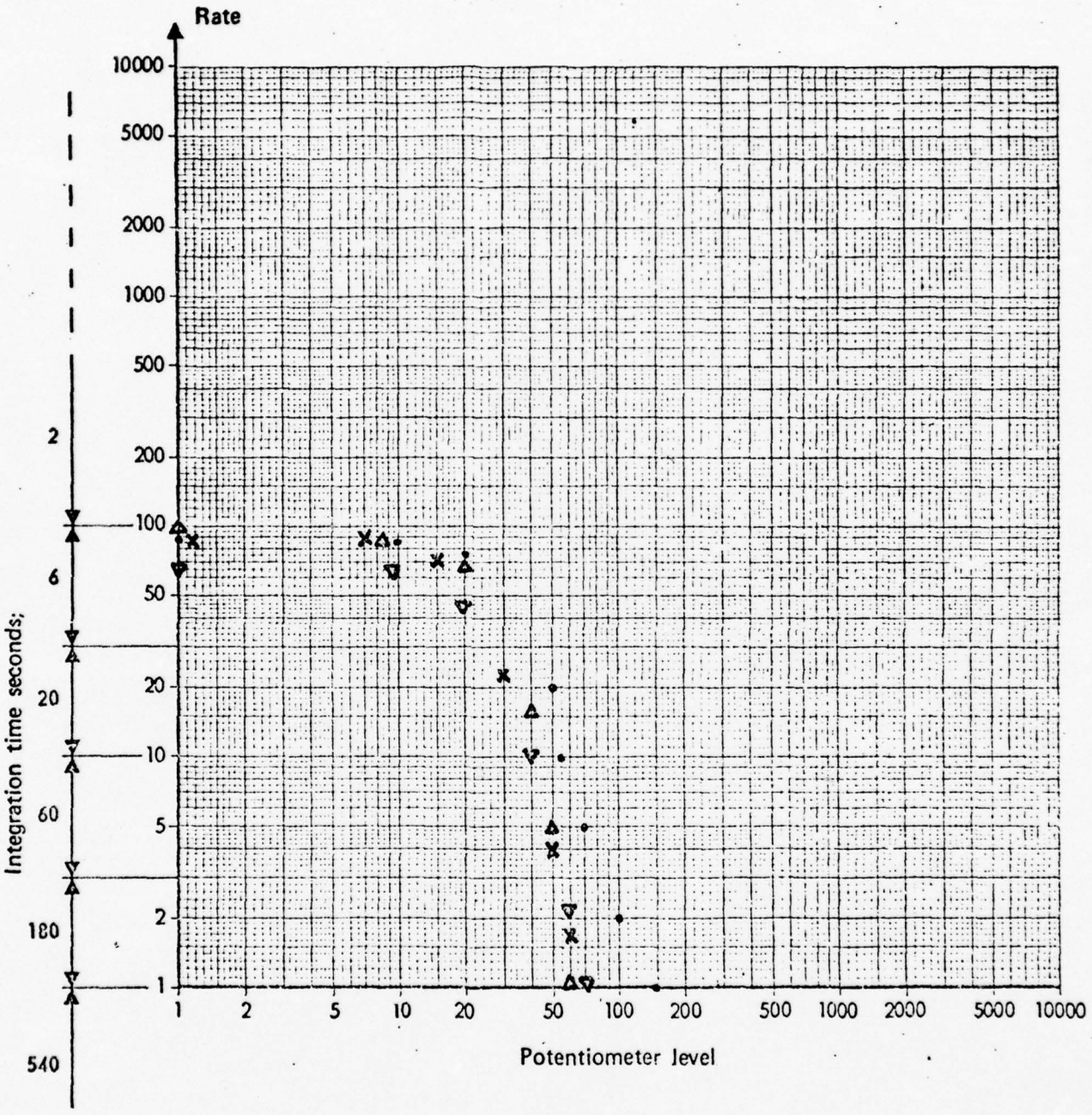


Effect of Sensor Mounting
On Mast Bearing Reading

Ft. Rucker, Al.

13 June 74

42° Gear Box

#B13-4312 (F-B)
A/C BC 13
6600 RPM $N_2$

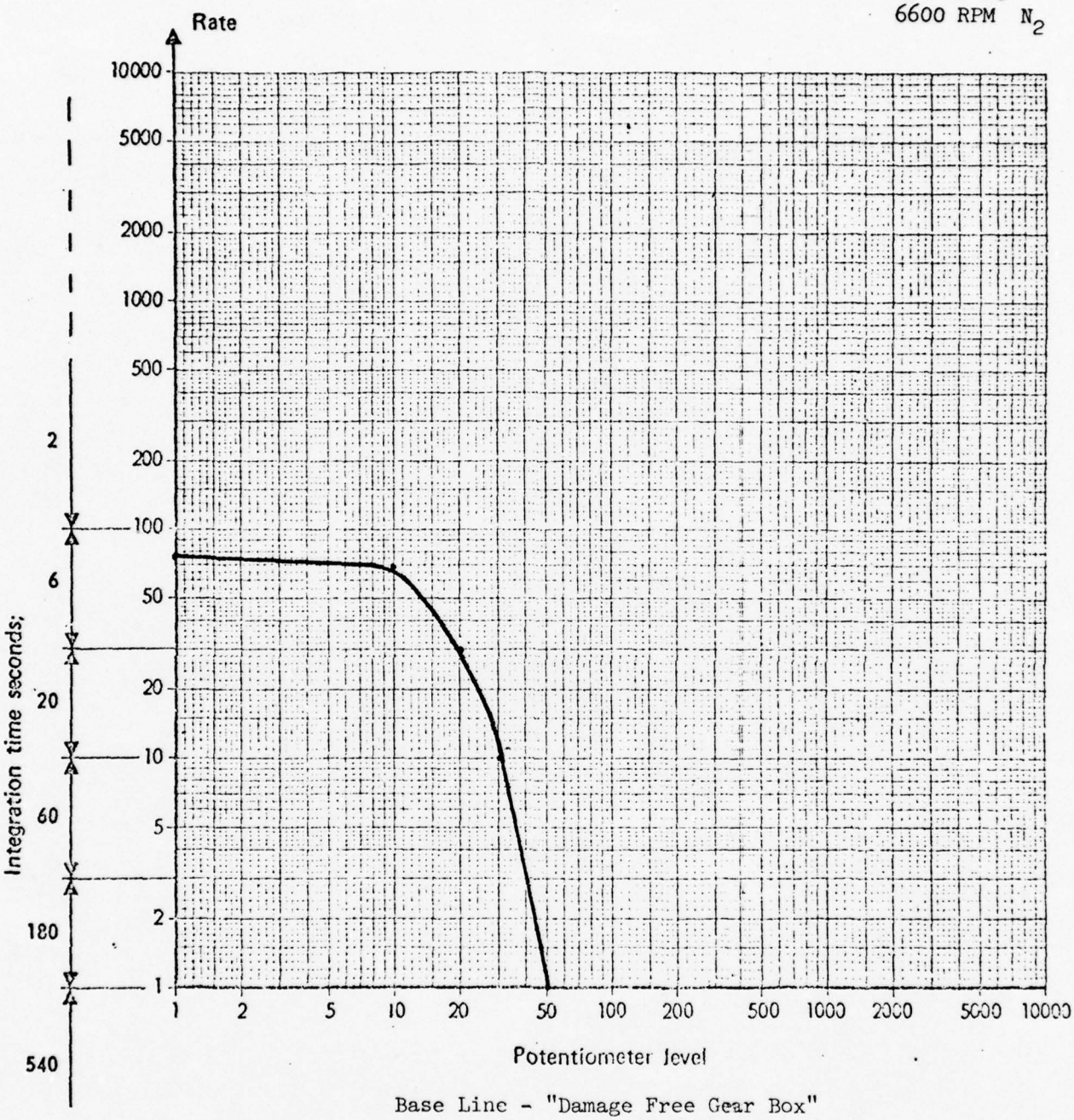


Base Line - "Damage Free Gear Box"

Ft. Rucker, Al.

13 June 74

42° Gear Box

S/N B13-9881 (F-6)
A/C BC-14
6600 RPM $N_2$

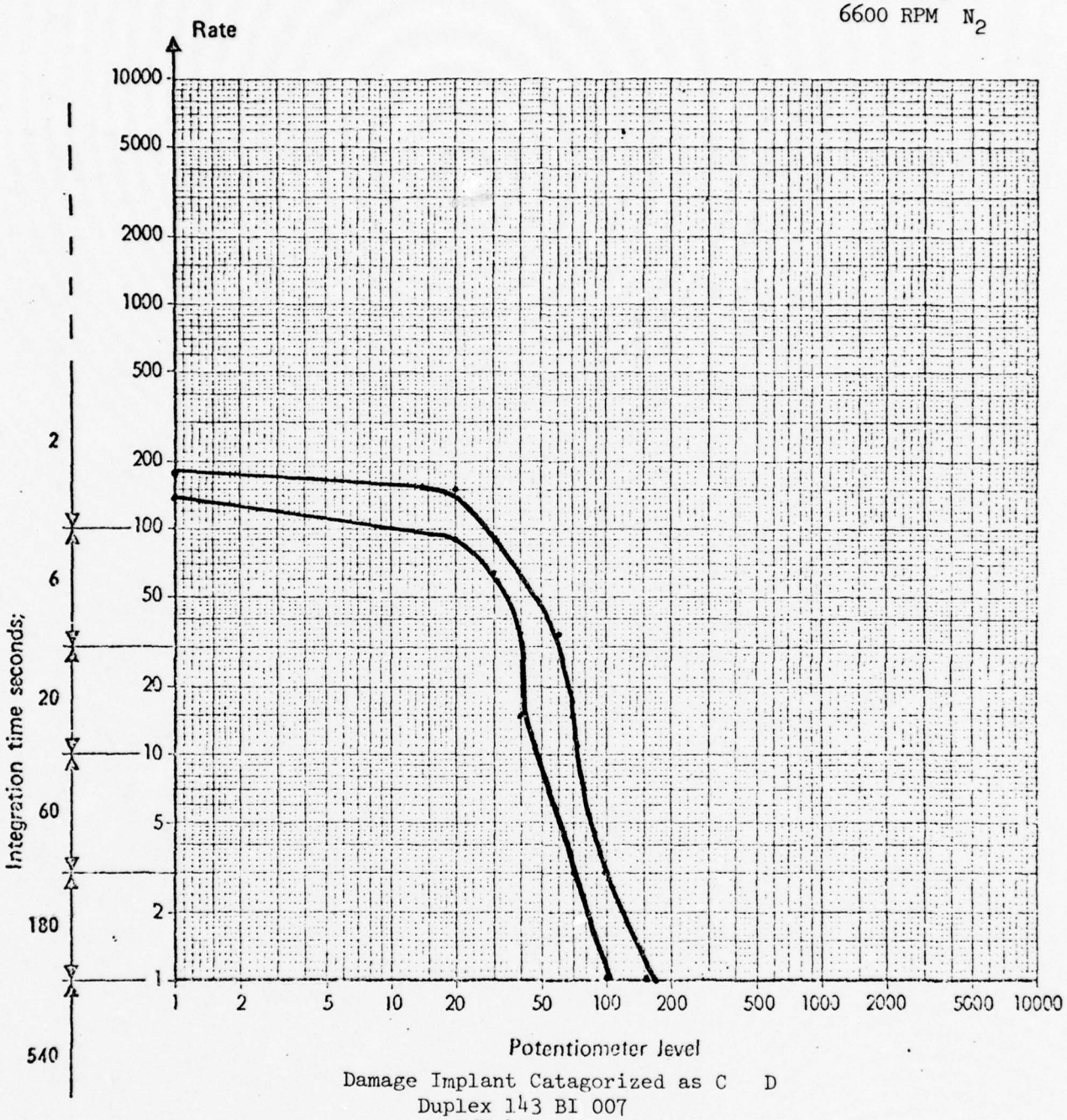


Damage Implant Catagorized as C D
Duplex 143 BI 007
S/N 41100 - 1 & 2
Average Data Scatter of 3 runs

Ft. Rucker, Al. (U.S. Army Test Board) 13 Jun 74

$42^{o}$ g/b

A/C - BC 14
6600 RPM $N_2$

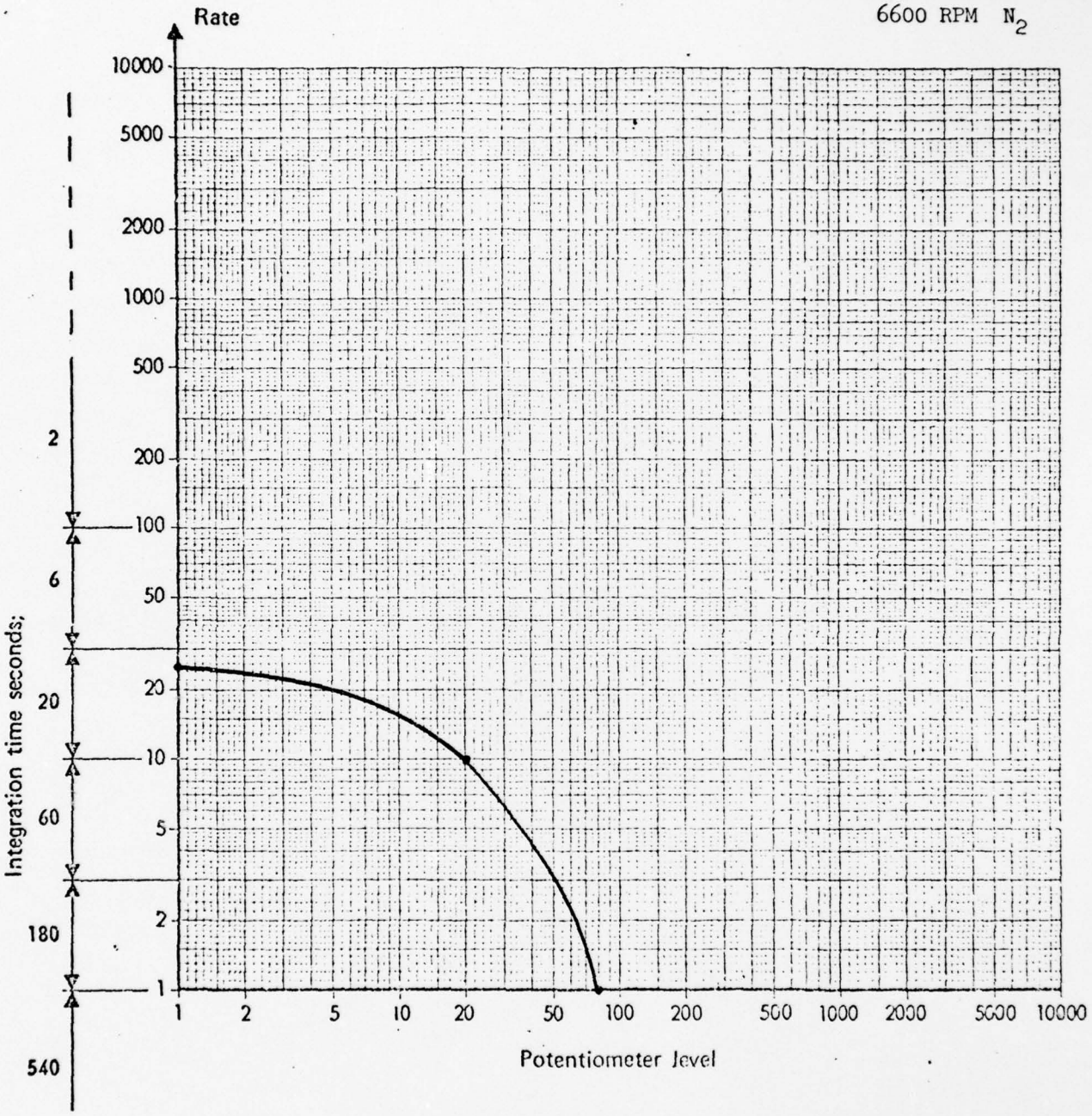

$42^{o}$ g/b

A/C - BC14
6600 RPM $N_2$

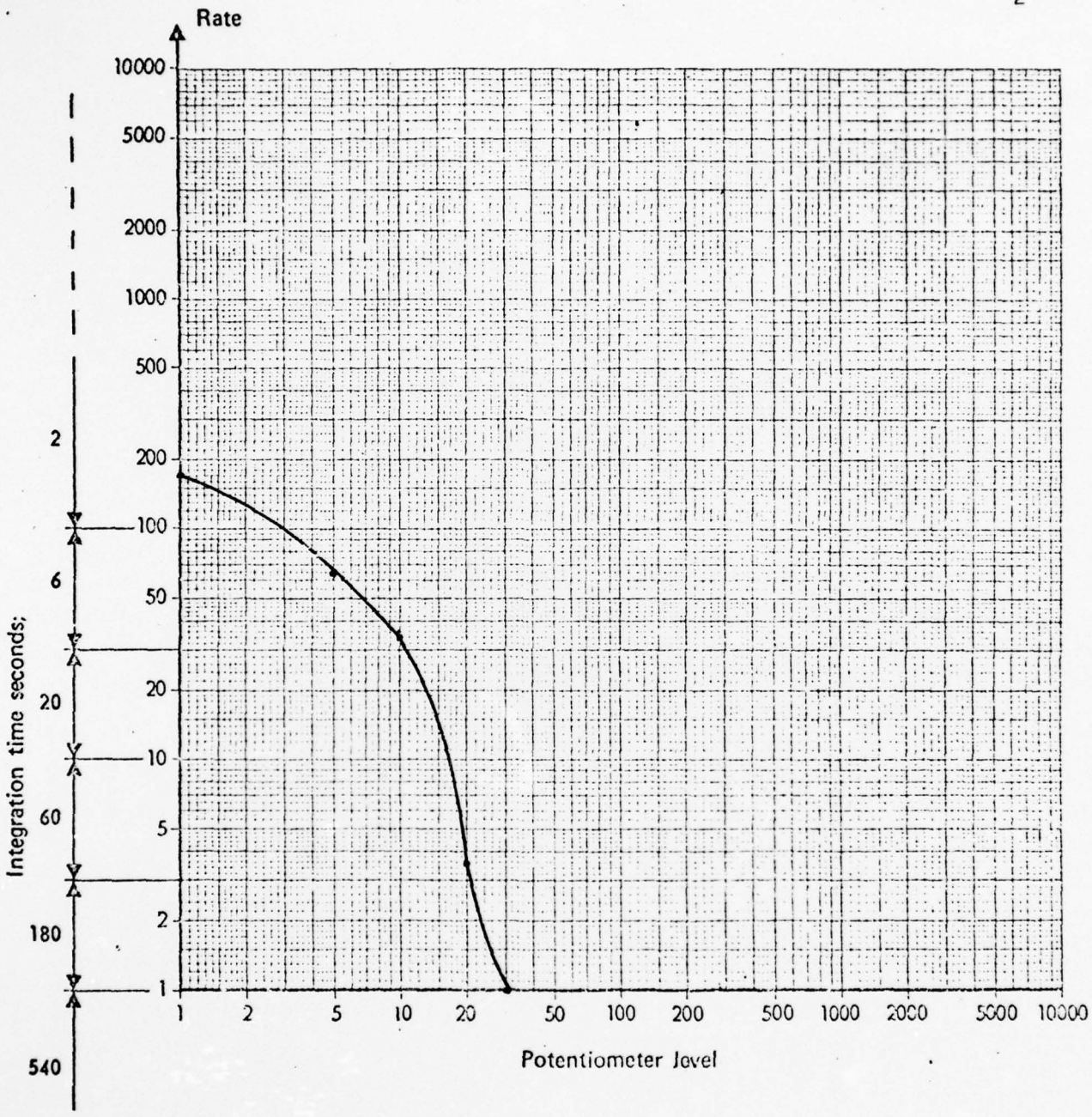

Ft. Rucker, Al. (U.S. Army Test Board) 13 Jun 74

42° Gearbox

A/C - BC 14
6600 RPM $N_2$

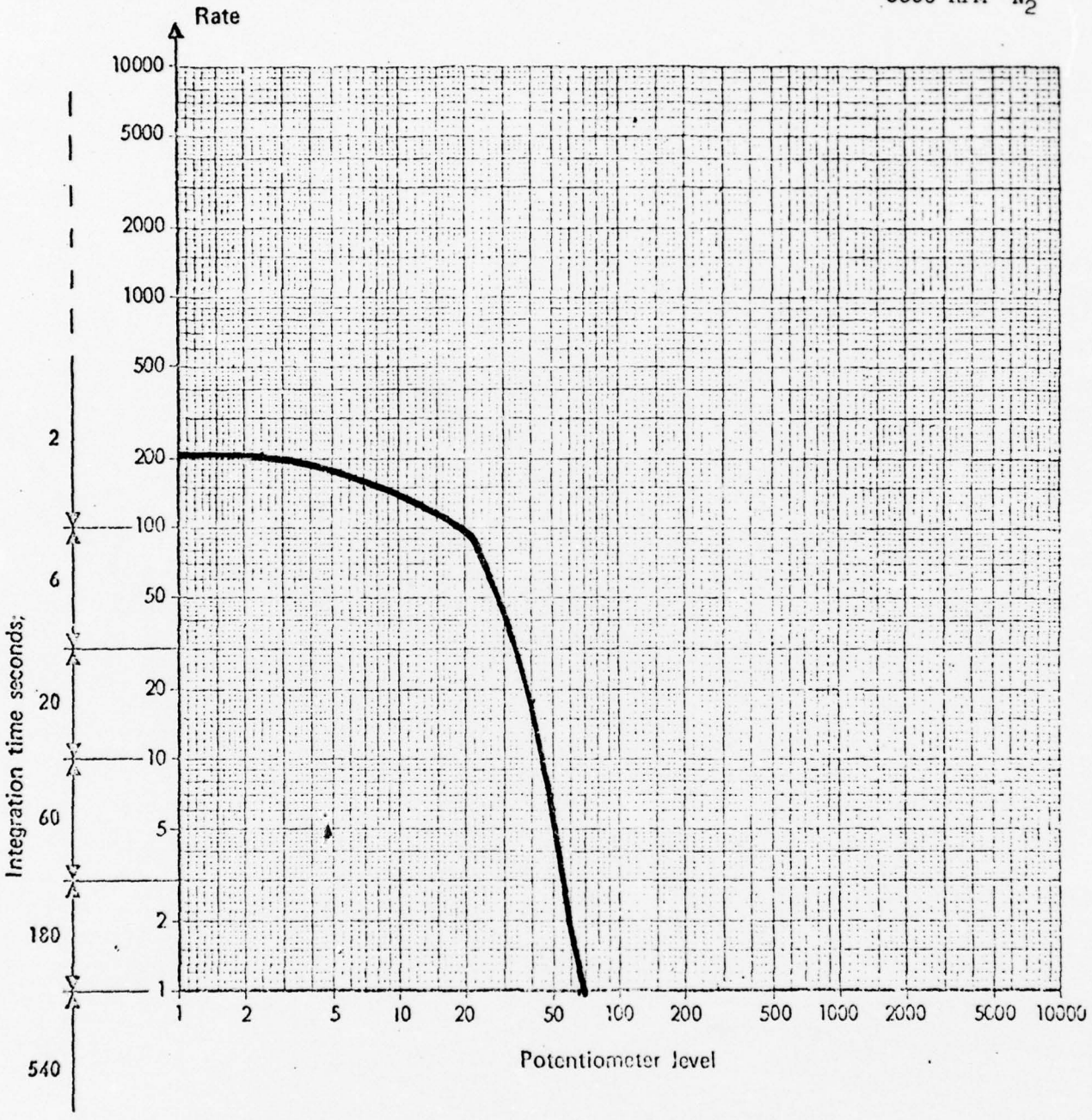

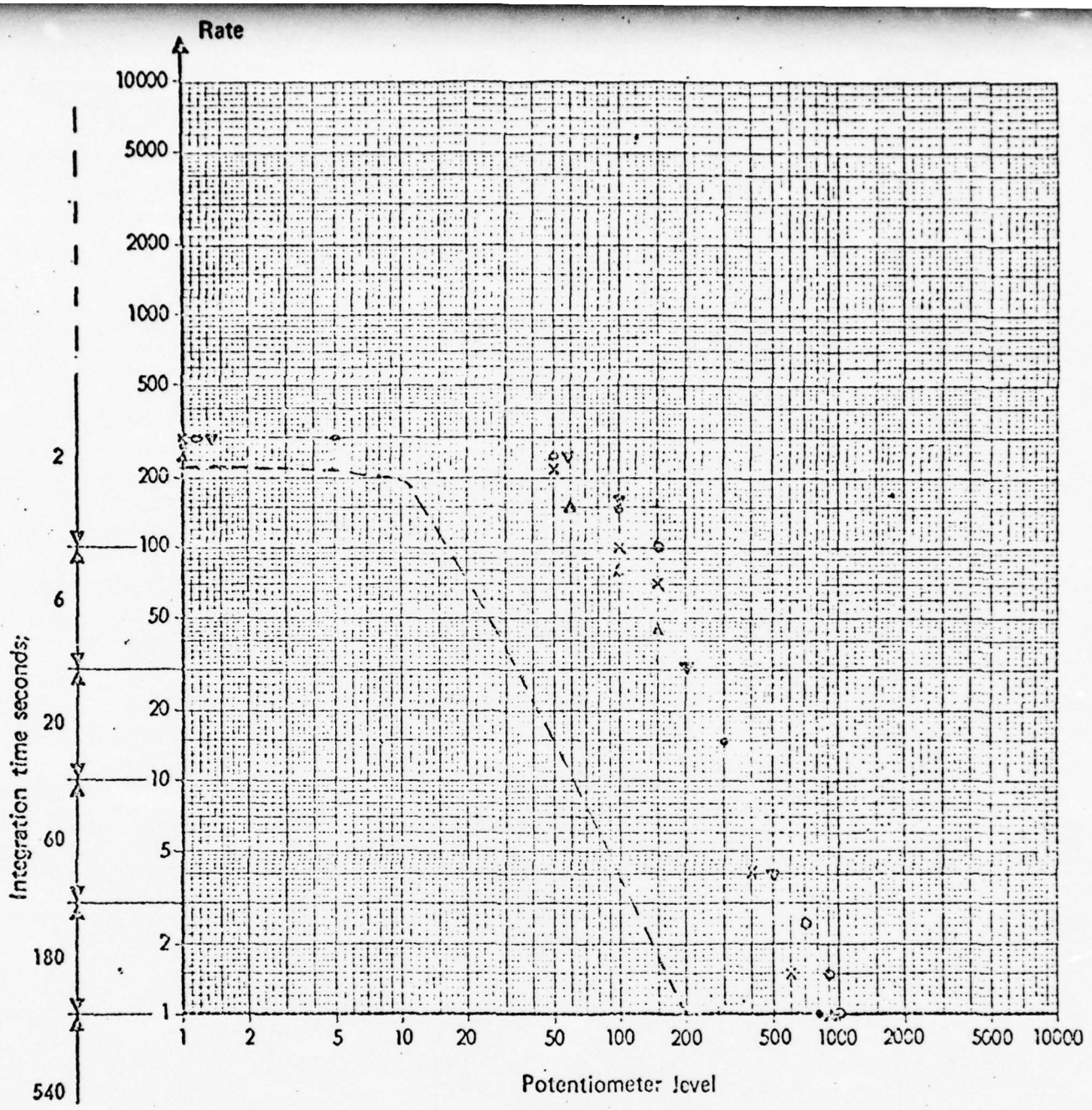


TIE-DOWN TESTS FORT RUCKER, AL.

BEARCAT 14 (S/N 65-9846)

| run | symbol | engine rpm | rudder pedal |
|---|---|---|---|
| 1 | ---- | flight idle | neutral |
| 2 | • | 6400 | full right |
| 3 | Δ | 6400 | full left |
| 4 | x | 6600 | neutral |
| 5 | o | 6600 | full right |
| 6 | ▼ | 6600 | full left |

Ft. Rucker, Al. (U.S. Army Test Board) 14 Jun 74

Input Drive Quill ABU-11067 (M-6)

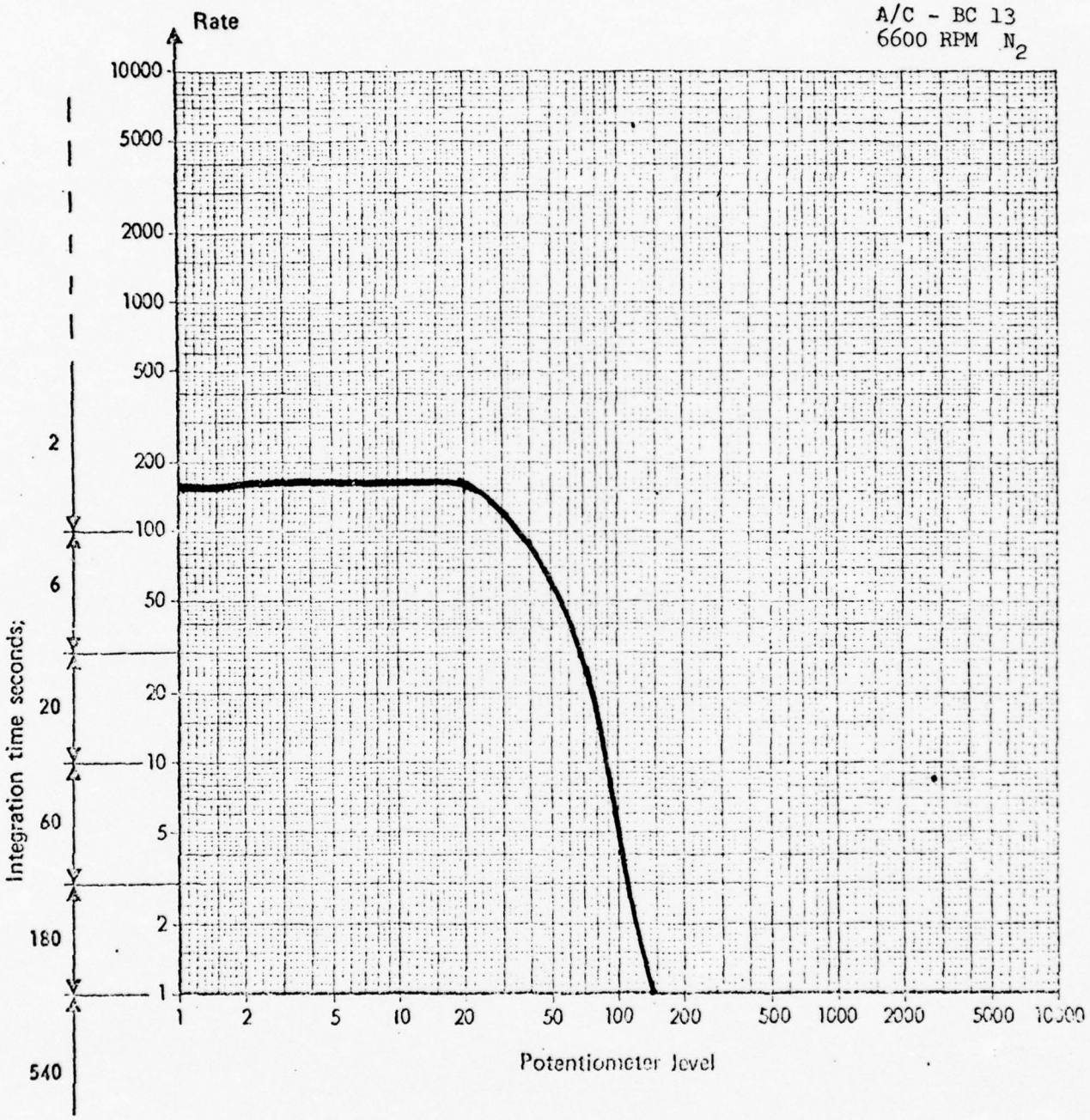

Ft. Rucker, Al. (U.S. Army Test Board) 14 Jun 74

Mast Bearing

A/C - BC 13
6600 RPM $N_2$

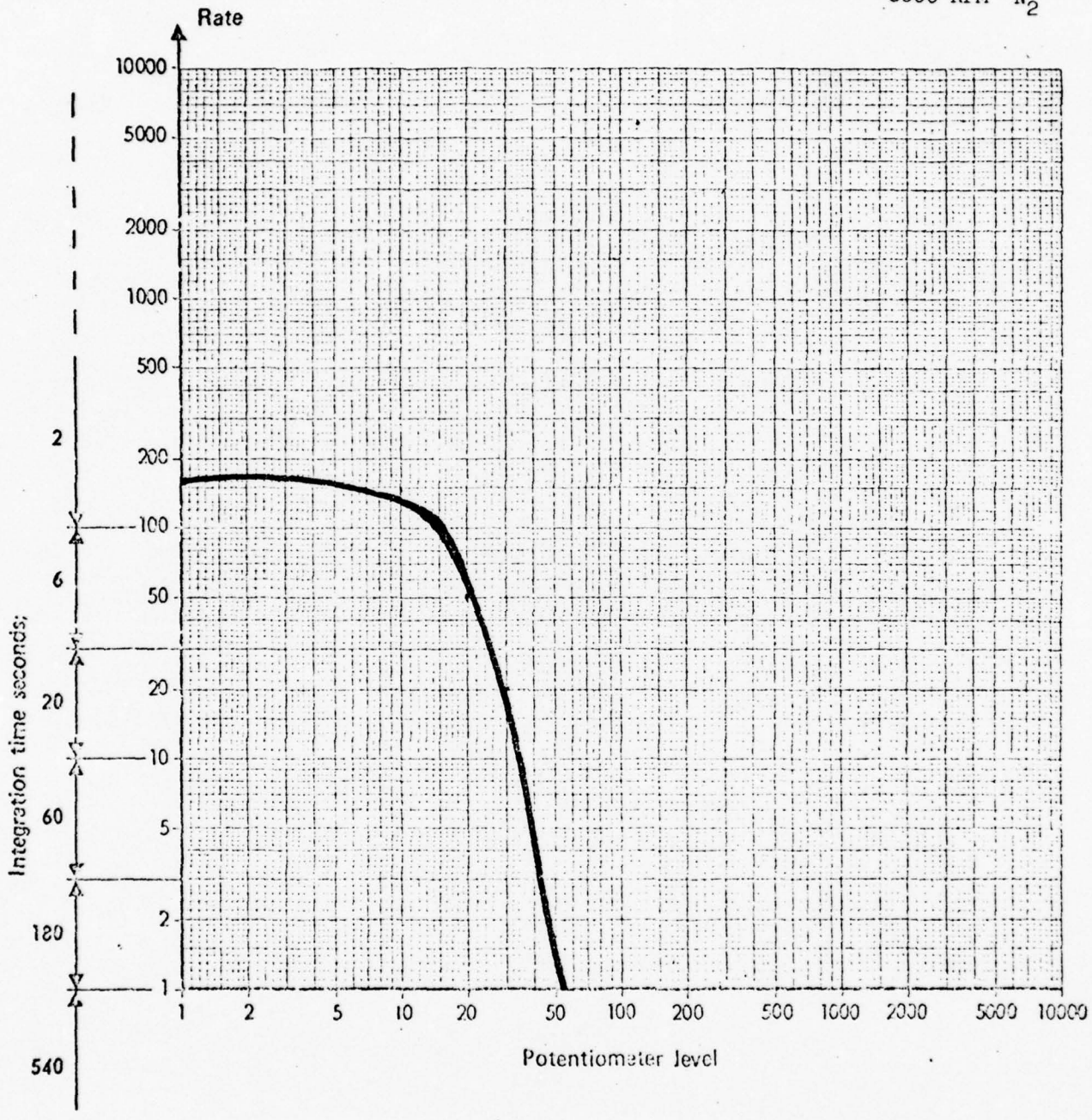

## 7.6 DAMAGED GEARS

Mean Profiles- Damaged Gears

42° Gear Box

SN B13-1561

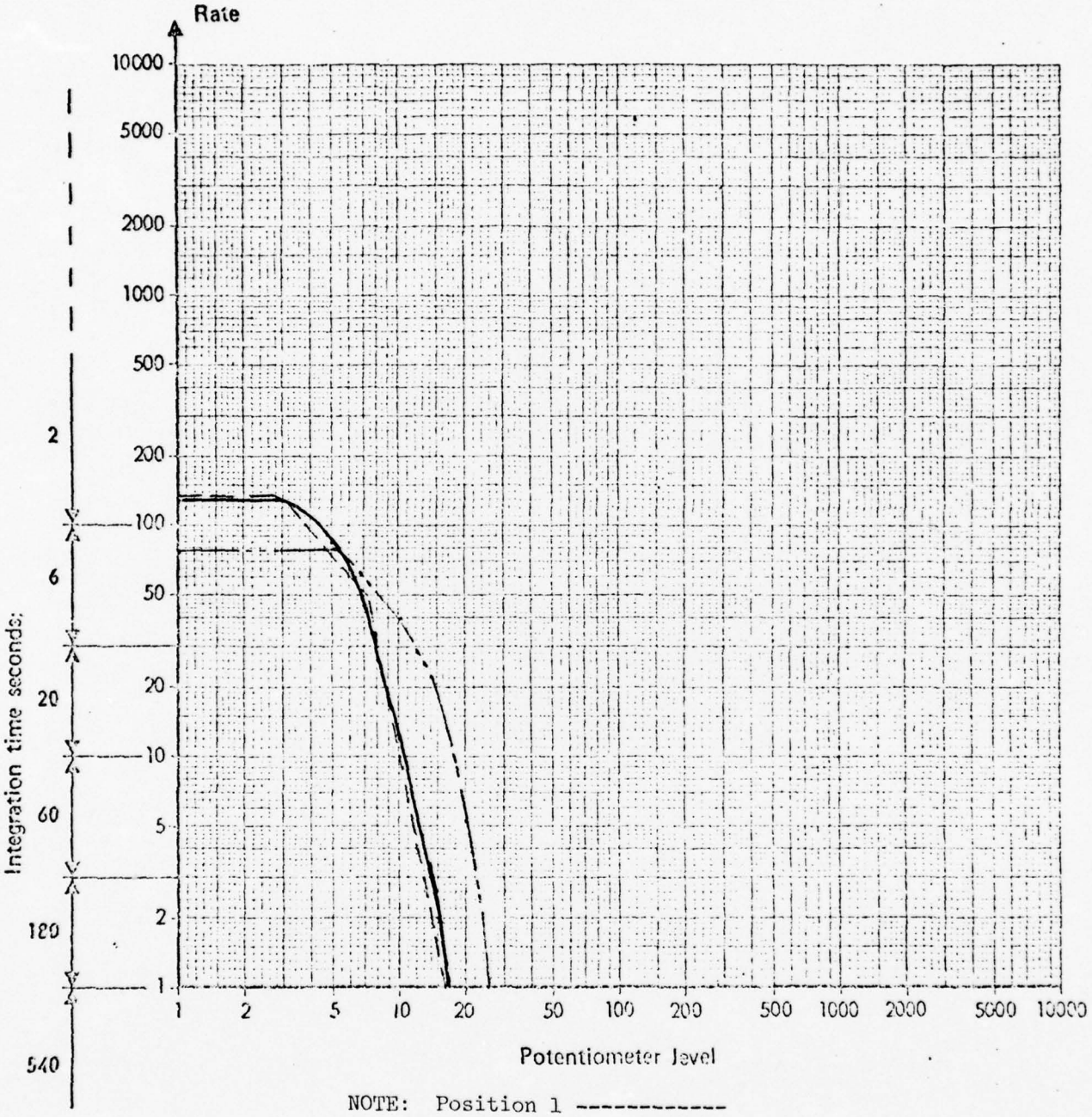


NOTE: Position 1 ----------

Position 2 _____ _ _ _ _____

Parks designed attachment_____

Mean Profiles - Damaged Bearing

$42^{o}$ Gear Box

SN B13-1561

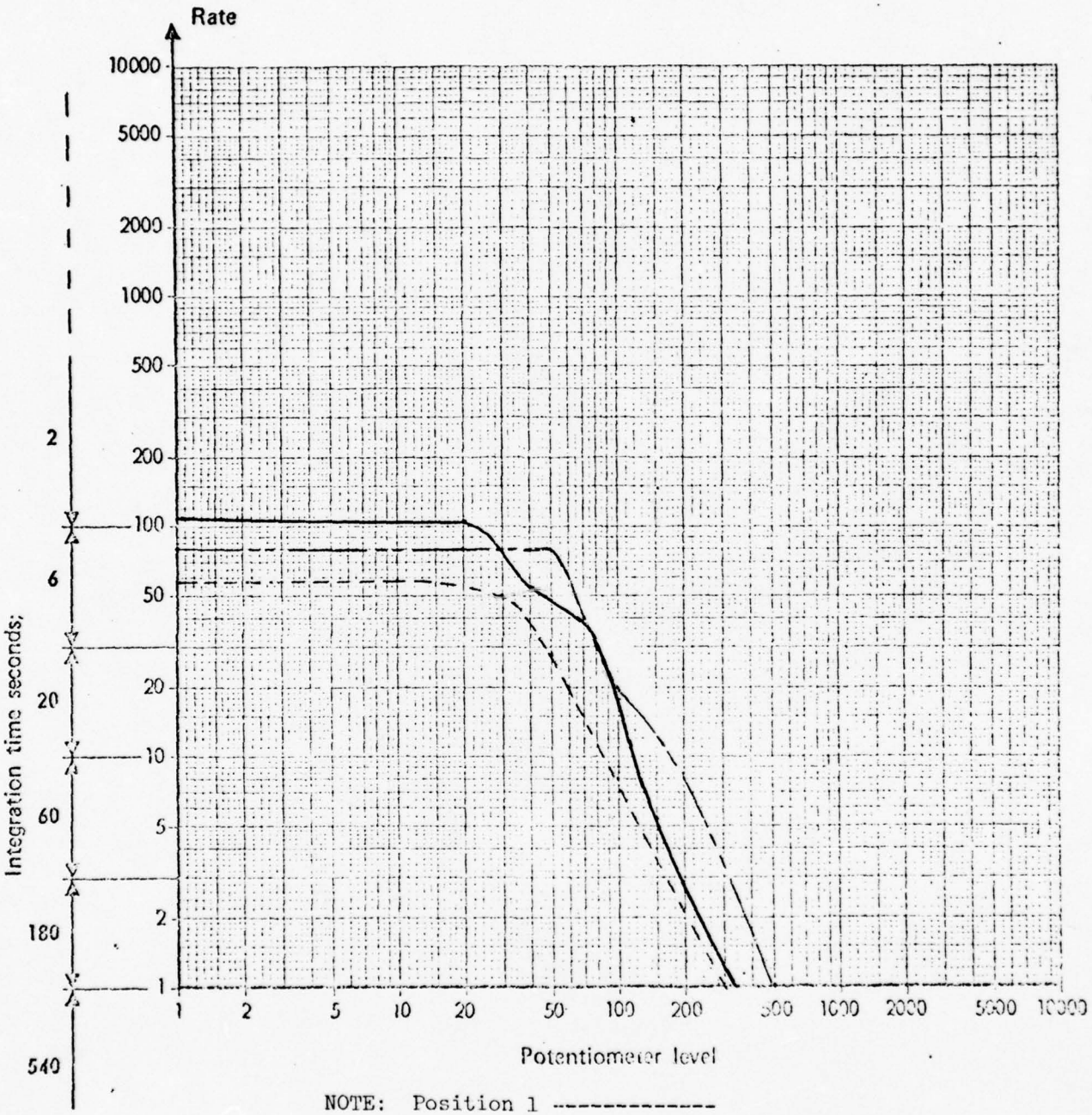


NOTE: Position 1 ----------

Position 2 ____ - - _____ - . _____

Parks designed attachment_____

## 7.7 SKF Report

# FINAL REPORT

ON

# THE APPLICATION OF THE SHOCK PULSE METER IN DETECTING GEAR DAMAGE ON THE UH-1 42° GEAR BOX

FEBRUARY 1975

Reported: [signature]

Approved: [signature]

Released: [signature]

SKF Report: AL75Q002
SKF Code:
Contract No.: P.O. 9716

Submitted to:

Parks College of Aeronautical Technology
St. Louis University
Cahokia, Illinois 62206

Table of Contents

I. Test Objective and Approach:

In the past, damage detection has consisted mainly of vibrational data analysis. A new diagnostic tool in the field of bearing damage detection that has been recently introduced is the SKF MEPA-10A Shock Pulse Meter. The principle of operation of this unit is that a damaged bearing in a machine generates mechanical shocks, which cause brief, high frequency vibrations to emanate from the point of impact. The pulse of energy is governed in its travel by the speed of sound in the structural material, not by the spring-mass characteristics of the mounting structure. It is attenuated at each mechanical interface and decays in amplitude in proportion to the distance and damping characteristics of the material through which it is travelling. A resonant accelerometer is used as the pulse sensor and its output is fed into an amplifier tuned to the accelerometer's resonant frequency. After signal processing, the output is displayed on a meter having a 20,000:1 dynamic range. The meter displays shock pulse, rate of occurrence and amplitude. It is then possible to plot a curve of these two parameters, which is a revealing measure of bearing condition.

Because of the successful results obtained in detecting rolling bearing damage, SKF Industries was contracted by Parks College of St. Louis University to establish the feasibility of, and determine a diagnostic approach for, the use of mechanical shock emissions to determine the condition of gears in an operating helicopter gear box. The tests were conducted on three UH-1 42° gear boxes. Each gear box was tested on an SKF test fixture which had been suitably modified for this series of tests. The fixture is shown in Enclosure 1. As shown, the drive motor is belt coupled to a pulley which was changed to vary the gear box speed. The input quill was coupled to

this pulley and was driven by it. The output quill was connected to a hydraulic pump which served to dissipate the energy transmitted, and whose pressure, and therefore load, could be varied with a manually operated valve.

The gear boxes were driven initially by a 15 horsepower induction motor and drove an IMO 3D hydraulic pump (with 156 rotor.)

Enclosure 2 shows a curve of oil viscosity as a function of temperature for the oil used in both pumps during testing. Enclosure 3 relates oil viscosity to horsepower as a function of the pump pressure for the IMO 3D pump, and Enclosure 4 does this for the IMO A6D pump.

Thus, by controlling pump pressure and monitoring oil temperature, the gear box applied load was determined. The gear boxes tested were operated at speeds of 3560 RPM and 1500 RPM. These speeds were held within 2%. At each speed two different loads, 2 horsepower and 4 horsepower at the lower speed and 2 horsepower and 10 horsepower at the higher speed, were applied. Early test results indicated that a greater load was desirable to more nearly approximate flight loads of 25 to 90 horsepower. Therefore an IMO A6D pump (with 137 rotor) and a 50 horsepower induction motor were installed on the fixture. This increased the drive and load capability of the test rig to 34 horsepower.

Shown in Enclosure 36 is a listing of the tests performed during the program in the order in which they were done. Test speeds, loads applied and gear implant conditions are also tabulated. This enclosure serves as a reference and guide for the following Test Results section.

## II. Test Results

The first step in the program was to establish optimum sensor locations for detecting gear damage. After examination of the gear box drawing, four candidate positions were chosen. Data obtained from these points in initial testing was not sufficiently different to clearly indicate one location as superior. Consequently, in accordance with the theory of shock pulse operation, a location was selected which had the most direct mechanical path to the gear mesh. A spot located over the roller bearing on the input quill was selected. An aluminum block conforming to the shape of the housing was fabricated and after the paint was removed from that area of the gear box housing, the block was bonded to the housing. A second or backup spot was selected on the base opposite to the oil level gage. This location was selected because the gear box structure in this location was suitable for mounting an accelerometer and there was also a direct mechanical path to the gear mesh. Enclosure 5 shows the sensor locations.

The test results are presented for each of the three gear boxes tested and sequentially for each gear box tested.

### A. Gear Box S/N A13-830

Gear Box S/N A13-830 was the first gear box tested. Enclosures 6 and 7 depict the base line data obtained for this gear box. At 1480 RPM, shock emission profiles were taken with 2.9 and 4.25 horsepower loads and at 3560 RPM with 2.6 and 10.4 horsepower loads. During Test 1, as can be seen from the data, the shock level increased mainly as a function of speed and not of load.

Test 3 was then conducted after damaged gears had been installed into this gearbox. The gear box was operated at 1480 RPM and 3580 RPM and loaded with 2.9 horsepower and 4.25 horsepower at the lower speed and 2.6 and 10.4 horsepower respectively at the higher speed.

Enclosure 8 shows a picture of these gears prior to their insertion into the gear box. The upper picture is that of the output gear, which has pieces of gear teeth missing. This was due to an earlier gear failure in another gear box. These gears had not, however, been previously run as a set in this gear box. Test 3 data with the damaged gears is shown in Enclosures 9 and 10. Position 2 data in Enclosure 9 at 1480 RPM shows higher shock levels with the damaged gears than with the undamaged ones, shown in Enclosure 6. At the higher speed, however, the shock level was slightly lower for damaged gears than for undamaged gears as is seen when comparing Enclosure 10 with Enclosure 7.

Since these damaged gears had not been operated as a set previously, the severity of shock generation by any given damage and the specific kinematics of the contact between the damaged surface is not known. In addition, the 2 to 10 horsepower load placed on the gear box was much less than the 25 to 90 horsepower load presented to the gear box in a helicopter. To provide a more representative load the previously discussed motor and pump change was made. Test 4 was then conducted at 3540 RPM and with the same damaged gears as in the previous tests, however, new higher loads were applied to the gear box. Tests at these new loads indicated approximately a 20% increase in the shock level for this gear box for both position 1 and position 2, as can be

seen by comparing Enclosure 11 to Enclosure 10 data. When comparing Enclosure 11 data with that for undamaged gears installed in the same gear box, at the same speed, however (Test 1 - Enclosure 7), no significant shock level trend is evident as a function of increased load.

A third set of gears was installed in this same gear box. These were also damaged gears. The severity of damage is shown in Enclosure 12. Test 5 was run at the test speeds of 1510 and 3540 RPM with the new applied loads of up to 34 horsepower. Data obtained is shown in Enclosures 13 and 14.

The curves taken for damaged gears in Enclosure 11 and the lower value curves in Enclosure 14 show only a slight variation when compared to Baseline undamaged gear data of Enclosure 7. Enclosure 13 data, at lower speed for damaged gears, when compared to Enclosure 6 data, at the same RPM for undamaged gears, also shows only a small change in shock level between damaged and undamaged gear sets at the 4 horsepower to 5 horsepower applied load level.

One event of significance that occurred early in test number 5 at 3540 RPM and at 13 HP load was a sharp increase in shock level for a period of about 2 minutes. The data obtained during this time period is shown in Enclosure 14 as the higher shock value curves. The rapid increase in shock level did not recur during further testing. A post-test examination of the oil in the gear box showed fine metal particles throughout the oil. The probable cause of the increase in shock level is, therefore, believed to be the passage of the particulate matter through the bearing load zone since bearing rolling element encounter with particulate matter is known to generate shock pulses.

B. Gear Box S/N B13-1561

The second gear box for which base line information was taken was S/N B13-1561. This baseline test is designated as Test 2 and the results are shown in Enclosures 15 and 16. This baseline data was obtained while the test rig was in the low horsepower configuration. The test was conducted at the same speeds and applied loads as the baseline test of gear box S/N A13-830. The data is similar to the baseline data obtained from gearbox S/N A13-830 during Test 1 (Enclosures 6 and 7). The largest shock level difference observed was that the position 2 shock level at 3580 RPM, Enclosure 16, was about one half that of S/N A13-830 gear box baseline value shown in Enclosure 7.

This second gear box, SN B13-1561, was also retested with the higher 13 to 33 HP loads (Test No. 2). Enclosure 17 shows the Baseline data obtained at 3540 RPM. There was again no distinct trend of shock level to follow load. Slight changes in shock level data compared to that in Enclosure 16 were observed in an increase in position 1 data and a decrease in position 2 readings. Because the data showed no marked change with these higher loads at 3540 RPM, the lower speed runs were not repeated.

This gear box was then removed from the fixture and the gears removed. They are shown in Enclosure 18. An artificial damage was inflicted on the output quill gear with a hand grinder. The damage was approximately 1/4" long, 1/16 inch wide and was placed in the contact area of one gear tooth.

After the gear box was remounted in the fixture, Test 6 was conducted. Data taken at 1520 RPM, and 5 and 14.5 horsepower loads is presented in Enclosure 19. Position 1 data indicates a high rate of shocks at low shock levels which is traditionally indicative of solid particulate matter in the lubricant.

Position 2 data was slightly lower in shock level than experienced in previous baseline runs for this speed.

A second part of Test 6 was conducted to assure the reliability of data obtained from position 2 (verify that the bonding of the accelerometer block did not adversely affect the data), a hole was drilled and tapped in the Gear Box housing at the Position 2 location, to mount the accelerometer block directly to the gear box, thereby eliminating any potential interface effect of the glue. Data was obtained with the block bonded on. The test was conducted at 3540 RPM and 13.25 horsepower loads. The hole was then drilled and tapped, the accelerometer stud mounted and the test repeated. The data obtained with the block bonded on and the repeat data are shown for comparison in Enclosure 20. There was a slight increase in both rate and level with the stud mounted accelerometer. The difference, however, lies within the normal 10% to 20% variation of readings from run to run.

Test 6 was continued with the accelerometer stud mounted. Enclosure 21 presents the shock emission data obtained for the artificially damaged gear implant at a speed of 3540 RPM and 13.25 and 33.75 horsepower loads.

This gear box was operated for an extended period of time and data taken at position 2 periodically to monitor the trend or growth in shock level with time. Enclosure 22 shows data acquired

after running for 5, 10, 30 and 50 minutes respectively. There was a 4 to 1 growth in shock level which normally indicates damage growth. The gear box was run for an additional hour on the following day. The curve shape and shock level did not change from that shown for 50 minutes in Enclosure 22. Visual examination of the gear box oil revealed a large amount of fine metal particles. The most likely source of these is the gear which had been artificially damaged. Because of the roughness at the edges of the artificially damaged area of the gear metal burrs could break off quite easily. Gear wear and spalling occurring naturally will also exhibit the tendency to produce a particulate debris which would have a similar effect on shock emission, introducing the possibility that the shock pulse technique may monitor gear wear or damage growth by monitoring the shock pulse affect of particulate matter in the oil or observed shock emission levels.

Test 7 was conducted using an input quill assembly with artificial damage on the gear implanted in this same gear box. The damage had been inflicted on the gear with a carbide scribe. Burring that occurred during the scribing was not removed. A photo of this gear is shown in Enclosure 23. The output quill in which the gear had been previously artificially damaged by the hand grinder remained in the gear box. Initial readings showed a shock level of about 9 at position 2. This quickly changed to about 25 within a minute or two after the Test was started and took the shape of the curve shown in Enclosure 24. Enclosure 25 shows data obtained at position 1 while Enclosure 26 shows data obtained using a Parks College type VD-3 accelerometer holder mounted to a bolt on the input quill housing. There was some variation in shock rate with time as can be seen in the three enclosures. This type of variation had not been

observed in the past. Also, there were occasional but regular spikes observed which gave readings of up to 2000 pulses per second. Increases in the rate of small shocks is characteristic of particulate contaminant in the lubricant passing through the bearings.

Upon request by Parks College, a 7th Test was performed with an "unknown condition" input quill assembly supplied by Parks College. It was implanted in the gear box and data again taken. This time the rate readings were also variant. The data is shown in Enclosures 27, 28 and 29. The readings obtained also showed extremely high shock levels indicative of bearing damage. This implant rather than having a gear damage had a bearing implanted with damaged balls, a picture of which is shown in Enclosure 30. The ability of the MEPA-10A to isolate bearing damage in an operating gearbox was again demonstrated.

C. Gear Box S/N BBB-1253

A third gear box was tested at the standard test speeds and loads. Baseline data was obtained to establish consistency of baseline level from gear box to gear box. The data is shown in Enclosure 31 and 32.

D. Summary of Results of Shock Pulse Testing

The baseline shock level determined on the three gear boxes at 1490 RPM varied from 25 to 35 in value while at 3580 RPM the variation was between 50 and 200.

Baseline shock level and its variation from gear box to gear box are so low compared to bearing damage levels that they do not markedly affect the ability of the shock pulse technique to detect bearing implant exhibited shock levels of ten times the baseline values, thus variations of 30% or even four to one in baseline level

do not affect the capability of the shock pulse meter to detect bearing damage.

The results of this test program, however, indicate that the same consistent correlation does not exist for the gear-damaged implants tested.

The tenfold increase in shock level experienced during Test 5, a test of damaged gear implanted in gear box S/N A13-830, and the growth in shock level from 65 to 160 in Test 6, a test of an artificially damaged gear in gear box S/N B13-1561 serve as evidence of the capability of the shock pulse technique to detect the growth of damage or wear in a gear set by measuring the effect of wear debris on emitted shock pulse level.

A correlation of a specific gear damage severity to a specific shock level emitted is not evidenced in the test data.

Gear mesh shocks (those occurring at gear mesh frequency) were not sensed as evidenced by the fact that they occur at 3 to 5 times the maximum shock rates observed during testing. This indicates they were not of sufficient magnitude to be sensed by the standard MEPA-10A Shock Pulse Meter.

Gear damage sourced shocks are similarly not evidenced in the data taken again, presumably because they are too small in amplitude to be sensed by the standard MEPA-10A Shock Pulse Meter.

E. Results of Vibration Measurements on Operating Gear Boxes

In addition to the testing with the MEPA-10A, single axis vibration measurements were also made. This was done using an SKF Industries MEB-17A Vibration Amplifier, which determines vibrational velocity from an accelerometer input signal. This unit has three frequency bands (50 to 300 HZ, 300 to 1800 HZ and 1800 to

10,000 HZ) and is used for production vibration testing of bearings at SKF. The sensor used was the accelerometer located at position 2. The data obtained is shown in Enclosure 33. It is evident that vibration velocity levels are not a conclusive measure of gear damage. Although there appears to be some correlation between damaged and vibration readings, this is true only for certain damaged gears and not for all. At the same time, a tape recording of the vibrational velocity signal output was made. This data was later analyzed on a B&K 1/3 Octave Frequency Spectrum Analyzer.

The B&K traces are shown in Enclosures 34 and 35. As can be seen from the data, the gear mesh frequency predominates, but damaged gears do not show marked differences (increase in amplitude) as compared to undamaged gears, confirming the statement that vibration measurements are an inconclusive measure of gear damage.

CONCLUSIONS:

Three UH-1 helicopter 42 degree gear boxes with several different types of gear damage have been subjected to shock pulse monitoring during runs at two different loads and at two speeds. From the data obtained during testing, the following has been determined:

1. The MEPA-10A as used can supply warnings as to the onset of damage in a gear box. If damage originates in the bearings, an indication directly correlated with damage is received. If the damage originates in gears, the indication is due to the sensing of particulate dontaminant passing through the bearings.

2. The MEPA-10A appears capable of detecting a secondary effect of gear damage in an operating 42° UH-1 helicopter gear box since, in this gearbox, the lubricant is captive in the gearbox. Metal chips and particles are the products of the mesh of damaged gear teeth and tend to pass through the bearings as the oil in the gear box circulates. Shock level and rate increases accompany their passage.
3. The shock pulse technique has again proven successful in isolating a damaged bearing in a gear box. Standard shock pulse analysis techniques (shock emission profile) using the MEPA-10A were not found in the present study to provide a direct indication of the degree of gear damage.
4. Vibrational velocity measurement, analyzing the signal either in three, two and one-half octave bands, or one-third octave analysis of the audio-frequency spectrum has failed to provide any consistent indication of damage.

RECOMMENDATIONS

The following further work is recommended:

1. To establish fully whether shock pulse indications due to debris entering the lubricant correlate with the gear damage condition from inception through advanced stages:
   (a) Modify the existing test fixture to permit higher gear box loading. Conduct gear endurance tests to obtain naturally caused damage and allow damage to grow. This will allow realistic observation of damage progression by shock pulse monitoring.

(b) Measure the effect of the gear emitted debris on shock emission profiles and correlate through periodic gear box examination to level of gear damage including wear. Also, correlate with analysis results of debris content in the oil.

2. As a more advanced approach to the establishment of a gear damage detection capability, work is recommended toward the development of more sophisticated shock pulse analysis techniques capable of examining the gear damage emitted shocks in time intervals between the main gear mesh shocks.

It is apparent from the B&K traces that the amplitude of vibration emitted at the gear mesh frequency is very high, due to the meshing impact. The damaged areas come in contact only as the teeth slide across one another. It appears that the impact of the damage as compared to the impact of the teeth mesh is quite small. The shock pulses emitted by the damage also would occur at a higher frequency. Since the MEPA-10A has proven so successful in the measurement of bearing damage, modification of the electronics should be considered to investigate the shock pulses emitted in time segments between the meshing of teeth, as a measure of gear damage severity.

A diagnostic approach that would permit this and also provide automated analysis of the shock emission data can be implemented by the following method.

The data taken during testing indicates shock rates on the order of several hundred per second, using the present lower threshold limit of "1" on the MEPA-10A. The gear mesh should have caused shock rates 3 to 7 times higher than these values. The shock rate due to damage, therefore, must have occurred at levels less than "1.0." To measure these small shocks it is necessary first, to increase the sensitivity of the MEPA-10A input circuitry, thereby allowing levels of less than 1.0 to be measured.

Next, by using signals with a level greater than one as an "inhibit" on the Pulse Integrator circuitry, the MEPA can be made to look only at shock levels less than one. The length of time of the inhibit would have to be determined empirically. This approach will permit analysis of smaller shocks occurring in the time segment between the larger shocks. It would then only be necessary to add level discrimination and logic circuitry to the design to enable automatic data analysis.

Enclosure 1

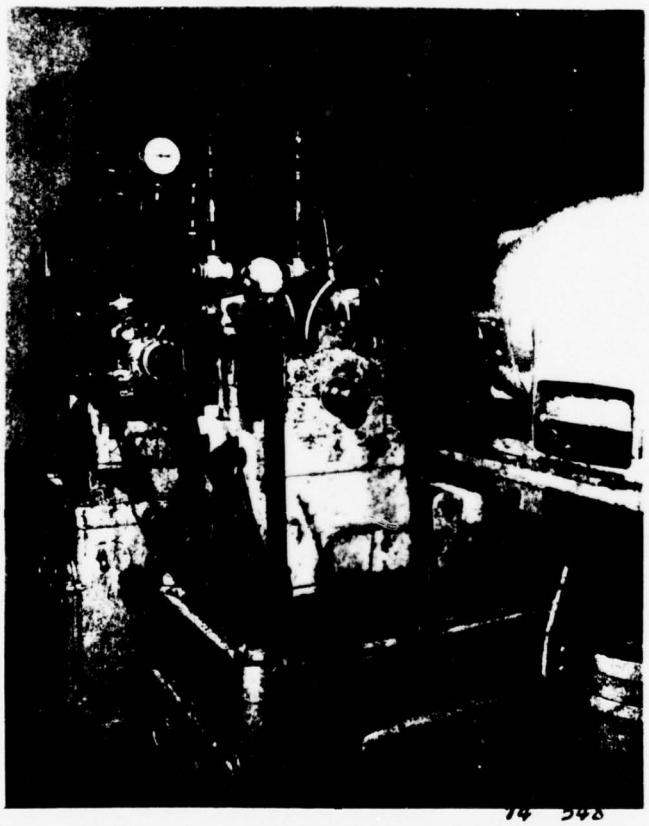

GEAR BOX
TEST FIXTURE

F-4186A R100

RESEARCH LABORATORY SKF INDUSTRIES, INC.

Enclosure 2

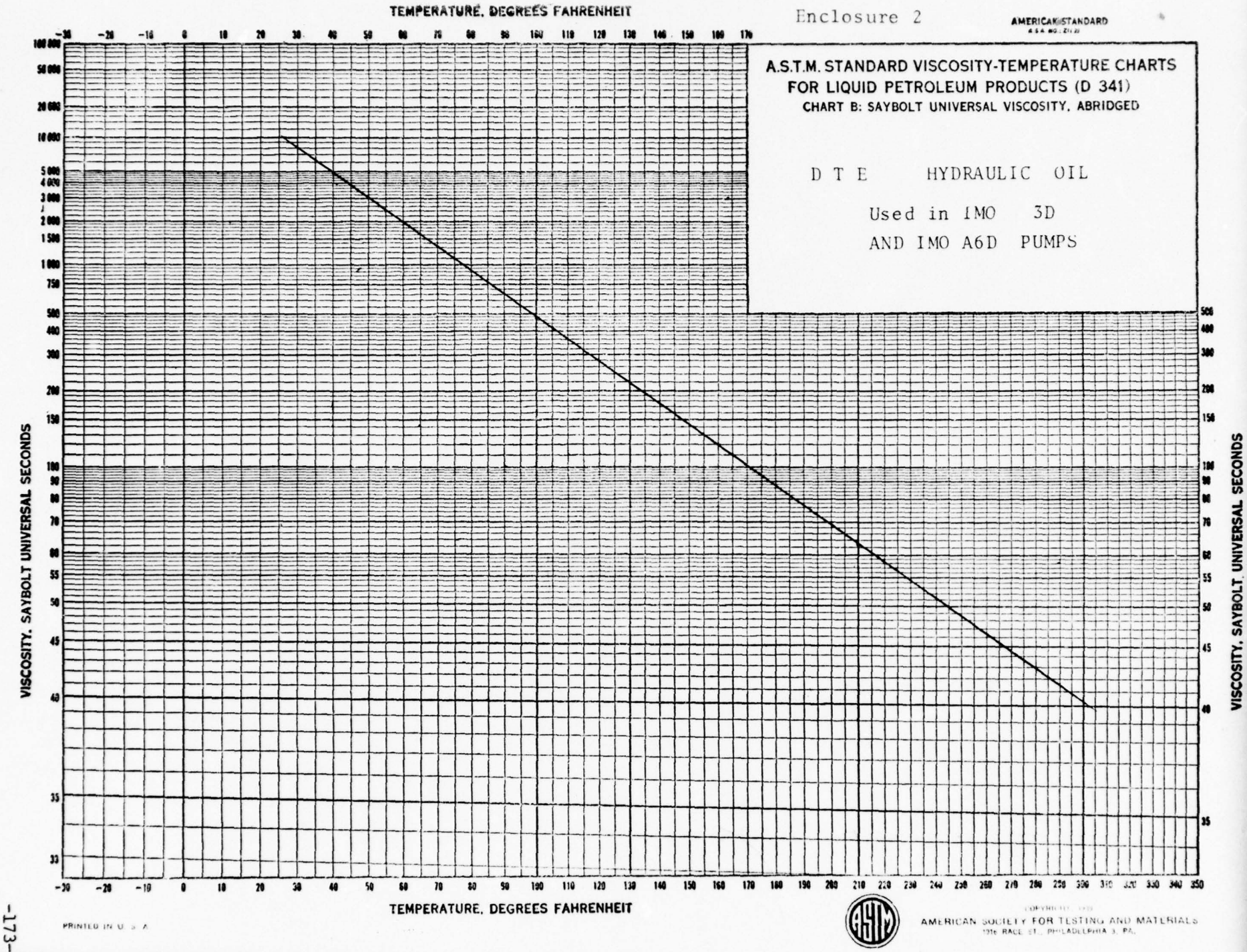
TEMPERATURE, DEGREES FAHRENHEIT
AMERICAN STANDARD
A.S.T.M. STANDARD VISCOSITY-TEMPERATURE CHARTS
FOR LIQUID PETROLEUM PRODUCTS (D 341)
CHART B: SAYBOLT UNIVERSAL VISCOSITY, ABRIDGED
D T E HYDRAULIC OIL
Used in IMO 3D
AND IMO A6D PUMPS
VISCOSITY, SAYBOLT UNIVERSAL SECONDS
TEMPERATURE, DEGREES FAHRENHEIT
PRINTED IN U. S. A.
AMERICAN SOCIETY FOR TESTING AND MATERIALS
1916 RACE ST., PHILADELPHIA 3, PA.

# IMO 3D PUMP (WITH 156 ROTOR)

ENCLOSURE 3

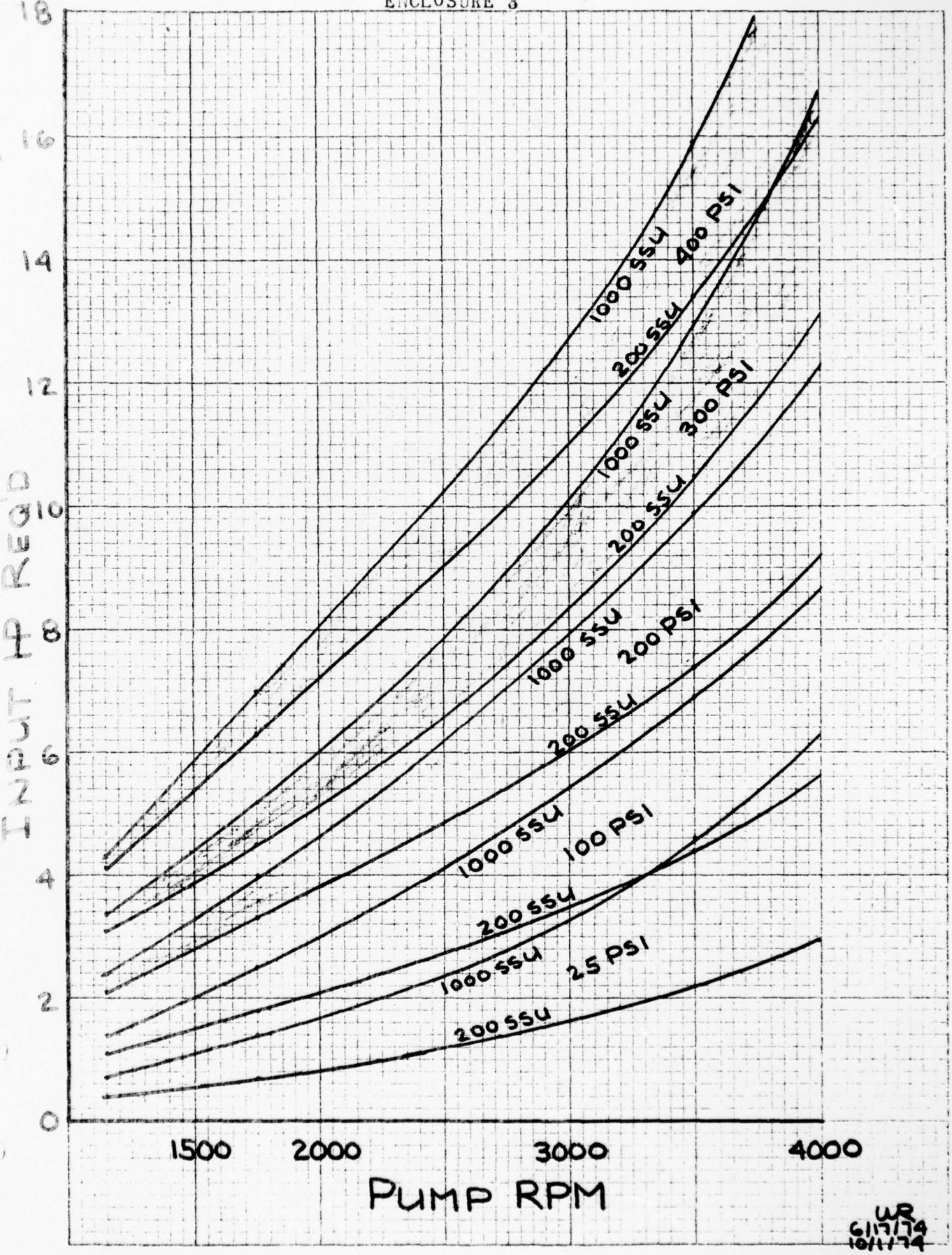


WR
6/17/74
10/1/74 174

# IMO A6D PUMP (WITH 137 ROTOR)

ENCLOSURE 4

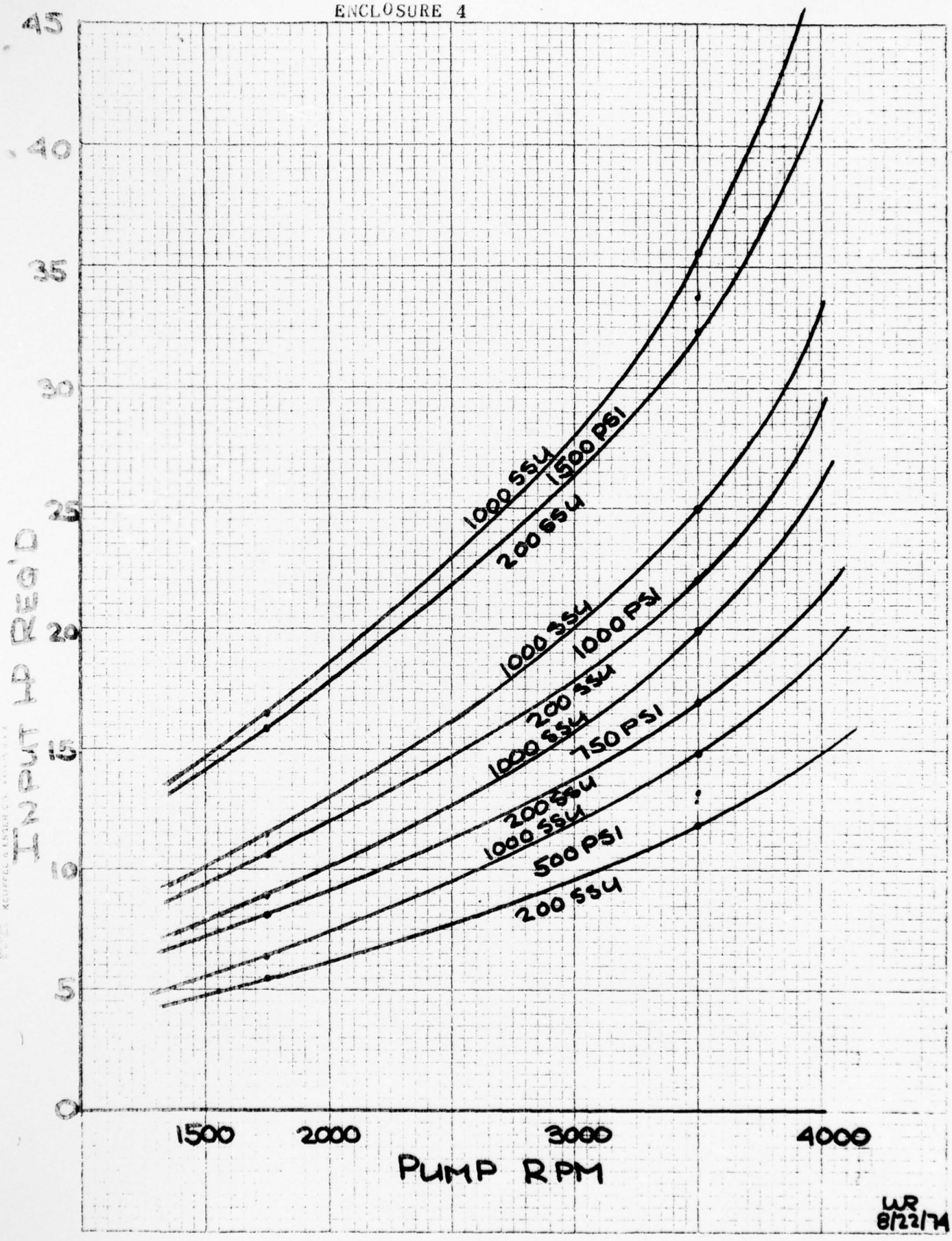


WR 8/22/74

ENCLOSURE 5

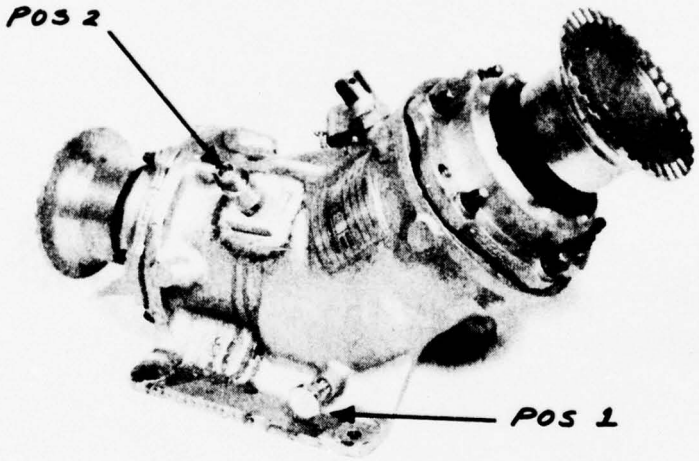


74 348

42° Gear Box

S/N A13 - 830

BASELINE DATA

SPEED: 1480 RPM
AMBIENT: 82° F
GEAR BOX TEMP: 103° F

ENCLOSURE 6

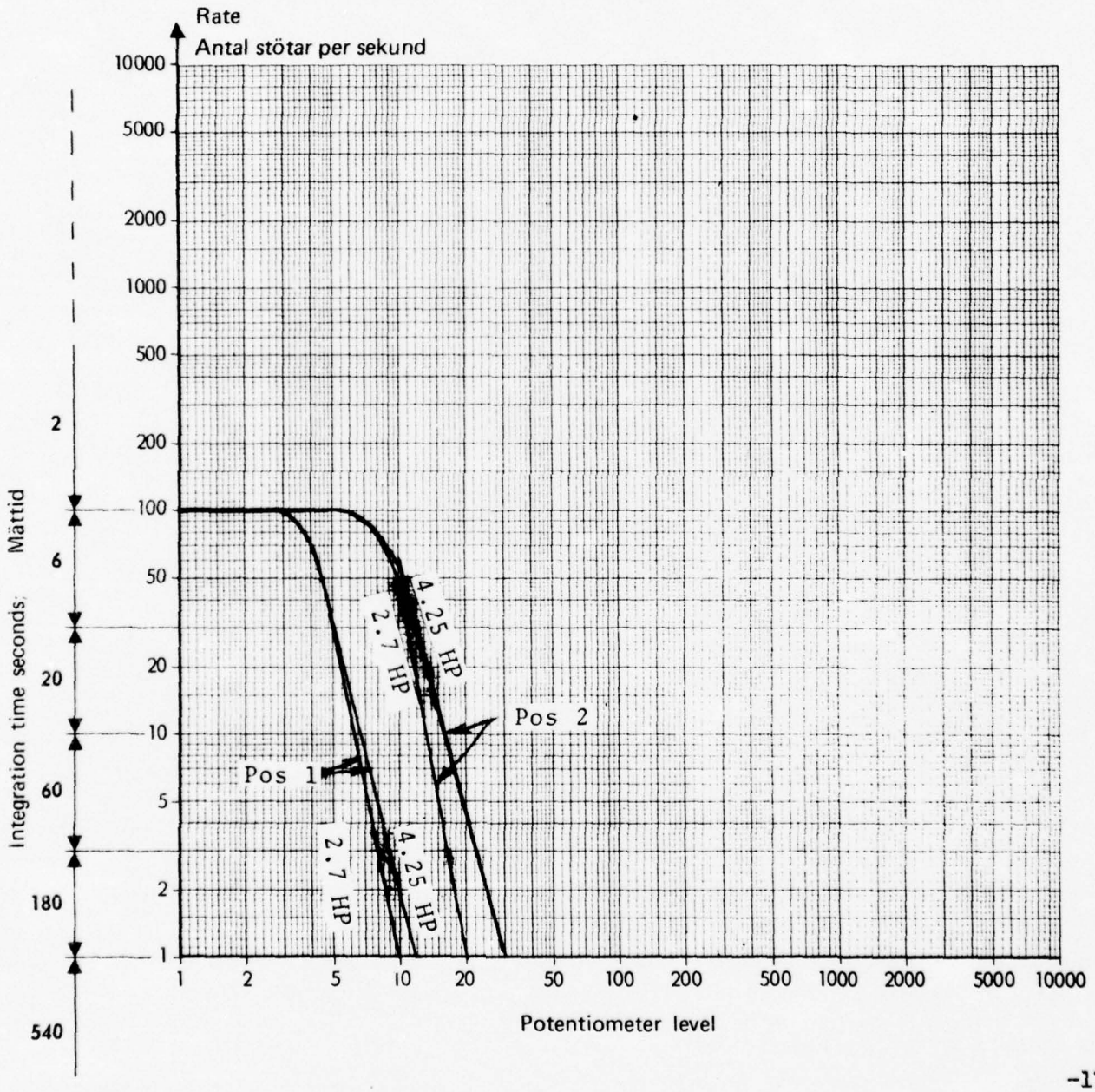


SKF Kl 169 Art. 1048-4 Repro 16959 7500 7103

S/N A13 - 830

BASELINE DATA

SPEED: 3560 RPM

AMBIENT: 35°F

GEAR BOX TEMP: 138°F at 2.6HP
150°F at 10.4HP

ENCLOSURE 7

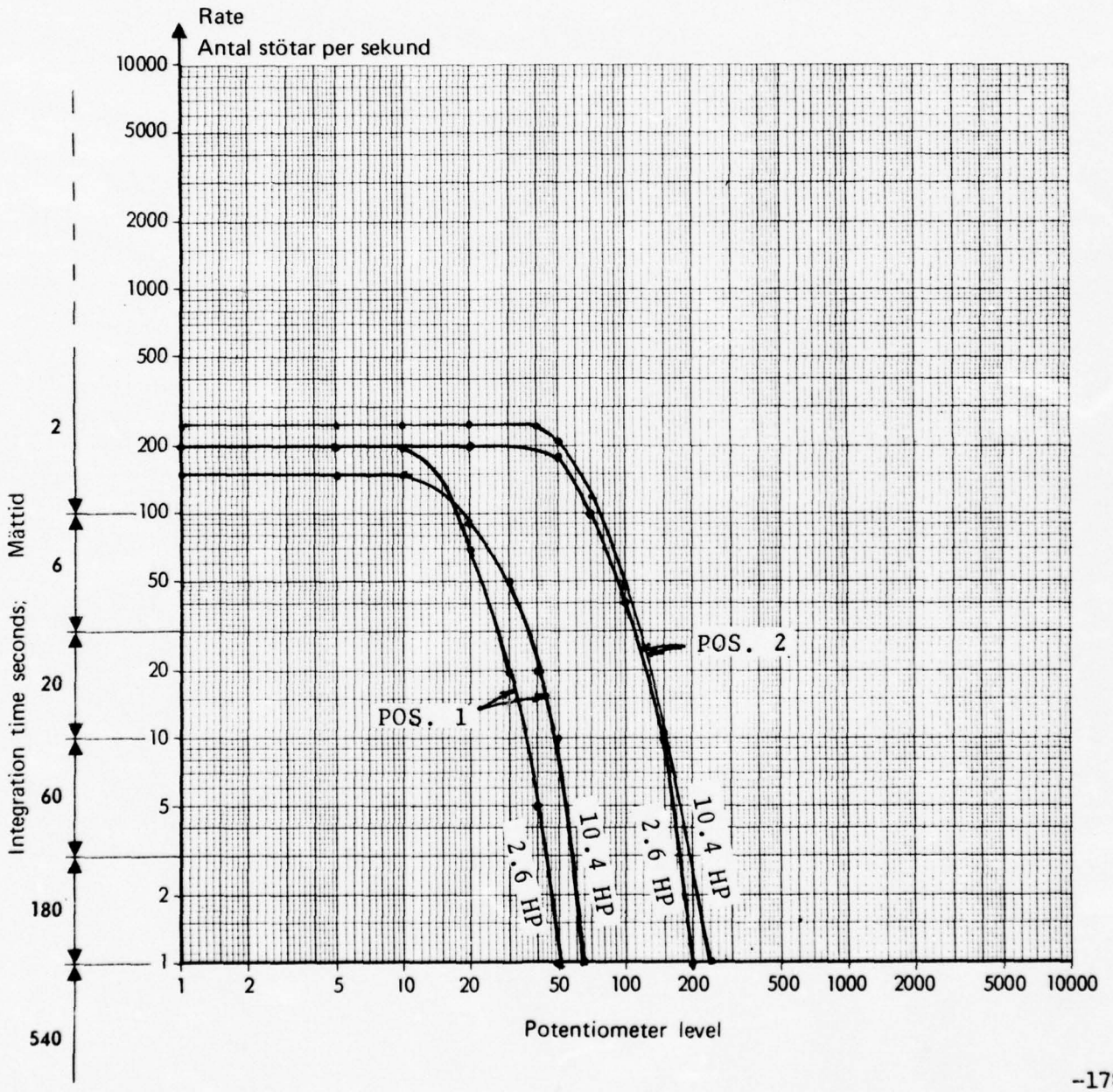

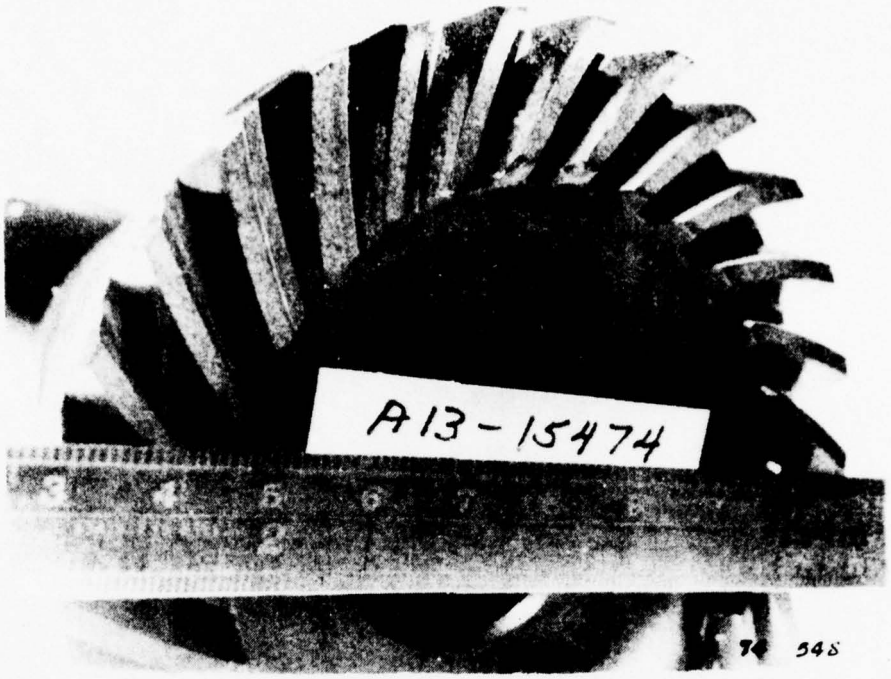


OUTPUT GEAR - Test 3

---

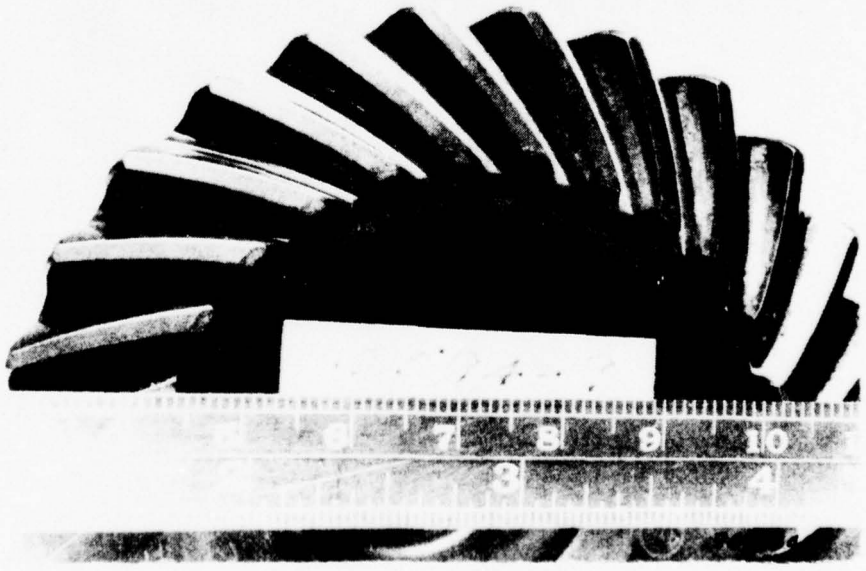

INPUT GEAR - TEST 3

RESEARCH LABORATORY SKF INDUSTRIES, INC.

F-4185A R100

S/N A13 - 830

HEAVILY DAMAGED GEARS

SPEED: 1480 RPM

AMBIENT: 72°F

GEAR BOX TEMP: 100°F

ENCLOSURE 9

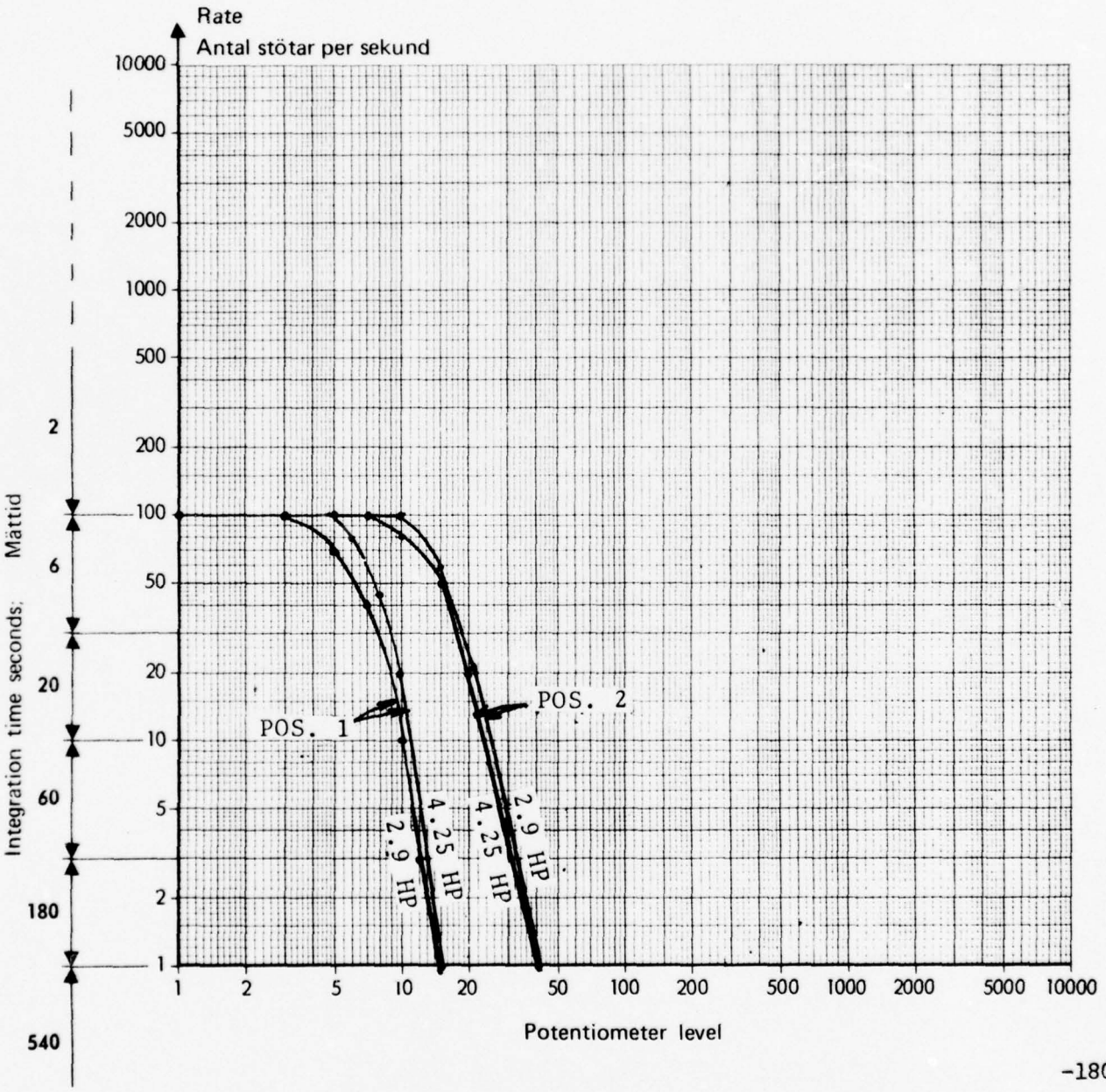

S/N A13 - 830

HEAVILY DAMAGED GEARS

SPEED: 3580 RPM

AMBIENT: 76°F

GEAR BOX TEMP: 140°F at 10.4 HP

128°F at 2.6 HP

ENCLOSURE 10

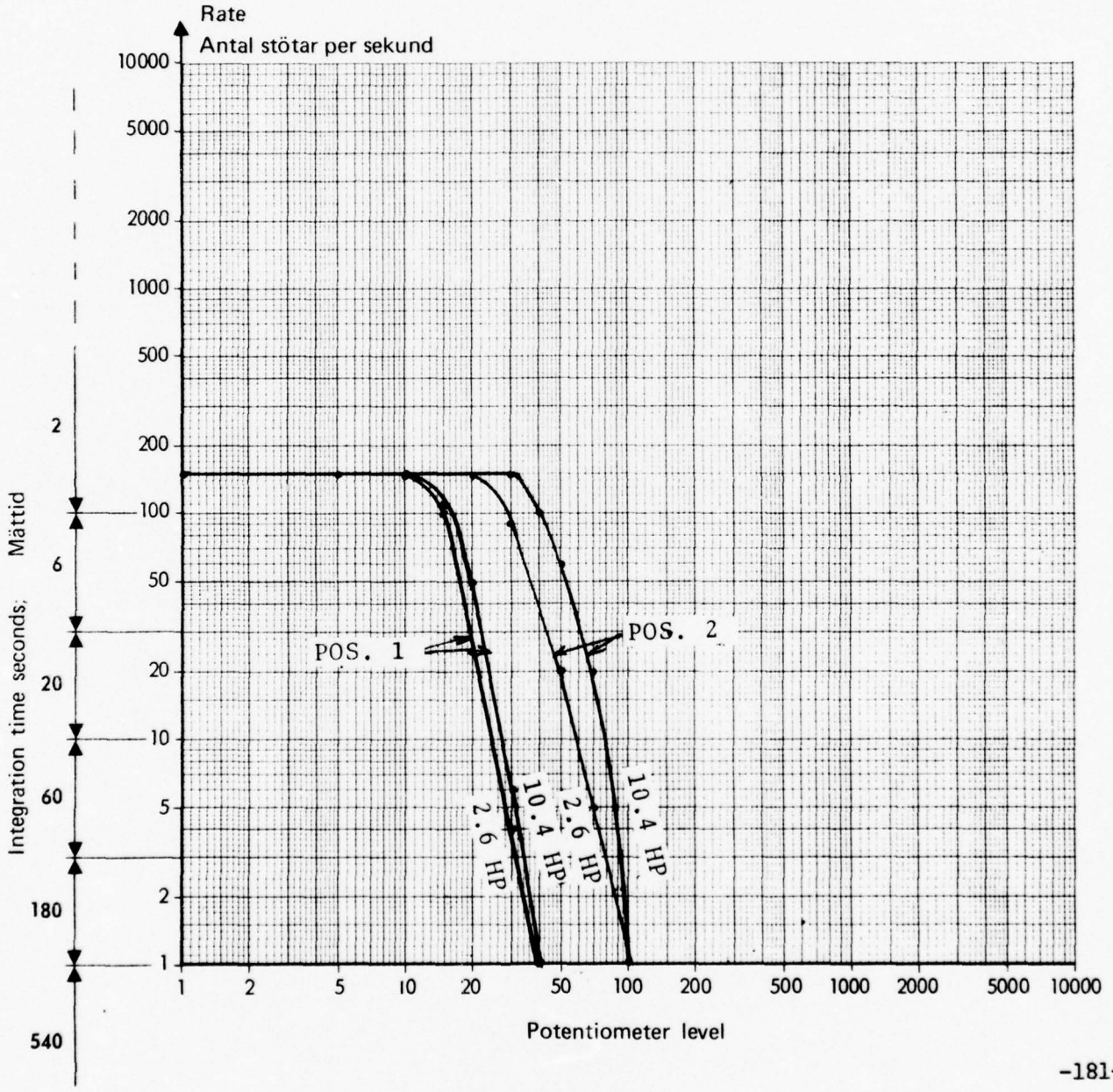


SKF Kl 169 Art. 1048-4 Repro 16959 7500 7103

S/N A 13 - 830

HEAVILY DAMAGED GEARS

SPEED: 3540 RPM

AMBIENT: 86° F

GEAR BOX TEMP: 165°F at 33.75 HP
157°F at 13.25 HP

ENCLOSURE 11

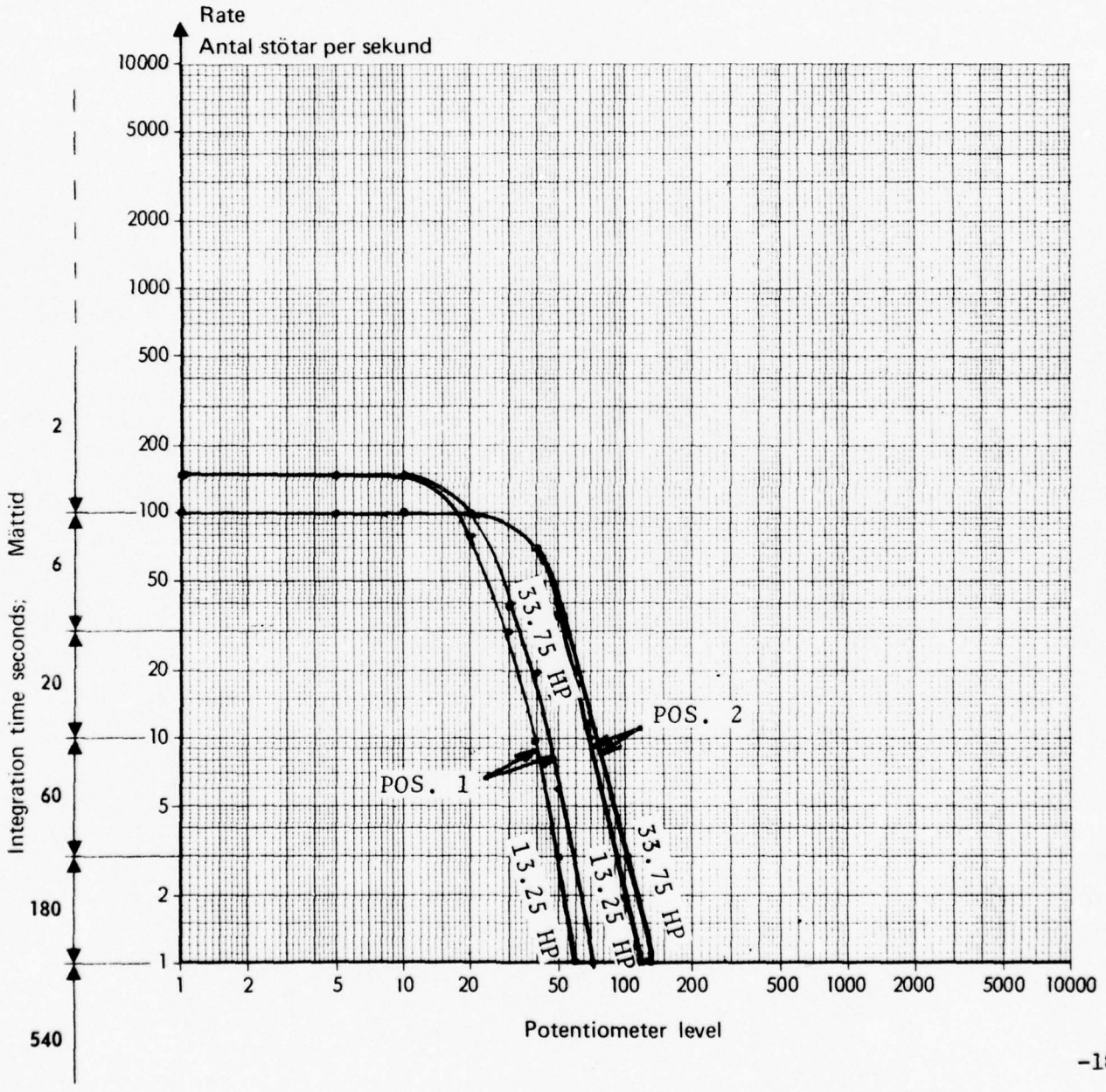


SKF KI 169 Art. 1048-4 Repro 16956 7500 7103

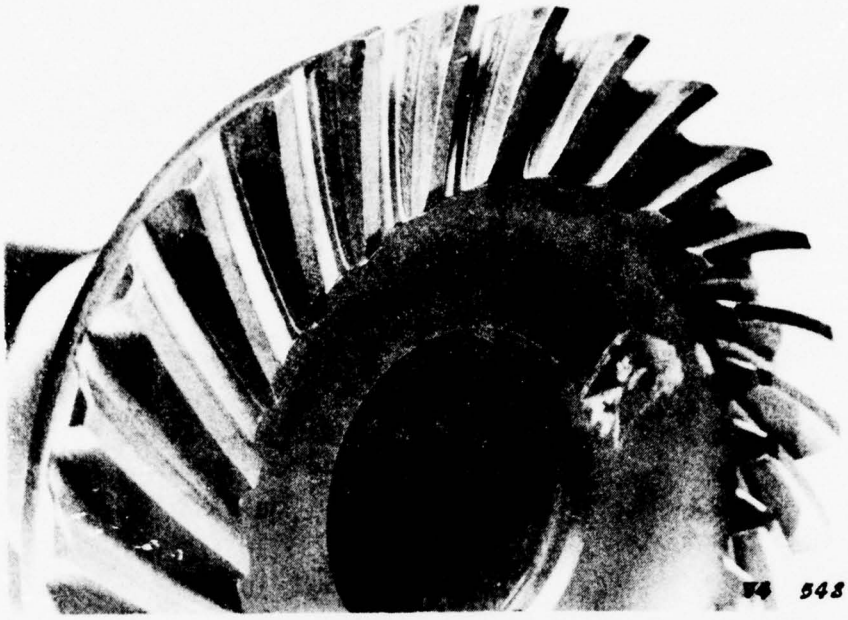


OUTPUT GEAR - Test 5

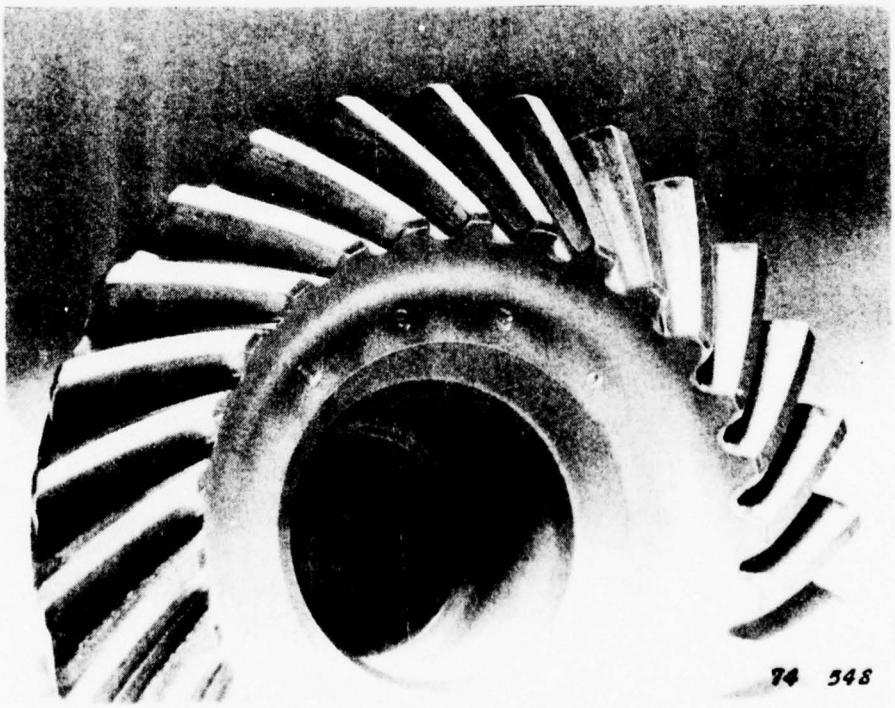


INPUT GEAR - TEST 5

S/N A 13 - 830

DAMAGED GEARS (2nd set)

SPEED: 1510 RPM
AMBIENT: 72°F
GEAR BOX TEMP: 103°F at 14.25 HP
99°F at 5 HP

ENCLOSURE 13

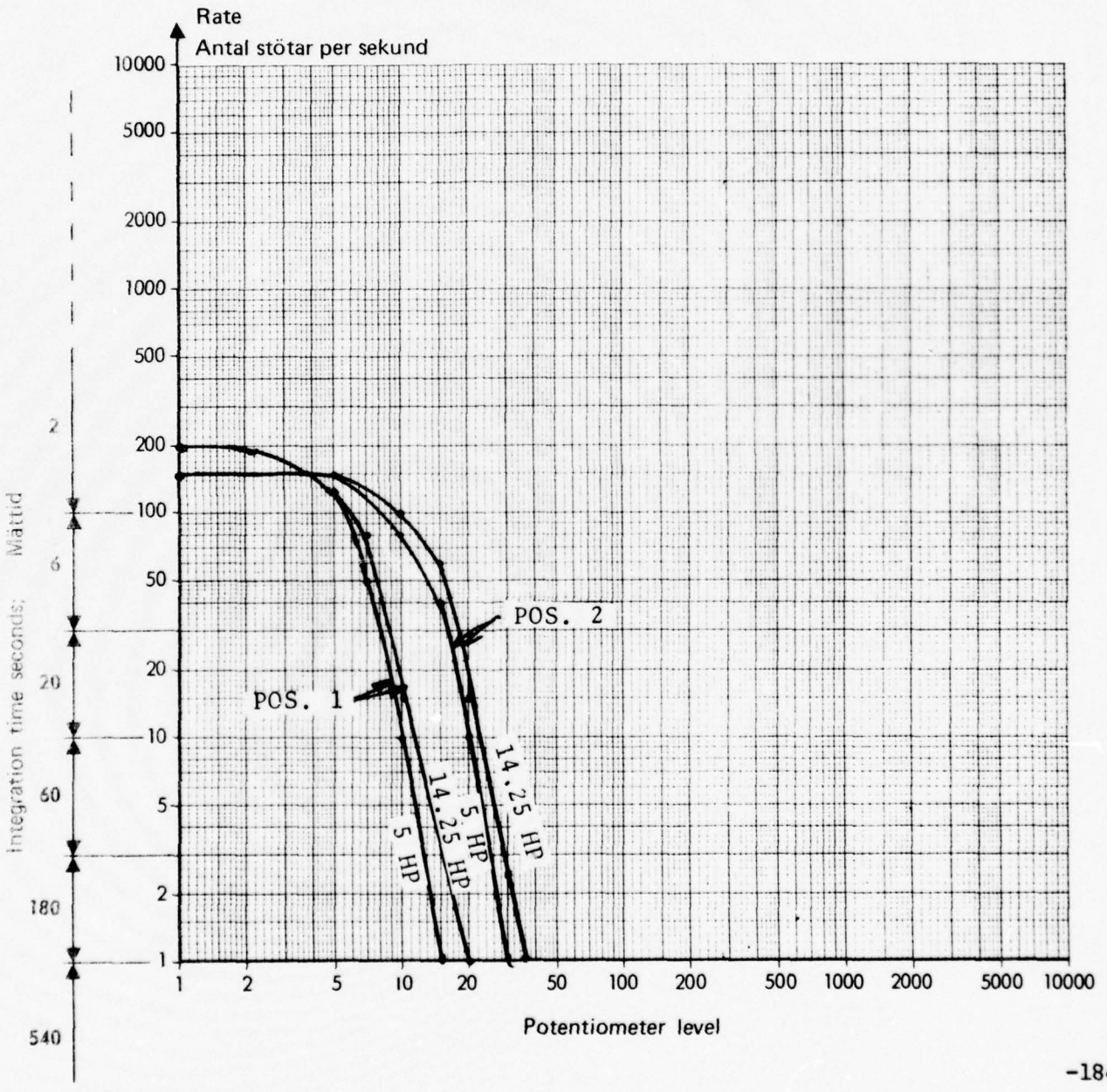


SKF Kl 169 Art. 1048-4 Repro 1695115907103

S/N A13 - 830

DAMAGED GEARS (2nd SET)

SPEED: 3540 RPM

AMBIENT: 82°F

GEAR BOX TEMP: 162°F at 33.75HP
153°F at 13.25HP

ENCLOSURE 14

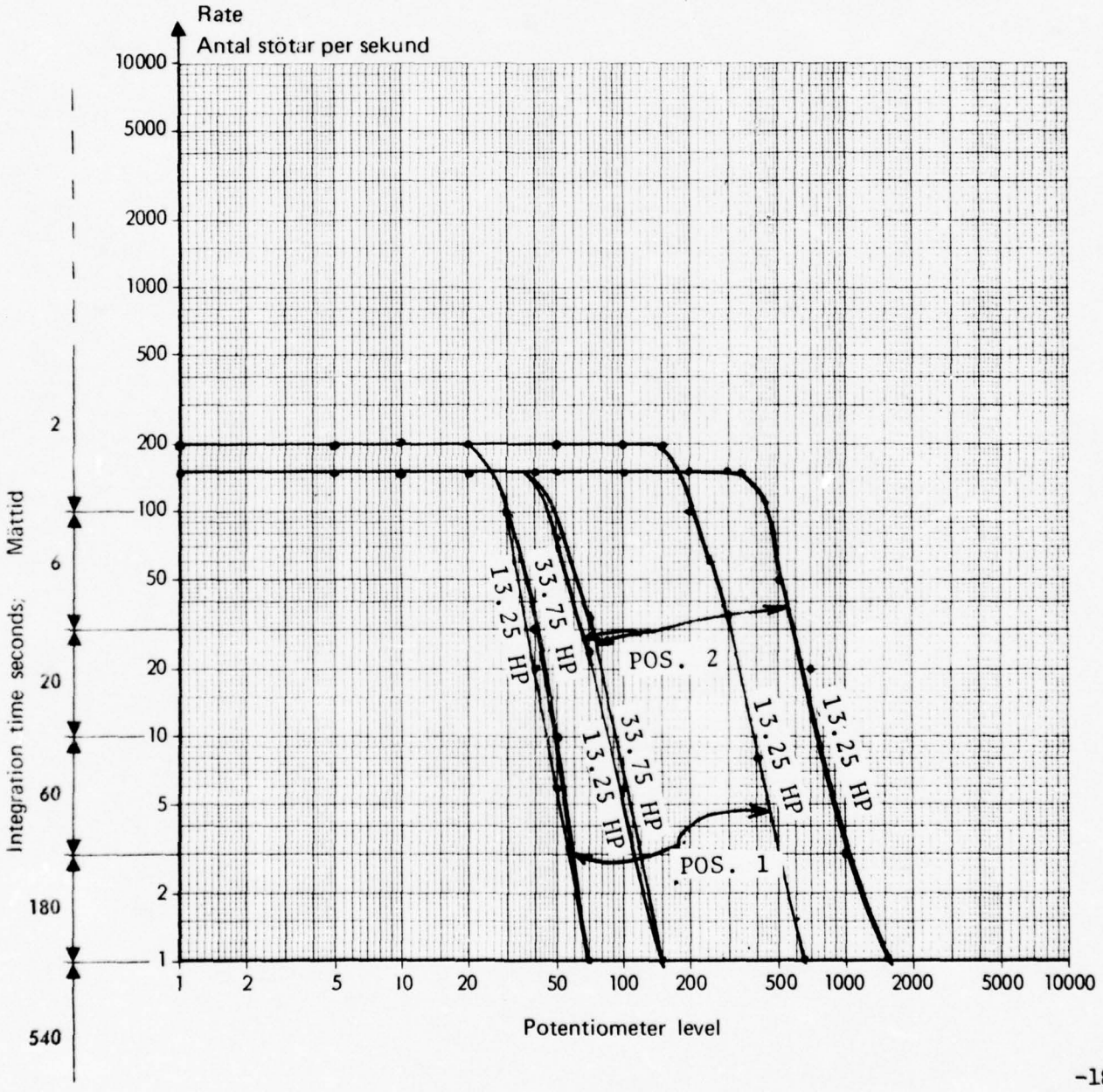

S/N B 13 - 1561

BASELINE DATA

SPEED: 1490 RPM

AMBIENT: 85°F

GEAR BOX TEMP: 108°F at 4.25 HP

107°F at 2.9 HP

ENCLOSURE 15

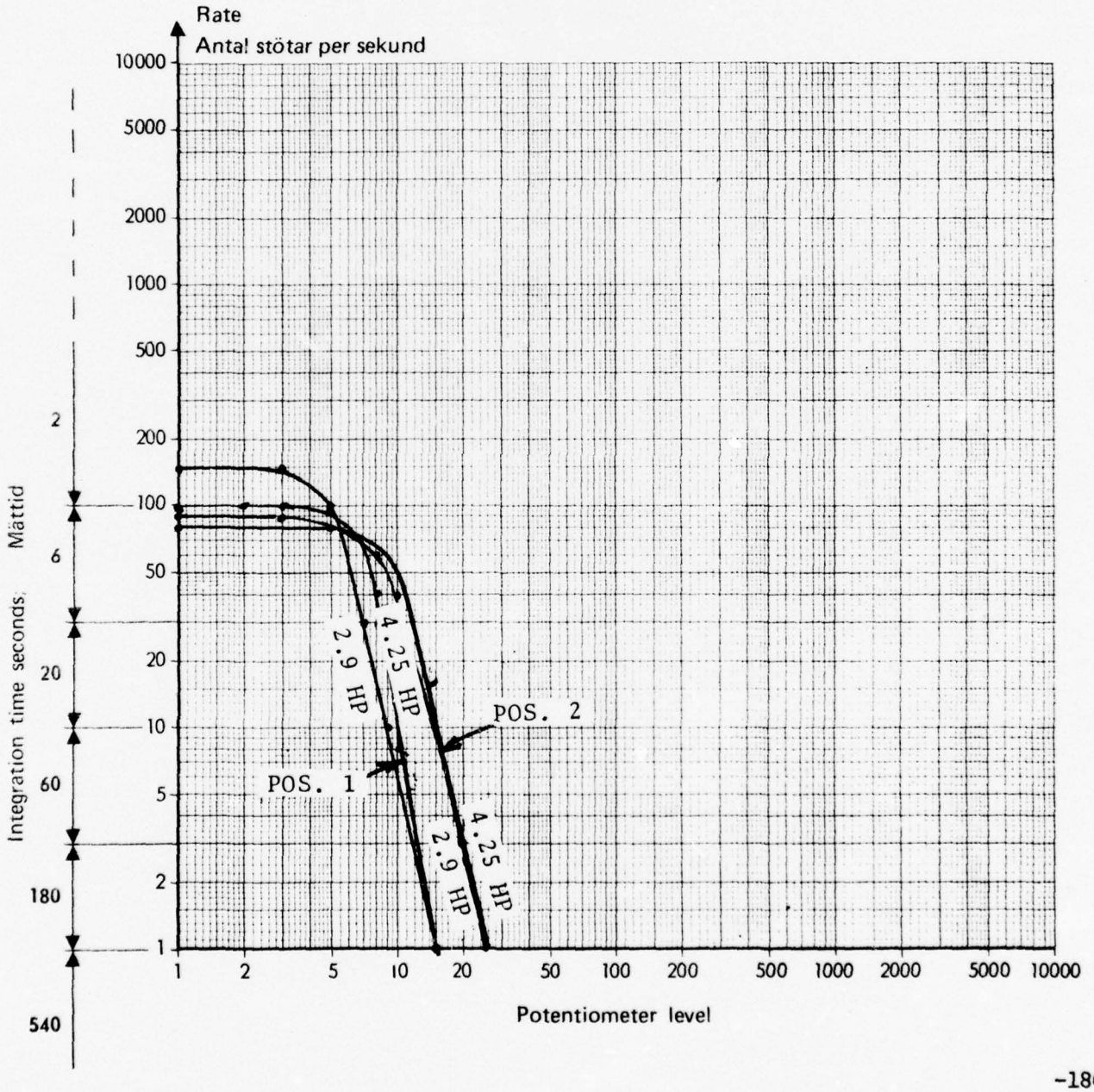

S/N B13 - 1561

BASELINE DATA

SPEED: 3580 RPM

AMBIENT: 75°F

GEAR BOX TEMP: 143°F at 10.4 HP

128°F at 2.6 HP

ENCLOSURE 16

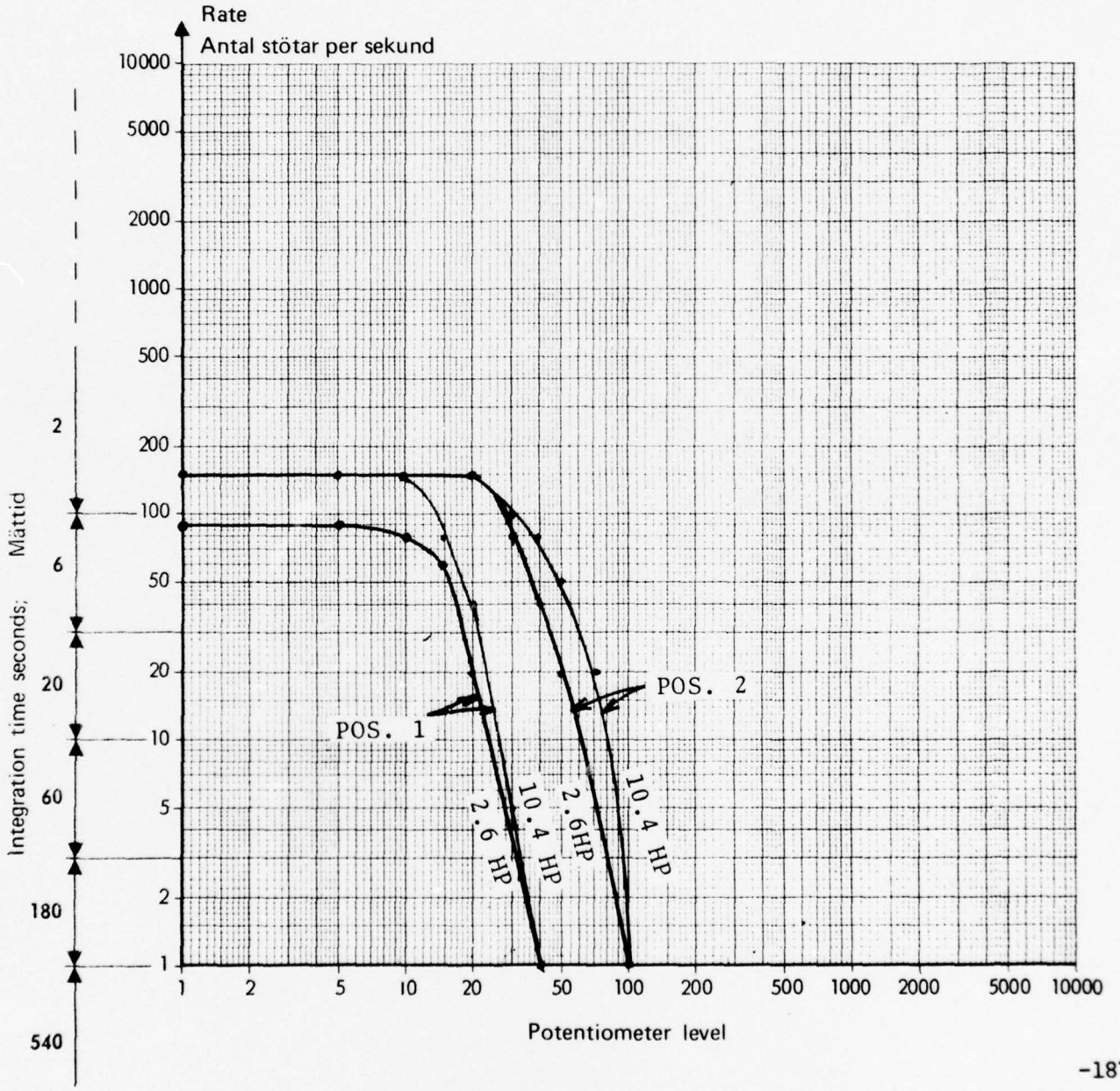

S/N B13 - 1561

BASELINE DATA

SPEED: 3540 RPM

AMBIENT: 86°F

GEAR BOX TEMP: 186°F at 33.75 HP
180°F at 13.25 HP

ENCLOSURE 17

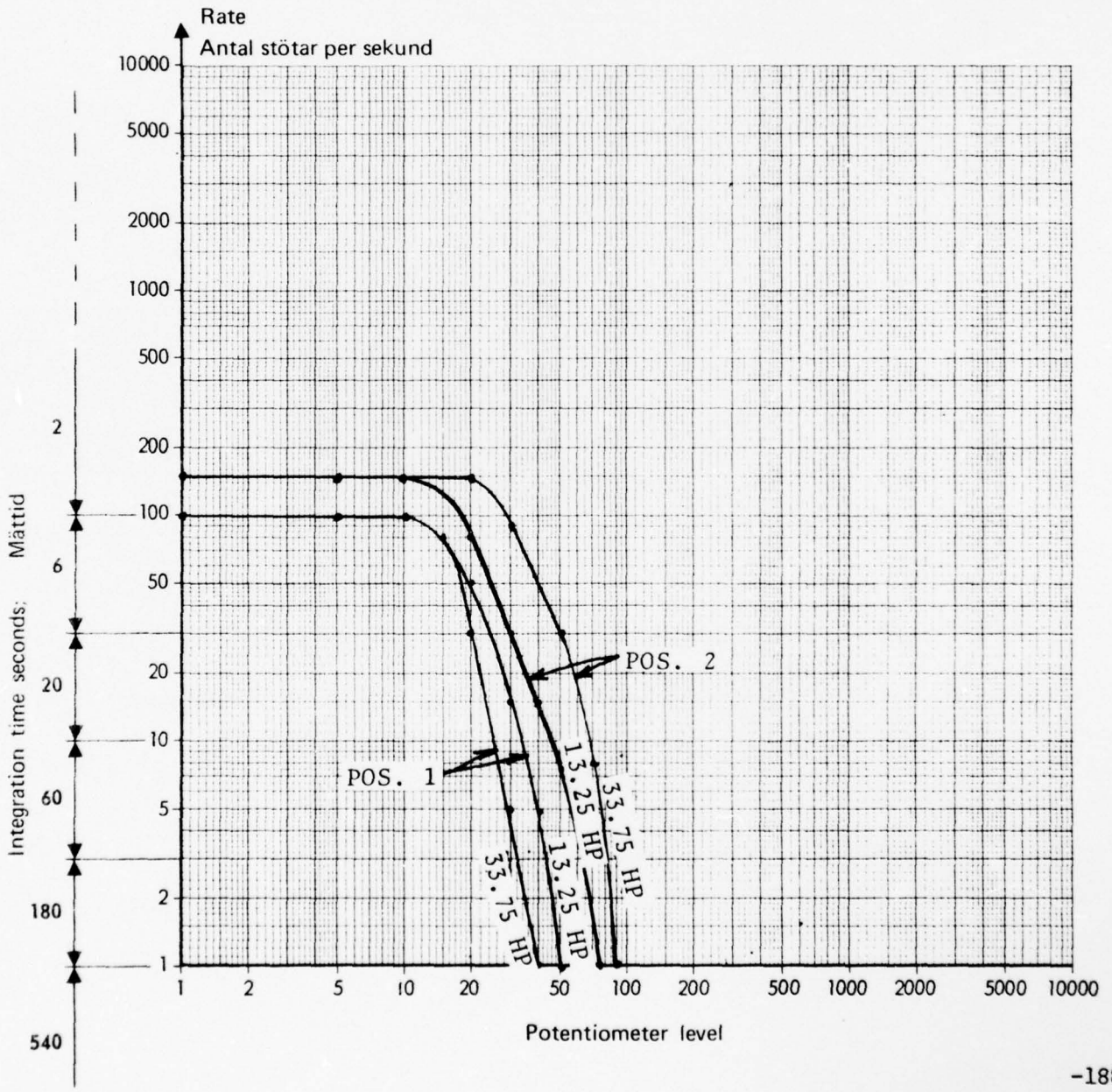


SKF Kl 169 Art. 1048-4 Repro 1695-7500-7103

ENCLOSURE 18

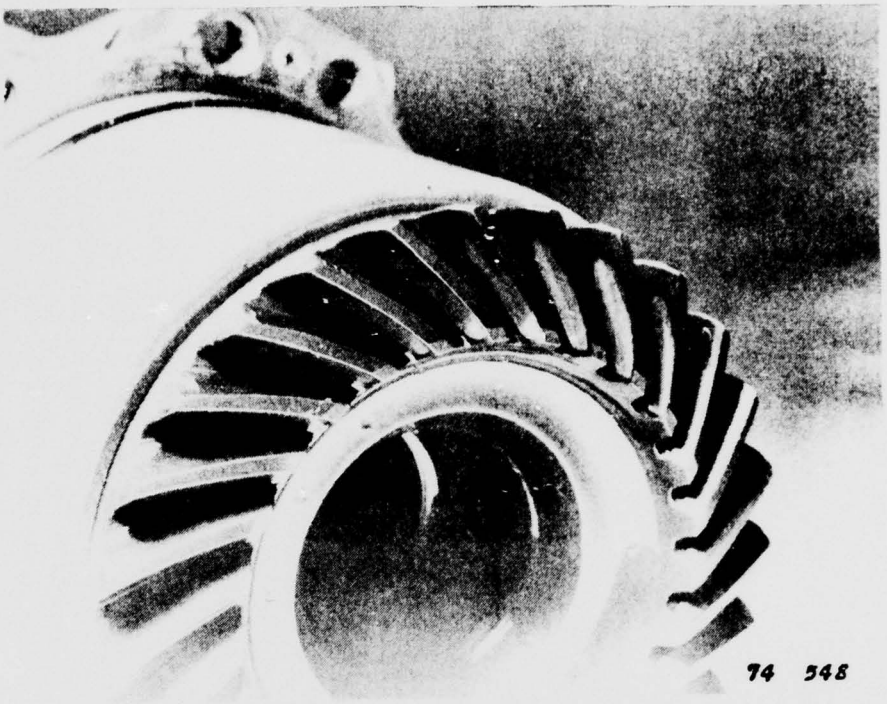


INPUT GEAR - TEST 2

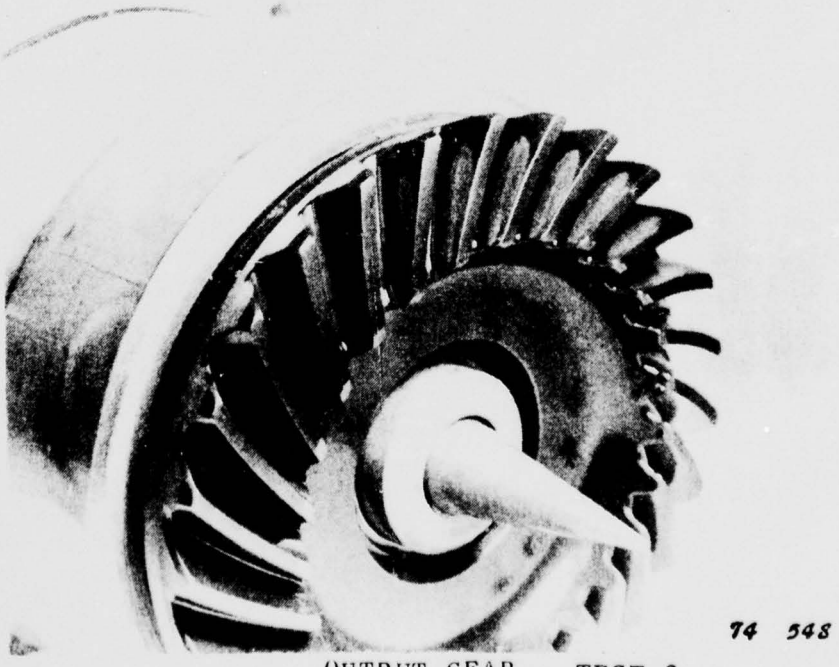


OUTPUT GEAR - TEST 2

F-4185A R100

RESEARCH LABORATORY SKF INDUSTRIES, INC.

S/N B13 - 1561

ARTIFICIALLY DAMAGED GEARS

SPEED: 1520 RPM

AMBIENT: 73° F

GEAR BOX TEMP: 107°F at 14.5 HP
105°F at 5 HP

ENCLOSURE 19

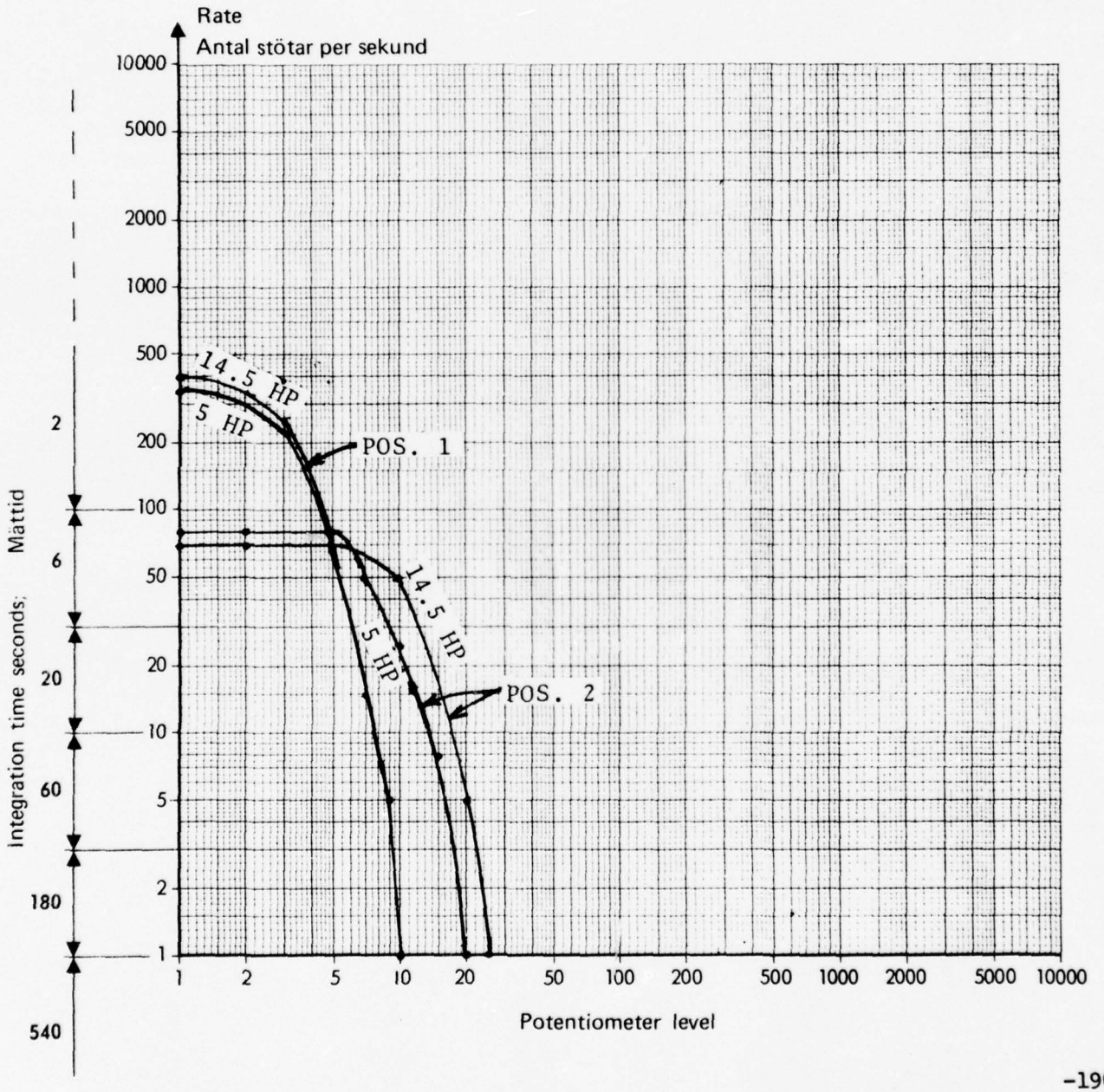

S/N B13 - 1561

ARTIFICIALLY DAMAGED GEARS

SPEED: 3540 RPM

AMBIENT: 78°F

GEAR BOX TEMP: 108°F at 13.25HP

ENCLOSURE 20

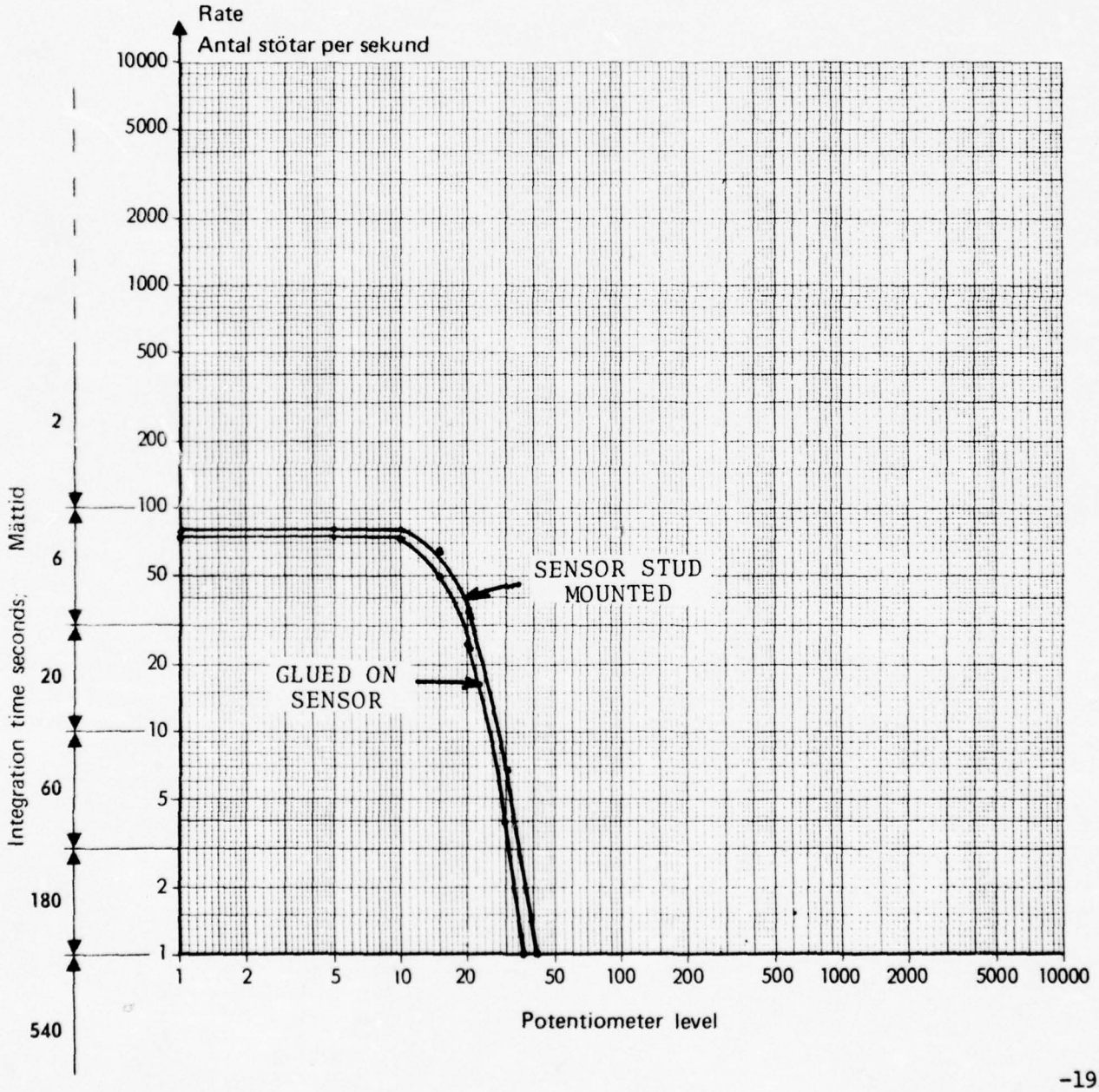


SKF KI 169 Art. 1048-4 Repro 16959 2500 7103

S/N B13 - 1561

ARTIFICIALLY DAMAGED GEARS

SPEED: 3540 RPM

AMBIENT: 78°F

GEAR BOX TEMP: 160°F at 33.75 HP
153°F at 13.25HP

ENCLOSURE 21

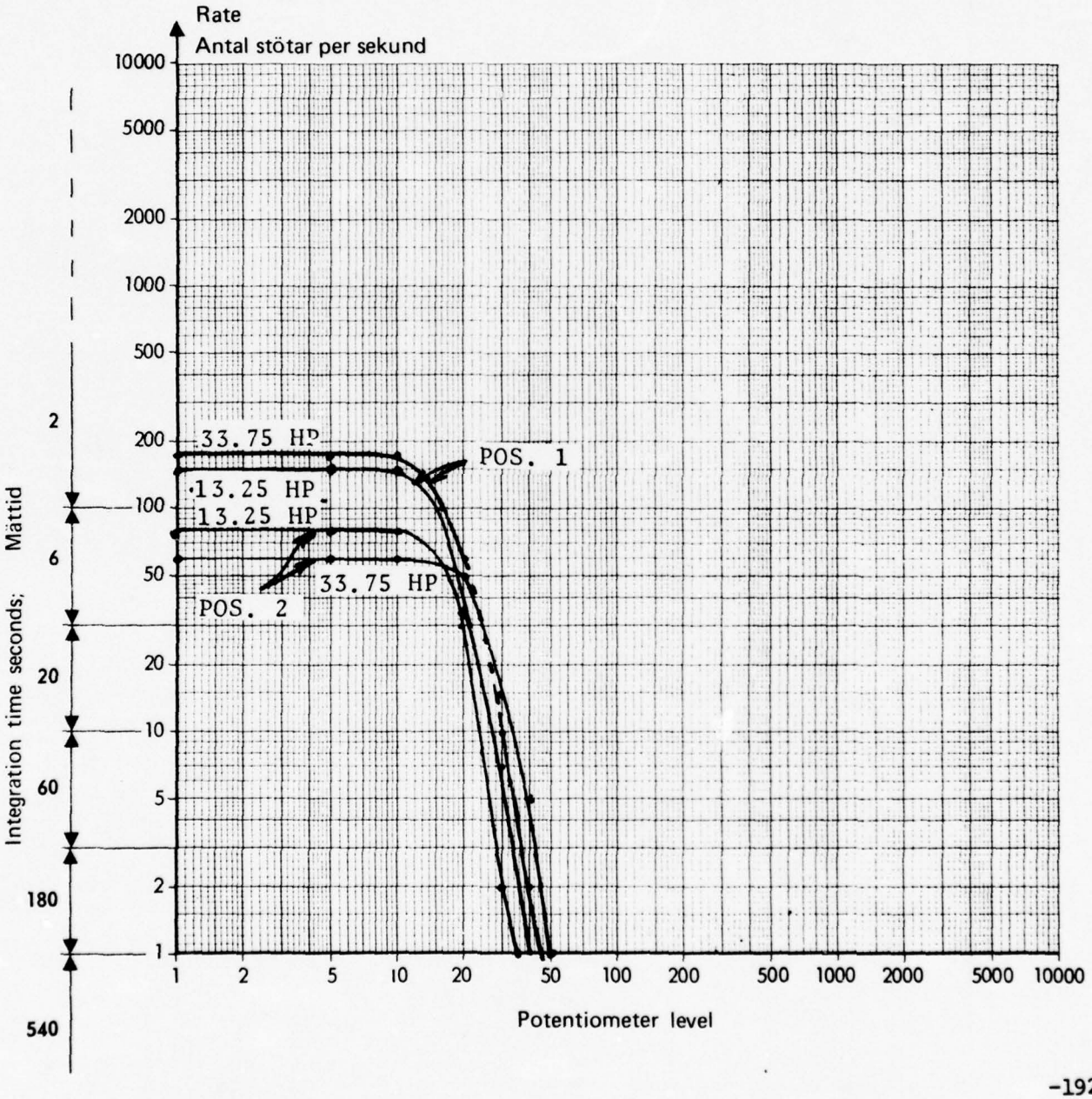


SKF Kl 169 Art. 1048-4 Repro 16959 7500 7103

S/N B13 - 1561

ARTIFICIALLY DAMAGED GEARS

SPEED: 3540 RPM

ENCLOSURE 22

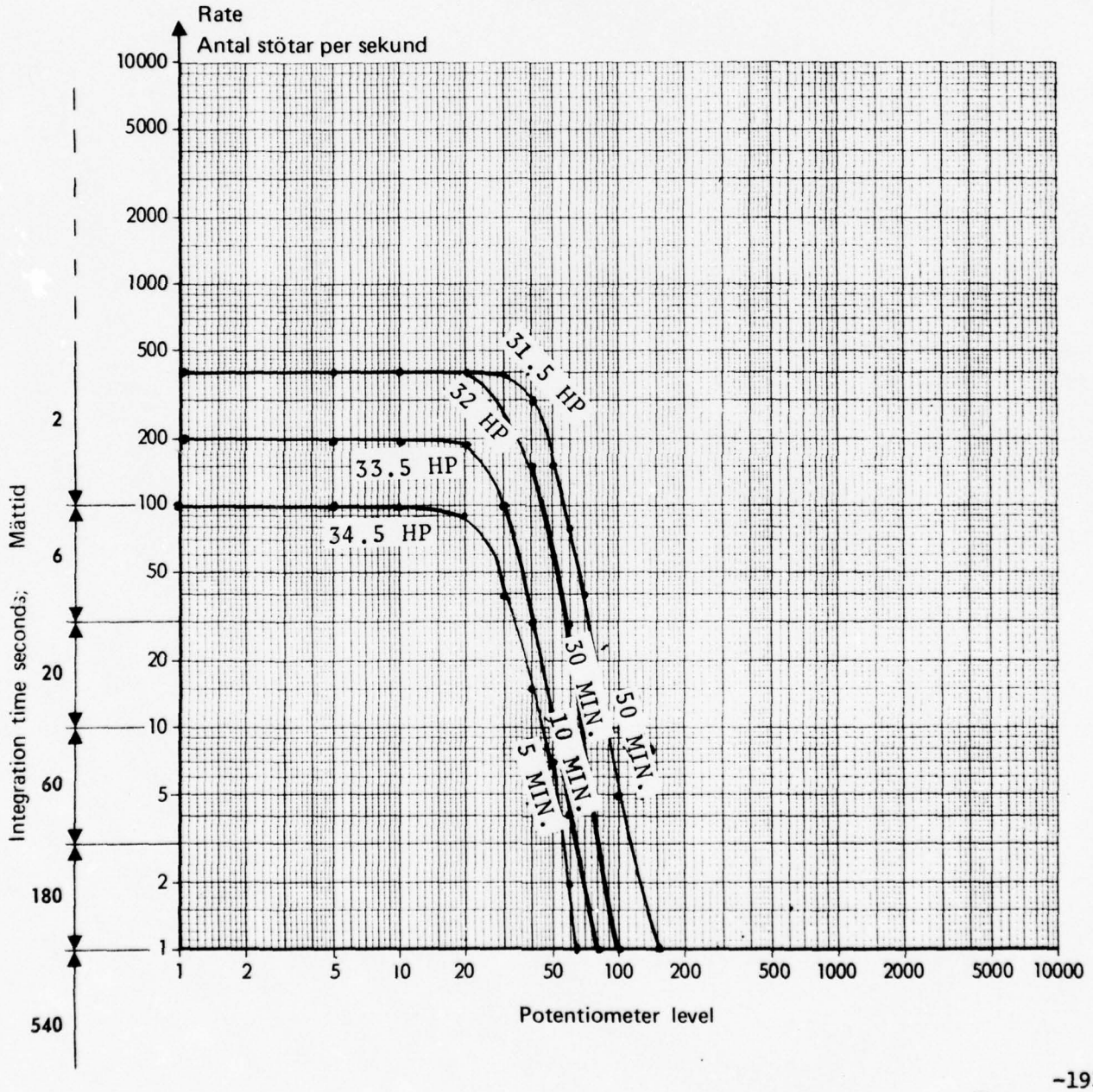


SKF Kl 169 Art. 1048-4 Repro 16959 7500 7103


INPUT GEAR WITH SCRIBE MARKS - TEST 7

Enclosure 23

F-4136A R100

S/N B13 - 1561

DAMAGED GEAR

SPEED: 1490 RPM

AMBIENT: 66°F

GEAR BOX TEMP: 102°F

POSITION 2

*ENCLOSURE 24*

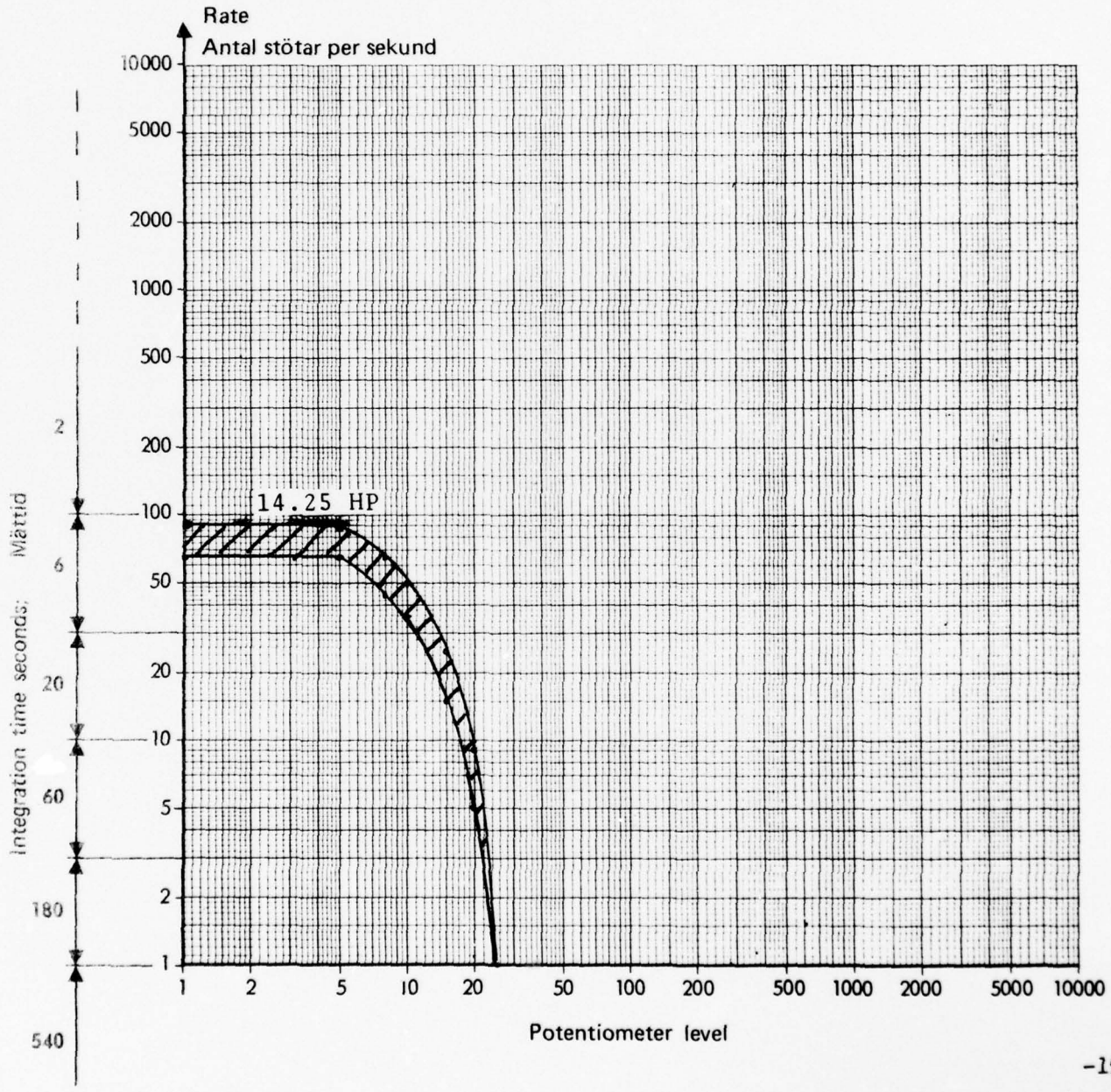


SKF Kl 169 Art. 1048-4 Repro 16950 7500 7103

S/N B13 - 1561

DAMAGED GEARS

SPEED: 1490 RPM

AMBIENT: 68°F

GEAR BOX TEMP: 103°F

POSITION 1

ENCLOSURE 25

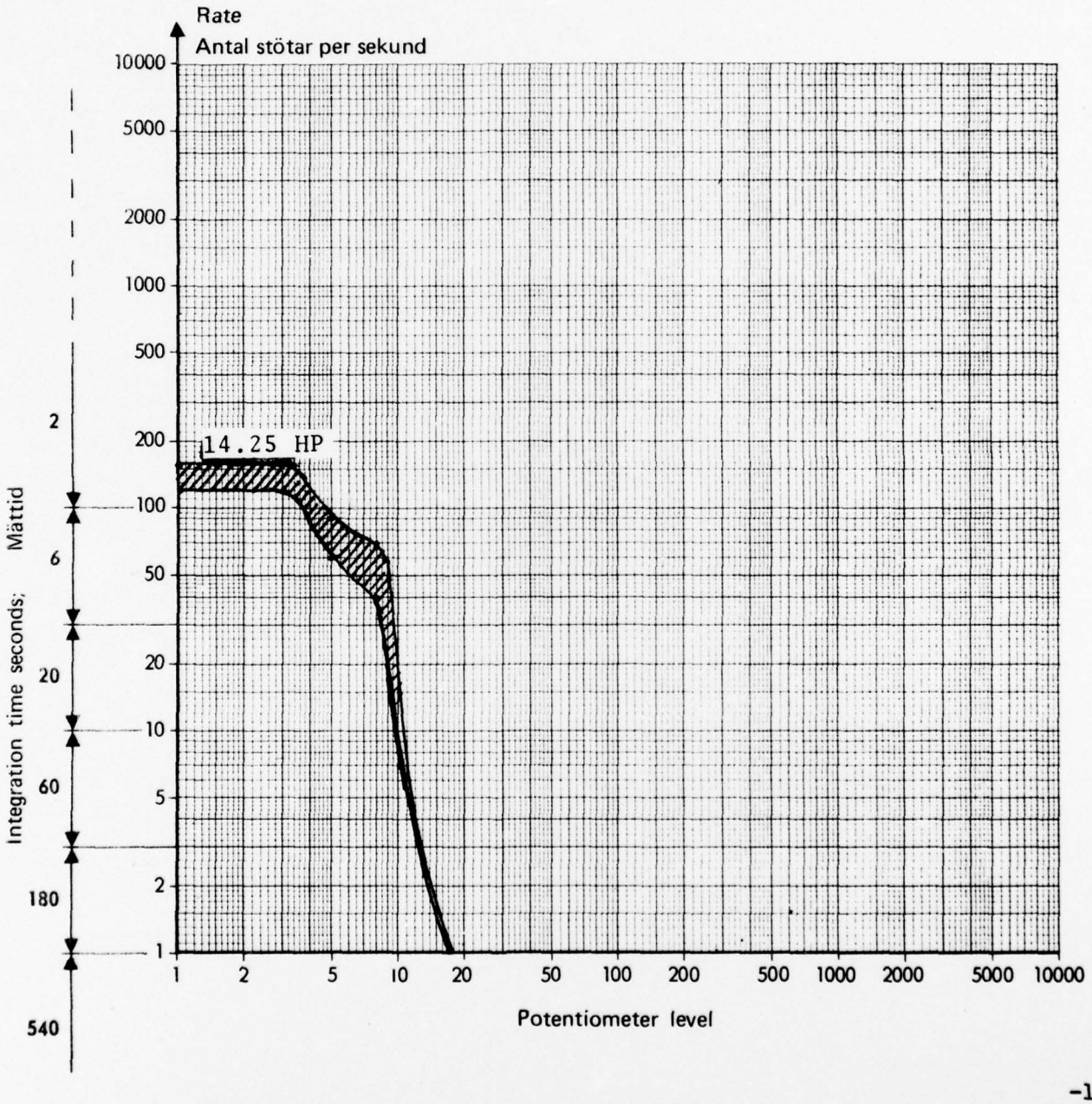


SKF KI 169 Art. 1148-4 Repro 1695y 7500 7103

S/N B13 - 1561
DAMAGED GEARS
SPEED: 1490 RPM
AMBIENT: 68°F
GEAR BOX TEMP: 104°F

POSITION 3

ENCLOSURE 26

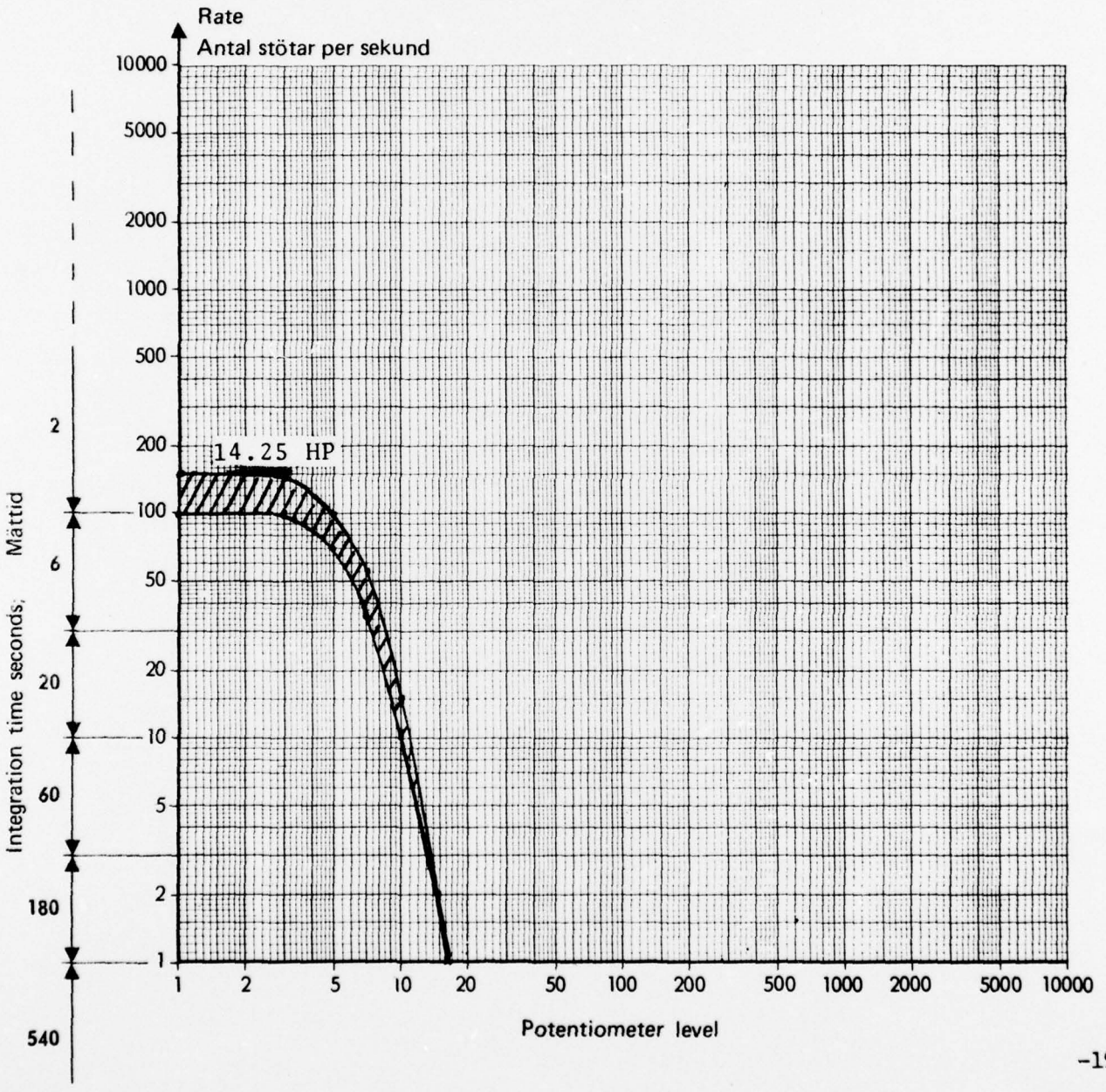

S/N B13 - 1561

DAMAGED BEARING

SPEED: 1490 RPM

AMBIENT: 70°F

GEAR BOX TEMP: 82°F

POSITION 2

ENCLOSURE 27

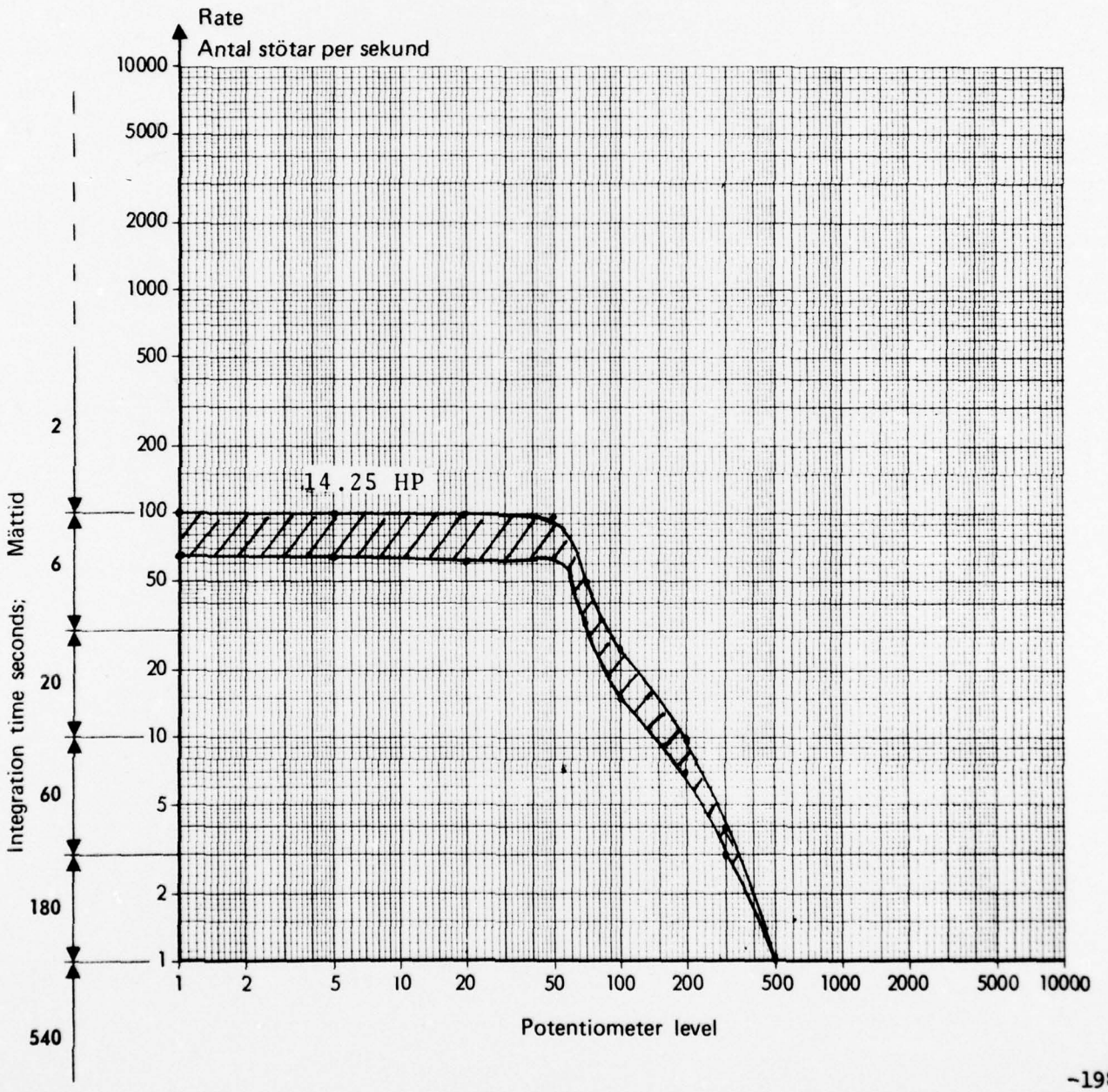


SKF Kl 169 Art. 1048-4 Repro 16959 7500 7103

S/N B13 - 1561

DAMAGED BEARING

SPEED: 1490 RPM

AMBIENT: 71°F

GEAR BOX TEMP: 90°F

POSITION 1

ENCLOSURE 28

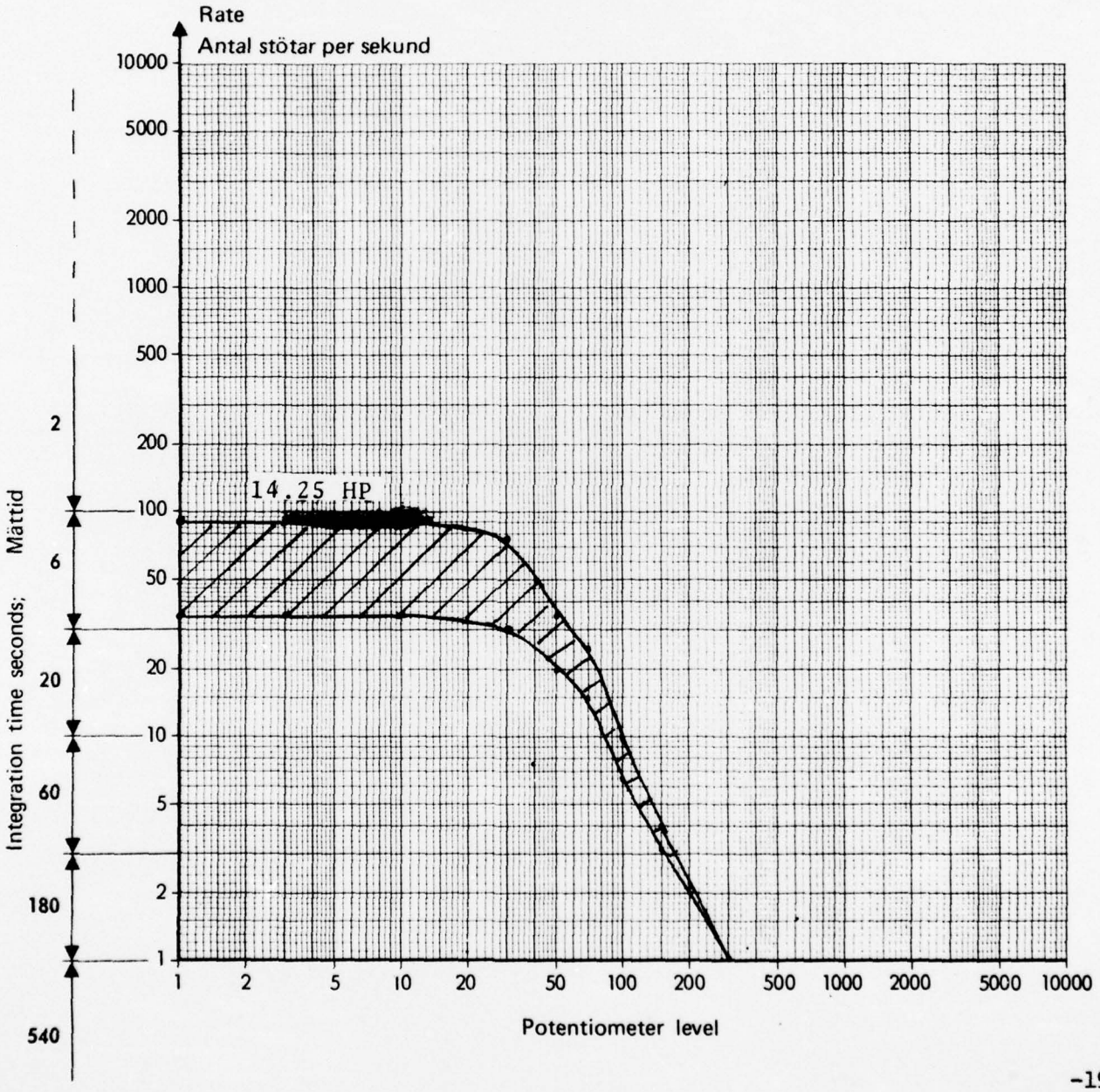


SKF Kl 169 Art. 1048-4 Repro 16959 7500 7103

S/N B13 - 1561

DAMAGED BEARING

SPEED: 1490 RPM

AMBIENT: 71°F

GEAR BOX TEMP: 95°F

POSITION 3

ENCLOSURE 29

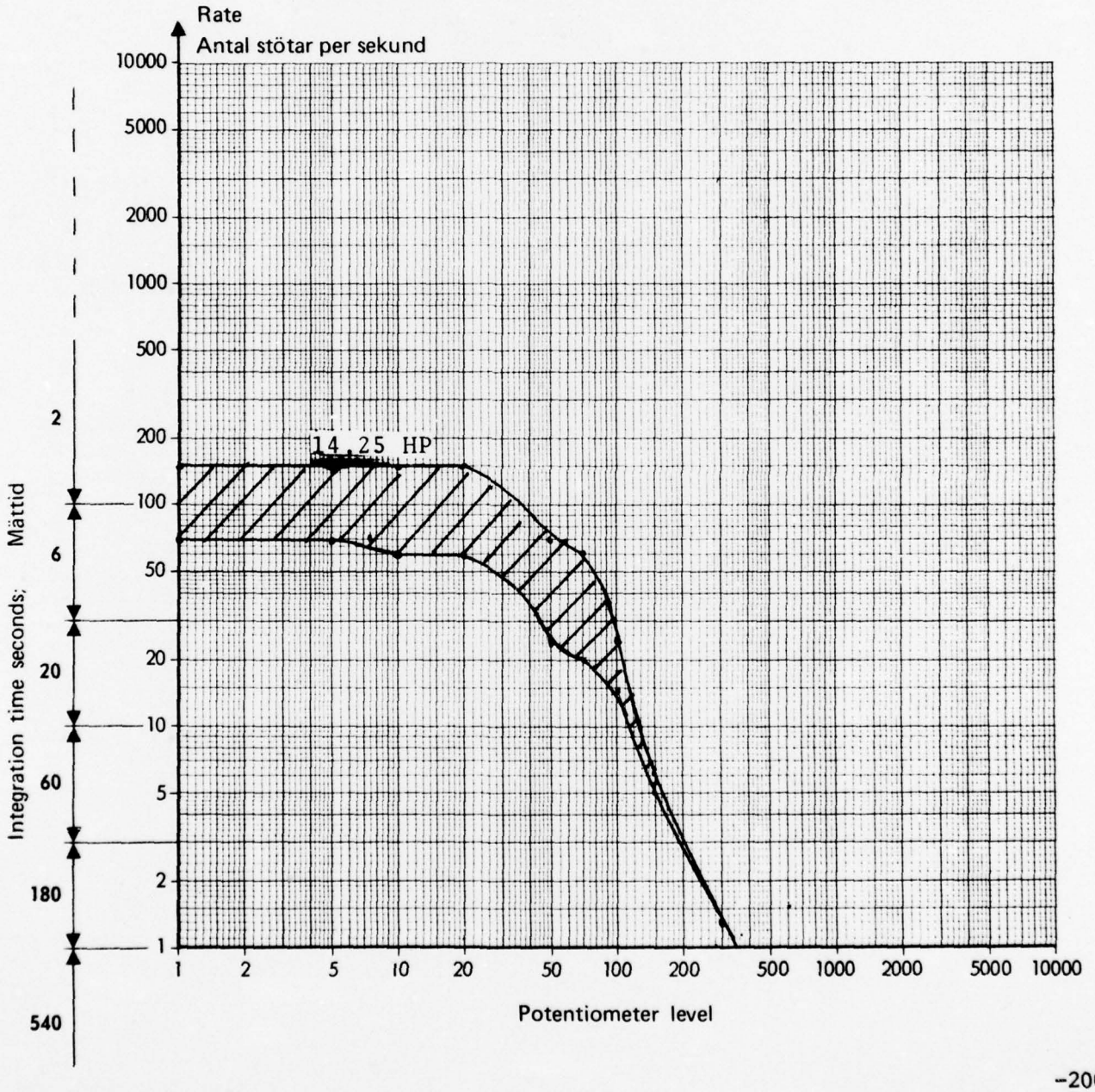


SKF Kl 169 Art. 1048-4 Repro 16959 2500 7103

ENCLOSURE 30

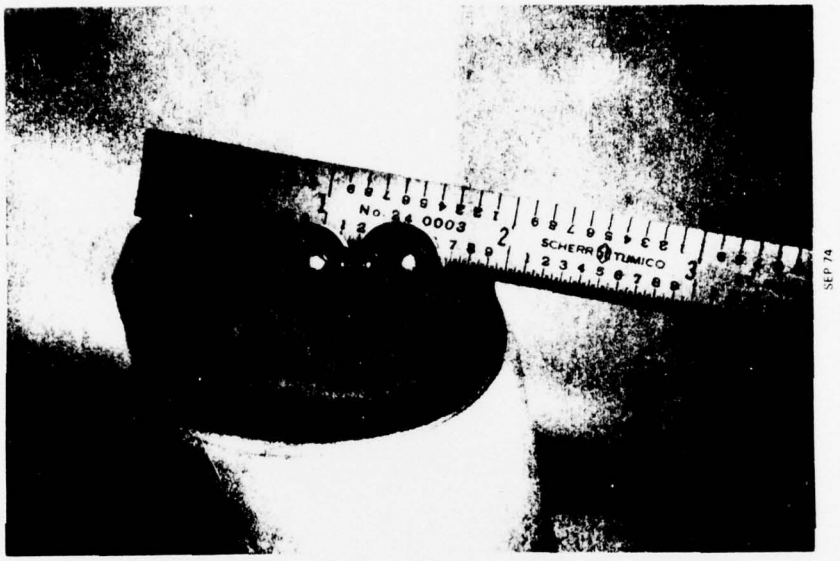


TEST 8 - BALL DAMAGE

F-1364 R100

S/N BBB - 1253

BASELINE DATA

SPEED: 1520 RPM

AMBIENT: 70°F

GEAR BOX TEMP: 98°F at 5 HP
103°F at 14.5HP

ENCLOSURE 31

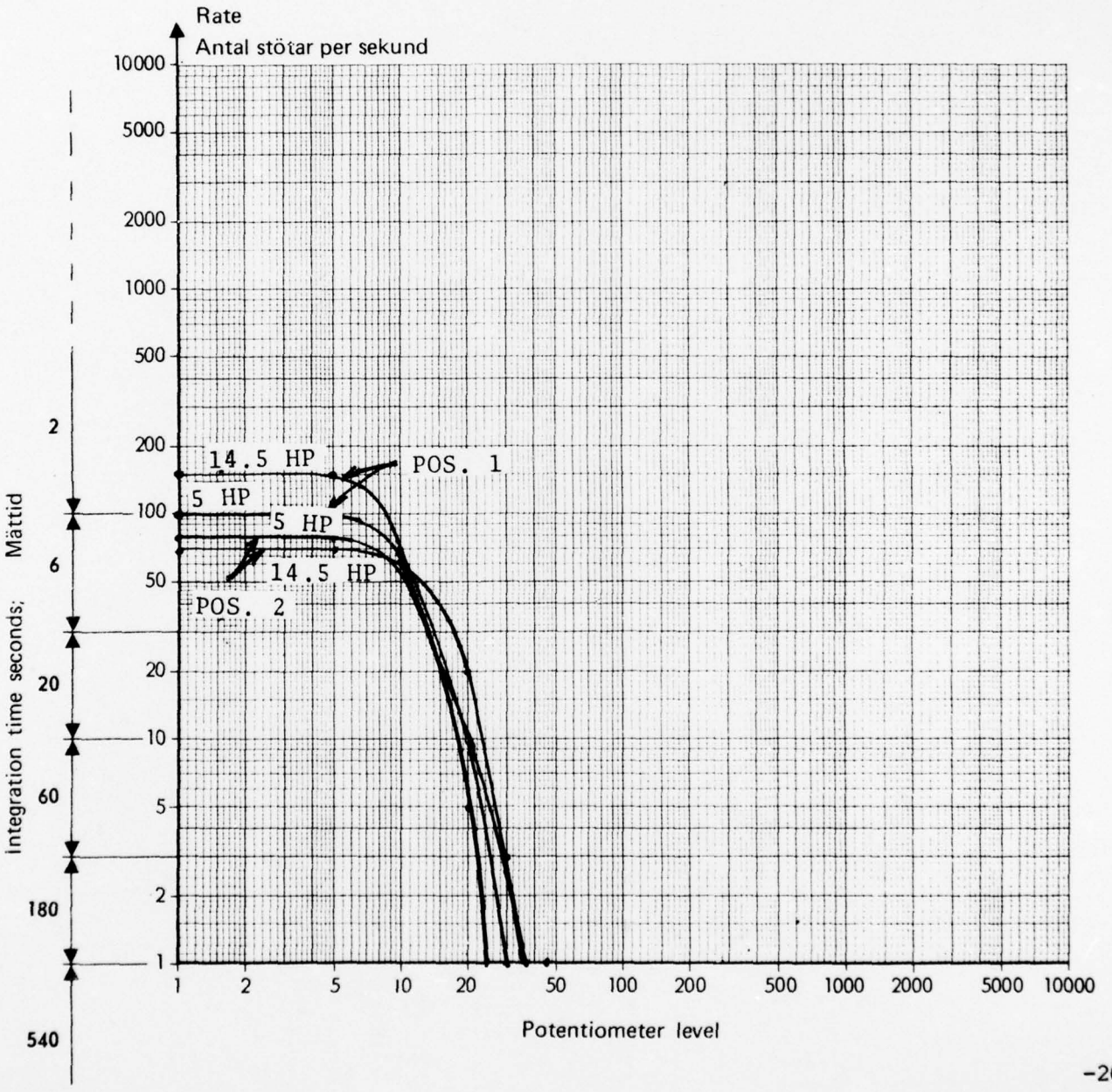


SKF KI 169 Art. 1048-4 Repro 16959 7500 7103

S/N BBB - 1253

BASELINE DATA

SPEED: 3540 RPM

AMBIENT: 92°F

GEAR BOX TEMP: 173°F at 13.25HP
180°F at 33.75HP

ENCLOSURE 32

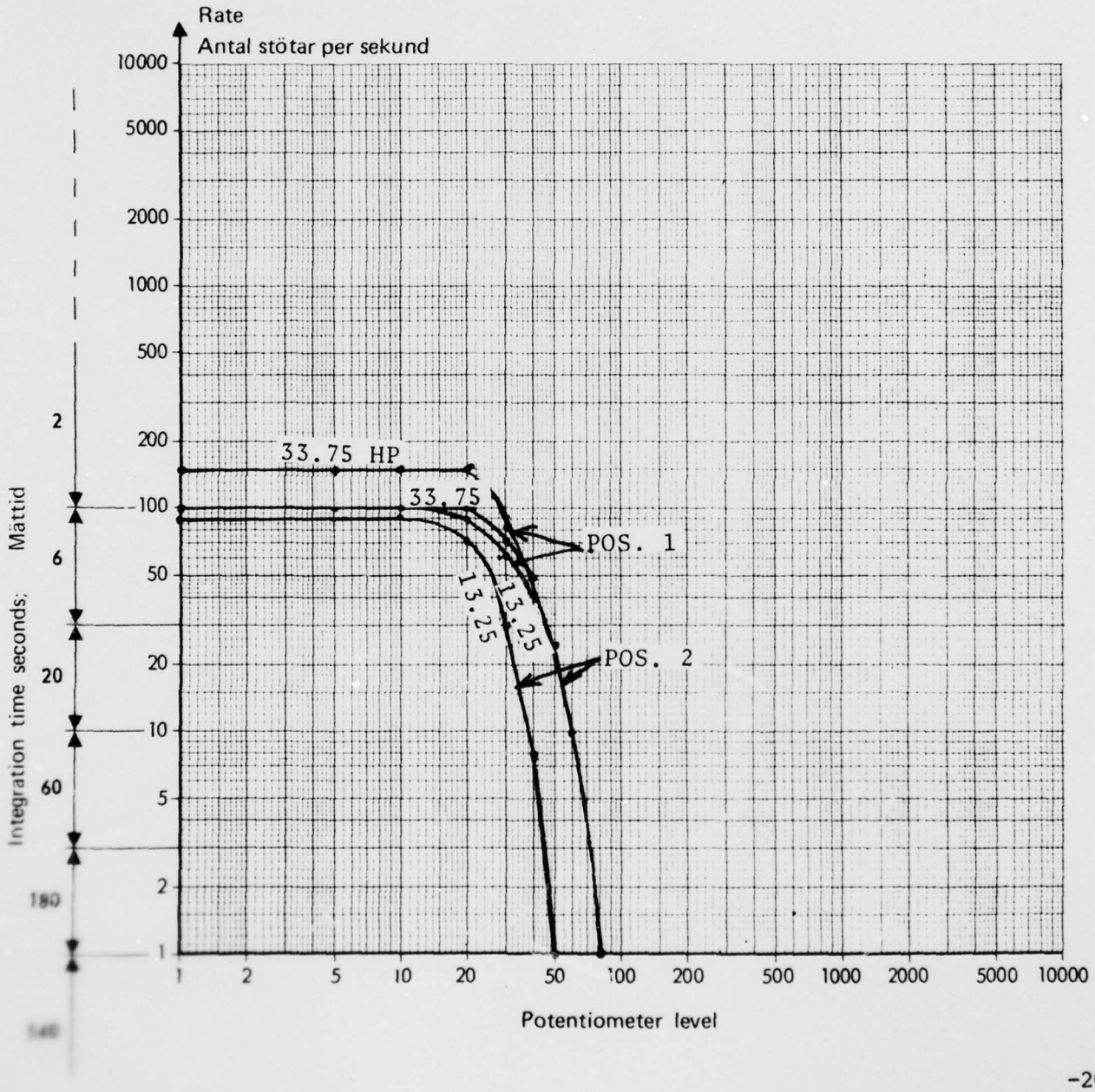

| GEAR BOX | CONDITION | LOAD (HP) | SPEED (RPM) | LOW BAND 50-300 cpa (μ in/sec) | MID BAND 300-1800 cps (μ in/sec) | HIGH BAND 1800-10000 cps (μ in/sec) |
|---|---|---|---|---|---|---|
| S/N A13-830 | DAMAGED GEARS | 33.75 | 3580 | 34k TO 64k | 183k | 128k |
| S/N B13-1561 | UNDAMAGED | 33.75 | 3540 | 64k TO 102k | 274k | 150k |
| S/N BBB-1253 | UNDAMAGED | 33.75 | 3540 | 60k TO 144k | 348k | 256k |
| S/N B13-1561 | ARTIFICIAL DAMAGE | 33.75 | 3540 | 238k | 293k | 220k |
| S/N A13-830 | DAMAGED GEARS (2nd Set) | 33.75 | 3540 | 219k | 549k | 402k |
| S/N BBB-1253 | UNDAMAGED | 14.5 | 1520 | 40k TO 56k | 121k | 44k |
| S/N B13-1561 | ARTIFICIAL DAMAGE | 14.5 | 1520 | 48k | 311k | 33k |
| S/N A13-830 | DAMAGED GEARS | 14.25 | 1510 | 220k | 220k | 37k |

ENCLOSURE 33

S/N A13-830
SPEED - 1520RPM
LOAD - 9.75HP

DAMAGED

40 DB = 1.16 in/sec

S
RH
9/30/74
RMS
-40DB
20 CPS
50 DB

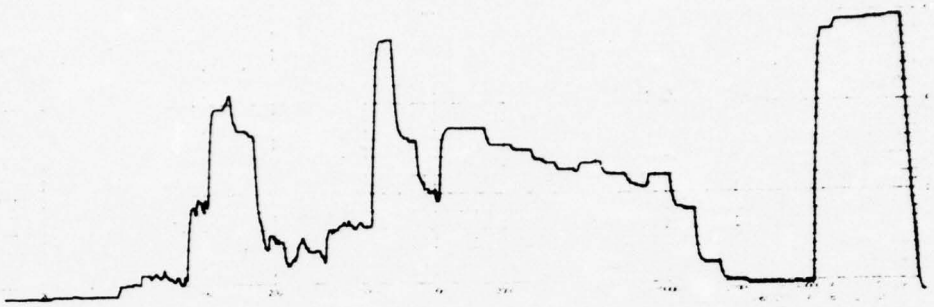

S/N BBB-1253
SPEED-3840 RPM
LOAD - 38.25 HP

NO DAMAGE

50DB = 1.16 in/sec

2
8/30/74
RMS
-50 DB
20 CPS
50 DB

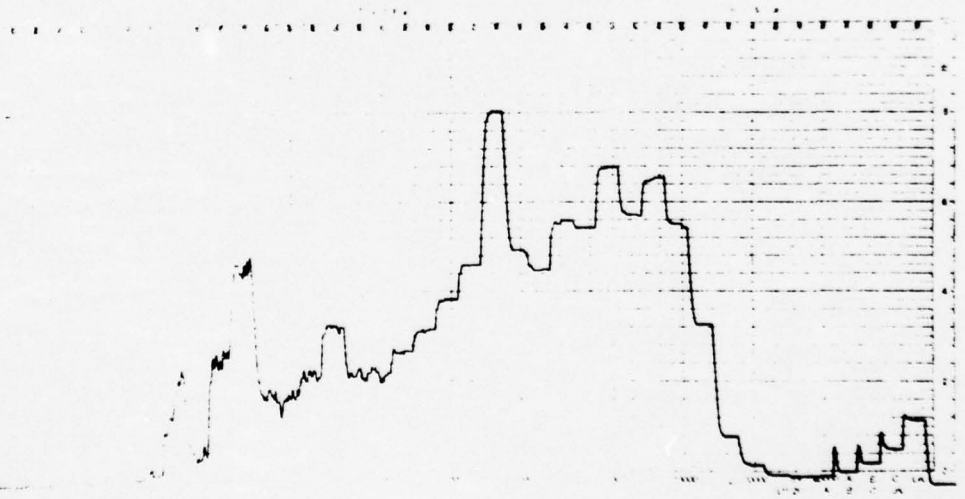

ENCLOSURE 34

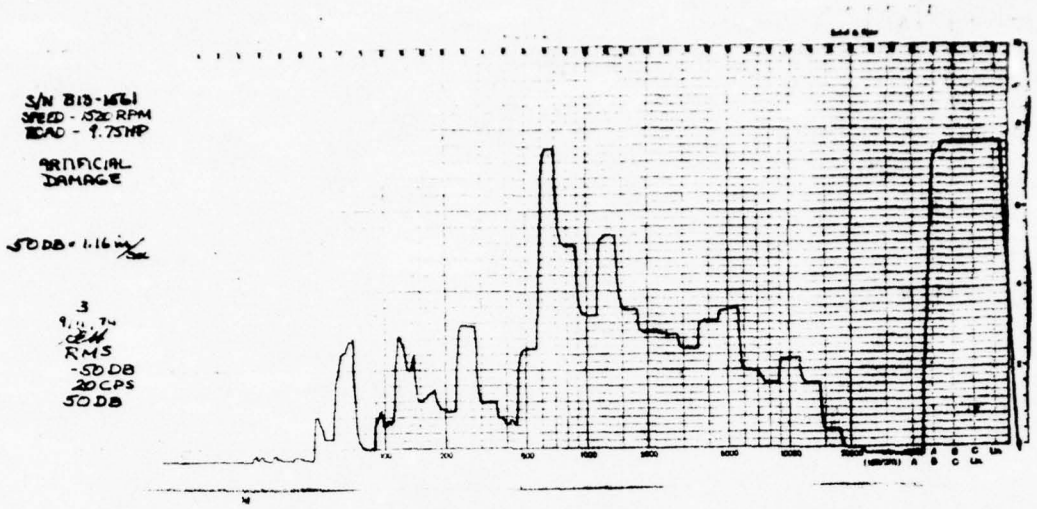


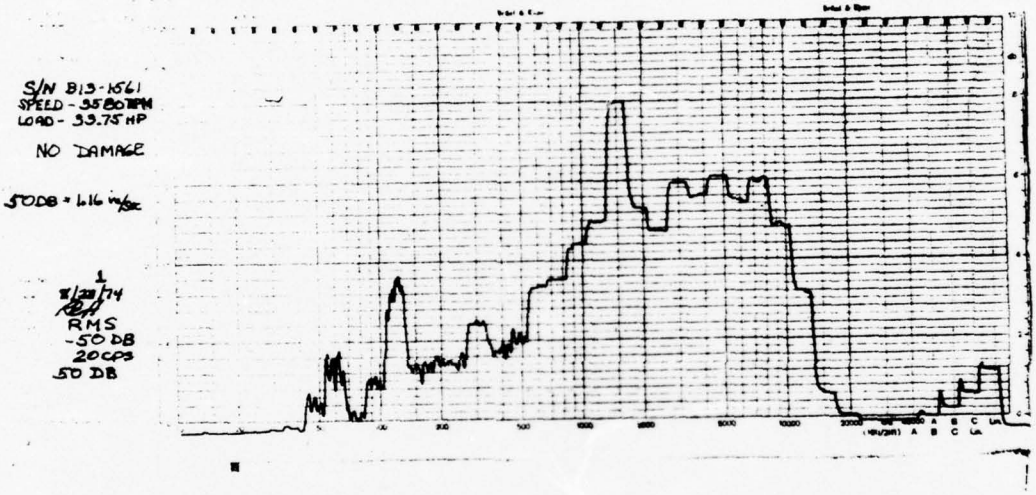


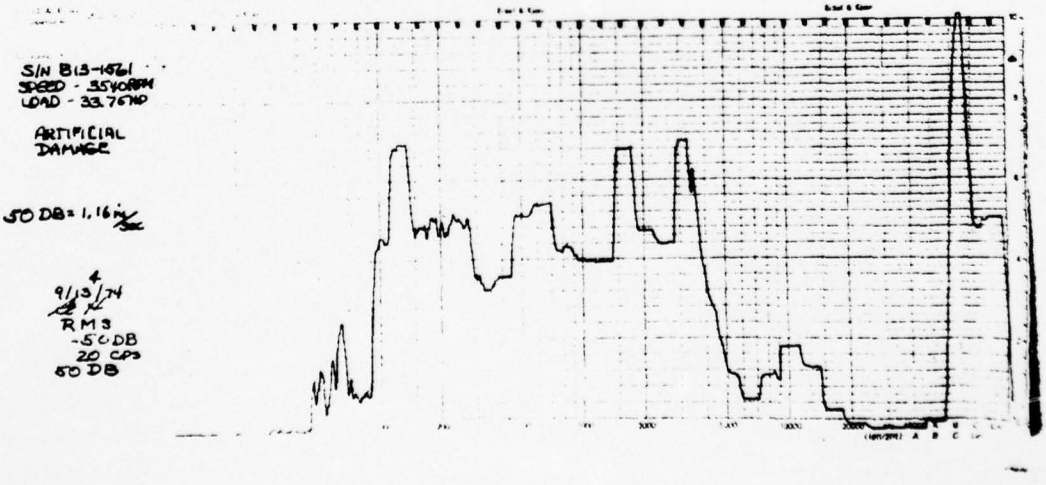


ENCLOSURE 35

RESEARCH LABORATORY SKF INDUSTRIES, INC.

| TEST | ENCLOSURES | GEARBOX | GEAR CONDITION | SPEED (RPM) | LOADS (HP) 1 | 2 | |
|---|---|---|---|---|---|---|---|
| 1 | 6 | A13-830 | Baseline | 1480 | 2.9 | 4.25 | |
| | 7 | A13-830 | Baseline | 3560 | 2.6 | 10.4 | |
| 2 | 15 | B13-1561 | Baseline | 1490 | 2.9 | 4.25 | |
| | 16 | B13-1561 | Baseline | 3580 | 2.6 | 10.4 | |
| | 17 | B13-1561 | Baseline | 3580 | 13.25 | 33.75 | |
| 3 | 9 | A13-830 | Heavily Damaged | 1480 | 2.9 | 4.25 | |
| | 10 | A13-830 | Heavily Damaged | 3580 | 2.6 | 10.4 | |
| 4 | 11 | A13-830 | Heavily Damaged | 3540 | 13.25 | 33.75 | |
| 5 | 13 | A13-830 | Damaged (2nd Set) | 1510 | 5 | 14.25 | |
| | 14 | A13-830 | Damaged (2nd Set) | 3540 | 13.25 | 33.75 | |
| 6 | 19 | B13-1561 | Artificial Damage | 1520 | 5 | 14.5 | |
| | 20 | B13-1561 | Artificial Damage | 3540 | 13.25 | | |
| | 21 | B13-1561 | Artificial Damage | 3540 | 13.25 | 33.75 | |
| | 22 | B13-1561 | Artificial Damage | 3540 | 31.5 | to34.5 HP | (load varied with temp.) |
| 7 | 24 | B13-1561 | Damaged Gear | 1490 | 14.25 | | Pos. 2 |
| | 25 | B13-1561 | Damaged Gear | 1490 | 14.25 | | Pos. 1 |
| | 26 | B13-1561 | Damaged Gear | 1490 | 14.25 | | Pos. 3 |
| 8 | 27 | B13-1561 | Damaged Bearing | 1490 | 14.25 | | Pos. 2 |
| | 28 | B13-1561 | Damaged Bearing | 1490 | 14.25 | | Pos. 1 |
| | 29 | B13-1561 | Damaged Bearing | 1490 | 14.25 | | Pos. 3 |
| 9 | 31 | BBB-1253 | Baseline | 1520 | 5 | 14.5 | |
| | 32 | BBB-1253 | Baseline | 3540 | 13.25 | 33.75 | |

Enclosure 36

## 7.8 STATISTICAL SUMMARY OF SHOCK PULSE DATA

| ITEM | | $\bar{x}$ | SD | SE |
|---|---|---|---|---|
| Hanger Bearings Total | Rate | 185.19 | 85.76 | 11.67 |
| | Level | 502.4 | 943.14 | 128.35 |
| $42^{o}$ G/B | Rate | 149.05 | 121.71 | 18.78 |
| | Level | 106.5 | 79.59 | 12.28 |
| $90^{o}$ G/B | Rate | 114.375 | 31.1 | 10.99 |
| | Level | 75.0 | 54.71 | 19.34 |
| Mast Bearing | Rate | 87.27 | 38.82 | 11.7 |
| | Level | 72.73 | 29.61 | 8.93 |
| Input Drive Quill | Rate | 161.81 | 37.37 | 11.27 |
| | Level | 190.91 | 67.89 | 20.47 |
| Hanger Bearings Removed | Rate | 273.64 | 52.06 | 15.7 |
| | Level | 1836.36 | 1575.61 | 475.06 |
| Hanger Bearings Not Removed | Rate | 172.0 | 78.59 | 12.43 |
| | Level | 147.93 | 189.46 | 29.96 |
| OH-58 Hangers | Rate | 95 | 50.79 | 20.736 |
| | Level | 77 | 37.79 | 15.427 |
| Hanger Bearings Not Removed | Rate | 170.23 | 84.35 | 12.86 |
| | Level | 159 | 213.45 | 32.55 |
| Hanger Bearings Removed | Rate | 271.67 | 72.37 | 20.89 |
| | Level | 2254.17 | 2126.83 | 613.96 |
| $42^{o}$ G/B Not Removed | Rate | 111.32 | 73.11 | 12.54 |
| | Level | 102.147 | 124.24 | 21.31 |
| $42^{o}$ G/B Removed | Rate | 337.22 | 195.02 | 65.01 |
| | Level | 180.0 | 85.99 | 28.66 |
| $90^{o}$ G/B Not Removed | Rate | 159.4 | 167.71 | 55.9 |
| | Level | 68.3 | 54.94 | 18.31 |
| Input Drive Quill High & Low Rate and corresponding levels removed | Rate | 161.81 | 37.37 | 11.27 |
| | Level | 189.1 | 70.21 | 21.17 |
| $90^{o}$ G/B Total High & Low Levels removed and corresponding Rates | Rate | 160.625 | 179.253 | 63.38 |
| | Level | 750 | 54.71 | 19.34 |